NASA CP-2017

An Assessment of Technology for Turbojet Engine Rotor Failures

A workshop held at
Massachusetts Institute of Technology
Cambridge, Massachusetts
March 29-31, 1977

NASA CP-2017

An Assessment of Technology for Turbojet Engine Rotor Failures

Edited by
Emmett A. Witmer
Massachusetts Institute of Technology

A workshop sponsored by
Lewis Research Center
Cleveland, Ohio
and held at
Massachusetts Institute of Technology
Cambridge, Massachusetts
March 29-31, 1977

PREFACE

In order to provide a convenient forum for assessing the technology available to cope with turbojet engine rotor failures and to obtain advice from engine manufacturers, airframe manufacturers, and airline operators on information needed in the 5-10-15 year future period to enhance safety with respect to engine rotor burst fragments, the NASA Lewis Research Center requested the MIT Aeroelastic and Structures Research Laboratory to host a Workshop on An Assessment of Technology for Turbojet Engine Rotor Failures. This Workshop was held at the Massachusetts Institute of Technology, Cambridge, Massachusetts during March 29, 30, and 31, 1977. The meeting agenda was essentially as shown in Appendix A. A list of attendees is given in Appendix B. The Workshop consisted of four sessions.

Session 1 was devoted to restating the nature and scope of the safety problems posed by turbojet engine rotor burst fragments; also, design considerations, objectives, and various approaches taken to cope with this safety problem were discussed.

Session 2 was devoted to examining the current state of the art for providing protection from engine rotor burst fragments. Included here were the use of layout arrangements and redundancies to provide continued safe operation in the event of fragment penetration following non-containment, selective escape of fragments in harmless directions, and local shield protection of aircraft components exterior to the engine casing. Protective structures consisting of single-layer metals, fiber composites, or layered multimaterial configurations were considered; experiments involving the responses of such structures to fragment impact were reviewed as were theoretical methods already developed or in the process of being developed to predict the attendant structural responses. (Current prediction capabilities and experimental data as well as anticipated needs in the 5-10-15 year future period, both experimental and theoretical, were considered.) The need to evaluate the effects of typical operating environments on newer containment/deflection materials and concepts was emphasized.

Session 3 centered attention on a variety of measures intended to prevent or to reduce the frequency and severity of engine rotor bursts. Design concepts tailored to insure that the first failure to occur (if at all) will produce small rather than large energetic fragments. The use of non-destructive test/inspection techniques to improve the quality of delivered items as well as vigilant inspection procedures which the airline operators can employ were indicated to be particularly effective measures to reduce failure incidence. Improvements in both access and inspection techniques for in-service monitoring of engines to detect trouble before a severe failure with large energetic fragments occurs were urged.

Session 4 was devoted to summarizing the main points raised in the three earlier sessions. A. K. Forney and J. J. Shea of the FAA presented a Summary of Design Considerations, Objectives, and Approaches. S. A. Sattar of Pratt & Whitney Aircraft was asked (with his associates) to summarize the status of Analysis and Experiments, Prospects, and Needed Research pertaining to Rotor Burst Protection. B. L. Koff and his GE colleagues presented a Summary of Status, Prospects, and Needed Research pertaining to Rotor Burst Prevention. At the conclusion of the Session 4 discussion, Mr. Solomon Weiss of the NASA Lewis Research Center closed the Workshop, expressing NASA's appreciation to all speakers and participants for their generous sharing of their experience and views for coping with engine rotor burst safety problems.

Included in these Proceedings are written versions of the presentations; in some cases, only an abstract and/or copies of the presentation slides were provided. Following each paper in these Proceedings are the questions and answers which followed each presentation in Sessions 1, 2, and 3 at the Workshop. These questions and answers were transcribed as well as feasible from tape recordings, and have been submitted to the persons involved for editing, clarification, and elaboration as deemed advisable; the purpose is to convey and to transmit information, not to have simply a verbatim account of those discuss ons.

Information from Session 4 (the "summary session") is not included here; there was no recording or reporting of the discussions in Session 4.

Emmett A. Witmer,
Workshop General Chairman
and Proceedings Editor

ACKNOWLEDGMENT

The NASA Lewis Research Center wishes to express its appreciation to the Session Chairmen, the presenters and their colleagues who assisted their preparations, those who presented the respective session summaries in Session 4, and all attendees who participated with gusto in all of the discussion periods. We are especially pleased by the generous participation and sharing of information and experience by the following individuals who traveled from far overseas: Gordon L. Gunstone of the Civil Aviation Authority of the United Kingdom, Denis McCarthy of Rolls-Royce (Derby) Ltd., and J. C. Wallin of the British Aircraft Corporation, Ltd. Professor Emmett A. Witmer, Director, MIT Aeroelastic and Structures Research Laboratory, was mainly responsible for the breadth and scope of the meetings. The hosting of this Workshop by MIT and the work of personnel in the MIT Aeroelastic and Structures Research Laboratory in preparing for this Workshop are much appreciated. Assisting Professor Witmer they included: Marilyn F. Bryant, Allen M. Lush, Diane E. McLaughlin, Fred Merlis, José J. A. Rodal, and Thomas R. Stagliano.

CONTENTS

FEDERAL AVIATION ADMINISTRATION'S APPROACH TO ENGINE ROTOR INTEGRITY

A. K. FORNEY*

INTRODUCTION

Close review of the record shows that aircraft engine failures are not a major contributor to commercial aircraft accidents today. This position has been arrived at by the concerted effort and resources of the entire industry, and the results are such that everyone in the industry can rightly have a feeling of pride and a sense of accomplishment. That is not to say, however, that now is the time to relax the effort. Engine problems, while not major, do occur occasionally. These include engine surge at or soon after rotation on takeoff, the need for engine shutdown after ingesting birds and an occasional rotor disk failure.

*Chief, Engine Section
Propulsion Branch
Flight Standards Service
FAA, Washington, D.C.

Even though engine failures are not a major contributor to airline accidents, the FAA is intensely interested in engine rotor integrity. This interest is demonstrated by the fact that there are several active programs under FAA sponsorship relating to this subject. Of particular interest to the FAA is the NASA Rotor Burst Protection Program. It is hoped that this program will result in a significant reduction in engine rotor failures.

The approach of the FAA to the protection of aircraft from uncontained engine rotor fragments is threefold. First, design and test requirements are imposed on engines for the purpose of ensuring to the maximum extent practicable the integrity of the engine rotor. Second, because the possibility always exists that the rotor will fail, design and test requirements are imposed on the engine to ensure some containment capability. Finally, because complete containment of all high energy fragments has been considered inpracticable up to now, design requirements are imposed on transport type aircraft to minimize the hazard to the aircraft from uncontained engine rotor fragments.

ENGINE DESIGN AND TEST REQUIREMENTS

The engine design and test requirements are covered in the United States Code of Federal Regulations, Title 14, Aeronautics and Space,

Part 33, Airworthiness Standards; Aircraft Engines. There are several sections of these Airworthiness Standards that contribute to rotor integrity.

Section 33.14, entitled "Start-Stop Cyclic Stress (Low-cycle Fatigue)," presents the low-cycle fatigue requirements. At the present time the engine manufacturer is required by this section to determine the predicted safe life of each rotor disk and spacer in the engine. An initial service life is then established at one-third of the predicted safe life. The section also describes the procedure to be used if it is desired to extend the initial service life to some higher value. To do so, three disks and spacers of each part number that have reached the initial life in service must undergo an additional number of cycles equal to at least twice the number of cycles comprising the increase in the limit desired.

Section 33.27, entitled "Turbine, Compressor, and Turbo-Supercharger Rotors," presents the overspeed design and test requirements for these engine components. The overspeed required is 120 percent of the maximum limiting rpm if the rotor is tested on a rig, or 115 percent of its maximum limiting rpm if it is tested on the engine.

Section 33.62, entitled "Stress Analysis," requires that a stress analysis be performed on each turbine engine showing the design safety margin of each turbine engine rotor disk, spacer and rotor shaft.

Section 33.75, entitled "Safety Analysis," requires it to be shown by analysis that any probable malfunction or any probable single or multiple failure, or any probable improper operation will not cause the engine to:

(a) catch fire;

(b) burst (penetrate its case);

(c) generate loads greater than those specified in §33.23; or

(d) lose the capability of being shutdown.

Section 33.83, entitled "Vibration Test," requires that each engine must undergo a vibration survey to determine the vibration stresses. This section further requires that these stresses may not exceed the endurance limit stress of the material from which these parts are made.

CONTAINMENT REQUIREMENTS

Section 33.19, entitled "Durability" requires that "the design of the compressor and turbine rotor cases must provide for the containment of damage from rotor blade failure." Traditionally, the demonstration

of compliance with this requirement was accomplished in an evacuated spin pit. In October 1974, as part of a major revision of the engine airworthiness requirements, a change was made to require that demonstration of compliance with the containment requirements be accomplished on an engine.

AIRCRAFT DESIGN REQUIREMENTS

The requirements relating to transport type aircraft are covered in the United States Code of Federal Regulations, Title 14, Aeronautics and Space, Part 25, Airworthiness Standards; Transport Category Airplanes. Section 25.903(d)(1) reads: "For turbine engine installations design precautions must be taken to minimize the hazards to the airplane in the event of an engine rotor failure...."

This requirement is very general and gives no guidance on what to do to comply with the requirement. In such cases, the general practice is for FAA Headquarters to prepare and distribute what is called "guidance material" describing one or more ways of complying with a general requirement. Guidance material has been distributed for this requirement and includes such considerations as:

1. Location of the engines relative to each other and to critical portions and systems of the airplane.

2. Location and separation of critical components and redundant systems.

3. The strategic location of protective armor and deflector shields.

More details on what is actually done in any given airplane to meet the FAR 25.903(d)(1) requirement can best be obtained from the airplane manufacturer.

CURRENT FAA ACTIVITY

The aircraft industry is not a static industry. Consequently, the FAA regulations are not static. We have underway, therefore, study contracts that will help improve the regulations. One of these contracts is with an engine company and will determine the weight penalty for two different levels of increased containment. The other contract is with an airplane company and is studying the penalties associated with protecting critical structure and systems, the passenger cabin and the flight deck by strategic location of armor shields or deflector plates. Results of these two contracts are not yet available, but they will be used to propose revisions to the regulations as appropriate.

CONCLUSION

The FAA has watched the NASA Rotor Burst Protection Program with interest for several years. In fact, the two contracts mentioned above require the contractor to evaluate and use to the degree practicable all the reports published under the Rotor Burst Protection Program. It is our hope that this workshop will somehow provide what is needed to make a significant reduction in uncontained rotor failures.

DISCUSSION

J.C. Wallin, British Aircraft Corporation

I am interested in your comments on the studies that you had done on looking at the weight penalty for increased levels of containment on the engine as against improved methods of protection on the airframe. In the UK, we were getting together a similar study with the CAA and Rolls Royce to put to our government for some funding. I'd be interested to know, how soon you expect to get some results from your present study, whether in fact you already have some results which are leading you to conclusions, and whether it is worthwhile trying to press my government for additional funding to do a study of this sort. Intuitively, I think we believe that the aircraft protective methods are likely (in the majority of the present day aircraft configurations) to result in the lightest form for improving protection. We think that increased protection in the engine is likely to lead to weight increases which are unjustified, on the whole, on typical North American subsonic configurations. I think perhaps in the case of special configurations, particularly of the Concorde kind, increased containment on the engine might be the lightest way of doing it. We had to add on something like about a thousand pounds of additional weight on the Concorde to look after non-containment problems.

A.K. Forney, FAA

Well, we should have reports available for distribution within three to six months on both of our projects. I'm not sure of the exact schedule. For one of them we do have the draft final report for review now, so the report should be available fairly soon. Our objective is the same as yours, it's to determine the trade-offs between increased containment on the engine and doing it on the airplane. And we just had no studies in hand that gave us any indication at all; that was the purpose of undertaking them. We confined the study to a wide-bodied jet with a high bypass ratio engine. You are fully aware of the current status of SST activity in the United States so we did not address that question. The draft report that I've seen (which was from the air frame study) does recommend continued effort. The results of the work to date uncovered fruitful areas for further work. So I would heartily endorse your continuing to try to press for effort in that area because, apparently it would be fruitful. Does that answer all your questions?

Guy Mangano, Naval Air Propulsion Test Center

I'd like to comment on Ken's statements regarding the conclusions that we drew in the cited report.

It's a matter of interpretation. The report means to imply that of all the different types of fragments generated at burst (disk and fan blade fragments) constitute the major threat to the welfare and safety of passengers. Taken out of context, as Mr. Forney has, this can of course be misconstrued to mean that "... disk and blade fragments (are a) major threat to welfare and safety of passengers". The intent was simply to identify which fragments present the worst threat. Whether or not rotor burst fragments or the incidence of rotor burst is a major threat in commercial aviation is a judgment that is clearly beyond the stated purpose or scope of the report being discussed.

A.K. Forney, FAA

The problem, Guy, of course, is that that report got some distribution and there was reaction, and we had to respond, you see. I don't know how much you got but I know we did, and it's difficult to respond to. Your statement claims to be based on FAA data, and so it is kind of difficult for us to answer the criticisms that we got. Clearly if your intent is what you have just stated, you can't tell it by reading that report; that's my point.

G.J. Mangano, NAPTC

All right, we'll take these recommendations under advisement and perhaps be more explicit in our future statements. Again, the intent of the report was to identify the extent of the problem, that's all. The conclusions made are so generally stated that they are subject to different interpretations by different people. I just wanted to explain what was meant by a major threat. By considering all of the fragments that were generated, the disk and the fan blades were the major threats, not that rotor burst per se is a major threat. I think we'll leave it up to the FAA to make that judgment. All that we do is to present the statistics of the situation. If I interpret Ken's words correctly, rotor burst is not a major threat. Again, I'll leave that judgment to the regulating agencies.

J.H. Enders, FAA

One might note that in these comments on the first paper we've exposed a very basic and common problem in research: human factors. Communication difficulties between human beings are increasingly recognized as a culprit in our business; one group trying to understand the other, whether it's the lay public vs. the technical community, or segments within the technical community itself.

Gordon Gunstone, CAA-UK

I just wanted to say that perhaps to save time on that particular point, if you'd comport yourselves with patience for ten minutes, I have some figures which I hope will illustrate exactly what the problem is or isn't.

ENGINE NON-CONTAINMENT -- THE UK CAA VIEW

G. L. Gunstone

Head, Power Plant Department
UK Civil Aviation Authority

SUMMARY

Present turbine engine non-containments happen too frequently for comfort, although fortunately the world-wide fatal accident level from this cause has not been excessive.

By far the majority of turbine engine induced accidents lie in non-containments, and therefore if the engine industry is to contribute to improved airworthiness, this is the problem it must tackle.

Because -

(a) the world-wide non-containment rate shows no sign of diminishing over the last decade,

(b) there seems to be no immediately obvious engineering avenues which will confidently lead to a quick reduction of incidents,

(c) the weight penalty of total containment is high,

the only valid solution for the immediate future seems to be to provide an adequate level of aircraft invulnerability.

This the CAA has attempted to achieve by introducing a requirement which it believes to be objective and capable of rational analysis. It can be applied to new designs without undue economic penalty and will enable an acceptable level of airworthiness to be achieved.

PART 1 The Perspective

At first sight, the reader may wonder what FIG 1 has to do with the title of this paper or the purpose of this 'Workshop'. In fact it shows that for more than 200 years we have been throwing pieces of hot metal at each other! FIG 2 shows that we are still at it. We can, of course, take comfort from the fact that the present situation is unintentional and not done with 'malice aforethought', but it must still be obvious to anyone closely engaged in the aviation business that not infrequently an aircraft hazard is created by the energetic debris arising from an engine rotor disintegration. This hazard was introduced at the same time as turbine engines and may perhaps be regarded as fundamental to them, since the rotation at high speed of the sort of mass typical of modern engine spools ties up huge amounts of energy. Some idea of the destructive potential is given by the realisation that the energy of rotation of a large modern engine can now be reaching 20 million ft.lb. and that across an aircraft can be approaching the energy rejected into the brakes during an abandoned take-off. (FIG 3).

The potential for hazardous damage is therefore obvious, although it will be shown later that this particular hazard has not been responsible for large numbers of fatal accidents. Therefore while it is proper, in fact necessary, that the Industry and Authorities should look into the whole situation, it is important that perspective is maintained so that in a world where resources are not infinite, a good balance of effort will be maintained.

Let us therefore spend a few minutes putting the whole problem into some kind of perspective. FIG 4 shows an analysis of a large number of 'accidents' to public transport (ie air carrier) turbojet aircraft. It is not an exhaustive survey but it is based on world-wide accident records to a given list of aircraft over a period from 1966 to 1976 inclusive.

(An accident here is that defined in Annex 13 of ICAO Standards and Recommended Practices, ie, one in which -

(a) any person suffers death or serious injury as a result of being in or upon the aircraft or by direct contact with the aircraft or anything attached thereto,

or

(b) the aircraft receives substantial damage).

The total number of accidents in the survey is 513, and the estimated aircraft hours involved, 103 million. The total accident rate is thus running at about 5 per 10^6 aircraft hours and the fatal rate at 1.4. The accident causes may be broken down into -

299	due to operational reasons	(58%)
134	due to airworthiness reasons	(26%)
80	due to other (or undetermined) reasons	(16%)

The airworthiness accidents, which are the sort of prime interest to this Workshop, thus account for roughly a quarter of the total, at a rate of 1.3 per 10^6 aircraft hours, and which may again be broken down (FIG 5) into:-

55 due to powerplant reasons	(41% of the airworthiness accidents)
79 due to other than powerplant reasons	(59% of the airworthiness accidents)

FIG 6 then subdivides the powerplant reasons into further detail, the chief message of which, for the purpose of this paper, is that by far the majority of powerplant caused accidents are attributable to or directly involve an engine non-containment of some form. The non-containment caused accident rate is 0.4 per 10^6 aircraft hours, the rate involving fatalities being fortunately lower at 0.03, this failing to meet our current suggested airworthiness target of 1 per 10^8 aircraft hours (for a single engineering cause) by a factor of 3.

This leads to the first main point I wish to make (FIG 7) viz that -

> "any significant improvement to the overall accident scene by virtue of action in the powerplant area must best lie in the direction of diminishing the danger arising from non-containment."

PART 2 Engine Statistics

Having decided (and I am sure my 'Workshop' hosts will be gratified to hear it!) that we have a problem worth attacking, it is now necessary to dig deeper to see if we can ascertain where the problems are arising. For a number of years now, the Power Plant Department of the CAA has kept a record of all non-containment incidents it could lay its hands on. For UK produced engines, we have complete records, but of course our accuracy is less for other countries. We are however, fairly sure that the hours used for determining the statistics are accurate enough to allow fairly confident use to be made of the data.

FIG 8 shows the non-containment rate, world-wide, for the past 10 years or so. Two obvious conclusions strike one immediately from the data, ie that the rate is about 1 non-containment per 10^6 engine hours, and that the rate has been reasonably constant over the period.

FIG 9 shows the same data broken down into incidents arising from compressors (including fans) as against those arising from turbines. The curves show that there is little to choose between the two, though perhaps in view of the larger number of compressor stages compared with turbines, it could be said that individually turbine rotors are more prone to failure than compressor rotors.

Non-containments involving only blades represent to some extent a failure to meet existing international engine requirements which all demand blade containment. However, the tests conducted are only required to demonstrate containment of one blade, and obviously many real failures involve more than this. Additionally, some non-containments of blades are produced by the blade being punched through the casing rather than breaking through ballistically, and these types are of a less dangerous nature, since the emergent energy is low. As might be expected, and as is borne out in practice, non-containments involving a failure of some part of the disc are generally more dangerous than those involving blades. FIG 10 shows the rate of such failures and FIG 11 the same data divided again as between compressors (with fans) and turbines. The conclusions to be drawn are that about half of non-containments involve a failure of some part of the disc, again that the compressor/turbine rates are not dissimilar, and again that there is no great sign of improvement over the years.

There are two other data that might be useful. FIG 12 shows non-containments grouped by 'phase of flight'. The criterion of prior to or post V_1 is not always determinable from incident reports, but the volume of statistics is probably enough to swamp minor errors. The data may be interpreted in a crude way as showing incidents divided into four roughly equal flight phases, viz prior to V_1, V_1 to power reduction, climb, remainder of flight. Paragraph (f) below gives the data more accurately but in a way less easy to remember. FIG 13 attempts to show the underlying causes. Here we are on much more difficult ground, since causes are treated very subjectively. For example, it may be easy to see that a failure had its origin in combustion chamber distortion, but whether the cause of that was due to poor operation, faulty material, errors of overhaul, fundamental design, etc, is often not clear and can depend on who is making the judgement! It is, of course, almost always the fault of someone else! However, the Figure is attached for what it is worth, and primarily because of one main conclusion which can be drawn from it - that is that there is no obvious single item which if tackled successfully would in itself produce a dramatic improvement in the non-containment scene - a point to which we shall return later.

All the above data was recently presented to a UK committee comprising the UK engine and aircraft industries as well as the CAA, and I append below the conclusions of that committee in summary form. (In case you think I am passing the buck, I should perhaps say I was a member of the committee).

(a) The average (world-wide) non-containment rate from all causes is 1 per million engine hours. This figure has been fairly constant for 10 years.

Note Roughly one-quarter of these non-containments have caused aircraft damage outside the confines of the nacelle. The 'significant' non-containment rate may therefore be regarded as about 1 per million aircraft hours. It might be noted, by referring back to FIG 6, that about half the 'significant' non-containments are serious enough to be classified as reportable accidents.

(b) Of all non-containments, about half involve a disc failure of some degree. The non-containment rate for disc failure is, therefore, 1 per 2 million engine hours. As might be expected, discs contribute more 'significant' non-containments than blades, in fact twice as many.

(c) Of all non-containments about one-eighth have resulted in the release of debris approaching or equal to a third of a disc. The major fragment rate is, therefore, about 1 in 8 million engine hours (say 1 per 2 million aircraft hours).

(d) Compressors and turbines make about equal contributions to non-containments. Fans provide perhaps 10% of the total (based on less experience obviously).

(e) Although depending on a somewhat subjective judgement, it appears that about half the disc failures are of a secondary nature.

Of the primary failures, nearly half are attributable to HCF (High Cycle Fatigue). No other single cause stands out on either the primary or secondary failures.

(f) As to phase of flight, the following is broadly true (although with the advent of engines whose rpm increase with altitude to the extent that cruise rpm may exceed that of take-off, this breakdown may be modified).

Phase:	T O before V_1	V_1 to power reduction	Climb	Remainder
% :	35	20	22	23

(g) No single predominant cause can be identified the cure of which would give a dramatic decrease in non-containment incidents. However HCF accounts for a high proportion and should therefore be given special consideration.

PART 3 Possible Solutions

In considering what might be done to minimise potential accidents due to non-containment, there are three immediately apparent solutions (FIG 14) -

(i) We may work on the root causes of the failures and attempt to eliminate them.

(ii) We may assume that the failures will continue to occur at a rate higher than is tolerable, and attempt to contain all the debris within a strengthened engine casing.

(iii) We may accept that uncontained debris will continue to be generated and make the aircraft design acceptably invulnerable to the debris by such means as deflection, the judicious siting of critical parts and structure, suitable duplication where appropriate, armouring, etc.

The first solution, being basic, seems right and attractive but as will be shown later, a reduction in present non-containment rates of at least an order of magnitude is necessary for this solution to be viable. Unfortunately, as FIG 13 indicates, something like a third to a half of all disc failures are from causes to which the disc failure is secondary, and we felt it would unrealistic to believe that any overwhelming improvement could be made to such a large number of unrelated prime causes. Even taking those cases where the disc failure is itself primary, there are still six or seven fundamentally different causes, none of which carries any obvious promise of easy solution and cure. Perhaps the relatively low number of basic LCF failures is interesting since this is a subject to which, after a few early failures, a great deal of attention has been paid, obviously to good effect. However, HCF, which now probably accounts for more failures than LCF, is much more difficult to cater for, since it tends to arise in much less predictable ways. I hope some other papers at this Workshop will be devoted to that subject.

It was therefore reluctantly concluded in the CAA that there could be little confidence in the engine industry's ability to produce engines which within the foreseeable future (by which we mean the next ten years) would achieve significantly reduced levels of non-containment incidents, and nowhere near the order of magnitude reduction we would need. I say reluctantly in the sense that regarding myself as a member of the engine fraternity, I am disappointed that we cannot guarantee to deliver engines free from this endemic disease. However, we must be honest enough not to try to avoid the truth and to admit, even with red faces, our inability to be certain of doing much better in the immediate future. (And I hope nothing here said will in any way diminish the desire and intent of this Workshop to prove me completely wrong).

Moving to the second solution, this is also an attractive one to an Airworthiness Authority since if we cannot stop the debris being generated, it would be almost as good to keep it inside the engine. It also has merit in lessening the danger arising from such unavoidable incidents as large bird ingestion where the benefit of total containment is obvious. Unfortunately, after numerous discussions with both the engine and aircraft industries, we were left with little hope, in the present state of the art, of effecting containment without swingeing increases in engine weight, except possibly on quite small engines or APU's. Estimates of 1 pound per 10,000 ft.lb. of energy to be absorbed or 2/3 pound per pound of bladed disc weight have been variously calculated, the final results implying an increase of bare engine weight of anything up to 50%. Of course containment does not have to be total, and it is interesting to look into partial containment, for example of the smaller debris, together with possible deflection. NAPTC may be able to suggest ways of reducing these figures, and I will be interested to hear of their recent work, but of course if the consideration of the larger pieces dictates the design, containment of the smaller ones may be less attractive.

However, the conclusion we reached, in association with our manufacturers was that the most reliable, practicable and cost-effective solution is the third, ie to make the aircraft relatively invulnerable to any likely debris which may affect it. (Though this decision was one which we felt we had to take in the time scale we were considering, it would be quite premature to abandon all hope of someday achieving solutions one or two, and such efforts as are being made by this Workshop are to be encouraged to keep this difficult task in active play).

PART 4 The UK Requirements

The CAA, having reached the conclusion that the only practicable requirement for the immediate future was to achieve a reasonable degree of aircraft invulnerability then gave thought to the form which the requirement should take. Phrases like "Shall minimise the risk" are very easy to put into requirements and are attractive in that they can be agreed with industry without too much argument since the broad principles involved are so obviously sensible. Unfortunately, when the crunch comes, it soon becomes apparent that there is a considerable conflict of opinion as to where minimising should stop!

The aim of the requirement in its simplest form is clear, viz, that unless an engine will contain any likely debris that it might generate, the chance of catastrophe occurring to an aeroplane from being struck by such debris should be something less than 10^{-8}/aircraft hour. While this provides a good aim, it was much more difficult for the aircraft industry to see a way of being able to demonstrate compliance in a convincing way, since of the two components contributing to the risk, ie 1) the probability of debris being generated and 2) the probability of the debris causing catastrophic damage, the former and more critical component was completely outside the competence of the aircraft constructor to assess. It was therefore decided to write the requirement such that only the latter term would be quoted, the former being assessed by the CAA and appearing only implicitly in the requirement.

I have already shown that a figure for debris generation of 1 per 10^6 engine hours was well founded as an average, and not subject to a particularly wide variation over a range of current engines. Knowing that about a quarter of the incidents caused 'significant' aircraft damage, ie damage outside the nacelle, the 'significant' rate may be expressed as being in the order of 1 per 10^6 aircraft hours. Starting from this precept therefore, the aircraft constructor needed to provide an additional factor of about 1 per 100 against a 'significant' engine non-containment ending in catastrophe.

Thus the aircraft constructor would be left with an assessment to make which was well within engineering judgement. The only further point remaining to him was to have a definition of the sort of non-containment debris that he had to consider, ie a freedom from catastrophe of 1 in 100 against what? We again decided that this judgement was also outside the area of knowledge of aircraft designers and in fact we doubt if even the engine designers can do much in the way of valid prediction since their avowed intent is to produce engines which <u>never</u> fail in this way.

We therefore decided that past experience was the only valid guide available to us, and although the requirement should be written in a way flexible enough to allow any peculiarities of an engine to be taken into account, the failures to be considered would be based on past history.

Thus the task was to provide a failure 'model' with which the aircraft constructor could assess his design against the 1/100 factor. Initially we tried very complex models which became so sophisticated that they defeated their own purpose. In the end we decided to revert to a simple model even though, as would be expected, it would be somewhat arbitrary - that is to say

that we would never claim that it represents the actual way in which any given engine is most likely to fail - only that it provides a yard-stick against which the aircraft design can be measured.

One of the obvious pieces of debris to be considered seemed to be the 1/3rd disc piece (this being very near the mathematically maximum energy of translation sector and also coinciding with current FAA thinking on FAR 25.903(d)). We then studied the distribution of debris which had been shed in a selection of previous non-containment incidents and chose one further piece to represent the mean of all the residual pieces which could not be considered to be covered by the 1/3rd piece.

Thus, starting with the distribution of the size of non-containment debris from a number of incidents where Rolls-Royce were able to recover the debris and assess the mass (and this is not a common state of affairs - often, thank goodness, a lot of the debris disappears into thin air!) we were able to construct a probability curve. (FIG 15). Having decided already that one of the model pieces should be the 1/3rd disc, and wishing to represent the remainder by one other arbitrary piece, it can be shown that this should be of 1/20 disc mass. From the probability of each of these types of failure occurring, we could then devise a figure which described the desired level of invulnerability of the aircraft design such that if engines continue to fail at the sort of rate which has applied in the past, the aircraft will have an acceptable level of airworthiness against this particular hazard.

Reference back to the data shows that the probability of the smaller (1/20 disc mass) piece is about twice that of the larger piece. We therefore had the equation : there is a significant non-containment (ie one causing damage outside the nacelle) every million aircraft hours, two out of three of which may be regarded as releasing a 1/20 piece, and one in three a piece getting into the 1/3rd disc size ballpark. If the target risk from this cause for catastrophe is to be less than 10^{-8} per aircraft hour, simple mathematics show that the invulnerability factors if the allowance is equally proportioned must be 1/133 for the smaller and 1/66 for the larger piece respectively.

$$\text{ie } \frac{2}{3}\,(1 \times 10^{-6}) \times \frac{1}{133} + \frac{1}{3}\,(1 \times 10^{-6}) \times \frac{1}{66} \simeq 1 \times 10^{-8}$$

We tested these factors against as much experience as we could and we concluded they were a bit tough since even aircraft which had good records could not meet them. We felt that this was probably because in estimating 'catastrophe', honest people were forced to be somewhat pessimistic, and that aircraft did on occasion survive incidents which any prudent engineer would have graded catastrophic. As a result we issued a paper for discussion with factors of 1/100 and 1/30, to test as it were, the temperature of the water.

Discussion with the aircraft industry still left doubt whether these figures were within the state of the art. Fortunately, in the course of our general work in dealing with incidents of a type which were potentially catastrophic when they occurred but which could be expected to occur at a low, unpredictable, frequency (ie of a type which have become to be described as 'unlikely though possible') we had been developing the idea that they can be dealt with by ensuring that if the unpredictable low frequency event does occur, there must be a 'reasonable' chance of a survival, enabling the problem to be exposed and corrected so as to avoid any possibility of a second occurrence. The choice of a number for such a 'chance' is arbitrary and subjective and depends to some extent on the average risk applicable to the 'unpredictable' event, but we had concluded that a chance of survival of 19 out of 20 was not unreasonable.

Taking the above into account, it was therefore decided we could reduce the 1 in 30 figure to 1 in 20 and the 1 in 100 to 1 in 60. It is this figure that now appears in our Requirements. It is expected that it will result in airworthiness risks in line with our target, but it cannot be too strongly emphasised that the risks are not intended to apply for the life of the aircraft, but assume that IMMEDIATE CORRECTIVE ACTION WILL BE TAKEN SHOULD ANY INCIDENT OCCUR. There must be no question of continuous exposure, or of living with a problem once it is exposed.

Of course, we would be naive if we assumed that in real life failures will cause debris like our model. We are not, and they won't. What we have done is created a requirement against which a non-subjective estimate of a design can be made. It is no more likely to represent the exact truth than an aircraft is likely to fly through a flock of exactly 4oz birds all perfectly spaced at 1 per 50 sq in. We do feel the requirement will act as a good yard-stick against which the non-containment danger can be assessed.

One or two further refinements serve to make the requirement complete:-

(a) Dimensions. In many cases the debris will not be stopped but will lead to what I call the infinite hole - that is the part passes through all intervening structure. In this case, the cross section area of the hole is important, and can of course in theory be as large as the section of the failed rotor. Here again we have been arbitrary and assumed that some blade bending will take place and that as a mean the two model pieces should be assigned maximum dimensions of R and ½R (R being the bladed disc radius) respectively. FIG 18 summarises in pictorial form the sort of analysis which results.

(b) Energy. We have made the simplified assumption that the prescribed pieces will leave the engine with their full, theoretical, energy of translation intact. This means that we have struck a rough balance between the casing absorption and the neglected energy of rotation. I would be glad to have any ideas for improvement on this if better generalised assumptions would be preferable.

(c) Averaging. Since the non-containment rate used has been per engine and not per disc, we are saying that a disc will fail at the frequency quoted, but we don't know which. It therefore seemed fair to allow a certain amount of averaging in assessing the overall risk, allowing a disc presenting a relatively high vulnerability to be offset by one with a low potential. Further, the same sort of thinking seemed permissible, and is allowed, over the various phases of flight, whereby the risk which varies depending for example on whether the fuselage is pressurised or not can be averaged over the various regimes provided the through flight total meets the requirement.

(d) Dispersion. FIG 17 shows a distribution made of particle sizes against the angle through which they had been deflected during their flight from the engine. We chose $\pm 3^{\circ}$ for the 1/3rd disc mass piece and $\pm 5^{\circ}$ for the smaller one. These may appear a little on the small side, but we feel that deflection is likely to be greatest as the speed and energy drops, and that the damaging energy is likely to be confined within these limits.

(e) Duplication. One last consideration completes the model. Since we have settled for a stylised failure involving only single pieces, it is obvious that an automatic solution would be to duplicate any vital part. To prevent this being possible in a foolish way, we have added a further clause requiring consideration of three pieces, dispersed randomly to each other, in respect of duplicated items only. The required factor for the 3 piece case has been adjusted accordingly.

SUMMARY

Present turbine engine non-containments happen too frequently for comfort, although fortunately the world-wide fatal accident level from this cause has not been excessive.

By far the majority of turbine engine induced accidents lie in non-containments, and therefore if the engine industry is to contribute to improved airworthiness, this is the problem it must tackle.

Because -

(a) the world-wide non-containment rate shows no sign of diminishing over the last decade.

(b) there seems to be no immediately obvious engineering avenues which will confidently lead to a quick reduction of incidents.

(c) the weight penalty of total containment is high,

the only valid solution for the immediate future seems to be to provide an adequate level of aircraft invulnerability.

This the CAA has attempted to achieve by introducing a requirement which it believes to be objective and capable of rational analysis. It can be applied to new designs without undue economic penalty and will enable an acceptable level of airworthiness to be achieved.

ACKNOWLEDGEMENTS

I would like to thank the CAA for permission to publish this paper. It is conventional to dissociate one's employers from any views expressed. In this case I am happy to say I do not need to. I would however express my thanks to all my colleagues who have contributed whether directly or through their normal work, to whatever merit this paper may possess.

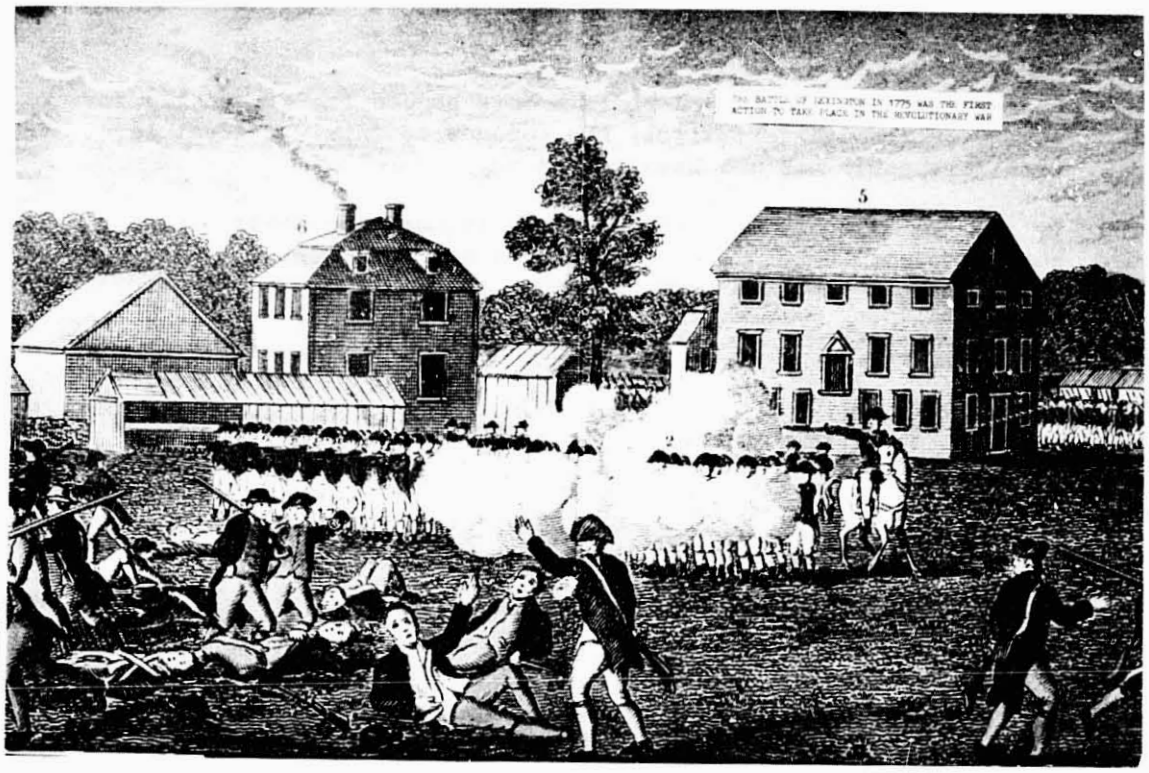

Figure 1. - Debris circa 1775.

Figure 2. - Debris circa 1975.

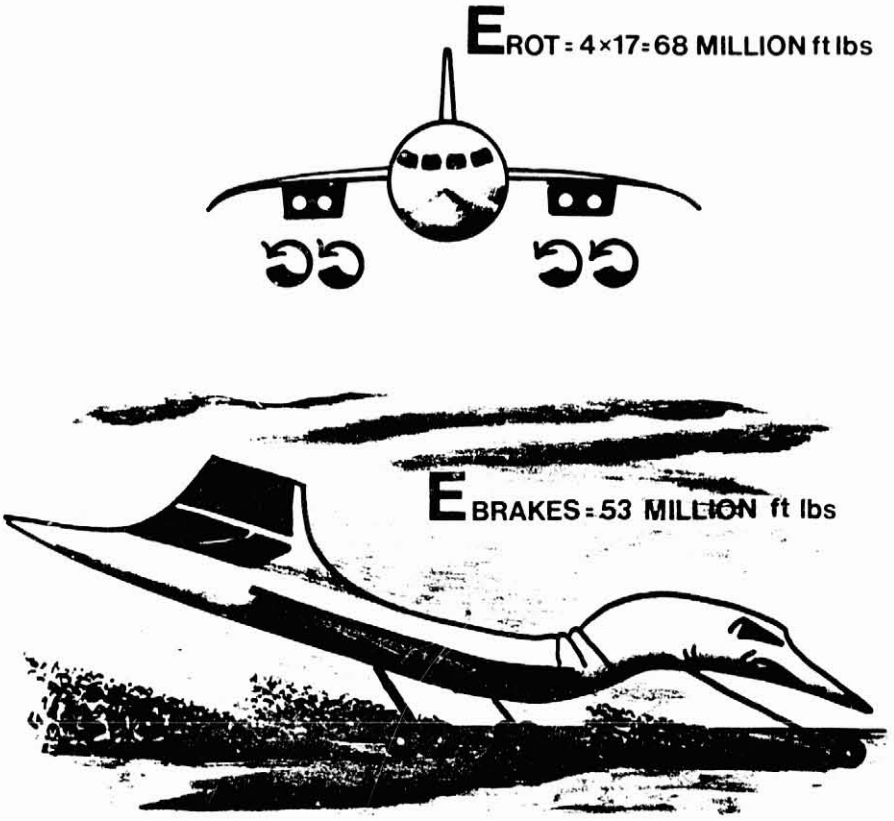

Figure 3. - Comparison of Energy of Rotation of Engines with Energy Rejected to Brakes on Abandoned Take-off.

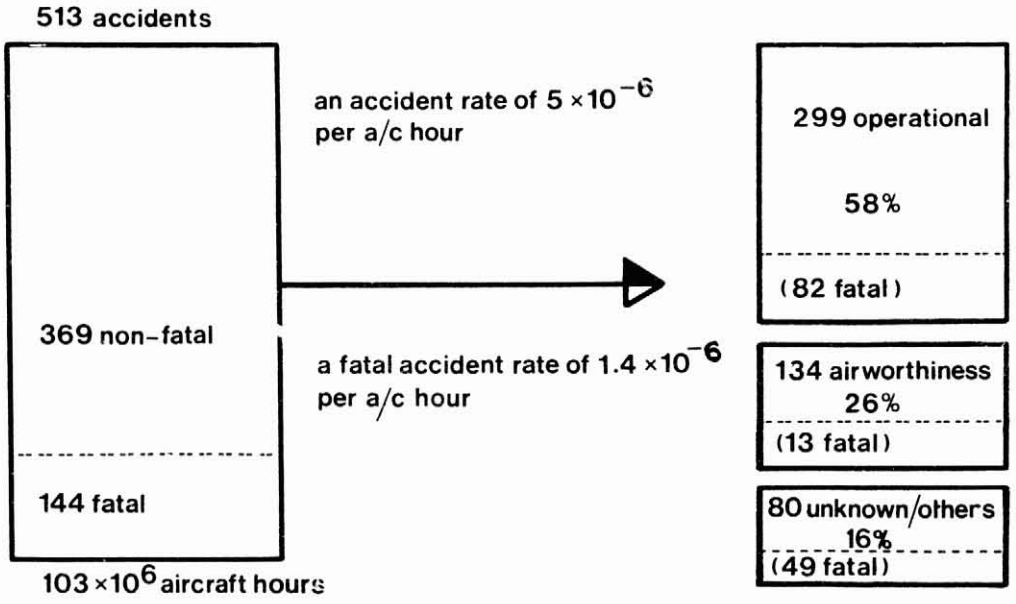

Figure 4. - Reasons for Jet Aircraft Accidents 1966-76.

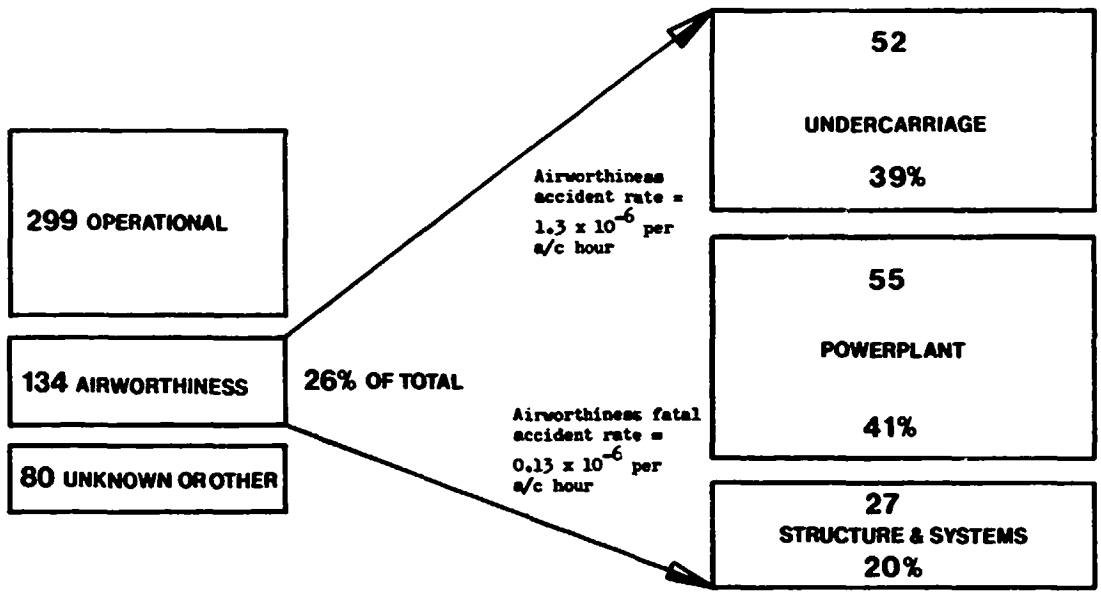

Figure 5. - Causes of 'Airworthiness' Accidents, Jet Aircraft 1966-76.

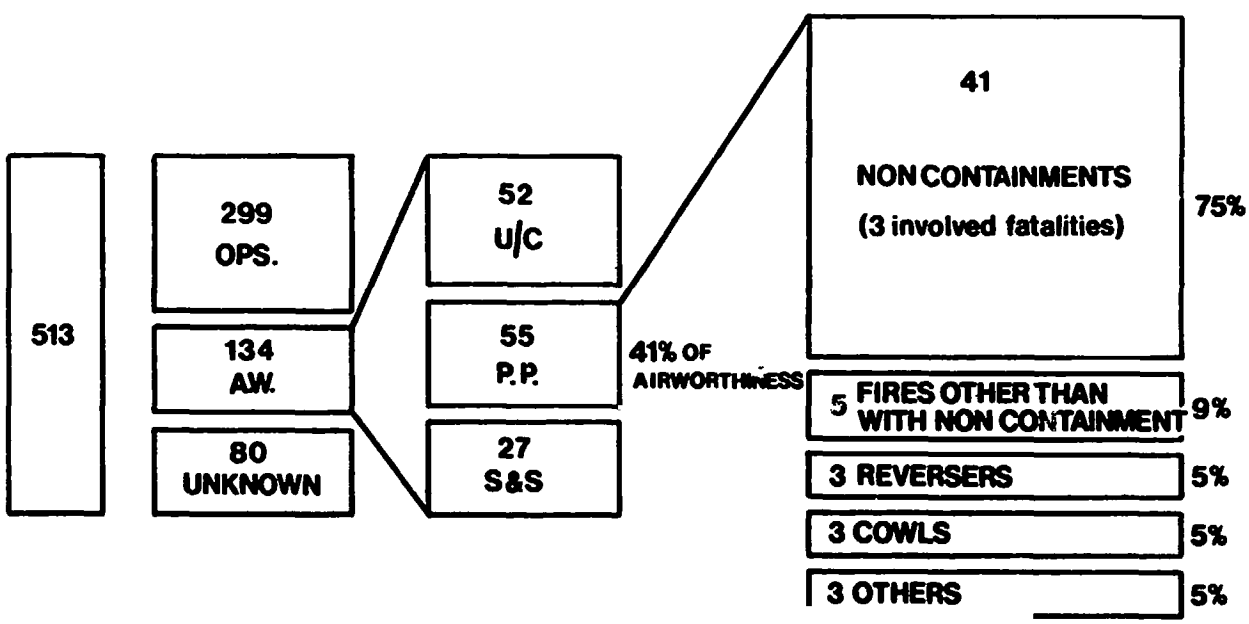

Figure 6. - Causes of Airworthiness Accidents Attributable to Powerplant, Jet Aircraft 1966-76.

"Any significant improvement to the overall accident scene by virtue of action in the Powerplant area must best lie in the direction of diminishing the danger arising from Non-Containment"

Figure 7. - Statement Deriving from Engine Accident Statistics.

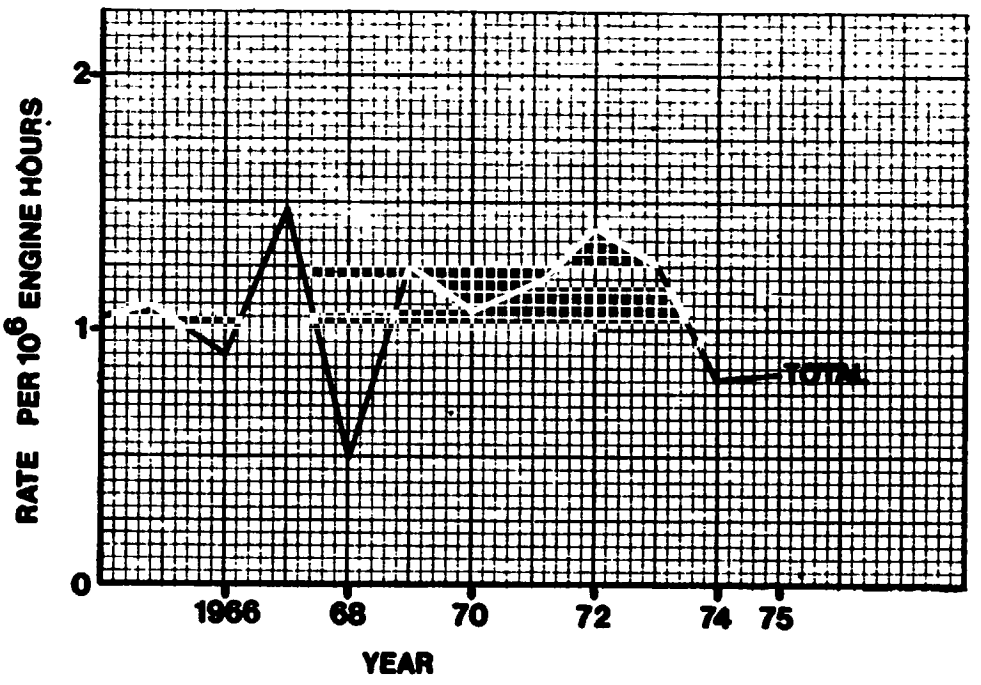

Figure 8. - Combined (World-Wide) & US (USA Register) Engines Total Non-containment Rate.

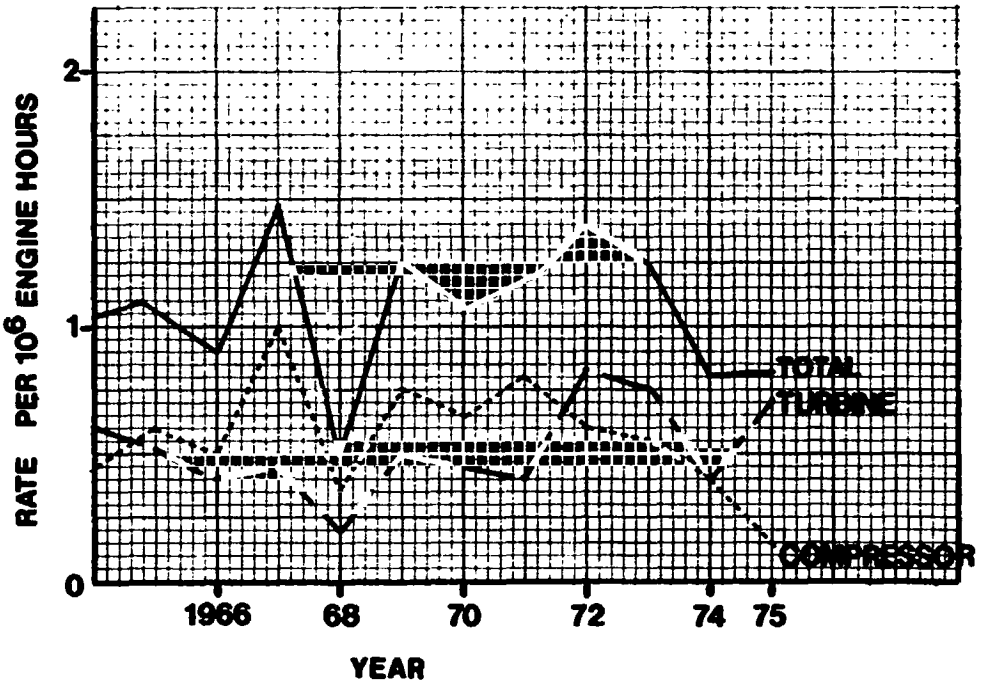

Figure 9. - Combined (World-Wide) & US (USA Register) Engines Total Non-containment Rate (showing rates for turbines and compressors separately).

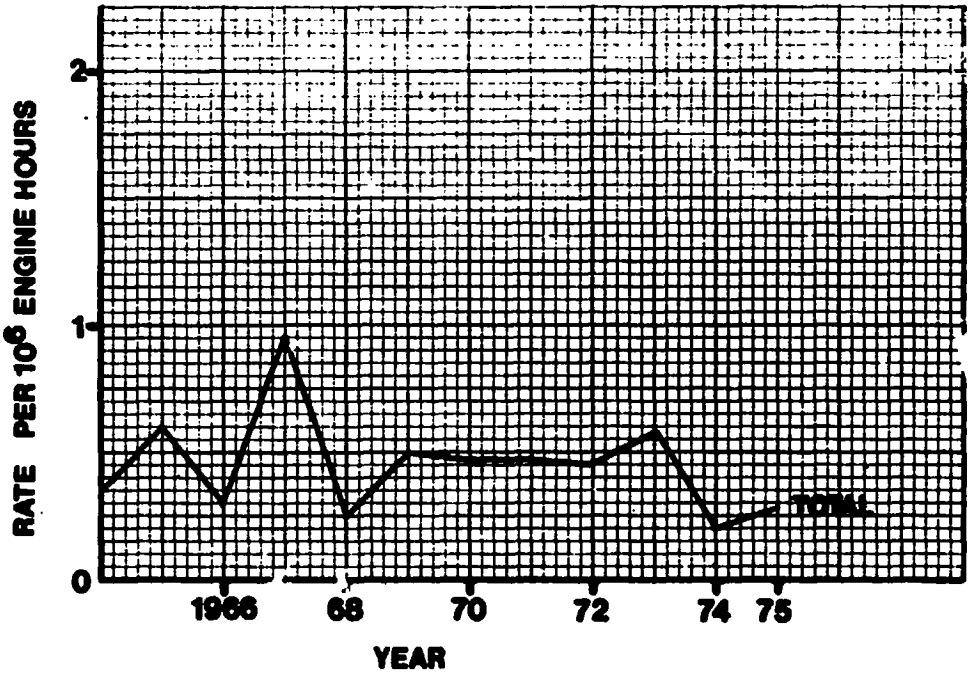

Figure 10. - Combined (World-Wide) & US(USA Register) Engines Disc Fragment Non-containment Rate.

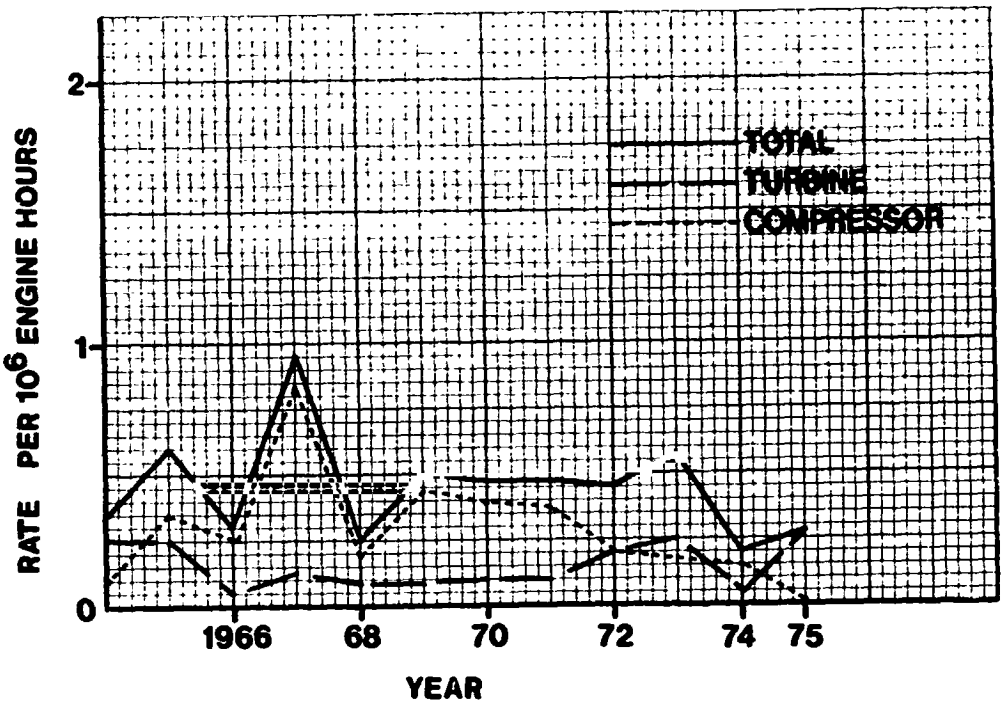

Figure 11. - Combined (World-Wide) & US (USA Register) Engines Disc Fragment Non-containment Rate (showing rates for turbines and compressors separately).

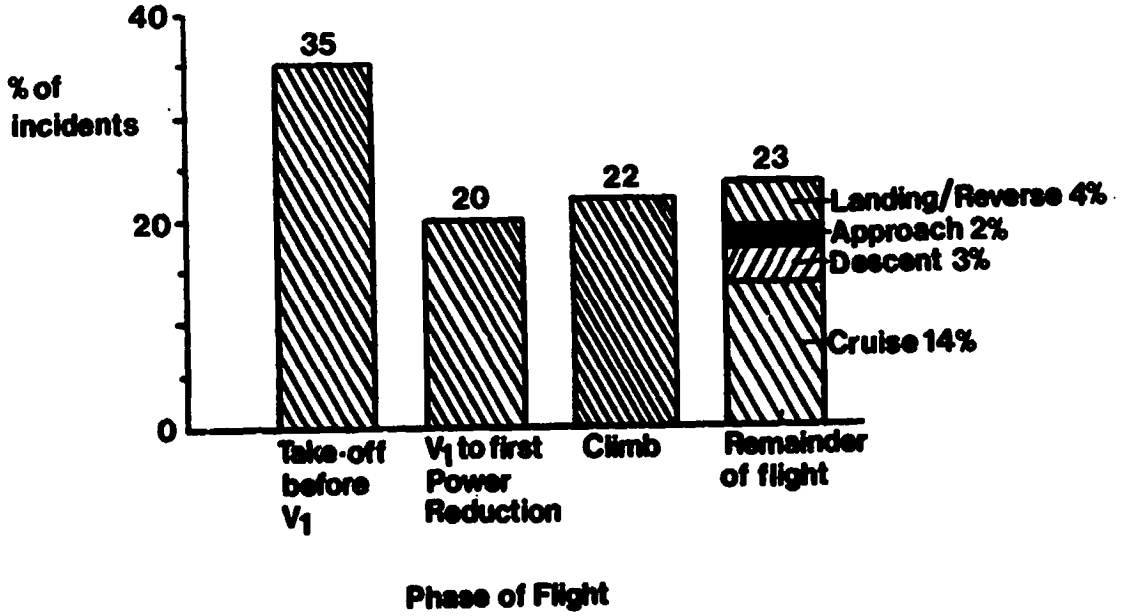

Figure 12 - Non-containments by Phase of Flight

	DESCRIPTION OF FAILURE	UK ENGINES %	US ENGINES %
PRIMARY	MATERIAL DEFECTS	6	25
	MANUFACTURING DEFECTS	0	
	MISASSEMBLY	0	10
	HIGH CYCLE FATIGUE	33	15
	LOW CYCLE FATIGUE	9	
	COMBINATION HCF/LCF	3	
	OVERHAUL PROCEDURES	16	
SECONDARY	OVERTEMPERATURE	9	50
	FOREIGN OBJECT DAMAGE	3	
	DETACHMENT DUE SHAFT OR BOLT FAILURE	3	
	RUBBING AGAINST STATIC PARTS	9	
	OVERSPEEDING	3	
	HCF DUE BLOCKAGE	6	

NOTE: FOR US ENGINES, 20% 'UNKNOWN CAUSES' HAVE BEEN ALLOCATED IN THE ABOVE SUB-DIVISIONS IN THE SAME PROPORTION AS FOR THE KNOWN ONES.

Figure 13. - Causes of Disc Failures.

1) Eliminate Prime Failures
2) Contain any Released Debris by Suitable Shielding
3) Make Aircraft Invulnerable to Possible Strikes

Figure 14. - Acceptable Airworthiness Solutions Against Non-containment Problem.

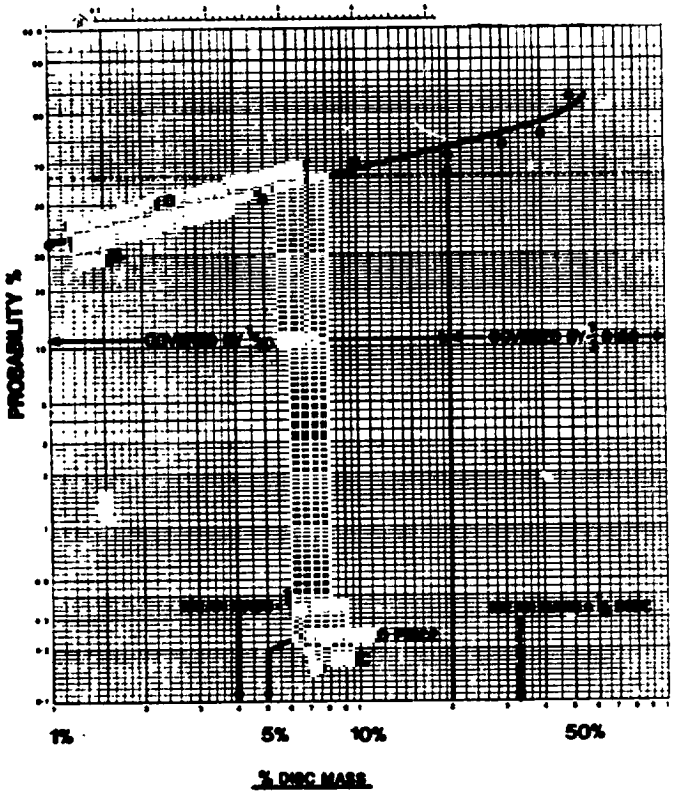

Figure 15. - Probability that Debris Mass is below a Given Proportion of Disc Mass.

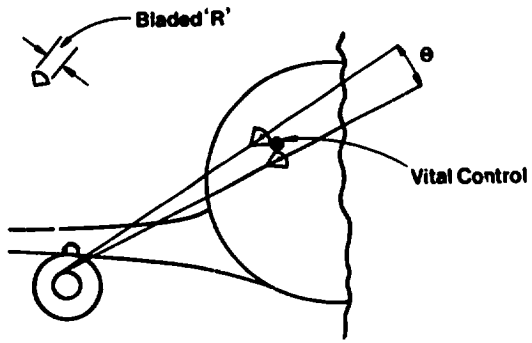

Probability of Strike in $\frac{1}{3}$ Disc Case = $\frac{\theta}{360}$

Probability of Control Failure leading to Catastrophe = $\frac{1}{y}$

Then Vulnerability = $\frac{\theta}{360} \times \frac{1}{y}$

Figure 16. - Vulnerability Analysis.

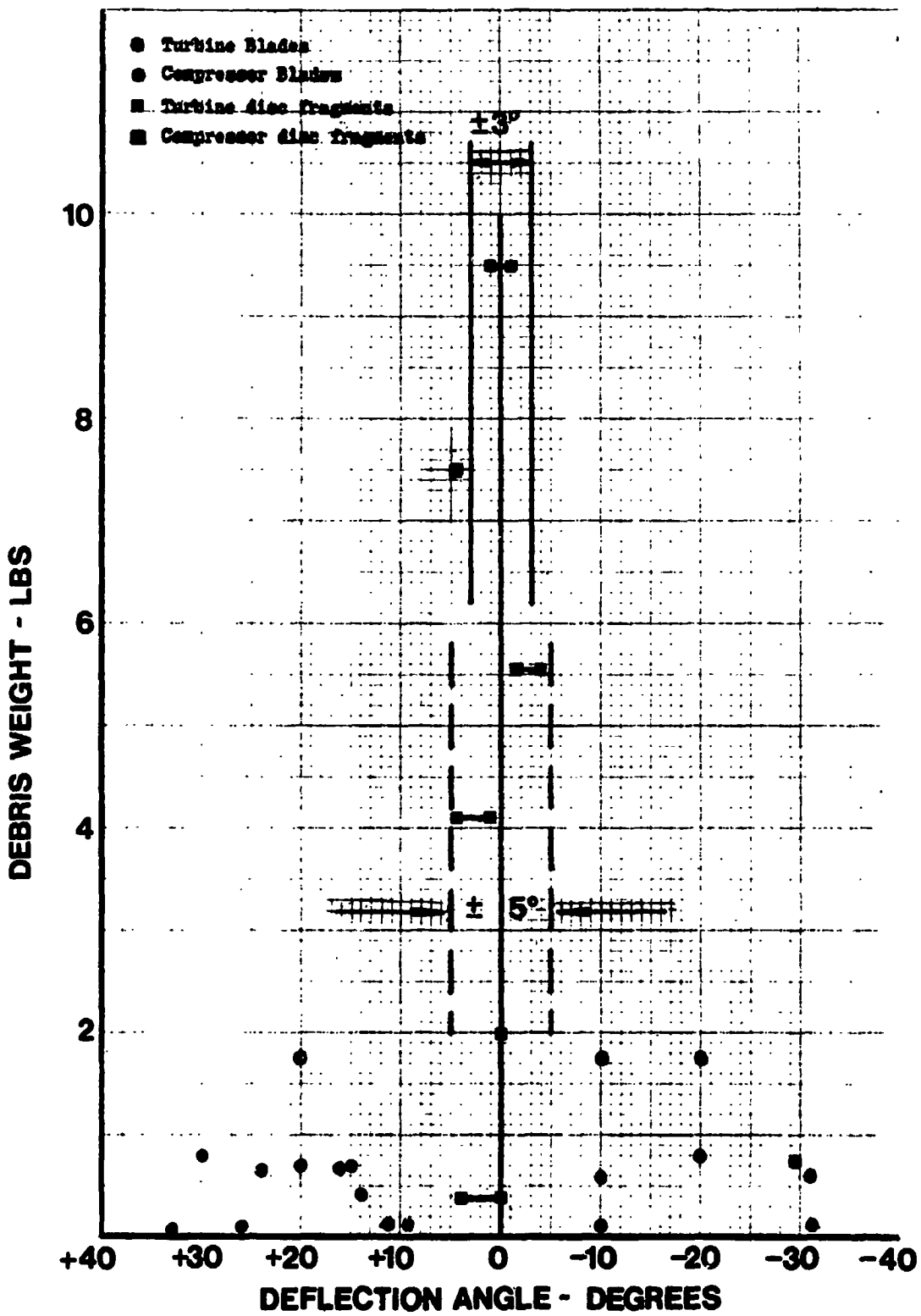

Figure 17. - Deflection of Debris versus Debris Mass.

DISCUSSION

Tom Horeff, FAA

Gordon, in your statistics you referred to 55 accidents due to power-plant reasons, of which 75% involved engine non-containment, or roughly forty in the period between 1966 and 1976. A rather simplistic view would be to say four non-containments per year. You added that one in four non-containments penetrates the cowl, or roughly one per year. My question, Gordon, is do you have corresponding data for passenger fatalities pertaining to the non-containment cowl penetration accidents that you referred to?

G.L. Gunstone, CAA-UK

Well, I think that we have just a slight misunderstanding of my figures. I know that it's been very unfair to push so many figures at you all at once but there are copies of my paper available which I'm sure you'd like to study later. What I would say, Tom, is that in my definition an accident is not necessarily a non-containment and a non-containment is not necessarily an accident. An accident in the ICAO definition is one which causes a serious injury to a passenger or substantial damage to an airplane, and there are very many more non-containments than there are accidents. I think that goes part way to answer your question. I have studied about a hundred million engine hours in the period taken, and in this hundred million engine hours (which could be perhaps 30 million aircraft hours) there have been 41 non-containment accidents and three fatal non-containment accidents. I did not, in the charts show those non-containments which did not become classified as accidents.

J.H. Enders, FAA

Gordon, I have a question that was posed by the "no-improvement" charts you showed. I don't interpret that data as implying that there has been no improvement in engine technology from a containment point of view. Rather, the growth in engines: that is, the larger diameter and larger thrust engines have continually posed a tougher problem to the designer to solve, and he's really improving in an absolute sense. To put it another way, he's really keeping up with the problem, not letting it get worse. Now some people might not agree with me, but truly the large diameter engine of today pose tougher containment design problems than did the smaller aircraft engines of a decade ago.

G.L. Gunstone, CAA-UK

I basically agree. But I think there is in all aircraft engine design a process of "brinksmanship". That is to say you push the design as far as you dare. Your constraints are economics, thrust, ...and so on, and you do not (unfortunately) apply all of the knowledge which you've acquired from previous experience to making an engine or aircraft safer. You use some of it, but the rest goes into making it cheaper. It is a matter of some judgment as to where the proper balance lies, and I was simply quoting what the facts are.

Could I just say, gentlemen, that I could bring only about 30 or so of these papers with me. They are up there for distribution. If anybody can easily share with a colleague I would ask him to do so for the moment. But I will get a clip-board put next to them, and if anybody fails to get a copy but would like one, if he will write his name and address I will have one posted as soon as I get back.

AIRCRAFT ENGINE CONTAINMENT -- SAE COMMITTEE FINDINGS

S. A. Sattar*, Chairman SAE Ad Hoc Committee

ABSTRACT

This presentation summarizes the study made by the Ad Hoc Committee on aircraft turbine engine containment under the auspices of the SAE. The committee is composed of individuals in the fields of engine and aircraft design, and airline operation. The study was directed to commercial aircraft service and covered the period from 1962 through 1975. The uncontained rotor data were gathered and analyzed for their cause, the consequence of failure, and mode of flight. The resulting aircraft damage for all the incidents were categorized by degrees of damage ranging from just penetration of the affected nacelle to severe aircraft damage. The committee also evaluated the penalties and benefits for aircraft systems to achieve greater levels of containment.

* Commercial Products Division, Pratt & Whitney Aircraft Group, United Technologies, East Hartford, Connecticut 06108

DISCUSSION

A. Holms, NASA-Lewis

How did you know which failures were high-cycle fatigue, and which were low-cycle fatigue? How did you distinguish between types?

S. Sattar, P&W

Since there were four engine manufacturers represented on this committee, we looked into our own data base and fixes that were finally arrived at for these failures. We determined that these were high-cycle fatigue failures. Some of that information is on the public record; the others, we were able to get from the engine manufacturers on the committee.

J. Gausselin, Rockwell International

I noticed your study paralleled the National Transportation Safety Board's study. I was going to ask you whether you have considered information in this report in your study. I think you may have answered the question when you remarked that your study showed that containing three blades was not a significant improvement, and I believe this could be a controversial issue between you and their conclusion, where they recommended that engine containment be improved by going to the three-blade containment.

S. Sattar, P&W

I think that the committee's work on the effectiveness of increased containment, three blades as you pointed out, does come from the National Transportation Safety Board and they refer to some aircraft manufacturer's report. We believe that increased containment (for the 49 events which involved significant aircraft damage) would have had insignificant improvement. We would be carrying 400 pounds of weight for little improvement. We asked ourselves, what are we trying to prevent?

Unknown Speaker

When the National Transportation Safety Board says that 3-blade containment should be done, they are actually requesting that the feasibility of this should be investigated.

Those recommended measures would be effective to some degree.

S. Sattar, P&W

I guess the other related comment that I could not make because of the time limitations was that we also made a very gross estimate of what would be required to contain a tri-hub disk failure. The answer was very similar to what Mr. Gunstone said. It would be extremely large weight penalty....40 - 50% weight. God knows what other problems we would introduce in and around the engine.

Don Haskell, Army-BRL

I don't know much about the aircraft engine rotor fragment containment business but I want to ask a question. What was the basis for 400 lbs. for this containment? Was that done by analysis, or test data, or how do you arrive at that?

S. Sattar, P&W

It was done by analysis. Each manufacturer used its own design system which, in all cases, is calibrated against testing different size fragments. But it was done by us strictly on an analytical basis.

G. Gunstone, CAA-UK

Just eyeballing those numbers of yours, it seemed to me that about one third of the failures were attributed to quality control, misalignment, manufacturing defects, so on and so forth. Was there any attempt to correlate these failures with a learning curve? Is there any trend with calendar time in this particular segment which accounts for roughly one-third of the total?

S. Sattar, P&W

We talked about it but, no, we didn't do that in the SAE study. If I may wear a different hat right now. We had made such a study at P&W and have found that indeed there is a significant downward trend in terms of failures due to material defects primarily due to the quality control, vacuum melting, titanium and so on. Result: a significant downward trend. As a matter of fact, no non-contained disk failure due to material defects has occurred in disks that were shipped after 1967.

Tom Stagliano, MIT-ASRL

You looked at the problem of containing the three blades and two posts and came up with a 400 pound weight by analysis. Did you look at the problem of deflecting these blades and posts away from the area you're trying to protect, when they were not contained within the engine?

S. Sattar, P&W

No, we did not. We limited our study to the engine portion and the scope that I showed you earlier was part of our work statement we had agreed upon. We did not include that.

G. Gunstone, CAA-UK

We have had to wait 20 years for data like this, and we need good data to make good decisions. I would strongly recommend that you in this country consider very carefully the possibility of creating a centralized source for this information. The data can be made "nondimensional", in the sense that companies need not be mentioned and also the type of engine need not be mentioned. We gain nothing by secrecy, in fact, we all lose by it. One of the big problems in this overall problem is the lack of feedback. We need a permanent source of accurate well-founded information from the engine and airframe constructors.

S. Sattar, P&W

I think that this is a very good suggestion.

ROTOR BURST PROTECTION CRITERIA AN IMPLICATIONS

RALPH B. MCCORMICK
BOEING COMMERCIAL AIRPLANE COMPANY

- ABSTRACT -

Due to the high energy content of the rotating compressor and the turbine assemblies in a turbine engine, the possibility of an engine burst was recognized as a potential hazard from the earliest development days. Recognition of the potential for engine burst has led to definitive FAA certification regulations and specific considerations in the design of current aircraft. This design philosophy is continued today and historically proved very effective. However, rotor burst protection must be considered an important element of overall aircraft safety and continued effort to reduce the frequency and minimize the consequence of non-contained rotor failures is justified. This paper reviews current aircraft design practices to minimize the hazard from rotor bursts, and discusses the consequences of non-contained engine failures and the impact of rotor burst protection systems on aircraft design.

INTRODUCTION

The high energy content of the rotating compressor and the turbine assemblies in a turbine engine and the possibility of an engine burst was recognized as a potential hazard to turbine powered aircraft from the earliest development days. For this reason, the FAA has developed stringent regulations for engine certification which requires special testing to substantiate rotor integrity. Recognition of this potential for engine burst has also led to definitive FAA certification regulations and specific considerations in the design of current aircraft.

This design philosophy is continued today and historically has proved very effective. The U. S. commercial air carrier record of one fatality attributed to non-contained rotor fragments in over 400 million turbine engine hours of flying shows that engine rotor failure is, in fact, statistically a very small hazard to the welfare and safety of commercial aircraft passengers.

However, to further improve flight safety, it is necessary to continually look for means of eliminating or reducing the potential for accidents, including the non-containment of turbine engine fragments. Consideration of the potential hazard of an engine rotor burst is an important factor in overall aircraft safety and continued efforts to reduce the potential hazard is warranted.

CURRENT DESIGN PRACTICES

Although considerable effort is being expended by engine manufacturers to reduce the number of engine rotor failures, it is believed that the rate will not be reduced to zero. Rotor failures may continue to occur at a rate near the current level of approximately one non-contained failure per million engine hours. Therefore, continued effort to minimize the hazard to the aircraft of non-contained engine fragments is required.

Current design practices to minimize this hazard include configuring the aircraft to reduce the risk of: (1) loss of additional thrust, (2) fuel fed fires, (3) loss of critical systems, and (4) loss of structural integrity. These objectives are accomplished by: (1) controlling the relative location and spacing of engines and critical systems, (2) use of redundant systems, (3) use of dual load path structure, and (4) use of fire protection systems. In addition, where configuration peculiarity indicates, consideration is given to special shielding of critical components. The application of these concepts is of course very dependent upon the basic airplane configuration. The success of this design approach is a matter of record.

CONSEQUENCE OF AN ENGINE BURST

Boeing has recently completed a study to identify the consequence of engine non-contained failures and to determine if there is a correlation between damage

severity and fragment type. Information on aircraft damage resulting from non-contained engine fragments was obtained from FAA, NTSB, and CAA reports (References 1 through 5). All current Boeing aircraft models were included in the study as well as available data on DC-8, DC-9, DC-10, CV880, CV990, and L-1011 aircraft. Damage data were collected on 366 jet engine non-containments that occurred between January 1964 and February 1976.

For this study, "non-containment" was defined as the release of internal parts of an engine with sufficient force to puncture or split the engine outer case with or without fragments passing through the case. Generally, non-containments that involve fragments that exit the nacelle with the potential to damage aircraft structure other than the affected nacelle are of primary concern. However, the broad definition of non-containment used in this study was selected to give consideration to all non-contained occurrences.

Various other studies (References 6 and 7) have examined non-contained engine failures from the standpoint of the cause of failure. The Boeing study was an attempt to analyze the consequence of non-contained failures with respect to the hazard to the aircraft and its passengers. Since all commercial aircraft certified under FAR Part 25 are capable of continued safe operation after the loss of thrust from one engine during any phase of flight, this study was concerned with damage to the aircraft other than the affected nacelle.

A method was developed which attempted to relate the aircraft damage caused by an engine non-containment to the potential hazard to the aircraft resulting from that damage and to the class of fragment causing the damage. The method generated a "relative damage severity rating" for each occurrence. This rating was in the form of a number by which the hazard associated with one occurrence could be compared to that of another occurrence. The rating has no absolute meaning. It was offered only as an aid in relating occurrences to each other.

The relative damage severity rating is a subjective measure of what could have happened in a particular occurrence, given the actual damage caused by the engine non-containment. Thus, it is a means of identifying the potential hazard. Since it is subjective, each occurrence could be rated differently by different analysts. However, it was felt that by applying the same criteria by the same analyst to all occurrences, a reasonable picture of the criticality could be obtained. After the numerical values for the relative damage severity were determined for each occurrence, the data were divided into four general categories shown in Table 1. It is apparent that Categories 1 and 2 damage severity presents no hazard to the welfare and safety of the commercial airline passenger. It is also apparent that if a meaningful reduction in the hazard to the aircraft from non-contained rotor failure is to be achieved, Categories 3 and 4 type damage must be significantly reduced.

It should be recognized that Boeing has no first hand knowledge of the vast majority of these occurrences and while for purposes of this study the information reported and the conclusions reached by the investigating authority or operator involved are assumed to be correct, they may not be so.

The results of the study are summarized in Figure 1. Of the 366 non-contained occurrences classified, 283 were judged to have caused minor damage severity, 53 moderate damage severity, 19 significant damage severity, and 11 extreme

damage severity. These data indicate that a relatively small percentage of engine non-contained failures result in significant or extreme damage severity. Only limited data was available covering the number of blades released, the size of the rim or disk segment or how many pieces were involved in a failure. For this reason only general categories of fragment size were used in plotting the data. The fragment categories used are: single blade, multiple blades, rim segments, and disk segments. Only occurrences where measurable aircraft damage occurred and where the fragment class was known are plotted. The figure shows that the majority of non-contained occurrences with high damage severity ratings (significant or extreme) involved large fragments with high energy levels (rim or disk segments) while very few smaller fragments (blades) were involved in significant or extreme damage severity. Thus to measurably reduce the hazard of non-contained rotor failures by the use of containment would require containment of the majority of the large high energy fragments.

These analyses indicated that the majority of non-contained engine bursts released fragments with relatively low energy levels. Although the installation of increased containment capability could significantly reduce the number of non-contained engine bursts to which the aircraft structure and system are exposed, reducing the number of non-contained burst does not directly imply an equivalent reduction in hazard to the aircraft. The hazard to the aircraft is a function of fragment size and energy. Containment of only the low energy fragments would not significantly reduce the hazard to the aircraft and could result in a significant weight penalty.

IMPACT OF ENGINE BURST PROTECTION

Substantial design effort has been expended by aircraft companies to retain a high degree of flight safety and at the same time minimize the penalties to the aircraft due to current design practices for engine burst protection. Any consideration of changes to the current design practices, such as increasing the containment capability must be evaluated on the basis of overall improvement in flight safety. The impact on air carrier operating cost must also be determined.

Improving the engine fragment containment capability or providing deflection capability in order to further protect vital aircraft areas impacts almost all aspects of aircraft design. The impact could include: nacelle weight, airframe weight, nacelle performance, nacelle and engine thermal balance, engine maintainability, aircraft weight and balance and aircraft structure including flutter. The amount of impact is dependent upon the configuration and the design of the specific aircraft being considered.

Increasing the containment capability presents an additional problem. Containing fragments within the engine case can cause increased damage to the rotor system and cause the release of more and larger fragments. This in turn could result in a greater hazard to the aircraft than the release of the initial fragment.

CONCLUSIONS

The Boeing study of non-contained turbine engine rotor failures resulted in the following conclusions:

1. Current design practices to: (1) reduce the number of turbine engine rotor failures, and (2) to minimize the hazard of a rotor failure to the aircraft has resulted in an outstanding safety record.

2. There was significant or extreme damage severity to individual aircraft in a relatively small percentage of engine non-containments.

3. The majority of non-contained occurrences with high damage severity ratings (significant or extreme) involved large fragments (rim or disk segments) with high energy levels. Containment of only low energy fragments (blades) would not have significantly reduced the hazard to the aircraft.

4. Any measure to reduce the hazard of non-contained engine fragments must be evaluated in terms of overall aircraft safety. In addition, economic effects must be evaluated.

REFERENCES

1. National Transportation Safety Board Report Number NTSB-AAS-74-4 Volume II, December 18, 1974: Turbine Engine Rotor Disk Failure Case Histories.

2. National Transportation Safety Board Report: Fan/Compressor/Turbine Disk Failure, 1963-1967.

3. National Transportation Safety Board: Briefs of Accidents/Incidents, All Turbine Engines Selected Cause/Factor, U. S. Civil Aviation 1964-1974.

4. Federal Aviation Administration AFS-140 January 1, 1974, Tabulation of Uncontained Rotor Disk Failure Cause in Civil Engines.

5. Civil Aviation Authority (United Kingdom): January 10, 1975: Tabulation of U. S. Uncontained Engine Failures, 1963 through September 1974.

6. National Transportation Safety Board Report Number NTSB-AAS-74-4, Volume I; December 18, 1974: Special Study - Turbine Engine Rotor Disk Failures.

7. Naval Air Propulsion Test Center Report NAPTC-PE-67, NASA/CR-134855, Rotor Burst Protection Program: Statistics on Aircraft Gas Turbine Engine Rotor Failures that Occurred in U. S. Commercial Aviation during 1974, September 1975.

TABLE 1. - DAMAGE SEVERITY.

- AIRCRAFT DAMAGE CLASSIFIED BY RELATIVE DAMAGE SEVERITY

  1. MINOR - DAMAGE TO AFFECTED NACELLE, NICKS AND DENTS IN AIRCRAFT STRUCTURE
  2. MODERATE - DAMAGE TO SECONDARY STRUCTURE AND SYSTEMS
  3. SIGNIFICANT - DAMAGE TO AIRCRAFT PRIMARY STRUCTURE AND SYSTEMS, MINOR INJURIES
  4. EXTREME - HULL LOSS, FATALITIES

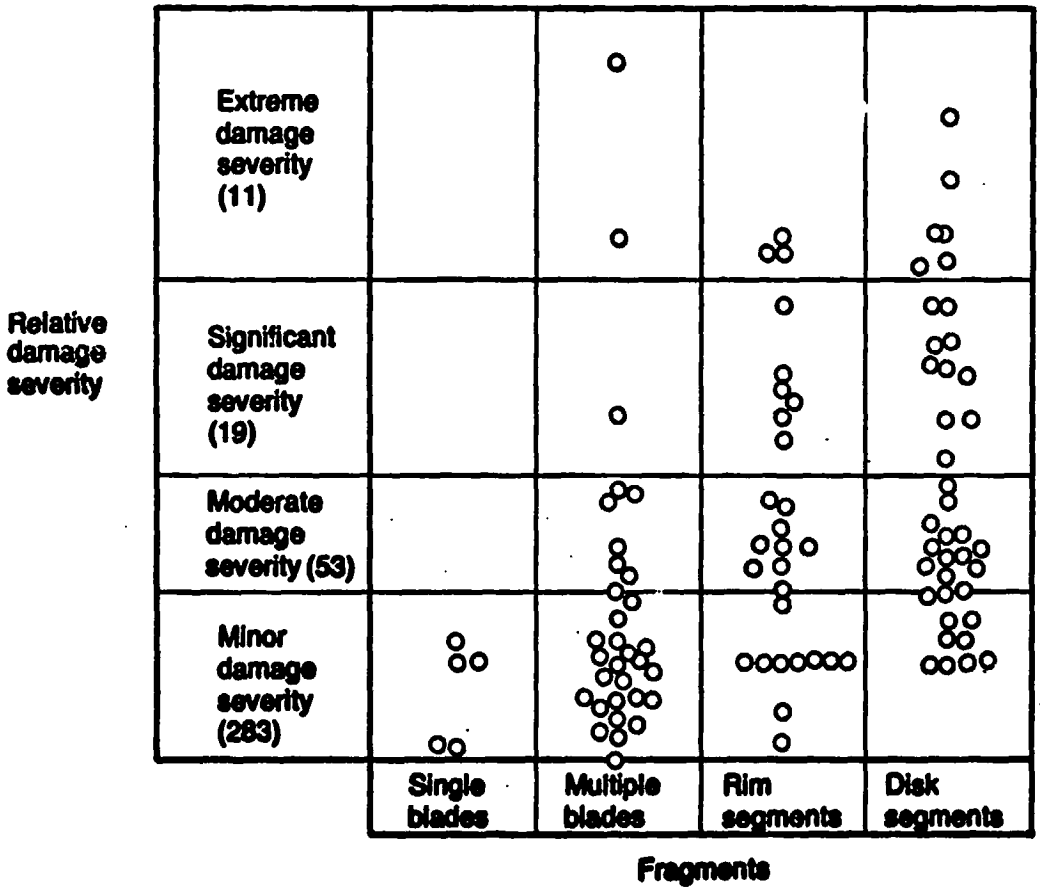

Figure 1. - Relative Damage Severity Versus Fragment Size.

DISCUSSION

E. Witmer, MIT-ASRL

Ralph, you talked about the occurrence of secondary damage that might develop as the result of primary fragment release. Are you suggesting that perhaps the use of deflectors rather than containers might be a preferable alternative?

R. McCormick, Boeing

I didn't mean to imply that. I suppose that may be a consideration. I intended to suggest that perhaps small fragments would do less damage by exiting out than if we contained them in the engine.

Unknown Questioner

Are you in a position to do more of a systems study of the effect of containment on these items that you talked about: flutter, increased weight, fuel consumption, those sorts of things?

R. McCormick, Boeing

We haven't done that type of study because we haven't looked at a containment system installation in an aircraft and we have no immediate plans to do so.

ENGINE NON-CONTAINMENT -- UK RISK ASSESSMENT METHODS

J. C. Wallin
Chief Propulsion Engineer
British Aircraft Corporation
Commercial Airplane Division

SUMMARY

In order to establish compliance with recent changes to British Civil Airworthiness Requirements it has been necessary to develop methodology for assessment of catastrophic risks resulting from uncontained turbine engine rotors.

The methodology was developed during the course of the Concorde SST certification programme, utilising an engine failure model for the Olympus 593.

In essence this work is applicable to any aircraft type, but it has been established that some of the data used produces unrealistically pessimistic assessments.

Work continues to develop realistic guideline data for use in these assessments, which can be used for future aircraft design.

1. Introduction

Gordon Gunstone in his paper "Engine Non Containment - The U.K. C.A.A. View" has explained the thinking which has led to the latest British Civil Airworthiness Requirement in respect of engine non-containment hazards.

Alongside this one has had to develop numeric methodology by the use of which compliance with the requirement can be shown. As will be appreciated new requirements cannot be imposed overnight, and in fact the present B.C.A.R. is the culmination of some years of joint work between CAA and the British Aircraft industry, so that the methodology has tended to be developed alongside the developing requirement.

Being a numeric method, somewhat greater precision can be given to answering the question "where should minimising the risk stop?" However it must be emphasised that a numeric answer is an aid to engineering judgement and can never entirely replace it. For example, if an assessment showed compliance with B.C.A.R., but one particular risk, which could be reduced without excessive penalties, constituted a major part of the total risk, it would be expected that design action to reduce this risk would be taken.

A summary of the foregoing appears in Figure 1.

It cannot today be claimed that the methods are perfect and indeed considerably more work is required to establish satisfactory data values in certain areas which require the use of judgements. However it is hopefully of interest to members of the workshop to have some idea of the present position.

2. Background

The current B.C.A.R. is summarised in Figure 2, and employs a relatively simple failure model.

This was not always the case, and the story of the practical development of the new requirement and its associated methodology really began with the Concorde. Here, because of the relatively unorthodox layout of the aircraft, the degree of hazard minimising required for parity with subsonic types was not immediately obvious. Additionally, although the aircraft in its conception in 1962 had accounted for the possibility of turbine rupture, accumulating evidence over the years indicated the necessity for considering compressor debris as well. Not unnaturally argument developed between the constructors and the ARB (as the CAA then was) as to the required precautions. Since numerical methods of airworthiness analysis were a fundamental part of Concorde certification, it seemed logical to extend this to consideration of engine non-containment risks. It was therefore agreed to make an assessment against an engine failure model to be derived by Rolls-Royce as the most probable failure debris based on previous non-containment experience and the knowledge of the Olympus construction. This resulted in the model shown in Figure 3, which took three years and numerous meetings to produce!

The requirement was that the probability of catastrophe should not be worse than 10^{-8} per aircraft hour, and in order to achieve this a number of changes were made to the aircraft, primarily as a result of the inclusion of compressor debris. These changes are shown in Figure 4 and 5 the former indicating the armour plate necessary to prevent penetration of the fuel tanks and the latter showing systems layout and fire precautions modifications.

It will be noted that the model did not include $\frac{1}{3}$ compressor disc pieces, since at the time the model was agreed, no Rolls-Royce axial engine had ever had a major compressor disintegration. Subsequent events, however, led CAA to review the situation and to require an assessment of the effect of the random release of two $\frac{1}{3}$ compressor disc pieces. Since there were insufficient statistics to define the probability of the event, it was not possible to include these pieces in the model, and a new requirement criterion had to be developed. At this stage, a requirement akin to the present BCAR was introduced for the compressor $\frac{1}{3}$ disc pieces, such that the probability of catastrophe per event, averaged across the flight should not be worse than a given number. Originally CAA would have liked to see 1 in 20, but this was not possible to achieve, the actual value being something like half of this. However an assessment, by the same methods and to the same standards, of a number of established aircraft showed that these aircraft had no better probability of catastrophe, and in some cases considerably worse. It was therefore apparent that parity at least with current aircraft types was established.

The final result of this effort, over a period of some six years was a certification report two inches thick and working documentation and drawings occupying over 50 cubic feet.

In retrospect this model was probably much too complicated and the precautions taken would have been similar had today's BCAR model been used, since $\frac{1}{3}$ disc pieces and disc rim fragments dominated the exercise. Nevertheless it did result in the development of methodology which with further refinement can be applied to any aircraft.

3. Methodology

3.1. Basic Work

The initial stages of the assessment consist of the following steps.

a) Establish a hazard tree (Figure 6). This will essentially be the same for all aircraft, but may vary in detail, particularly where methods of operation of flying controls differ.

b) Establish debris size for each stage of the engine (Figure 7).

c) Draw plan view of fly off zone (Figure 8) for each stage, identifying potential risk items (e.g. systems, fuel tanks, other engines etc.)

d) Draw section through fly off zone (Figure 9) establishing risk angles for each item potentially at risk. It is assumed that ½ disc pieces will not be stopped, but in the case of the disc rim pieces, structural analysis is required to determine whether at some structural interface the piece will be stopped. The example in Figure 10 shows that engine controls and fuel tank are potentially at risk but that flying controls and electrics are not.

3.2. Data and Assumptions

3.2.1. Flight Phases

It will be remembered that the hazard assessment is averaged throughout the flight, and there will be some risks which are only present during certain phases of flight. Hence it is necessary to break down the flight to well defined phases, and while this breakdown could vary with the aircraft mission, it has been found so far that the three phases shown in Figure 11 are suitable for jet transport types.

3.2.2. Failure distribution by flight phase

In assessing the overall risks it is necessary to consider the percentage of failures occurring in each phase. In practice this can only be established statistically and Figure 12 shows the values obtained from three sources. So far, in BAC's assessments, the Rolls-Royce values have been used, but these are identical with NTSB for the phases in use. CAA's analysis gives a slightly higher weighting to the take-off phase and some re-thinking here may be necessary.

3.2.3. Guidelines

In considering the potential hazards from individual contributory factors, some items can be dealt with as matters of fact. For example in systems areas the design of the aircraft will establish clearly whether a catastrophe can or cannot occur due to the loss of a given system or systems.

In other areas, notably loss of adequate thrust, fire, and structural damage an element of judgement is required. In these cases guidelines have been discussed and provisionally agreed with CAA.

3.2.4. Loss of adequate thrust

Figure 13 shows the probability of catastrophe (i.e. of not being able to land the aircraft safely) for the loss of multiple engines. Apparent inconsistencies will be noted, and these have resulted from CAA Flight Department knowledge of the handling of the particular aircraft types considered. It is thought that for design assessment of new types, a more consistent set of numbers needs to be established.

3.2.5. Fire Hazards

Figure 14 shows the factors considered in establishing fire hazards. In this I_R, the ignition probability is a powerful factor and Figure 15 gives the CAA guideline values.

3.2.6. Structural damage

Figure 16 shows the CAA guideline for the minimum static ultimate strength requirement to be used in considering the size of catastrophic holes in primary structure.

3.3. Calculations

Having completed the basic work of section 3.1. (establishing the risk angle) and assessed the risk factor for each hazard, using where appropriate, the assumptions from section 3.2., it is now possible to draw for each flight phase and each stage a diagram of risk angle versus risk factor as shown in Figure 17. (In practice it will probably be found that one diagram covers several stages, all producing the same angles and factors.)

The individual risks are then summed as shown at the bottom of the figure, using success theory for summing overlapping risks, i.e.

$$F_{1+2} = \left[1 - (1-F_1)(1-F_2)\right]$$

Thereafter the averaging method shown on Figure 18, will result in the mean catastrophic risk to the aircraft across a typical flight mission.

4. Results

In order to validate the above methods and assumptions, BAC have been analysing a range of current aircraft to evaluate the catastrophic risk level due to $\frac{1}{3}$ disc pieces. The results appear on Figure 19, and are indeed surprising, with risks varying from 1 in 6.9 for an underwing narrowbody twin to 1 in 27.8 for a widebody trijet, with only two of the types considered meeting BCAR!

The actual in-service world wide record derived from the number of fatal accidents compared with the number of major disc releases gives a value of approximately 1 in 30. In can be argued therefore that current aircraft on average must in practice be complying with BCAR, and hence the assessments must be pessimistic.

Work is continuing to identify and study the areas of pessimism, with the objective of modifying the guidelines where necessary. As an end result it is hoped to agree a set of realistic ground rules with CAA which will be suitable for future aircraft design assessment.

Reference to Figure 19 will show that the most recurring major contributory factors are structural damage and fires, and hence these are receiving major attention.

With particular regard to critical cut lengths in fuselage structure, work is leading to a more sophisticated analysis of the residual structural strength based on the fracture toughness of the skin material and the nominal axial stress before damage (Figure 20).

Even this may still be pessimistic in meeting the requirement of Figure 16, and perhaps this requirement should be further questioned. Who, for example, on the basis of analysis, would have believed that the aircraft shown in Figure 21 could have suffered this amount of damage and survived - but it did!

5. Conclusions

Methodology has been established to assess the catastrophic risks from uncontained rotor debris, but further work is required to refine the assumptions used so as to bring the results into accord with the known facts. When this is done it should be possible, using agreed standards of assessment, to produce cost effective design precautions against rotor failure on future aircraft types.

Acknowledgements

The author wishes to thank British Aircraft Corporation for permission to give this paper, and colleagues, particularly Mr. B. Tufnell, for help in its compilation.

Opinions expressed are those of the author and do not necessarily represent the view of British Aircraft Corporation.

- METHODOLOGY DEVELOPED TO MEET NEW C.A.A REQUIREMENTS.
- GIVES MORE PRECISION TO SAFETY ASSESSMENT-BUT:
- DOES NOT REPLACE ENGINEERING JUDGEMENT.

Figure 1. - Engine Non-containment U. K. Risk Assessment Methods.

DEBRIS TYPE	ACCEPTABLE * CATASTROPHIC RISK LEVEL	N° OF PIECES	SPREAD ANGLE	MASS	REMARKS
ONE-THIRD DISC FRAGMENT	1 in 20	1	± 3°	ONE-THIRD BLADED DISC MASS.	TRANSLATIONAL ENERGY (NEGLECTING ROTATIONAL ENERGY)
DISC RIM PIECE	1 in 60	1	± 5°	GREATER OF 1/20th BLADED DISC MASS OR MASS OF TWO BLADES WITH ROOTS.	TRANSLATIONAL ENERGY (NEGLECTING ROTATIONAL ENERGY)
MULTIPLE ONE-THIRD DISC FRAGMENTS	1 in 10	3	± 3°	AS FOR SINGLE ONE-THIRD DISC FRAGMENT.	APPLICABLE TO DUPLICATED OR MULTIPLICATED SYSTEMS ONLY. ENERGY AS DEFINED FOR SINGLE ONE-THIRD DISC FRAGMENT.

* 1. AVERAGE OF ALL DISCS & ALL ENGINES ACROSS TYPICAL FLIGHT PLAN.
2. NO SINGLE DISC MUST HAVE RISK GREATER THAN TWICE THE REQUIRED AVERAGE RISK.

Figure 2 - BCAR Engine Failure Model.

	DEBRIS TYPE	CONTRIBUTION PER 10^4 A/C HOURS		Nº OF PIECES	SPREAD ANGLE	REMARKS
TURBINE	1/3 BLADED DISC	·05	·75	2	±3°	EQUAL PROBABILITY OVER 360° TRANSLATIONAL ENERGY
	MINOR DISC FRAGMENTS	·20		1	±5°	RIM PIECE & BLADES WITH SIZE & ENERGY VALUE DEFINED FOR EACH STAGE.
	BLADES (HIGH ENERGY)	·08		2	±30°	MAX BLADE ENERGY
	BLADES (LOW ENERGY)	·40		1	±30°	55% OF MAX BLADE ENERGY
	MULTIPLE BLADES	·02		N/3-120° SPREAD N/12-30° SPREAD	±30°	ALL BLADES 100% ENERGY
COMPRESSOR	DISC RIM PIECE	·05	·25	1	±5°	RIM PIECE & BLADES WITH SIZE & ENERGY VALUE DEFINED FOR EACH STAGE
	BLADES (HIGH ENERGY)	·05		2	±30°	MAX BLADE ENERGY
	BLADES (LOW ENERGY)	·15		1	±30°	55% OF MAX BLADE ENERGY

Figure 3 - Olympus 593 Failure Model.

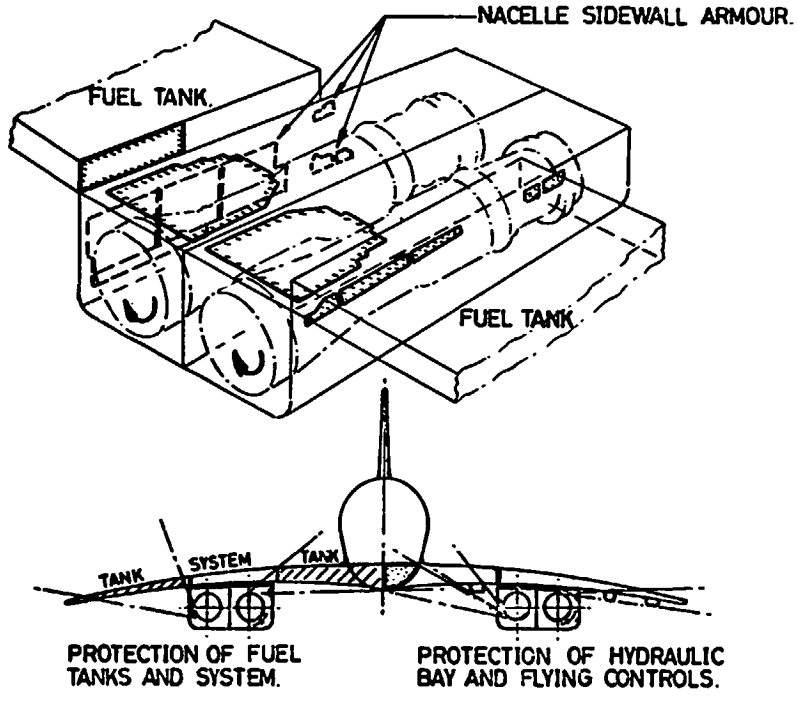

Figure 4 - Concorde-Armour Plate.

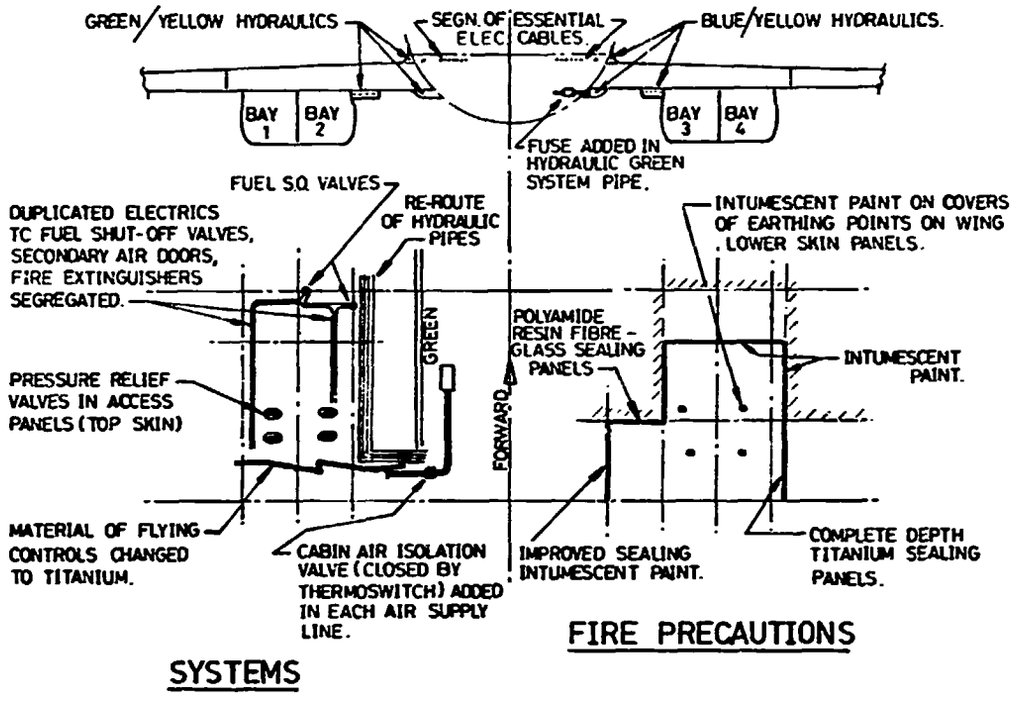

Figure 5. - Concorde - Design Precautions to Minimise Rotor Failure Damage.

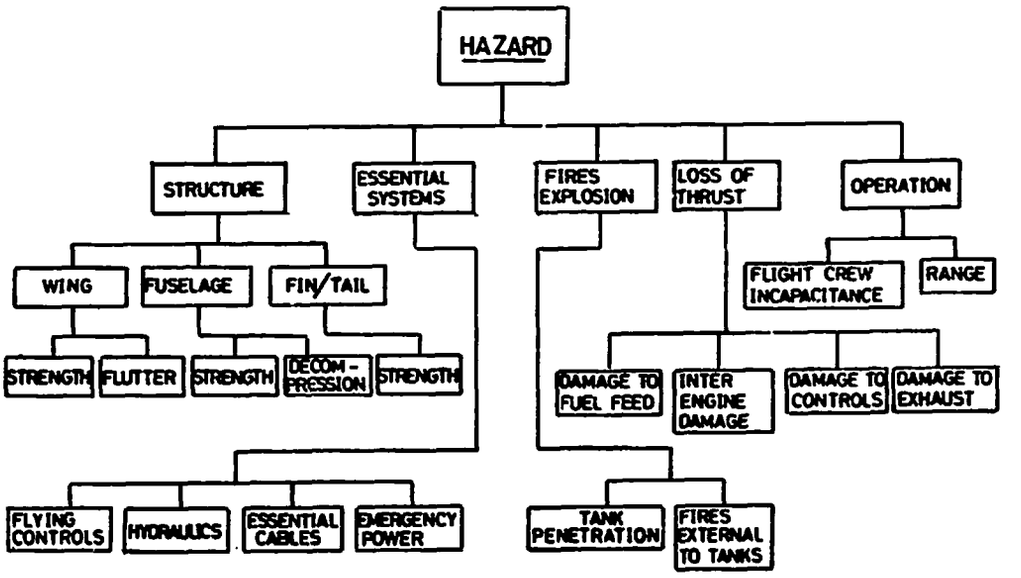

Figure 6. - Engine Rotor Failure - Hazard Tree.

r = BLADED DISC RADIUS

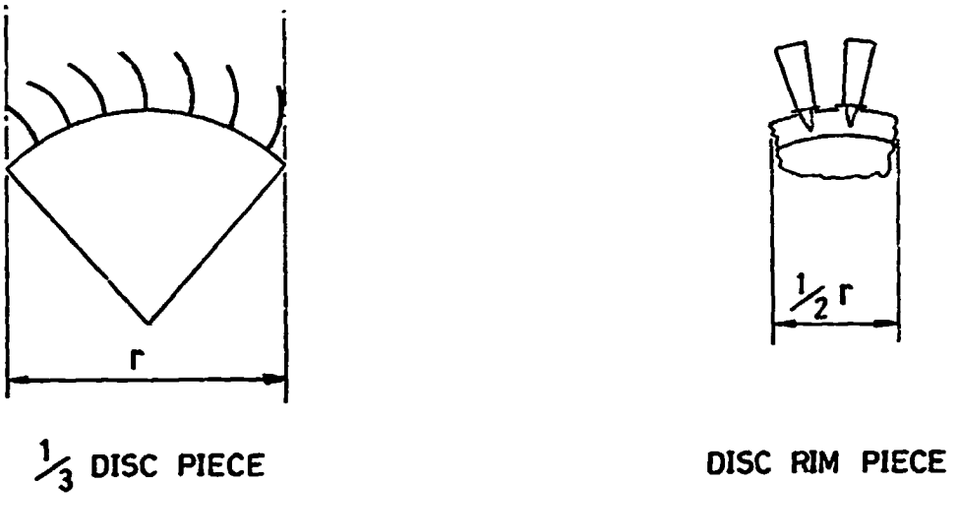

Figure 7. - BCAR Debris.

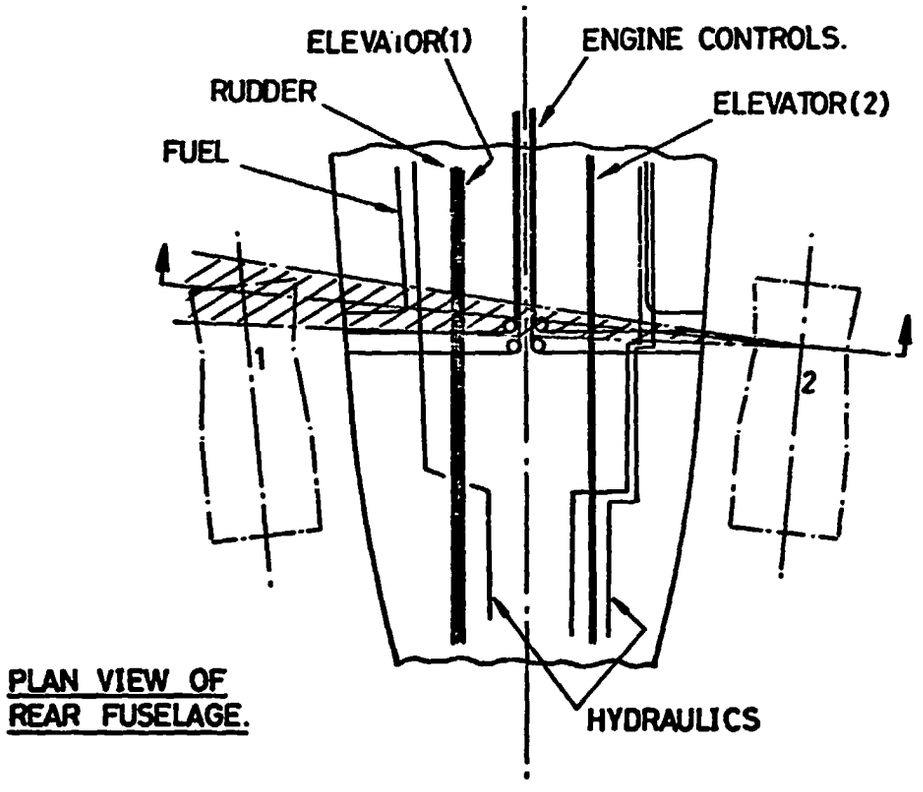

Figure 8. - Typical Fly Off Zone.

ITEM AT RISK.	ANGLE OF EMISSION.
ENGINE.	85° – 100°
CONTROLS (FLYING-ENGINE)	99° – 113°
STRUCTURE	53° – 62° and 126° – 139°

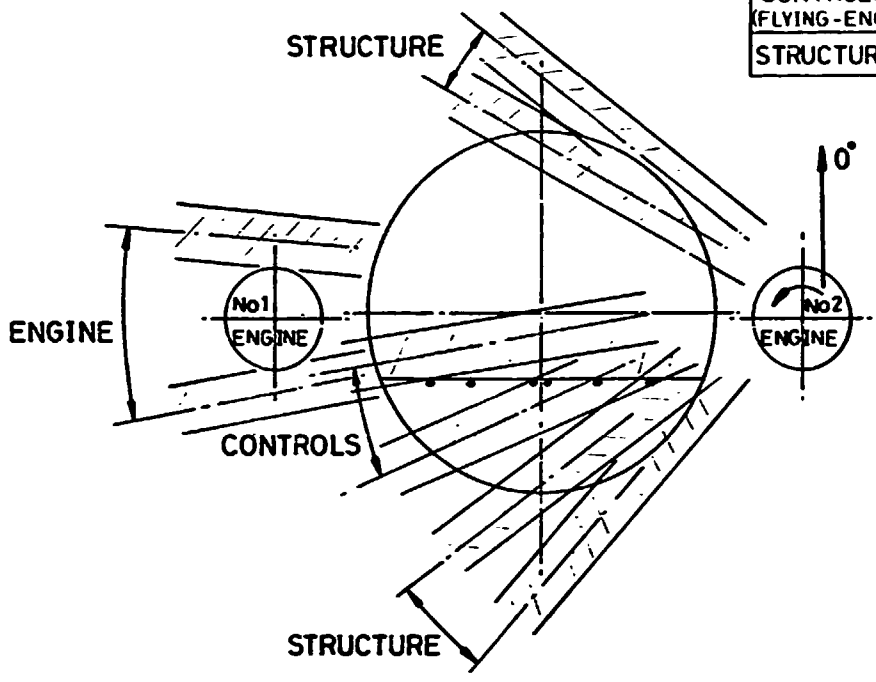

Figure 9. - Debris Trajectories.

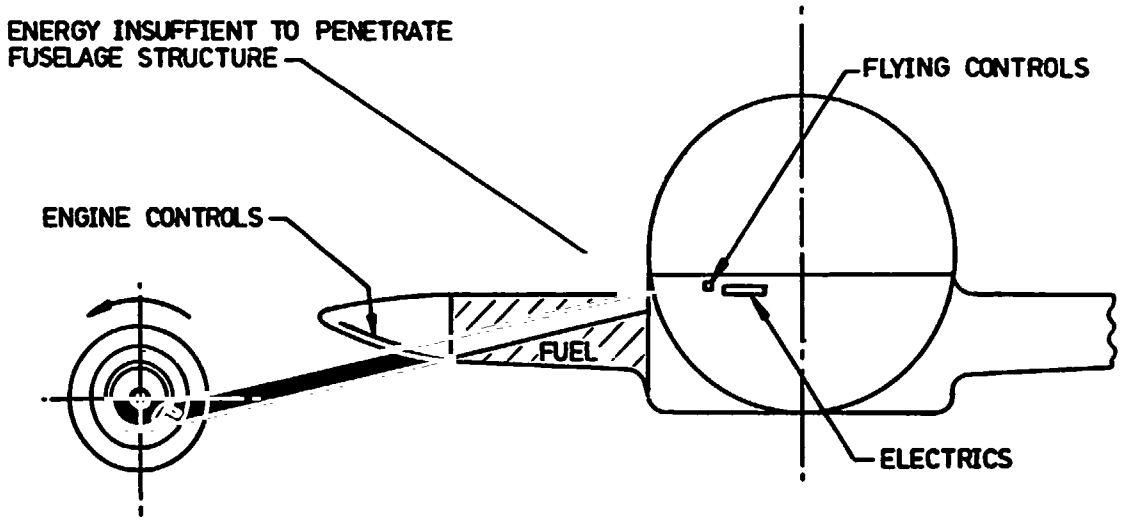

Figure 10. - Structurally Limited Trajectory.

1. TAKE OFF – START OF ROLL TO V_1.

2. TAKE OFF – V_1 TO 1,500 FT.

3. POST TAKE OFF – 1500 FT TO TOUCHDOWN.

Figure 11. - Flight Phase Breakdown.

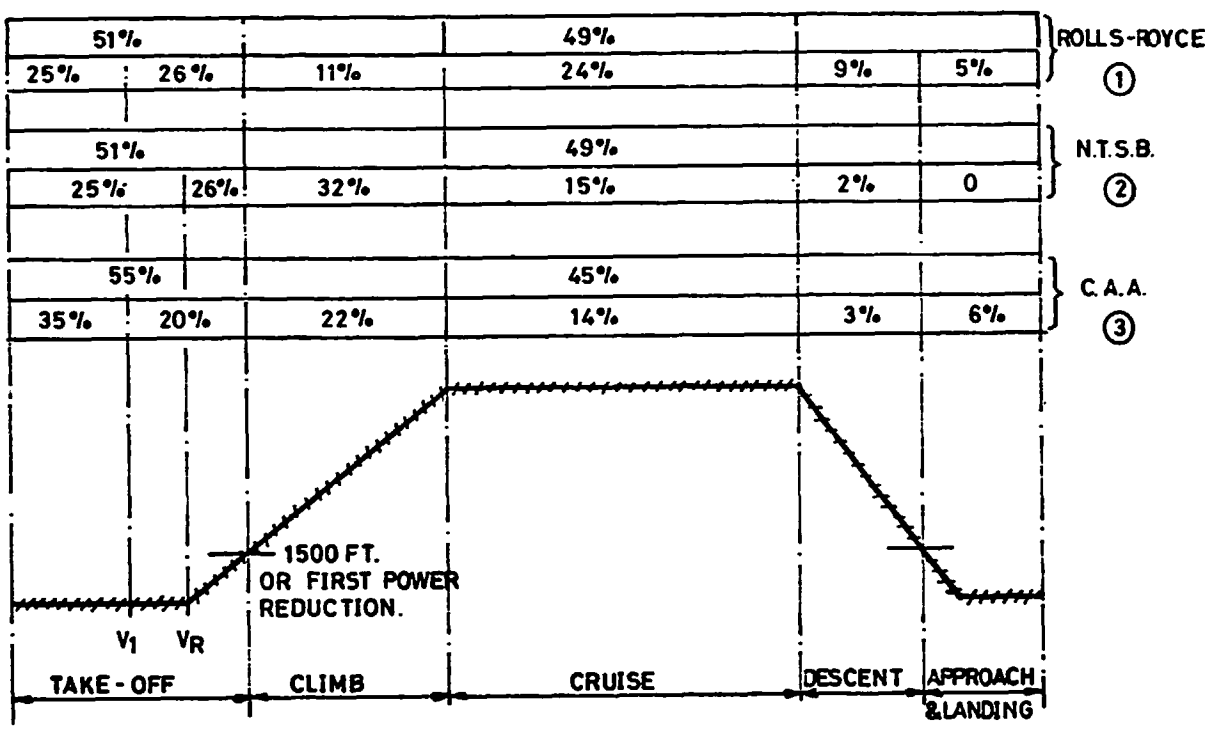

① ROLLS-ROYCE ENGINES (1954-1970 STATISTICS)

② N.T.S.B. REPORT NTSB-AAS-74-4.

③ CAA - GUNSTON, "ENGINE NON CONTAINMENT - THE UK CAA VIEW."

Figure 12. - Distribution of Uncontained Failures Over Flight Phases.

FLIGHT PHASE	NO OF ENGINES LOST				AICRAFT TYPE
	1	2	3	4	
0 TO V_1	0	0			REAR OR UNDERWING ENGINED TWIN-JET.
V_1 TO 1,500FT	0	·7			
POST 1,500FT	0	·6			
0 TO V_1	0	0	0		REAR ENGINED TRI-JET
V_1 TO 1,500FT	0	·4	·85		
POST 1,500FT	0	0	·75		
0 TO V_1	0	0	0	0	FOUR REAR MOUNTED ENGINES.
V_1 TO 750FT	0	·8	·8	·8	
750 TO 1500FT	0	·2	·5	·8	
POST 1500FT	0	0	·2	·7	
0 TO V_1	0	0	N/A	0	FOUR UNDERWING PODDED ENGINES.
V_1 TO 1,500FT	0	·25	N/A	·7	
POST 1,500FT	0	0	N/A	·6	

Figure 13. - Risk Factors for Loss of Thrust. (Expressed as a fraction of 1.)

RISK FACTORS / FLIGHT PHASE	T_R	I_R	H_R	L_R	E_R
GROUND ROLL TO V_1					
V_1 TO 1,500 FT					
POST 1,500 FT					

T_R = PROPORTION OF FLIGHT PHASE THAT FUEL IS PRESENT IN PENETRATED TANK.
I_R = IGNITION PROBABILITY.
H_R = PROBABILITY OF FIRE SITUATION BECOMING POTENTIALLY CATOSTROPHIC.
L_R = PROBABILITY OF NOT LANDING SAFELY AND EVACUATING PASSENGERS WITH POTENTIALLY CATASTROPHIC FIRE.
E_R = PROBABILITY OF A CATASTROPHIC EXPLOSION AT INSTANT OF PENETRATION = I_R X STRUCTURAL RESISTANCE TO OVERPRESSURE.

PROBABILITY OF CATASTROPHE = $(T_R \times I_R \times H_R \times L_R) + E_R$

Figure 14. - Risk Factors for Fuel Tank Fire and Explosion.

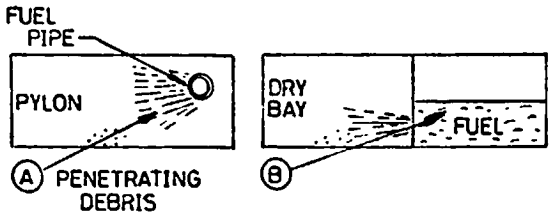

FUEL TEMP ABOVE LOWER FLAMMABILITY LIMIT FOR VAPOUR ASSUME 80% PROBABILITY OF FIRE.
FUEL TEMP WITHIN MIST REGION ASSUME 5% PROBABILITY OF FIRE AT -50°C RISING LINEARLY TO 80% AT LOWER FLAMMABILITY LIMIT FOR VAPOUR.

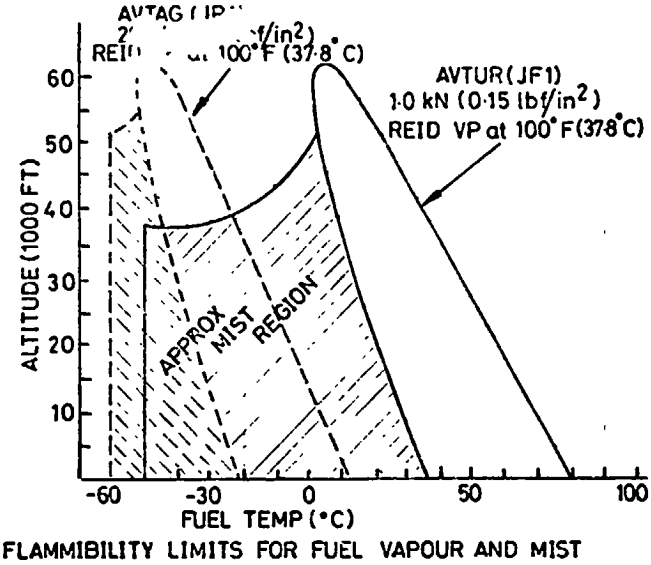

FLAMMIBILITY LIMITS FOR FUEL VAPOUR AND MIST

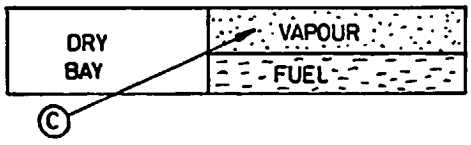

FUEL TEMP WITHIN FLAMMABILITY LIMITS FOR VAPOUR AND DEBRIS PENETRATES ULLAGE SPACE WITHOUT PASSING THROUGH FUEL. ASSUME 90% PROBABILITY OF AN EXPLOSION.

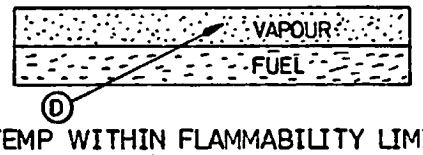

FUEL TEMP WITHIN FLAMMABILITY LIMITS FOR VAPOUR AND DEBRIS PENETRATES TANK BELOW FUEL SURFACE AND PASSES THROUGH ULLAGE SPACE, ASSUME 70% PROBABILITY OF EXPLOSION. IF FUEL TEMP IS WITHIN MIST REGION ASSUME 5% PROBABILITY OF AN EXPLOSION AT -50°C RISING LINEARLY TO 70% AT LOWER FLAMMABILITY LIMIT FOR VAPOUR.

Figure 15. - Ignition Risk Factors, I_R.

A. 70% LIMIT FLIGHT MANOEUVERING LOAD.
20 FT/SEC EAS GUST (VERTICAL OR LATERAL) AT Vc
COMBINED WITH MAXIMUM CABIN DIFFERENTIAL PRESSURE (PLUS AERODYNAMIC SUCTION).

B. 1·1 (MAXIMUM NORMAL CABIN DIFFERENTIAL PRESSURE AT TIME OF INCIDENT PLUS AERODYNAMIC SUCTION) PLUS 1g FLIGHT LOAD FREEDOM FROM FLUTTER UP TO Vc.

Figure 16. - Minimum Static Ultimate Strength Requirement.

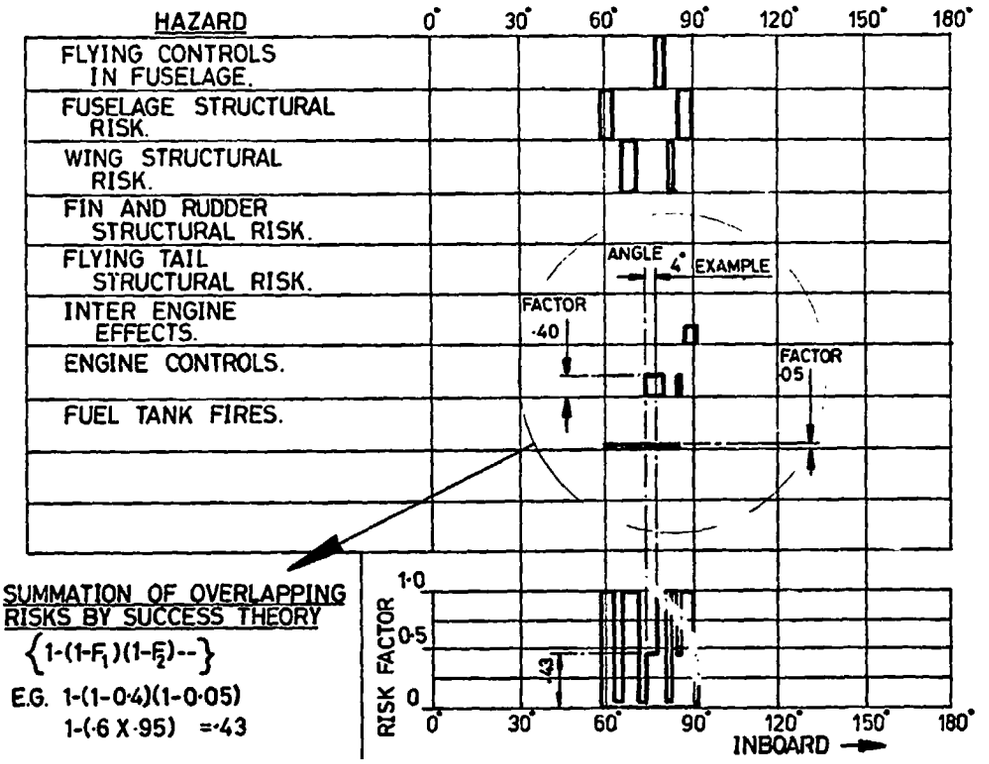

Figure 17. - Hazard Summary Diagram.

FOR EACH ENGINE STAGE IN EACH FLIGHT PHASE

- DERIVE POTENTIALLY CATASTROPHIC ANGLES (α) FOR EACH HAZARD.
- DERIVE RISK FACTOR (F) FOR EACH HAZARD.
- CALCULATE COMBINED RISK FACTOR (C_{SP}) FOR THE PHASE AND AVERAGE OVER 360° (n RISKS)

$$C_{SP} = D_P \times \left(\alpha_1 F_1 + d_2 F_2 \cdots \alpha_n F_n\right) \qquad D_p = \text{PHASE FAILURE DISTRIBUTION.}$$

THEN

- SUM COMBINED RISK FACTOR FOR THE STAGE OVER THE TOTAL FLIGHT ('P' PHASES) TO OBTAIN OVERALL STAGE RISK (C_S).

$$C_S = C_{SP_1} + C_{SP_2} \cdots C_{SP_p}$$

- AVERAGE ALL STAGES OVER THE TOTAL ENGINE ('S' STAGES) TO OBTAIN MEAN ENGINE RISK (C_E)

$$C_E = \frac{C_{S_1} + C_{S_2} \cdots C_{S_S}}{S}$$

- AVERAGE ALL ENGINES OVER THE AIRCRAFT ('E' ENGINES) TO OBTAIN MEAN AIRCRAFT RISK (C_A)

$$C_A = \frac{C_{E_1} + C_{E_2} \cdots C_{E_E}}{E}$$

Figure 18. - Engine Rotor Failure - Risk Evaluation.

AIRCRAFT TYPE	CATASTROPHIC RISK RATIO	MAJOR CONTRIBUTARY FACTORS.
TWO REAR ENGINES – NARROWBODY	1 IN 23·3	1. LOSS OF ADEQUATE THRUST. 2. FUSELAGE STRUCTURAL DAMAGE.
TWO UNDERWING ENGINES – NARROWBODY	1 IN 6·9	1. FUEL TANK FIRES.
THREE REAR ENGINES – NARROWBODY	1 IN 9·2	1. FUSELAGE/FIN STRUCTURAL DAMAGE 2. FIRE. 3. LOSS OF ADEQUATE THRUST.
FOUR REAR ENGINES – NARROWBODY	1 IN 12·7	1. LOSS OF ADEQUATE THRUST.
FOUR UNDERWING ENGINES- NARROWBODY	1 IN 15·8	1. WING STRUCTURAL DAMAGE. 2. FUSELAGE STRUCTURAL DAMAGE.
ONE REAR, TWO UNDERWING ENGINES- WIDE BODY	1 IN 27·8	1. FUSELAGE STRUCTURAL DAMAGE. 2. WING STRUCTURAL DAMAGE.
FOUR UNDERWING ENGINES WIDE BODY	1 IN 15·9	1. WING STRUCTURAL DAMAGE. 2. FUSELAGE STRUCTURAL DAMAGE.

ALL TYPES - WORLDWIDE STATISTICS	APPROX. 1 IN 30	—

Figure 19. - Summary of BAC Assessments for Single 1/3 Disc Piece.

AN APPROXIMATION OF CRITICAL CRACK LENGTH FOR CATASTROPHIC CIRCUMFERENTIAL FUSELAGE DAMAGE IS GIVEN BY THE FOLLOWING, AND MAY BE USED FOR CRACKS OF UP TO 100 INCHES IN LENGTH.

$$\text{CRACK LENGTH } 2ac = \frac{2}{\pi}\left(\frac{1{\cdot}74\ Kc}{\sigma}\right)^2$$

WHERE Kc = FRACTURE TOUGHNESS OF SKIN MATL.

σ = NOMINAL AXIAL STRESS BEFORE DAMAGE UNDER CRITICAL LOADING CASE

Figure 20. - Catastrophic 1/3 Disc Fuselage Damage.

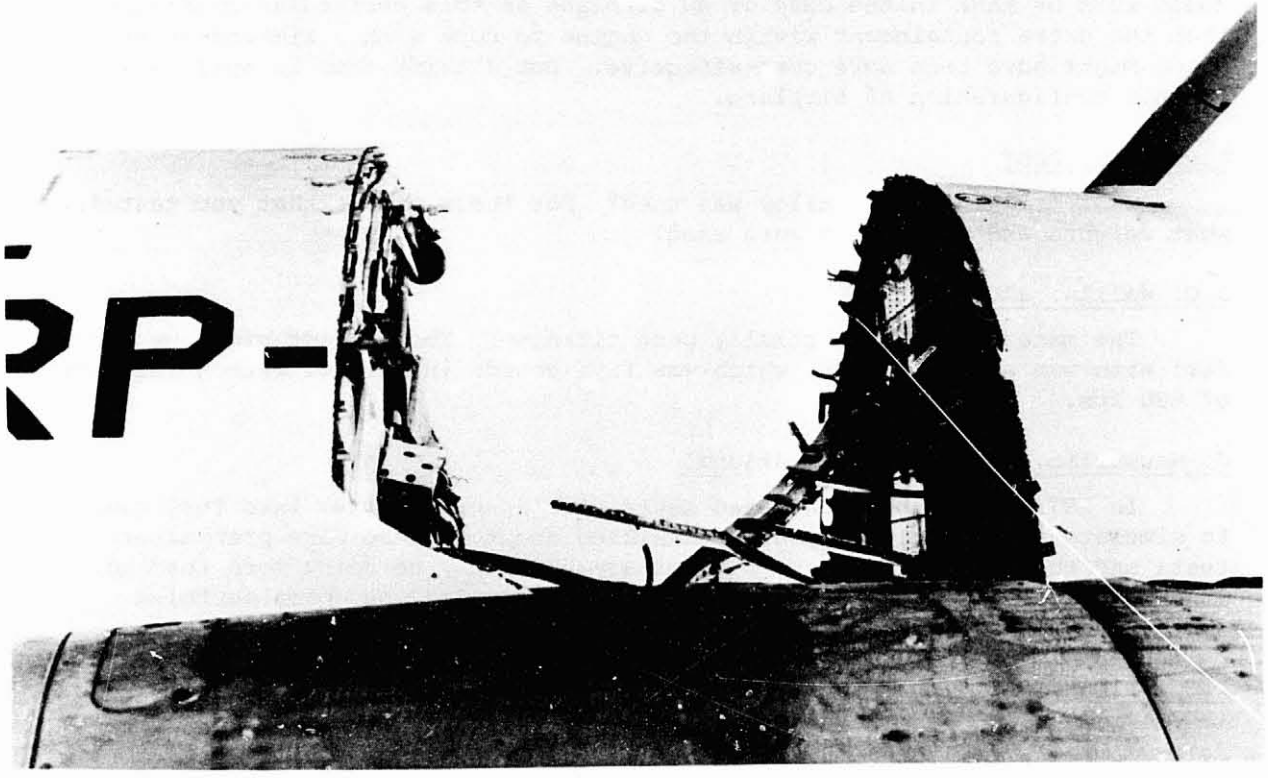

Figure 21. - Fuselage Damage - BAC 1-11.

John Meaney, Rohr

I have a question on the armor plate slide that you showed on the Concorde. What material is that and what total weight impact was it, and what was the largest energy magnitude that your're trying to absorb?

J.C. Wallin, BAC

The material was titanium. We looked at a number of different materials including non-metallics and so on, and found in the end that titanium was the lightest that we could use. For our testing the fragment that we dealt with was a full energy single blade which in the failure model was the equivalent (in energy terms) of a disk ring piece plus a couple of blades, (which having penetrated the casing, will have lost some energy).

From the point of view of armor design, the single blade was a critical piece because, of course, you had the highest impact pressure (acting on the small area). We designed on that criterion. The actual weight we added to the airplane was something of the order of a thousand pounds. I said earlier (when I was commenting on I think it was Ken Forney's talk this morning) it could well be that in the case of an airplane of this particular configuration that the extra containment within the engine to cope with a rim-and-three-blades piece might have been more cost-effective. But I think that is applicable only to this configuration of airplane.

J. Meaney, Rohr

What titanium metal alloy was used? For these pieces that you tested, what weights and velocities were used?

J.C. Wallin, BAC

The material is commercially pure titanium. The biggest piece we had to deal with was an LP 1 blade, which was five pounds in weight, with a velocity of 680 fps.

J. Gausselin, Rockwell International

In 1972 you people conducted tests, firing projectiles into fuel tanks, to simulate the fan blades you were talking about. These were preliminary tests and the conclusions were preliminary. You may be doing more testing. I haven't seen anything further in this program. Are you doing anything further and if so, where can the results be obtained?

J.C. Wallin, BAC

At the time we had to deal with the fuel tanks because we thought that blades being fired into fuel tanks (where the blade passed through the fuel before it got into the vapor space), was probably not a very high ignition risk. So we started doing these tests to try to generate some data to prove our case if you like. Now, in point of fact what we came up with was that

within the first six firings, we generated four explosions, due to titanium blades nicking structure. We had been looking at the prime ignition source as being the blade temperature. What we found was that when we fired the blade into a representative tank, as soon as the blade hit the structure inside the tank, even though it passed through the fuel in the first place, we actually generated sparks of sufficient magnitude to set off the explosion. At that point we abandoned our original line of thinking and, therefore, abandoned the tests. I think in that respect, even if we had been right in our original thinking, the cost of the testing we would have had to have done to prove our case would have been so high that we would probably have abandoned it anyway. This was because we would have needed to do it a thousand times or so with no ignition to prove the case statistically. Since we could, in fact, get explosions in the tank if titanium blades were being fired into it, we faced up to the facts and decided to develop our armor for the tanks.

One other thing that we found in general, both in the case of firing into tanks and also doing our armor testing, was that a lot of the information which you get from ballistic firings (typical of military projectiles) is totally irrelevant to the engine burst case where one is dealing with non-uniform shapes and sharp corners. With things of that sort, the results can be very different from those derived from bullet firings.

TYPES OF ROTOR FAILURE AND CHARACTERISTICS OF FRAGMENTS

D. McCarthy
Rolls-Royce Limited
Aero Division
Derby, United Kingdom

INTRODUCTION

There are three obvious ways of reducing the hazard of non-contained engine failure. One is to find ways of preventing the types of failure that lead to non-containment, another is to make the engine casings strong enough to prevent the release of high-energy debris, at least in harmful directions, and a third is to design the aircraft in such a way that the probability of high-energy debris creating a hazard is acceptably low.

The prevention of primary failure, particularly of the type that may escalate to non-containment has always been a natural aim in engine design and development and it will continue to be so. Prevention of non-containment by providing engine casings strong enough to contain the highest energy fragments would require an increase in engine weight that is generally regarded as quite unacceptable and would create problems of thermal lag in the casings and substantially increased loads in the engine mountings. Limited strengthening of casings, especially local strengthening designed to prevent the release of debris in harmful directions, might offer some advantage provided that containing larger or more numerous bodies did not cause greater problems downstream.

The remaining action open to the engine manufacturer is to provide the aircraft designer with the most accurate information available upon the probability of non-contained failure and upon the type of debris a given engine is capable of releasing. This information can be taken into account, along with all other constraints, when the positioning of engines and the location of vital services are being determined for a new aircraft. In the case of established aircraft, a re-appraisal of current precautions against non-containment can be conducted with a view to making any adjustments that might improve on the current level of safety.

In this presentation I propose to concentrate upon the types of non-contained rotor failure experienced in U.K. engines and upon the characteristics of fragments released, including their size, shape, weight, velocity, energy and direction. Developments in the prevention

of rotor failure and in the technique of containment or deflection of fragments comes up for discussion later at this meeting, therefore they are not included here.

SAFETY RECORD

Although non-contained failures account for only a small proportion of aircraft accidents, their spectacular nature makes non-containment an emotive subject. Anyone who has been near a turbine engine when it has produced a non-contained failure will know why. It is an alarming experience. The explosive release of energy appears to have enormous destructive potential. Yet in nearly all cases of non-contained engine failure in commercial service the aircraft landed safety and no one was hurt.

This record is partly due to aircraft/engine layout geometry which, to varying degrees in different aircraft types, minimises the chances of a fragment from the engine striking a vulnerable part of the aircraft. It is also partly due to the ability of the aircraft to withstand the impact or to deal with the consequences of any damage caused by the impact in all but the most serious cases. Less than one non-containment in 10 has caused injuries or affected the airworthiness of the aircraft. This is in 146 million hours of service operation.

To put the part played by non-containment in aircraft accidents into perspective for U.K. engined aircraft, FIG.1 lists the known causes of

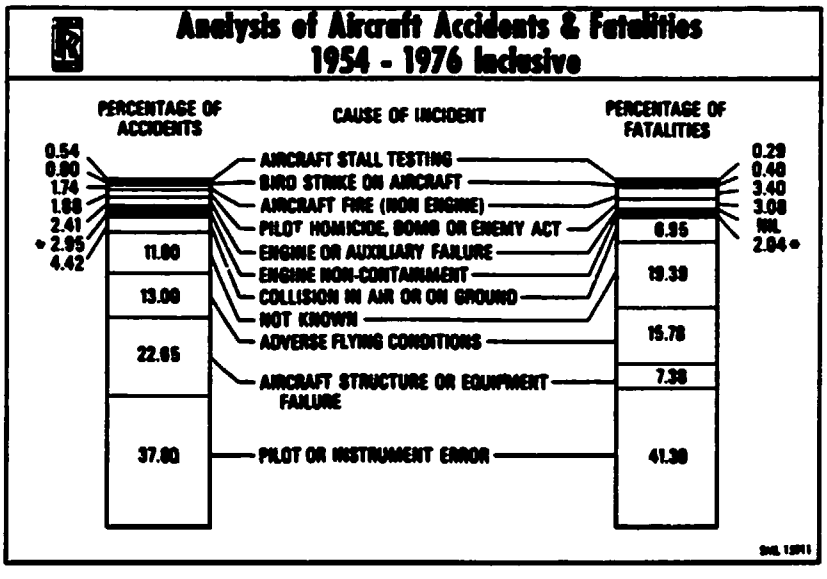

FIG.1

aircraft accidents (defined as involving damage to wing, fuselage or vital services) expressed in the left hand column as a percentage of total accidents and in the right hand column as a percentage of total fatalities. It illustrates that non-contained engine failure accounted for 2.95% of accidents and 2.04% of fatalities from the beginning of commercial flying to the end of 1976. These are not large numbers but it is clear that research and development to eliminate non-containment or to minimise its effect must continue at high priority.

FAILURE RATE

In a machine based upon high energy rotating masses carried inside relatively lightweight casings, a degree of risk of non-contained failure is bound to exist. The level of that risk does not appear to have changed very much since the early days of gas turbine flight. FIG.2 illustrates that during the initial three years of gas turbine

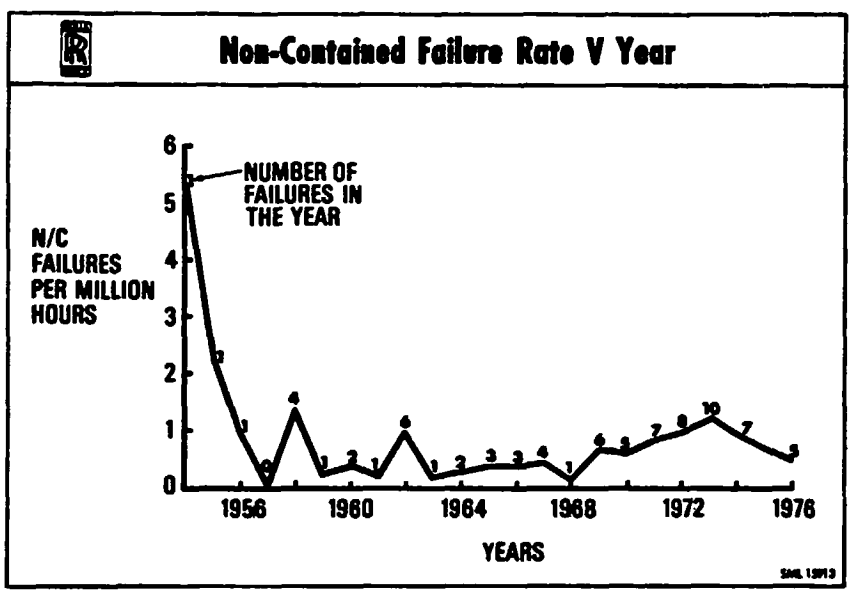

FIG.2

operation there was one Category D (i.e. not contained within engine or cowling) failure per year. The rate looks high because the running time was low. Thereafter the rate was generally below 0.5 per million engine hours. In spite of the progressive elimination of the causes

of earlier non-containments, engines continued to find new ways of producing non-contained failure. The hump in the curve in the 1969 to 1973 period was not due to the introduction of new engines, it was the result of a crop of new modes of failure appearing on long-established engines.

It would be unrealistic to expect the rate of non-contained failure to be appreciably better than 0.5 per million hours in the foreseeable future, the constant demand for higher engine efficiency and reduction in weight involves increasingly arduous engine conditions and the development of new materials without any substantial background of service experience. These factors tend to offset the benefits derived from the elimination of the causes of past non-contained failures. Further, it should be remembered that the figure of 0.5 is an average for all engines and there could be considerable variations in the rate between different engine types.

TYPES OF ROTOR FAILURE

In this presentation we are concerned with the fragments released by engines when non-contained engine failure occurs, rather than with the causes of failure, and for this purpose the types of rotor failure, as affecting the shape of fragment, can be divided into three categories.

1. Low cycle fatigue (LCF)

2. LCF with superimposed high cycle fatigue (HCF)

3. Failure due to overheating and/or overspeeding

LOW CYCLE FATIGUE

Cracks which propagate to eventual failure at a rate related to flight cycles and not to total running time are categorised as LCF failures. The resulting fracture surfaces can be expected to exhibit fatigue striations indicating an extension of the crack for each flight cycle after crack initiation. For the purpose of this study the category includes LCF failures initiated by defects in material, manufacture or assembly, as well as those that occurred where no such defects existed.

FIG.3 shows the types of rotor failure known to have been caused predominantly in LCF. Diagram A shows a failure from an origin in the

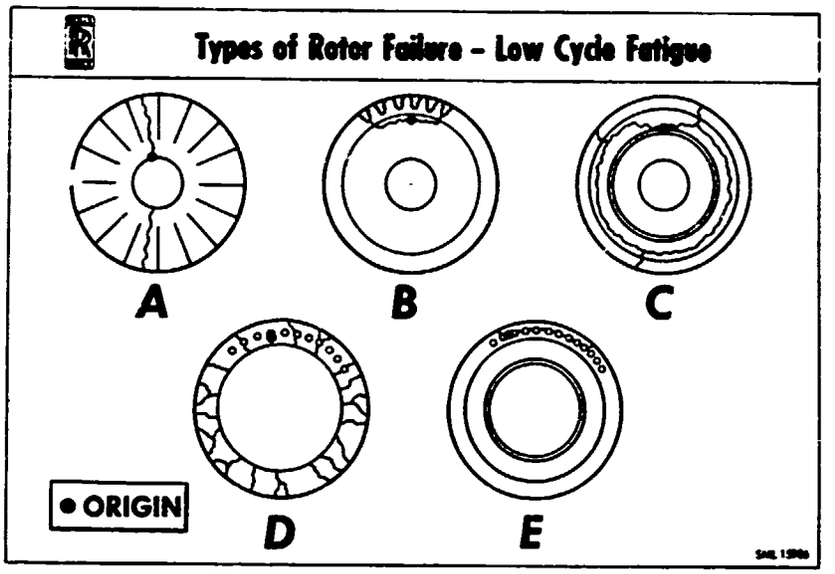

FIG.3

hub of a disc. This mode of failure, which can release the most potentially destructive fragment an engine is capable of producing, is fortunately extremely rare because the cyclic life of a given disc can be predicted with reasonable accuracy in terms of disc bore life, when based upon calculation and the results of rig and engine cyclic tests carried out at appropriate levels of stress in the disc bore. Occasionally a disc has failed from the hub in service but all such failures have been traced to defects in the disc material or processing.

The measures taken to eliminate them make similar problems less likely to occur in the future. But it is impossible to guarantee that there will never be another failure from a disc hub.

Diagrams B and C illustrate LCF failures from an origin in the disc diaphragm. This failure can be initiated in a region of high radial stress when some additional factor has increased the stress beyond a tolerable level. For example, natural concentration of stress in a disc neck can be unacceptably increased by the presence of machining

marks or handling damage or by the unintentional axial displacement of the disc hub relative to the rim. As a result, a crack may initiate and develop into the disc rim (Diagram B) or propagate right round the disc to release the entire disc rim either in one piece or in series of lengths (Diagram C).

Diagram D is a type of failure of which only one has occurred. A compressor drum carrying pin-fixed blades cracked from an origin in the bore of a pin hole. The crack ran into the bore of the drum which proceeded to break-up into a large number of pieces.

Diagram E shows a type of LCF failure experienced on discs with pin-fixed blades. Cracks propagated from hole to hole in one of the two flanges on the disc rim eventually releasing blades and a local piece of disc flange.

LCF WITH SUPERIMPOSED HCF

Under engine conditions all rotor discs are subject to some degree of alternating stress superimposed upon the speed-related steady stress. The steady stress is reasonably predictable but the level of alternating stress has to be arbitarily assumed at the design stage on the basis of previous experience and measurement on other discs. Its level depends upon the dynamic characteristics of the bladed disc and the likely magnitude and frequency of the exciting forces. When alternating stresses are low enough for the cycles to failure to be related only to flight cycles, the failure mode is labelled LCF. When the superimposed alternating stresses are high enough to propagate fatigue cracks at a rate related only to the number of alternating cycles, it is a case of HCF. But this is an over simplification because both LCF and HCF play a part in most disc fatigue failures, one or the other being predominant during the whole or part of the crack propagation process. FIG.4 Diagram F shows an early alum centrifugal impeller with a fatigue origin in a region of high alternating stress created by a vibration mode in the impeller. The 'striation count' method of inspecting fractures had not been developed at the time but it is likely that, as the crack propagated inward, the initial predominance of HCF was superseded by LCF as the crack moved into the hub region which is little affected

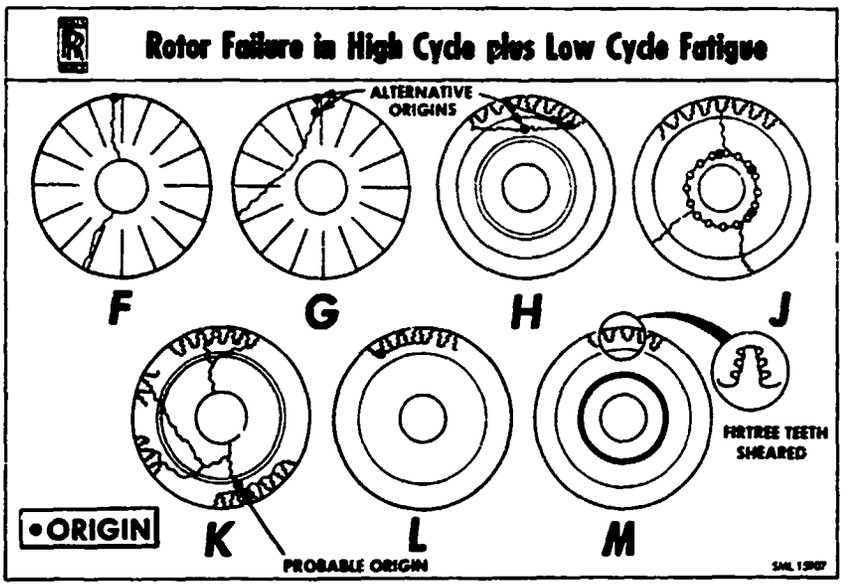

FIG.4

by impeller vibration but is subject to a high steady hoop stress. The crack proceeded to propagate into the bore, to release a large sector of the impeller.

Diagram G illustrates an impeller failure initiated in a similar way but in this case the crack turned circumferentially under the influence of low cycle radial stress combined with the high cycle bending stress arising from the impeller vibration mode. The crack eventually ran outwards and released a relatively light piece of disc, compared with the previous case. Similar cracks developed in compressor and turbine discs with dovetail or firtree fixings (Diagram H).

Diagram J shows a more serious type of failure, predominantly in HCF. Cracks initiated in the ring of holes in the disc hub, run around their pitch circle and radially outwards through the disc rim, releasing three large sectors of disc but leaving the hub, inboard of the holes, in position in the engine. This failure and other similar less severe failures occurred when the wake created by local blockage of nozzle guide vanes excited diametral-mode resonance in the bladed disc. Similar vibration can be caused by the disturbance created when a nozzle guide

vane is missing, or when a fuel burner becomes blocked, or even when a local rub occurs, say an axial rub on the blade tip shroud, and such failures may release a substantial piece of disc. The cure is to design low diametral mode resonances out of the running range because disc failures in such modes tend to release large fragments. Disc failures in higher diametral modes, say 5D and over tend to release much smaller fragments and they are also more difficult to excite.

Another way in which high levels of alternating stress have been generated in discs is the repeated deflection of a bladed disc in an umbrella mode due to engine surge. Each surge causes a cycle of stress unrelated to flight cycles by contributing to the accumulation of fatigue. The result can be the detachment of the disc rim resulting in the release of pieces of disc rim with blades, as in the case of LCF failure in the disc neck.

Diagram K shows a turbine disc nearing time-expiry which was judged to have been exposed to a degree of high-cycle alternating stress for a long period due to a minor blade vibration problem. Fatigue cracks perdominantly in LCF but with indications of superimposed HCF, developed in the bottom of a large number of disc grooves. Disc failure occurred shortly before the full service life of the disc had been achieved. One of the cracks propagated inwards far enough to become critical and the disc broke into six pieces, the largest fragment being almost half a disc.

Diagram L is an example of disc failure in blade-excited fatigue in which a group of disc lobes failed in the neck and released the lobes together with the corresponding group of blades. Diagram M shows a case in which firtree teeth on the disc failed and released blades. In both types of failure the largest fragment likely to be released by the engine is a single complete blade.

DISC FAILURE DUE TO OVERHEATING (FIG.5)

Three types of disc failure have occurred as a result of loss of material properties due to overheating. The causes were:-

(a) Loss of cooling air

(b) Rub against a static part

(c) Internal oil fire

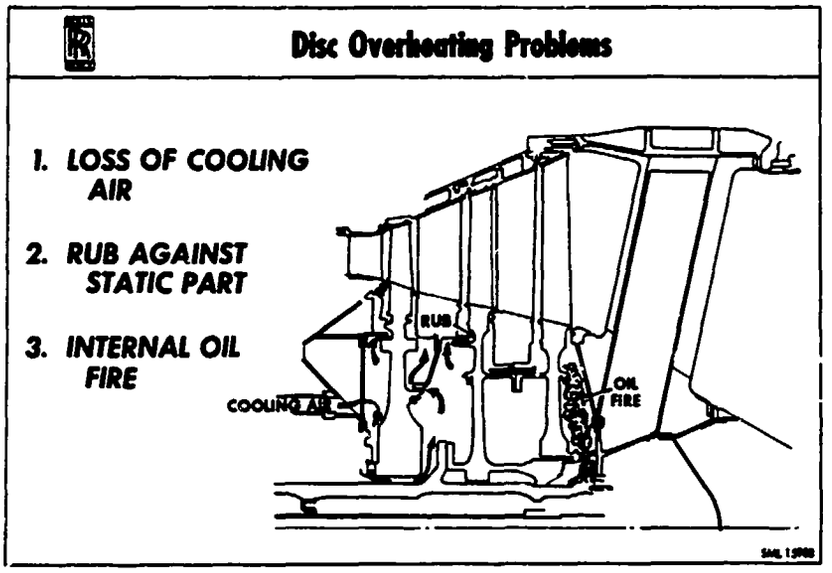

FIG.5

Disc failures under these headings have occurred only in turbines. Turbine discs in UK engines are traditionally cooled by enveloping them in cool air which exhausts into the gas annulus fore and aft of the disc. It has the dual purpose of cooling the discs and of preventing the ingress of hot gas into spaces surrounding them. On rare occasions this system has been disrupted by loss of cooling air pressure, in a typical case due to the failure of an external cooling air supply pipe and in another due to the loss of interstage seals following turbine blade failure. In both cases the result is overheating of the disc due to the inflow of hot gas into spaces adjacent to it. The form of failure depends upon the design of disc and blades. In some cases the overheated disc stretches and releases all its blades and the largest fragments released are single complete blades. In other cases the disc fails first in the neck, releasing the disc rim with blades attached and the largest fragments are pieces of disc rim with blades. The latter failure is much more serious, in terms of the

likely energy of the largest fragment released, than the loss of blades alone, the fragments being capable of cutting through the engine casings throughout the entire circumference of the engine and proceeding to inflict heavy damage on any aircraft parts in the line of flight.

Disc failures due to axial rubs were typically rubs between the disc diaphragm and a stationary component such as a static seal. This causes overheating of the diaphragm at the seal diameter and the release of the portion of the disc outboard of the rub which includes the entire disc rim and some of the diaphragm. The result is similar to the previous case.

The third cause of overheating, the oil fire, again results in stretching of the disc which either releases the blades or fails in the diaphragm.

MULTIPLE BLADE RELEASE (FIG.6)

In addition to disc overheating, multiple turbine blade release has been brought about in two other ways -

(a) Shelling-out of blades

(b) Overspeed of turbine

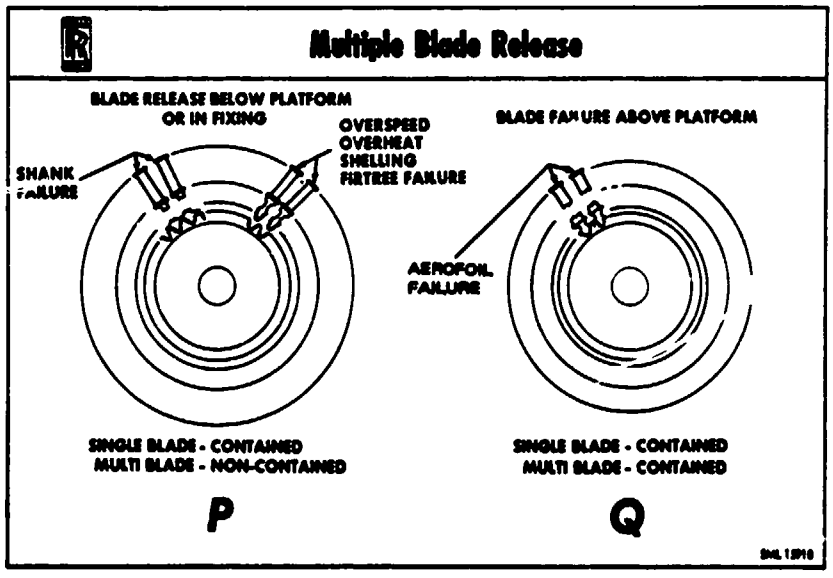

FIG.6

If sufficient tangential force be applied to a blade it will bend over or break, or it will be wrenched out of its fixing. The result depending upon the relative strengths of blade and fixing. In some cases the fixing will fail first so that an obstruction in the blade path or a heavy rub against adjacent vanes will cause the complete row of blades to shell out of a disc. If such a failure be non-contained the largest single fragments to be released by the engine are likely to be single complete blades.

In the event of turbine overspeed to failure the result is that either the disc bursts, probably from the bore, or it stretches sufficiently to release its blades. The outcome depends upon factors such as the ductility of the disc material, the fineness of the firtree teeth and the stress distribution in the disc. Clearly, the release of the blades is preferable to the disc burst in terms of the destructive potential of the fragments released, but multiple blade release provides the greater probability of striking any vulnerable aircraft item in the general plane of the rotor.

The requirement that engine casings shall be capable of containing a single blade released from immediately above its fixing, determines the minimum strength required in the casings. If the casings just meet this requirement we would not expect two adjacent blades released together to be contained but we might expect two blades 180° apart, and perhaps four or more blades, 90° or less apart, released simultaneously, to be contained up to the point where the bulge in the

casing caused by one blade did not encroach upon the bulge created by the next. The energy of a contained blade is used up in stretching and bulging the casing and if a second blade attempts to use up energy in the same bulge the casing is likely to fail. In virtually every case of multiple turbine blade release from below the platform the blades have been non-contained, even where casings have been substantially thicker than the minimum required for single blade containment because of structural or pressure requirements. Multiple blades released from above the platform, in the aerofoil, normally have been contained, presumably because of their light weight compared with complete blades. It would be useful to know how strong a casing would have to be to contain the multiple release of complete blades.

The release of all blades from a disc does not normally result in their emerging uniformly from the engine in 'Catherine Wheel' style but rather in the release of groups of blades through random arcs of casing, typically as shown in FIG.7, presumably because the first blades to

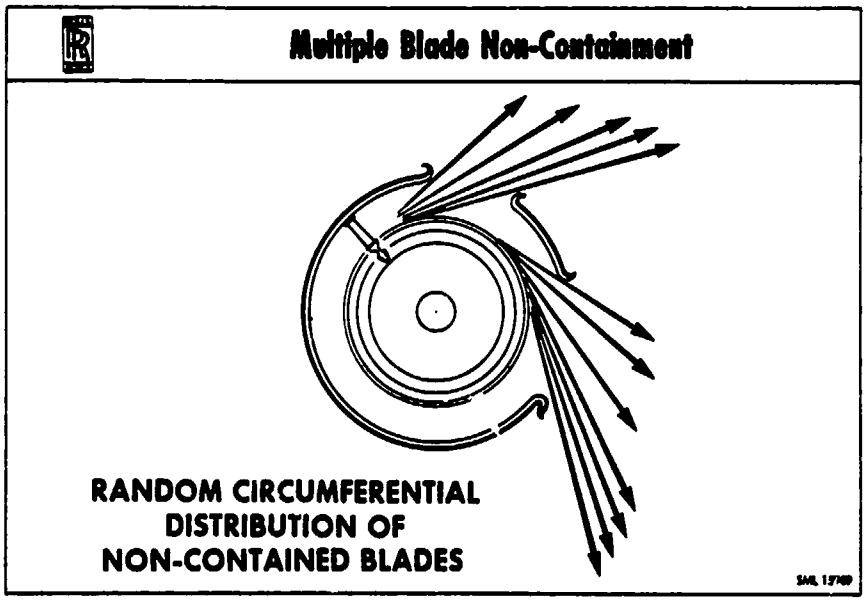

FIG.7

touch the casing tend to interfere with following blades. The result, from the aircraft point of view, is that the assumption must be made that the engine may throw complete blades either singly or in groups, and a number of impacts may occur almost simultaneously within a small target area.

CHARACTERISTICS OF ROTOR FRAGMENTS

At an early stage in the evolution of the design of a new engine the approximate diameters, speeds and weights of compressor and turbine rotors can be defined. From the information generated by all non-containment incidents, these three parameters can be used to predict the range of fragments the new engine could conceivably release, including weight, size, shape, velocity and direction, together with the probability of release of given fragments. The prediction should give the aircraft designer the best chance of minimising the possible effect of non-containment upon aircraft safety.

An analysis of all UK engine failures not contained within engine casings or cowlings, since turbine engine flying began in 1953 is given below.

SHAPE OF FRAGMENT

Diagram R in FIG.8 shows the shape of fragments released when a compressor

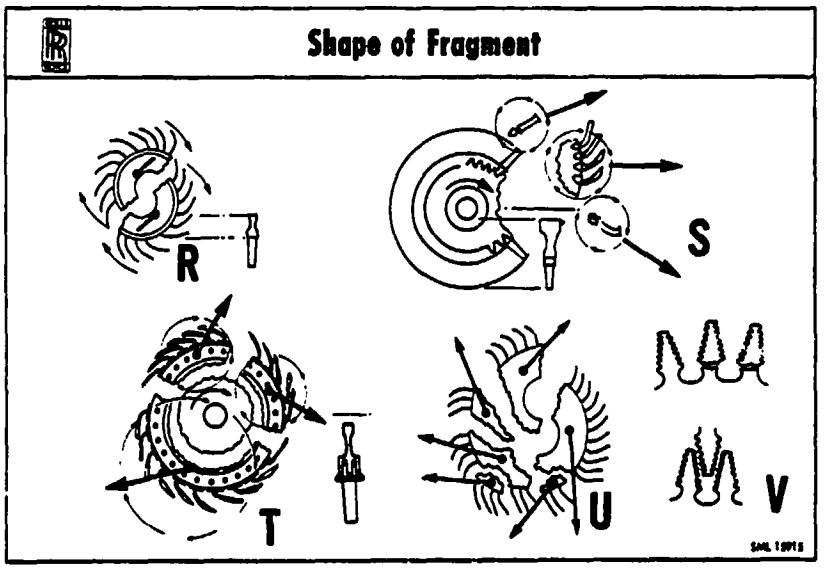

FIG.8

disc fails through the bore. It could equally well be a turbine disc. The origin of failure might be anywhere along the line of fracture in the fatigue case or it might be from the bore in the overspeed case. Two sectors of rotor are released with very high energy, capable of slicing through almost any aircraft structure in their path, each rotating about its own c of g and travelling along a line tangential to the circle described by its c of g before release.

Diagram S shows a failure where the fragment released comprises a group of blades held in a piece of disc, additional separate blades are released at the same time. This type of failure is likely to be the result of low or high cycle fatigue or a combination of both. The fragment again rotates about its own c of g and travels along the appropriate tangential line. It has a much less energy than a half disc and it may strike its target in any attitude probably the most damaging being when a jagged piece of disc rather than the relatively flexible blades, make first contact.

Diagram T shows the case where the complete rim of a disc is released in a number of lengths. This type of failure can be the result of fatigue cracks in the diaphragm propagating circumferentially right round the disc. A failure with similar results is the circumferential failure of a disc diaphragm due to overheating caused by a local rub on the diaphragm say by a static air seal or due to general overheating due to loss of disc cooling air. This type of failure can cut an engine in half in the case of a disc with a heavy rim section. But rims of light section, when released from discs, have often been contained by the casings, notably in the case of H.P. compressor disc rims. In other incidents the rim has penetrated the casing locally and unwrapped itself to emerge from the engine in a straight line, like a spear.

Diagram U shows the fatigue break up of a disc into a number of irregular fragments. This type of failure has been observed particularly in the case of discs reaching the end of their fatigue life. It presents some formidable fragments, distributed around the engine.

Diagram V shows other types of fatigue failures in blade fixings, including failure through the firtree neck and failure of the firtree

teeth. These failures release one or more blades which may or may not be contained, but the largest fragment released is a single blade.

The failure of a turbine disc due to overspeed, say due to shaft failure, will produce a type of failure dependent upon the disc design. In some cases the disc will fail from the bore and release sectors at higher velocity than the normal maximum but in most engines the design aim is to release blades rather than allow the disc to fail in the ultimate overspeed case.

SIZE OF FRAGMENT

With regard to the size of fragments, the maximum dimension of a missile affects the probability of its striking a given part of the aircraft and an analysis of fragment sizes has been carried out.

FIG.9 shows a breakdown of all non-containments in terms of number of

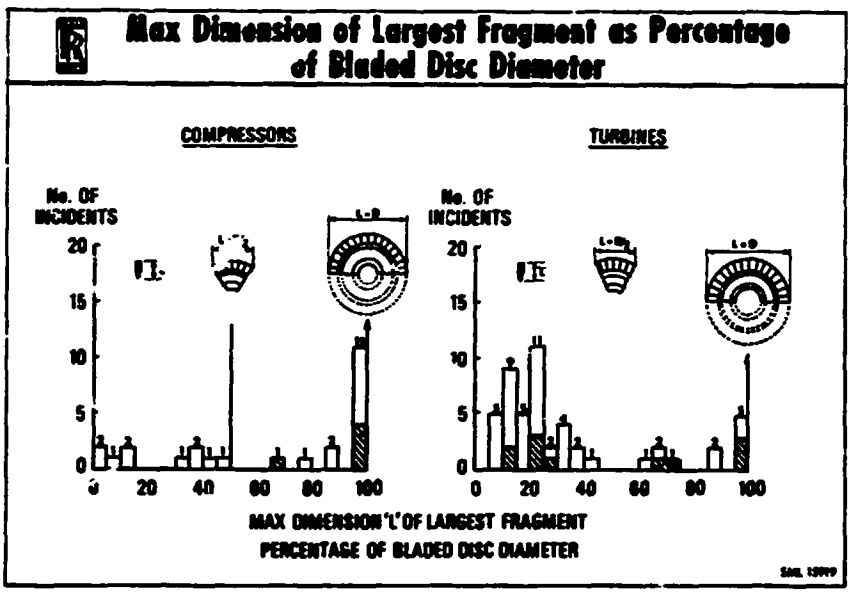

FIG.9

incidents against the maximum dimensions of the largest fragment expressed as a percentage of the bladed disc diameter, ignoring the effect of bent-over blades which is unpredictable. Compressors and turbines are shown separately. It can be seen that for compressors,

fragments with a maximum dimension equal to the overall diameter of the bladed disc, i.e. a half-disc and above, less the effect of bent blades, tend to predominate. The shaded areas in the figure show the incidents that caused injuries or affected the airworthiness of aircraft. Not surprisingly the large fragments did the most damage, not the least because, in the case of compressors, large fragments were released more frequently than small ones.

In the case of turbines, about twice as many non-containments overall have occurred (although in recent years compressors and turbines have produced approximately equal numbers of non-containments) and the tendency has been for turbines to release small fragments more often than large. The small pieces include single blades or part blades or small pieces of disc with blades attached.

Clearly, large fragments are more likely to damage the aircraft and, based upon the limited number of incidents for which fragment sizes are known, this tendency is confirmed. But small fragments have been released in far more incidents than large and they have caused service aircraft problems in a greater total number of cases.

WEIGHT OF FRAGMENT

FIG.10 shows the number of incidents in which the heaviest fragment

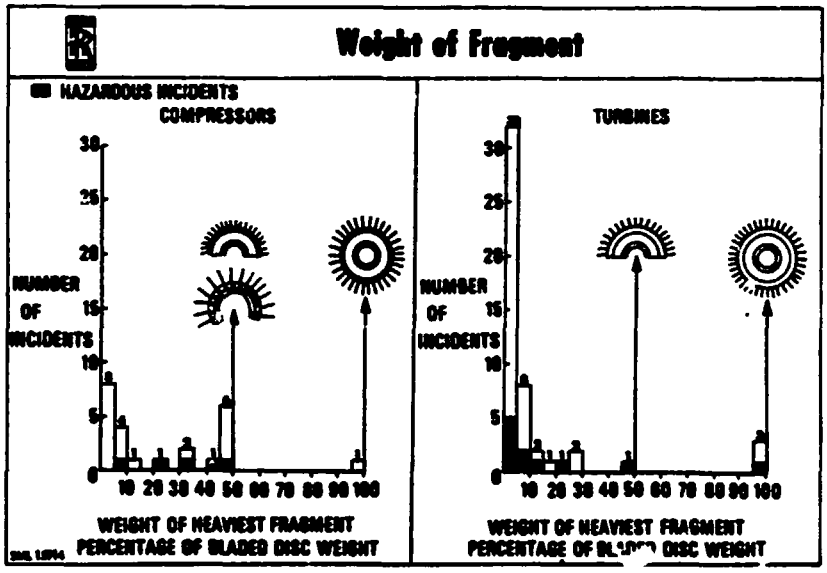

FIG.10

released was a given percentage of the bladed disc weight. The weights are taken in 5% steps. The heaviest fragment is chosen because it has the greatest destructive potential of all the fragments released in a given incident. In this plot the heaviest fragment in a non-containment in which all the blades in a disc are released, is taken as a single blade.

The shaded areas show the number of incidents in which injuries were caused or the airworthiness of the aircraft was affected. In the case of compressors the release of fragments weighing up to 5% of the bladed disc weight was not, in this experience, responsible for creating any hazard. Incidents involving the release of heavier fragments weighing more than 5% of bladed disc, proved to be hardous or non-hazardous in a random way, probably because the aircraft/engine layouts provide favourable odds against single heavy fragments striking a vital part of the aircraft.

In the case of turbines, of the total of 50 incidents in which the weight of fragments released is recorded, 32 involved the release of fragments weighing not more than 5% of their bladed disc weight and 5 of the 32 caused sufficient damage to affect the airworthiness of the aircraft. Larger fragments in the range 10 to 50% of the bladed disc weight appear in only 7 incidents but, as might be expected with larger fragments, they proved more likely than small fragments to affect airworthiness and this they did in 3 of the 7 incidents. Looking more closely at the manner in which the aircraft was affected in these events we find that the incidents involving the release of fragments weighing no more than 5% of the bladed disc weight were all cases of multiple blade release, two causing damage to aircraft hydraulics, one damaging an adjacent engine, one starting an extensive fire and one causing cabin depressurisation. In the case where the heaviest fragment released weighed 50% of the bladed disc the result was penetration of the fuselage and of a wing tank causing a fire. In one case of full disc release the pressure hull was punctured and an adjacent engine was damaged but in the other two cases damage was not serious.

On this evidence heavy fragments present an occasional serious threat and lighter fragments present a less serious but more frequent threat capable of causing enough damage to create an aircraft hazard in some cases. This experience involves some of the older aircraft and the results might be different with later designs, but it shows that there are two vital factors affecting airworthiness in the non-containment case, the first is the aircraft/engine layout and the way it affects the probability of damage to vital parts of the aircraft and the second is the number of fragments released in a non-contained failure. Clearly there is a need to pay a lot more attention to the problem of multiple blade release.

VELOCITY OF FRAGMENT

In designing armour or deflectors to provide protection against missiles, it is important to have some knowledge of the likely approach velocity of the missile as this will determine the type of armour or deflector required. FIG.11 gives the maximum rim speeds of rotors in UK engines.

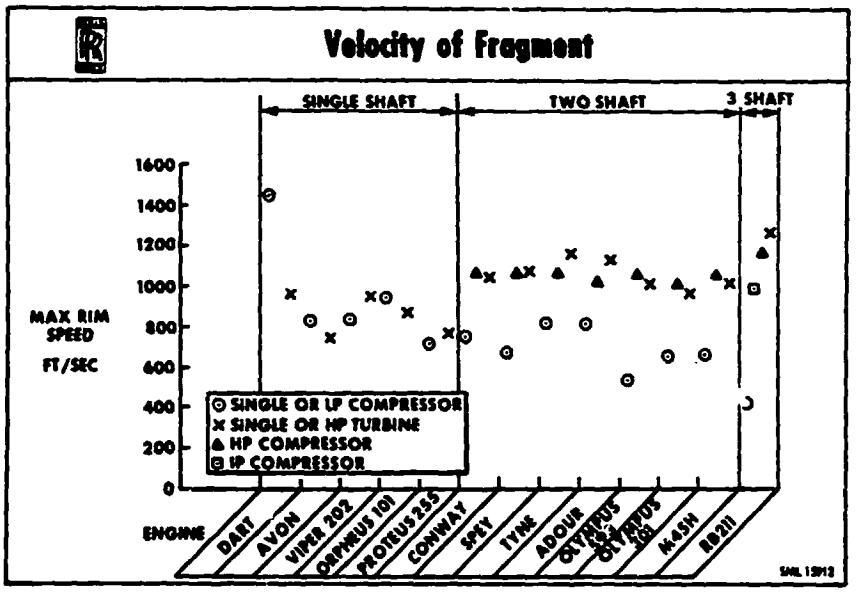

FIG.11

Rim speeds were chosen because a fragment is released at approximately the tangential velocity of its centre of gravity at the instant of

release and the centre of gravity of a rim piece with blades attached is likely to be near the radius of the rim and travelling at rim speed. Corrections can be made for fragments with centres of gravity at smaller or larger radii. Note that the velocities lie between about 400 and 1300 ft/sec. which is within the range that can be stopped or deflected by conventional armour like steel or titanium plate, and does not require the more exotic armour developed against missiles with much higher approach velocities. It will be shown later that non-contained fragments weighing above about 6% of the bladed disc weight are likely to emerge from an engine with a tangential velocity equal to the tangential velocity of the c of g of the fragment at the instant of release from the disc.

ENERGY OF FRAGMENT (FIG.12)

A fragment released from a rotor has kinetic energy along its line of flight plus rotational energy about its own c of g. Plotting the

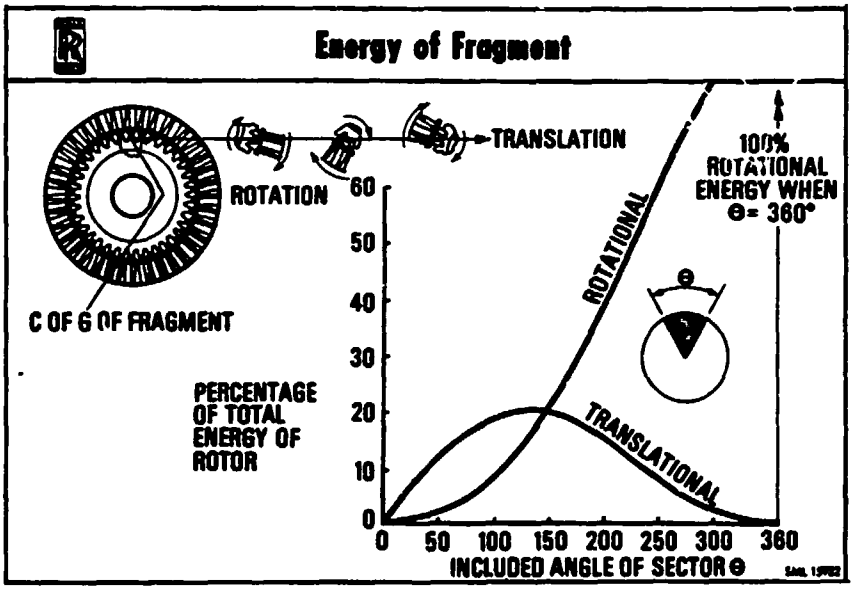

FIG.12

translational and rotational components of energy for a disc sector against the included angle of the sector shows that translational energy reaches a peak when the sector angle is about 134°. But the rotational

energy increased with sector angle until at 360° we have a full disc with all its energy in rotation and none in translation.

Engine experience and tests on armour and deflectors used against rotor fragments show that translational energy is the more important factor in the case of fragments comprising up to four blades and a piece of disc. Rotational energy may have a greater effect in the case of large fragments involving half a disc or more but this has yet to be established by test. Another point to note about the shape of the curve of translational energy is that any sector angle between 90° and 180° has energy within 10% of the maximum. Evidently a fragment of near-maximum translational energy would be produced if a rotor released anything between a quarter and a half of a disc.

In passing through an engine casing, a fragment uses up energy in damaging itself and the casing. Recent containment tests in which representative fragments were released from a rotating arm inside an engine casing showed that a fragment with an energy level just beyond the containment capability of the casing lost 90% of its translational energy in getting through the casing. But when a portion of rotor, comprising four blades and a piece of disc weighing 6.5% of the bladed-disc weight, was released inside a casing designed to contain a single blade, the fragment passed through the casing without measurable loss of translational energy. It was thought at the time that the energy expended by the fragment in bursting through the casing was too small to be measured in terms of fragment velocity before and after penetration. But on further study of high-speed films of the fragment passing through the casing, it was observed that although no translational energy was lost there was a 10% to 20% loss of rotational energy and this would account for the energy used up in damaging the fragment and the casing. There is no evidence that this loss of rotational energy would reduce potential damage to the aircraft.

It is notable that when complete discs were released, usually as a result of heavy unbalance due to blade or other failure, in the majority of cases no serious aircraft damage was sustained. Any disc released with virtually all its energy in rotation is unlikely to develop more than a small amount of translational energy, say by being thrown sideways by

friction between rotor and static parts. The main danger of a free disc is its ability to act as a cutter, capable of severing vital services in its path.

DEFLECTION OF FRAGMENTS BY CASING

When a fragment passes through an engine casing it tends to be deflected from its path. The deflection is equally likely to be in an axial or in a circumferential direction as shown in FIG.13. Observations of

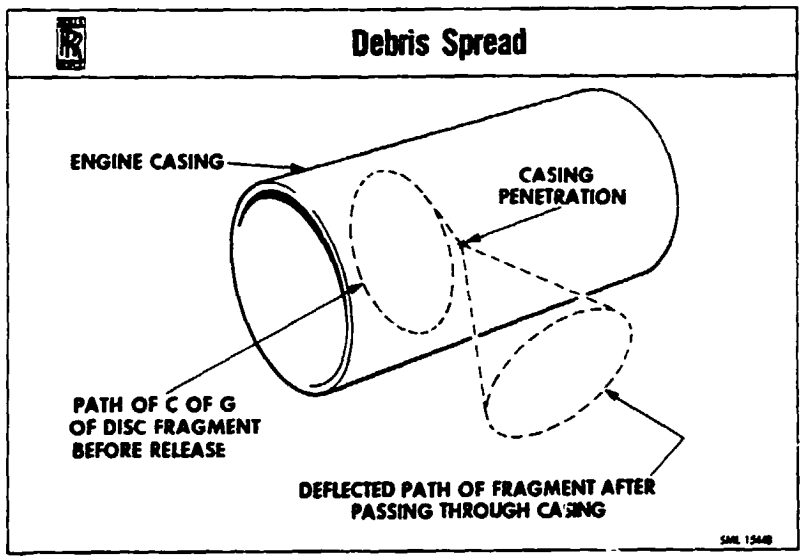

FIG.13

damage to surroundings caused by actual non-containment incidents show that heavy fragments tend to remain within $\pm 5^{o}$ of the plane of the rotor FIG.14. Much greater deflections have been recorded with lighter

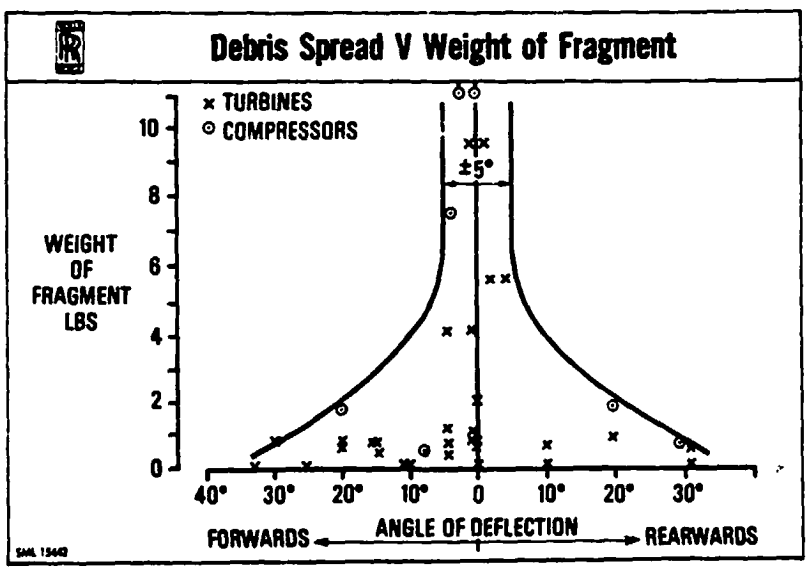

FIG.14

fragments but those deflected by more than 33° appear to have lost virtually all their energy.

If we assume that in striking the casing, a fragment loses the component of velocity perpendicular to its final line of flight, this does not wholly account for the loss of translational energy observed in practice when deflection exceeds 33°. There must be another factor and this is likely to be the decelerating impulse induced by friction between fragment and casing. We can derive this frictional factor from the knowledge that the final velocity is virtually zero when deflection exceeds 33°. FIG.15 shows the translational energy of fragments for

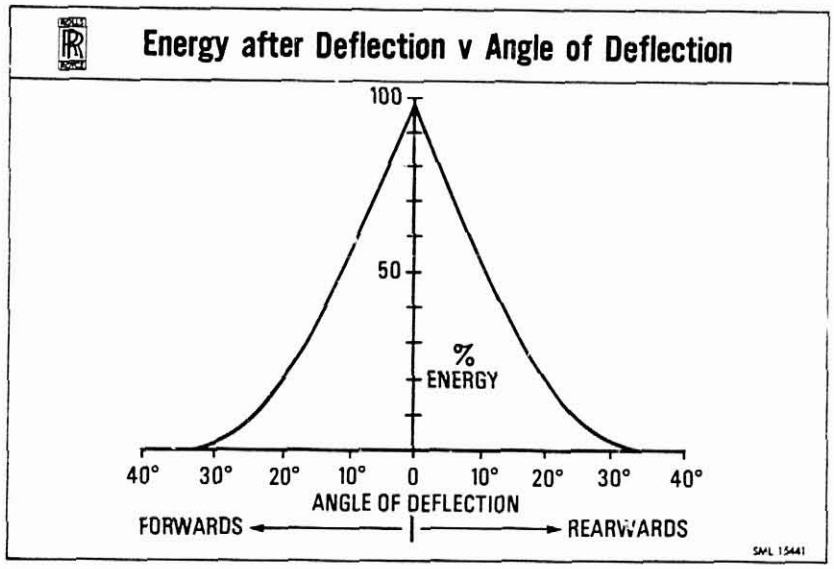

FIG.15

various degrees of deflection derived in this way. From the aircraft point of view the potential spread of debris is as shown in FIG.16.

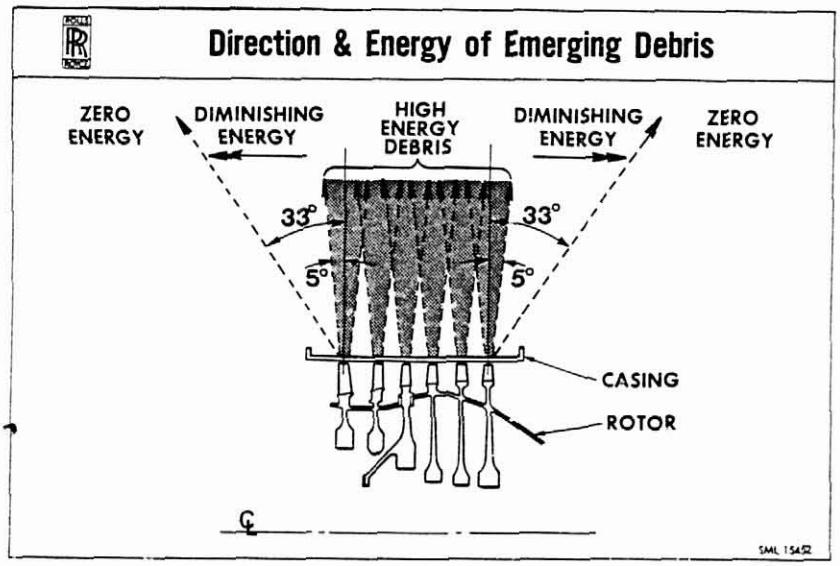

FIG.16

The distribution of energy can be established for a given engine. High energy fragments emerge within $\pm 5^{\circ}$ of the plane of the rotor, fragments deflected beyond 5° have energy that diminishes with angle of deflection and fragments deflected by more than 33° have zero energy.

SUMMARY AND CONCLUSIONS

1. The rate of non-contained engine failure in UK engined aircraft has remained sensibly constant at 0.3 per million engine hours for the past 20 years. The progressive elimination of tangible causes of non-containment has been offset by the development of new modes of failure. To reduce the rate of non-contained failure, or even to hold it down to the present level, requires work on the prevention of rotor failure to be continued at high priority. In addition, research and development in the field of containment of high-energy debris should continue to be pushed ahead and measures taken in aircraft design to minimise the hazard of non-containment should begin to reflect a more complete knowledge of the characteristics of fragments likely to be released by a given engine.

2. Types of rotor failure leading to non-containment include low and high cycle fatigue, disc material and processing defects, disc overheating due to rubs or loss of cooling air and disc over-speeding due to shaft failure or engine overspeed. It is not possible to guarantee the permanent elimination of them all.

3. Rotors are capable of breaking up in a wide variety of ways, producing non-contained debris ranging from maximum energy sectors to single blades or part blades. Complete discs have been released in some cases of shaft or bolt failure, sometimes precipitated by the primary failure of another rotor.

4. Large heavy fragments released by an engine are naturally more prone to damage the aircraft than small fragments and the damage tends to be more extensive. But small fragments are also capable of doing enough damage to create airworthiness problems, they are released more frequently than large fragments and because

of the greater number released per non-containment, the probability of impact on a vulnerable item in the aircraft is increased. Multiple blade release has proved to be particularly damaging and this type of non-containment calls for special attention.

5. The velocities at which engine fragments are released fall within the range that can be arrested or deflected by armour developed to provide protection against low velocity projectiles. There would be no advantage in using advanced armour developed for use against very high speed projectiles.

6. Large fragments, certainly those weighing over 6% of the bladed disc weight, tend escape from the engine without losing any of the translational velocity they possessed at the instant of their release from the disc. But they lose a small proportion of their rotational energy. Small fragments lose some translational energy in getting through the casing unless they escape through a previously created hole.

7. Large fragments tend to emerge from the casing within $\pm 5^{\circ}$ of the plane of the rotor but small fragments can be substantially deflected axially and circumferentially and they lose energy in the process. They appear to lose virtually all translational energy if deflected more than about 33°.

8. From these results the distribution of possible fragments and the energy with which they are likely to emerge from any given engine can be predicted with reasonable accuracy and used in assessing the threat to the aircraft.

ACKNOWLEDGEMENTS

I acknowledge the support of the Procurement Executive of the Ministry of Defence in the research work referred to in this Paper and thank colleagues at Rolls-Royce, both in Derby and in Bristol, who did the work and carried out much of the analysis.

DISCUSSION

H. Rubel, Lockheed-Georgia

Thank you for a very enlightening discussion. I have a question on the very last statement that you made with regard to multiple blade release and I wonder if the turbine blade release you referred to is associated with the retention of the turbine blade and not necessarily with the difference inherent between compressor and turbine. What I have in mind is your Fig. 6 -- how many of these cases, five, were category three and four (if I may use the SAE Ad Hoc Committee terminology) and were due to overspeed or overheat causing shelling of the fir tree because of the retention having small teeth? Specifically, in the designs discussed because the teeth were very fine, a slight overspeed causing yielding of the disk would permit the whole blade to come out. By the same token, if there were a fatigue failure and the retention was very fine, the impact from the failed blade could cause other blades to snap out or unlatch. Whereas, in America, we have gone to two or three fir trees and, normally, have a failure above the attachement in the first fir tree or airfoil. With this type of failure (similar to the compressor), energy is used up in breaking all the other blades. So, the question I raise is, do you really need to beef up the turbine case for multiple blade release or should we prevent the unlatching of the multiple blades?

D. McCarthy, Rolls-Royce

Our experience is that breaking up blades absorbs very little energy. We design blades so that in the event of a blade being bent over it will break in the shank or in the aerofoil before it breaks in the fir tree fixing. Some of our turbine discs are designed with fine fir tree teeth so that, in the event of overspeed, the disc releases its blades before bursting speed can be reached. This blade-release is achieved only after very substantial plastic growth of the disc, just short of ultimate failure. The situation is quite different under normal running conditions when the fir tree teeth are fully engaged and the difference between fine and coarse fir tree teeth is like the difference between fine and coarse screw threads.

Our reference to blade "shelling" in early engines covers cases where blades were successively wrenched out of their fixings by a tangential force, like shelling peas. Later blade fixing designs do not have this problem.

Turbines tend to release blades more frequently than do compressors because turbines are open to overspeeding or overheating whereas compressors, in general, are not.

H. Rubel, Lockheed-GA

Energy can be used up in breaking blades. Is it better to have blades break off before releasing? Should we put more weight into the aircraft to protect against multiple release or should we work on preventing multiple release?

D. McCarthy, Rolls-Royce

We should be doing both. There are some things the engine man can do to avoid known problems but he can never guarantee that non-containment has been entirely eliminated. The aircraft man should protect vulnerable items in his aircraft and he should not ignore small fragments.

In Mr. McCormick's paper the statistics showed that in a total of eleven serious (SAE definition) accidents, six were due to the release of disc sectors but no less than five others were due to impact from small fragments. I suggest that the aircraft man cannot afford to ignore the cases involving the release of small fragments.

S. Sattar, P&W

One question I had concerns fan blades. Could you comment on those designs where one has the same mode of failure below the platform at the dovetail where some designs tend to result in multiple blade loss failures and others don't? Have you in your studies come across some significant parameter (say there's something about a particular airfoil configuration or airfoil geometry) that makes one more prone to a multiple blade loss failure than others, assuming that both fail below the platform?

D. McCarthy, Rolls-Royce

We have experience of a fan blade failure in the root releasing the blade which leaned upon the adjacent following blade and caused it to fail in the fixing due to asymmetrical loading. The process did not go beyond the release of the two blades. The problem was overcome by strengthening the fir tree teeth and by improving the circumferential support of the blades at the platform. It was later demonstrated that a failed fan blade no longer dislodged its neighbour, nor any other blade in the rotor.

Alan Weaver, P&W

You showed fragment impact velocities between 400 and 1200 feet per second in your armor design work. Are these blade tip or disk rim velocities?

D. McCarthy, Rolls-Royce

Rim velocity is plotted because the centre of gravity of a rim-piece with blade attached is approximately at the rim radius. A factor could be used in the case of a fragment with a centre of gravity at a different radius.

J.C. Wallin, BAC

Damage depends on the way that engines actually can break up (or have broken up). From the point of view of the assessment methods that I was describing earlier, we consider one-third disk piece, or a piece of rim with a couple of blades. If we take blade shelling, the assessment would be the same as if you were using a one-third disk. Indeed, the one-third disk might be a bit over-pessimistic, so I don't think there's an inconsistency here. The one particular inconsistency that one sees is perhaps the question of the blades which will come out over a 33 degree fore and aft sector and which in the CAA model we don't take account of. Again, I think that one perhaps doesn't

have to take account of that because the energy gets lower as you move away from the five degrees. One hopes that there won't be single articles in the way of a single blade that could in fact lose the airplane. I'm quite sure that if we did Concorde over again today (and bear in mind we're talking about airframe design that's really fifteen years old) we would not put a flight control system in, where all three hydraulic systems came together at a single point. I'm sure my colleagues in the aircraft design industry would agree, we just wouldn't do that today. So in that case you don't really need to consider the single-blade effect because you wouldn't have single vulnerable articles.

D. McCarthy, Rolls-Royce

In the case of multiple blade release, some of the blades are deflected in passing through the engine casing. The likely spread of emerging debris has been indicated, together with the likely energy of the fragments. These factors affect the provision necessary in the aircraft. Beside affecting the extent of the target area, the amount of deflection given to a fragment may be important in determining the angle at which to mount a deflector to ensure that all fragments that strike it will be deflected in a harmless direction.

J.H. Gerstle, Boeing

Do you have any data on the range of residual velocities that the fragments have in the case of multiple releases?

D. McCarthy, Rolls-Royce

In the event of multiple blade release, the blades that first strike the casing can lose as much as 90% of their energy in penetrating the casing. The remaining blades tend to come out through the hole or holes created by the first impacts. A few blades may emerge with full energy, having come through the casing without touching it. But the majority will lose energy in sliding round inside the casing and the measured residual translational energy in these blades, when they emerge from the casing, is not more than 55% of their original energy.

J.H. Gerstle, Boeing

Would you suspect that the rotational energy lost would be a function of the fragment type -- that a rim fragment would lose a greater fraction of the rotational energy than a pie-shaped fragment?

D. McCarthy, Rolls-Royce

We have released a fragment consisting of four blades and a piece of disc from a rotor rotating at full speed inside a casing designed to contain a single blade. On that test we measured a zero loss of translational energy and a 10% to 20% loss of rotational energy in the fragment when it emerged from the casing. Presumably the rotational energy was absorbed in bending the blades and damaging the casing. We would expect the corresponding loss of rotational energy in the case of non-containment of a high energy disc sector to be proportionally less, because the casing has limited energy-absorbing capability.

In the case of a small fragment like a single blade, its rotational energy after release is unpredictable.

J.H. Gerstle, Boeing

I might just remark on a very slender piece of evidence that we have from some films taken at the Naval Air Propulsion Test Center involving impact against a Kevlar shield by a rotor disk burst with six equal-size fragments, the portions of rotational and translational energy loss were roughly comparable. This surprised us.

D. McCarthy, Rolls-Royce

Were you using a metal drum with a Kevlar wrapping?

J.H. Gerstle, Boeing

Yes.

D. McCarthy, Rolls-Royce

So the angles would be somewhat different from the case of going through a casing close to the blade?

J.H. Gerstle, Boeing

That's correct.

BLADE FRAGMENT ENERGY ANALYSIS

M. A. O'Connor, Jr.

Douglas Aircraft Company
McDonnell Douglas Corporation

Douglas effort in the field of blade fragment energy analysis has dealt primarily with two classes of fan blade fragments. The first is of relatively small size (.15 pound) and energy, and tends to rebound from the fan and case when liberated in an FOD encounter. These small fragments have relatively low secondary damage potential and are less demanding in terms of protection. The larger fan blade fragments are ejected in a more direct release trajectory with higher energy and hence can represent a higher potential hazard. Using available empirical and analytical techniques, plus additional Douglas analysis and testing, protection has been developed for both classes of fragment.

Some of the more basic work accomplished includes evaluation of the penetration resistance of composites, determination of armor coverage and weights if protection were aircraft furnished (FAA contract), and development of lightweight local protection concepts.

Simplified analytical methods have been used to describe blade fragment energy transfer kinematics, establish fragment energy levels, evaluate damage potential and configure protection. The approach, methodology, and application are discussed as a possible building block for other applications. Development of effective local protection using Kevlar is also discussed. Analysis methods developed and applied to the rebound fragment problem and to the large direct release fragment problem are described. Douglas testing yielded useful data on the capability of existing structures and verified the GE Watertown Arsenal energy absorption curve and British Aircraft Company empirical energy absorption curve and British Aircraft Company empirical energy absorption relationships as usable tools.

With the necessary tools available, an assessment of aircraft "designed-in" protection was made. This included assessment of the consequences of penetration of the engine section ahead of the inlet flange and assessment of the probability of penetration outside the nacelle. Areas of concern and protective features provided to handle failures from whatever cause, are reviewed. It was concluded that the fan blade fragments did not constitute an airworthiness issue but that, for an aft engine installation, fuel line protection of some form would further complement fire safety even though completely within a designated fire zone.

Analysis and testing of large high velocity fan blade fragments were also conducted to determine energy and penetration characteristics. This evaluation again resulted in the conclusion that damage potential was within design margins. However, as for the smaller fragments, additional protection for systems traversing the zone ahead of an aft engine inlet flange can substantially reduce the exposure to secondary damage and was considered a desirable improvement.

In examining design concepts for protection of the aft engine inlet area it was concluded that there had to be a better approach than plain metallic armor. A "flack jacket" concept using Kevlar cloth as the energy absorbing medium was selected as offering the most promise. By using a complete belt around the inlet bellmouth, the uncertainties and design and installation complications of armor support were avoided. The concept also offered a potentially lighter weight installation.

Because of the extreme variation in vendor design data and claims, a decision was made to undertake an in-house development program starting with the basic purchased cloth. The number of lamina required for containment was determined using a compressed air gun firing 1.1 pound "design fragments" at the selected 900 fps design velocity. Additional firings were made with the final thickness and construction to assure repeatability, and to demonstrate successful containment with respect to protection of adjacent systems.

Additional firings were accomplished to determine the energy absorption characteristics of commonly used honeycomb inlet materials. Firings were also made with steel plate targets to check the Watertown Arsenal curve and empirical energy absorption equation.

In summary, we believe that we have developed a simple analysis methodology adequate for our needs, added to the experimental data base, and developed an efficient and effective concept for local protection of areas ahead of the engine flange.

DISCUSSION

A. Holms, NASA-Lewis

What did you mean by dynamic shear strength? How is it measured?

M.A. O'Connor, Jr., McDonnell-Douglas

This is a property that differs from the normal static shear strength of a material; it is determined by actual ballistic testing. It is the shear strength exhibited by a material under dynamic penetration conditions (as against static shear). Each material has a characteristic value: e.g., steel = 188,500 psi, aluminum = 30,450 psi, titanium = 145,000 psi. It is the constant derived by dividing the energy loss of the test projectile by the product of the impact perimeter of the projectile and the square of the thickness of the material penetrated. Maybe the BAC folks can shed some more light on the actual test methodology they used; I believe they pioneered this approach.

DESIGNING THE L-1011 TO MINIMIZE ROTOR FAILURE EFFECTS

J. E. Wignot
Lockheed California Co.

Despite the considerable emphasis on containment, and the effort spent in analysis, research, and design development testing in attempting to achieve same, the experience of the aircraft industry is that an uncontained fragment of significant size and energy is to be anticipated at some time in the life of an aircraft type. In recognition of this fact, the Federal Aviation Regulation Special Propulsion Condition P-I states, in part: "The airplane must incorporate design features to minimize hazardous damage to the airplane in the event of an engine rotor failure ..." The L-1011 incorporates numerous design features that provide a high level of protection against rotor fragments. Some of these features are reviewed herein.

Protection against rotor fragments may be provided in one or more of the following ways: (1) By incorporating design features into the rotor that tend to promote small fragments if failure occurs, (2) By containing the fragments within the engine shell or greatly reducing the energy content of those fragments that are eventually uncontained, (3) By shielding vulnerable elements or systems with heavy structural members that tend to stop or deflect high velocity fragments, and (4) By incorporating redundant and/or "backup" systems into the basic design and separating these systems so as to minimize the probability that more than one system will be damaged by an uncontained rotor fragment. The L-1011 utilizes all of these design philosophies.

Some of the design features that have been incorporated into the Rolls-Royce RB211 engine are discussed briefly and two in-service experiences are considered in order to illustrate the practical operation of these features. The penalties

that would be imposed by trying to design for 100% containment are assessed. Designing for 100% containment is found to be: (1) less effective than a rational integration of all techniques and (2) prodigally wasteful of our energy resources.

The aircraft systems such as flight controls, engine controls, fuel, hydraulic, and electrical control systems are considered and shown to be located and multiplicated so as to maximize the protection and availability of these vital systems. Special attention is given to the location of fuel lines, fuel shut-off valves, and the fuel valve control systems to minimize fire hazard.

Secondary equipment possessing high speed rotating elements are reviewed to illustrate the design philosphies followed, the design features utilized, and the in-service results attained.

The L-1011 has, to date accumulated close to a million flight hours with an excellent safety record showing the viability of the design philosophy utilized in designing the L-1011 to minimize rotor failure effects.

DISCUSSION

G. Gunstone, CAA-UK

I would like to ask Mr. Wignot if he could give some indication of the cost he feels has been allocated in the 1011 design against meeting the fragment protection requirement. In other words, trying to estimate the cost effectiveness of various solutions, what penalty is he paying now for having had to design the airplane the way it is, or would the aircraft have been just the same without a containment requirement?

J.E. Wignot, Lockheed-California

I think that's a very fair question. I think the answer is that, to date, the airplane proper has had very little weight added to it for containment. The additional weight that is associated with containment lies primarily in the engine.

J.C. Wallin, BAC

I couldn't help noticing that in your statement you said that there were certain systems, I think, that were protected by the structure. Now, that would presume based on your philosophy that you were not going to have more than a certain size disk piece coming out. I think that in an overall assessment (even with the best will involved and the best that Denis and his boys can do to the engine) one is unrealistic if one doesn't allow for the fact that one day there could be a failure of a disk piece and I don't believe that any structure, however heavy, will stop a disk piece. Having said all that, I will say that in our assessment, the L-1011 was one aircraft that would meet the current CAA requirements without any changes.

J.E. Wignot, Lockheed-Cal.

I want to thank Mr. Wallin for his comments and to acknowledge the pertinence of his question. Yes, we do have to face up to the possibility that a large fragment of a disk may be released. But after all, it's a matter of probability, isn't it? And here we're talking about the probability that we will have a bit of a disk come out, escape with the proper energy in the correct direction and do more than the damage that we have anticipated.

I would like to add that although philosophically we have to accept a rotor fragment size of one-third of the disk, it has been demonstrated many

times that when a contributing problem is recognized, such as excitation of the lower disk modes by partial local blockage, it is possible to alter the design to promote smaller fragment production in the event of a failure. It would be hoped that through the efforts of this group, that the technology base and the theoretical base that is developed will tend to make the probability of the release of a third of a disk negligible. If we design so as to keep the rotor burst fragments small it makes all the other design problems that much easier.

APPROACHES TO ROTOR FRAGMENT PROTECTION

M. A. O'Connor, Jr.

Douglas Aircraft Company
McDonnell Douglas Corporation

In recent years there has been a substantial increase in regulatory attention in the area of rotor fragment protection. Concern appears to stem primarily from an apparent nearly constant per year occurrence of incidents involving uncontained fragments, large fan blade masses of the large high bypass ratio turbofans, and degree of secondary damage produced in some instances. Increase emphasis is evident from NASA and FAA activities including their sponsorship of some industry activities.

It is essential that the containment question be examined in the correct perspective. The commercial record is a fairly convincing argument that the requirements and practices in place today are reasonably effective. Since Douglas' entry into the jet transport field in 1956, two hulls have been lost and a single fatality incurred in a third incident involving rotor/blade failures. In none would additional "armor" isolation, or redundancy have affected the outcome. However, this is not to imply that there is no room for improvement. Some ideas that may provide insight include review of key controlling requirements, armor as a brute force approach, and an integrated airframe and engine solution.

As part of the approach to rotor/blade fragment protection, key airworthiness design criteria/considerations for fragment protection are reviewed. Various FAA requirements in FAR Parts 25 and 33, plus interpretive 8110 orders, deal with engine and installation requirements specifically aimed at minimizing this type of hazard. These requirements cover such features and design areas as engine isolation, containment of damage from rotor blade failures, containment of fire, and design of other features of the aircraft to permit continued flight and safe landing in the event of more serious engine failures.

Armor represents one end of the spectrum of protection approaches. An FAA sponsored study is in process at Douglas to evaluate the impact of providing aircraft armor in lieu of engine armor for typical 3 and 4 engine wide bodied transports. The initial area of discussion deals with protection within the length of the engine case. Protection from fragments exiting ahead of the engine inlet flange has some unique considerations and is therefore treated separately.

For protection within the length of the engine case, armor weight penalties, plus fuel burned and dollar cost of carrying the armor protection are defined. Immediately ahead of the inlet flange, direct tangential impacts are predominant, but further forward, rebound impacts predominate. Armor thickness requirements and fuel cost impact of protection are shown.

The right answer is a balanced or "system" approach involving both the aircraft and engine design. This approach whether formalized or not is basically

responsible for the demonstrated success to date. Accomplishment involves nothing more than the systematic recognition of the problem during the basic design and development of both the aircraft and engine. Key steps in the aircraft design are delineated.

Design considerations relative to a tail engine installation are delineated. Limited armor is used for specific applications, i.e., tail engine fuel line protection, and tail engine inlet "flack jacket".

Results of demonstration testing and weight penalties are reviewed and areas of engine design which might be examined for optimum overall solutions are suggested.

This paper attempts to place the containment issue in better perspective and is felt to show that we are not faced with problems which would justify major regulatory and/or basic design concept changes. Based on Douglas' experience, however, areas where future effort could be directed productively are suggested.

DISCUSSION

J.H. Gerstle, Boeing

You showed the figure of eight million dollars a year as a fuel cost penality to carry the added containment weight on a quad-jet. Could you amplify on the assumptions that went into that figure?

M.A. O'Connor, Jr., McD-D

Basically, there were 971 aircraft in the estimate (635, 3 engine and 336, 4 engine wide bodied transports). We assumed a representative flight profile (based on an airline cross section) for the fleet and then merely calculated the fuel consumed to carry the armor weight. The total armor weights shown represent an upper bound (i.e., armor weights were not discounted for inherent and/or intentional containment capability of the engine cases. Each stage was assumed equally critical and armor weights were calculated and included for full protection).

METALLIC ARMOR FOR BALLISTIC PROTECTION FROM STEEL FRAGMENTS

Donald F. Haskell

Ballistic Modeling Division
U.S. Army Ballistic Research Laboratory
Aberdeen Proving Ground, Maryland 21005

ABSTRACT

Perforation information for compact cylindrical steel fragments impacting on each of six alloys are presented. The bulk of the experimental data, developed by Project THOR and presented herein, is characterized by fragment sizes from 0.32 to 53 grams, striking velocities from 152 to 3658 m/sec and angles of striking obliquity from zero to 80 degrees. Additional tests have also been conducted with 0.06 and 0.14 gram steel fragments fired against mild steel and aluminum alloy targets from 373 to 2020 m/sec and 65, 194, and 324 gram steel fragments fired at rolled homogeneous alloy targets from 367 to 1234 m/sec. Empirical formulas of a given type have been fitted to these data to relate fragment limit velocity, fragment residual velocity and fragment residual weight to important impact parameters. Information is presented for the following target alloys: magnesium, aluminum, titanium, face-hardened steel, mild steel, and rolled homogeneous armor steel. This information has been found useful in the selection of metallic armor type and thickness required for a specific degree of ballistic protection.

DISCUSSION

J.H. Gerstle, Boeing

Did you say that the data shown here are available?

D. Haskell, Army-BRL

Yes, from unclassified BRL reports.

ROTOR BURST PROTECTION PROGRAM: EXPERIMENTATION TO PROVIDE GUIDELINES FOR THE DESIGN OF TURBINE ROTOR BURST FRAGMENT CONTAINMENT RINGS*

G. J. Mangano

J. T. Salvino

R. A. DeLucia

Naval Air Propulsion Test Center

Princeton, New Jersey 08628

ABSTRACT

ABSTRACT

Presented are the results of a program of rotor burst containment experimentation that provides guidelines for the design of optimum weight turbine rotor disk fragment containment rings. These guidelines were derived by establishing the relationships between a measure of the ring's capability to contain fragment energy with respect to it's weight (the specific contained fragment energy - SCFE - derived by dividing the rotor burst energy by the weight of ring required to contain this energy) and other significant ring and rotor variables such as the: rotor tip diameter; number of rotor fragments; and ring radial thickness and axial length. The experiments consisted mainly of bursting 14 and 31 inch diameter turbine rotors into encircling containment rings made from centrifugally cast 4130 steel. Rules are given for achieving optimum weight ring designs.

*Prepared under NASA Defense Purchase Request C-41581-B, Modification No. 6, for the NASA Lewis Research Center. Solomon Weiss, Robert D. Siewert, and Arthur G. Holms of the Lewis Research Center served as program managers and technical consultants for this program. Also published as NASA CR-135166, 1977.

SUMMARY

The program of parametric rotor burst containment experimentation being reported was developed and conducted by the Naval Air Propulsion Test Center (NAPTC) under National Aeronautics and Space Administration (NASA) sponsorship. The program was structured to develop guidelines for the design of optimum weight turbine rotor disk fragment containment rings. The design guidelines were generated by experimentally establishing the relationship between a specific energy variable that provides a measure of ring containment capability, and several select variables which characterize those configurational aspects of the containment rings and rotor fragments that significantly influence the fragment containment process.

The program consisted of a series of rotor burst containment experiments in which rotors of two different diameters were modified to burst at their respective design speeds into various numbers (2, 3 and 6) of pie-sector shaped fragments. These fragments impacted rings made from 4130 cast steel that encircled the rotors at a radial clearance of 0.5 inches (0.0127 m). The ring axial lengths were varied in three discrete steps of 1/2, 1, and 2 times the rir axial length of the rotors used. The radial thicknesses of the rings were varied until fragment containment was achieved, thus establishing the weight of ring required. The results of test provided the guidelines necessary to design an optimum weight steel containment ring for small rotors. The optimum weight ring was 8.6 lbs (3.9 kg) for a 14 inch (0.356 m) diameter rotor having a burst energy of 10^6 in-lbs (3511.6 J) at its design speed of 20,000 rpm (2094 rad/s). This weight decreased slightly with the number of fragments generated at burst in the range of from 2 to 6. The results also indicated that the weight of steel ring required to contain the pie-sector fragments from an average size commercial engine turbine rotor (31 inch (0.787 m) diameter) having a burst energy of 10 X 10^6 in-lbs (. '16 J) would be in excess of 168 lbs (76.2 kg) for 2 and 3-fragment bursts and in the neighborhood of 150 lbs (68 kg) for a 6-fragment burst. Unlike the small rotor containment ring characteristics, the weight of ring required to contain these larger rotors was clearly dependent on the number of fragments generated at burst.

It was also found that a composite ring made from boron carbide backed with filament wound fiberglass in an epoxy matrix contained the fragments from the small rotor burst at a weight reduction of 30% compared to steel. This represents a significant weight reduction configuration that warrants further exploration.

It would appear from the results of this effort that the steel rings required to contain the fragments generated by the burst of an average size turbine rotor (the larger of the two rotors tested) from a commercial engine would be heavy for aircraft application. However, the use of optimally configured composite rings for fragment containment and partial rings for fragment deflection, which are systems that show great promise for light-weight protection, should be thoroughly investigated.

INTRODUCTION

This is a report on the Rotor Burst Protection Program (RBPP), which is sponsored by the National Aeronautics and Space Administration (NASA) and conducted by the Naval Air Propulsion Test Center (NAPTC). The objective of this program is to develop guidelines for the design of devices that will be used on aircraft to protect passengers and the aircraft structure from the lethal and devastating fragments that are generated by gas turbine engine rotor bursts.

Presented in this report are the results of a parametric test program that was conducted by the NAPTC to provide guidelines for the design of turbine rotor fragment containment rings. This program was a sequel to, and to a large extend guided by, the exploratory testing that was conducted by NAPTC and reported in reference (a).

CONCLUSIONS

1. Regarding the containment of typical, relatively small (14 inch (0.356 m)) diameter, axial flow turbine rotors that burst at their design speeds into various numbers of pie-sector shaped fragments having a total energy of approximately 10^6 in-lbs (3511.6 J):

a. Containment of these fragments can be achieved using rings described as follows:

(1) Rings made from 4130 cast steel weighing 8.6 lbs (3.9 kg).

(2) Laminated rings consisting of boron-carbide backed with fiberglass weighing 6.02 lbs (2.71 kg).

b. Optimum weight for the steel containment ring configuration was achieved when the ring axial length was made equal to that of the rotor; making the ring twice or half as long as the rotor axial length resulted in containment rings that were heavier and therefore less than optimum with respect to weight.

c. With the steel ring axial length at it's optimum value with respect to weight, the ring thickness and therefore its weight is, for practical purposes, independent of the number (ranging from 2 to 6) of equal pie-sector shaped rotor fragments generated at burst.

2. Regarding the containment of typical relatively large (31 inch (0.787 m)) axial flow turbine rotors that burst at their design speeds into various numbers of pie-sector shaped fragments having a total energy of approximately 10 X 10^6 in-lbs (35116 J):

a. Rings made from relatively brittle 4130 cast-steel weighing in excess of 168 lbs (76.2 kg) will be required to contain 2 and 3 fragment rotor bursts. A ring of the same material weighing in the neighborhood of 150 lbs (68 kg) will be required to contain a 6-fragment burst.

b. The optimum weight of 4130 cast-steel ring required for containment is dependent on the number of pie-sector shaped fragments generated at burst in the range of from 2 to 6 fragments. The weight will increase as the number of such fragments decreases.

RECOMMENDATIONS

1. Experimentation and analysis should be continued on a limited basis to establish the baseline or reference steel ring weight required to contain 2 and 3 fragment large rotor bursts.

2. Because the weight of steel rings required to contain the pie-sector shaped burst fragments from an average size commercial engine turbine rotor appears to be excessively high, the following two facets of rotor burst protection should be further investigated and design guidelines developed:

a. The use of multi-layered, multi-material rings for containment applications, and

b. The use of partial rings to control the trajectories of rotor burst fragments (directing them away from the more vital areas of the aircraft into the less or negligibly sensitive areas) as a means of providing a "degree" of protection at reduced weight.

PROGRAM DESCRIPTION

A. Concept Development

1. The program of parametric turbine rotor fragment containment testing that is being reported was structured to develop empirical guidelines for the design of minimum weight turbine rotor disk fragment containment rings made from a monolithic metal.

The empirical design guidelines were generated by experimentally establishing the relationship between a variable that provides a measure of containment ring capability and several other variables that both characterized the configurational aspects of the rotor fragments and containment ring; and had been found from exploratory testing to have had significant influence on the containment process.

The variable that provided this measure of containment ring potential or capability was termed the Specific Contained Fragment Energy (SCFE) and was derived by dividing the rotor fragment energy at burst by the ring weight required to contain this energy. The SCFE was the dependent variable of test.

2. The four ring and rotor characteristics that were chosen for test because of their suspected influence on the containment process, and varied during test to establish what this influence was (as measured by the SCFE) were as follows:

a. The ring inner diameter. Two diameters, one approximately twice as large as the other (31.64 and 15 inches) were used for test with rotors having correspondingly larger and smaller tip diameters (the CWJ65 and GET58 engine turbine rotors having tip diameters of 30.64 (.778 m) and 14 (0.356 m) inches, respectively). The burst energies of these rotors at their nominal design speeds were 10×10^6 and 10^6 in-lbs (35116 and 3511.6J) for the larger and smaller rotor, respectively. Burst fragment energy (speed) was held constant from test to test as a function of rotor size; the larger rotor having the higher energy.

b. The ring axial length. Three lengths were used that corresponded to 1/2, 1 and 2 times the rim axial lengths of the large and small rotors which were nominally 1.25 and 1 inch (.032 and .0254 m), respectively.

c. The number of rotor fragments generated at burst. The rotors were modified to fail at their respective design speeds of 8,500 rpm (890. rad/s) (J65 rotor) and 20,000 rpm (2094 rad/s) (T58 rotor) and produce pie-sector shaped fragments having included angles of 60° (1.0472 rad), 120° (2.0944 rad) and 180° (3.1416 rad). These were termed 6, 3 and 2-fragment rotor bursts, respectively.

d. The ring radial thickness. The ring thickness was varied until fragment containment was achieved for the different combinations of ring (rotor) diameter; ring axial length; and number of rotor fragments.

The resultant test matrix for this test program is shown in Figure 1; and the procedure for ring thickness variation to achieve containment is shown schematically in Figure 2.

3. Other variables which would, in some way, influence the magnitude and orientation of the forces that create the deformations and displacements of the ring and rotor fragments, and therefore govern the containment process are as follows:

a. The mechanical properties of the rotor and ring materials.

b. The fragment velocities.

c. The fragment masses and mass distributions.

d. The rotor-to-ring radial tip clearance.

e. The rotor tip-to-hub diameter or radius ratio.

Although these factors would significantly influence the containment process, with the exception of the ring material used for containment, the variability of these factors, as a function of rotor size, are constrained within relatively narrow limits by the dictates of rotor aerothermal and structural design. For all practical purposes then, for a given rotor size, these factors would be essentially invariate and the results generated by the experiments conducted would be generally applicable to all turbines as a function of rotor size. This would be so because the experimental scheme presented incorporates, either purposely through the variables of test or inherently because actual rotors are used, all of the factors that could (with the exception of ring material properties) significantly influence the rotor fragment containment process.

Although the mechanical properties of the materials used to make a containment ring can vary widely and are considered to be important factors in containment ring design, the ring material used in most of the tests conducted was the same from one test to another. The material was 4130 cast steel. This was done to generate a baseline for materials comparison in subsequent tests, and to establish the effects of the other variables on the containment process exclusive of material influences. Later when these effects are firmly established, the influence of ring materials will be more fully explored. In fact, during the tests conducted the use of composite rings as containment devices were cursorily investigated.

B. Design Guidelines Synthesis

1. The conceptual functional relationship between the dependent (SCFE) and independent (t, ALR, NF, ID) variables of test are presented conceptually in Figure 3. Once these relationships are established through test, they provide all the information that is needed to design an optimum weight steel ring for a turbine rotor fragment containment application. Given these relationships, the procedure would be as follows:

a. Three basic things would have to be known about the rotor to proceed with the design analysis:

(1) The kinetic energy (KE_R) of the rotor at burst

(2) The rotor tip diameter, and

(3) The rotor rim axial length.

These are characteristics that are usually known or can be easily calculated by a designer.

b. The relationships between the SCFE, the number of fragments and rotor diameter, with the ratio of ring to rotor rim axial length as the parameter, provide an indication of the worst combination of burst conditions for the size rotor being considered; i.e., the lowest SCFE. For a given analysis, this value of SCFE would be obtained from the curves in Figure 3 (or equations derived from regression analyses of the data points developed through test) for the size rotor being considered; the number of rotor fragments that result in producing the most adverse containment condition with respect to weight of ring (the lowest SCFE value in the SCFE-NF plane; and the optimum ring to rotor rim axial length ratio ($L_{RG}/L_{RT} \equiv ALR$)), which is represented by the highest contour line. The SCFE value that is obtained by this exercise is divided into the total anticipated energy of the rotor to yield the optimum (lowest) weight steel ring that will be required to contain the fragments. This procedure is expressed in equation (1).

$$(1) \quad W_t = \frac{KE_R}{SCFE}$$

The weight so derived is then used in the following equation (2) which expresses the thickness of ring required for containment as a function of all the other known dimensional variables.

$$(2) \quad t = \left[R_i^2 + \frac{W_t}{\rho \pi L_{RG}} \right]^{\frac{1}{2}} - R_i$$

Of course the value of weight derived in equation (1) can be substituted in equation (2) to yield perhaps a more useful form; equation (2a)

$$(2a) \quad t = \left[R_i^2 + \frac{KE_R}{\rho \pi L_{RG}\ SCFE} \right]^{\frac{1}{2}} - R_i$$

where

t = ring radial thickness required for containment

R_i = ring inner radius, which, for practical considerations, equals the rotor tip radius because rotor-to-casing operational clearances and considerations of minimum ring weight dictate that the ring and rotor radius be equivalent as possible.

L_{RG} = ring axial length: Derived by the multiplication of the optimum ALR (parameter of highest contour in Figure 3) and the rotor rim axial length L_{RT}.

c. This data synthesis and design analysis would provide the lightest weight steel ring configuration (ID, radial thickness, and axial length) that would be needed to contain the fragments generated by a turbine rotor burst of known size and energy. The analysis is generally applicable to axial flow turbines from aircraft gas turbine engines because, as mentioned previously, of the inherent operational and configurational similarities between turbines of a given size.

C. Test Procedures and Methods of Analysis

1. Test Procedures

Testing was conducted in the NAPTC Rotor Spin Facility (RSF), the detailed capabilities and description of which are contained in reference (b). The test set-up and procedures were basically the same for each test conducted: Rings being evaluated for their containment capability as measured by the SCFE were sandwiched between rigid steel plates and positioned so that they concentrically encircled rotors that were vertically suspended (plane of rotation horizontal) in the spin chamber from the output shaft of the air turbine motor used to spin the rotors to their burst speed. This set-up is shown in Figure 4. The radial tip clearance between the rotor and ring was maintained at 0.50 inch (1.27 cm). The two different size rotors described previously were modified, as shown in Figure 5, to fail into 2, 3 and 6 pie-sector shaped fragments at their nominal operational design speeds.

During test, the spin chamber was evacuated to a vacuum pressure of 10mm Hg to minimize the drive power required to accelerate the rotors to burst speed.

2. Methods of Analysis

Because of the nature of the test program conducted, the analysis of results was relatively straight forward; it depended on two things:

a. Whether or not the ring being subjected to test contained the rotor fragments generated.

b. And if it did contain, what was the associated ring SCFE (by definition no SCFE could be derived for a ring that did not contain the fragments).

As previously mentioned, the SCFE for a ring is derived by dividing the rotor fragment burst energy by the ring weight required for containment. For the tests conducted, two axial flow turbine rotor configurations having different tip diameters (14 and 30.64 inches) bursting at their respective operational design speeds (20,000 and 8,500 rpm) were used. Therefore, from test to test, the rotor burst energy was held constant as a function of rotor size. However, variations in burst energy for a given rotor size did occur during test because of small unpredictable variations in rotor burst speed. These variations stemmed from such factors as: material property scatter; dimensional tolerance differences; flaws or cracks (scrap turbine rotors from high time military engines were used); and other such inherent and induced rotor to rotor anomalies. To account for these "experimental" variations in analyzing the burst test results, the policy was adopted whereby results which had a speed variation greater than $\pm$ 2.5% of the design burst speed were not used for analytical purposes; i.e., assessment of a ring's SCFE. The reason for not using the results of a low burst speed (and therefore low energy) test is obvious: It would mistakenly give a lower and therefore erroneously conservative SCFE value for a particular ring configuration. The reason for rejecting the results of a higher burst speed was more subtle and was based on the fact that materials exhibit strain rate sensitivity. Under singularly optimum conditions, it might be possible to derive an erroneously high SCFE from a higher than "rated" burst speed because of a favorable material rate sensitivity. This would indicate that a lighter than required ring would be suitable for containment when in fact at rated speed it would not.

3. In this report, the results of analysis will be presented graphically by indicating the range of SCFE based on the acceptable speed variation ($\pm$ 2.5%) and the SCFE based on the actual burst speed.

4. The other element beside speed that established the rotor energy at burst was the mass moment of inertia of the two turbine rotors used for test. The values of inertia for each rotor were determined experimentally using the well known torsional pendulum method (reference c).

RESULTS AND DISCUSSION

A compendium of the pertinent test and calculated data used in this report are presented in Appendix A.

The results of test are presented in plotted form in Figures 6, 7, 8, 14 and 15. These plots are actually plane sections of the conceptual three dimensional (variable) plot shown in Figure 3, but in these instances using the test data developed. The intent here is to clearly show, where possible, the functional relationship between the SCFE and the significant test variables: inner ring diameter (ID_R); number of fragments (NF); and ring axial length (ALR).

a. SCFE - NF Relationship for Small Rotors; Figure 6. It can be seen from these curves that for small rotor containment the SCFE is for all practical purposes independent of the number of pie-sector shaped fragments generated at burst. This indicates that rings of the same weight would be required for containment regardless of the number of fragments generated at rotor burst in the range of from 2 to 6 fragments and having a total (translational and rotational) energy content of approximately 10^6 in-lbs. A corollary to this would be that a worst fragment number condition for small rotor containment with respect to ring weight does not exist.

b. SCFE - ALR Relationship for Small Rotors; Figure 7. The relationship shown in this Figure indicates that an optimum value for ring axial length exists. For the size rotor tested, an optimum lightweight ring for containment is derived when the axial length of the ring is made equal to that of the rotor; that is where ALR = 1.

c. SCFE - ID_R Relationship for 2, 3 and 6 Fragment Bursts at ALR = 1; Figure 8. First of all, these relationships are incomplete except for the 6-fragment data because the radial thickness required for large rotor containment of the 2 and 3-fragment bursts exceeded that which was available from inventory (4130 cast steel circular rings with an ID of 31.64 inches (0.804 m) and having a maximum radial thickness of 4.1875 inches (.106 m)). The relationship shown in Figure 8 indicates that the amount of fragment energy that a pound of ring material can contain decreases when the rotor size and energy content increases; that is for the same ring to rotor axial length ratio, ring material, and number of fragments generated at burst, the containment capability of the larger ring, as measured by the SCFE (on a contained energy per unit weight basis) is lower than a small ring. This indicates that the practice of extrapolating small rotor containment ring results to large rotor containment ring applications would be very tenuous. To provide some feel for the ring and fragment distortions that normally accompany the containment process, the post-test conditions of rings and rotors from several selected tests (both contained and uncontained) are shown photographically in Figures 9 through 13.

d. SCFE - NF Relationship for Large Rotor Containment at ALR = 1; Figure 14. The relationship in this figure, though not definitive because containment was not achieved for the 2 and 3 fragment burst, indicates that the SCFE is dependent on the number of fragments (NF) generated at burst. This differs from the small rotor results, which indicated that the SCFE and NF were almost independent. The trend of this relationship indicates that the capability of a ring increases as the number of fragments generated increases or in other words, as the number of fragments generated at burst decreases the containment situation with respect to ring weight become more adverse, i.e., more weight is required.

e. SCFE - ALR Relationship for Large Rotor Containment of 2-Fragment Bursts; Figure 15. Only limited tests were conducted to explore this relationship because trends indicated that the weights of ring required for containment were becoming very high. Figure 15 tends to show that an optimum axial length might exist in the neighborhood of ALR = 1. This is consistent with the results of the small rotor results, which because of the abundance of test data, was more conclusive in indicating an optimum ALR = 1.

f. General Observations and Results:

(1) Comparison Between Large and Small Rotor Containment Ring Deformation/Displacement Characteristics During Fragment Impact: Figure 16 shows high-speed photographic results that depict the mechanics of large and small rotor containment in which a 3-fragment rotor burst is involved. It can be seen from these data that the gross deformations and displacements experienced by the steel rings are quite independent of size. In fact, in a general sense, the deformation/displacement characteristics for the large and small rotor containment rings are approximately identical. On the basis of this data, it was anticipated that a functional relationship between SCFE and rotor diameter/ring ID could be experimentally derived and be generally applicable.

(2) Exploratory Tests of a Small Rotor Composite Containment Ring: Data for these tests can be found in Appendix A under test numbers 143, 144, 183 and 208. These tests were conducted using the smaller T58 engine turbine rotors modified to burst into three fragments at their design speed of 20,000 rpm and impact concentrically, encircling rings that were made from three types of materials or material configurations: (a) filament wound fiberglass in an epoxy matrix; (b) circular boron carbide segments backed by filament wound fiberglass in an epoxy matrix; and (c) a segmented, hardened 4130 steel ring backed by filament wound fiberglass in an epoxy matrix. The fiberglass and steel-fiberglass rings did not contain the fragments; however, the boron carbide-fiberglass ring did contain at a weight savings of 30% over an optimally configured steel ring subjected to identical burst conditions. Post-test photographs of these rings are shown in Figures 17 through 19. On the basis of these exploratory tests, it appears that composite rings may serve to reduce the weight penalty associated with rotor disk fragment containment. To determine what these weight reductions might be, will require an extensive program of experimentation using multi-layered material rings.

REFERENCES

1. REPORT - Mangano, G. J., "Rotor Burst Protection Program - Phases VI and VII; Exploratory Experimentation to Provide Data For The Design of Rotor Burst Fragment Containment Rings", Naval Air Propulsion Test Center, NAPTC-AED-1968 of March 1972

2. REPORT - Martino, A. A. and Mangano, G. J., "Turbine Disk Burst Protection Study", Final Phase II-III Report on Problem Assignment NASA DPR #R105, Naval Air Propulsion Test Center, NAPTC-AEL-1848 of February 1967.

3. TEXT - Freberg, C. R. and Kemler, E. N., "Elements of Mechanical Vibration", John Wiley & Sonce, Inc., New York, 1949 (Page 23).

		ID 15			ID 32		
		NF 2	NF 3	NF 6	NF 2	NF 3	NF 6
ALR 1/2	t_1						
	t_2						
	t_3						
	t_4						
ALR 1	t_1						
	t_2						
	t_3						
	t_4						
ALR 2	t_1						
	t_2						
	t_3						
	t_4						

WHERE: ALR = RING TO ROTOR RIM AXIAL LENGTH RATIO (NUMBER DENOTES RATIO)

ID = RING INNER DIAMETER (SUBSCRIPT DENOTES NOMINAL DIAMETER IN INCHES)

t = RING RADIAL THICKNESS (SUBSCRIPT REFERS TO NO. OF TRIALS TO ESTABLISH CONTAINMENT THICKNESS)

NF = NO. PIE SECTOR SHAPED ROTOR FRAGMENTS (SUBSCRIPT DENOTES NO. FRAGMENTS)

Figure 1. - Small/Large Rotor Containment Test Matrix.

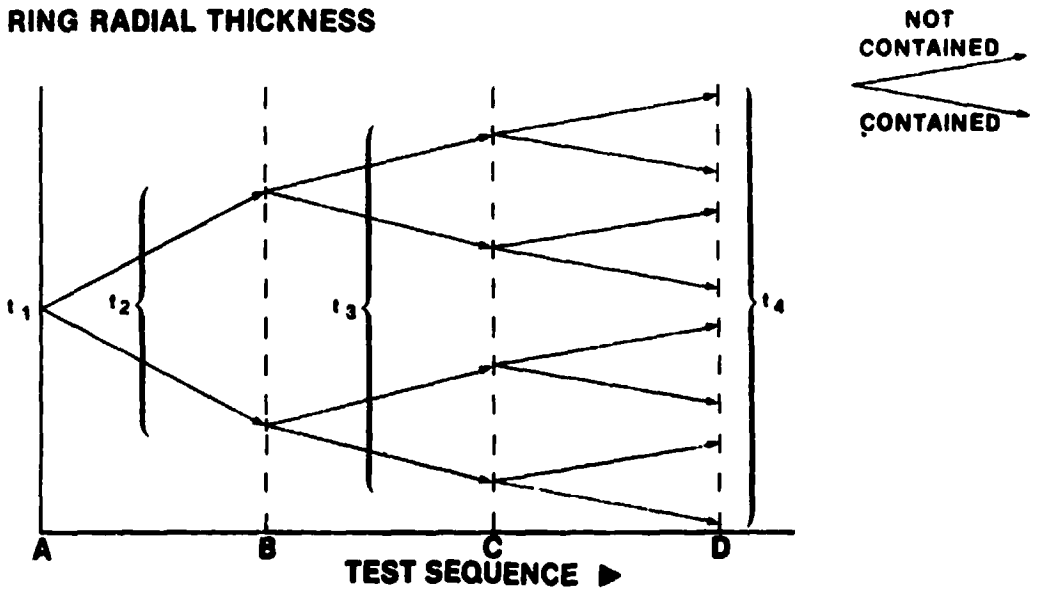

Figure 2. - Ring Thickness Variation Scheme.

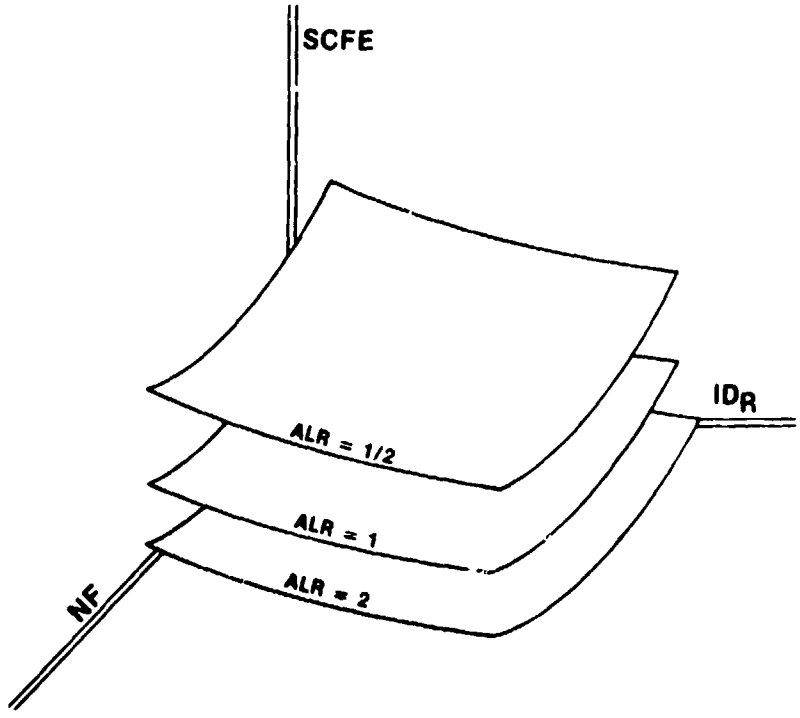

Figure 3. - Conceptual Relationships Between Containment Program Test Variables.

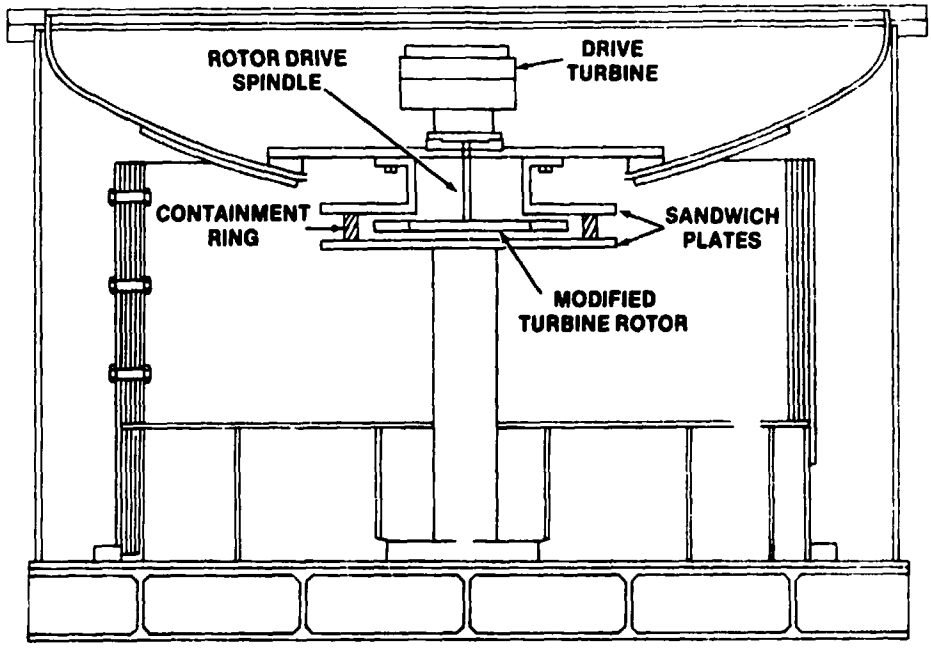

Figure 4. - Typical Containment Test Set-Up.

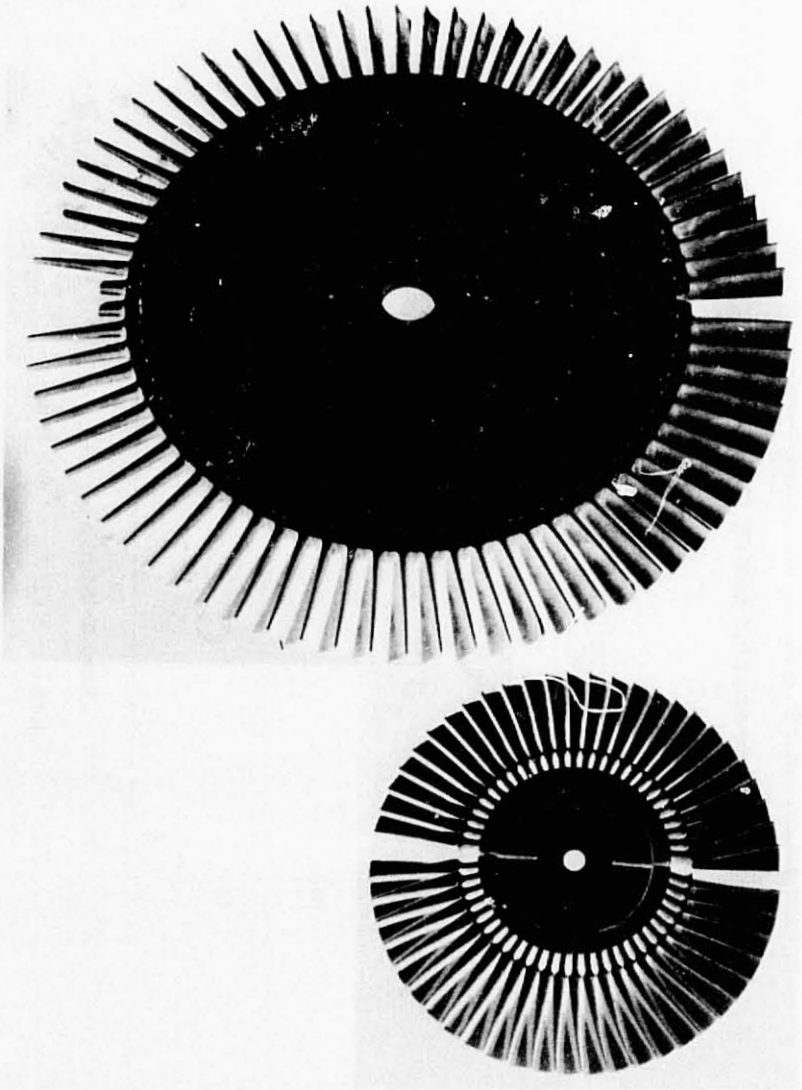

Figure 5. - Typical Rotor Modifications For Containment Tests.

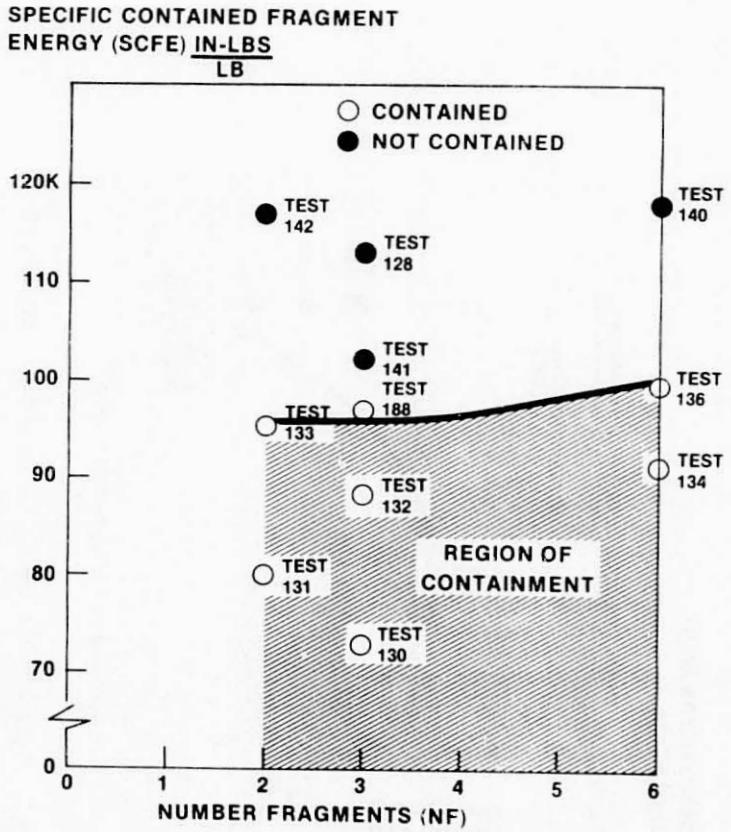

Figure 6. - SCFE-NF Relationship For Small Rotor Containment.

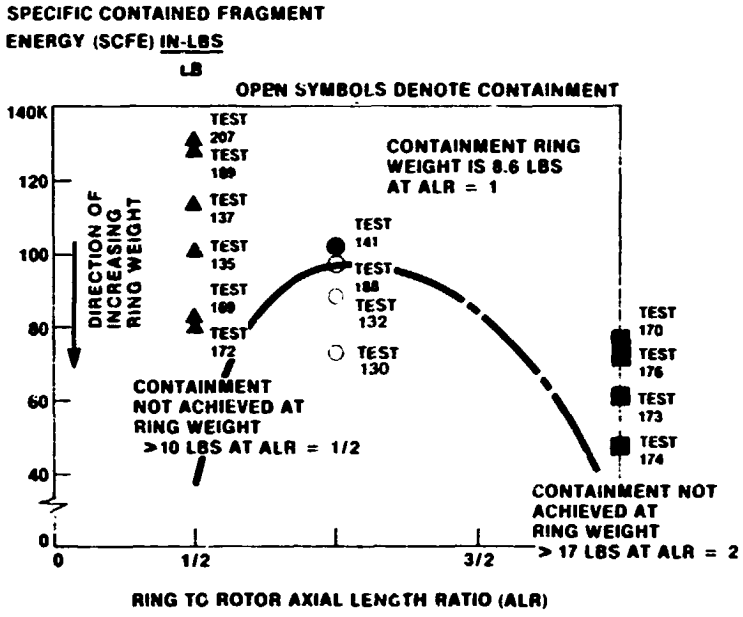

Figure 7. - SCFE-ALR Relationship For Small Rotor Containment.

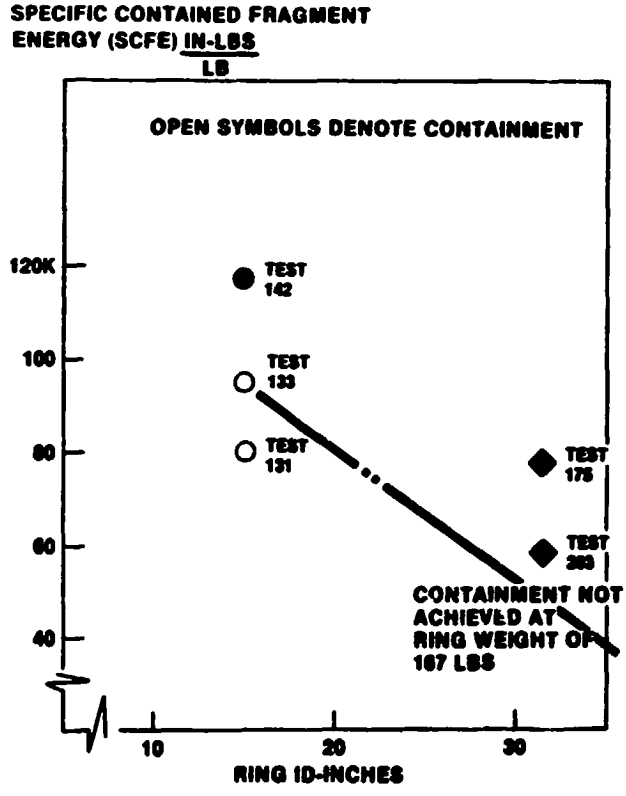

Figure 8. - SCFE-ID_R Relationship.

RING AND ROTOR FRAGMENTS IN PLACE FOLLOWING TEST

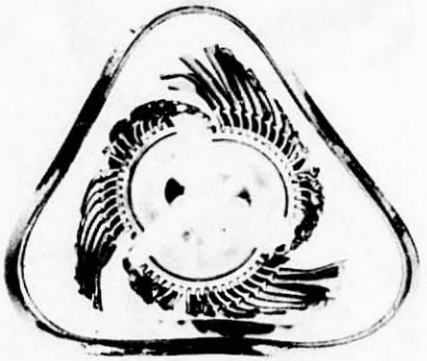

Figure 9. - Small Rotor 3 Fragment Containment Post Test Results.

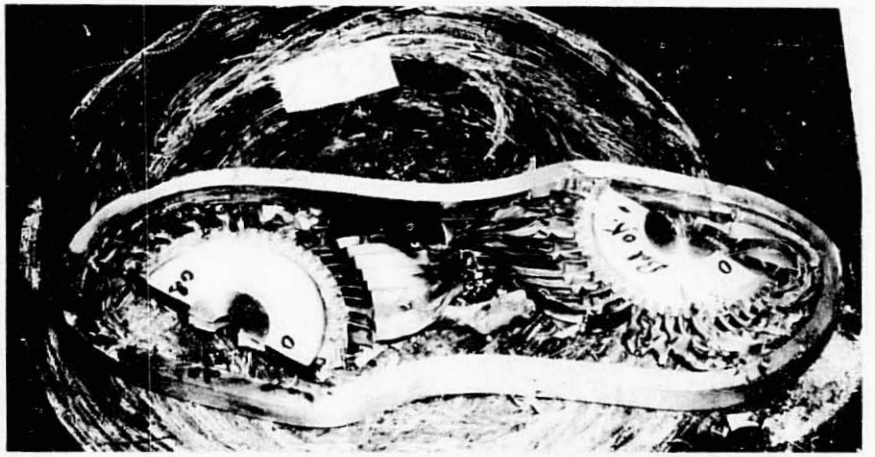

RING AND ROTOR FRAGMENTS IN PLACE FOLLOWING TEST

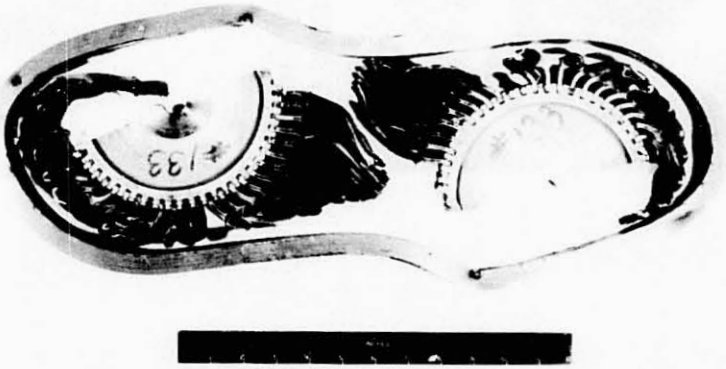

Figure 10. - Small Rotor 2 Fragment Containment Post Test Results.

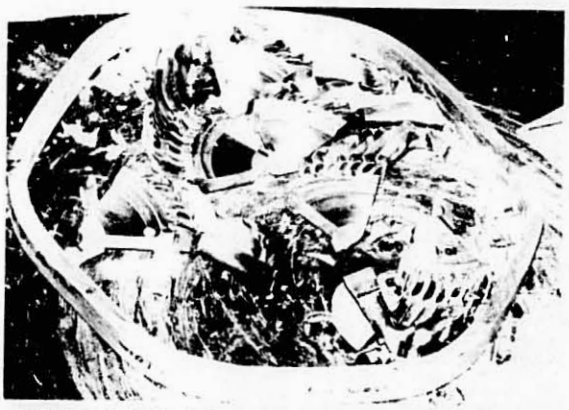

RING AND ROTOR FRAGMENTS IN PLACE FOLLOWING TEST

Figure 11. - Small Rotor 6 Fragment Containment Post Test Results.

Figure 12. - Small Rotor 2, 3 and 6 Fragment Containment Post Test Results.

Figure 13. - Large Rotor 2, 3 and 6 Fragment Containment Post Test Results.

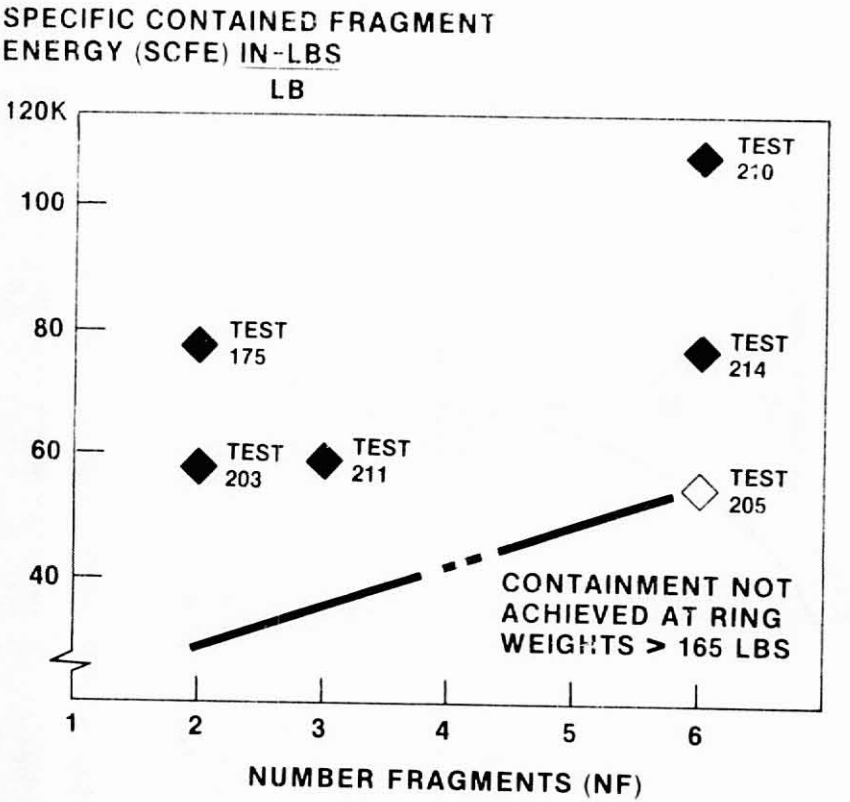

Figure 14. - SCFE-NF Relationship For Large Rotor Containment.

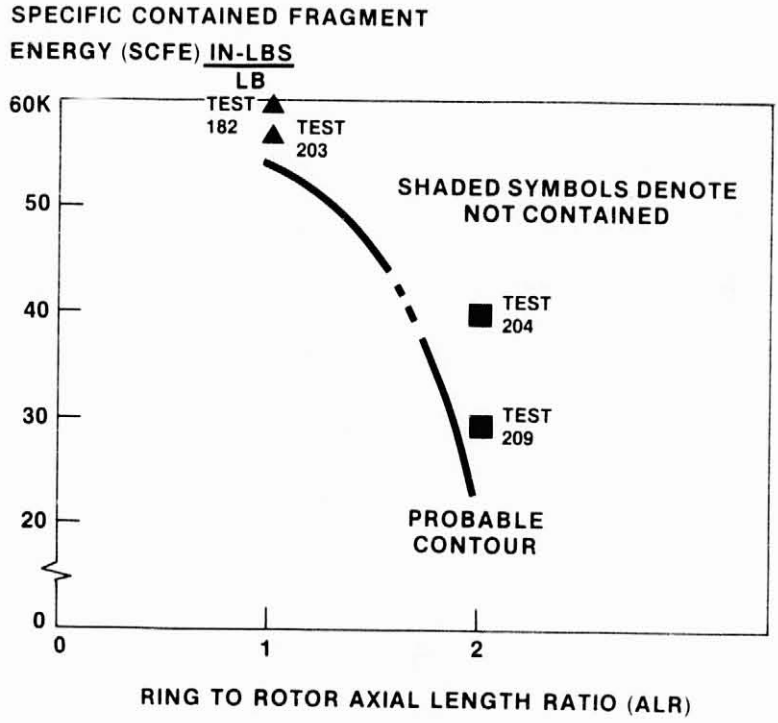

Figure 15. - SCFE-ALR Relationship For Large Rotor Containment 4130 Cast Steel Ring (NF = 2).

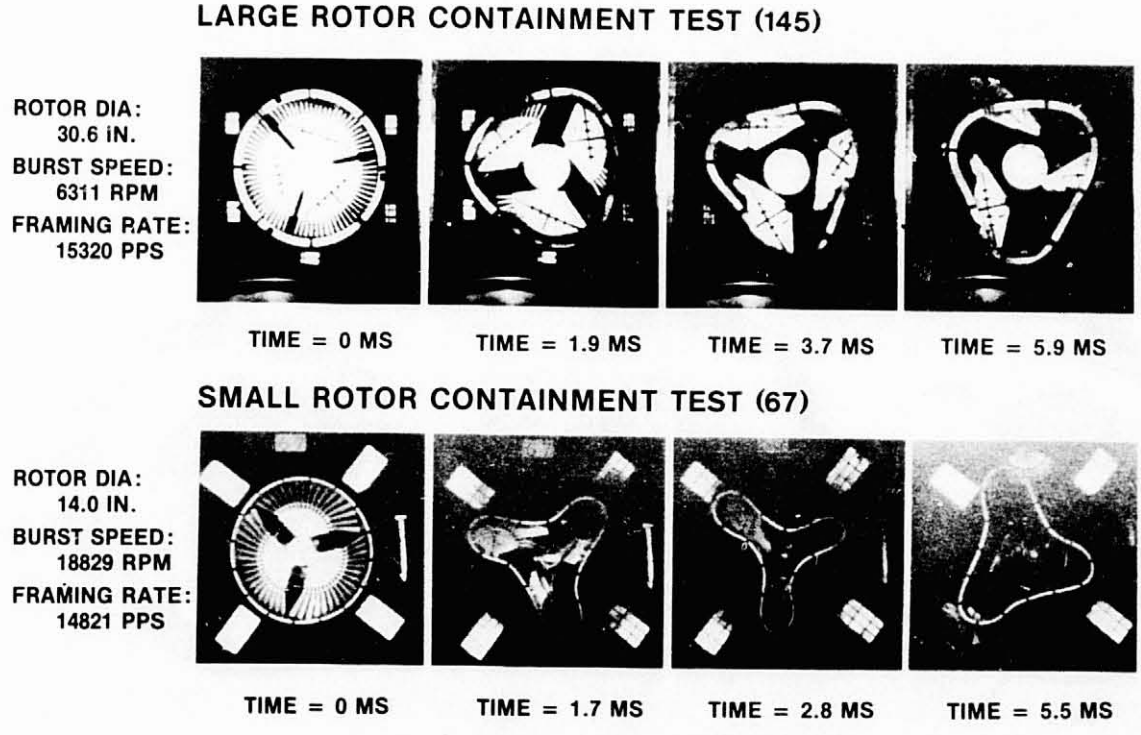

Figure 16. - Rotor Burst Fragment Containment Ring Deformation Characteristics.

Figure 17. - Small Rotor 3 Fragment Containment With A Fiberglass Ring Post Test Results.

Figure 18. - Small Rotor 3 Fragment Containment With A Boron Carbide/Fiberglass Composite Ring Post Test Results.

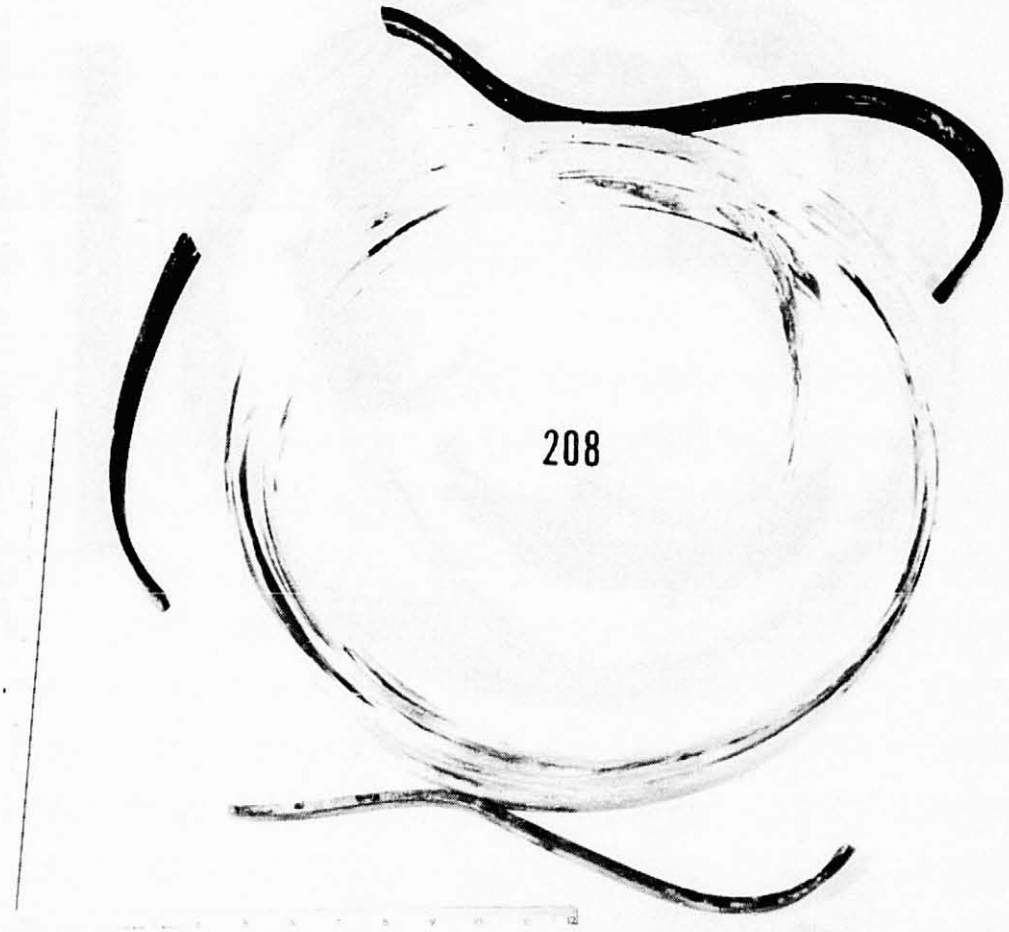

Figure 19. - Small Rotor 3 Fragment Containment With A Steel/Fiberglass Composite Ring Post Test Results.

APPENDIX A

Rotor Burst Protection Program Experimental Test Data Compilation

DATA COMPILATION NOTES:

(1) GE T58 Engine Power Turbine Rotor - Refer to Figure A-1 for dimensional and physical details.

(2) SRCT Ring Diameter = 15.0 inches.

(3) NF - Centrifugally cast 4130 steel billet produced by National Forge Company, refer to Figure A-2 for stress-strain char.

(4) ACIPCO - Centrifugally cast 4130 steel billet produced by ACIPCO, refer to Figure A-3 for stress-strain char.

(5) Fiber Glass - Composite ring manufactured by Eshbaugh Corporation; construction - E-glass roving in an epoxy resin matrix.

(6) B/C-Glass - Composite ring manufactured by Reflective Laminates/ Fansteel; construction - Boron Carbide segments backed with E-glass tape in an epoxy resin matrix (see Figure A-4).

(7) STL-Glass - Composite ring; construction-4130 plate steel segments backed with E-glass roving in an epoxy matrix (see Figure A-5).

(8) Curtiss-Wright J65 Engine Stage 2 Turbine Rotor; Refer to Figure A-6 for dimensional and physical details.

(9) LRCT Ring Diameter = 31.64 inches.

(10) Centrifugally cast 4130 steel billet produced by ACIPCO. Refer to Figure A-7 for stress-strain char.

(11) C - Contained
NC - Not Contained

SMALL ROTOR[1] CONTAINMENT TESTS (SRCT):

	RING DATA (2)				ROTOR DATA			RESULTS	
TEST NO.	AXIAL LENGTH IN	RADIAL THICKNESS IN	WEIGHT LBS	MATERIAL	NO. FRAGMENTS	BURST SPEED RPM	BURST ENERGY IN-LBS	SCFE IN-LBS/LB	CONT. COND.
129	1.0	0.560	7.68	NF[3]	2	18,630	722,424.0	94,065.6	NC
131	1.0	0.750	10.44	NF	2	20,022	834,413.6	79,924.7	C
133	1.0	0.625	8.63	NF	2	19,899	824,193.1	95,503.3	C
142	1.0	0.5625	7.77	NF	2	20,889	908,242.4	116,890.9	NC
126	1.0	0.250	3.41	NF	3	19,754	799,831.1	234,554.6	NC
127	1.0	0.375	5.14	NF	3	19,720	797,080.2	155,074.0	NC
128	1.0	0.507	7.0	NF	3	19,665	792,640.2	113,234.3	NC
130	1.0	0.750	10.49	NF	3	19.416	772,694.3	73,660.1	C
132	1.0	0.625	8.67	NF	3	19,342	766,815.6	88,444.7	C
138	1.0	0.625	8.62	NF	3	21,363	935,433.0	108,518.9	C
139	1.0	0.561	7.76	NF	3	18,897	731,937.4	94,321.8	NC
141	1.0	0.561	7.78	NF	3	19,719	796,999.4	102,442.1	NC
188	1.0	0.625	8.72	ACIPCO[4]	3	20,347	848,572.5	97,313.4	C
134	1.0	0.625	8.60	NF	6	20,056	786,168.2	91,414.9	C
136	1.0	0.5625	7.69	NF	6	19,775	764,292.8	99,387.9	C

SMALL ROTOR[1] CONTAINMENT TESTS (SRCT):

	RING DATA (2)				ROTOR DATA			RESULTS	
TEST NO.	AXIAL LENGTH IN	RADIAL THICKNESS IN	WEIGHT LBS	MATERIAL	NO. FRAGMENTS	BURST SPEED RPM	BURST ENERGY IN-LBS	SCFE IN-LBS/LB	CONT. COND.
140	1.0	0.500	6.89	NF	6	20,420	814,963.7	118,282.1	NC
135	0.5	1,200	8.53	NF	2	20,437	869,362.2	101,561.0	C
137	0.5	1.075	7.71	NF	2	20,559	879,772.7	114,108.0	(a)
168	0.5	1.402	10.17	NF	3	19,164	752,766.9	74,018.4	C
169	0.5	1.352	9.81	NF	3	20,000	819,976.0	83,575.5	NC
172	0.5	1.394	10.18	NF	3	19,978	818,073.3	80,360.8	NC
177	0.5	0.868	6.20	NF	3	19,103	747,982.4	120,642.3	C
178	0.5	0.883	6.13	NF	3	20,975	901,762.5	147,106.4	NC
207	0.5	0.874	6.16	ACPICO	3	19,880	810,067.1	131,504.4	NC
189	0.5	0.885	6.33	ACPICO	3	19,933	814,392.1	128,655.9	NC
170	2.0	0.375	10.81	NF	3	20,243	839,920.0	77,698.4	NC
173	2.0	0.497	13.57	NF	3	20,206	836,852.5	61,669.3	NC
174	2.0	0.6105	17.01	NF	3	20,032	822,501.8	48,354.0	NC
176	2.0	0.432	11.96	NF	3	20,559	866,347.6	72,437.1	NC
143	1.0	1.50	6.03	B/C-GLASS[6]	3	19,058	744,462.5	123,459.8	C

(a) CONTAINMENT QUESTIONABLE - UNDETEMINED

SMALL ROTOR[1] CONTAINMENT TESTS (SRCT):

	RING DATA (2)				ROTOR DATA			RESULTS	
TEST NO.	AXIAL LENGTH IN	RADIAL THICKNESS IN	WEIGHT LBS	MATERIAL	NO. FRAGMENTS	BURST SPEED RPM	BURST ENERGY IN-LBS	SCFE IN-LBS/LB	CONT. COND.
144	1.0	1.375	5.9	FIBER GLASS[5]	3	21,826	976,419.6	165,494.9	NC
208	1.0	.183	6.88	STL-GLASS[7]	3	19,556	783,877.6	113,935.7	NC
183	1.0	1.388	5.4	FIBER GLASS	3	20,680	876,575.4	161,135.2	NC

LARGE ROTOR[8] CONTAINMENT TESTS (LRCT):

	RING DATA (2)				ROTOR DATA			RESULTS	
TEST NO.	AXIAL LENGTH IN	RADIAL THICKNESS IN	WEIGHT LBS	MATERIAL	NO. FRAGMENTS	BURST SPEED RPM	BURST ENERGY IN-LBS	SCFE IN-LBS/LB	CONT. COND.
167	1.25	2.750	105.0	ACIPCO[10]	2	8,044	8,649,195	82,373.2	NC
175	1.25	3.250	125.5	ACIPCO	2	8,581	9,842,544	78,426.6	NC
180	1.25	1.800	70.5	ACIPCO	2	7,798	8,119,958	115,176.7	NC
181	1.25	1.939	74.0	ACIPCO	2	8,592	9,867,795	133,348.5	NC
182	1.25	4.000	160.0	ACIPCO	2	8,416	9,541,828	59,636.4	NC
203	1.25	4.1875	166.6	ACIPCO	2	8,500	9,657,585	57,968.6	NC
211	1.25	4.183	168.25	ACIPCO	3	8,614	9,918,373	58,950.2	NC
205	1.25	4.231	168.75	ACIPCO	6	8,316	9,243,994	54,779.2	C
210	1.25	2.500	95.0	ACIPCO	6	8,764	10,266,808	108,071.6	NC
214	1.25	3.250	123.0	ACIPCO	6	8,458	9,562,381	77,743	NC
204	2.5	3.000	232.0	ACIPCO	2	8,270	9,142,011	39,405	NC
209	2.5	4.225	330.0	ACIPCO	2	8,499	9,655,313	29,259	NC

FIGURE A-1

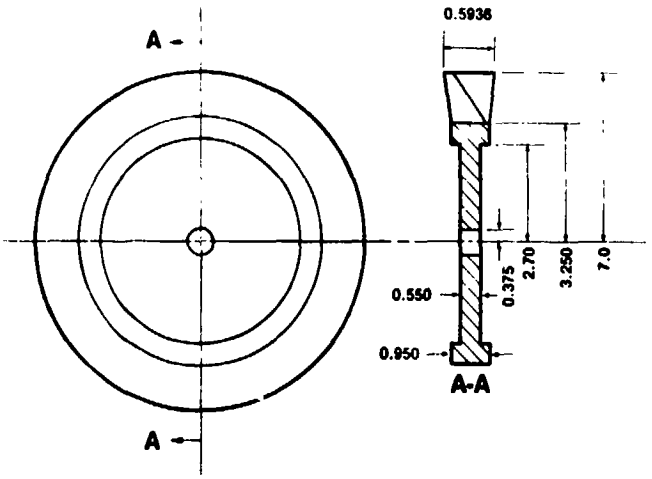

TYPE ROTOR: T-58 POWER TURBINE (MODIFIED, UNSLOTTED)
ROTOR WEIGHT: 11.8 LBS (AVG.)
ROTOR INERTIA: 151 LB-IN^2 (NOMINAL)

	DISK	BLADES
MATERIAL:	A-286	SEL-5
PROPERTIES:		
SU	157K psi	136K psi
SY	110K psi	116K psi
EU	12%	12%
HD	313 BHN	313 BHN

FIGURE A-2

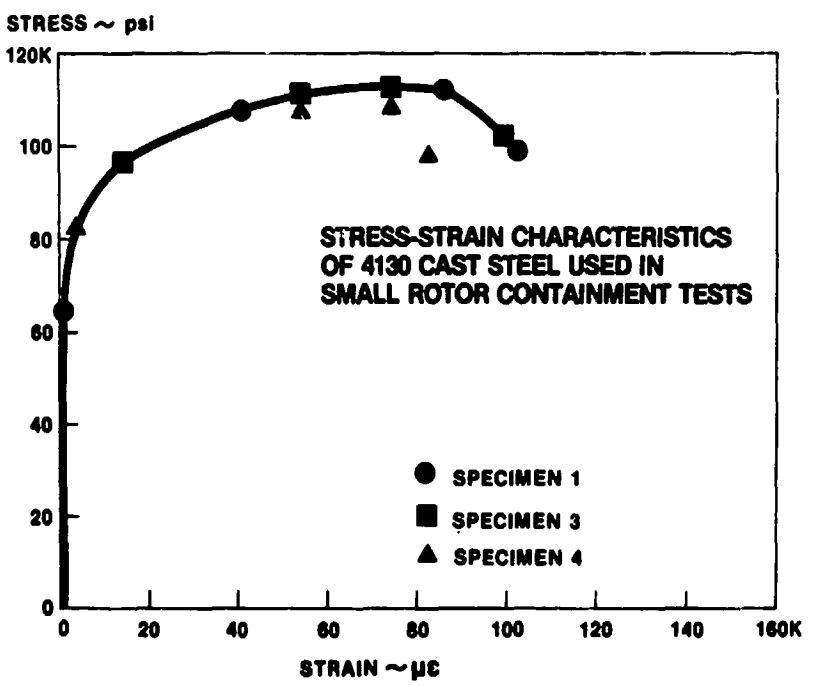

FIGURE A-3

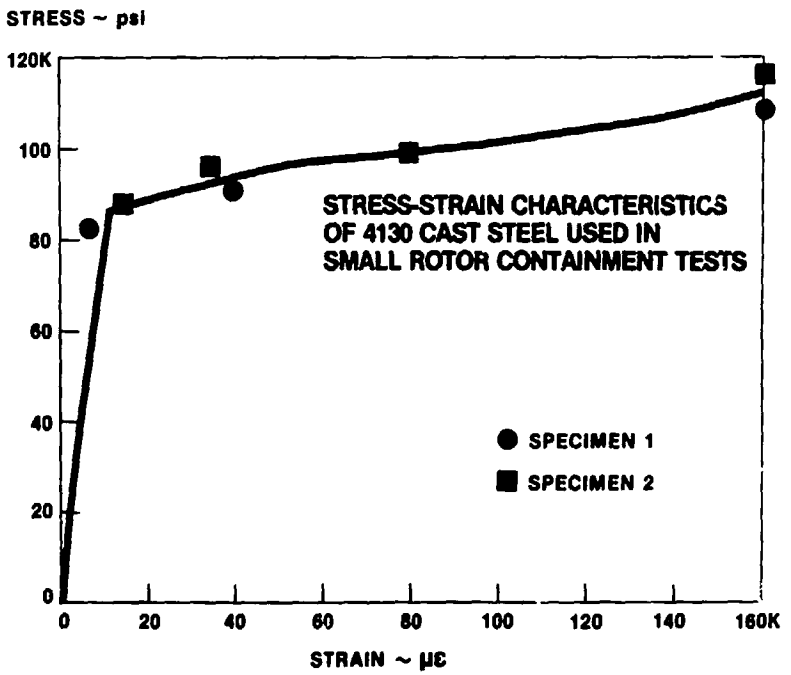

FIGURE A-4

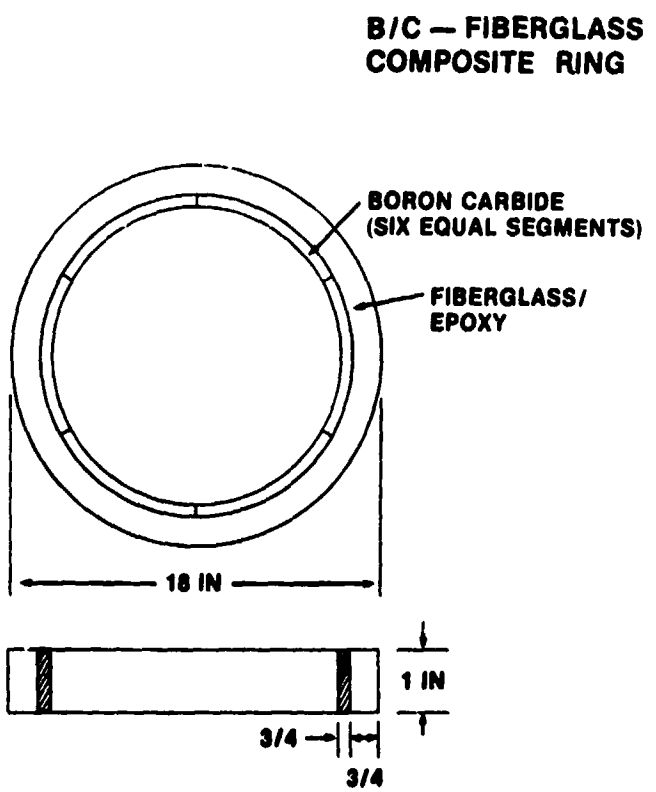

FIGURE A-5

STL-FIBERGLASS COMPOSITE RING

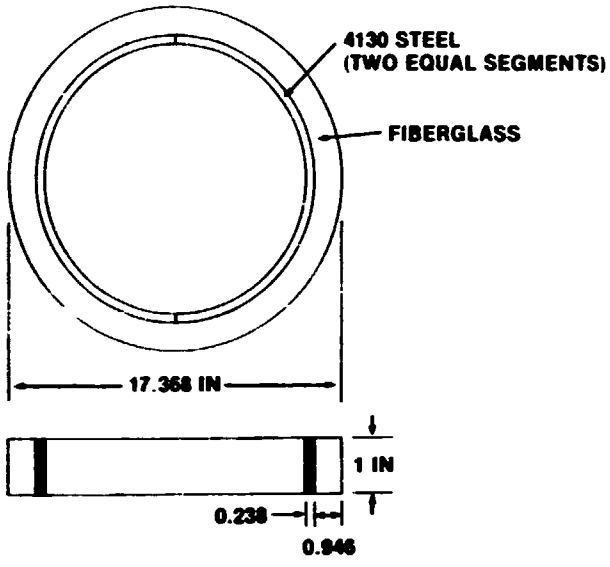

FIGURE A6

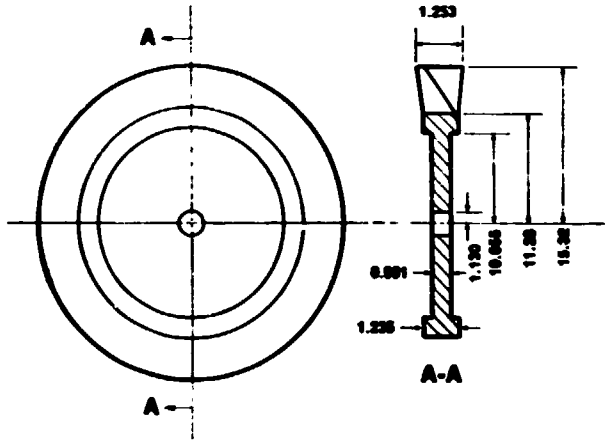

TYPE ROTOR: J-85 SECOND STAGE TURBINE
(MODIFIED, UNSLOTTED)

ROTOR WEIGHT: 127.75 LBS (APPROX.)

ROTOR INERTIA: 9410 LB-IN^2 (NOMINAL)

	DISK	BLADES
MATERIAL:	17-22A FERRITIC STEELS	INCONEL 700
PROPERTIES:		
SU	142K PSI	146.5K PSI
SY	128.5K PSI	132K PSI
EU	18%	18%
HD	311 BHN	311 BHN

FIGURE A-7

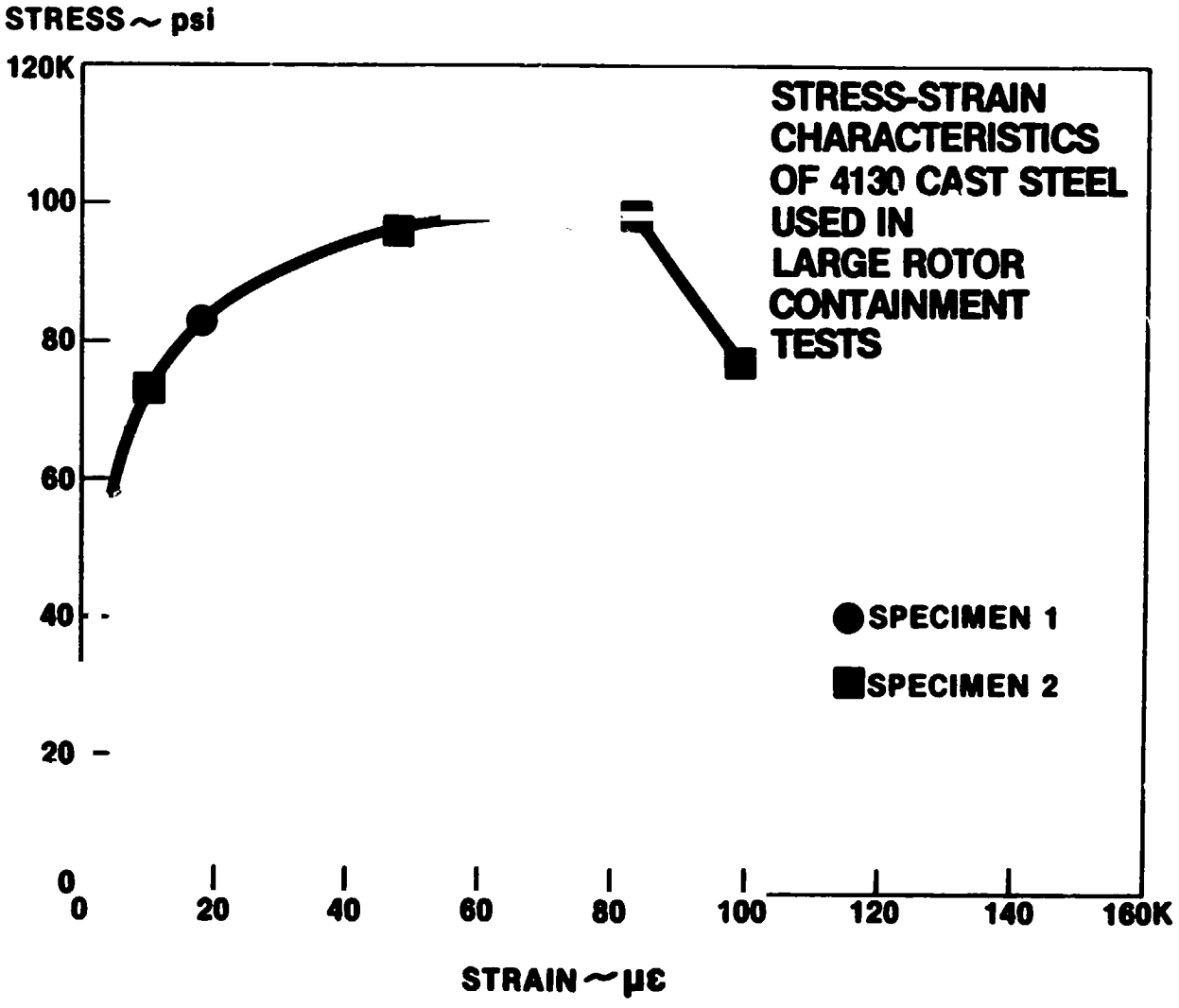

MOTIVATION FOR RBPP STEMS FROM THE ROTOR FAILURE SITUATION IN COMMERCIAL AVIATION.

POWERPLANT

DATE	STATUS	CAUSE	ATA	AIRCRAFT TYPE	AIRCRAFT NO.	SEQUENCE NO.
12-27-76	Orig-Open	PAR	7230	CV-580-31	73102	01107023

TEXT:
BIL. On arrival, crew reported the left engine oil quantity went to zero. Feathered the left prop. Maintenance found metal in the engine tail pipe. Replaced left engine.

SPECIFIC PART CAUSING PROBLEM

PART NAME	PART NUMBER	MANUFACTURER	SERIAL NO.
[redacted]	[redacted]	[redacted]	[redacted]

COMPONENT/APPLIANCE HAVING PART INSTALLED ON	PART LOCATION	BUS PART NO.
[redacted]	[redacted]	[redacted]

CONDITION CODE	MANUFACTURER	BUS PART NUMBER	SERIAL NO.
[redacted]	ALLSN	501D13H	501671

DATE	STATUS	CAUSE	ATA	AIRCRAFT TYPE	AIRCRAFT NO.	SEQUENCE NO.
12/26/76	ORIG OPEN	UNK	7200	DC-10-10	1002U	01107024

TEXT DEN-NO. 2 ENGINE FLAMED OUT ON TAKEOFF. FOUND METAL IN SCREEN. REPLACED UNDER INVESTIGATION

SPECIFIC PART CAUSING PROBLEM

PART NAME	PART NUMBER	PART DESCRIPTION	PART LOCATION
[redacted]	[redacted]	[redacted]	[redacted]

COMPONENT/APPLIANCE HAVING PART INSTALLED ON	PART NO.	ITEM NO.
	[redacted]	[redacted]

CONDITION CODE	MANUFACTURER	BUS PART NUMBER	SERIAL NO.
	[redacted]	CF6-6	A51368

DATE	STATUS	CAUSE	ATA	AIRCRAFT TYPE	AIRCRAFT NO.	SEQUENCE NO.
12/26/76	Orig-Open	MMAS	72-30	B720-027	7209U	01107025

TEXT

New: Aborted takeoff DTW due to suspected #4 engine compressor stall on power application. Cause under investigation.

SPECIFIC PART CAUSING PROBLEM

PART NAME	PART NUMBER	PART DESCRIPTION	PART LOCATION
[redacted]		[redacted]	[redacted]

COMPONENT/APPLIANCE HAVING PART INSTALLED ON	PART NO.	ITEM NO.
	[redacted]	[redacted]

CONDITION CODE	MANUFACTURER	BUS PART NUMBER	SERIAL NO.
[redacted]	PWA	JT3C-7	682772

THE INCIDENCE OF UNCONTAINED ROTOR BURSTS IN U. S. COMMERCIAL AVIATION 1962 – 1976

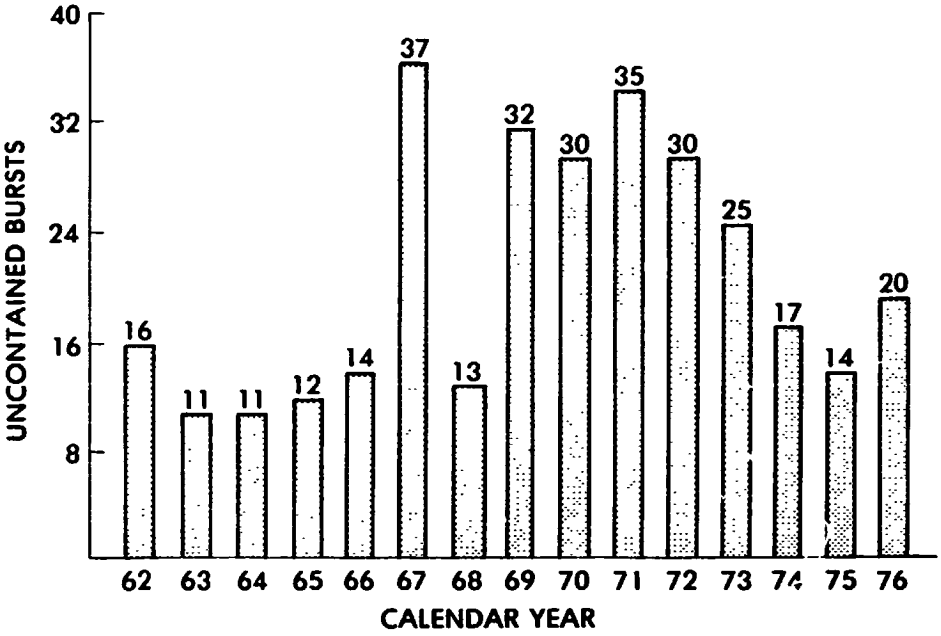

INCIDENCE OF ROTOR FAILURE/BURST IN U. S. COMMERCIAL AVIATION 1975

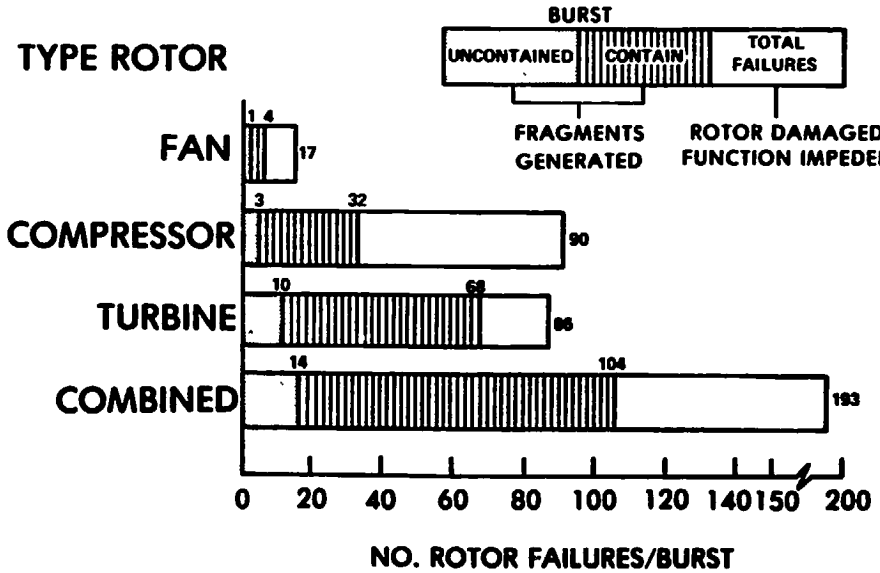

COMPONENT AND FRAGMENT TYPE DISTRIBUTIONS FOR CONTAINED AND UNCONTAINED ROTOR BURSTS[1]—1975

ENGINE ROTOR COMPONENT	TYPE OF FRAGMENT GENERATED								TOTALS	
	DISK		RIM		BLADE		SEAL			
	TF	UCF	TF	UCF	TF	UCF	TF	UCF	TF	UCF
FAN	0	0	0	0	4	1	0	0	4	1
COMPRESSOR	1	1	1	0	30	2	0	0	32	3
TURBINE	5	5	1	0	60	4	2	1	68	10
TOTALS	6	6	2	0	94	7	2	1	104	14

(1) FAILURES THAT PRODUCED FRAGMENTS

TF - - TOTAL FAILURES
UCF - - UNCONTAINED FAILURES

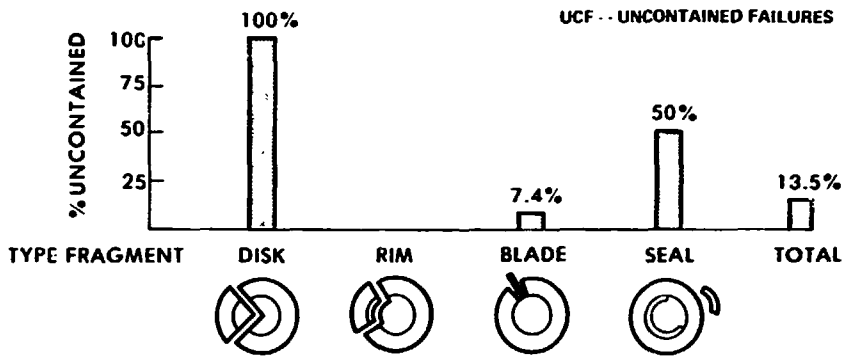

THE INCIDENCE AND RATE OF ROTOR BURST[1] IN U.S. COMMERCIAL AVIATION ACCORDING TO ENGINE TYPE AFFECTED — 1975

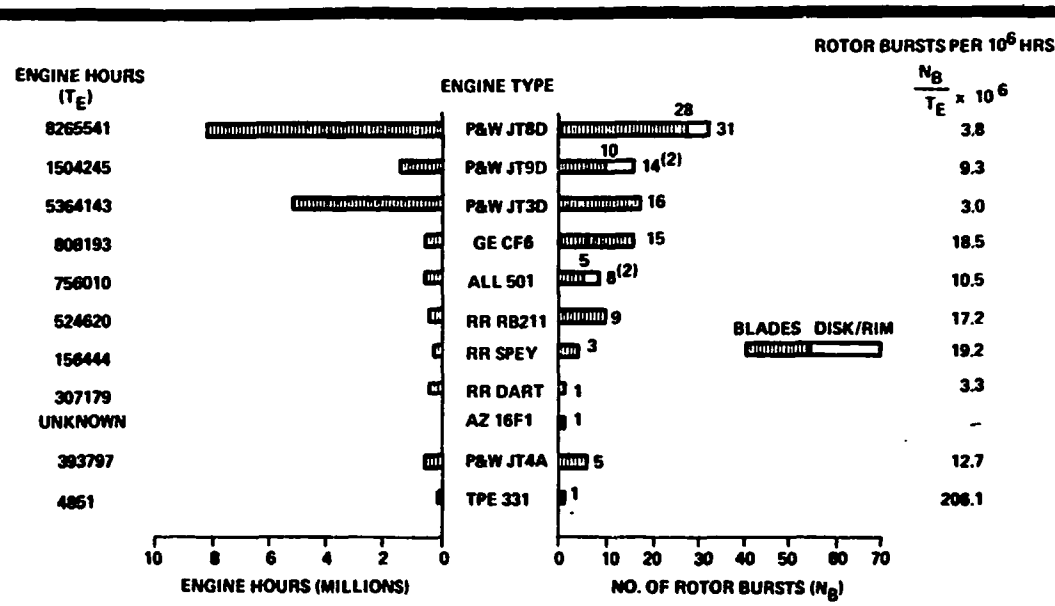

(1) Failures that produced fragments
(2) 1 Seal Burst included in Disk/Rim compilation

ROTOR FAILURE/BURST CAUSE CATEGORIES — 1975

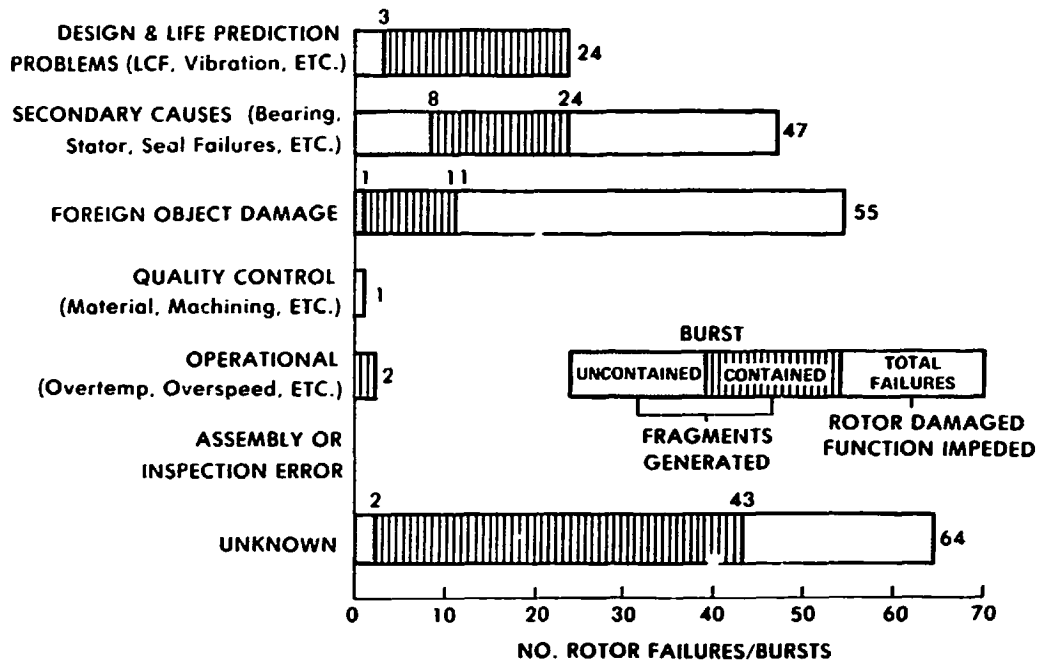

FLIGHT CONDITION AT ROTOR FAILURE/BURST — 1975

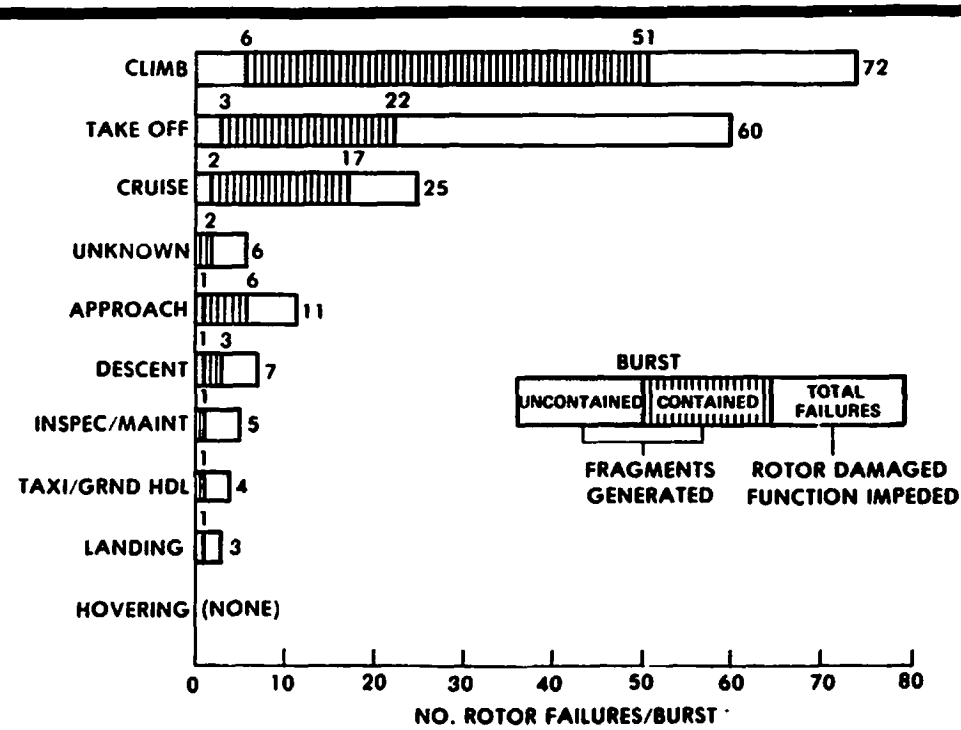

SUMMARY ANALYSIS OF ROTOR BURST
INCIDENCE AND RATE FOR 1975

FACTS:

- TOTAL NO. ENGINE SHUTDOWNS - 2305
- NO. ROTOR FAILURES - 193
- NO. ROTOR BURSTS (1) - 104
- NO. UNCONTAINED ROTOR BURSTS - 14
- A/C FLIGHT HOURS - 6×10^6
- ENGINE FLIGHT HOURS - 19.2×10^6

ANALYSIS:

- PERCENT ROTOR FAILURE INDUCED ENGINE SHUTDOWNS - 8.4%

	PER 10^6 A/C HRS	PER 10^6 ENGINE HRS
• ROTOR FAILURE RATE	32	10
• ROTOR BURST RATE	17	5.4
• UNCONTAINED ROTOR BURST RATE	2.3	.73

(1) FAILURES THAT GENERATED FRAGMENTS

DATA ON AIRCRAFT FLIGHT HOURS AND UNCONTAINED ROTOR BURST RATE, U.S. COMMERCIAL AVIATION 1971-1976

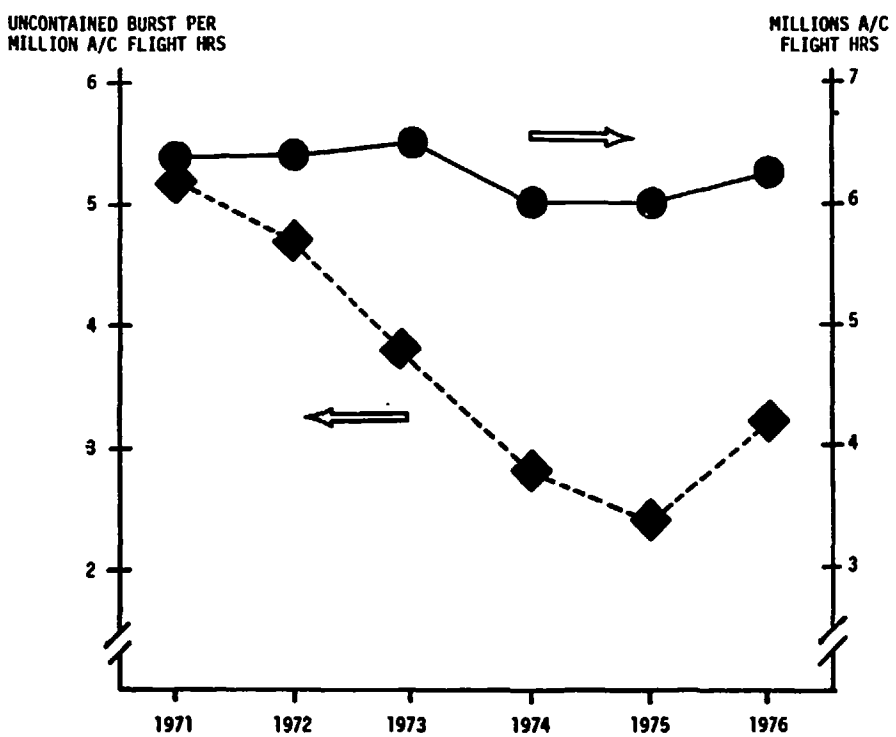

DISCUSSION

J. Meaney, Rohr

First, was the Kevlar ring made with epoxy binding? Second, did you ever test these rings with radial supports; don't you feel that not having radial supports could be unconservative inasmuch as you allow the ring to deform to a much greater manner than if it were part of a "long" container?

G.J. Mangano, NAPTC

In answer to the first question, the Kevlar that we used was a fabric wound on a diagonal with no binder. A thin inner aluminum cylinder was used to provide shape.

Concerning the second question, some preliminary tests in which we purposely added radial constraints were conducted. We found that it wasn't a weight-effective configuration. That is, it weighed more than a freely-supported ring that provided the same degree of containment for identical burst conditions.

J. Meaney, Rohr

Well, the point I was trying to get at was that some of the rings that you showed that actually contained the fragments were greatly deformed. But if the ring had a "large axial length" and was supported on casing or bracket structure, would not this support influence the containment ability?

G.J. Mangano, NAPTC

That was why we went through the exercise of trying to determine the optimum ring axial length with respect to weight. An optimum was found when the axial length ratio between the rotor axial length and the ring axial length was one. Ratios of one-half, one, and two were investigated for a one-inch wide rotor. We evaluated the effect of axial length on the containment process and found an optimum with respect to weight at a rotor to ring axial length ratio ratio of one.

R. Bristow, Boeing

I would like to make a comment on that last question. A Kevlar shield must deform quite a bit more than a steel shield, and we were worried about how some of the aircraft structure might restrain the Kevlar shield such that the fragment punches a hole or chews its way through. We put some honeycomb material behind the Kevlar on some of our tests to simulate the sound suppression material. On some of these, we had two layers of sixteenth inch aluminum with honeycomb in between, so that the whole honeycomb panel was about an inch thick. The Kevlar did not fail under that condition; it blew the honeycomb apart and continued to expand. These were ballistic type impact tests, not engine rotor burst impacts.

B.L. Koff, GE-Cincinnati

These disk impact tests were conducted by bursting a rotor between two

steel plates and having the segments impact on a steel ring. In an actual engine, that ring cross-section is not held rigidly and would roll and let the disk segments slip by. As a result, it would take three or four times the ring weight if the axial length effect is included to achieve containment, because in the engine the disk is not guided between two solid steel plates. The disk moves radially outward but the fragment could twist the ring and deflect right past it. That's one point.

The second point is that if you're talking about containing turbine disks, it seems that you should only experiment with materials (if you're going to pack it down tight around the rotor) that can take the temperature environment in the turbine section of the engine.

G.J. Mangano, NAPTC

Yes, I agree. These tests are somewhat abstract; they are not intended to provide final design information, but rather to explore containment ring behavior under conditions of actual engine rotor fragment attack. Because this was a first attempt at providing general design guidelines, it didn't take into account more specific variables such as engine mounting effects, temperature effects, etc.

S. Sattar, P&W

To follow up the previous question -- in an engine, you may not get an axisymmetric failure where fragments are trying to load the ring in a hydrostatic pressure manner. Quite often the fragments want to apply not only hydrostatic pressure on the ring, but want to twist it. If you had supported the containment ring in the manner that the engine sees it, quite often I think a Kevlar ring which might be very effective to contain pressure, may buckle under the very large torque loads that these pieces will impart. An engine rotor may not burst perfectly; all the pieces may not be released. You might lose maybe one-third of it in pieces, and the other two-thirds might stay on the rotor. I wonder if you'd like to comment on that.

G.J. Mangano, NAPTC

High-speed photo results taken of the containment process and examination of the rings after testing indicate that ring loading by a symmetrical rotor burst is not hydrostatic. In fact, highly local and considerable bending of the ring occurs outwardly at the disk impact sites and inwardly at points approximately midway between the impact sites. A symmetrical three-fragment burst, for example, will cause six local bending sites: three inward and three outward. For two-, three-, and six-fragment symmetrical bursts, the loading is symmetrical to be sure but is far from being what can be considered hydrostatic. This is evident from Figs. 9, 10, 11, and 16 of our paper. As the numbers of fragments involved in the burst increases much beyond six, the ring loading would tend to be hydrostatic, but within the scope of our experience, highly fragmented disk bursts in service tend to be the exception rather than the rule.

I have no direct experience with the mechanics of asymmetric burst containment, but it would seem that this type of failure would more likely load larger areas of the ring in a hydrostatic manner than would a symmetric burst.

In order to minimize the weight of ring used for containment, whether it is made of steel or Kevlar, the ring should be allowed to deform and displace freely during the fragment interactions so as to take maximum advantage of the energy that can be absorbed in the distortion process. Where weight is to be minimized, this concept dictates that the ring installations on an engine should approach that which was used for test; namely, freely supported. Under these conditions the Kevlar ring did admirably well in containing the fragments at minimum weight.

P. Gardner, Norton Co.

Why did you limit your studies of Kevlar to Kevlar 29 and not 49?

G.J. Mangano, NAPTC

We did only exploratory testing of Kevlar: Boeing has provided us with the rings. We have conducted only four or five tests to date. Kevlar 29 was supplied and used.

J.H. Gerstle, Boeing

I might just add a comment to that. Boeing has tested both Kevlar 29 and 49. We did not see substantial differences.

A. Weaver, P&W

Concerning the weight effectiveness, with the increased axial widths of your rings, above the ratio of 1:1 that you cited, although the long rings are heavier, did the actual thickness for threshold containment decrease when compared with the 1:1 ratio case?

G.J. Mangano, NAPTC

Thickness required for containment at an axial length ratio of 2 was greater than for a ratio of 1. This is a surprising result.

Sol Weiss, NASA-Lewis

As you presented the containment data on the small wheel, I got the impression (I think you said this) that apparently the threshold containment weight did not depend upon the number of equal-size fragments. I think yesterday we heard some people intuitively say (and I think we all believe this) that if you decrease the size of the fragments and increase the number of fragments, you may have a better opportunity for containment at lower containment ring weight. Now, when you went to a large wheel, it seems that the number of fragments did have an effect upon containment capability. Now, with what we've done so far, can we conclusively say, that the number of fragments did not affect containment in the small wheel tests, but did in the large wheel tests?

G.J. Mangano, NAPTC

For the small-rotor containment tests, the results definitely indicate an independence between the weight of ring required for containment (or SCFE) and the number of fragments generated at burst. The large rotor test results tend to indicate the opposite.

A.K. Forney, FAA

Guy, if I may, I'd like to go back to the motivation portion of your presentation because I'd hate to have these experts leave here with an incorrect impression about the FAA sitting on all of this beautiful data. First, I'd like if you could, to put your slide back up that shows the causes of the uncontained rotor bursts. Could you, I'm going to ask you to show two things: one that SDR, and second: your causes.

Now, since he's found the SDR I'll go ahead with it first. I wanted you to see that you get very little information on an SDR; here you see just about all that you really ever get. Now, a few things about it that maybe you wanted to know. This one is "open"; it does mean that there will be a subsequent report. It says "under investigation" so that there will be another one that will close it. All three of these happen to be open and so we do get a subsequent report; it's interesting what some of these subsequent ones say. This one could very well say "engine torn down and inspected, insufficient stall margin". We have a little difficulty determining how the airline's overhaul shop determines by inspection that the hardware had an insufficient stall margin (that it obviously did have insufficient stall margin under the conditions that caused it to stall). We in FAA engineering have found that we cannot use the SDR's to provide us with any engineering information. All the SDR's can do is tell us that something happened, and if we want to get details, we really do not depend on the SDR. Now there are several reasons. One is they don't have very much more detail than you see here. Secondly, all of this is fed into a computer and the computer is not programmed, for example, to let us pull out "uncontained failures". So if it does not specifically happen to mention it (and frequently you can't tell from the SDR whether the rotor failure was contained or not) the SDR really is of no value there. Then (and maybe I should have started out here) these things are submitted by an air carrier (that's the FAA term for airlines). They are required by the regulations to report certain things that occur, and one of the things they are required to report is all of the in-flight shutdowns of engines. Now, it's interesting, what is in-flight; there's a fuzzy area. If something requires them to shut an engine down before rotation, then some of the airlines don't record it; it wasn't in-flight so it wasn't an in-flight shutdown. But you know, we're interested in what happens to the engines just the same but we don't often get the reports. So having made my comment, I would like to ask you how you determined the causes. Did you attempt to determine the causes from SDR's, or did you do it like we do, use the SDR to alert yourself to an incident and then go back not even to the airline but to the engine company? Experience has shown us that we get the best information on what really happened and what the causes were by going back to the engine manufacturer whose engine was involved. I do not know enough of your work to know how you're doing that.

G.J. Mangano, NAPTC

Let me explain our procedures to you. I agree with you, there isn't very much information in the SDR, but there is enough to give us some measure of what's happening. When there's any controversy as to whether or not a fragment was contained or if fragments were generated, we just don't include it in our analysis. We operate to the limits of what the SDR has to offer, nothing more. If the SDR doesn't have the cause (and this is FAA data), if it doesn't stipulate what the cause is, then we do not use it. This is evidenced

by the preponderance of "unknowns" that we have here; the "unknown" category is far and away the largest category. We compile data to the level of what the SDR provides. However, this compilation gives a reasonably good indication of what's going on. I do not think that our compilation is nearly as extensive as that of the SAE committee; theirs is a very fine effort, and a very welcome one. Our tabulation is intended to keep our finger on the pulse of the situation; the data are no better than the information provided by the FAA. Now, Bob DeLucia is in charge of reducing this information, I would like to ask if he has any comments to make.

R. DeLucia, NAPTC

I'd just like to address one point. As of June of last year we got together with the FAA in Washington and explained the problem that we're having identifying uncontained rotor bursts. They are sympathetic and as of last year, they have included a code letter T, which means "engine case punctured". So any subsequent SDR, say from about last June to the present will have a code letter "T" in the computer runoff sheet if a fragment penetrated the engine casing and came out.

A.K. Forney, FAA

I would like to express publicly my appreciation to the Navy for that. First of all, I didn't know that; I'd be interested in knowing who in FAA headquarters you talked to. But our maintenance people, not engineering, looked after this program. When the SAE Committee's activities started, we asked them to pull out of the computer all of the uncontained failures, and they couldn't. We tried officially from engineering and maintenace to get the program changed to identify uncontained failures, and we were unsuccessful. So the fact that you now have done it, I want to express my appreciation publicly, but I'd like to know who you did it with so I can find out the details of it.

G. Gunstone, CAA-FAA

I would just like to say that the last question reinforces yesterday's plea that the constructors should get together to supply a consistent set of data which could be used by all. We are all fumbling around with insufficient, incomplete, inaccurate data. It is quite silly that we should be in that position, and I hope that a strong recommendation for a consistent data input will come from this meeting.

H. Garten, GE-Lynn

I would just like to reinforce some of the other technical comments about the tests. It seems to me that the first series of tests with the small turbine wheel were really hydrostatic tests. If you had bothered to measure the length of the shield after testing, you might have found that it was quite long, (circumferentially long) as compared to the original circumference, because most of the strain energy went into tension. Now, when you got to the larger rotor, you had to build your ring shield very deep, and the shield failed before it ever could support the hydrostatic load in tension, and it failed in bending. So I just wonder if you had considered comparing a metal shield with a Keval shield, building a metal shield in layers so that you would get more strain energy into tension and less strain energy into bending?

G.J. Mangano, NAPTC

Herb, in fact, we did run layered rings. The results were not presented here because those tests were exploratory and not part of a systematic testing effort. As an abstract idea they worked well but appear not to be a practical configuration.

J.H. Gerstle, Boeing

I'd like to make a comment about the separate-rings tests -- I happen to have seen those three concentric rings which the Navy tested, and which worked. I believe that the three rings responded similarly to a Hopkinson bar apparatus with the outer ring doing the momentum trapping. That is, the stress waves will first propagate in the thickness direction of the three rings and will be trapped in the outer ring after it separates, causing it to break while leaving the second ring intact. However, this is not a practical method.

G.J. Mangano, NAPTC

There was a question about the relative ductility of the ring material for the small rotor vs. the large rotor containment tests.

As a matter of fact, I think the materials used for the large rotor tests were less ductile. We have some curves and they're contained in the paper. The material was centrifugal cast 4130 steel. Random samples of the material were taken and subjected to standard ASTM X-ray tests for defects -- none were found. We were concerned about porosity problems. We ran some containment tests on wrought steel rings, and found large rotor threshold containment at a weight of about 135 pounds vs. about 168 pounds for the cast 4130 steel. We did not use titanium for containment tests. As someone mentioned, containment testing under high temperature conditions would be useful.

What we'd like to do to close the loop is, perhaps, run a few more baseline tests using a better steel, perhaps such as a wrought alloy that isn't subject to defects and has better ductility. Then we plan to go on to composites, which Art Holms is going to cover, in a paper later on. We shall explore Kevlar. We are not looking at a particular design but want to provide generally applicable guideline information that will be useful. We would welcome your comments on how we can make the tests more realistic without incurring excessive costs, and without focussing on a particular application or problem. We are looking for rules that will be generally applicable and useful to the aircraft community.

H. Garten, GE-Lynn

I don't know why you're not looking at titanium because titanium is incorporated in some of the fan engines.

G.J. Mangano, NAPTC

We agree with you and Denis McCarthy that titanium does appear to merit attention for containment applications. Some selected testing would be useful.

A. Holms, NASA-Lewis

I have a comment. One question dealt with unsymmetrical bursts. It seems

to me that the symmetrical burst is the more severe test of the ring. Mainly with an unsymmetrical burst, you probably have one piece flying out with a lot of translational energy and velocity, but the big piece has a lot of stored rotational energy which it can give up over a longer period of time, dissipating its energy with rubbing friction. So it seems to me that an unsymmetrical burst would be a less severe test than a symmetrical burst.

On the question of the X-rays of the castings, the pieces that were X-rayed were about one and a quarter inch thick with the X-ray beam going through the one and a quarter inch direction. I think that was a reasonable nondestructive test of the material. It is true that the larger castings were more difficult castings than the small castings. The elongation in the tensile specimens from the small casting was quite a bit larger than the elongation from the large casting specimens. That may explain our size effect. But, on the other hand, workers in fracture mechanics often do find size effects in the work they do.

The body armor data that's been gathered by the Dept. of Defense shows that titanium is much superior to most steels for high velocity impact in the range of 2,000 or 3,000 feet per second. Put if you get down around 500 feet per second, titanium is no longer superior.

ANALYSIS OF SIMPLE 2-D AND 3-D METAL STRUCTURES SUBJECTED TO FRAGMENT IMPACT*

E.A. Witmer, T.R. Stagliano, R.L. Spilker, and J.J.A. Rodal

Aeroelastic and Structures Research Laboratory
Department of Aeronautics and Astronautics
Massachusetts Institute of Technology

SUMMARY

Reviewed in this paper are studies carried out and/or in progress at the MIT Aeroelastic and Structures Research Laboratory to develop theoretical procedures for predicting the large-deflection elastic-plastic transient structural responses of metal containment or deflector structures to cope with rotor-burst fragment impact attack. Most of the past effort was devoted to containment/deflector (C/D) structures whose axial dimension is comparable to that of the attacking fragments and hence the associated structural responses are essentially two-dimensional. Recent effort has been applied to analyzing C/D structures whose "axial dimension" is much larger than that of the attacking fragments; thus, the associated structural response to be analyzed is essentially three-dimensional.

For two-dimensional C/D structures both finite-element and finite-difference analysis methods have been employed to analyze structural response produced by either (a) prescribed transient loads or (b) fragment impact. For the latter category, two time-wise step-by-step analysis procedures have been devised to predict the structural responses resulting from (a succession of) fragment impacts: (1) the collision force method (CFM) whereby one utilizes an approximate prediction of the force applied to the attacked structure during fragment impact (also equal and oppositely to the fragment itself) and (2) the collision imparted velocity method (CIVM) in which one computes the impact-induced velocity increment acquired by a region of the impacted structure near the impact point (and the attendant velocity decrement suffered by the attacking fragment). The merits and limitations of these approaches are discussed. For the analysis of 3-d responses of C/D structures, only the CIVM approach is being investigated.

Experimental data for assessing the accuracy, limitations, and versatility of these analyses have been obtained from two sources. The Naval Air Propulsion Test Center has provided data on the responses of containment rings to (a) a single T58 turbine rotor blade and (b) to tri-hub burst fragment attack from a T58 turbine rotor. Simpler impact experiments involving a "non-deformable fragment" (a solid steel sphere) against simple aluminum beams and panels have been conducted at the MIT Aeroelastic and Structures Research Laboratory. Comparisons of predictions with observed structural response data are discussed.

* This research has been supported in large part by the NASA Lewis Research Center under NGR 22-009-339; the authors wish to acknowledge also the help of their various colleagues (see co-authors cited in references of Appendices A and B).

1. Introduction

Engine rotor burst fragments may impact against the engine casing and/or against special protective structures. These structures may be intended either to contain or to divert the fragment and to allow it to escape along a "harmless" path; the respective behavior is termed as being either fragment containment or fragment deflection. Of principal interest in this paper is the theoretical prediction of container or deflector structures (C/D structures) which are subjected to fragment impact. Further, attention is restricted to single-layer metallic protective structures; the use of non-metallic materials for protective structures undergoing fragment impact is addressed by several other papers in this Workshop.

If the dimension of the protective structure in the direction parallel to the axis of rotation of the turbojet engine is comparable to the corresponding dimension of the attacking fragment, the deflection of the attacked structure will be essentially the same at all locations along that axial direction; in this case, the deformation is termed two-dimensional (2-D). However, if that protective-structure dimension is large in the above comparative sense, the structure will undergo general three-dimensional (3-D) structural deflections.

For preliminary design and parametric studies of C/D structures, it may be useful to idealize the transient structural response as 2-D, as depicted schematically in Fig. 1. Here the effect of the structure which supports the C and/or D structure is represented by a normal and tangential spring foundation; also, various support conditions can be provided in this type of idealized 2-D model. This type of model tends to include the main structural response features while minimizing the computational burden. Accordingly, a series of 2-D structural response codes for partial and/or complete rings of arbitrary initial shape, with uniform or nonuniform thickness, and subjected to initial-velocity distributions, prescribed externally-applied loads, or fragment impact have been developed. The capabilities and features of these computer codes [1-5]* are summarized in Appendix A. Some illustrative examples of the use of some of these codes are shown later in this paper.

For structural response conditions wherein the use of a 2-D idealization is an excessive over-simplification and where one seeks to predict the response in greater detail, the structure needs to be modeled as an assemblage of shell elements (and stiffeners) [6-8] to enable an accounting of the 3-D shell

*References are indicated by numbers in square [ ] brackets.

structural deflections which are present. On the other hand an excessively fine modeling such as the use of 3-D solid elements to represent a single-layer shell, stiffeners, etc. leads to an excessive computational burden for many purposes. Hence, "shell behavior" modeling serves as a logical "next improvement" over 2-D modeling of C/D structures. Accordingly, theoretical prediction methods to compute the responses of plates and shells to initial velocity distributions and prescribed externally-applied transient loads [6] are being adapted to predict structural response to fragment impact [9].

In order to evaluate the accuracy and adequacy of these structural response prediction methods, various experiments have been carried out. The Naval Air Propulsion Test Center (NAPTC) has provdied data on the responses of aluminum and steel containment rings to (1) impact by a single T58 turbine rotor blade and (2) to tri-hub burst fragment attack from a T58 turbine rotor ([10-13], for example); in these cases the attacking fragment is complex and undergoes a considerable amount of deformation during its impact interaction with the containment ring. A cleaner, less-complex set of impact experiments has been conducted at the MIT Aeroelastic and Structures Research Laboratory, involving steel-sphere impact against (1) beams, (2) uniform-thickness initially-flat square aluminum panels, and (3) panels of type (2) but with integral stiffeners of rectangular cross section; transient strain, permanent strain, and permanent deflection data of good reliability and accuracy for comparison with predictions were obtained [14,15]. Some of these studies are described briefly in the following.

At the present time, theoretical-experimental correlation studies utilizing the NAPTC and the MIT-ASRL experimental data are in progress for the 2-D cases; for these cases the CIVM-JET 4B computer code is being employed. For fragment-impact panels (which undergo 3-D responses), some preliminary calculations are under way using the breadboard CIVM-PLATE code; systematic testing and checking of this code will be required before it can be used with confidence.

Figure 2 serves as a concise outline of most of the MIT-ASRL studies which have been carried out to date concerning the theoretical prediction of the responses of metallic C/D structures to fragment impact. Listed in Appendix B are the associated MIT-ASRL reports and papers, as well as the status and availability of the pertinent structural response computer codes.

Section 2 is devoted to describing two of the analysis methods (the collision imparted velocity method CIVM, and the collision force method CFM) studied for predicting the large-deflection, elastic-plastic, transient responses of 2-D structures which are subjected either to impulse loading or to fragment impact attack; illustrative examples of the application of these methods are shown, with emphasis on the CIVM approach. Section 3 deals with theoretical and experimental studies of fragment-impact-induced responses of panels which undergo 3-D structural responses. Comments are given in Section 4 concerning the status of structural response prediction procedures for 2-D and 3-D single-layer metallic C/D structures, as well as observations concerning analysis needs for multilayer multimaterial C/D concepts and configurations being considered as lighter weight candidates to cope with energetic engine rotor burst fragments.

2. 2-D Structural Response Studies

Some representative analyses and results will be illustrated here concisely; more extensive results and discussion may be found in the cited references. Analysis of 2-D structural response to fragment impact will be discussed for two approaches: the collision imparted velocity method (CIVM) and the collision force method (CFM); for illustration, both approaches are applied to analyze the transient response of a containment ring to impact by a single blade of a turbine rotor. Next, a more complex fragment attack is analyzed by using the CIVM approach; this involves T58 tri-hub turbine rotor burst attack against a steel containment ring. Because of the complexities arising mainly from severe changes in the geometries of the attacking fragments during the impact and interaction process, it became advisable to obtain experimental data for a more clearly defined impact situation in order that the measured transient response information could be used to make a clear assessment of the adequacy of the basic building blocks contained in the theoretical prediction procedure. Accordingly, described next are experimental and theoretical studies of the transient responses of simple beams to impulse loading or to steel sphere impact attack.

2.1 Single Rotor Blade Impact Against a Containment Ring

In these studies of 2-D structural response to impact, use is made of finite element and finite difference methods which have been shown to produce

reliable predictions for large-deflection, elastic-plastic, transient response of simple beams and rings subjected to known impulsive loading [16,17]. For impact-induced structural response analysis, the principal added ingredient to be taken into account is the impact/interaction itself; two methods (CIVM and CFM) explored for treating this matter are discussed next.

To illustrate these approaches, impact of a single blade from a T58 turbine rotor against a containment ring will be studied. High speed photographic data for such a case have been obtained at the spin-chamber facility of the Naval Air Propulsion Test Center [10]. Ring configuration data and blade orientation as a function of time at intervals about 30 microseconds apart were obtained and are used for illustrative comparisons.

2.1.1 Analysis with the Collision Imparted Velocity Method

Figure 3 illustrates a containment ring which is modeled by a number of finite elements and subjected to impact attack by an idealized single rotor blade. The equations of motion for the ring and for the fragment are solved in small increments Δt in time by an appropriate finite-difference time operator scheme. For this analysis, the fragment is regarded as being rigid. Impact is regarded as being an instantaneous local effect between the fragment and a small region of the structure in the vicinity of the impact point; for present purposes, the size of this small ring region on either side of the impact point is estimated as being the product of Δt and the longitudinal elastic wave speed in the ring. Impulse/momentum and kinetic energy conservation equations are used to calculate the "post-impact" (or collision-imparted) velocities of the fragment and of this impact-affected structural region; by employing the concept of the coefficient of restitution (e) this local impact can be treated as perfectly elastic (e=1), perfectly inelastic (e=0), or intermediate ($0<e<1$).

Figure 4 is an information flow diagram illustrating the use of this "collision-imparted velocity method" (CIVM) in the calculation of transient structural response produced by fragment impact. Typically, a succession of impacts is predicted. Fuller details of this approach are given, for example, in Refs. 4, 17, and 18.

Table 1 summarizes the containment ring and fragment data for the illustrative case: NAPTC Test 91. Shown in Fig. 5 are predicted and measured deformed ring configurations and blade locations at 150, 570, and 810 microseconds after initial impact. In the impact quadrant the ring was modeled by 10 equal length

cubic-cubic elements; 6 equal-length elements were used in each of the 3 other quadrants. For these calculations, coefficients of restitution of e=0 and e=1 were used. The 6061-T6 aluminum ring material was regarded as elastic, perfectly-plastic, with a strain-rate (EL-PP-SR) dependent yield stress σ_y given by the following approximation:

$$\sigma_y = \sigma_o[1 + |\frac{\dot{\varepsilon}}{D}|^{\frac{1}{p}}]$$

where σ_o is the static yield stress, $\dot{\varepsilon}$ is the strain rate, and D and p are material constants. For these calculations, D=6500 sec^{-1} and p=4 were assumed. Also, frictionless impact and interaction (μ=0) between the ring and the blade was assumed for the cases illustrated here. Fairly good agreement between the predicted and observed deformed ring configuration is noted, but the predicted vs. observed fragment motion is not good. This latter disagreement stems mainly from ignoring friction and the changing mass moment of inertia of the actual deforming blade. Later calculations included these effects.

2.1.2 Analysis with the Collision Force Method

In this method the attacking fragment is treated as being deformable. Shown, for example, in Fig. 6 are some postulated idealized configurations to represent a deformable impacting blade. The straight rigid blade model was used in the previous case. Explored in Ref. 19 were the following two idealizations -- the blade was assumed (a) to remain straight but to shorten in an elastic, perfectly-plastic (EL-PP) fashion or (b) to curl in a simple plausible assumed-mode fashion; these are termed, respectively, the elastic, perfectly-plastic shortening blade model (EL-PP-SB) and the elastic, perfectly-plastic curling blade model (EL-PP-CB). These modes of behavior combined with a step by step collision inspection set of rules permitted following this process. At any given instant, applicable values of governing geometric deformed-blade-configuration parameters were identified. These in turn were related via energy methods to the component of the force applied by the blade perpendicular to the surface of the attacked containment ring and equal-and-oppositely to the fragment itself. Similarly, equal and opposite tangential forces (from friction) were postulated to be μ times the normal-to-the-surface component. A self-explanatory information flow chart for the CFM process is given as Fig. 7.

Shown in Fig. 8 are defomed ring predictions at two instants after initial

impact for the EL-PP-SB model and the EL-PP-CB model for the case in which the friction coefficient μ is assumed to be .15 and the perfectly-plastic yield stress of the steel-alloy blade is assumed to be σ_{y_f} = 160,000 psi. Fairly good agreement between experiment and these EL-PP-CB model predictions is observed. Reference 19 shows the ring response to be rather insensitive to (plausible) values of friction coefficient used. The motion of the blade, however, is much more sensitive to μ -- as Fig. 9 indicates.

The curling blade model [19] devised by plausible engineering rules and approximations appears to represent rather well the behavior and the observed deformed configuration of the actual single blade in NAPTC Test 91. One must keep track of the time-varying geometry of both the deforming blade and the deforming containment ring in order to determine when and where the successive collisions (i.e., attempted simultaneous occupancy of some regions of space) occur. Hence, it is evident that if one were to use this method to analyze structural response to impact by, for example, a disk-rim fragment with perhaps 3 to 10 attached blades (each of which will undergo sequential different deformations), one would be faced with a substantial book-keeping job to define the space occupancy of this complex deforming fragment; the advisability of seeking a less complex scheme is clear. Accordingly, subsequent attention has been given to the use of greatly-idealized rigid fragments in conjunction with the CIVM analysis scheme.

2.2 CIVM Analysis of Tri-Hub Rotor Burst Attack Against a Containment Ring

One type of postulated engine rotor fragment attack which has received much discussion is that in which the rotor bursts into 3 equal segments (termed a tri-hub burst). One fragment of this type is shown schematically in Fig. 10. The NAPTC has conducted many tests involving tri-hub burst attack against various single-layer and multilayer containment rings. Recently NAPTC Test 201 involving tri-hub burst attack of a T58 turbine rotor at 19,859 rpm against a cast 4130 steel containment ring of 7.50-in inner radius, 0.625-in thickness, and 1.50-in axial length was conducted [13]. Figure 11 shows the post-test deformed-ring configuration. High speed photographs showed the severe deformation incurred by many of the blades during the impact/interaction process; this is depicted schematically in Fig. 10.

For convenience and geometric simplicity, each such fragment has been idealized for use in the CIVM-JET 4B computer code [4] as a rigid circular body

of the same mass and mass moment of inertia as the pre-impact fragment, with the same CG location, translational velocity, and rotational velocity as the actual fragment at postulated release. As indicated in Fig. 10, one might elect to represent the actual fragment by an idealized fragment of "properly selected radius r_f". An examination of this rotor indicates that reasonable minimum and maximum values for r_f would be about 2.56 and 4.20 inches, respectively; the use of these as well as an "intermediate" value of 3.36 inches was explored.

Figure 12 indicates the geometric, test, and modeling data for this case. The ring has been modeled by 48 equal-length ring elements. The point of initial impact of each of the three fragments is indicated in Fig. 12; element numbers and node identification are also given. The uniaxial static stress-strain properties of 4130 cast steel were approximated by piecewise linear segments with the stress-strain pairs: (σ,ε) = 80,950 psi, .00279; 105,300 psi, .0225; and 121,000 psi, .200 via the mechanical sublayer model; strain rate effects were approximated by using D = 40.4 sec^{-1} and p=5. Shown in Fig. 13 is the predicted ring configuration at 1000 microseconds after initial impact. The predicted inner surface and outer surface strains at the midelement location of elements 1, 4, and 6 are given in Fig. 14; for this calculation, frictionless impact μ=0 and r_f=2.555-in were employed. Figure 15 shows the circumferential distributions of inner-surface and outer-surface strain at 2400 microseconds after initial impact.

The effects of friction for otherwise identical modeling are indicated roughly by the Fig. 16 comparison of deformed ring configurations at 1200 microseconds after initial impact for μ=0 and μ=0.3. Similarly, the effects of idealized fragment radius r_f are seen in Fig. 16 where deformed ring profiles at 1200 microseconds after initial impact are shown for r_f=2.555-in and r_f=3.360-in. It is evident that if one chooses an unduly large idealized fragment radius r_f, this "rigid fragment" will constrain the ring to restrict its bending strain contribution so that unrealistically small total strains will be produced at the "convex lobes" -- compared with that which the actual "effectively-smaller-radius" fragment will produce.

The use of an idealized fragment of constant radius will clearly make it impossible to obtain complete time history agreement between predicted and measured inner-surface and/or outer-surface strains. However, the hope is that a properly-chosen effective r_f will lead to reasonable predictions vs. experiment

of maximum strains produced as a function of circumferential location. Further calculations and measurements are needed to assess the reliability with which this can be done. However, at the cost of greater complexity and computational expense, one can devise and use a fragment model which more closely simulates the behavior of the actual fragment.

Note, finally, that a comparison between the predicted and observed permanently-deformed ring configuration is not shown. This is the case because the calculation at Δt=1 microsecond has been carried out only to 2400 microseconds after initial impact. Whereas peak response occurred near 1200 microseconds, the ring is still springing back considerably at the 2400 microsecond time. A longer calculation would be necessary in order to permit making a reasonable estimate of the permanent-deformation configuration.

2.3 Beam Response to Steel Sphere Impact

In order to obtain appropriate and detailed 2-D transient structural response data under well-defined impact conditions so that a definitive evaluation could be made of the adequacy of the approximate collision-interaction analysis employed in the CIVM scheme, some simple experiments have been conducted at the MIT-ASRL. Beams of 6061-T651 aluminum with nominal 8-in span, 1.5-in width, and 0.10-in thickness and with both ends ideally clamped (see Fig. 18) have each been subjected to midspan impact by a solid steel sphere of one-inch diameter [14]. Impact velocities ranged from those sufficient to produce small permanent deflection to those needed for threshold rupture of the beam. Spanwise-oriented strain gages were applied to both the upper and the lower (impacted) surface of the beam at various spanwise locations. In each test, transient strain measurements were attempted for 8 of the gages; after each test, permanent strain readings were obtained for all surviving gages. Also, permanent deflection measurements were made.

An inspection of each specimen indicates that except near the point of impact itself (i.e., where $|x| \gtrsim 0.8$-in), the beam underwent essentially 2-D deflection behavior; pronounced 3-D behavior occurs near the point of initial impact. Hence, the 2-D structural response code (CIVM-JET 4B) may be expected to provide valid comparisons for $|x| \gtrsim 0.8$-in. Accordingly, such calculations and comparisons are in progress, and some preliminary results are shown next.

For the test and specimen identified as CB-18 in Ref. 14, the entire beam has been modeled with 43 equal-length cubic-cubic finite elements. The beam

material has been modeled as having either elastic, strain-hardening (EL-SH) or EL-SH-SR behavior where the uniaxial static stress-strain curve has been approximated by the σ,ε pairs: σ,ε= 41,000 psi, .0041; 45,000 psi, .0012; and 53,000 psi, .1000. For EL-SH-SR conditions, D=6500 sec^{-1} and p=4 have been assumed. For CB-18 initial steel-sphere impact occurred at a velocity of 2974 in/sec; a state of large permanent deflection was produced.

Shown in Fig. 19 are predicted and measured strains at spanwise stations x=1.50 and 1.20-in from the midspan impact point. At these 2-D structural response locations, there is fairly reasonable agreement between predicted and measured strains. Figure 20 shows the predicted transient vertical displacement response at x=1.0-in for both the EL-SH and the EL-SH-SR case. From these and longer-duration plots, the estimated respective permanent deflection is 0.63 and 0.58-in; the measured value is 0.60-in. While the comparisons shown here indicate encouraging agreement, more extensive calculations and comparisons are needed before a firm assessment can be made of the adequacy of the procedure embodied in the CIVM-JET 4B computer code [4].

3. 3-D Structural Response Studies

Of concern here are situations in which the fragment-impacted structure undergoes pronounced 3-D rather than 2-D deformation. Appropriate methods of structural response analysis and corresponding well-defined experimental transient structural response data which will serve to permit making a clear evaluation of the adequacy and/or accuracy of proposed prediction schemes are needed. Some contributions to this process are described here.

Although structural response analyses for fragment impact against initially-curved as well as initially-flat target structures are of interest, it is useful to minimize the complexities while checking the adequacy of the basic building blocks in the analysis process. Hence, attention has centered on impulse and impact experiments and theoretical analysis of initially-flat structures. Experiments involving steel-sphere impact against (1) narrow-plate (or beam) specimens [14] as well as (2) square uniform-thickness panels with four clamped edges and (3) panels of type (2) but with integrally-machined stiffeners of rectangular cross-section [15] have been conducted.

Two of the type (2) initially-flat specimens have been subjected to well-defined impulse loading by the sheet explosive loading technique to produce large-deflection, elastic-plastic transient structural response data for checking

the basic finite-element and transient response prediction aspects -- independent of impact itself. Also, steel sphere impact tests of this type of panel have been conducted. Thus, transient strain, permanent strain, and permanent deformation data of high quality are available for checking the prediction procedures of Refs. 6 and 9; the latter pertains to the breadboard computer codes PLATE and CIVM-PLATE which hopefully will enable one to predict 3-D transient large-deflection elastic-plastic, structural responses of panels caused by impulse and impact, respectively. If future correlation calculations reveal these codes to provide reliable transient response predictions, these codes will be upgraded to a condition convenient for routine use.

To illustrate the general character of the panel deformations produced for this purpose, Fig. 21 shows the permanent deflection along the centerline of specimen CP-2, a 0.062-in thick square initially-flat 8-in by 8-in panel of 6061-T651 aluminum with all four edges ideally clamped. The sheet explosive loading technique was used to impart essentially a uniform initial normal velocity of 16,235 in/sec over a 2-in by 2-in region centered at the panel center. Strain gages were also applied at various locations on the non-loaded side of the panel; both transient and permanent strain data were recorded. In addition, a pattern of lightly scribed grids was applied to a 3-in by 3-in region centered at the panel center on the non-loaded surface. Measurements of pre-test and post-test spacings of these grid lines enable one to make a rough determination of the permanent relative elongation on that surface as a function of location from the center of the panel. Some results from these determinations are shown in Fig. 22.

Steel sphere impact against a square 8-in initially-flat 6061-T651 aluminum panel of 0.063-in thickness with all four sides ideally clamped results in permanent deformation conditions wherein severe permanent deformation is concentrated near the point of initial impact itself as Fig. 23 shows for panel specimens CP-8 which suffered 1-inch diameter steel-sphere impact at 2435 in/sec. Photo-etched grids spaced 0.020-in apart on the non-impacted surface permitted making the permanent relative elongation measurements indicated in Fig. 24; the "large strains" are seen to be concentrated near the impact location and decrease rapidly with distance from the center of impact.

Finally, some illustrative preliminary results from applying the breadboard CIVM-PLATE code to steel-sphere-impacted narrow-plate (or beam) specimen

CB-18 are presented here; the steel-sphere impact velocity was 2794 in/sec initially. For computational thrift, one quarter of the specimen (see Fig. 18) was modeled by a 2 by 11 mesh of flat plate elements having 6 degrees of freedom per node, with symmetry conditions imposed along x=0 and y=0; this finite element mesh is shown in Fig. 25. Initial impact was assumed to occur at (x,y)=(0,0) whereas it actually occurred at about .06-in from this location. Relative elongation time histories predicted in this calculation along y=0 at stations x=0.6-in and x=1.2-in are compared with experimental measurements in Fig. 26. Figure 27 demonstrates that this 3-D structural response model exhibits 3-D deflection predictions -- vertical displacements predicted along y=0 (the centerline), y=.375-in, and y=.75-in as a function of spanwise location x are shown at 800 microseconds after initial impact. The anticipated larger displacement is seen to occur along y=0, with decreasing displacements (at given x-locations) more remote from the center of impact. Finally, Fig. 28 shows the predicted lateral transient deflection of the center of the plate (x,y)=(0,0) and the observed permanent deflection at this location; reasonable agreement is evident.

4. Summary Comments

Presented here is an overview of some of the work carried out to develop simple methods for predicting the 2-D transient large-deflection elastic-plastic structural responses of metal containment or deflection structures subjected to impulse loads or fragment impact; many more details may be found in the cited references. This 2-D type of idealization may serve as a good representation of certain fragment/structure impact/interaction situations or as a reasonable first approximation to other more complex cases. This 2-D idealization is relatively inexpensive to apply and may be useful for preliminary design, parametric studies, materials screening, etc. Structural configurations of 2-D type included in this discussion consist of complete rings, partial rings, constant or variable thickness, and uniform or arbitrarily-varying initial curvature, with various elastic foundation or various local support conditions provided. The associated computer codes (see Appendices A and B) are:

Structure Subjected to Prescribed Transient Loads or Initial Velocity Distributions

JET 3: Single-Layer Structures

JET 5A: Multilayer Bernoulli-Euler Structures

Structure Subjected Only to Fragment Impact

CIVM-JET 4B: Single-Layer Structures

CIVM-JET 5B: Multilayer Bernoulli-Euler Structures

Comparisons between experiment and predictions indicate good theoretical-experimental agreement for JET 3 predictions and a very encouraging but incomplete assessment for CIVM-JET 4B; further assessment studies are in progress.

For cases in which the impulsively-loaded structure [6] or fragment-impacted structure [9] undergoes significant 3-D structural responses, this more complex behavior must be modeled accordingly. Excellent theoretical-experimental agreement has been demonstrated [6] for finite-element analysis of plates and curved shells which undergo large-deflection elastic-plastic deformations in response to known severe impulse loading. Shown in this paper are encouraging preliminary comparisons between theory and experiment for fragment-impacted structures exhibiting 3-D structural response. Appropriate high quality experimental data on steel-sphere-impacted narrow beams, square uniform thickness panels, and longeron-stiffened initially-flat panels are available for near-future theoretical-experimental correlation studies to assess the accuracy and/or adequacy of the proposed prediction procedures. These studies are expected to suggest useful prediction modifications and improvements. Extensions to include fragment-impacted initially-curved 3-D structures would comprise a useful logical addition to the prediction capability.

Although this discussion has pertained to initially-isotropic metallic protective structures, many but not all of these analysis features can be carried over to the analysis of multilayer multimaterial protective structures -- such configurations are of potential future interest, as other papers in this Workshop indicate. Although such configurations will be much more complex and difficult to analyze, a validated structural response analysis capability would be of considerable value for preliminary design, materials screening, parametric studies, and to reduce the amount of ad hoc testing which otherwise would be required. The development and checking of accurate prediction methods to accommodate structural configurations and materials such as those cited at this Workshop in the presentations, for example, of Gerstle, Gardner, and Holms will be a difficult and lengthy process but will represent a highly useful state-of-the-art advance. This development and validation will require making

careful and detailed transient response observations and measurements for well-defined targets (geometry, boundary conditions, material mechanical and failure properties) and impact conditions. Realistic types of rotor-burst fragments should be used in exploratory experiments and in evaluation experiments; such experiments are essential to reveal the principal phenomena and to insure that important response features are not overlooked -- as might be the case if only highly simplified impact experiments were to be conducted. However, simpler better-defined fragments should be used to minimize uncertainties when obtaining detailed transient response data which are intended to serve as a definitive test of the accuracy and/or adequacy of the key building blocks of the procedures proposed for predicting the "threshold containment levels" of structural responses of multilayer multimaterial C/D structures.

REFERENCES

1. McCallum, R.B., Leech, J.W. and Witmer, E.A., "Progress in the Analysis of Jet Engine Burst-Rotor Containment Devices", ASRL TR 154-1, Aeroelastic and Structures Research Laboratory, Massachusetts Institute of Technology, August 1969. (Available as NASA CR-107900.)

2. McCallum, R.B., "Simplified Analysis of Trifragment Rotor Dist Interaction with a Containment Ring", AIAA Journal of Aircraft, Vol. 7, No. 3, May-June 1970, pp. 283-285.

3. Wu, R.W.-H. and Witmer, E.A., "Computer Program - JET 3 - to Calculate the Large Elastic-Plastic Dynamically-Induced Deformations of Free and Restrained, Partial and/or Complete Structural Rings", ASRL TR 154-7, Aeroelastic and Structures Research Laboratory, Massachusetts Institute of Technology, August 1972. (Available as NASA CR-120993.)

4. Stagliano, T.R., Spilker, R.L. and Witmer, E.A., "User's Guide to Computer Program CIVM-JET 4B to Calculate Large Nonlinear Transient Deformations of Single-Layer Partial and/or Complete Structural Rings to Engine Rotor Fragment Impact", MIT ASRL TR 154-9, March 1976. (Available as NASA CR-134907.)

5. Wu, R.W.-H., Stagliano, T.R., Witmer, E.A. and Spilker, R.L., "User's Guide to Computer Programs JET 5A and CIVM-JET 5B to Calculate the Large Elastic-Plastic Dynamically-Induced Deformations of Multilayer Partial and/or Complete Structural Rings", MIT ASRL TR 154-10, February 1977.

6. Wu, R.W.-H. and Witmer, E.A., "Finite Element Predictions of Transient Elastic-Plastic Large Deflections of Stiffened and/or Unstiffened Rings and Cylindrical Shells", AMMRC CTR 74-31 (also MIT ASRL TR 171-4), April 1974.

7. Pirotin, S.D., Berg, B.A. and Witmer, E.A., "PETROS 3.5: New Developments and Program Manual for the Finite-Difference Calculation of Large Elastic-Plastic Transient Deformations of Multilayer Variable-Thickness Shells", BRL CR 211 (MIT ASRL TR 152-4), February 1975.

8. Santiago, J.M., Wisniewski, H.L. and Huffington, N.J. Jr., "A User's Manual for the REPSIL Code", BRL Report No. 1744, October 1974 (AD A003176).

9. Spilker, R.L., Witmer, E.A. and French, S.E., "Finite Element Nonlinear Transient Response Analysis of Panels Subjected to Impulse or Impact Loads", MIT ASRL TR 154-13 (in preparation).

10. Private Communication from A. Martino, U.S. Naval Air Propulsion Test Center, Phila, Pa., 1970.

11. Mangano, G.J., "Rotor Burst Protection Program -- Phases VI and VII: Exploratory Experimentation to Provide Data for the Design of Rotor Burst Fragment Containment Rings", NAPTC-AED-1968, March 1972. (Available as NASA CR-120962).

12. --- "Rotor Burst Protection Program". (Study for NASA Lewis Research Center on NASA DPR-105 and NASA Interagency Agreement C-41581-B), U.S. Naval Air Propulsion Test Center, Aeronautical Engine Dept., Progress Reports Sept. 1969 - Jan. 1977.

13. Private communications from G.J. Mangano, R. DeLucia, and J. Salvino, U.S. Naval Air Propulsion Test Center, Trenton, New Jersey 1975-1976.

14. Witmer, E.A., Merlis, F. and Spilker, R.L., "Experimental Transient and Permanent Deformation Studies of Steel-Sphere-Impacted or Impulsively-Loaded Aluminum Beams with Clamped Ends", MIT ASRL TR 154-11, October 1975. (Available as NASA CR-134922.)

15. Witmer, E.A., Merlis, F., Rodal, J.J.A. and Stagliano, T.R., "Experimental Transient and Permanent Deformation Studies of Steel-Sphere-Impacted or Impulsively-Loaded Aluminum Panels", MIT ASRL TR 154-12, March 1977.

16. Balmer, H.A. and Witmer, E.A., "Theoretical-Experimental Correlation of Large Dynamic and Permanent Deformations of Impulsively-Loaded Simple Structures", MIT, AFFDL-TDR-64-108, July 1964.

17. Wu, R.W.-H. and Witmer, E.A., "Finite-Element Analysis of Large Transient Elastic-Plastic Deformations of Simple Structures, with Application to the Engine Rotor Fragment Containment/Deflection Problem", ASRL TR 154-4, Aeroelastic and Structures Research Laboratory, Massachusetts Institute of Technology, January 1972. (Available as NASA CR-120886.)

18. Collins, T.P. and Witmer, E.A., "Application of the Collision-Imparted Velocity Method for Analyzing the Responses of Containment and Deflector Structures to Engine Rotor Fragment Impact", MIT ASRL TR 154-8, August 1973. (Available as NASA CR-134494.)

19. Zirin, R.M. and Witmer, E.A., "Examination of the Collision Force Method for Analyzing the Responses of Simple Containment/Deflection Structures to Impact by One Engine Rotor Blade Fragment", ASRL TR 154-6, Aeroelastic and Structures Research Laboratory, Massachusetts Institute of Technology, May 1972. (Available as NASA CR-120952.)

TABLE 1

DATA CHARACTERIZING NAPTC RING TEST 91

Ring Data	Test 91
Outside Diameter (in)	17.619
Radial Thickness (in)	0.152
Axial Length (in)	1.506
Material	2024-T4
Elastic Modulus E (psi)	10^7
PP Yield Stress σ_o (psi)	50,000

Fragment Data	
Type	T-58 Single Blade
Material	SEL-15
Outer Radius (in)	7.0
Fragment Centroid from Center of Rotation (in)	4.812
Fragment Tip Clearance from Ring (in)	1.658
Fragment Length (in)	3.5
Fragment Length from CG to Tip (in)	2.188
Fragment Weight (lbs)	0.084
Fragment Moment of Inertia about its CG (in lb sec^2)	2.163×10^{-4}
Failure Speed (RPM)	15,644.4
Fragment Tip Velocity (ips)	11,467.
Fragment Centroidal Velocity (ips)	7,884.
Fragment Initial Angular Velocity (rad/sec)	1,638.3
Fragment Translation KE (in lb)	6,756.
Fragment Rotational KE (in lb)	290.3

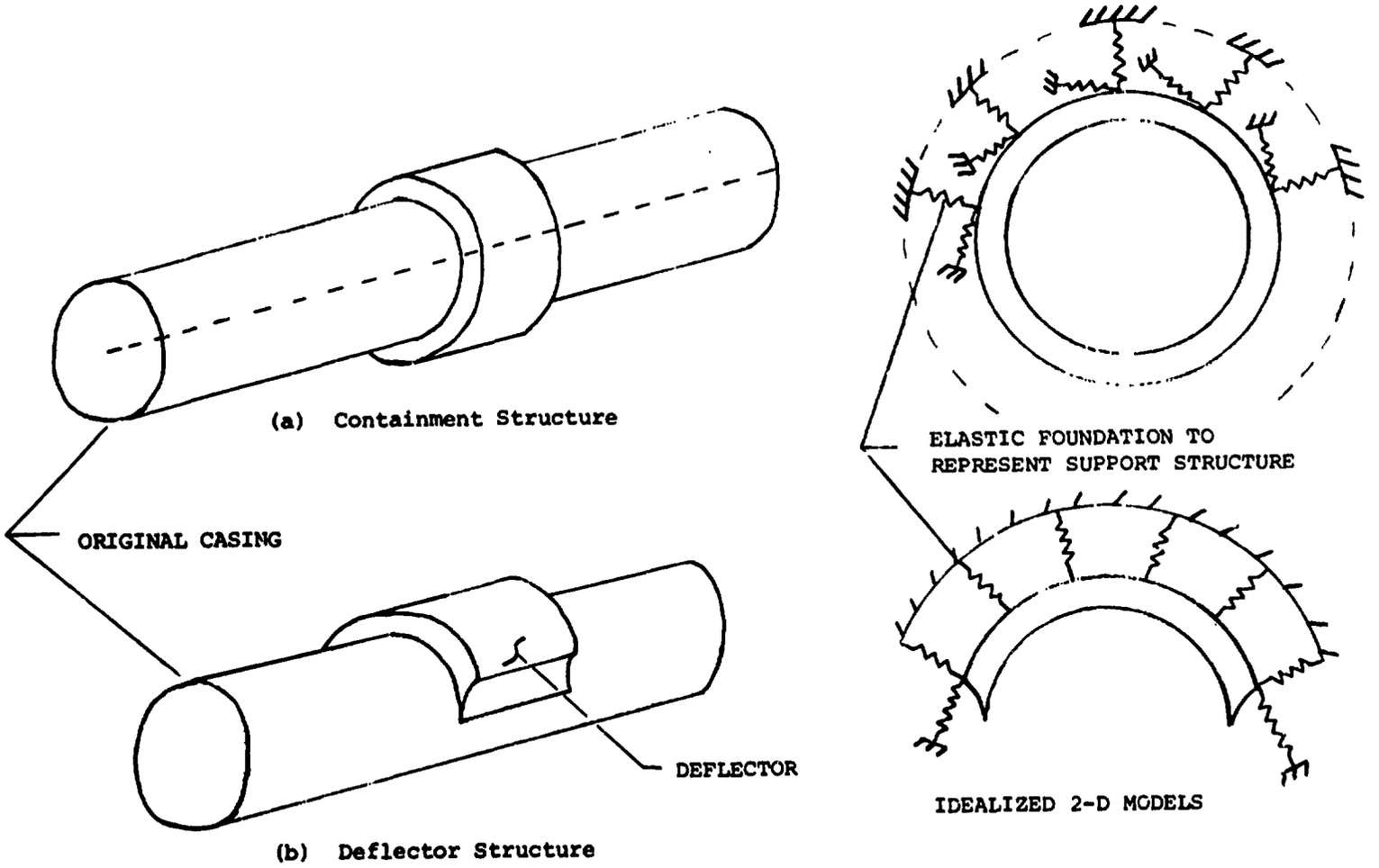

FIG. 1 SCHEMATICS OF CONTAINMENT AND DEFLECTOR STRUCTURES, AND ASSOCIATED IDEALIZED 2-D STRUCTURAL MODELS

- DEVELOPMENT OF PREDICTION METHODS FOR STRUCTURAL RESPONSE
  - TO PRESCRIBED TRANSIENT LOADS OR INITIAL VELOCITIES → JET CODES (FINITE ELEMENT)
  - TO FRAGMENT IMPACT → CIVM-JET CODES
  - ANALYSIS OF 2-D STRUCTURES
    - SINGLE-LAYER RINGS → NEAR COMPLETION
    - MULTILAYER RINGS → IN PROGRESS
  - ANALYSIS OF GENERAL PANEL RESPONSE
    - SINGLE LAYER → IN PROGRESS
    - MULTILAYER → NEXT

- EXPERIMENTS
  - SMALL SCALE SIMPLIFIED IMPACT TESTS AT MIT TO SUPPLEMENT COMPLEX FULL-SCALE TEST AT THE NAPTC
    - OBTAIN DATA TO MAKE IN-DETAIL EVALUATION OF ADEQUACY OF PREDICTION METHOD
    - IMPACT OF STEEL SPHERE AGAINST
      - BEAMS
      - FLAT SINGLE-LAYER PANELS
      - WAFFLE-STIFFENED PANELS

      } CLAMPED EDGES

- THEORETICAL-EXPERIMENTAL CORRELATION STUDIES
  - USE OF MIT-ASRL EXPERIMENTS
  - USE OF NAPTC DATA

- COMPUTER CODES
  - PARAMETRIC AND SCREENING STUDIES
  - TO ASSIST PRELIMINARY DESIGN OF CONTAINERS AND DEFLECTORS

FIG. 2 SUMMARY OF MIT-ASRL STUDIES ON ENGINE ROTOR FRAGMENT IMPACT ON C/D STRUCTURES

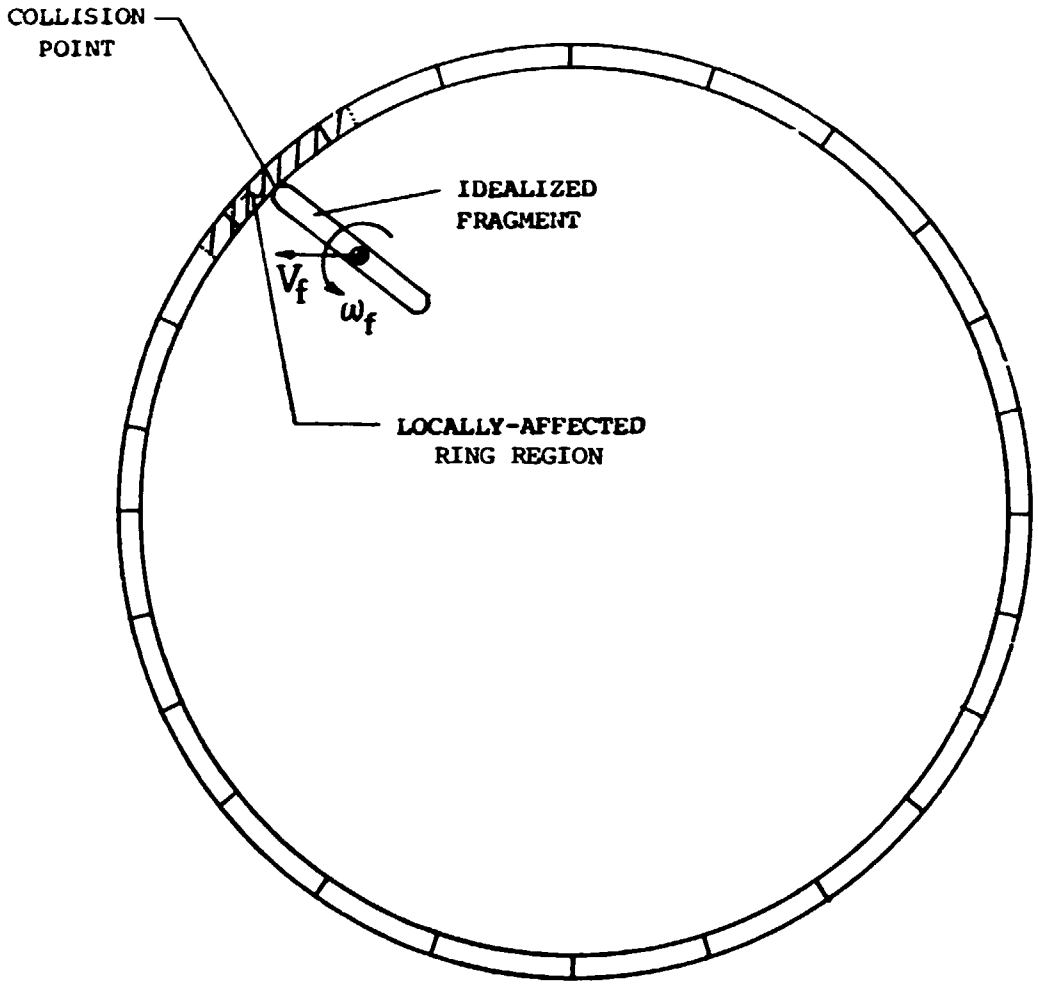

FIG. 3 SCHEMATIC OF A CONTAINMENT RING SUBJECTED TO SINGLE-FRAGMENT IMPACT

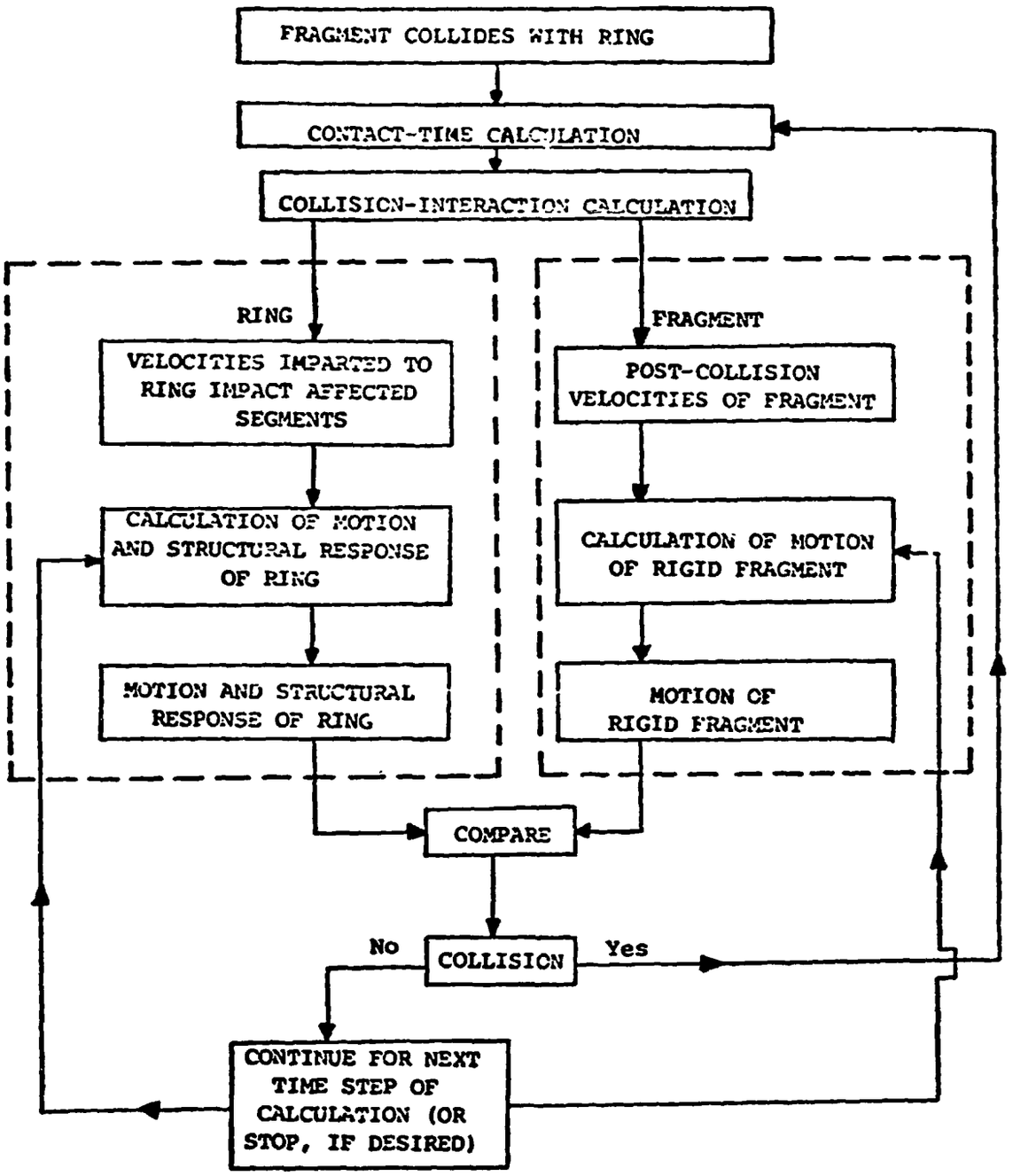

FIG. 4 INFORMATION FLOW SCHEMATIC FOR PREDICTING RING AND FRAGMENT MOTIONS IN THE COLLISION-IMPARTED VELOCITY METHOD

o —·— EXPERIMENT

x ----- CASE CR-11B (EL-PP-SR, e = 0)

Δ —— CASE CR-10B (EL-PP-SR, e = 1)

——— RING BEFORE INITIAL IMPACT

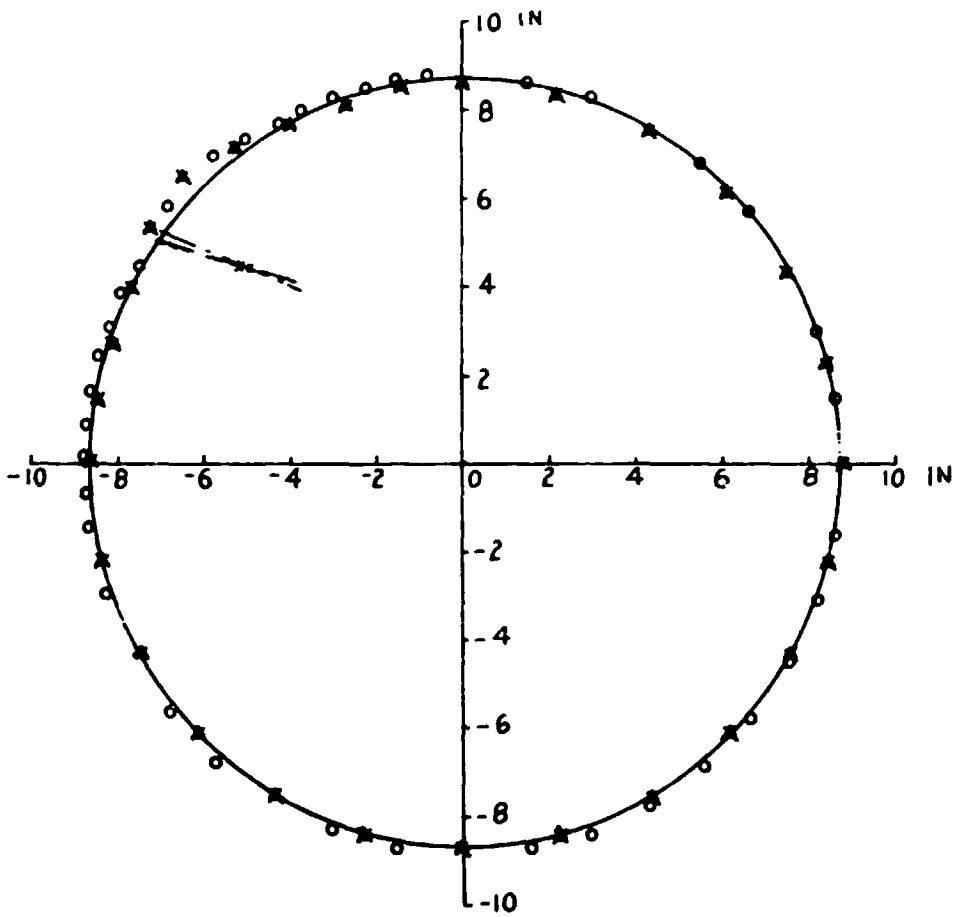

(a) TAII = 150 μsec

FIG. 5 COMPARISON OF CIVM PREDICTIONS WITH EXPERIMENT FOR THE FREE COMPLETE RING SUBJECTED TO SINGLE-BLADE IMPACT IN NAPTC TEST 91

o —·— EXPERIMENT

x ---- CASE CR-11B (EL-PP-SR, e = 0)

Δ —— CASE CR-10B (EL-PP-SR, e = 1)

——— RING BEFORE INITIAL IMPACT

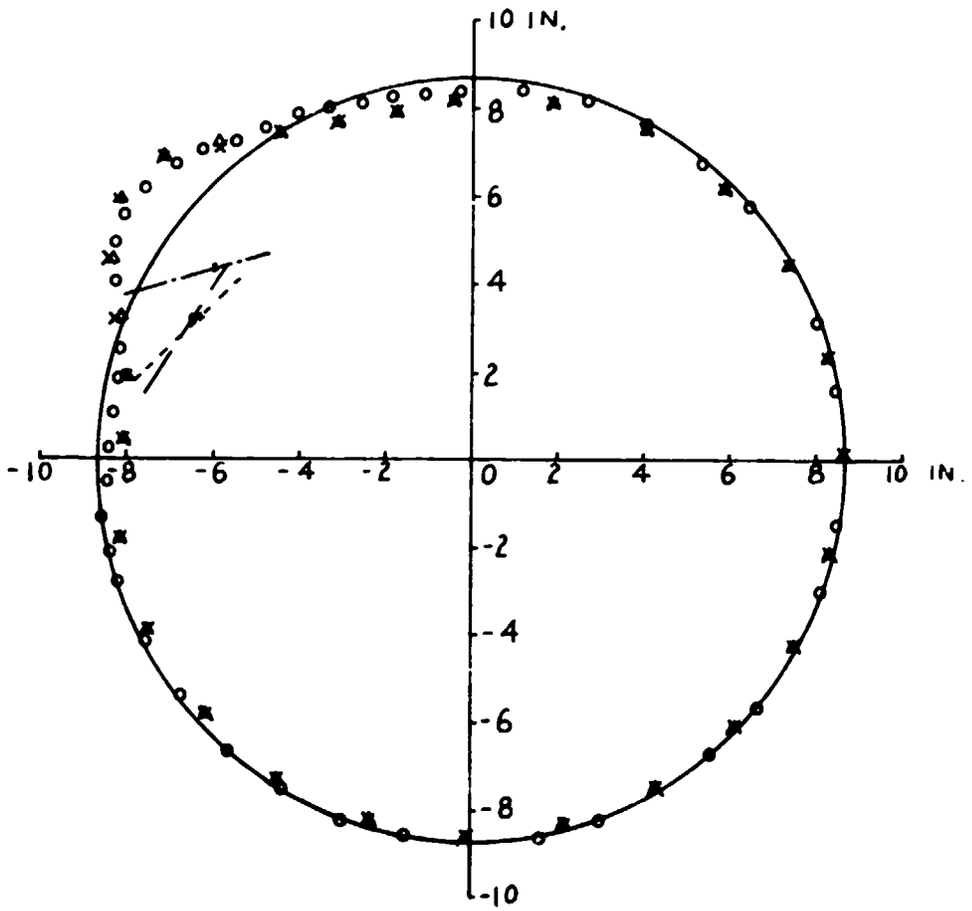

(b) TAII = 570 μsec

FIG. 5 CONTINUED

o — · — EXPERIMENT

x - - - - CASE CR-11B (EL-PP-SR, e = 0)

Δ — — CASE CR-10B (EL-PP-SR, e = 1)

——— RING BEFORE INITIAL IMPACT

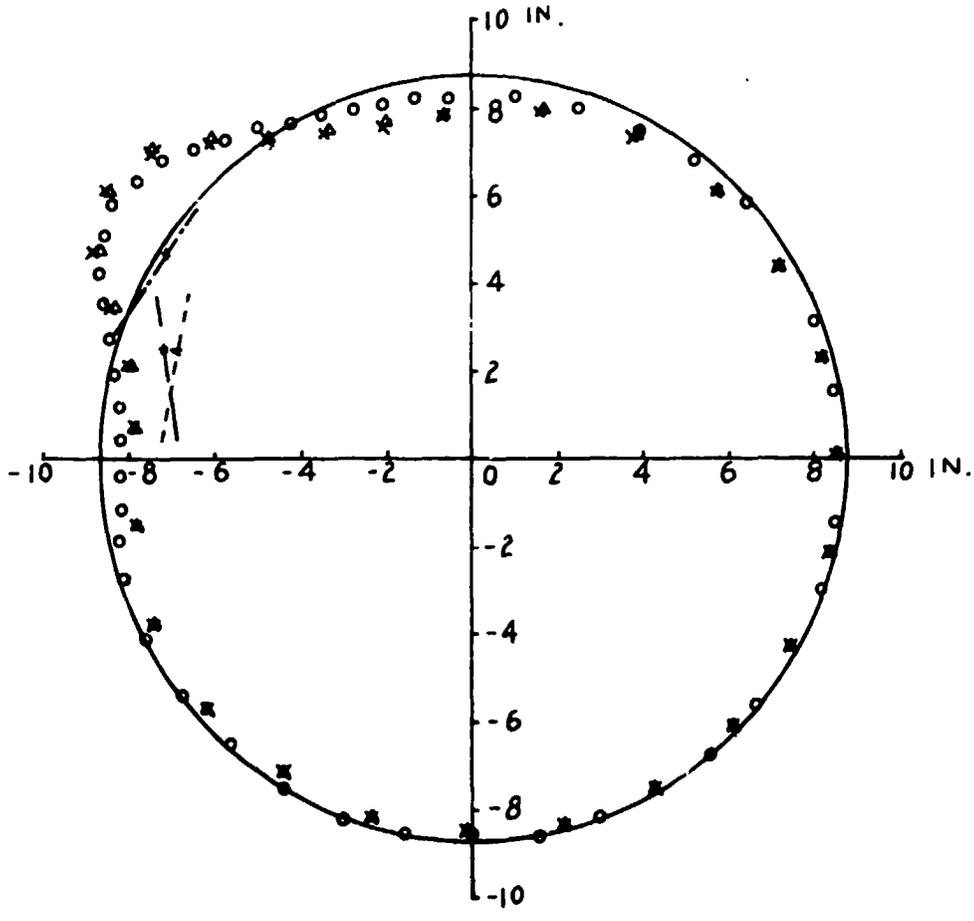

(c) TAII = 810 μsec

FIG. 5 CONCLUDED

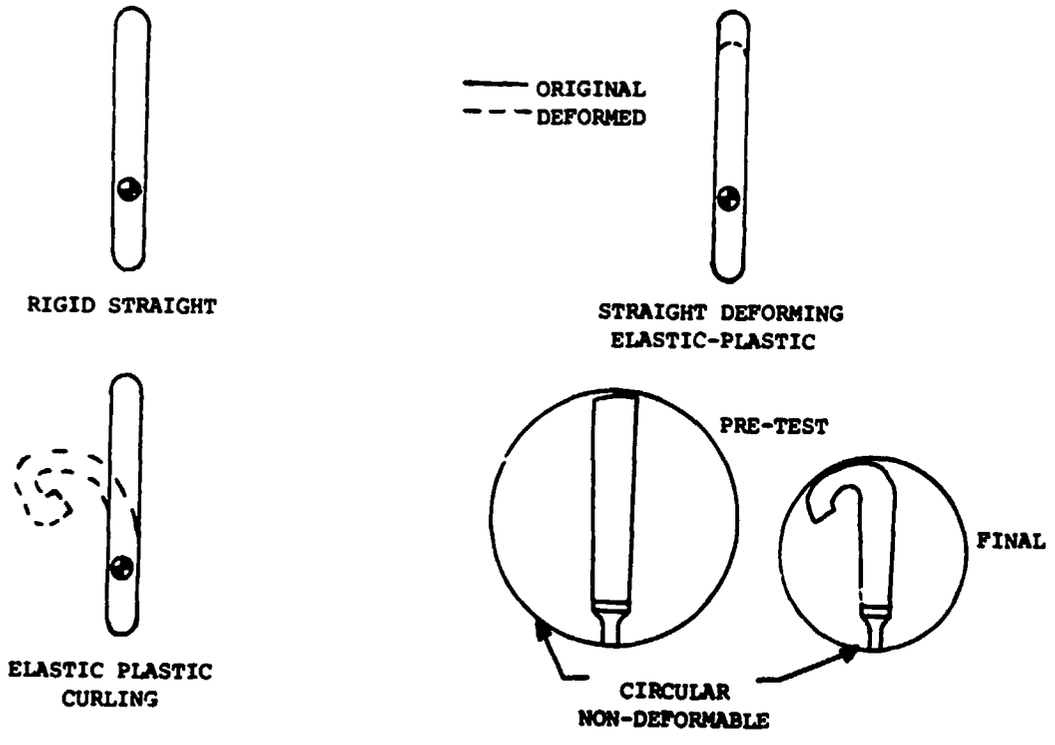

FIG. 6 SCHEMATICS OF ACTUAL AND IDEALIZED FRAGMENTS

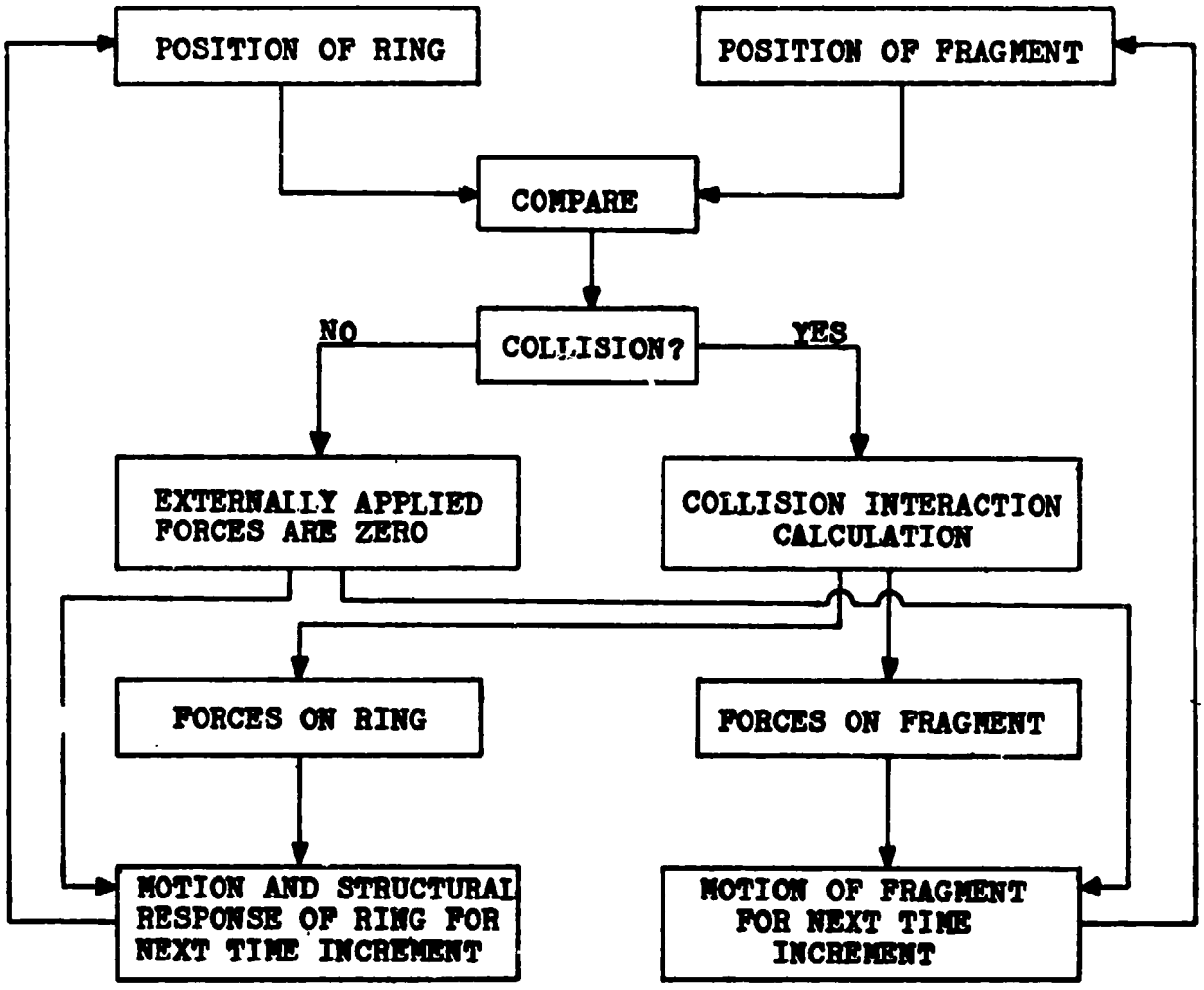

FIG. 7 INFORMATION FLOW SCHEMATIC FOR PREDICTING RING AND FRAGMENT MOTIONS IN THE COLLISION FORCE METHOD

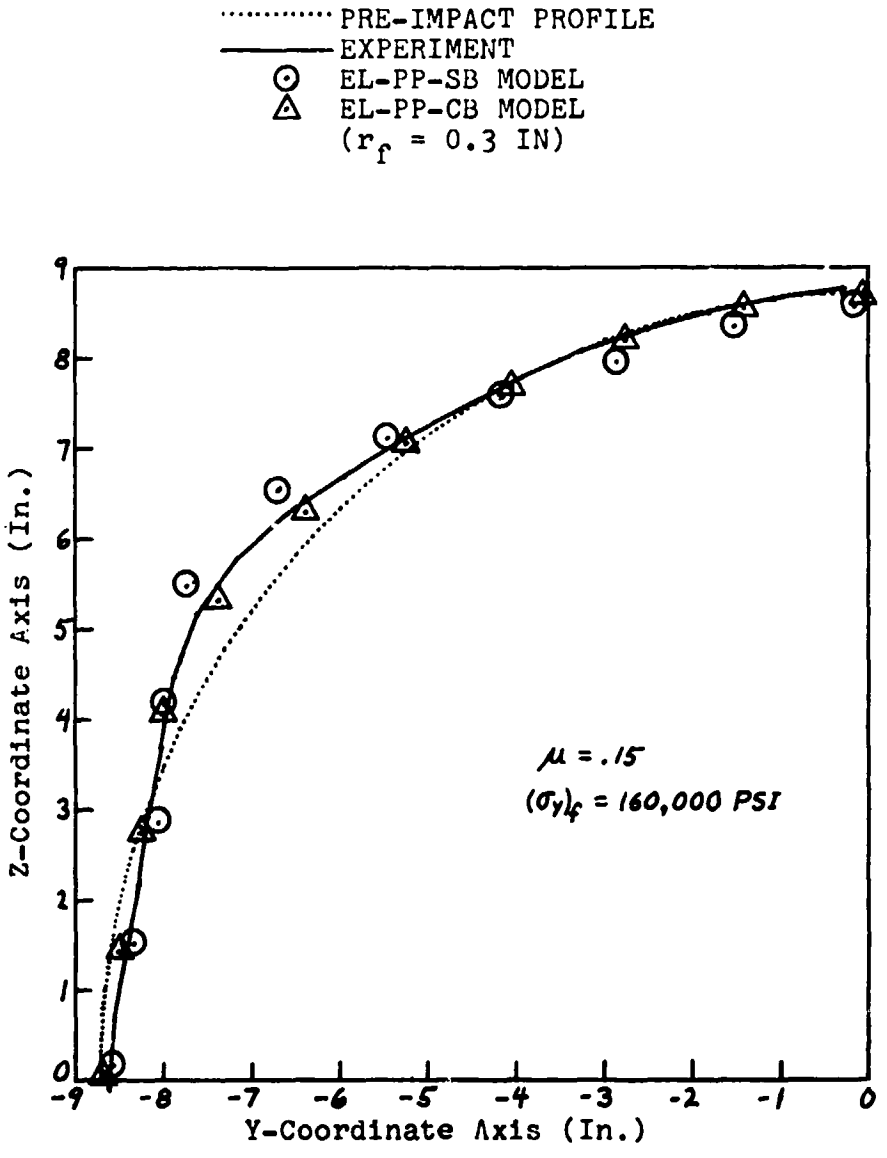

(a) First Quadrant of the Deformed Ring at TAII = 326 μsec.

FIG. 8 COMPARISON OF CFM PREDICTIONS FOR EL-PP-SB AND EL-PP-CB BLADE MODELS FOR μ=.15 BLADE/RING IMPACT VERSUS EXPERIMENTAL DEFORMED RING DATA

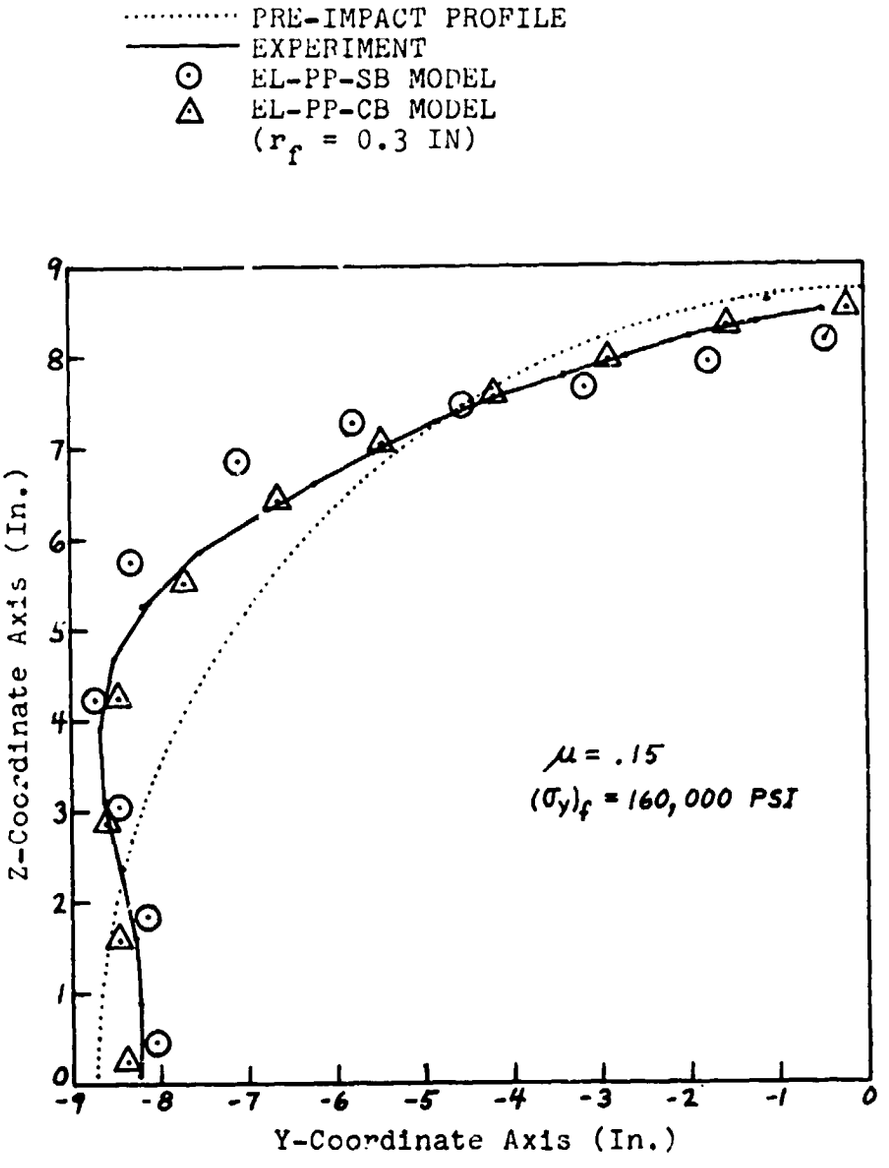

(b) First Quadrant of the Deformed Ring at TAII = 626 μsec.

FIG. 8 CONCLUDED

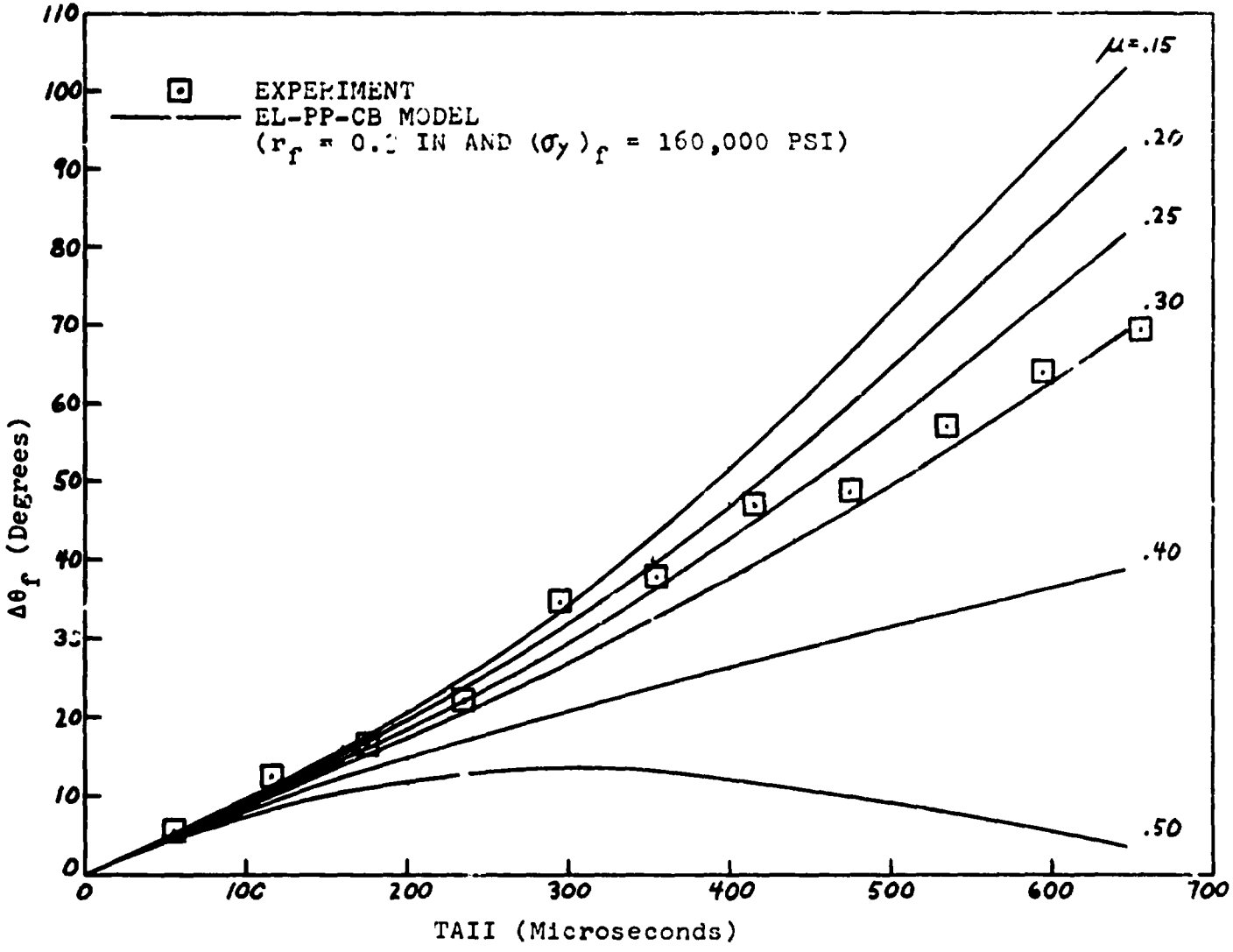

FIG. 9 COMPARISON OF CFM PREDICTIONS OF BLADE MOTION FOR THE EL-PP-CB BLADE MODEL AND VARIOUS VALUES OF THE FRICTION COEFFICIENT μ VERSUS OBSERVED BLADE ANGULAR ROTATION

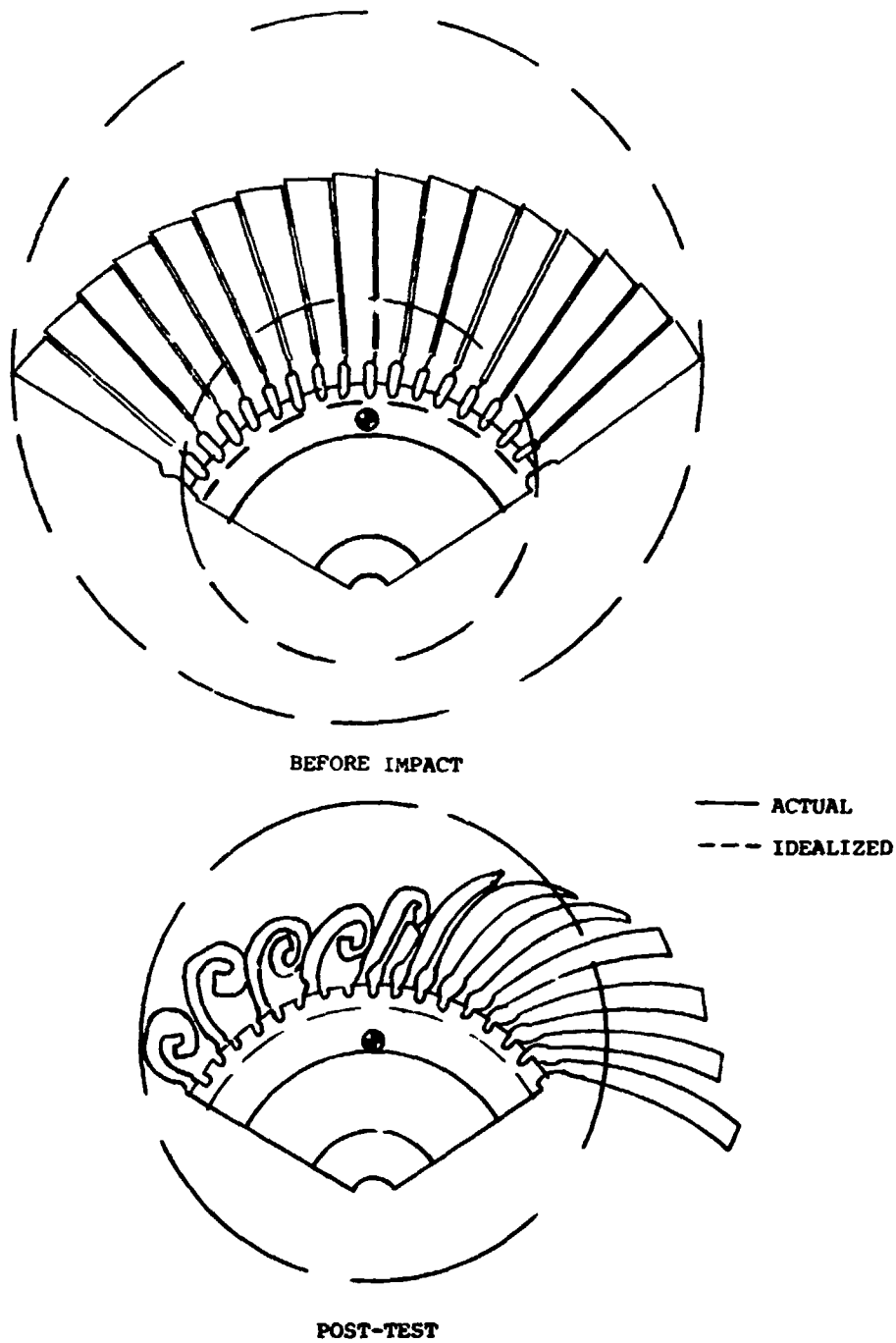

FIG. 10 SCHEMATICS OF PRE-TEST AND DEFORMED TRI-HUB DISK/BLADE FRAGMENTS, AND IDEALIZED MODELS

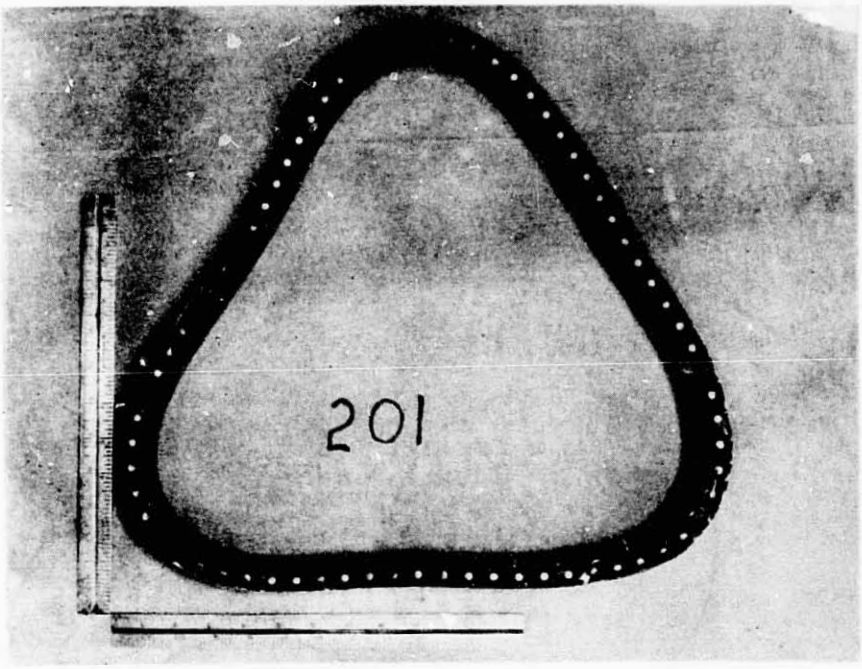

FIG. 11 POST-TEST CONFIGURATION OF THE STEEL CONTAINMENT RING SUBJECTED TO T58 TURBINE ROTOR TRI-HUB BURST IN NAPTC TEST 201

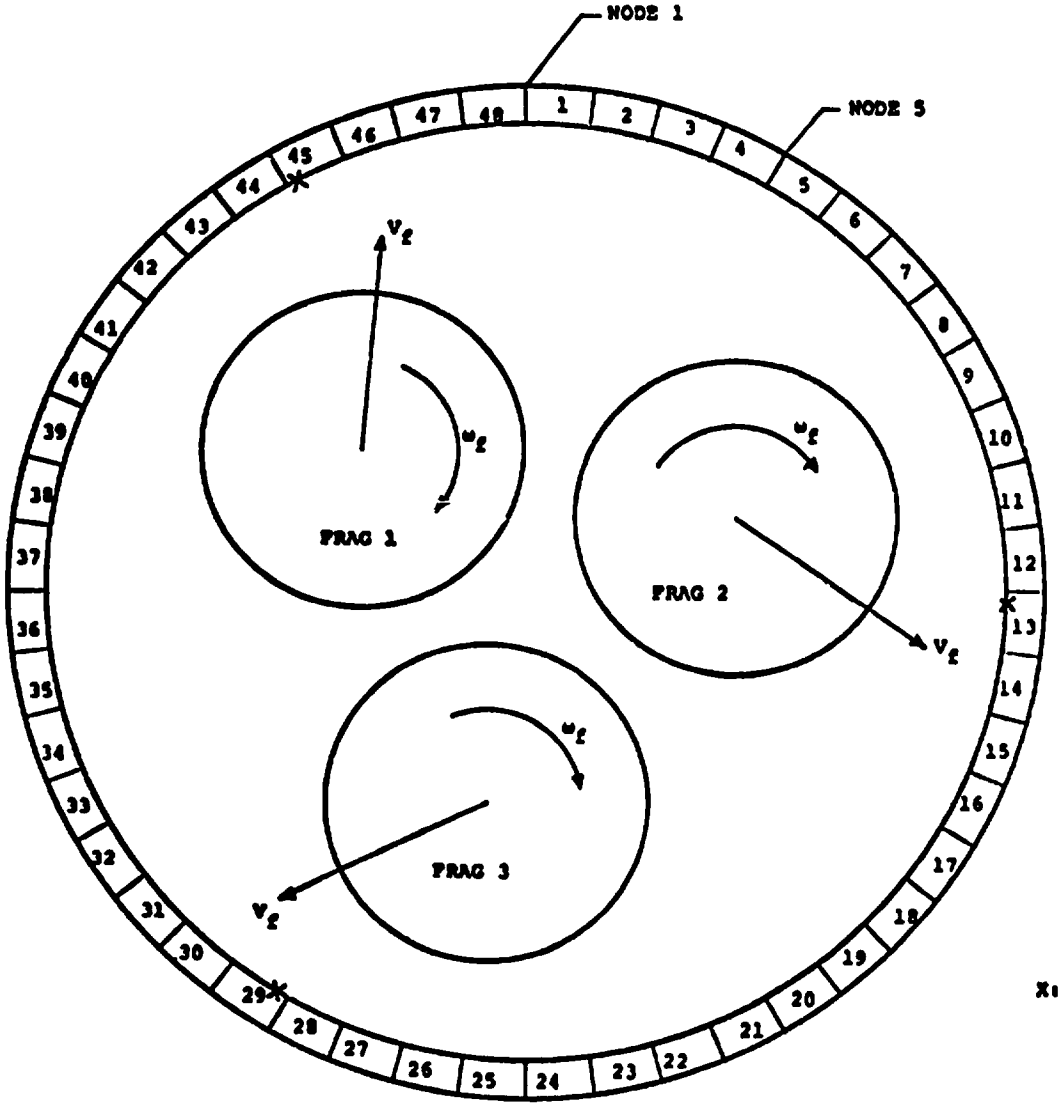

4130 STEEL RING

INNER RADIUS = 7.50 IN
THICKNESS = 0.625 IN
AXIAL LENGTH = 1.50 IN

FINITE-ELEMENT ANALYSIS

48 EQUAL ELEMS (FULL RING)
4 DOF/NODE
EL-SH-SR

FRAGMENTS: 3 EQUAL CIRCULAR
AT 120-DEG. SPACING

FOR EACH FRAGMENT

RADIUS = 2.555 IN
MASS = 0.009395 (LB-SEC^2)/IN
MASS MOM. INER. = 0.06899 IN-LB-SEC^2
TRANSL. VEL., V_f = 5816.7 IN/SEC
ROT. VEL., ω_f = 2079.6 RAD/SEC
INITIAL KINETIC ENERGY
TRANSLATIONAL = 158,942 IN-LB
ROTATIONAL = 149,177 IN-LB
TOTAL = 308,119 IN-LB

X: POINT OF INITIAL IMPACT

FIG. 12 GEOMETRIC, TEST, AND MODELING DATA FOR THE 4130 STEEL CONTAINMENT RING SUBJECTED TO TRI-HUB T58 ROTOR BURST IN NAPTC TEST 201

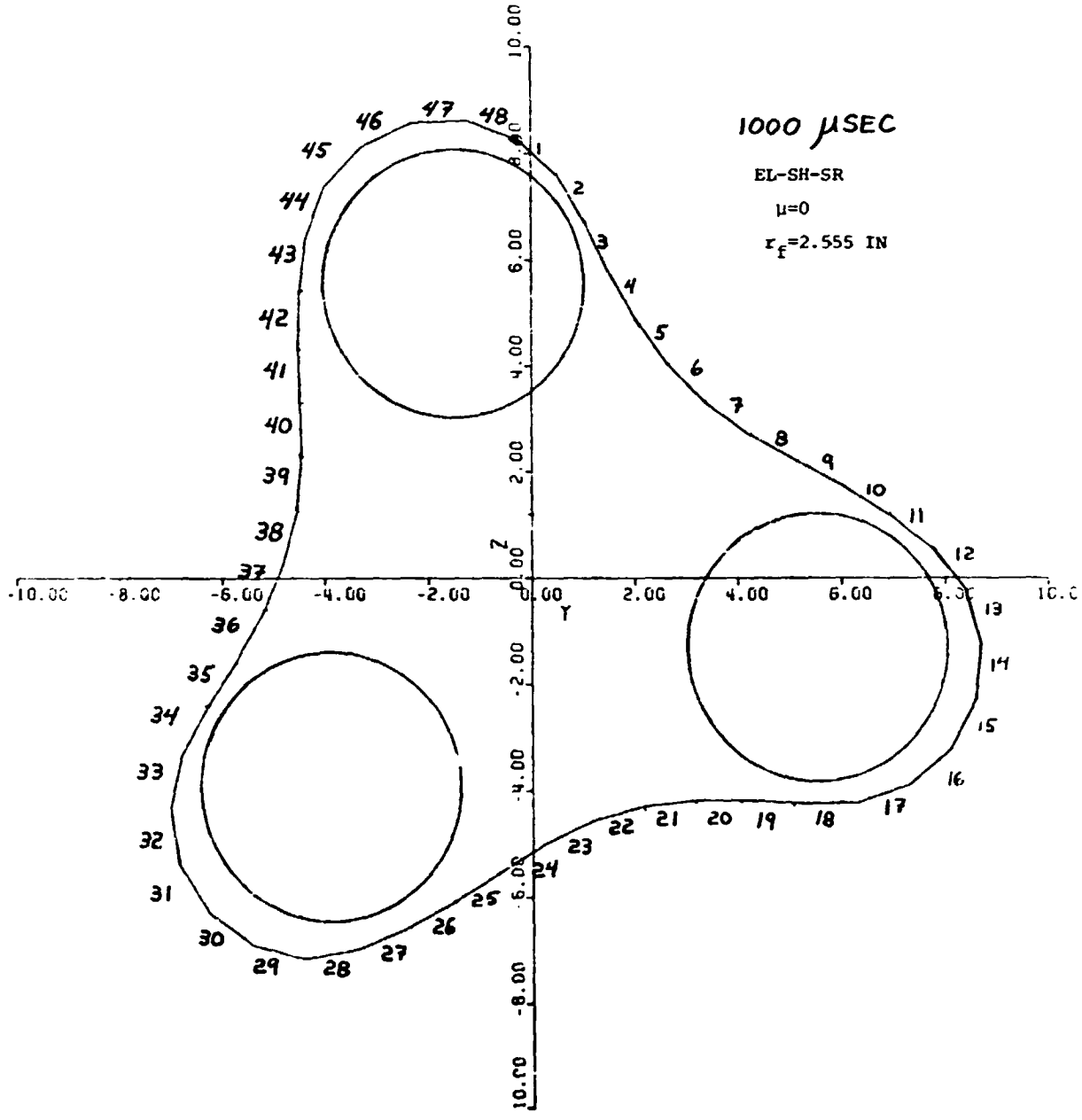

FIG. 13 PREDICTED DEFORMED RING CONFIGURATION AT 1000 MICROSECONDS AFTER INITIAL IMPACT FOR THE NAPTC TEST 201 CONTAINMENT RING

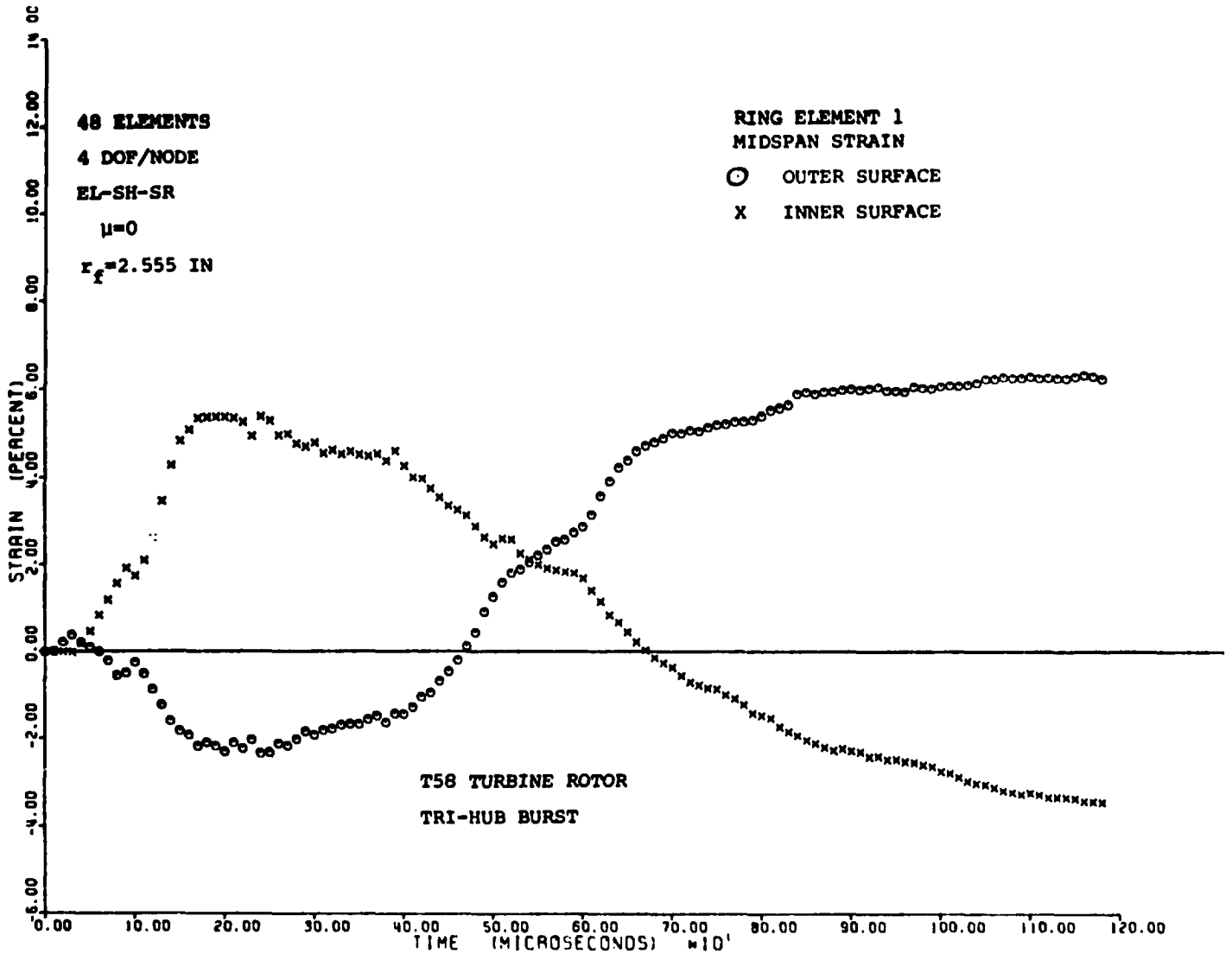

(a) Element 1 Midspan Strain

FIG. 14 PREDICTED TRANSIENT STRAIN ON THE NAPTC TEST 201 CONTAINMENT RING

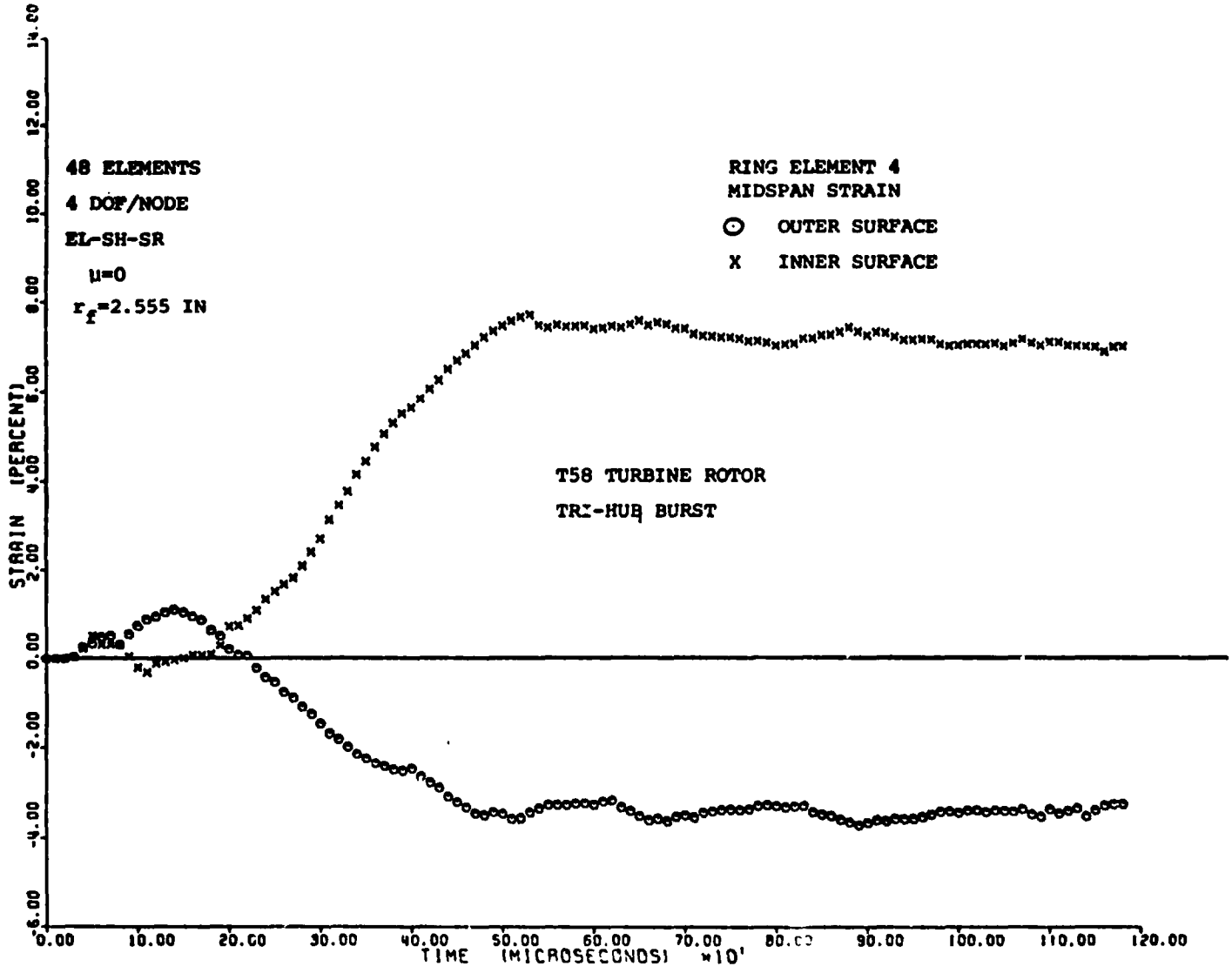

(b) Element 4 Midspan Strain

FIG. 14 CONTINUED (NAPTC TEST 201 RING)

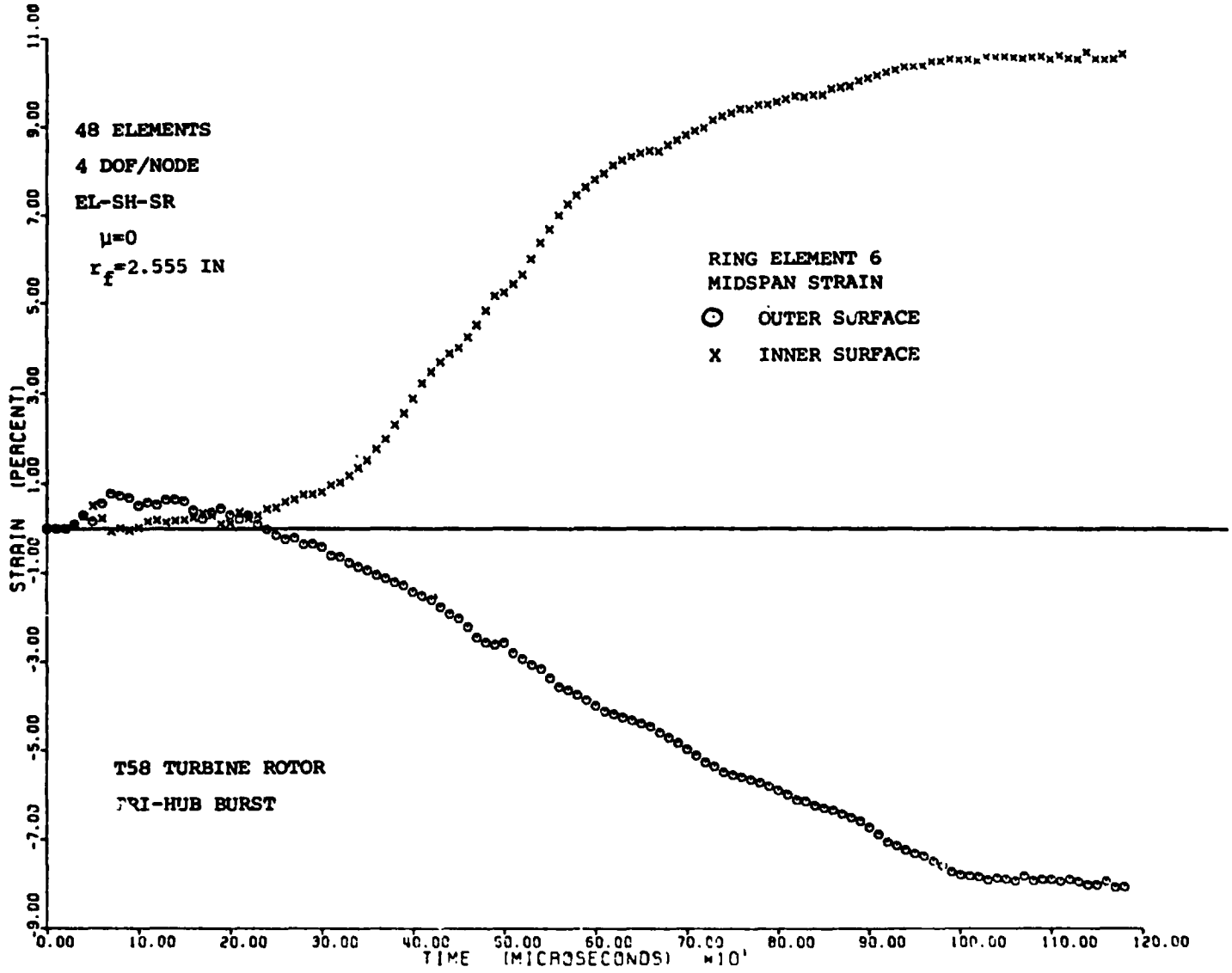

(c) Element 6 Midspan Strain

FIG. 14 CONCLUDED (NAPTC TEST 201 RING)

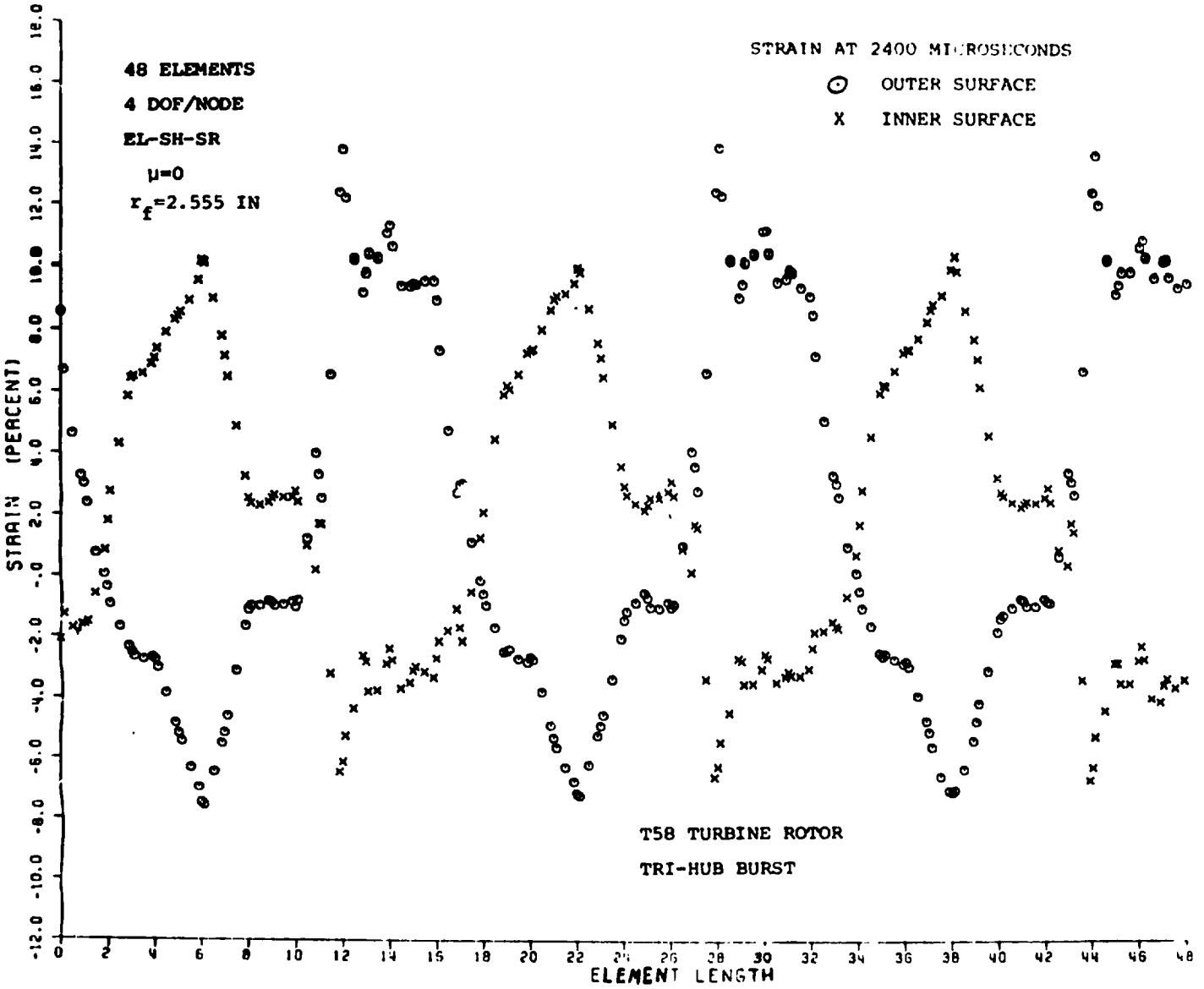

FIG. 15 CIRCUMFERENTIAL DISTRIBUTION OF PREDICTED INNER-SURFACE AND OUTER-SURFACE STRAIN AT 2400 MICROSECONDS AFTER INITIAL IMPACT FOR THE NAPTC TEST 201 CONTAINMENT RING FOR r_f=2.555 IN AND μ=0

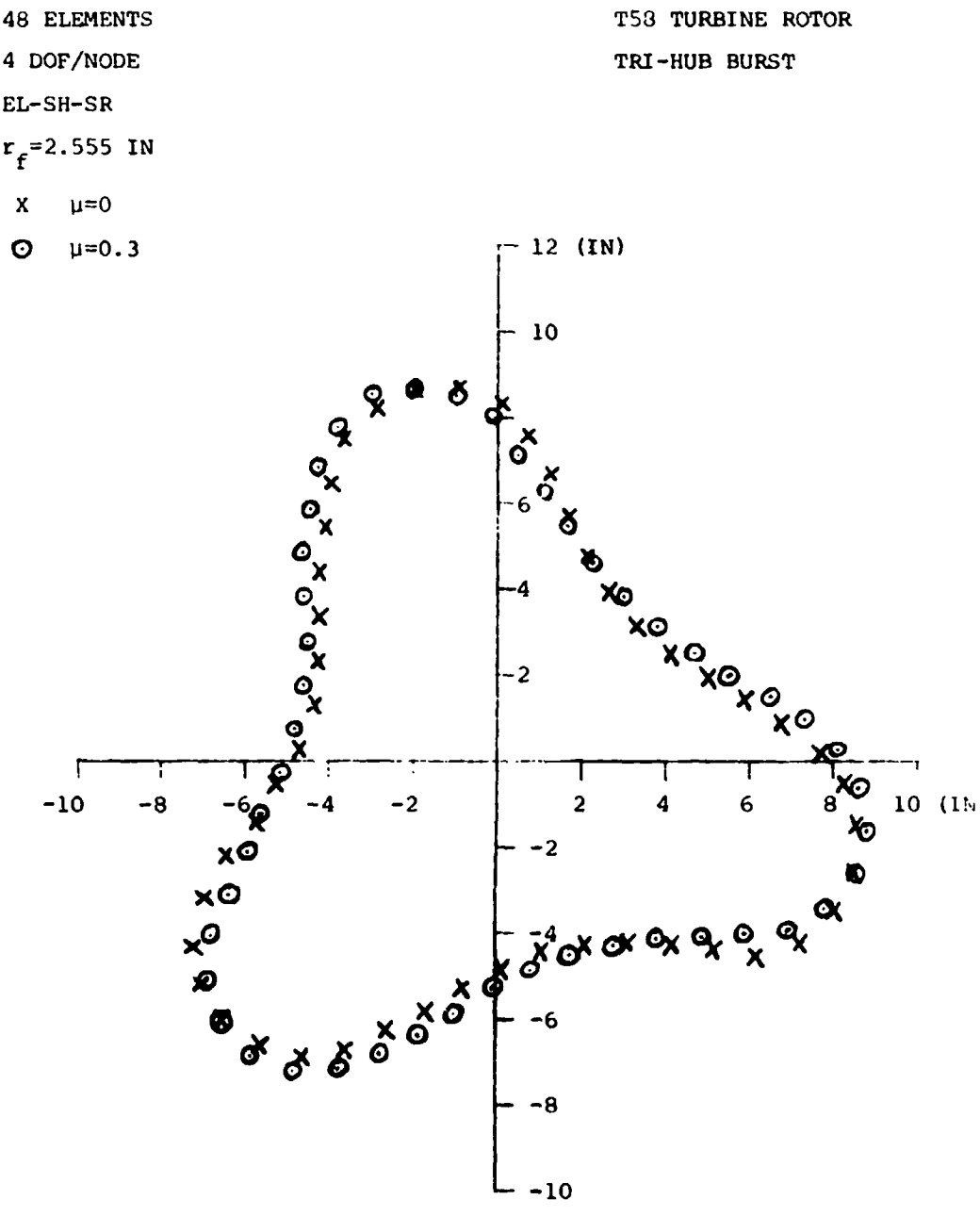

FIG. 16 COMPARISON OF PREDICTED DEFORMED RING CONFIGURATIONS AT 1200 MICROSECONDS AFTER INITIAL IMPACT FOR μ=0 AND μ=0.3 WITH r_f=2.555 IN FOR THE NAPTC TEST 201 CONTAINMENT RING

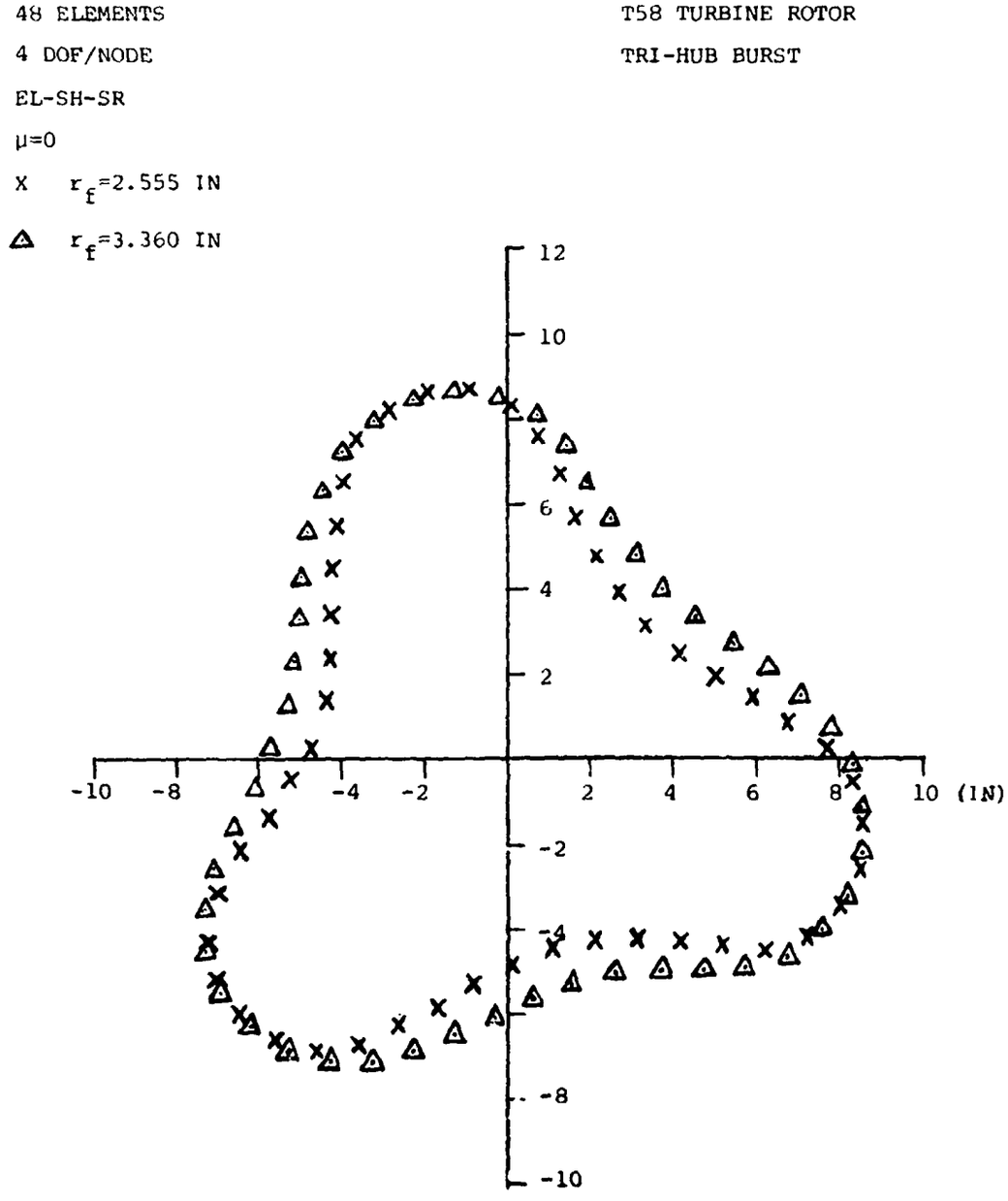

FIG. 17 COMPARISON OF PREDICTED DEFORMED RING CONFIGURATIONS AT 1200 MICROSECONDS AFTER INITIAL IMPACT FOR TWO DIFFERENT FRAGMENT-SIZE MODELINGS AND FRICTIONLESS IMPACT CONDITIONS FOR THE NAPTC TEST 201 CONTAINMENT RING

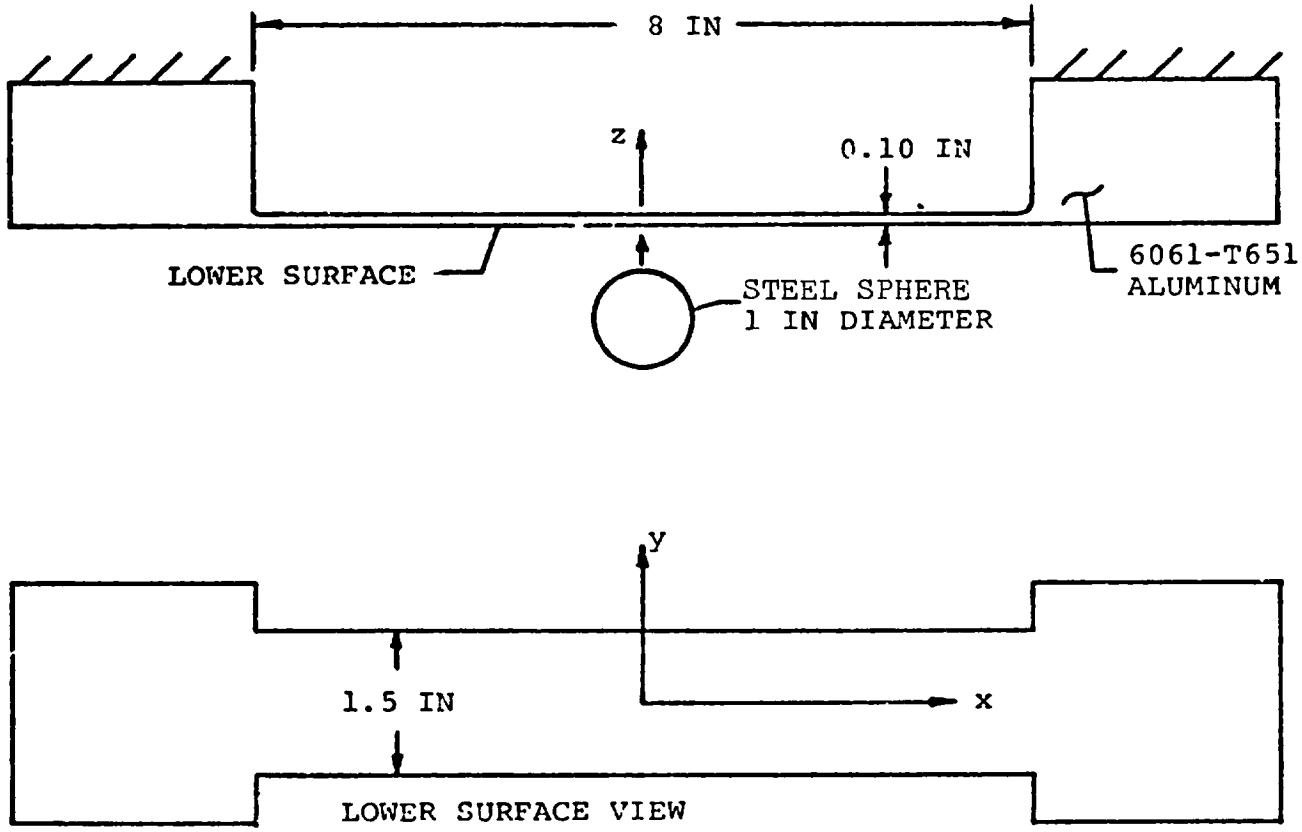

FIG. 18 SCHEMATIC OF 6061-T651 NARROW PLATE OR BEAM MODEL SUBJECTED TO IMPACT BY A ONE-INCH DIAMETER STEEL SPHERE

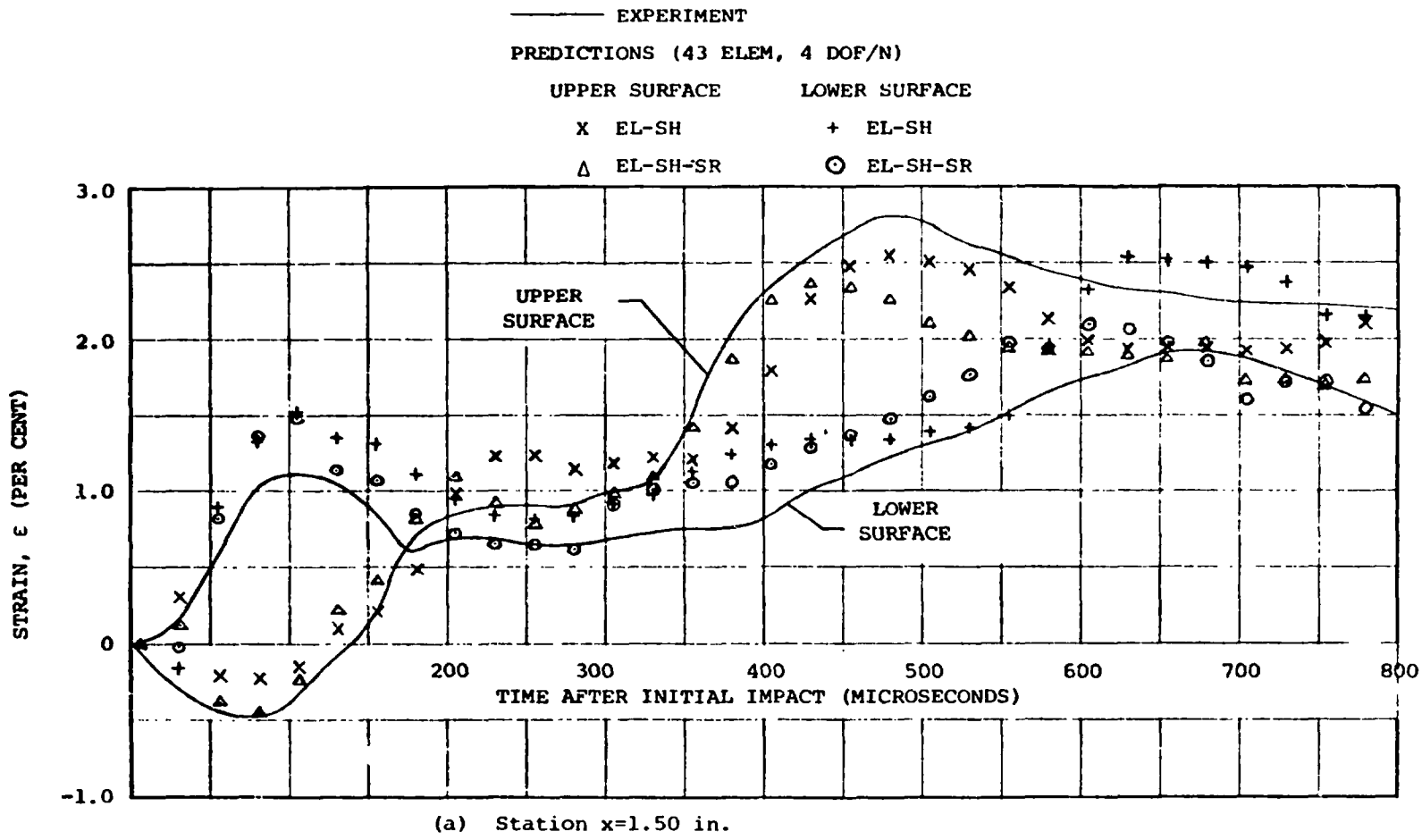

(a) Station x=1.50 in.

FIG. 19 TRANSIENT STRAIN AT VARIOUS SPANWISE STATIONS OF STEEL-SPHERE-IMPACTED 6061-T651 ALUMINUM ⅄ AM MODEL CB-18

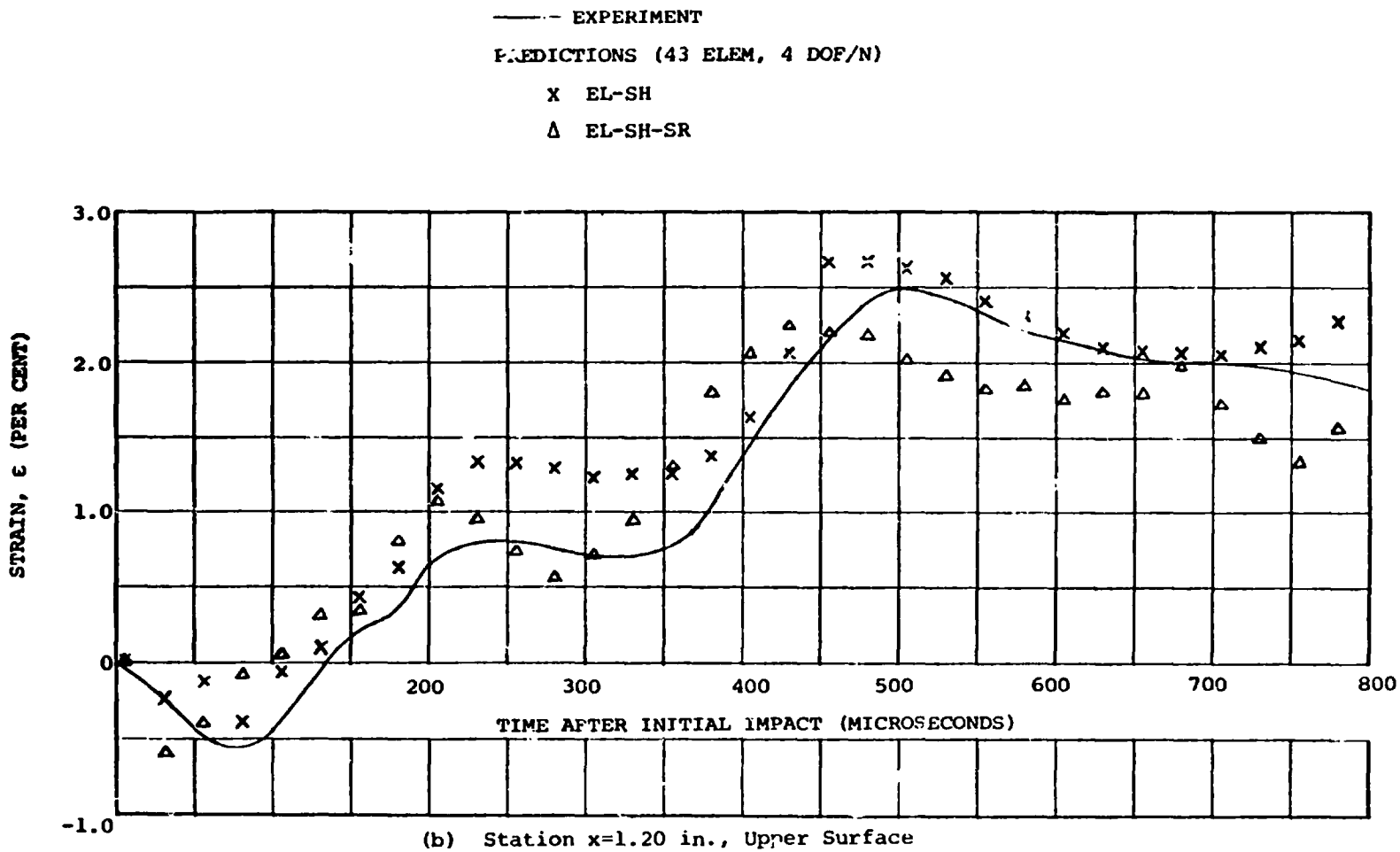

(b) Station x=1.20 in., Upper Surface

FIG. 19 CONCLULED (CB-18)

C-3.

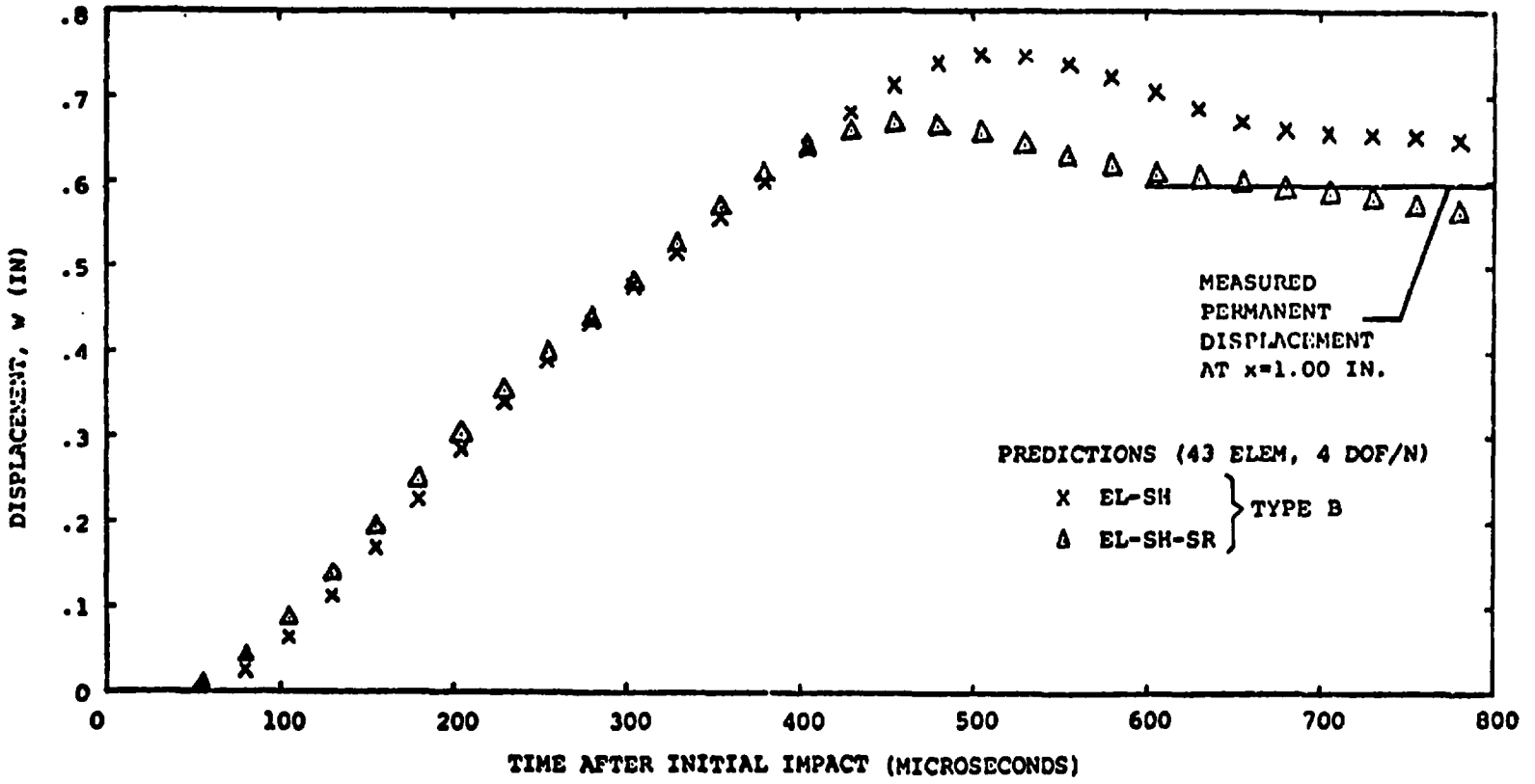

FIG. 20 PREDICTED TRANSIENT AND OBSERVED PERMANENT LATERAL DEFLECTION w AT SPANWISE STATION x=1.0 IN FOR STEEL-SPHERE IMPACTED 6061-T651 ALUMINUM BEAM SPECIMEN CB-18

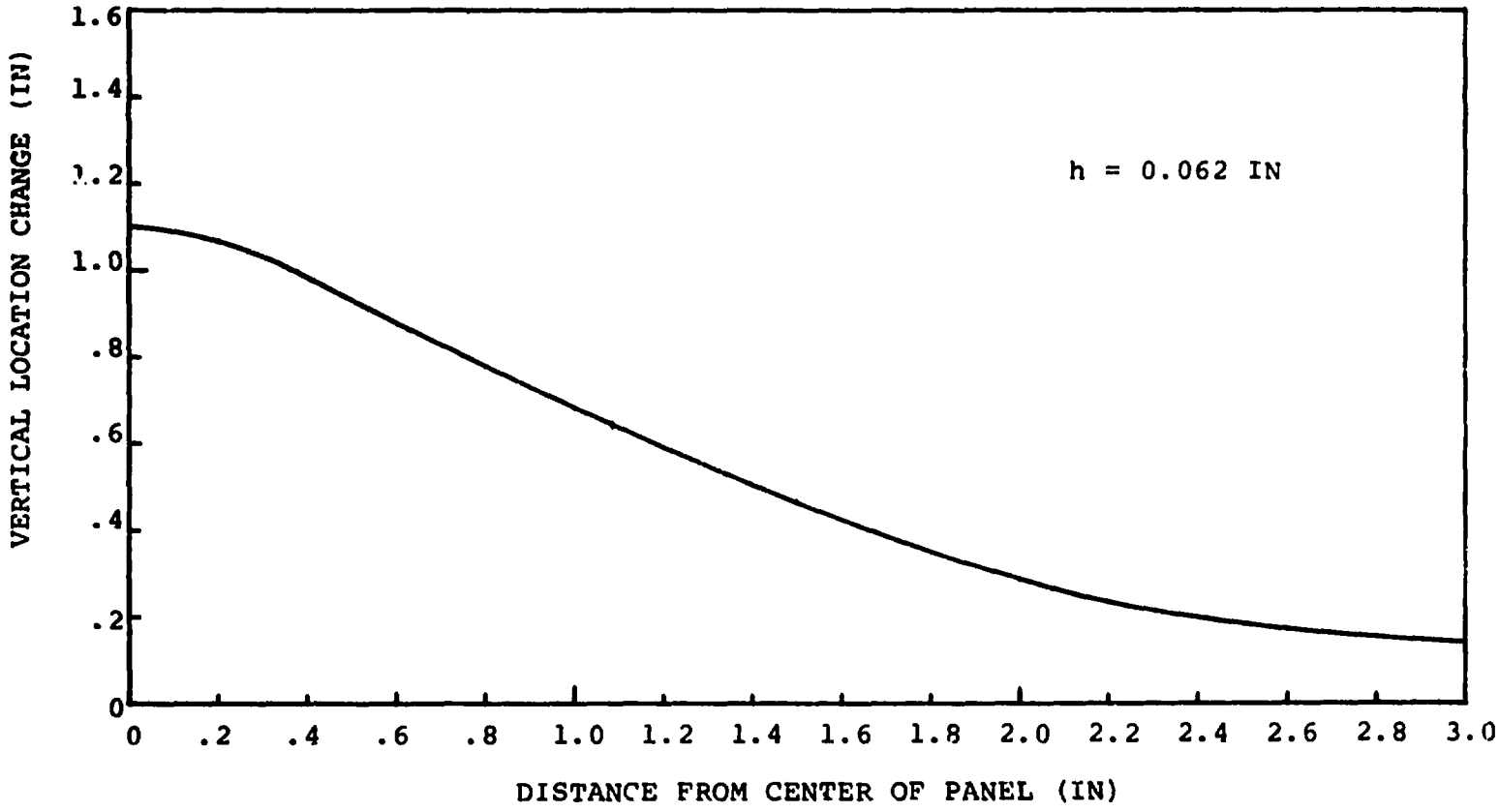

FIG. 21 PERMANENT LATERAL DEFLECTION OF IMPULSIVELY-LOADED SQUARE 6061-T651 ALUMINUM PANEL MODEL CP-2 WITH ALL FOUR SIDES IDEALLY CLAMPED

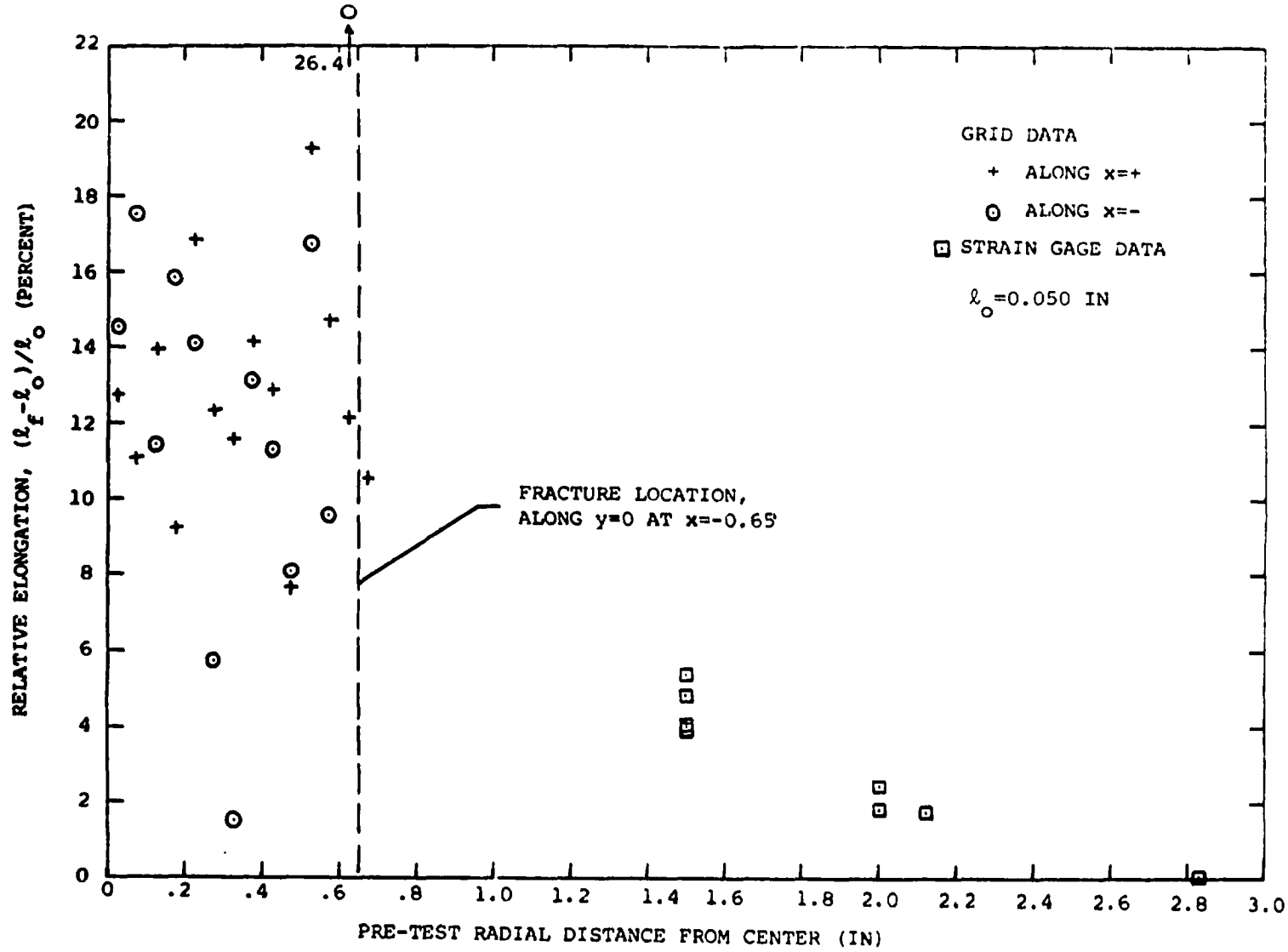

FIG. 22 UPPER SURFACE PERMANENT RELATIVE ELONGATION DATA FOR IMPULSIVELY-LOADED PANEL MODEL CP-2

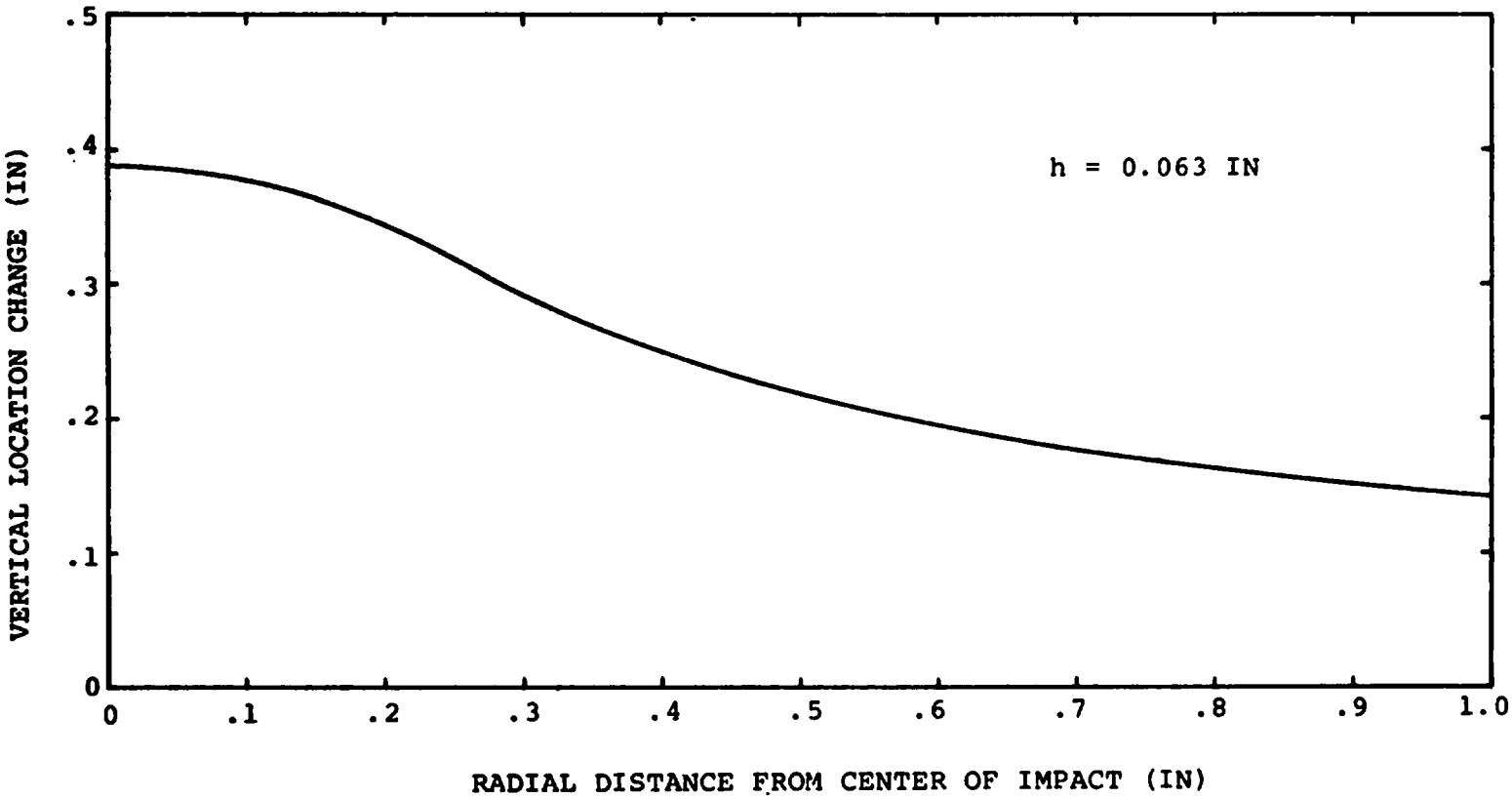

FIG. 23 PERMANENT LATERAL DEFLECTION OF STEEL-SPHERE IMPACTED 6061-T651 ALUMINUM PANEL MODEL CP-8

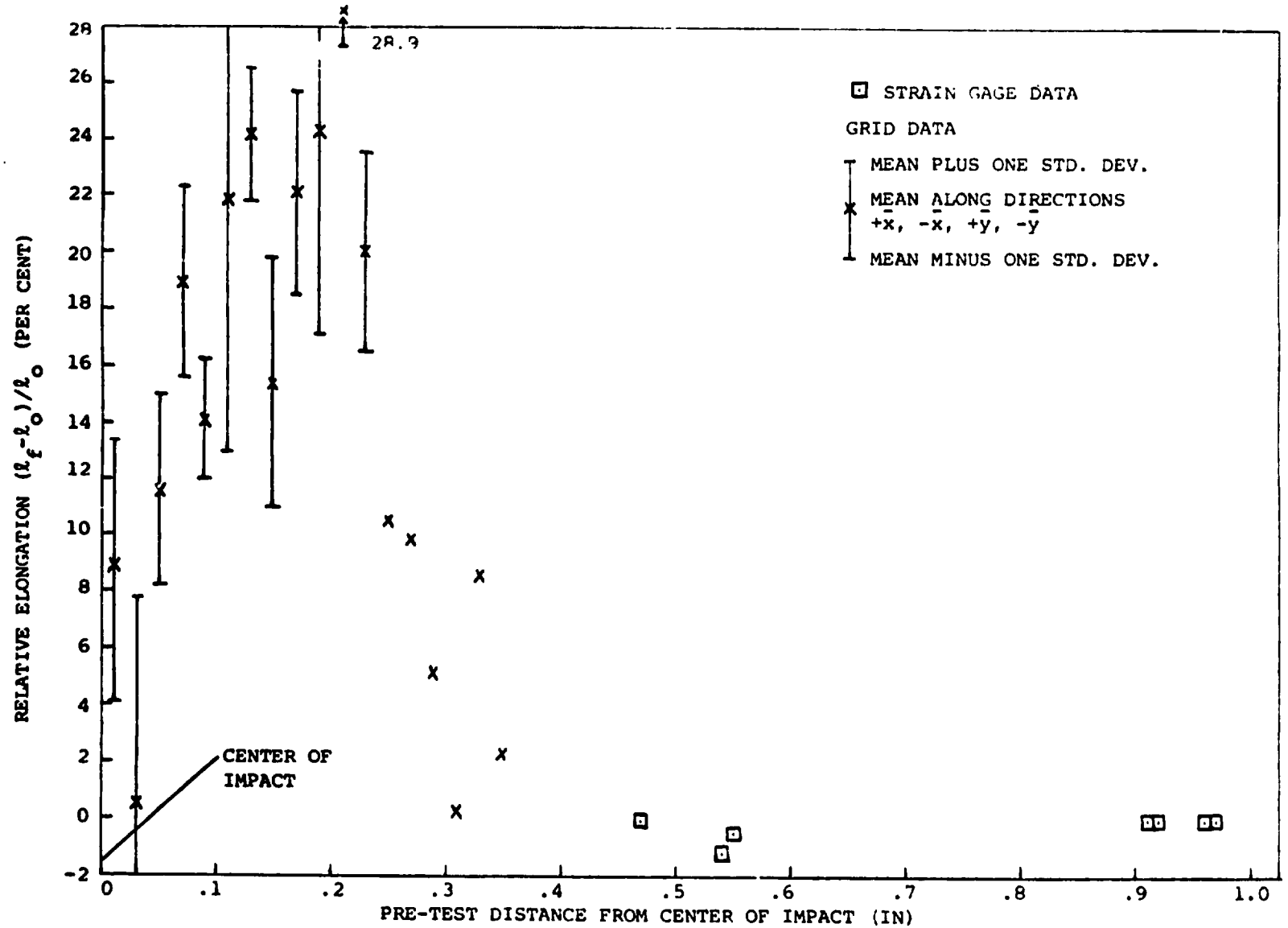

FIG. 24 UPPER SURFACE PERMANENT RELATIVE ELONGATION DATA FOR STEEL-SPHERE-IMPACTED PANEL MODEL CP-8

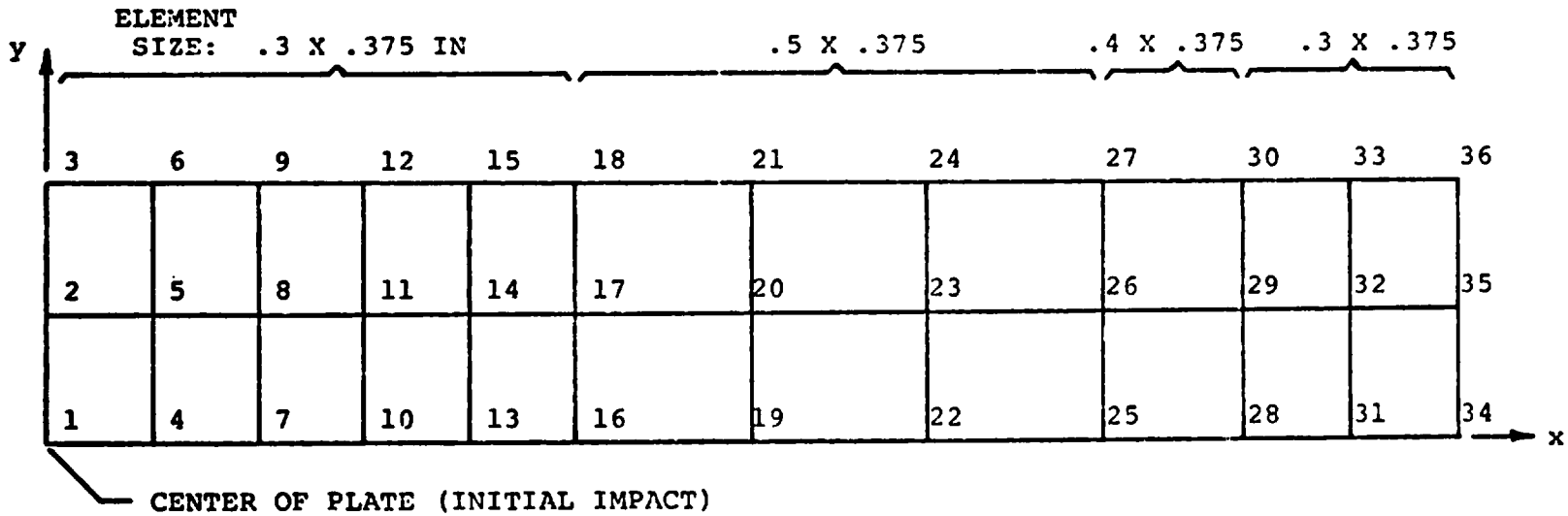

FIG. 25 FINITE ELEMENT ARRAY USED TO REPRESENT ONE QUARTER OF NARROW-PLATE SPECIMEN CB-18

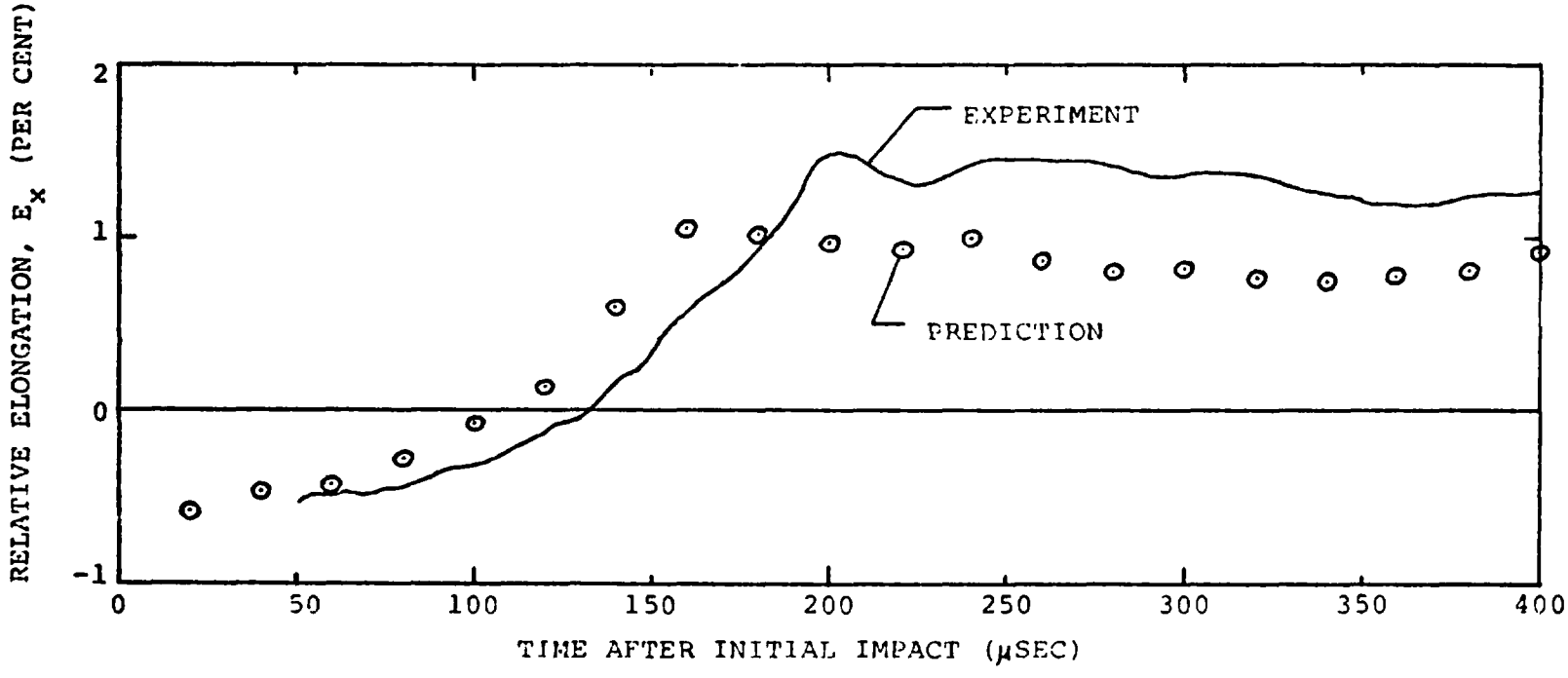

(a) x = 0.6 IN; UPPER SURFACE

FIG. 26 COMPARISON OF PREDICTED AND MEASURED TRANSIENT RELATIVE ELONGATIONS E_x AT VARIOUS SPANWISE STATIONS x ALONG y=0 FOR STEEL-SPHERE-IMPACTED NARROW-PLATE SPECIMEN CB-18

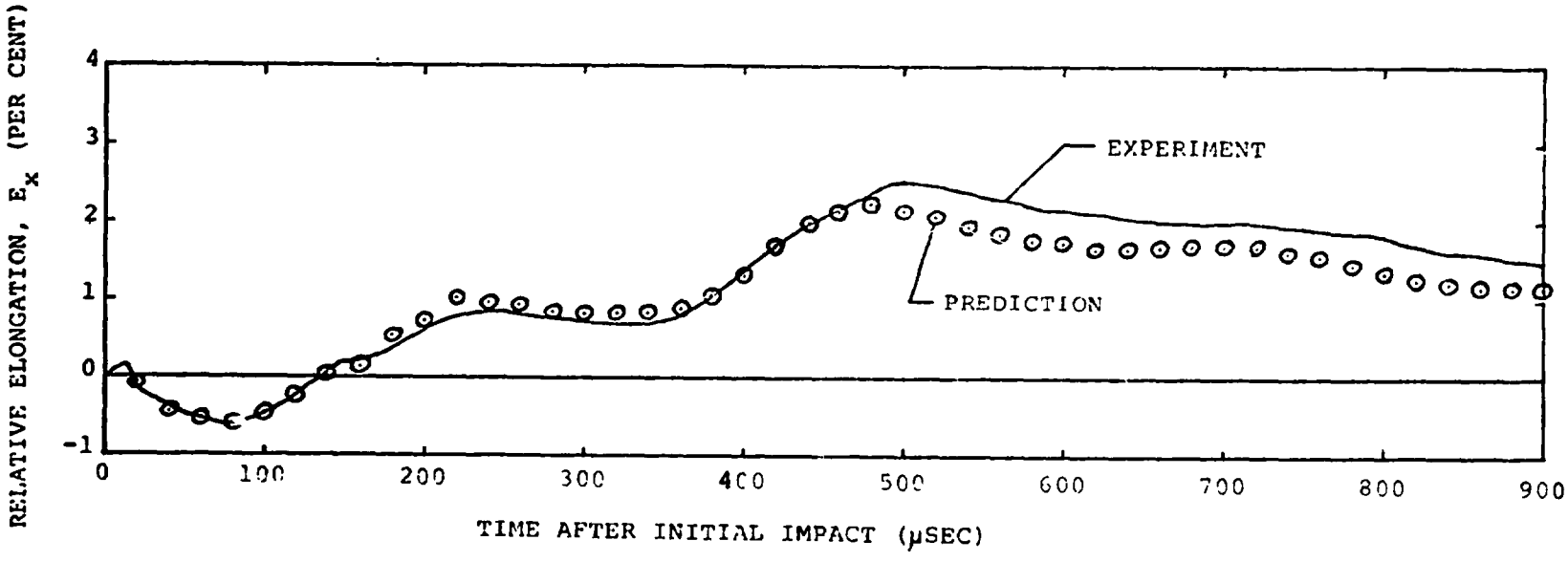

(b) x = 1.2 IN; UPPER SURFACE

FIG. 26 CONCLUDED (NARROW PLATE CB-18)

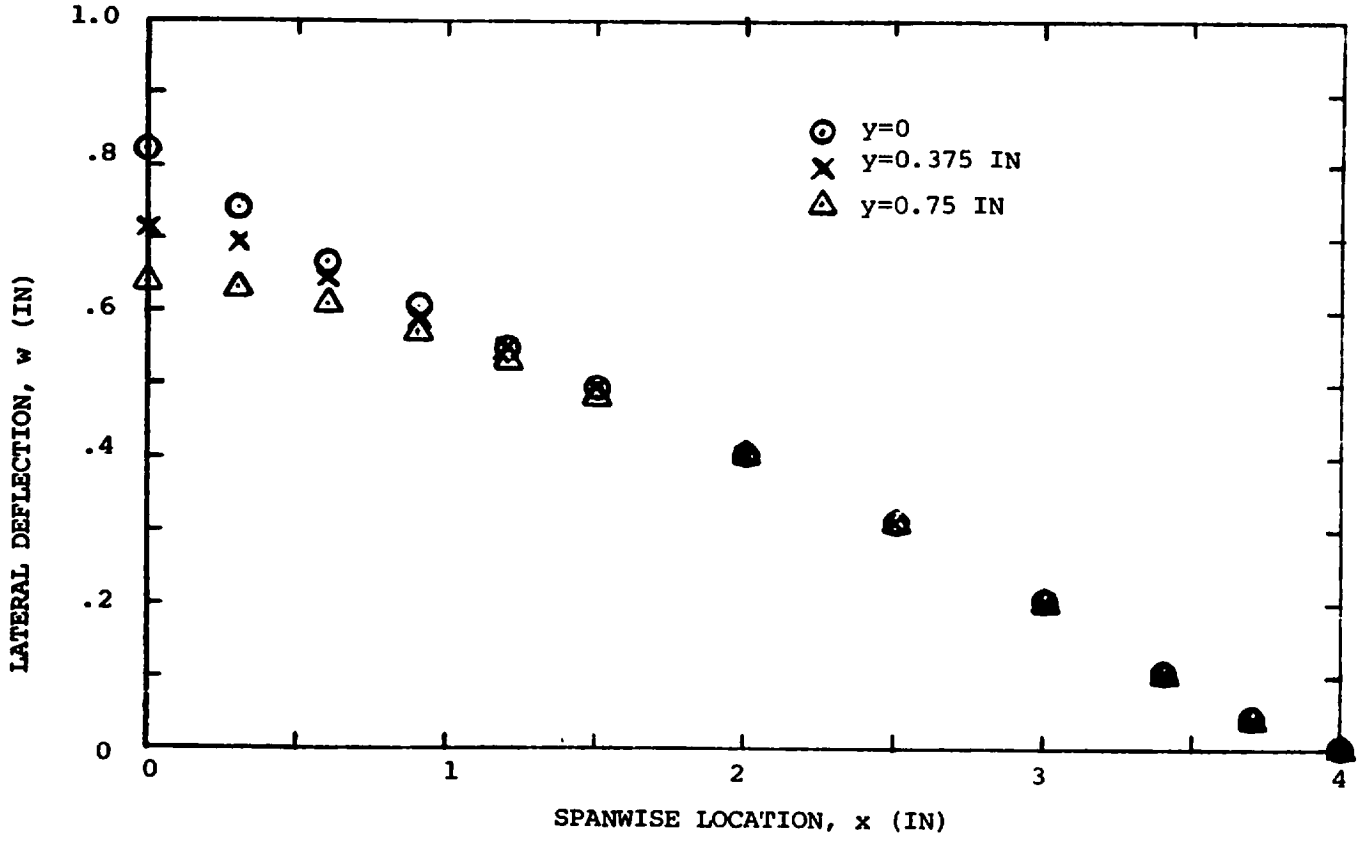

FIG. 27 PREDICTED LATERAL DEFLECTION DISTRIBUTION AT 900 MICROSECONDS AFTER INITIAL IMPACT FOR NARROW-PLATE SPECIMEN CB-18

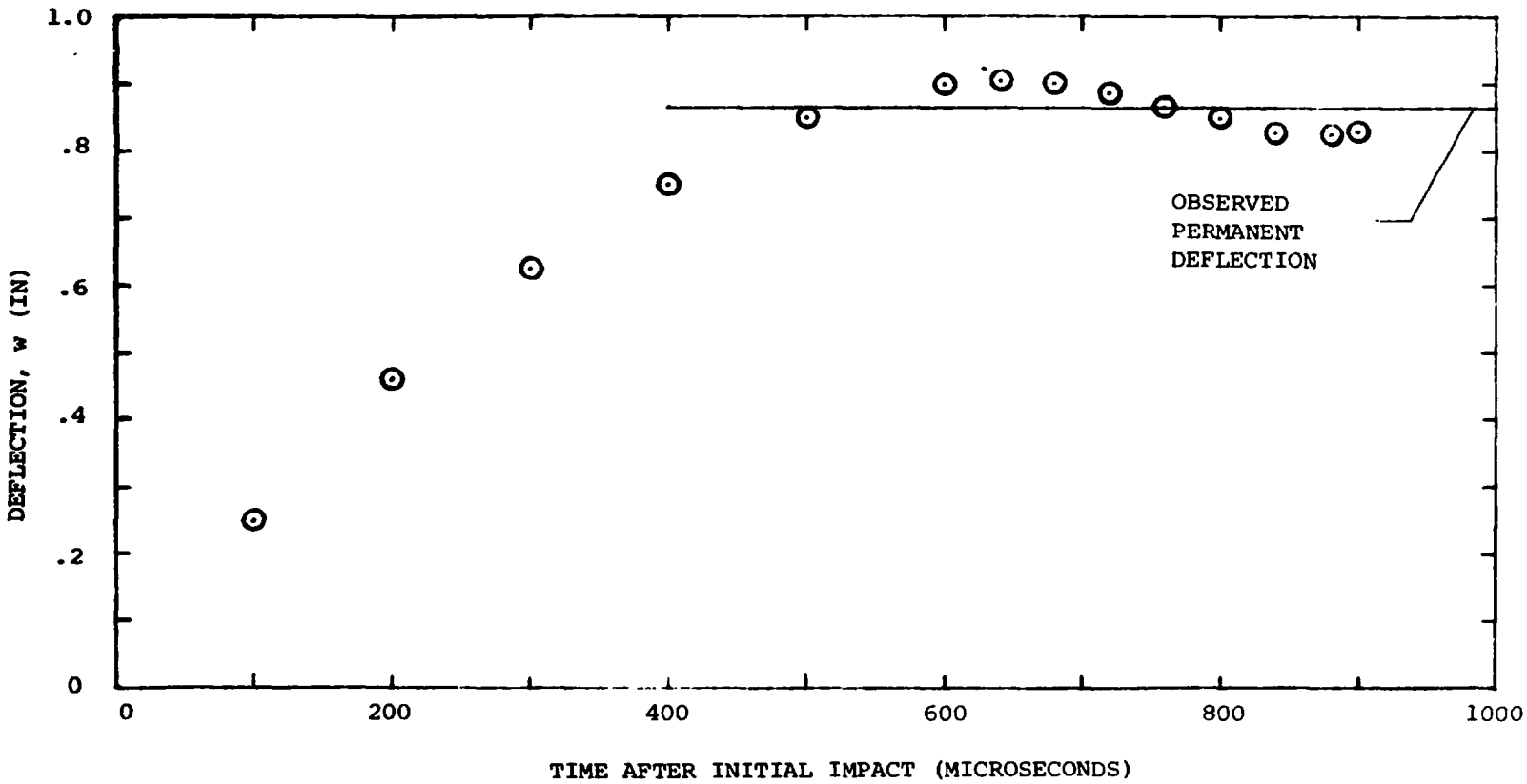

FIG. 28 PREDICTED TRANSIENT AND MEASURED PERMANENT DEFLECTION OF NARROW-PLATE SPECIMEN CB-18 AT PANEL CENTER (x,y)=(0,0)

APPENDIX A

SUMMARY OF THE CAPABILITIES OF MIT-ASRL COMPUTER CODES FOR PREDICTING TWO-DIMENSIONAL LARGE-DEFLECTION ELASTIC-PLASTIC TRANSIENT RESPONSES OF RING STRUCTURES

This description is intended to provide for the reader a convenient tabular summary of the principal features and capabilities of the two-dimensional transient large-deflection elastic-plastic structural response ring codes JET 1 (Ref. 1), JET 2 (Ref. 2), JET 3A-3D (Ref. 3), CIVM-JET 4B (Ref. 4), and JET 5A and CIVM-JET 5B (Ref. 5) developed under NASA NGR 22-009-339.

The JET 1 code of Ref. 1 pertains to single-layer complete, uniform-thickness, initially-circular rings of either temperature-independent or temperature dependent material properties. These rings may be subjected to prescribed: (a) initial velocities, (b) transient mechanical loading, and/or (c) steady nonuniform temperatures. The finite-difference method employed in this code had been shown previously (Ref. 6) to provide reliable predictions for the case of temperature-independent material properties.

The JET 2 code was written in order to extend this finite-difference analysis capability to treat multilayer rings -- cases anticipated to be of future concern. In the interests of efficiency and the minimization of computer storage requirements, temperature-dependent material properties and thermal loading features were omitted from JET 2; if these omitted features should turn out to be needed urgently, they could be added later.

Since the JET 1 and JET 2 codes pertained to initially-circular, complete rings of uniform thickness whereas there was interest also in variable-thickness, arbitrarily curved, partial as well as complete rings, the JET 3 series codes was developed. To accommodate these latter features as well as a variety of types of (1) boundary conditions, (2) elastic-foundation supports, and (3) point elastic supports, the more versatile finite-element analysis procedure was developed and employed. For efficiency and user convenience, four versions of the JET 3 program were developed; each version accommodates both complete rings and partial rings. JET 3A and JET 3B pertain to uniform-thickness, initially-circular rings, and employ, respectively, the central-difference and the Houbolt finite-difference time operator; for certain cases, the latter finite-difference time operator may permit more economic converged transient response predictions than the former. The codes JET 3C and JET 3D are corresponding codes which accommodate variable-thickness, arbitrarily-curved rings.

In most of these codes (JET 1 through JET 3D and JET 5A), the stimuli: (1) initial velocity or impulse conditions and/or (2) transient mechanical loading must be prescribed by the user or analyst. The externally-applied forces experienced by a complete or a partial ring from fragment impact are not provided within these codes. The user must supply his own estimate of the distribution and time histories of these forces. However, in the CIVM-JET 4B and CIVM-JET 5B codes, fragment/ring interaction and response effects are handled internally automatically, for the idealized single-fragment and n-fragment cases provided and discussed in the Appendices of Refs. 4, 5, and 7.

The CIVM-JET 4B code (Ref. 4) was developed from a modified version of the JET 3C code, using the central difference timewise operator. The CIVM (collision imparted velocity method) handles a fragment-structure impact as a series of quasi-static momentum transfers between the attacking fragment and the local-impact-affected portion of the impacted structure. The solution proceeds as though a series of impulses has been applied to the impacted region of the structure. This code provides strain output at each Gaussian station, nodal location, and designated additional points for user convenience, and calculates the reaction forces at each constrained degree of freedom. Another feature of this code is the ability to accommodate branches which are used as additional structural supports. These branches can have material properties either the same or different from those present in the main structure.

The JET 5A and CIVM-JET 5B codes (Ref. 5) were written in order to extend the capabilities of the JET 3D and CIVM-JET 4B codes to multilayer structures which are assumed to be hard-bonded and to deform in the Bernoulli-Euler fashion. Both codes contain the Houbolt timewise operator and all the additional strain and reaction force output and structural support capabilities utilized in the CIVM-JET 4B code.

In convenient tabular form, the principal features and capabilities of the codes JET 1, JET 2, JET 3A-D, CIVM-JET 4B, JET 5A, and CIVM-JET 5B are given in the following:

REFERENCES

1. McCallum, R.B., Leech, J.W. and Witmer, E.A., "Progress in the Analysis of Jet Engine Burst-Rotor Containment Devices", ASRL TR 154-1, Aeroelastic and Structures Research Laboratory, Massachusetts Institute of Technology, August 1969. (Available as NASA CR-107900.)

2. McCallum, R.B., Leech, J.W. and Witmer, E.A., "On the Interaction Forces and Responses of Structural Rings Subjected to Fragment Impact", ASRL TR 154-2, Aeroelastic and Structures Research Laboratory, Massachusetts Institute of Technology, September 1970. (Available as NASA CR-72801.)

3. Wu, R.W.-H. and Witmer, E.A., "Computer Program - JET 3 - to Calculate the Large Elastic-Plastic Dynamically-Induced Deformations of Free and Restrained, Partial and/or Complete Structural Rings", ASRL TR 154-7, Aeroelastic and Structures Research Laboratory, Massachusetts Institute of Technology, August 1972. (Available as NASA CR-120993.)

4. Stagliano, T.R., Spilker, R.L. and Witmer, E.A., "User's Guide to Computer Program CIVM-JET 4B to Calculate the Transient Structural Responses of Partial and/or Complete Structural Rings to Engine Rotor Fragment Impact", MIT ASRL TR 154-9, March 1976. (Available as NASA CR-CR-134907.)

5. Wu, R.W.-H., Stagliano, T.R., Witmer, E.A. and Spilker, R.L., "User's Guide to Computer Programs JET 5A and CIVM-JET 5B to Calculate the Large Elastic-Plastic Dynamically-Induced Deformations of Multilayer Partial and/or Complete Structural Rings", MIT ASRL TR 154-10, February 1977.

6. Balmer, H.A. and Witmer, E.A., "Theoretical-Experimental Correlation of Large Dynamic and Permanent Deformations of Impulsively-Loaded Simple Structures", Massachusetts Institute of Technology, AFFDL-TDR-64-108, July 1964.

7. Collins, T.P. and Witmer, E.A., "Application of the Collision-Imparted Velocity Method for Analyzing the Responses of Containment and Deflector Structures to Engine Rotor Fragment Impact", ASRL TR 154-8, MIT, August 1973. (Available as NASA CR-134494.)

Feature	JET 1 (Ref.1)	JET 2 (Ref.2)	JET 3A (Ref.3)	JET 3B (Ref.3)	JET 3C (Ref.3)	JET 3D (Ref.3)	CIVM-JET 4B (Ref.4)	JET 5A (Ref.5)	CIVM-JET 5B (Ref.5)
Type of Spatial Analysis Formulation									
Finite Difference	x	x	-	-	-	-	-	-	-
Finite Element	-	-	x	x	x	x	x	x	x
Type of Finite-Difference Time Operator									
Central Difference	x	x	x	-	x	-	x	-	-
Houbolt (Backward Difference)	-	-	-	x	-	x	-	x	x
Ring Geometry									
Complete Ring	x	x	x	x	x	x	x	x	x
Partial Ring	-	-	x	x	x	x	x	x	x
Initial Configuration									
Circular	x	x	x	x	x	x	x	x	x
Arb. Curved	-	-	-	-	x	x	x	x	x
Constant Thickness	x	x	x	x	x	x	x	x	x
Variable Thickness	-	-	-	-	x	x	x	x	x
Single Layer	x	x	x	x	x	x	x	x	x
Multilayer Hard-Bonded (1 to 3 layers)	-	x	-	-	-	-	-	x	x
Boundary Conditions									
Ideally Clamped	-	-	x	x	x	x	x	x	x
Hinged Fixed	-	-	x	x	x	x	x	x	x
Symmetry	-	-	x	x	x	x	x	x	x
Free	-	-	x	x	x	x	-	x	-
Other Support Conditions									
Distributed Elastic Foundation	-	-	x	x	x	x	x	x	x
Point Elastic Springs	-	-	-	x	x	x	x	x	x
Structural Branch	-	-	-	-	-	-	x	x	x

Feature	JET 1	JET 2	JET 3A	JET 3B	JET 3C	JET 3D	CIVM-JET 4B	JET 5A	CIVM-JET 5B
Material									
Single Material	x	-	x	x	x	x	x	x	x
Different for Each Layer	-	x	-	-	-	-	-	x	x
Homogeneous	x	x	x	x	x	x	x	x	x
Initially Isotropic	x	x	x	x	x	x	x	x	x
Temperature Independent	x	x	x	x	x	x	x	x	x
Temperature Dependent	x	-	-	-	-	-	-	-	-
EL	x	x	x	x	x	x	x	x	x
EL-PP	x	x	x	x	x	x	x	x	x
EL-LSH	x	x	x	x	x	x	x	x	x
EL-SH	x	x	x	x	x	x	x	x	x
EL-SH-SR	x	x	x	x	x	x	x	x	x
Stimulii									
Initial Velocity									
Arbitrary	x	x	x	x	x	x	-	x	-
Half-Sine over each of Selected Regions	x	x	x	x	x	x	-	x	-
Mechanical Loading									
Arbitrary Spatial Distribution with Arb. Time History	-	x	x	x	x	x	-	x	-
Half-Sine over each of Selected Regions	x	x	x	x	x	x	-	x	-
Triangular Time History	x	x	x	x	x	x	-	x	-
Arbitrary Time History	-	x	x	x	x	x	-	x	-
Thermal Loads (Temp. Distribution)									
Distribution Thru Thickness	x	-	-	-	-	-	-	-	-
Time-Independent Prescribed Circumferential Distribution	x	-	-	-	-	-	-	-	-
Impacting Fragments									
Single	-	-	-	-	-	-	x	-	x
Multiple	-	-	-	-	-	-	x	-	x
Friction	-	-	-	-	-	-	x	-	x

Feature	JET 1	JET 2	JET 3A	JET 3B	JET 3C	JET 3D	CIVM-JET 4B	JET 5A	CIVM-JET 5B
Deflections: Bernoulli-Euler Type Only									
Small	x	x	x	x	x	x	x	x	x
Arbitrarily Large	x	x	x	x	x	x	x	x	x
OUTPUT INFORMATION									
At Selected Times									
Energy/Work Type and Amount	x	x	x	x	x	x	x	x	x
Nodal Station Data									
Locations Y,Z	x	x	x	x	x	x	x	x	x
Displacements	-	-	x	x	x	x	x	x	x
Moment Resultant	x	x	x	x	x	x	x	x	x
Circum. Force Resultant	x	x	x	x	x	x	x	x	x
Circumferential Strains									
Inner Surface	x	x	x	x	x	x	x	x	x
Outer Surface	x	x	x	x	x	x	x	x	x
Location where Prescribed Value is Exceeded	-	x	x	x	x	x	-	-	-
Strain at Gaussian Stations	-	-	-	-	-	-	x	x	x
Strain at Additional Location	-	-	-	-	-	-	x	x	x
Support Reaction Forces	-	-	-	-	-	-	x	x	x
At Certain Other Times									
Time of First Yielding	x	x	-	-	-	-	-	-	-
Time when Strain First Exceeds a Prescribed Value	-	x	x	x	x	x	-	-	-
Time, Location, and Value of Largest Strain Reached During Run	-	-	x	x	x	x	x (For Each Substructure)	x	x
CAPACITY INFORMATION									
Maximum No. of Finite-Difference Stations[a]	100	100	-	-	-	-	-	-	-
Maximum No. of Finite Elements[a]	-	-	50	50	50	50	50	50	50

[a] These limits can be circumvented by altering the dimensions of appropriate program variables (see each source reference).

APPENDIX B

PUBLICATIONS AND TRANSIENT STRUCTURAL RESPONSE COMPUTER CODES BY THE MIT-ASRL ON NASA-SPONSORED FRAGMENT CONTAINMENT/DEFLECTION RESEARCH

1. McCallum, R.B., Leech, J.W. and Witmer, E.A., "Progress in the Analysis of Jet Engine Burst-Rotor Containment Devices", ASRL TR 154-1, Aeroelastic and Structures Research Laboratory, Massachusetts Institute of Technology, August 1969. (Available as NASA CR-107900.)

2. McCallum, R.B., "Simplified Analysis of Trifragment Rotor Disk Interaction with a Containment Ring", AIAA Journal of Aircraft, Vol. 7, No. 3, May-June 1970, pp. 283-285.

3. McCallum, R.B., Leech, J.W. and Witmer, E.A., "On the Interaction Forces and Responses of Structural Rings Subjected to Fragment Impact", ASRL TR 154-2, Aeroelastic and Structures Research Laboratory, Massachusetts Institute of Technology, Sept. 1970. (Available as NASA CR-72801.)

4. Wu, R.W.-H. and Witmer, E.A., "Finite Element Analysis of Large Elastic-Plastic Transient Deformations of Simple Structures", AIAA Journal Vol. 9, No. 9, Sept. 1971, pp. 1719-1724.

5. Leech, J.W., Witmer, E.A., and Yeghiayan, R.P., "Dimensional Analysis Considerations in the Engine Rotor Fragment Containment/Deflection Problem", ASRL TR 154-3, Aeroelastic and Structures Research Laboratory, Massachusetts Institute of Technology, December 1971. (Available as NASA CR-120841.)

6. Wu, R.W.-H. and Witmer, E.A., "Finite-Element Analysis of Large Transient Elastic-Plastic Deformations of Simple Structures, with Application to the Engine Rotor Fragment Containment/Deflection Problem", ASRL TR 154-4, Aeroelastic and Structures Research Laboratory, Massachusetts Institute of Technology, January 1972. (Available as NASA CR-120886.)

7. Zirin, R.M. and Witmer, E.A., "Examination of the Collision Force Method for Analyzing the Responses of Simple Containment/Deflection Structures to Impact by One Engine Rotor Blade Fragment", ASRL TR 154-6, Aeroelastic and Structures Research Laboratory, Massachusetts Institute of Technology, May 1972. (Available as NASA CR-120952.)

8. Wu, R.W.-H. and Witmer, E.A., "Computer Program - JET 3 - to Calculate the Large Elastic-Plastic Dynamically-Induced Deformations of Free and Restrained, Partial and/or Complete Structural Rings", ASRL TR 154-7, Aeroelastic and Structures Research Laboratory, Massachusetts Institute of Technology, August 1972. (Available as NASA CR-120993.)

9. Wu, R.W.-H. and Witmer, E.A., "Approximate Analysis of Containment/Deflection Ring Responses to Engine Rotor Fragment Impact", AIAA Journal of Aircraft, Vol. 10, No. 1, January 1973, pp. 28-37.

10. Wu, R.W.-H. and Witmer, E.A., "Nonlinear Transient Responses of Structures by the Spatial Finite-Element Method", AIAA Journal, Vol. 11, No. 8, August 1973, pp. 1110-1117.

11. Collins, T.P. and Witmer, E.A., "Application of the Collision-Imparted Velocity Method for Analyzing the Responses of Containment and Deflector Structures to Engine Rotor Fragment Impact", MIT ASRL TR 154-8, August 1973. (Available as NASA CR-134494.)

12. Yeghiayan, R.P., Leech, J.W. and Witmer, E.A., "Experimental and Data Analysis Techniques for Deducing Collision-Induced Forces from Photographic Histories of Engine Rotor Fragment Impact/Interaction with a Containment Ring," MIT ASRL TR 154-5, October 1973. (Available as NASA CR-134548.)

13. Witmer, E.A., Merlis, F. and Spilker, R.L., "Experimental Transient and Permanent Deformation Studies of Steel-Sphere-Impacted or Impulsively-Loaded Aluminum Beams with Clamped Ends", MIT ASRL TR 154-11, October 1975. (Available as NASA CR-134922.)

14. Stagliano, T.R., Spilker, R.L. and Witmer, E.A., "User's Guide to Computer Program CIVM-JET 4B to Calculate Large Nonlinear Transient Deformations of Single-Layer Partial and/or Complete Structural Rings to Engine Rotor Fragment Impact", MIT ASRL TR 154-9, March 1976. (Available as NASA CR-134907.)

15. Wu, R.W.-H., Stagliano, T.R., Witmer, E.A. and Spilker, R.L., "User's Guide to Computer Programs JET 5A and CIVM-JET 5B to Calculate the Large Elastic-Plastic Dynamically-Induced Deformations of Multilayer Partial and/or Complete Structural Rings", MIT ASRL TR 154-10, February 1977.

16. Witmer, E.A., Merlis, F., Rodal, J.J.A. and Stagliano, T.R., "Experimental Transient and Permanent Deformation Studies of Steel-Sphere-Impacted or Impulsively-Loaded Aluminum Panels", MIT ASRL TR 154-12, March 1977.

STRUCTURAL RESPONSE COMPUTER CODE STATUS

Code	Capability	Status	Availability
JET 3	2-D Single-Layer Beams and Rings Subjected to Prescribed Transient Loads or Initial Velocity Distributions (No Fragment Impact)	Complete (Ref. 8)	a
CIVM-JET 4B	2-D Single-Layer Beams and Rings Subjected Only to Fragment Impact	Complete (Ref. 14)	b
JET 5A	2-D Multilayer Bernoulli-Euler Beams and Rings Subjected to Prescribed Transient Loads or Initial Velocity Distributions	Complete (Ref. 15)	b
CIVM-JET 5B	2-D Multilayer B-E Beams and Rings Subjected only to Fragment Impact	Complete (Ref. 15)	b
PLATE and CIVM-PLATE	3-D Single Layer Initially-Flat Panels Subjected, Respectively, to (1) Prescribed Transient Loads and/or Initial Velocity Distributions or (2) Fragment Impact Only	In Progress	--

a: Available from COSMIC, Barrow Hall, University of Georgia, Athens, GA. 30601; contact MIT for errata.

b: Available under a copyright licensing agreement from MIT. Contact Prof. E.A. Witmer, Room 41-219, MIT, Cambridge, Mass. 02139.

DISCUSSION

B.L. Koff, GE-Cincinnati

We have conducted tests and managed to collect pieces of blades that were deliberately failed to understand containment ring behavior. It is quite obvious that you don't get a three-lobe shape in the ring, because as soon as the ring starts deforming locally, all of the other blades in the rotor act as a bearing for the ring. This tends to keep the ring round, not three-corner or some other shape, by adding quite a bit of support to the ring. It suggests that there is more to be learned from the tests you are now running on panels, than in oversimplified tests run with a ring that is not supported in a manner similar to the engine. When you start adding other support, you might find that these simplified panel tests, in fact, more nearly duplicate what actually happens, than an oversimplified test with rotor burst fragments.

E.A. Witmer, MIT-ASRL

I think it would be very useful in this whole program, if we could have people like you, who could suggest to us proper models to use for supported structures, so that we simulate things in the right way. It's an excellent idea.

As I understand your described tests, you released 1 or 2 blade portions from a rotating fully-bladed rotor to impact a containment ring. Similar tests done at the NAPTC show behavior very similar to what you describe; the initial impact causes the ring to deform and then it comes in contact with the blades still attached to the spinning rotor. These blades also deform but do "support" the ring and tend to restrain it from deforming as severely as it would if a "free ring" were impacted only by the initial attacking fragments.

A. Weaver, P&W

As I understand this model, it does a fairly representative job of modelling deflections in simple structures, whether they are panels or rings. However, it doesn't get at the meat of the containment problem as I see it, which is failure. I don't always care about deflections, but I do care when and where the ring is going to fail, and how to model that. The 2-D analysis completely ignored the localized effects going on at the center of impact, which I believe are very important.

E.A. Witmer, MIT-ASRL

You're perfectly correct, there are 3-D effects present where failure initiates in the cited beam experiments, and 2-D is clearly an idealization. It's a convenient scheme to us to obtain some crude estimates but it certainly doesn't address the real problem. The 3-D problem is the important one. For the beams and rings discussed here, the structural response behavior is of the 2-D type essentially everywhere on the (narrow) rings and also everywhere on the steel-sphere-impacted beam specimens except near the "impact point" itself where 3-D effects are very prominent. Here at threshold rupture, a multiaxial

strain state involving very large strains exists. For such regions, the analysis must accommodate large strain plasticity effects and an appropriate "failure strain" or similar criterion. This is a matter that is receiving much attention now by various groups.

D. Oplinger, Army-AMMRC

Is it realistic to assume that you're going to get a structural problem rather than a penetration problem? Some of the velocities I saw were fairly low; they were a couple hundred feet per second, but when you get up to a thousand feet per second, you've got to treat the penetration problem first and then you can treat it as a structural response problem.

E.A. Witmer, MIT-ASRL

As I understood the fragment velocities cited, they represent the fragment tip and/or the CG velocities; not the velocity component perpendicular to the impacted surface at impact. For rotors with typical small clearance, the typical impact angle is very shallow -- somewhere in the vicinity of 20-25 degrees. Hence, for many cases, the typical normal-to-the-surface velocity component at impact might range up to perhaps about 420 fps. Depending upon the material properties of the structure being impacted, the subsequent behavior could involve "penetration" followed by structural response or could involve principally only structural response. For most of the containment structure materials being considered, I believe that the latter is the more prevalent case.

D. Oplinger, Army-AMMRC

I am not familiar with blade materials but what little I know would lead me to believe that it would be unusual to get such large curling as you were showing. Is that typical of common blade materials, that they can bend over like that without snapping into small pieces?

E.A. Witmer, MIT-ASRL

For the small T58 turbine rotor used in many of the NAPTC tests, this was the observed behavior. However, for the rotors of the newer larger engines, I will ask Mr. Koff of GE to respond -- he can give a better answer.

B.L. Koff, GE-Cincinnati

Some of the blades are high aspect ratio turbine blades, and are more typical of aft end turbine stages. The first stage of the HP has blades of low aspect ratio and the first stage of an air-cooled turbine consists of a hollow structure which usually fragments into many pieces upon impact. Titanium fan blades don't curl very much but break up into pieces.

S. Sattar, P&W

I want to remark on the basic philosophy or approach to fragment containment design. Would it make more sense for us to step back and ask ourselves that if you go through this analysis and you have to determine when these computer programs will predict penetration, you would have to calibrate them against tests? Might it not be easier to take a simpler approach to predict

whether the fragment will be contained or not? It is a case of strength of materials or solid mechanics approach, calibrated against spin-pit or specimen tests versus these codes to predict the deflections and strains, and then finding out at what strain value will the penetration finally take place -- which you will calibrate anyway, against some tests. I would like a comment on that.

E.A. Witmer, MIT-ASRL

Your point is, a valid one, however, I think that if one can afford to run experiments on every kind of configuration, material, and so forth, to obtain the data you seek, that's one way of proceeding. There is some hope that one need not go that far, but instead one can rely upon more basic material property information and methods of structural dynamic analysis (at least for simple cases) and have a reasonable prospect of predicting analytically when these containment-structure failures should occur. I believe that the 3-D structural response studies in progress represent a useful step in that direction.

Now, one can immediately dream up a new case which is too complicated for any available analysis to handle properly. In such cases one would have to appeal to selected experiments; it seems to me any good organization would always do that.

J.W. Leech, ERDA

Would you comment on why an aluminum alloy was used for the beam model, the panel models, and the containment ring which was subjected to single-blade impact.

E.A. Witmer, MIT-ASRL

We used 6061-T6 and 6061-T651 aluminum for these specimens for fabrication convenience and because their stress-strain properties are well known; very little strain hardening is present. We approximated these properties by piecewise linear segments and used them (via the mechanical sublayer model) in the transient response calculations.

Incidentally, the NAPTC had static stress-strain tests conducted on the 4130 cast steel used in their containment ring tests. As perhaps you noticed, we did not show any comparisons between our calculations and the experiment for NAPTC Test 201 (T58 tri-hub burst against the steel containment ring) because we have not concluded that work. You can see immediately that the idealization that we used for the fragment, will give us no hope whatever of predicting in detail the transient response. The hope is that a realistic selection of the idealized (rigid circular) fragment may enable us to predict the peak response reasonably well, but the actual physical situation is just so much different from the idealized model that the fine transient response details actually present can not be reproduced by this model. But that's really expecting too much of that simple model. Of course, the model can be refined. One can devise a more complicated fragment model -- one can put in the various curling blades (attached to the disk segment) and let them go ahead and curl and follow them; a tremendous amount of bookkeeping would be involved.

Hence, we elected to try to see the potential of this simple rigid-circular-fragment idealization. Also, one could modify this simple circular fragment to permit deformations approximating roughly the behavior of the blade/disk fragment itself to achieve a still simple, but better simulation of the actual attacking fragment.

DEVELOPMENT OF FIBER SHIELDS FOR ENGINE CONTAINMENT

by

R. J. Bristow and C. D. Davidson
Senior Engineers

THE BOEING COMPANY
Seattle, Washington 98124

SUMMARY

A partial review is given of the progress at Boeing toward achieving a lightweight means for containing engine burst debris. This paper describes only the empirical work. Another paper at this meeting, by Dr. J. H. Gerstle, deals with the Boeing theoretical approach. The testing described was conducted in both translational launchers and spin pits. Empirical model development relating fragment characteristics to shielding requirements is given. The change in relative importance of shield mounting provisions as fragment energy is increased is given.

INTRODUCTION

The current shield design concepts have resulted from an evolutionary development that began in the early 1960's. Since that time, a group at Boeing has developed shielding for a wide range of threats: meteoroids, bullets, blast, hail, rain, and free-falling rocks, to mention a few. In all of these efforts, it was clear that shielding weight could be reduced if the projectile deceleration distance was increased. For lower velocity regimes, this could be accomplished by combining the properties of high shear resistance and elasticity in the direction of projectile motion. Certain fibrous materials can provide these properties.

Various fibrous materials have been used since the days of spears and arrows to shield against projectiles. More recently, fibrous shields have been used as "flak vests". At Boeing, glass fiber blankets have been used experimentally as blast shielding. It was natural, then, to try fiber blankets for engine containment. The first fibers tried, glass, performed better than metallic shields but the data was inconsistent. DuPont's Kevlar fabric was then tried and has developed into today's design concept.

The development of the Kevlar shield has been undertaken with a two-pronged approach. An analytical computer model (EBCAP) was developed based on a theoretical approach, the M.I.T. Model JET 4B and other published data. The second approach used the empirical data to generate two empirical models that have in turn been used to solve design problems. The first empirical model (Figure 1) defined the weight of shield for various projectile sizes and the velocities at which the projectiles would be contained; this at a constant dynamic stiffness. The second model related the shield mount load to mount dynamic stiffness. Both approaches, analytical and empirical, were coordinated with the test program and are complementary.

BACKGROUND

In order to maintain continuity, earlier program results published in a previous paper* will be summarized.

Translational testing consisted of firing steel cubes from a smoothbore cannon into a test shield as shown schematically in Figure 2. Figure 3 is a photograph of the test range. The target assembly, shown in Figure 4, consisted not only of the test shield, but a series of thin aluminum plates. The plates, called "witness sheets," were used to determine the residual energy of the cube if the test shield was penetrated. The cubes were launched from the cannon by means of a polycarbonate sabot as shown in Figure 5. The ballistic limit was found by plotting penetration versus velocity as shown in Figure 6. (Ballistic limit is the limiting velocity below which shield penetration will not occur.) The figure shows the abscissa to be made up of shield layers plus numbers of witness sheets. The slanted line shows the number of witness sheets penetrated when the shield was removed. The "S"-shaped curve shows penetration with the shield in place. The number of Kevlar layers penetrated increased gradually with velocity until the ballistic limit was approached. At the ballistic limit, the penetrability of the cube increased greatly. At a velocity a little above the ballistic limit, the number of witness sheets penetrated was nearly equal to that with no shield at all. This signified that above the ballistic limit, the shield absorbed very little energy. From these data, the first empirical model was developed (Figure 1):

* Bristow, R. J., et al, "Advances in Engine Burst Containment, "AGARD-R-648, presented at the 42nd Structures and Materials Panel Meeting, NATO-AGARD, Ottawa, Canada, April 1976.

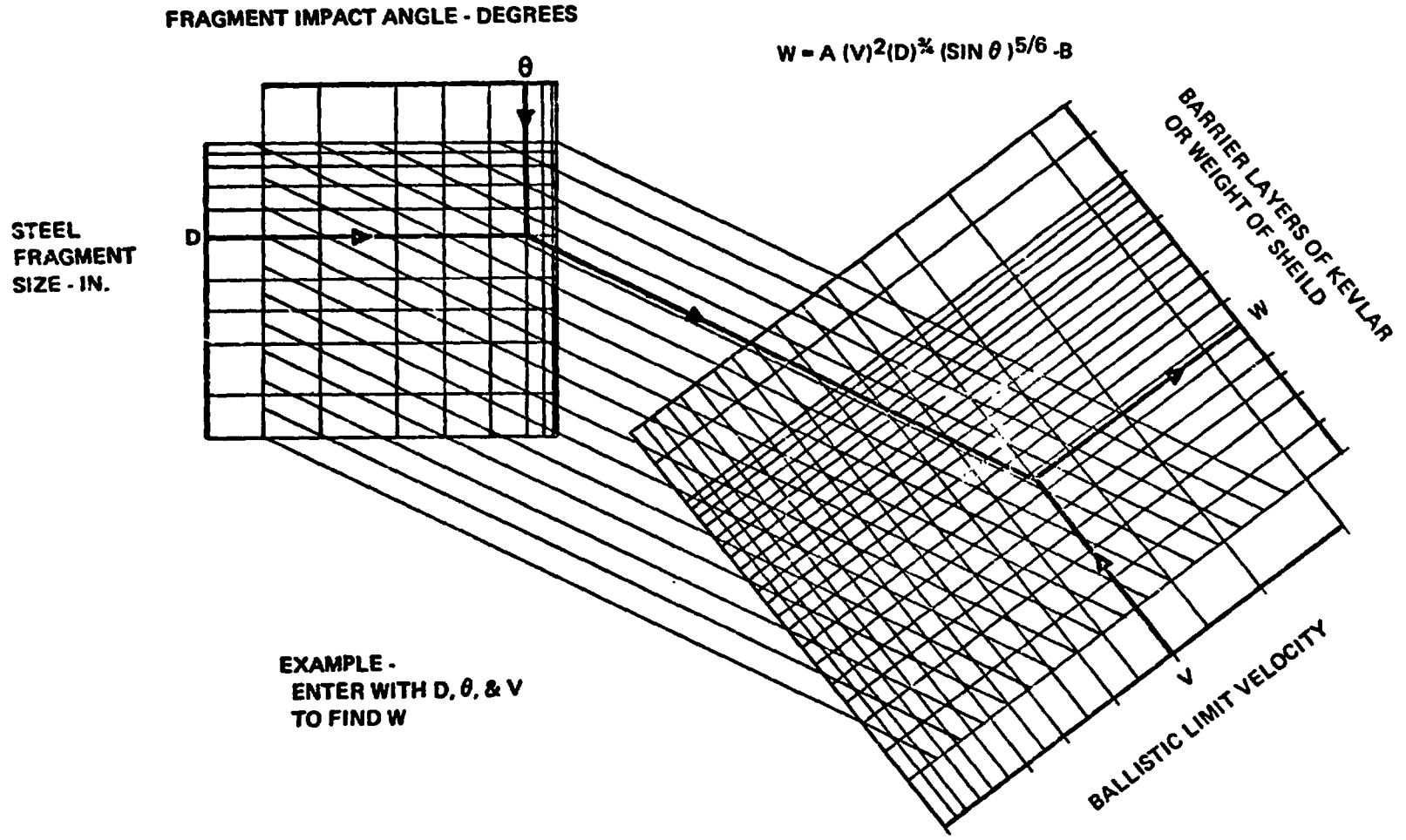

Figure 1. - Ballistic Limit Model.

$$N = A(V)^2(D)^{3/4}(\sin\theta)^{5/6} - B \qquad (1)$$

where:

N = number of shield layers (Kevlar)
V = cube velocity at ballistic limit - fps
D = cube size - inches
θ = angle between shield surface and flight path
A & B = constants.

Other areas covered by the previous paper include temperature effects and the effect of spinning on fragment penetration. Since neither of these areas are pertinent to the subject of the current paper, they will not be reviewed.

One of the major efforts during the last year was the development of an attachment load model. The load involved was that in the mount of a particular shield arrangement with a particular dynamic stiffness. However, the form of the model should be general in nature and provides a great deal of information on shield design requirements. The data for the model were obtained using the test arrangement shown in Figure 7. One post was calibrated to read equivalent load at the centerline of the shield. In order to change effective mounting stiffness, a series of nylon ropes were run through the shield ends and looped around the posts as shown in Figure 8. The stiffness was varied by changing the length or diameter of the ropes. The resulting model was of the form

$$P = CV(D)^3(K)^{1/2}(N + E)^{-1/2} \qquad (2)$$

where:

P = peak impact load (lb)
K = stiffness of mount + attachments (lb/in)
C & E = constants.

It should be pointed out that the form of the term involving the number of shield layers may be different for other shield arrangements.

Once an empirical model like the one above has been obtained, it is often constructive to examine it in detail in order to get an insight into the phenomenology involved. Notice that the peak load is directly proportional to the fragment velocity and mass. It is not too surprising that the load would be

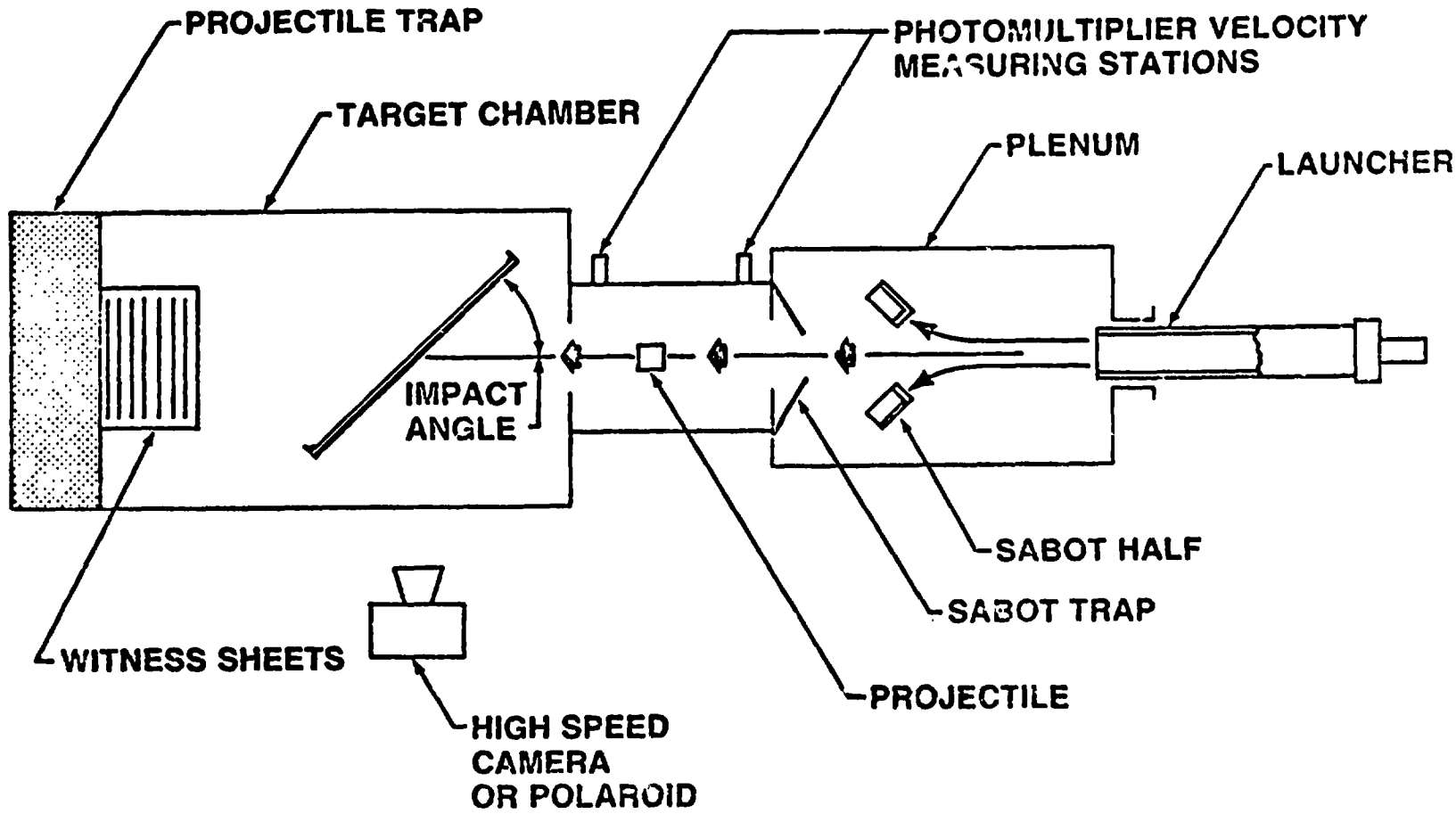

Figure 2. - Test Range Schematic.

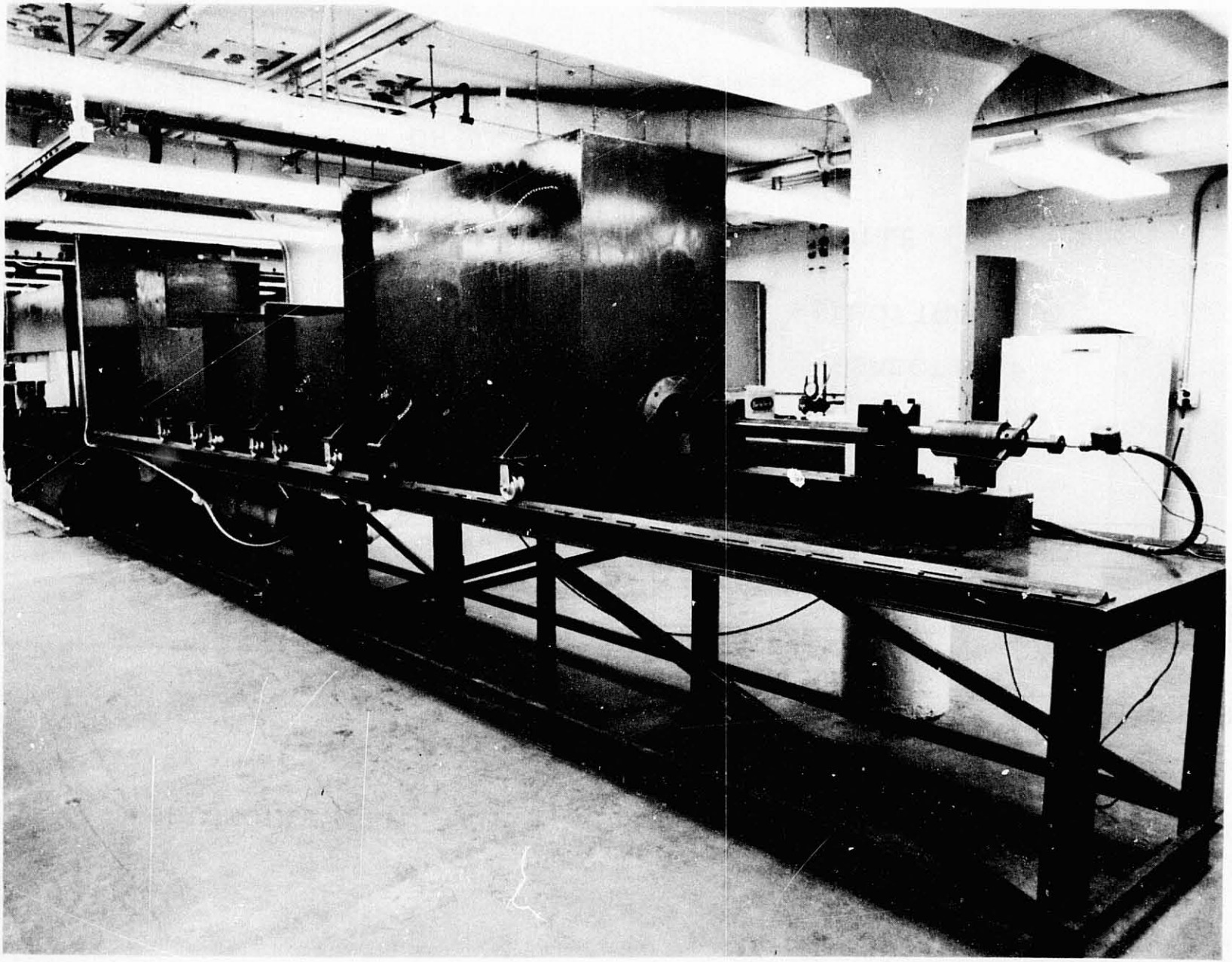

Figure 3. - Test Range No. 2.

Figure 4. - "Flat" Shield and Witness Sheets.

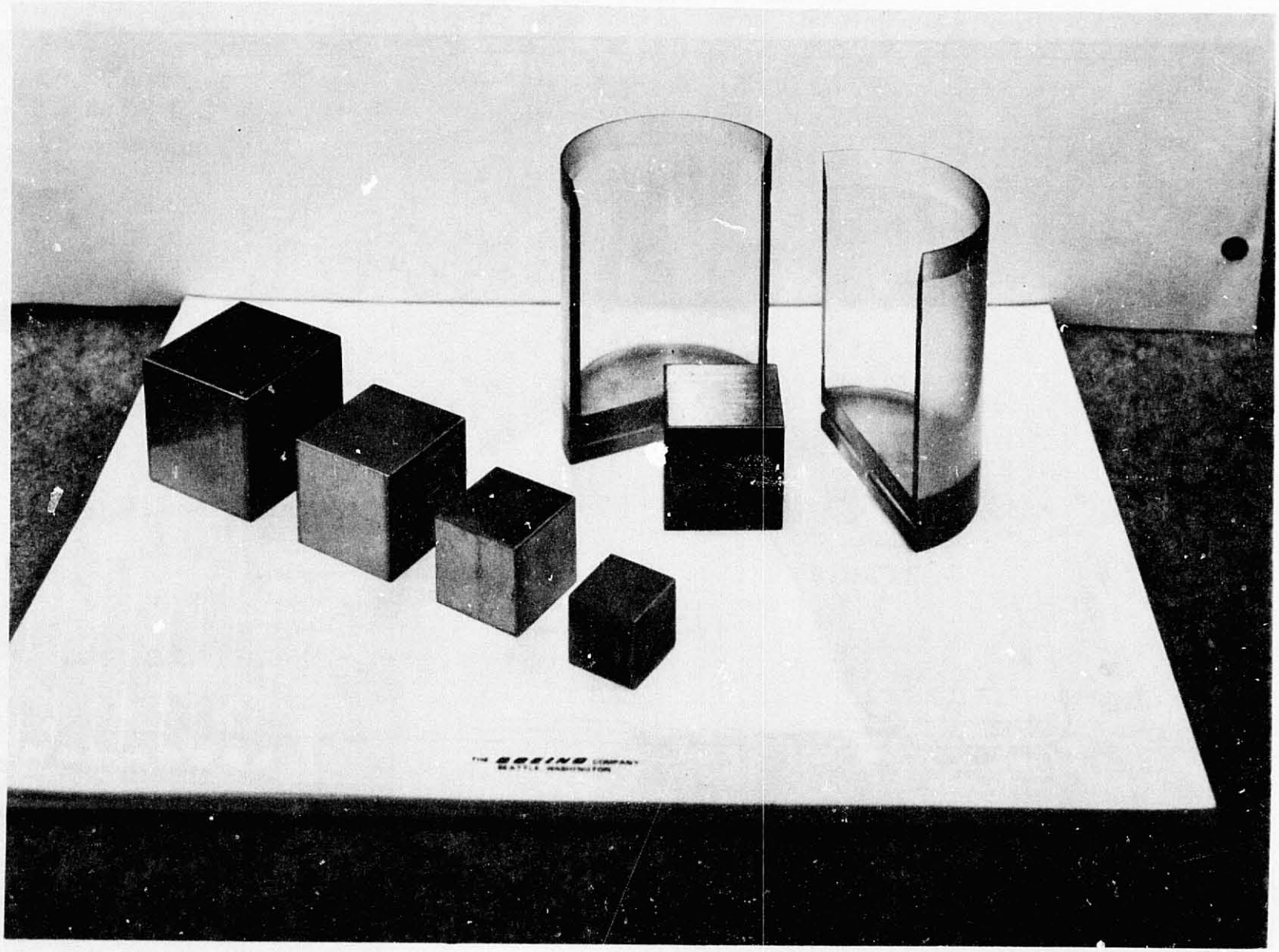

Figure 5. - Steel Cubes and Sabots.

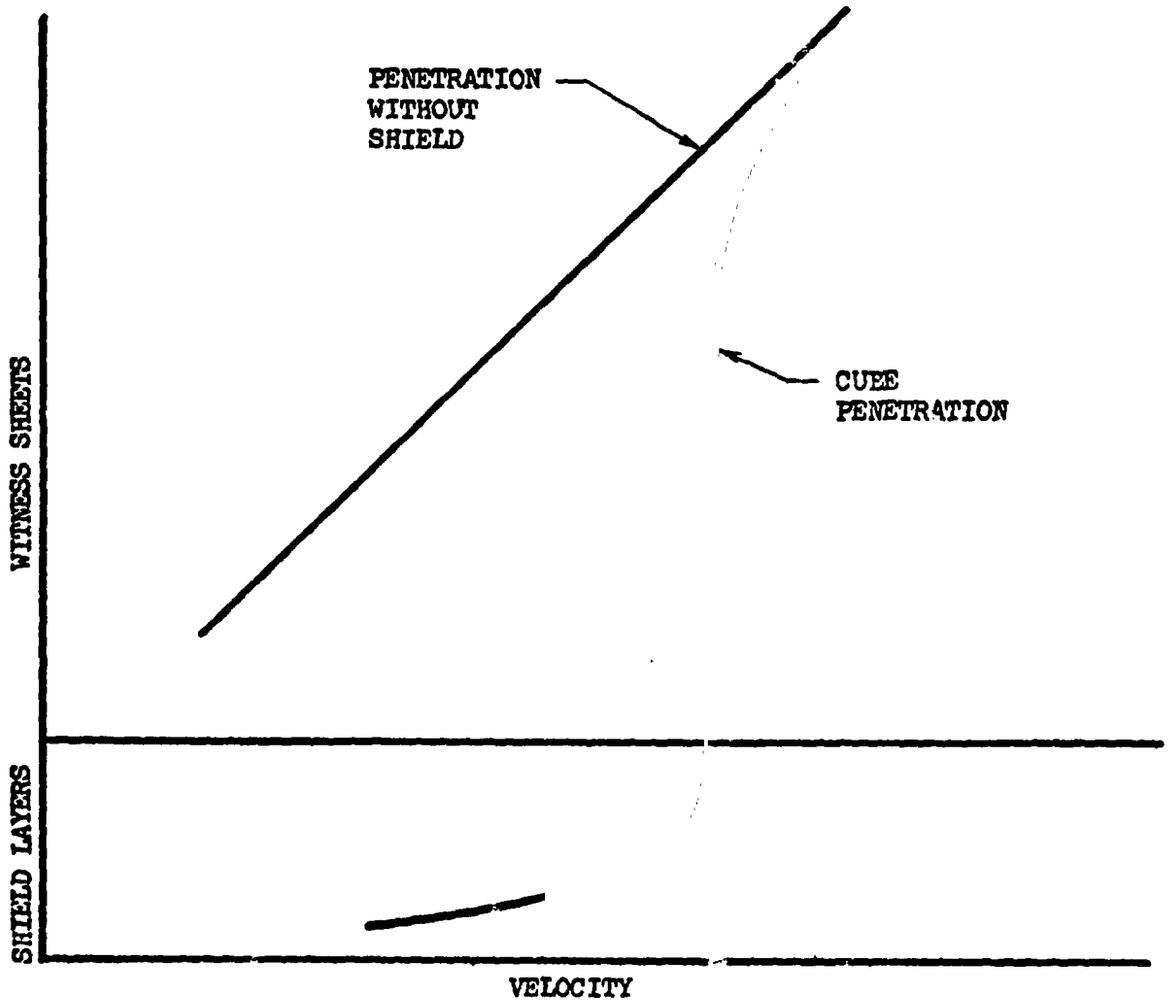

Figure 6. - Test Data.

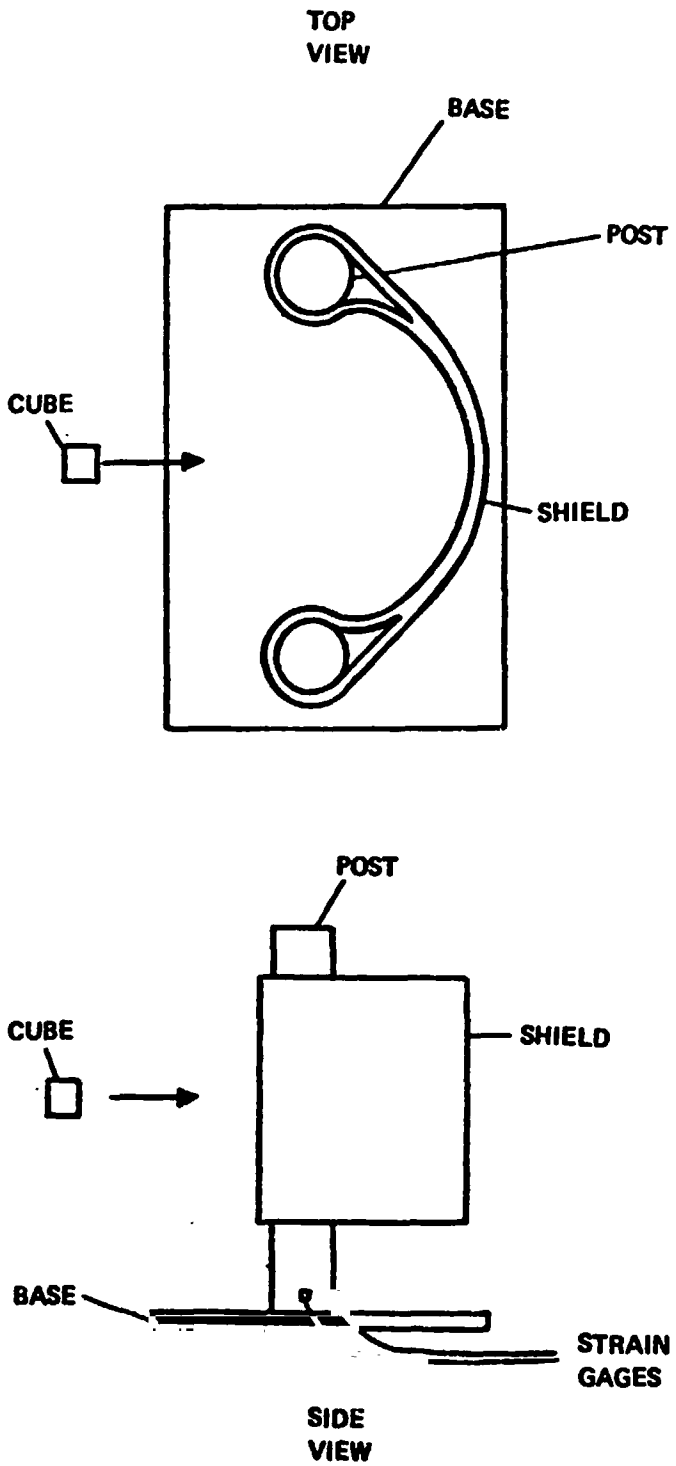

Figure 7. - Test Arrangement Schematic.

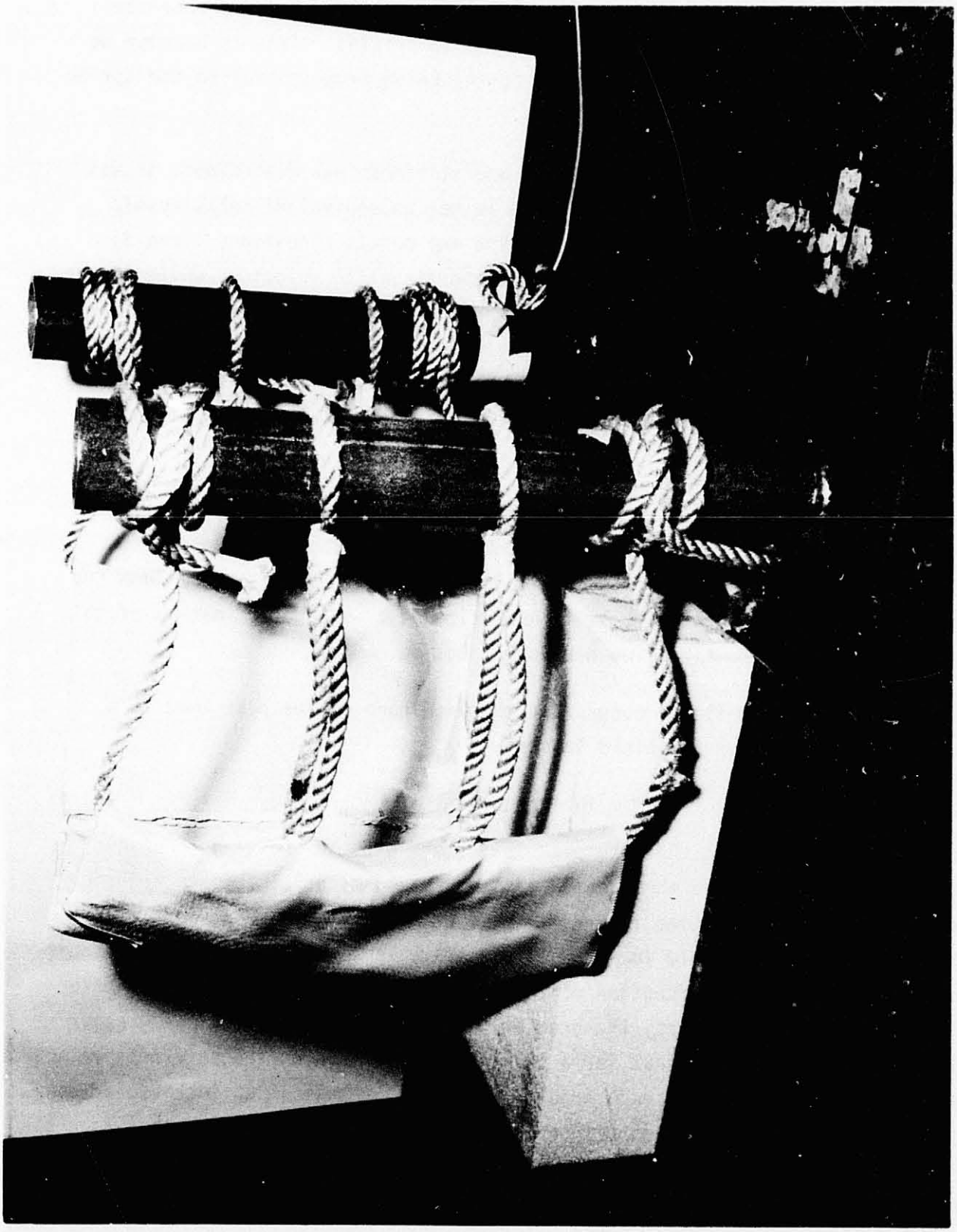

Figure 8. - Test Arrangements - Elastic Mount.

proportional to the fragment momentum. However, the load being proportional to the square root of the stiffness is a bit surprising. This is because we are accustomed to seeing the load in a spring being proportional to the spring constant times the deflection.

Once the relationship between peak load and stiffness was determined, it was tempting to try to use this relationship to get an equivalent relationship between stiffness and ballistic limit. The two models (Equations 1 and 2) show that in one case, load is directly proportional to velocity, while in the other, the number of shield layers required at the ballistic limit is proportional to the square of the velocity. Holding fragment size constant, and equating velocity between the two models, we get a relationship showing that the shield layers required should be directly proportional to the stiffness:

$$N \sim K \tag{3}$$

The above equation has not been substantiated. In fact, its validity is questionable because Equation 1 had to be simplified somewhat in order to derive the above equation. It is critical to any design procedure to know the relationship between ballistic limit and stiffness. The determination of this relationship is currently being derived at Boeing.

The last term in Equation 2 shows that the magnitude of the peak load is a function of the number of shield layers:

$$P \sim (N + \text{const})^{-1/2} \tag{4}$$

This equation indicates that the peak load drops with an increase in shield layers. This is because the greater mass of shield material acts to transfer the load over a longer time interval. However, Equation (4) does not mean that an increase in shield layers will always decrease the load. The stiffness of the shield is also a function of the numbers of shield layers. The greater the number of shield layers, the greater the stiffness and hence, the greater the load. The result is that for a shield with few layers, the stiffness effect predominates and an increase in shield layers will result in an increase in load. For heavier shields, the mass effect predominates and the peak load then tapers off with an increase in shield layers. Figure 9 shows the change in peak load with changes in shield layers.

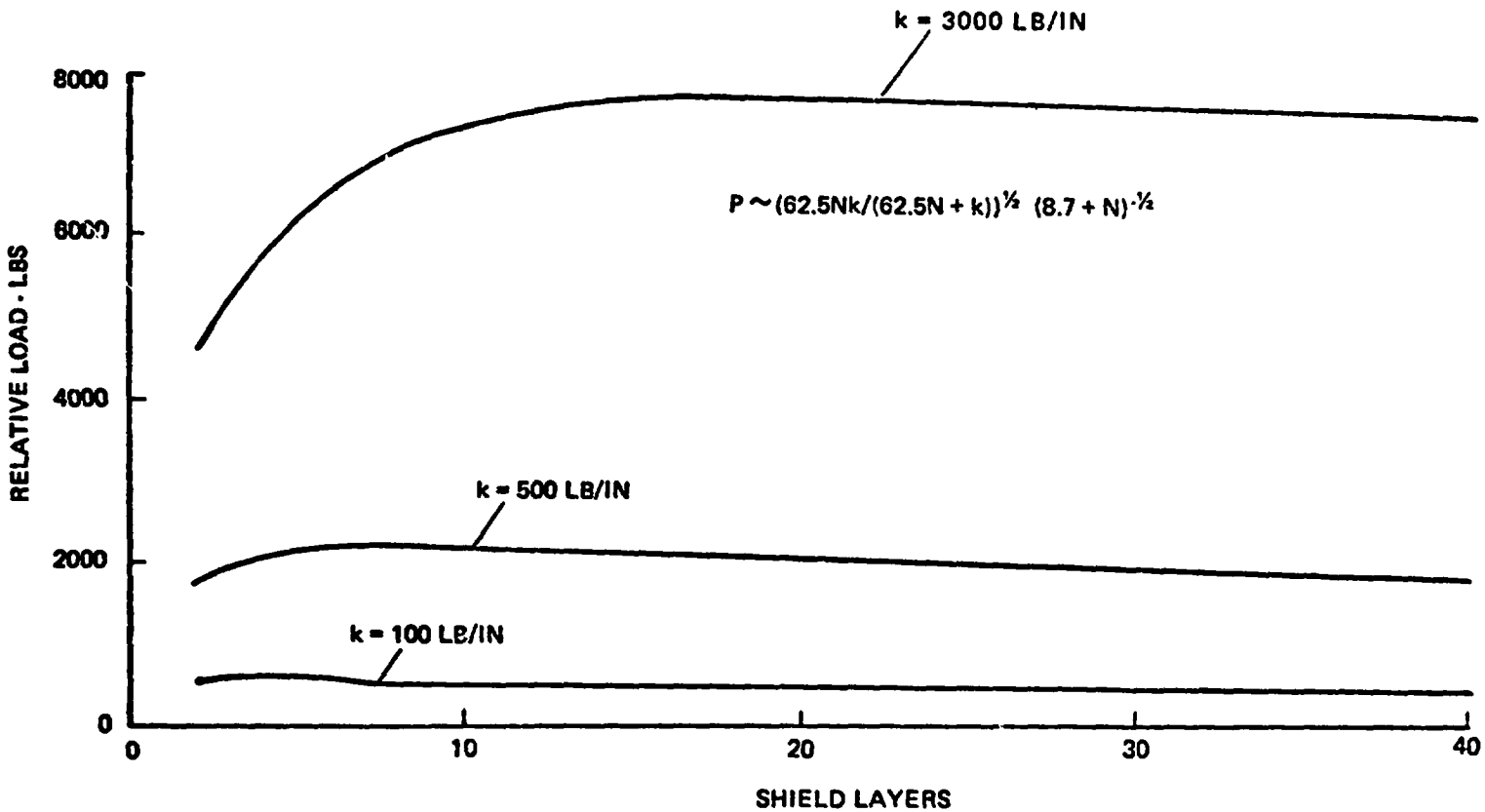

Figure 9. - Effects of Shield Density.

The above paragraphs have shown that stiffnes is an important consideration in any Kevlar fabric shield design. The stiffness, as viewed by the projectile, can be written:

$$[K] = [k_s] + [k_A] \tag{5}$$

where:

K = total equivalent dynamic stiffness (lb/in)
k_s = shield stiffness (lb/in)
k_A = attachment stiffness (lb/in).

Algebraically, Equation (5) becomes:

$$K = \frac{k_s + k_A}{k_s\ k_A} \tag{6}$$

As discussed previously, the shield stiffness (k_s) depends on the number of shield layers. Because of this, for a shield with few layers, the shield stiffness soon predominates over the attachment stiffness. This is shown in Figure 10. The four-layer shield in Figure 10 results in a rapidly increasing load at low attachment stiffness levels. However, the attachment stiffness soon becomes so high that only the shield stiffness needs to be retained in Equation (6). As can be seen in the figure, this is also true for heavier shields except that the point where the attachment stiffness can be neglected occurs at a higher total attachment stiffness.

Another area receiving emphasis during the last year concerned large fragments. Steel cubes up to 3.75 in. in size were launched in translational accelerators. These large cubes were contained at energy levels of up to 544,000 in. lb.

These tests were interesting in that a new failure mode was discovered. It was found that at high energy levels with large cubes, a tensile failure occurred at some distance from the impact point. (Before, the normal failure had been shearing or local tension around the periphery of the projectile.) However, it was further found that reduction of the effective shield stiffness would again switch the failure mode to one of local failure at the impact point. This local failure was desirable since it occurred at a higher energy level than the tensile failure.

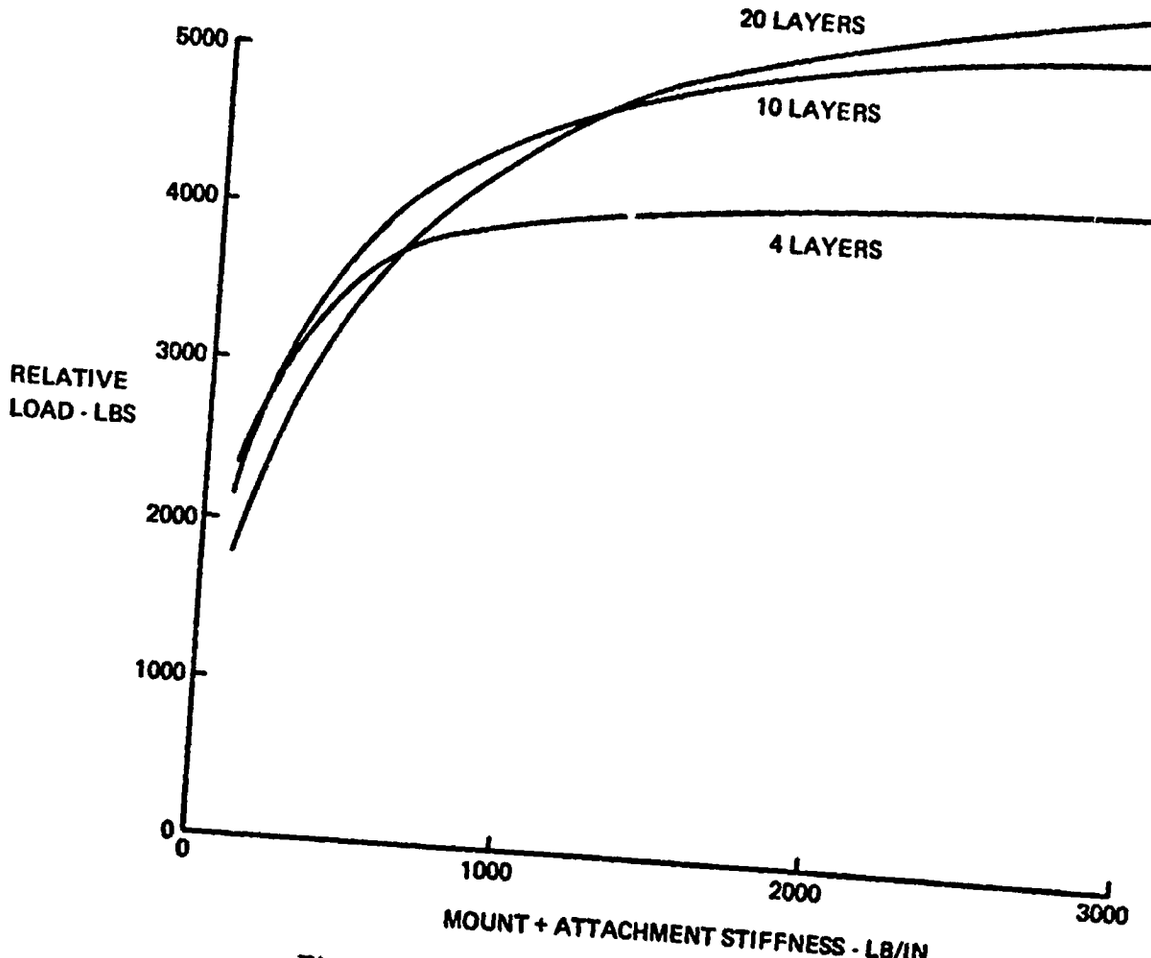

Figure 10. - Support Stiffness Effects.

The above tests, plus the load model, made it abundantly clear that stiffness is a major consideration in any fibrous shield design.

In order to check out the results obtained in the Boeing Impact Mechanics Laboratory translational accelerators, the Navy has been most cooperative with the use of the NAPTC spin pits. Several tests have been conducted with 14-inch-diameter rotors at about one million inch pounds of total energy. The shields consisted of a light aluminum ring (one pound) with a number of wraps of Kevlar (varying from 25 to 40). Recently, a successful test was made where a rotor with 8.7×10^6 in lb of total energy was contained by a 120 layer shield. It is expected that on later tests, this number of layers can be significantly reduced. In all cases, the spin pit test results were near those obtained with translational accelerators when adjusted for stiffness of the system.

FUTURE WORK

The largest task yet to complete is a model relating ballistic limit to stiffness. This model will then be combined with the earlier ballistic limit model to give required shield weight as a function of fragment size and velocity, angle of obliquity, and overall shield/mount stiffness. Another area of study involves techniques that will reduce the inherent Kevlar stiffness without losing its inherent strength. One method currently being examined involves wrapping the shield in such a manner that the material is stressed in the bias direction. Further tests in the spin-pit with the J 65 turbine are programmed; these will be useful in confirming the empirical models at higher energy levels and will identify the effects of multi-layer configurations. A number of other smaller study efforts will be made to fill in gaps or answer questions remaining from previous studies.

CONCLUSIONS

Boeing has been studying engine burst containment as part of a comprehensive damage mechanisms program. The last three years have been devoted to a study of Kevlar material as the basic containment medium. Models for ballistic limit and attachment load are available. The models have closely predicted the results obtained in spin pits. The importance of overall shield stiffness has been determined and shield designs are being worked out that will have the proper stiffness. Translational test energies have been pushed up to over 540,000 in lb,

while successful spin pit tests up to 8.7×10^6 in lb have been made. An areal weight of 1.7 lb/ft^2 was required for the spin pit rotor having one million inch pounds of energy while 8 lb/ft^2 was used for the 8.7 million inch pound energy rotor. This latter shield was not optimized and a lower areal weight is expected.

DISCUSSION

Unknown Speaker

What are the effects of moisture and temperature/time on Kevlar?

R.B. Bristow, Boeing

There is a report put out by du Pont on that subject, which indicates that Kevlar strength does indeed fall off with temperature and time. However, we were rather surprised during our tests to find that when we heated the Kevlar targets and fired the fragments into them, we actually had a higher ballistic limit. The reason being that the strain rate effects increased faster with higher temperature than does the degradation of the strength. This was covered in a previous paper that I mentioned, and is cited in my paper here as a reference. As far as moisture goes, I can't answer that.

D. Oplinger, Army-AMMRC

I was interested in your attachment or support load dropoff. With armor, that's usually considered to occur because the projectile shatters at a certain speed so that it becomes blunt. It's hard to visualize what would be causing this in the case of Kevlar.

R.B. Bristow, Boeing

I haven't been able to figure it out. One reason I brought it up was that we have many experts here and I'd like to find out what's causing it, if possible. I also might mention that I feel we've come a long ways with Kevlar but we're a long way from having something that's suitable for putting on an airplane. There's lots of design considerations that we haven't even begun to consider.

P. Gardner, Norton Co.

That projectile that you passed around, the large cube, had some blunted edges on it. Was that from the impact with the Kevlar or did it fall on the floor after going through the first test panel?

R.B. Bristow, Boeing

The steel projectile was not deformed by going through the Kevlar. We fired it in tests both below and above the ballistic limit, so we could find that dividing line. This one has gone through the shield and struck a steel plate behind, and suffered this blunting of the edges.

LIGHTWEIGHT ENGINE CONTAINMENT

A. T. Weaver

Pratt & Whitney Aircraft
United Technologies Corporation

SUMMARY

This presentation covers preliminary evaluation and development of Kevlar fabric as a lightweight containment material for use to contain blades released from gas turbine rotors. The evaluation and development included review and selection of fabric styles and weaves as well as methods of application for advanced gas turbine engines.

During this investigation effort, the Kevlar material was subjected to high speed impacts by simple projectiles fired from a rifle, as well as more complex shapes such as fan blades released from gas turbine rotors in a spin pit. Just contained data is developed for a variety of weave and/or application techniques and a comparative containment weight efficiency has been established for Kevlar containment applications. The data generated during these tests is being incorporated into an analytical design system that will allow a designer of future engines to make blade containment trade-off studies between Kevlar and metal case engine structures.

In addition to the evaluation of the containment efficiency of Kevlar, certain laboratory tests and engine environment tests were performed to determine the survivability of Kevlar in a gas tubine environment.

LIGHTWEIGHT CONTAINMENT

INTRODUCTION:

Current regulations require that blade containment be provided on all gas turbine engines certified for commercial flight. Since the structures that provide this are generally parasitic, engine technology dictates that they be as light as possible. In order to meet this requirement, new materials and new containment concepts are being explored. Initial data generated using fabrics as energy absorbing devices under high speed impact indicate that a significant weight improvement can be achieved. This presentation deals with the evaluation and development of fabric structures for blade containment applications for gas turbine engines.

DISCUSSION:

A cross section of a typical gas turbine engine is shown in Figure 1. The red outline represents a typical rotor stage for which a containment structure must be provided. The rotor is enclosed in a metal case which provides support for the engine weight and imposed thrust loads. Additionally, the case must provide the necessary containment in the event of a blade failure. This containment is provided by the energy absorbing capability of the impacted case structure which normally bulges or deforms when struck by a released blade. Sufficient material thickness must be employed in the containment structure to prevent the blade from exiting the case.

In current gas turbine engines, the metal case structure is fabricated with adequate thickness to provide the necessary containment. In future gas turbine engines, fabric wrapped thin metal cases may be used to provide the necessary level of containment capability with a minimum weight. (See yellow outline in Figure 2.)

The thickness of the engine cases, in the plane of the blades, can then be reduced to a value limited by normal engine loads such as thrust and rotor support.

DEVELOPMENT PROGRAM:

The following development program was performed at P&WA East Hartford to provide a data base for future applications of fabric containment structures for gas turbine engines:

- Ballistic Impact Evaluations
- Laboratory Tests
- Spin Pit Tests
- Engine Tests

The ballistic impact tests consisted of subjecting various fabric structures to impacts by projectiles fired from a gun. "Just-contained" data were developed for a wide spectrum of fabric weight densities and projectile velocities. (See Figure 3).

In this testing we were able to determine the degree of participation of Kevlar^{R} DuPont versus the associated metal structure. The results of this testing showed:

1. Kevlar impact resistance by itself is 5 more weight efficient than AISI 410 hardened steel.

2. Kevlar structures lose efficiency if the fabric is not allowed to deflect.

3. Kevlar fabric can absorb multiple hits closely spaced without apparent loss of containment strength.

The laboratory investigation included wicking and flammability tests to assess fire risk associated with Kevlar fabric around the outside of an aircraft gas turbine. The results of this testing showed:

Wicking

Kevlar 29, style 71 fabric, wicked engine oil and hydraulic fluid in an applicable bench test.

Flammability

Kevlar 29 was non burning by itself.

The spin pit testing consisted of wrapping Kevlar cloth around a thin metal engine case and subjecting this containment structure to an impact by a released blade from a spinning rotor. (See Figures 4 and 5). A thin aluminum witness case was mounted outboard of the Kevlar wrapped blade containment structure to determine if blades/pieces exited the Kevlar. "Just-contained" data were obtained for typical gas turbine speeds and several configurations of Kevlar fabric.

The fabric configurations evaluated were:

Kevlar 29	1:1 plain weave
Kevlar "	3:1 weave
Kevlar "	6:1 weave
Kevlar "	3D weave

The results of this testing showed that the blades would penetrate the thin engine metal cases; however, the blades were contained by fabric wrap. The containment weight efficiencies for the above Kevlar weave configurations were determined to be basically identical.

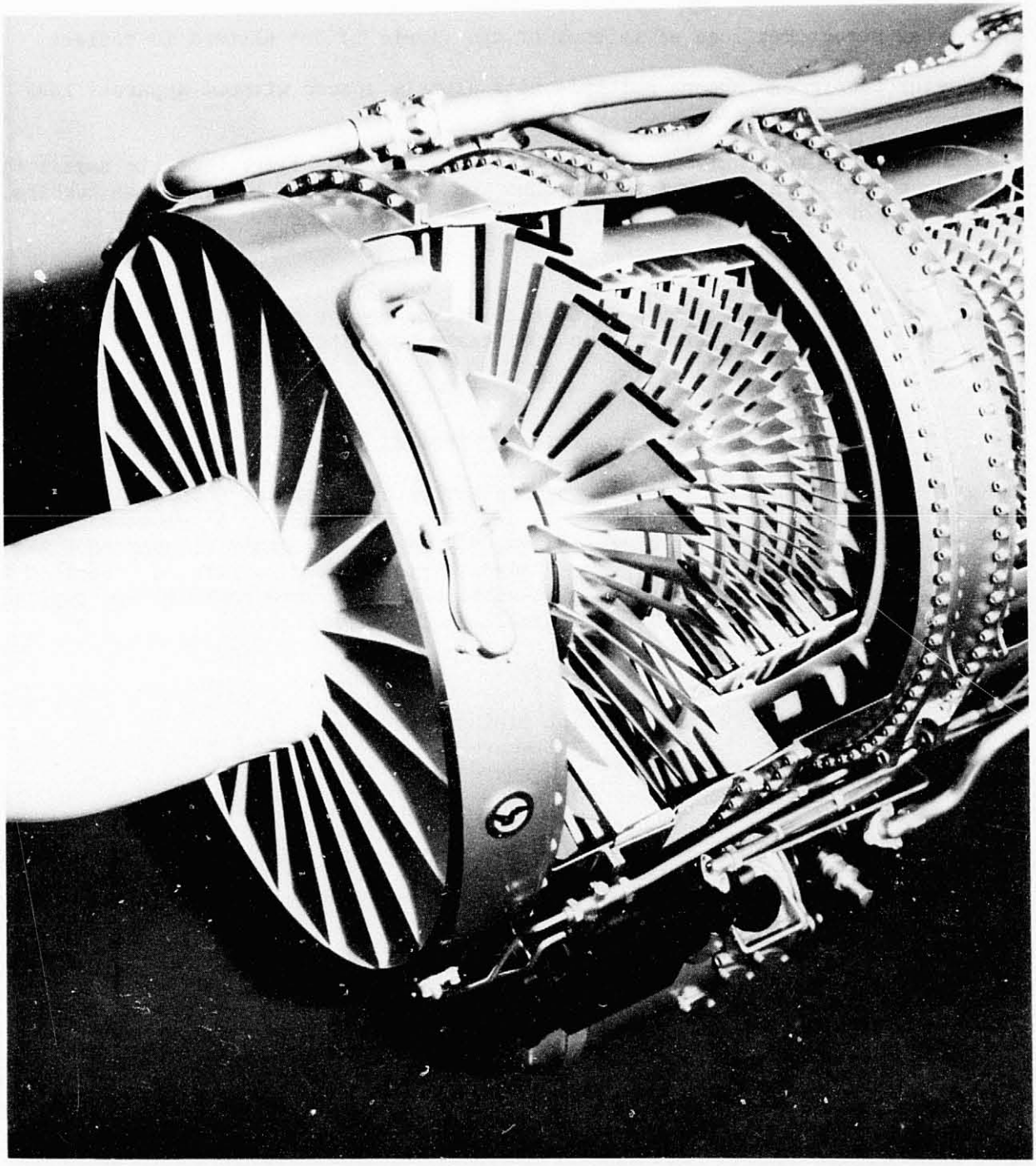

FIGURE 1
GAS TURBINE ENGINE SHOWING TYPICAL FAN STAGE
(RED BLADE TYPE).

77-441-0042-E

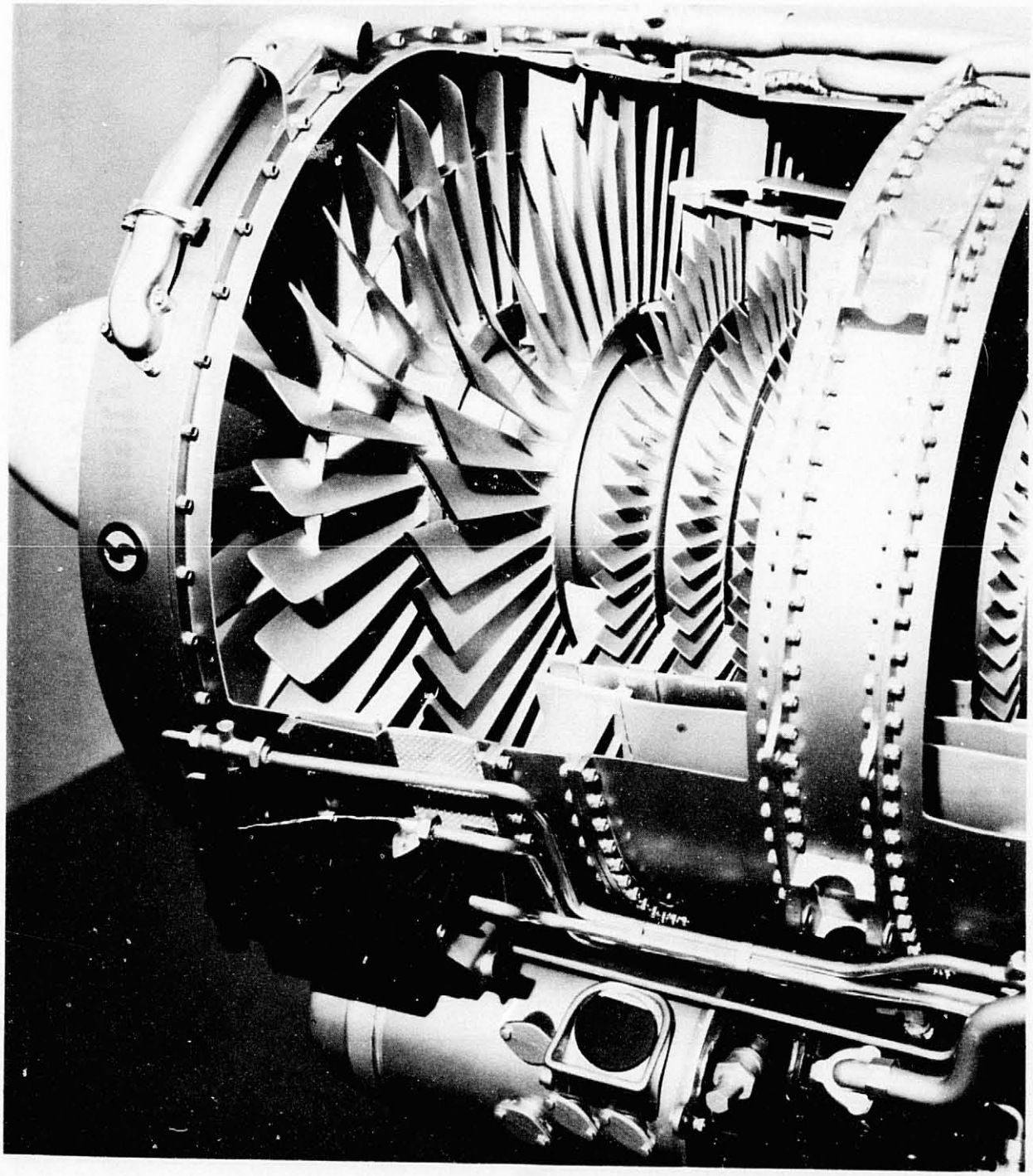

FIGURE 2
GAS TURBINE ENGINE SHOWING LOCATION OF FABRIC CONTAINMENT WRAP (YELLOW BAND).

77-441-0042-B

BALLISTIC IMPACT EVALUATION OF KEVLAR®

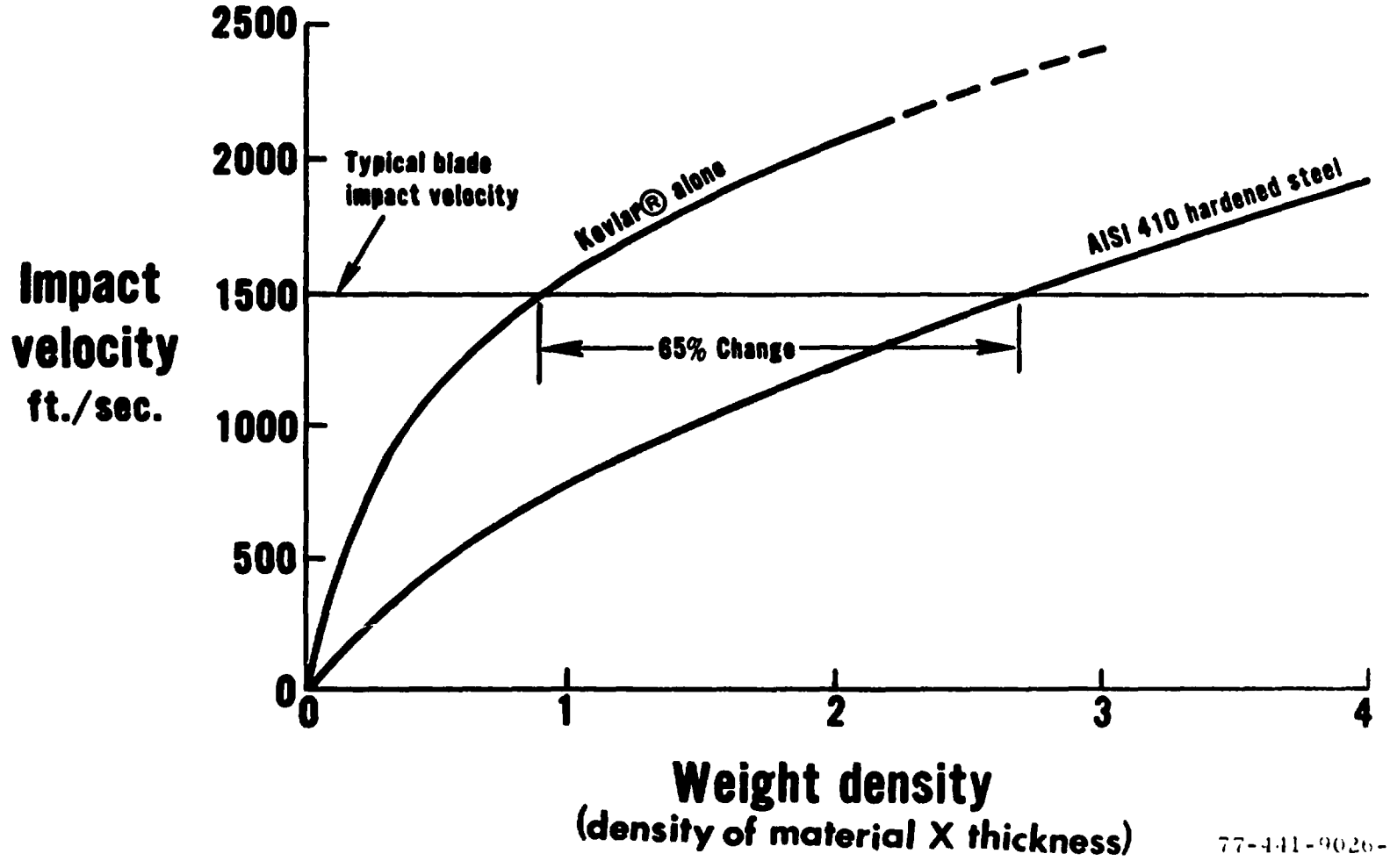

77-441-9026-B

FIGURE 3

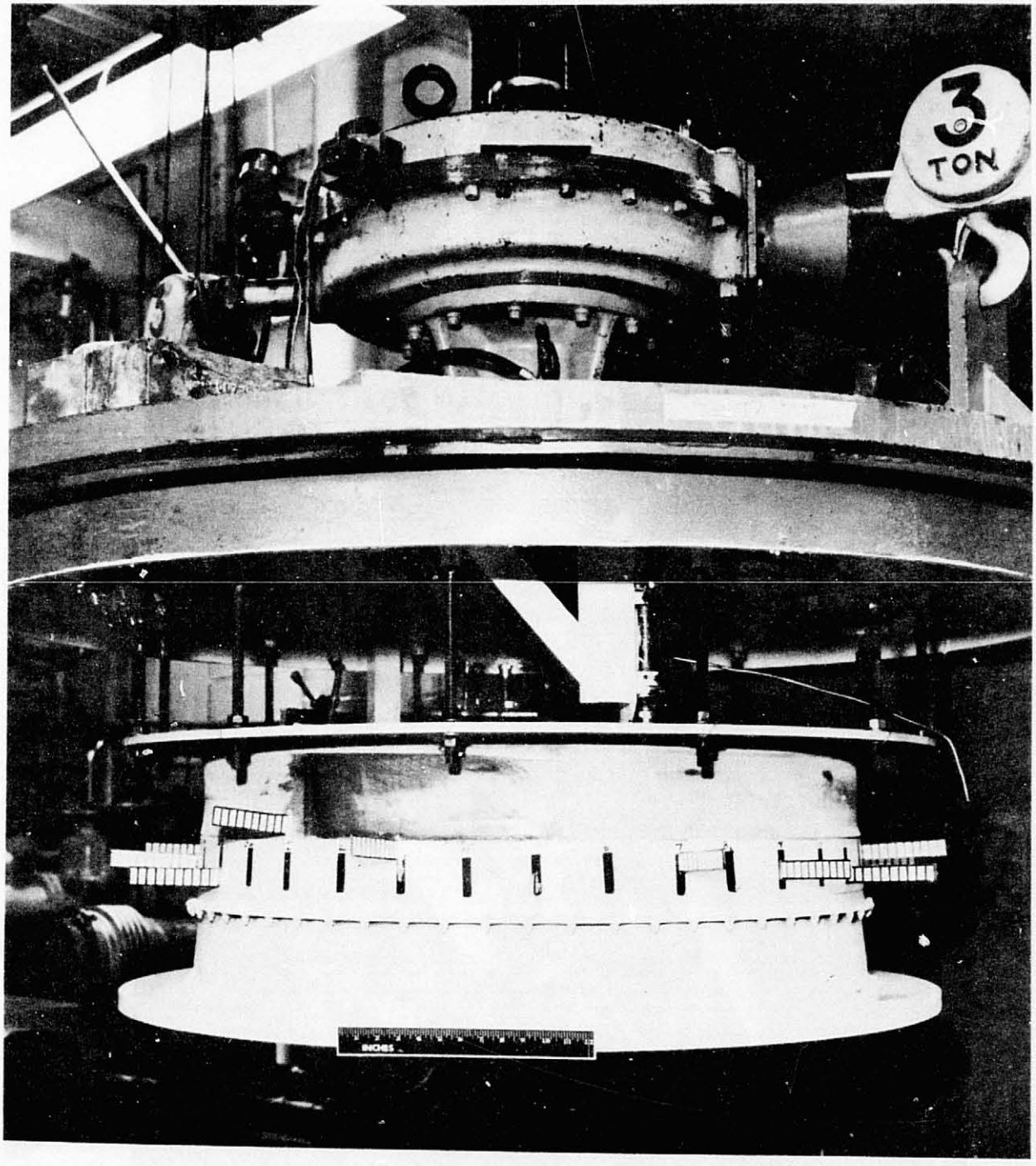

FIGURE 4
SPIN PIT CONTAINMENT TEST RIG SHOWING KEVLAR WRAPPED CASE.

CN-57214

FIGURE 5
SPIN PIT KEVLAR WRAPPED CONTAINMENT METAL CASE
AFTER TEST.

76-444-4047-C

DISCUSSION

J.C. Wallin, BAC

Al, as one who spends much time worrying about fires, I think you tossed off the absorbability of Kevlar pretty lightly. If the casing were wrapped around with asbestos, I'd be pretty unhappy. But as you described the wicking, I would not be any happier with Kevlar. I think that before you can have a practical system on the engine you've got to have some way of avoiding that soak-up (fire hazard) problem. Is there a suitable coating that can be used to prevent its soaking up fluids?

A. Weaver, P&W

I share your concern about the fires; an engine can experience some leakage of oil or fuel at some time. This leakage could be characterized as so many gallons of this flammable fluid; all the Kevlar played a part in was simply in wicking it. I'm not too certain if that's any more of a threat than allowing the fluid to collect in the bottom of the nacelle, although this can be drained off or trapped.

However, this is not going to take care of all of the leakage. Some of the engine parts are going to be covered with this liquid because of its natural adherence.

I'm not yet convinced about the Kevlar increasing the fire hazard. We do agree that it wicks, and probably is going to hold more of the fluid than a metal part would hold just because it sticks to it. But it still may be a small quantity and not an increased threat.

J.H. Gerstle, Boeing

Al, wouldn't it be possible to put a very lightweight nonabsorbent sheet around the Kevlar?

A. Weaver, P&W

That is a possibility that is being considered. One could also put in a certain amount of impregnation. This might result in some loss in containability, but with a 65% weight saving as it is, I can afford to give up some of that and still have it very attractive.

Some of these questions are long-range considerations that we'd like to pursue and get answers on. That's why we're quite a ways away from putting this out in the field.

H. Garten, GE-Lynn

How much weight saving do you think that you get as compared with a titanium shield?

A. Weaver, P&W

The data indicated a 65% weight saving compared with using 410 steel.

So, I think, the proper question would be: how does titanium compare with 410 steel? Then, obviously, how does it compare to Kevlar?

H. Garten, GE-Lynn

I thought you said that the actual engine test (the spinpit test) was surprisingly good. I thought that it inferred that it was better than the initial assessment of your ballistic test.

A. Weaver, P&W

Yes, there was some inference of that. We don't completely understand it whether it's because the ballistic test does not completely model what happens in the spinpit or not.

We have not pinned down in the spinpit the exact weight savings with the Kevlar. On the surface, it appears to me that the spinpit test results were going to be better than ballistic-test results. This may be due to the way we bookkeep the results. We have not completely understood the bookkeeping of the Kevlar versus the inner steel wrap that we have.

D. McCarthy, Rolls-Royce

We tested some Kevlar and found that when it was wetted with oil, its containment capability was seriously diminished; you suggested that the effect of oil wetting depended upon the shape of the missile. Have you done tests, firing blades at the Kevlar shield while it is oil-impregnated?

A. Weaver, P&W

No, we haven't; we certainly intend to do that. We would have done it some time ago had we not received the advice we did from Watertown saying, "you really don't have to worry about it -- your initial ballistic tests kidded you". We put that down to the lower part of our priority list, but it still remains to be done. We will not consider Kevlar to be fully developed unless we run tests in a spinpit with the blades impacting into the oil-soaked Kevlar.

R. Bristow, Boeing

I think you may very well find out that when you soak the Kevlar shield in oil that you're getting a similar effect to having a matrix, that is, the mass of the oil and the mass of the matrix is causing the problem.

E.A. Witmer, MIT-ASRL

Could you clarify the nature of the discussed test in the spin chamber: the way the failure was initiated and the sequence of events?

A. Weaver, P&W

We take a fully-bladed rotor, and purposely weaken a blade in the rotor so that when you operate it at red-line speed, that blade is running very near its ultimate tensile strength. The chamber is evacuated so the blade doesn't have a significant vibration imposed on its P/A stress, and it continues to remain intact. We then impose on the whole rotor a vibratory stress which

forces the one weakened blade to failure, usually in a second. That's the simple way we conduct most of those tests. We normally fail the blade in a root attachment or in the root airfoil. This would be a significant mass of blade.

I think in the particular photograph you looked at on the viewgraph, there was probably a root airfoil. Though, on the same rotor we've also run with the full root attachments released into the case.

J. Meaney, Rohr

I have two questions. First, had you spliced the Kevlar and in what direction? Second, you say that the Kevlar must deflect to work, but in the pictures of the engine you show a lot of pneumatic lines that run very close to the shield. Do the deflections exceed that distance?

A. Weaver, P&W

Concerning the first question, the Kevlar application that you were looking at is a very simplified application that I would think of as analogous to an ace bandage. When you put an ace bandage on your wrist, you take the one piece and you hold it and you wrap the other piece around, and you depend on the friction of the layers to keep it there; the last little end of the ace bandage you take a couple little hooks and you hook. That's all we've really done here. I propose to let the designer make it very simple; don't require him to add weight.

As to your second question, the particular engine case you saw was simply a vehicle for subjecting the Kevlar to the environment of an engine. This was not designed to be a mock-up of a final design. One must provide for adequate clearance because Kevlar must deflect appreciably to do its work.

We had put some structure outboard of the Kevlar (not against the Kevlar) and the Kevlar has deflected into these structures. At the present time in the number of tests we've run, we've seen no effect on the containability of the Kevlar if it was deflected into a structure. If you back the Kevlar up in intimate contact with the structure, yes, you would probably lose containability. But, if you don't back it up and you give the Kevlar a gap and allow it to deflect through that gap, then if you hit the structure it didn't really appear to affect the Kevlar. The Kevlar still did its job.

J. Salvino, NAPTC

In your spin pit containment test on Kevlar, where did you find the blade fragment? Was it between the Kevlar and the outer case?

A. Weaver, P&W

Typically, the Kevlar is ripped and torn, and many layers of it are penetrated; the blade is trapped in the layers. The blade is generally in one piece not including the root; it does not always break up.

NUMERICAL ANALYSIS OF PROJECTILE IMPACT IN WOVEN TEXTILE STRUCTURES

David Roylance*

INTRODUCTION

Textile structures have been used to provide protection against ballistic threats since the Second World War, with the development then of flak jackets for aircraft crewmen. Now used widely by military and police personnel, these devices have been constructed principally of ballistic nylon or impregnated fiberglass. In recent years, however, improved devices have been developed using aramid fibers (DuPont's Kevlar 29 or 49), and these are being considered for such additional applications as aircraft engine rotor-blade burst containment. Development and design of these devices has been largely empirical, and considerable effort has been expended to develop rational analytical tools which may be used in design, or at least in improving the designer's intuition.

Although closed form-mathematical analyses can be applied to the initial ballistic response of a single fiber [1], late-time effects arise due to stress wave interactions and reflections which make such closed-form analyses intractable. In the case of woven panels, each fiber crossover acts to reflect a portion of the stress wave which is propagating outward from the impact point, so here closed-form treatments

* Associate Professor, Department of Materials Science and Engineering, Massachusetts Institute of Technology, Cambridge, MA 02139.

are completely inapplicable. The complexity of these phenomena have resulted in the development in our laboratory of a series of computer codes, and these numerical treatments have proven to be of great value in understanding the ballistic event. These codes do not involve the idealizing approximations needed in many other treatments, such as modeling the woven panel as a membrane, so that the user is able to proceed directly from fiber material properties, weave geometry, projectile velocity, etc.

NUMERICAL ANALYSIS OF TEXTILE IMPACT

The computer method used in the numerical analysis of textile impact is an outgrowth of a technique pioneered by Davids et al. [2] and applied successfully to a variety of wave propagation problems. This approach, which is similar in final form to finite-difference analysis but markedly different in derivation, was first used by Lynch [3] to analyze transverse impact of single fibers and later extended by Roylance et al. to the study of viscoelastic fiber impact [4] and impact of woven textile panels [5]. Referring to Fig. 1, the woven panel is first idealized as an assemblage of pin-jointed, flexible fiber elements, each having a mass which makes the areal density of the idealized mesh equal to that of the panel being simulated. The initial projectile velocity is imposed on the node at the impact point, which causes a strain to develop in the adjacent elements. The tension resulting from this strain is computed from the constitutive law, and

this tension is used to calculate an acceleration in the neighboring elements. The computer proceeds outward from the impact point in this manner, using a momentum-impulse balance, a strain-displacement condition, and a constitutive equation to compute for each element the current values of tension, strain, velocity, position, and such ancillary but important quantities as strain energy and kinetic energy.

At the end of these calculations, a new projectile velocity is computed from the tensions acting on the projectile from the fibers, and the process is repeated for a new increment of time. In the development of such codes, due attention must be given to matters of efficiency, stability, and accuracy. As now developed, the fabric code produces data in excellent agreement with experiments, and does so at reasonable cost (approximately $15 for a typical impact event simulation, using MIT's IBM 370/168 system).

MATERIAL PROPERTIES

The numerical algorithm is finally terminated by simulated rupture of the fibers. Since the strain and tension histories are computed for each element in the mesh, a variety of failure criteria may be easily incorporated. The use of Eyring-type rate process fracture criteria [6] are particularly attractive, since they are computationally convenient and still provide good simulation of time and temperature effects.A simple but very useful such criterion is that due to Zhurkov, who states that

the lifetime τ of a solid subjected to a constant stress σ is:

$$\tau = \tau_0 \exp\left(\frac{U - \gamma\sigma}{kT}\right)$$

where k is Boltzman's constant and T is the absolute temperature. τ_0, U and γ are material constants related to the dissociation kinetics of the atomic bonds and the internal defect structure of the material. For time-varying stresses and/or temperatures, one may assume superposibility and write Zhurkov's equation in the form

$$\int_0^{\tau} \frac{dt}{\tau_0 \exp\left\{\frac{[U - \gamma\sigma(t)]}{kT(t)}\right\}} = 1$$

In our numerical treatment, the current value of the above integral is computed at each node. The time and location of rupture is determined when the integral value reaches unity at any node.

In the course of the iterative calculations, a constitutive material law must be evoked at each element in order to compute the element tension from its strain (or strain history). One would expect that a model incorporating viscoelastic effects would be necessary for proper simulation of polymeric structures and in fact, there is considerable evidence that relaxation does indeed occur in the ballistic time frame [8]. This is expected in light of the dynamic mechanical spectrum of nylon, in which

a beta relaxation is observed having an apparent activation energy of $\sim$ 14 kcal/mole [9]; this relaxation is calculated to occur in approximately five microseconds at room temperature.

A general viscoelastic model well suited for computing tensions from prescribed strains is the Wiechert model, depicted schematically in Fig. 2. This model takes the polymer response to be that of the shown array of Newtonian dashpots and Hookean springs. The differential tension-strain law for the jth arm of the model is

$$\dot{\epsilon} = \frac{1}{k_j}\dot{\sigma}_j + \frac{1}{\eta_j}\sigma_j$$

where the dots indicate time differentiation, σ is the tensile stress and ϵ is the strain. Casting this equation in finite difference form relative to a discrete time increment Δt and solving:

$$\sigma_j^t = \frac{1}{[1+(\Delta t/\tau_j)]}\left[k_j(\epsilon^t - \epsilon^{t-1}) + \sigma_j^{t-1}\right]$$

where the superscripts t and t-1 indicate values at the current and previous times respectively, $\tau = \eta_j/k_j$ is a characteristic relaxation time for the j^{th} arm. The total tension at time t is the sum of all the σ_j plus the tension in the equilibrium spring k_e:

$$\sigma^t = k_e\epsilon^t + \sum_j \frac{k_j(\epsilon^t - \epsilon^{t-1}) + \sigma_j^{t-1}}{1+(\Delta t/\tau_j)}$$

This tension-strain calculation is performed at each element node. In addition to storing all the k_j and τ_j, the computer must also store the previous strain and tension values at each node.

Finally, it should be noted that the above models for dynamic fracture and viscoelastic consitutive response may not be applicable to some materials. The modification or replacement of these models is very convenient in the computer code, since they exist as separate subroutines. The easy implementation of various material response models is one of the strongest advantages to this numerical treatment of impact.

RESULTS

The Fabric code has been used to perform computer experiments aimed at elucidating the influence of various material properties on the impact resistance of woven panels. The objective of this work has been to provide a tool for the designer of personnel armor devices, and to enhance his intuition as to the physics of the impact event. Certain related phenomena have also been explored, including the influence of nonlinear viscoelastic response and the role of backup layers in reducing dynamic deformation and blunt trauma. Certain findings from these studies will be described briefly here in order to illustrate the utility of the method.

Assessment of accuracy of the numerical analysis is somewhat problematical, as no closed-form mathematical analyses are available against which to check the code results. Certain experimental observations are available, however, one of which is shown in Fig. 3. This figure is a plot of residual projectile velocity after penetration of a Kevlar panel, as a function of initial velocity. The good agreement of the predicted and observed

results is especially satisfying, since it provides some assurance that both the transient response and the final fracture processes are being modeled reasonably. It might also be mentioned that this particular plot is one which plays an important role in the design process, so that the ability to generate it numerically without prior ballistic data or any idealizing assumptions is of considerable practical importance.

Figure 4 presents the results of a series of computer experiments in which the response of various ballistic candidate materials is compared. The principal parameters of interest here are the dynamic modulus of the material and its dynamic breaking strain. It is seen clearly that the energy absorption rate of a given fabric rises monotonically with the modulus, increasing in the order of nylon, Kevlar 29, Kevlar 49, and graphite. However, Kevlar 29 demonstrates the best balance of high modulus and reasonable breaking strain, with the result that it is the superior ballistic material. It should be mentioned that Kevlar 49 is not found experimentally to be as deficient as this figure would predict, indicating that an improved model of fracture for this material is needed.

CONCLUSIONS

Although the numerical method described above was developed for use in design and analysis of ballistic protection devices for personnel armor, its potential for use in a similar role in rotor blade burst containment at high velocity is obvious.

The speed range for which the code is well suited is that for which wave propagation effects become important: approximately 200 m/sec and above. The code is applicable at lower impact speeds, but would not be cost effective in comparison with structural dynamics approaches.

Certain alterations in coding would be required in treating burst containment problems. First, one would relax the present restriction to zero-obliquity impact. Such impacts are used as worst-case events in personnel armor, but a more general treatment would be needed for burst containment analysis. A loss of symmetry would result, accompanied by proportionally greater computation time, but the principles of analysis would be unchanged. Another coding alteration would involve the projectile size, and a provision for larger projectiles would be incorporated without major difficulty. Motion of the impacting fragment would likely be followed by an incremental rigid-body motion scheme.

It is this author's hope that the community concerned with hardening against rotor bursts will agree that the method described here would constitute a valuable addition to the techniques presently available or under development. The implementation and verification of the method for this type of problem would not be an overly large task.

REFERENCES

1. D. Roylance, Tex. Res. J., in press.
2. P. Mehta and N. Davids, AIAA J. 4, 112 (1966).

3. F. Lynch, TR70-16, Army Materials and Mechanics Research Center (1970).

4. D. Roylance, J. Appl. Mech., 40, 143 (1973)

5. D. Roylance et al., Tex. Res. J., 43, 34 (1973).

6. A. Krausz and H. Eyring, Deformation Kinetics, Wiley, 1975.

7. S. Zhurkov, Int. J. Fracture Mech., 1, 311 (1965).

8. J. Smith et al., Tex. Res. J., 35, 743 (1965).

9. N. McCrum et al., Anelastic and Dielectric Effects in Polymeric Solids, Wiley, 1967.

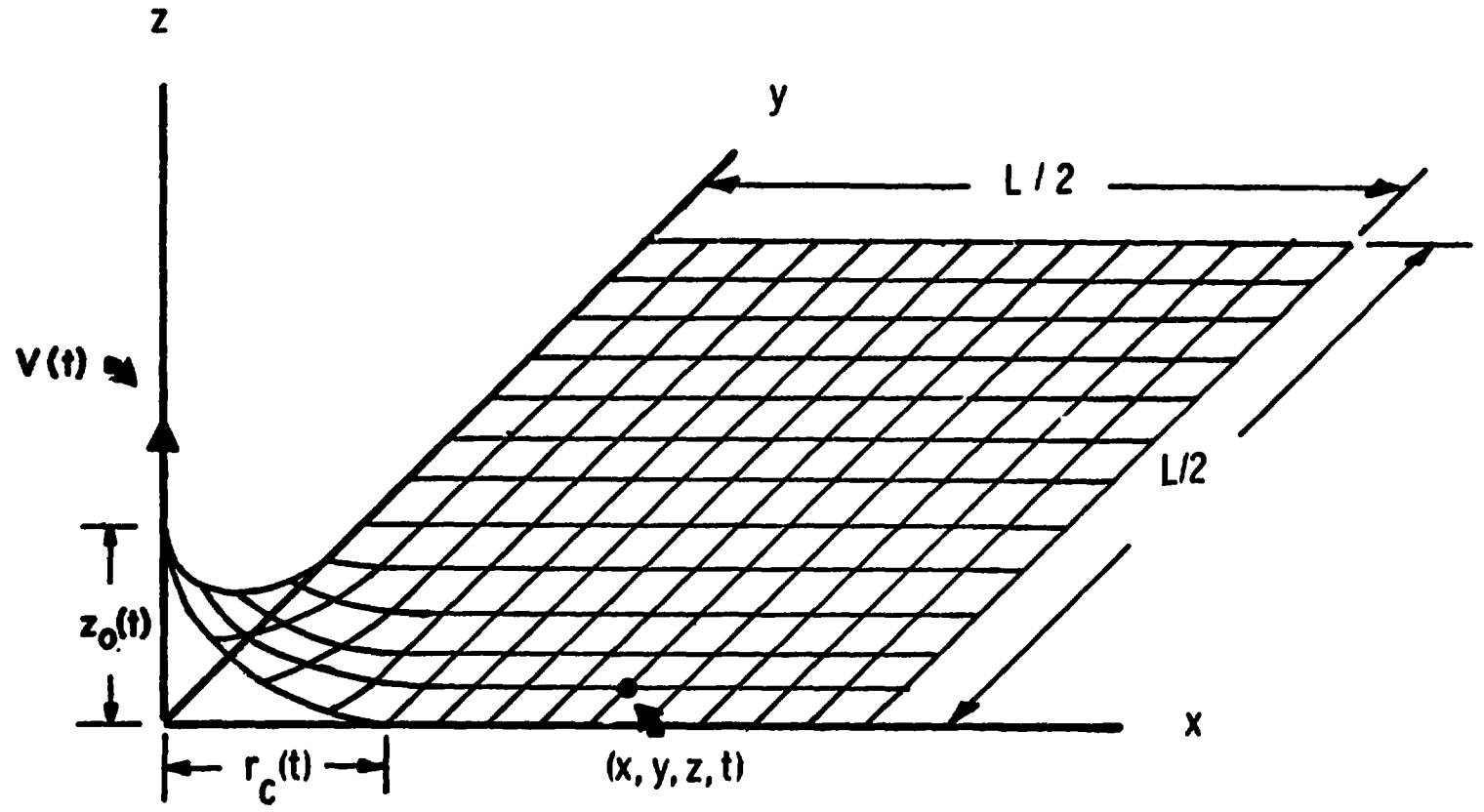

FIG. 1 DISCRETE-ELEMENT MESH USED IN NUMERICAL ANALYSIS OF IMPACT UPON WOVEN TEXTILE PANELS

WIECHERT MODEL

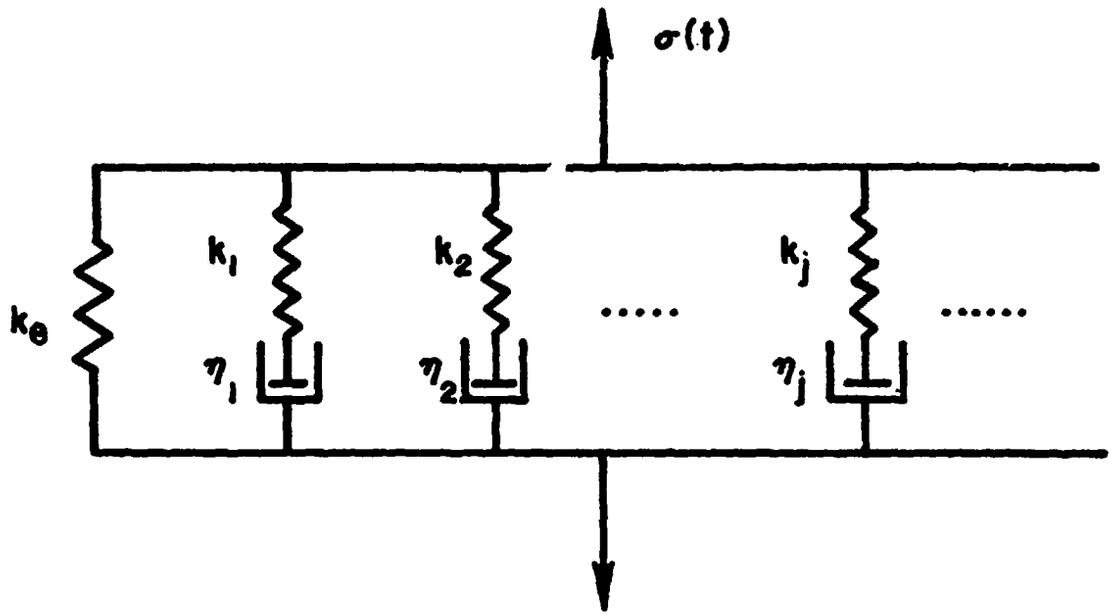

$$\sigma(t) = \left\{ k_e + \sum^{n} \frac{k_j D}{D + \frac{1}{\tau_j}} \right\} \epsilon(t)$$

$$(D \equiv \partial/\partial t \, , \; \tau_j = \eta_j / k_j)$$

$$\sigma^t = k_e \epsilon^t + \sum^{n} \frac{k_j (\epsilon^t - \epsilon^{t-1}) + \sigma^{t-1}}{1 + (\Delta t / \tau_j)}$$

FIG. 2 SCHEMATIC ILLUSTRATION OF WIECHERT VISCOELASTIC CONSTITUTIVE RELATION, USING SPRING-DASHPOT ANALOGIES

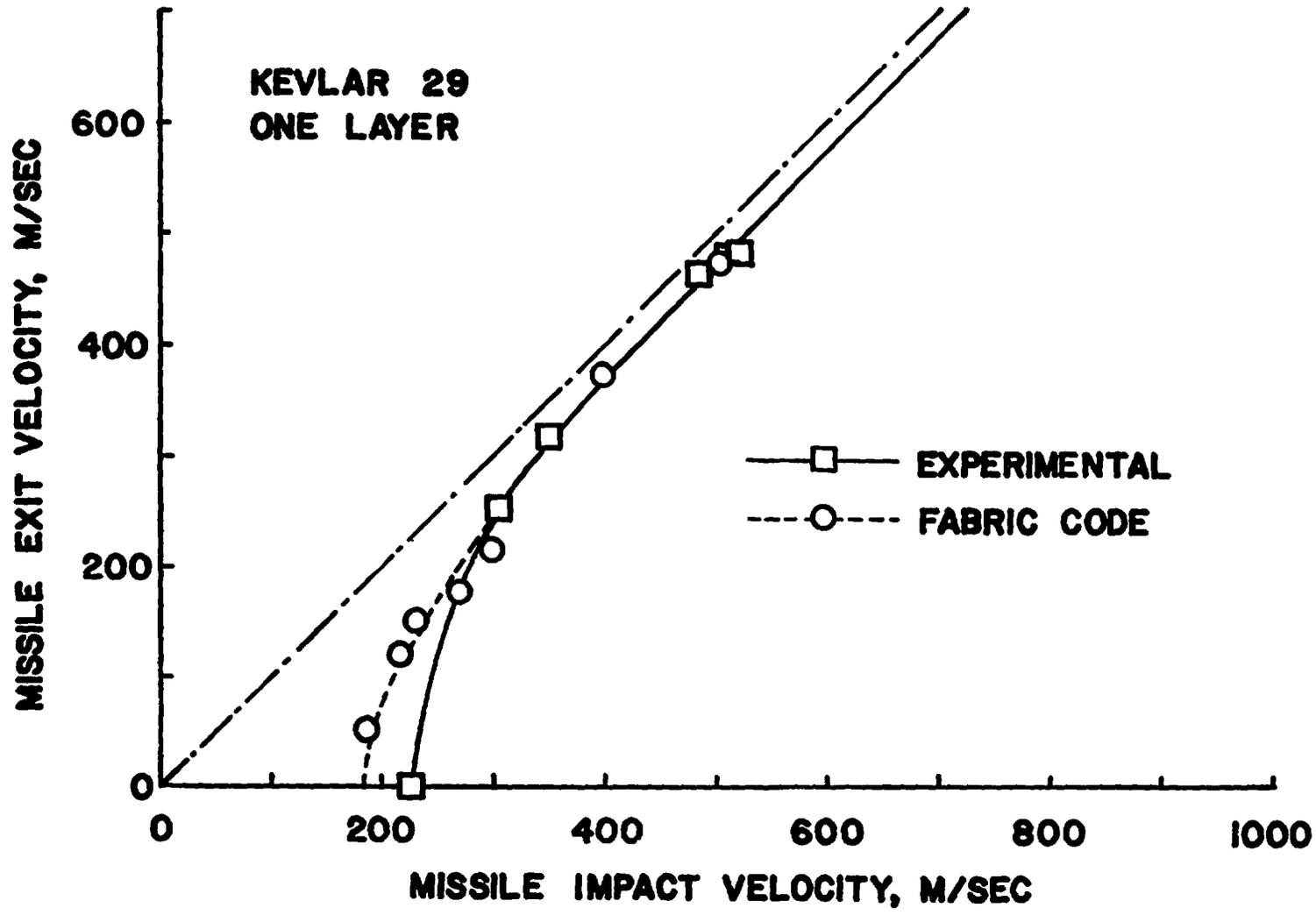

FIG. 3 V_s-V_r CURVE FOR A 2 x 2 BASKETWEAVE PANEL, WITH AREAL DENSITY OF 0.421 kg/m^2 AND PROJECTILE MASS OF 1.10 gms.

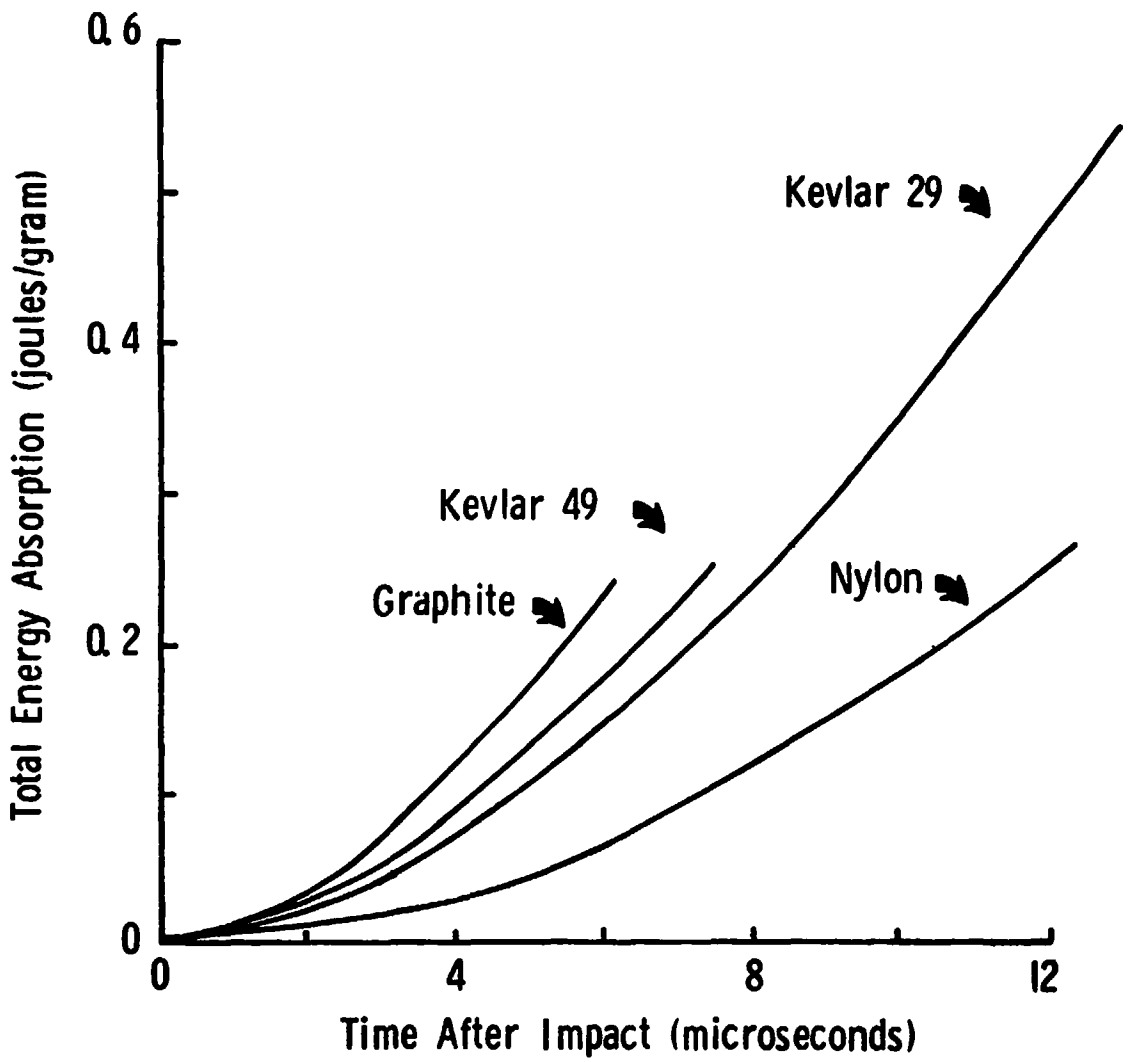

FIG. 4 COMPARISON OF BALLISTIC ENERGY ABSORPTION FOR VARIOUS CANDIDATE FABRICS; FABRIC WEIGHTS AND MISSILE MASS AS IN FIG. 3

DISCUSSION

D. Oplinger, AMMRC

Is the code capable of handling multiple-layer fabrics?

D. Roylance, MIT

As presently configured, the code simulates multiple layers only in that it uses a numerical mesh of weight equal to the fabric being simulated. Such an approach obviously misses any layer-layer interactions which might be present, but comparisons with limited experimental results using multiple-layer targets have been very promising.

ANALYSIS METHODS FOR KEVLAR SHIELD RESPONSE TO ROTOR FRAGMENTS

J. H. Gerstle
Boeing Commercial Airplane Company
Seattle, Washington

ABSTRACT

Several empirical and analytical approaches to rotor burst shield sizing are compared and principal differences in metal and fabric dynamic behavior are discussed. The application of transient structural response computer programs to predict Kevlar containment limits is described.

For preliminary shield sizing, present analytical methods are useful if insufficient test data for empirical modeling are available. To provide other information useful for engineering design, analytical methods require further developments in material characterization, failure criteria, loads definition, and post-impact fragment trajectory prediction.

INTRODUCTION

Over the last couple of decades, there have been numerous efforts to develop predictive methods for blade containment design. These efforts have helped to reduce the costly full-scale testing required for design integrity validation.

Many efforts at shield sizing formulas were based on the assumption that a rotor fragment's kinetic energy can be equated to the available strain energy in the engine casing and other structures in the path of the fragment. Test data and analysis[1] usually indicate that a factor is required, namely:

$$E_f = C \sum_n U_n$$

where $\sum_n U_n$ is the sum of ultimate strain energies for the n material to be deformed, E_f is the fragment energy, and the range of the factor is roughly

$$0.05 < C < 10$$

depending on case materials, blade type, etc., as well as assumptions regarding the extent of deformed material.

Semi-empirical containment criteria have also been developed that relate fragment energy to shield thickness as well as other relevant physical parameters. These criteria can be generalized as having the form:

$$E_f = \sum_n f_n (h^b, \sigma_u, e, A, \theta)$$

where h is the material thickness, σ_u is the ultimate tensile or shear strength, e is the elongation, A is the contact area, shear area, or contact surface length, and θ = the angle of impact. Typically for metals:

$$2 \leq b < 3$$

implying that the thickness is a function of velocity (or momentum) when b = 2.

These criteria appear to generally be adequate when based on sufficient test data.

To reduce the dependence on test data, many other methods have been developed to predict impact response, especially in the field of ballistics. Before the availability of large-memory high-speed computers, such methods relied principally on quasi-static theories wherein the deformation shape was assumed a priori and various assumptions were made regarding material behavior, e.g., rigid-plastic, etc. (See reference 2 for further discussion and extensive references.)

One analytical containment criterion has recently been proposed[3] that considers both the short-term compressive and shear energy absorption in the contact region followed by longer term energy absorption due to overall structural deformation. This model, as well as the others, still neglects the contribution of bending stiffness which has been observed to be significant, although correlation with very high energy spin pit tests was found to be satisfactory.

During the last decade, transient material and structural response computer codes have advanced to the point where in weapon effects and other aerospace applications, large deformation transient response calculations are made routinely. Whether such techniques can be applied to containment prediction and specifically to the problem of Kevlar containment shielding, and whether they offer any advantages over empirical methods, will be the subject of the remainder of this paper.

BOEING KEVLAR SHIELD DEVELOPMENT PROGRAM

In 1972, an experimental program was initiated at Boeing to develop lightweight containment technology.[4,5] The initial tests used multilayered flat shields made of "S" glass fabric. Subsequent tests used Kevlar 49, then Kevlar 29. From these early tests, it was apparent that the very high strength-to-weight ratio and excellent ballistic impact properties justified further investigation, but the impact and structural behavior of Kevlar would be very different from steel or titanium alloys and would pose major installation difficulties.

The Kevlar program has been undertaken with a dual approach to the development of (math) models for shield sizing. One approach, an empirical model, has already been discussed in a previous paper.[6] The other approach is analytical and is based largely on existing transient structural analysis methods.[7] As such, the two approaches served the test program by providing complementary but independent projections.

Transient finite difference and finite element computational techniques were first applied to rotor fragment impact by Witmer et al. Under NASA funding, successive refinements have culminated in the CIVM-JET series of codes.[2,8,9] A similar approach was also adapted at Boeing to an existing finite difference large deflection plate/shell code, PETROS 3.[10] The converted program, called EBCAP, was specifically developed to predict the containment of woven fiber shields.[11]

BOEING ANALYTICAL APPROACH

The principal assumptions in EBCAP are that:

1. Fragment deformation is negligible.
2. The impact process is inelastic (i.e., zero coefficient of restitution).
3. For rotating fragments, the instantaneous coefficient of friction is essentially infinite (this would be incorrect for smooth-surfaced metal shields).
4. Multilayered Kevlar shields can be idealized as single layer membranes.

The flow diagram shown in Figure 1 illustrates the numerical procedure used to predict the motion of the fragment and shield.

For given initial conditions of fragment angular velocity, translational velocity, and incidence angle, the post-impact velocities of the fragment and shield are calculated. Next, the nodal displacement components for the first time increment, $t = \Delta t$, are found from the nodal velocities. The midsurface geometric quantities at each mesh point are then calculated from the displacements, followed by the strain increments and then the stresses. A stress failure criterion is evaluated to determine if the shield fibers could have ruptured. If not, the stresses are used to calculate stress resultants from which the new velocities are found by solving the equilibrium equation, thus specifying the new displacements. Next, the fragment's position is updated to correspond to the new time according to equations of motion. A check is made to see if the effective fragment radius overlaps any mesh points. If not, the program flow cycle is repeated. Otherwise, a collision is assumed to have occurred and the impact analysis procedure is used to calculate velocity increments that are superimposed on the vibratory motion before entering a new cycle. The process ends if a failure is predicted, a maximum time is reached, or a numerical stability condition is violated.

A principal difference between EBCAP and the CIVM-JET codes is that momentum transfer occurs over an area of the shield larger than the immediate contact area due to stress wave propagation over the duration of the numerical time step, Figure 2.

FLAT PLATE IMPACT TEST PREDICTIONS

Kevlar shields dissipate the fragment energy almost wholly by tensile deformation. The mechanical energy is distributed rapidly throughout the fabric shield, relative to metal response, due to the fiber's high wave speed and membrane response. Transverse wave propagation, while not quantitatively predictable for a nonbonded structure, is attenuated extremely quickly. The in-plane compressive stresses cause buckling, which in these analyses are only crudely taken into account by setting the compressive stiffness to zero.

The measured peak displacement as a function of time from an early Kevlar test is shown in Figure 3. In this experiment, a 1-inch nonrotating steel cube was shot at the center of a rectangular flat shield with an incidence angle of 60 degrees with respect to the plane of the shield. The projectile velocity was reduced from 876 fps at impact to 250 fps after perforation. The shield was riveted to steel reinforcements at the top and bottom which in turn were bolted to a heavy steel frame. The shield was unattached at its two sides. The shield was composed of two materials. The first layer was a thin steel plate that may be regarded as simulating a support panel. This steel panel was experimentally found to reduce the residual projectile velocity by less than 10 percent for impact velocities above 800 fps. Twelve layers of Kevlar made up the rest of the shield. The deformation of the shield was obtained by high-speed photography. Experimental uncertainties are shown by error bars on the experimental data points.

To compare results, the predicted peak displacement time histories are also shown in Figure 3. In this analysis, the shield was idealized as a single layer of fabric clamped at the top and bottom edges. Since the fabric layers are neither bonded nor sewn together, only the initial transient response prediction is meaningful.

Details of this test comparison may be found in reference 7, but the principal conclusions were that the prediction of peak displacement did not vary significantly with node spacing and was consistently lower than measured. However, the actual shield deflections were also found to be partly due to buckling of the steel reinforcements and failure of some of the rivets, which unfortunately hinders the comparison. EBCAP will predict fastener failures, but cannot change the boundary conditions to physically model this effect. Another shortcoming of the analysis was probably the lack of material data, i.e., a linear stress-strain curve based on the static mechanical fiber properties of Kevlar was used.

The most direct computational approach for predicting containment limits is to start with very high fragment velocities and successively reduce velocity until the ballistic limit, the impact velocity at which the residual velocity is zero after perforation, can be estimated by extrapolation as shown in Figure 4. As the fragment velocity is lowered, the EBCAP calculations take more time steps to predict perforation, with the result that numerical inaccuracies build up and the physical simulation becomes increasingly more questionable.

The results from a series of tests to determine the ballistic limit are compared in Figure 4. It is seen that as impact velocities approach the ballistic limit of approximately 830 fps, the number of damaged (i.e., penetrated) fabric layers increases very rapidly for small increases in velocity.

To evaluate the effectiveness of the analytical method, the predicted residual velocities are again shown for two different mesh spacings. When the region of influence contains many mesh points, the predicted ballistic limits will generally converge with increasing numbers of mesh points.

In Figure 5, the correlation with higher energy flat Kevlar shield tests is compared to EBCAP predictions. Two sets of predictions are shown, one made with static properties, the other with modulus and ultimate stress measured at elevated strain rates. The use of this Boeing strain rate data did not shift the predicted ballistic limit significantly (although in other studies, the ballistic limit was raised up to 10 percent higher). The predicted ballistic limits are seen to be within 15 percent of the experimental ballistic limit.

In general, the analytical predictions for flat shield tests were comparable in accuracy to those from the empirical model.

CURVED SHIELD IMPACT TEST PREDICTIONS

A major analytical difficulty for either flat or curved shields is modeling flexible supports. Varying the material properties at nodes adjacent to the supports will lower the overall shield stiffness, but care must be taken to make the transition sufficiently gradual that large spurious stress waves are not generated by wave reflection.

As mentioned earlier, in many of our tests in the past two years, flexible supports have been successfully used to improve containment performance and also to simulate the response of ring shields by curved segment shields. In general, analytical predictions were not very satisfactory.

SPIN PIT TEST PREDICTIONS

In a recent test (No. 218) at the Naval Air Propulsion Test Center, three 120° pie segments from a T-58 rotor were contained at a burst speed of 20,550 rpm by a 6.7-lb ring shield made of 40 layers of Kevlar 29. The shield width of 6 inches was much larger than the blade chord length (approximately 1 inch) or disk thickness. The exact ballistic limit is unknown, but is regarded to be close to 20,550 rpm for this configuration. Figure 6 shows that perforation was predicted about 17,000-18,000 rpm, or equivalently, the predicted contained rotor burst energy is approximately 25 percent too low.

As discussed earlier, MIT has developed a series of special purpose finite element transient structural computer programs to simulate the response of rotor fragment/containment ring interactions. These programs restrict containment shield motion to be two dimensional, i.e., by a beam/ring idealization, in contrast to EBCAP, which allows for three dimensional geometry and motion. However, the latest code, CIVM-JET4B, has the capability of following the impact of up to 6 rotor fragments simultaneously, whereas EBCAP cannot model more than one fragment-shield interaction. In view of this, the CIVM-JET4B code was obtained with the hope that the use of both computer programs would lead to improved analytical predictions.

The Boeing version of the CIVM-JET4B program has incorporated several changes. Special logic was added to allow the idealization of Kevlar fabric as a membrane and the equivalent of buckling by not allowing compressive stresses. A shield failure criterion based on the maximum strain in an element is used to predict the shield failure similar to the logic used in EBCAP. The overall solution procedures are also similar.

Analyses of test 218 were also made with the modified CIVM-JET4B code. The results are shown in Figure 7 where the three points at each energy level indicate the residual energies calculated for each fragment. Containment is seen to be predicted approximately at 18,000 rpm.

No significantly different conclusions were drawn from predictions based on only the fragment translational energies.

As far as possible, the ECBAP and CIVM-JET4B runs were made using comparable mode spacing, time increments, and physical assumptions. The CIVM-JET4B results appear to be slightly better. The CIVM-JET4B results are expected to improve for lower ratios of shield width to fragment thickness.

A subsequent test, NAPTC test 221, was used to obtain an order of magnitude higher energy, approximately 10,000,000 inch-lbs. In this test, a 58-lb, 120-layer, 9-inch-width Kevlar shield was successfully used to contain at least two 120° fragments from a J65 rotor burst at 8100 rpm. (The shield was intact, but lack of photographic evidence makes it difficult to ascertain if the nonimbedded fragment tumbled around the edges of the shield.) This test, however, indicated that considerably more further development work is probably required, for neither EBCAP or CIVM-JET4B came close to providing as satisfactory shield sizing predictions as the empirical model.

If future needs indicate that Kevlar or other woven fiber materials warrant more detailed consideration, then such development work should be directed toward present shortcomings such as the idealization of multilayered Kevlar wraps as a membrane, and modeling of load transfer processes when inner layers of the shield are torn. More extensive material data for Kevlar would also be useful since so little is known about its fabric properties, damage tolerance, etc.

CONCLUSIONS

At present, special purpose structural dynamics computer programs for rotor fragment containment prediction are only advantageous for Kevlar or other woven fiber shield sizing when there is insufficient test data for empirical modeling.

To be useful for engineering design, analytical methods such as JET4B should continue to be developed under NASA sponsorship, but with emphasis on shield failure and attachment loads with consideration for structural behavior differences between metals and woven fiber and in the long-term, post-impact fragment path prediction.

Development of a 3D finite element program with similar emphasis should also be continued, which could offer the capability for analysis of off-center fragment impacts, one-sided displacement constraints, and varying shield thickness or material properties in both circumferential and axial directions.

REFERENCES

1. Many published papers are available on this subject. For a recent example, see: J. I. Goatham and R. M. Stewart, "Missile Firing Tests at Stationary Targets in Support of Blade Containment Design," ASME Paper No. 75-GT-47, March 1975.
2. R. W. H. Wu and E. A. Witmer, "Finite-Element Analysis of Large Transient Elastic-Plastic Deformation of Simple Structures, with Application to the Engine Rotor Fragment Containment/Deflection Problem," NASA CR-120886, January 1972.
3. A. C. Hagg and G. O. Sankey, "The Containment of Disk Burst Fragments by Cylindrical Shells," J. Engineering for Power, 96, 2, April 1974.
4. R. J. Bristow, C. D. Davidson, and J. H. Gerstle, "Advances in Engine Burst Containment," in AGARD Report No. 648, Sept. 1976.
5. C. D. Davidson, "Engine Burst Containment Kevlar Shield Development (1976) -- Phase III, Spin Pit Validation," Boeing Document D6-44264, March 1977.
6. R. J. Bristow and C. D. Davidson, "Development of Fiber Shields for Engine Containment," NASA Workshop on Assessment of Technology for Turbojet Engine Rotor Failures, March 29-31, 1977.
7. J. H. Gerstle, "Analysis of Rotor Fragment Impact on Ballistic Fabric Engine Burst Containment Shields," J. Aircraft, 12, 4, April 1975.
8. T. P. Collins and E. A. Witmer, "Application of the Collision-Imparted Velocity Method for Analyzing the Responses for Containment and Deflector Structures to Engine Rotor Fragment Impact," MIT, ASRL TR 154-8, CR-13494, Aug. 1973.
9. T. R. Stagliano, R. L. Spilker, and E. A. Witmer, "User's Guide to Computer Program CIVM-JET4B to Calculate the Transient Structural Responses of Partial and/or Complete Structural Rings to Engine Rotor Fragment Impact," NASA CR-134907, March 1976.
10. S. Atluri, E. A. Witmer, J. W. Leech, and L. Morino, "PETROS 3: A Finite Difference Method and Program for the Calculation of Large Elastic-Plastic Dynamically Induced Deformations of Multilayer Variable Thickness Shells," MIT, ASRL TR 152-2, Nov. 1971.
11. J. H. Gerstle, "EBCAP: A Computer Program to Analyze Rotor Fragment Impact on Plate/Shell Containment Shields," Boeing Document D6-44273, March 1977.

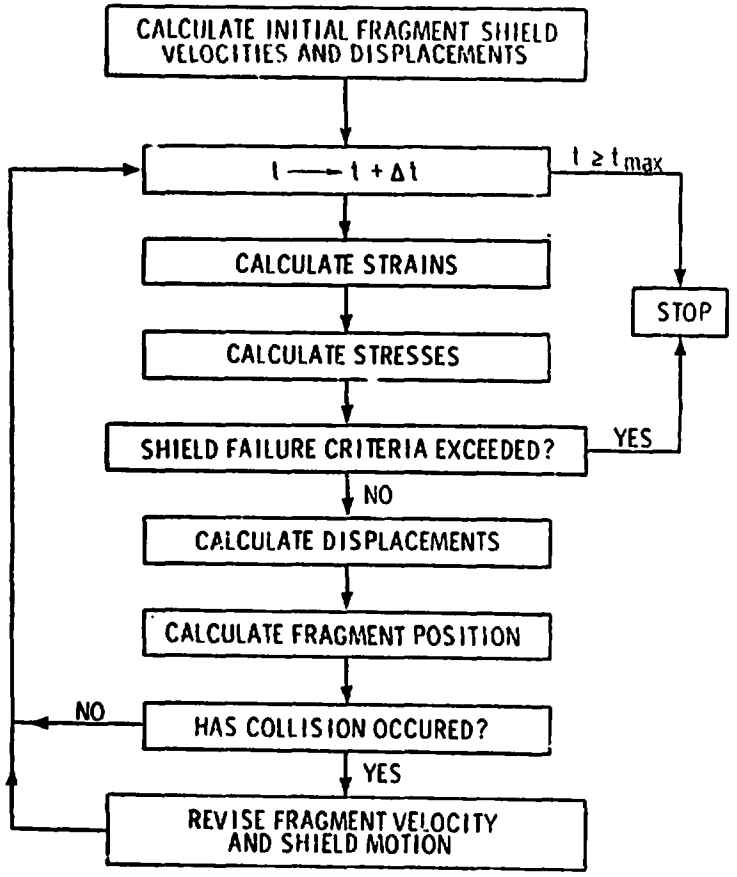

Figure 1. - Solution Procedure.

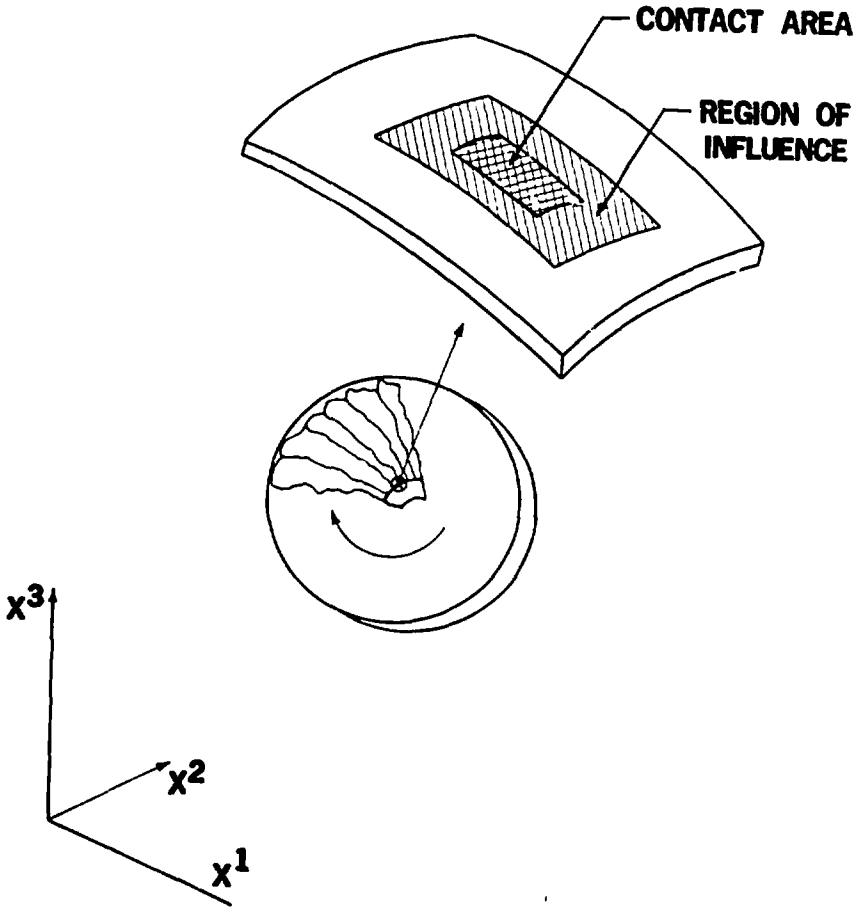

Figure 2. - Effective Instantaneous Structural Excitation Area.

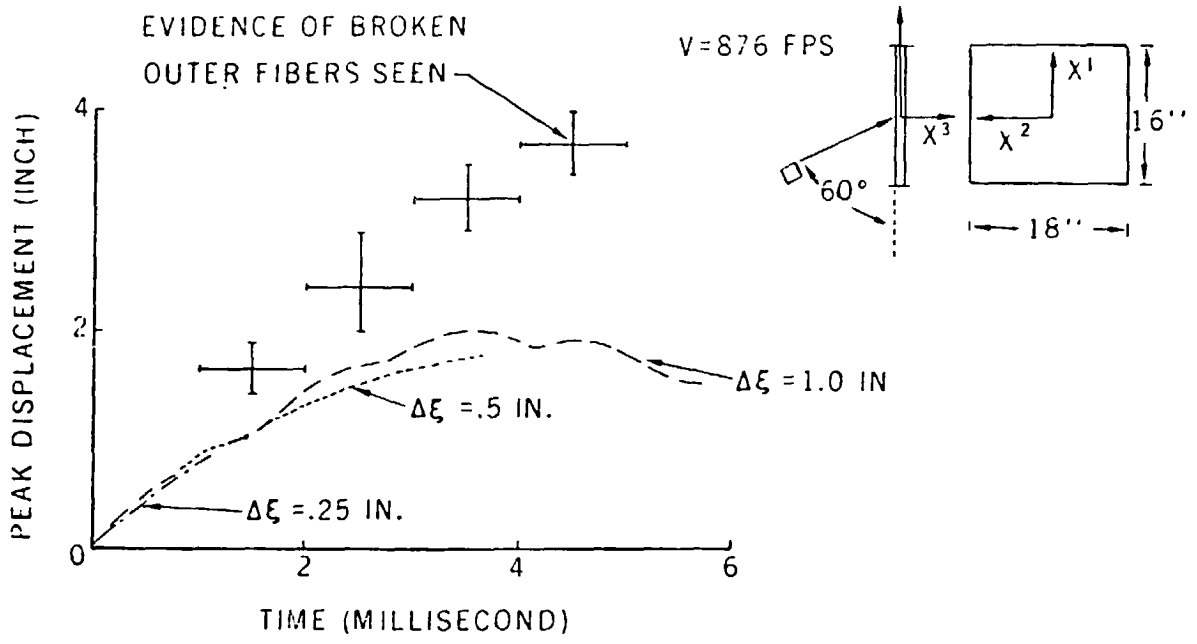

Figure 3. - Comparison of Predicted and Measured Peak Displacement in Oblique Impact Material Configuration Test.

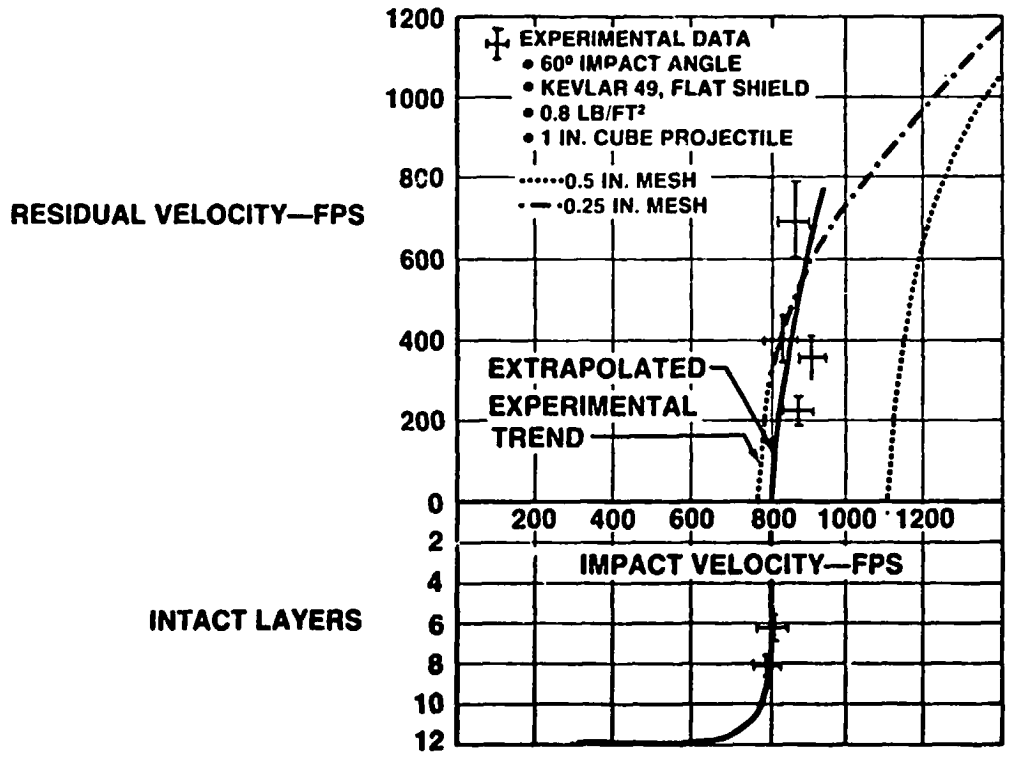

Figure 4. - Predicted and Measured Residual Velocities.

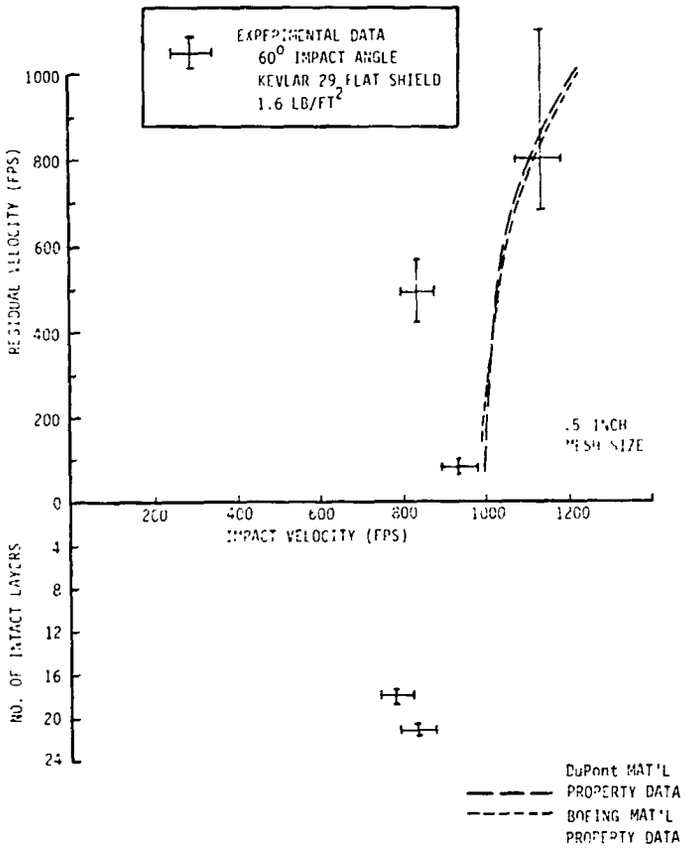

Figure 5. - Comparison of Predicted and Measured Residual Velocities For 1.5 Inch Cube Projectile.

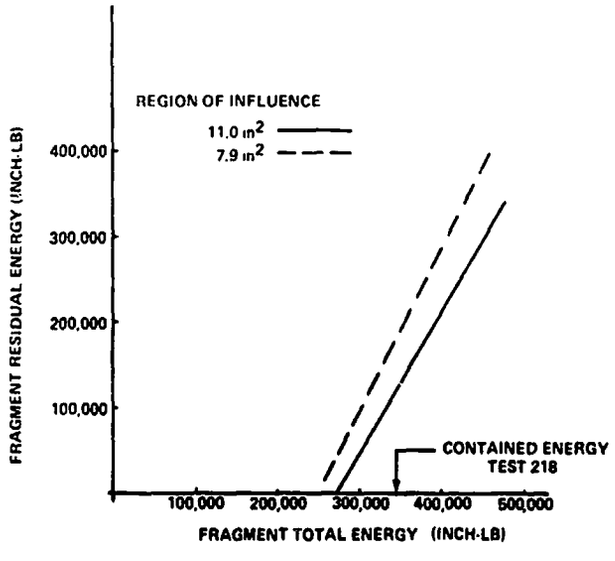

Figure 6. - EBCAP Predictions For NAPTC Spin Pit Tests.

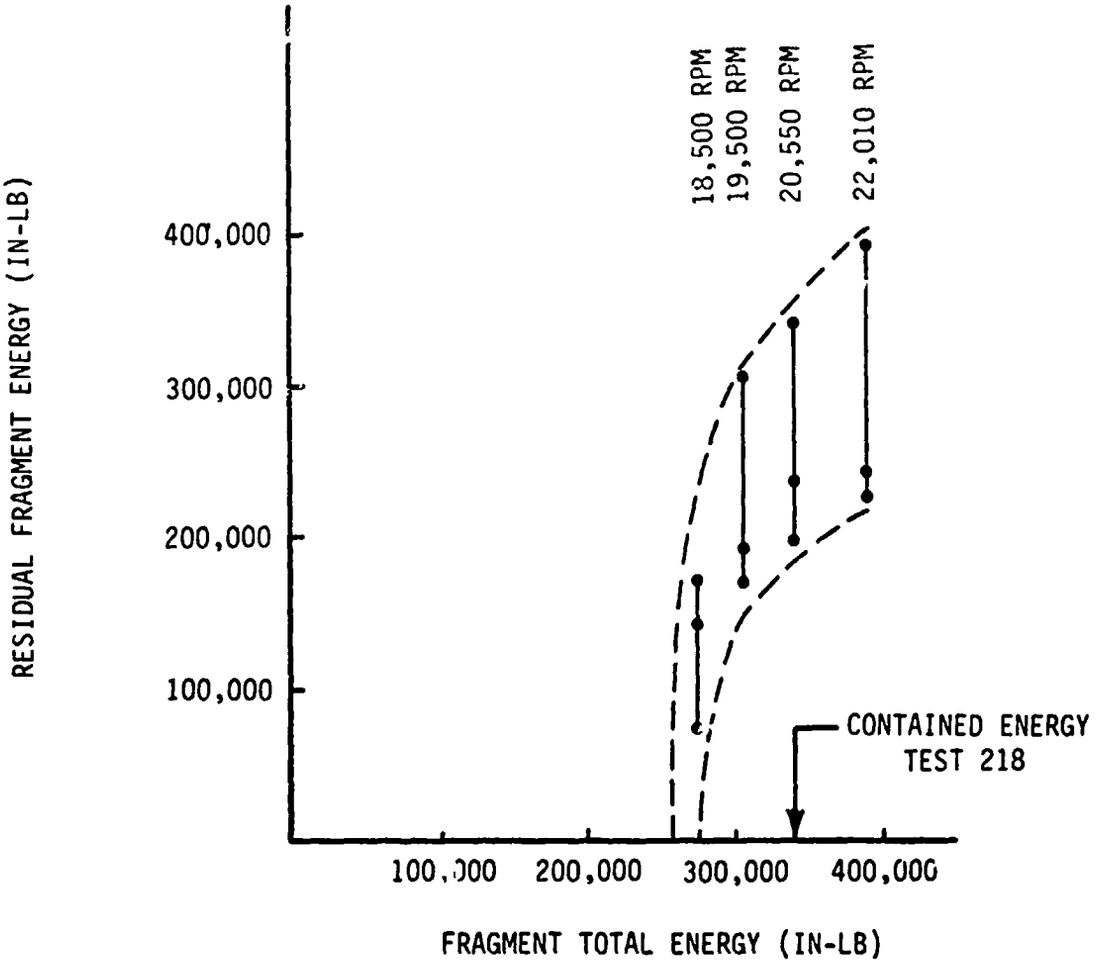

Figure 7. - JET4B Predictions For NAPTC Test 218.

CERAMIC COMPOSITE PROTECTION FOR TURBINE DISC BURSTS

P. B. Gardner
Industrial Ceramics Division
Norton Company

INTRODUCTION

Imagine yourself boarding an airbus with 300 other passengers heading off for a vacation trip when suddenly the in-flight certified auxiliary power unit bursts a turbine rotor during the take-off roll. Not a very happy start for your vacation is it?

This is what the civil authorities in Europe were concerned about prior to European certification of the A300B Airbus Commercial Transport.

The Hamburger Flugzeugbau Division of Messerschmitt-Bolkow-Blohm went to work on a solution to this potential problem since they had the installation responsibility for the Garrett supplied Auxiliary Power Unit (APU) for the A300B. In a program with Norton Company, a viable lightweight rotor containment system was developed and qualified for use in the production A300B aircraft.

The ceramic composite rotor containment system for the A300B application was totally developed and qualified for close to $60,000 with an addition to the aircraft weight of about 50 pounds. The cost per aircraft set is close to $2300. Compared to the integral containment system used on the L-1011 APU which cost close to 2 million dollars to develop at an increased unit cost per PT-6 engine much greater than the cost of the A300B panels, it can be readily determined that the ceramic composite rotor containment system provides an economical solution to the APU disc containment problem.

BACKGROUND

The Garrett TSCP 700-4 APU for the Airbus is the identical unit used in the Douglas DC-10. Unlike the L-1011 APU which Lockheed specified both integral blade and rotor disc protection for, the DC-10 unit was not designed to withstand rotor disc failures since the FAA TSO only required blade containment. Both the DC-10 and L-1011 APU's have high degrees of reliability, but Lockheed wanted the extra measure of safety provided with an integrally contained APU. Over two million dollars was spent to develop and qualify the L-1011 APU for this protection level.

The Garrett unit in the DC-10 installation apparently does not constitute a hazard to flight critical equipment in the immediate proximity of the tail installation location, but with the A300B location there could be some severe consequences from a turbine burst. Immediately beside the APU the triply redundant hydraulic actuators for the horizontal stabilizer surfaces are located. The rotating plane of the high energy rotors can be shown to pass through the flight control actuator locations. It was in these areas that MBB selected to locate rotor containment protection panels.

MATERIALS SEARCH

Having made the decision to provide protection with guards or panels located in the plane of the high energy compressor section of the APU, the next obvious task was to

find a lightweight material capable of stopping pieces of the high or low pressure compressor rotor discs.

This turned out to be a much greater task than originally anticipated by MBB. Their tests were conducted on over 25 different materials without success. In utter frustration, even reinforced concrete slabs were tested without success. Some limited success was obtained using rubber/metal composite laminates but not so much success as to allow their consideration for production. Finally, MBB contacted the ceramic composite armor manufacturers for information and selected Norton to work with them on a developmental effort to see if a modified ceramic composite armor system could do the job.

Norton's engineers determined analytically that a slight modification to the Armor System could possibly provide the high energy level protection required and various ceramic to backing ratios were proposed for testing to prove out the system design.

Essentially, four configurations were finally selected for testing against the high pressure and the low pressure wheels. Samples were provided to MBB and successful containment tests were conducted on the first try! All of the selected configurations passed the impact tests, and a final design was then optimized to combine both high pressure and low pressure protection in the same panel.

Final qualification impact and environmental testing was then jointly conducted and the Norton supplied rotor containment system was certified for use on the A300B aircraft against the FAA special conditions which required complete APU containment against rotor bursts to protect the complete aircraft.

PANEL DESIGN

As previously mentioned, Norton provided a modified Armor System design for the rotor containment panels. Basically, the modification of the design consisted of increasing the thickness of the fiberglass reinforced plastic backing material to achieve an optimum ratio of ceramic thickness to backing thickness for the different ballistic defeat condition.

CERAMIC COMPOSITE ARMOR SYSTEMS

Conventional Armor Systems of ceramic composites for Armor piercing projectile protection have been around for about 15 years. Much of the preliminary design of these systems was done on an empirical basis in ballistic test laboratories by both government and industry researchers.

The first lightweight Armor Systems to provide protection against ballistic projectiles were composed of a sintered aluminum oxide ceramic tile approximately one-third of an inch thick bonded to a ductile backing panel, usually aluminum or fiberglass reinforced plastic. In the early

1960's, the Norton Company entered the field of ceramic armor development with the hot pressed boron carbide armor system. Both the alumina and the boron carbide systems are similar in construction - the tile composition being the only difference, but the lower specific gravity of the boron carbide ceramic yields an armor system weighing approximately 30 percent less than the aluminum oxide system.

The most common lightweight armor systems, listed in the order of decreasing areal density (the weight per square foot necessary to provide a given ballistic protection level) follow:

- -Dual Hardness Steel (also identified as DPSA, or dual property steel armor)
- -Alumina (Aluminum Oxide, or Al_2O_3)/GRP Backing
- -Silicon/Boron Carbide/Silicon Carbide (Si/B_4C/SiC-Sintered/Impregnated)/GRP Backing
- -Boron Carbide (B_4C, also identified as SF B_4C, or silicon-free boron carbide - hot pressed)/GRP backing

All of the ceramic armor systems have one feature in common. Each is a two-component system consisting of a facing of hard brittle material and a backing of soft, deformable material such as fiberglass reinforced plastic. For dual hardness steel armor, the facing is a hardened austenitic steel, while the backing is a mild steel.

When either armor system is struck by an armor-piercing projectile, the core or penetrator is broken upon impact with the facing in the first few microseconds. The residual energy

is then absorbed by the backing material. The role of the backing has been likened to that of a "catcher's mitt" in this situation.

What was desired in the rotor containment application was to optimize the design to obtain a bigger "catcher's mitt" to contain the much greater kinetic energy of the impacting disc fragment. Unlike the piercing projectile situation, the impact "footprint" is very much larger for the disc fragment. The boron carbide ceramic acts to break-up the impacting disc fragment much like the armor piercing projectile, but the backing material plays a much greater role in absorbing the kinetic energy. Without the ceramic facing, the disc fragment's sharp edges would easily cut through the various plies of fiberglass causing easy defeat of the backing plate.

MODIFICATION OF THE DESIGN

By increasing the backing thickness of the rotor containment system to achieve a nearly 1/1 ratio of ceramic thickness to backing thickness, as opposed to the conventional projectile armor system which utilizes close to a 1.75/1 ceramic to backing ratio, a two-to-three fold increase in the kinetic energy protection level can be obtained for the same areal density system. For comparison purposes, an armor system for 50 caliber AP projectiles with an areal density of 13 pounds per square foot protects against 12,500 ft-lbs of energy whereas the rotor containment system of 13.5 pounds per square foot protects against 26,000 ft-lbs of energy.

BALLISTIC TEST PROGRAM

In order to develop the rotor containment system, Norton Company in conjunction with Hamburger Flugzeugbau in Hamburg, Germany, conducted an extensive test program utilizing an air cannon test rig. A plenum chamber was connected to the air cannon barrel by a fast acting pressure valve. The plenum chamber could be pressurized to varying levels to produce different impact velocities at the test panels.

The test fragments were unmachined 120° segments of the actual compressor discs weighing 1.25 Kg each. Impact velocities from 175 m/sec to 260 m/sec were used in the test program with the test criteria for success being total containment.

The test fragments were mounted in hard foam plugs which exposed the sharp edge of the disc fragment. These hard foam plugs are called sabots, and this is a common method for mounting test fragments of varying sizes for impact testing.

The test panels were rigidly mounted to an impact frame and subjected to a variety of impact tests which simulated various energy levels associated with the high and low pressure discs of the engine compressor.

The initial tests were conducted with the panels bolted directly to the impact frame, but the impact energy transmitted to the frame was so great that the mounting bolts were all sheared completely off. A revised mounting technique was then designed utilizing four straps which mounted the panel to the test frame. This mounting method was very successful and has been incorporated in the actual aircraft installation.

This transmitted energy to the mounting structure is a particularly troublesome problem for projectile armor systems as well. On the higher level kinetic energy threats such as the 50 caliber AP round, it can be a tough problem to solve. LTV Corporation spent considerable time and effort designing deformable bracketry to mount the armor panels on the USAF A-7D aircraft just to attenuate the energy levels transmitted to the aircraft structure. The Army's Natick Laboratories have also fretted over the problem in the design of a ballistic infantry helmet. Their problem is a bit tougher, however, because if they stop the round, the transmitted energy is great enough to break the helmet wearer's neck, and a helmet suspension system capable of attenuating the energy is also much too heavy to wear! For these reasons, the U. S. Army Infantry is still using the old "steel pot" helmet which makes a good coffee pot but not much else!

THE A300B APU INSTALLATION

In the absence of firm requirements for rotor disc containment and the fact that the APU compressor is not secured against the egress of debris; Hamburger Flugzeugbau required additional shielding over a given area. This shielding is installed between the adjacent fire walls and the airframe structure of the APU compartment. The shielding protects both the hydraulic systems and the airframe structure from damage, so that the free operation of the horizontal elevators remains unimpaired.

THE FINALIZED DESIGN - DUAL PROTECTION

After the complete survey of ballistic impact tests were conducted, it was determined that a single panel design could be provided to protect both the low pressure and high pressure disc fragments. Norton designed this system using a constant thickness backing with two different boron carbide ceramic thicknesses. The total thicknesses of the two segments are 25 mm and 30 mm respectively.

The backing material consists of various plies of armor grade woven roving fiberglass in a special high temperature resistant polyester resin. The high temperature resin was used since the panels are subjected to the high temperature levels of the APU compartment during operation.

This panel design was then subjected to full environmental testing per MIL-STD-810 which included the following tests:

-Structural Performance Load Tests

-Fungus Resistance

-Humidity Test

-Salt Fog Test

-Fluid Resistance (Hydraulic oil, fuel, lubricating oil and Halon 1301 fire extinguishant)

-High and Low Temperature (-60°C to +130°C)

-Acceleration (-4.5G to +9G)

-Vibration Test (Method 514, Procedure I, MIL-STD-810B)

Following the successful completion of the environmental test program, the rotor containment system was certified for use on the A300B Aircraft. The A300B aircraft entered commercial service in 1974 and over 50 aircraft are now in service with the European carriers.

RECENT ADVANCES IN ARMOR TECHNOLOGY - WEIGHT SAVINGS POTENTIAL

There has been a significant improvement made in the performance of ceramic composite armor systems since the rotor containment system was developed and qualified for the A300B APU. This improvement could be directly applicable to this system to achieve an areal density savings of about 12%. This could translate directly to a weight reduction of 7.0 pounds per aircraft set of panels today with a minimum of requalification testing required. This improvement involves the replacement of the woven roving fiberglass backing with DuPont's Kevlar-49 organic fiber. Norton Company is considered the pioneer in the development of advanced design

ceramic composite armor systems utilizing Kevlar-49 backing materials, and a summary of this development work applicable to crashworthy armored seats is discussed below.

BACKING MATERIAL IMPROVEMENTS

With the advent of the U. S. Army's request for proposals to industry for the Advanced Attack Helicopter, much emphasis was placed on eliminating parasitic armor completely or reducing the current areal densities required to defeat the specified ballistic projectile threats.

Theoretical penetration analysis techniques (THOR) indicated that a significant weight savings could be realized by replacing the conventional woven roving fiberglass (E-Glass) reinforced plastic with a newly developed synthetic fiber recently developed by DuPont.

Initial consultations began and soon various tests were underway by Norton to evaluate the validity of the hypothesis that a potential (7-8%) savings could be achieved by utilizing this material as a backing for the then "best" B_4C/E-Glass armor system.

Initially, the test results were not entirely encouraging, but inspired by DuPont, Norton attempted to reduce the variables affecting the performance of the backing to a minimum by utilizing essentially a one-for-one replacement of the E-Glass fibers alone by the Kevlar-49.

In a self-funded program, a comparable backing material was developed to the conventional E-Glass system with a resultant weight savings of about 30% over the E-Glass system. This program gained extreme interest and eventual further funding for ballistic verification by the U. S. Army's Natick Laboratories.

A number of ballistic verification tests were conducted to establish the validity of the initially encouraging results and the B_4C/Kevlar-49 system was approved by the Army for use as the armor system on the new advanced attack helicopter, thereby enabling the potential contractors a significant 10-12% weight savings in the Armor System.

The Kevlar-49 backing works well as an armor because of its outstanding physical properties as compared to E-Glass. As suggested by Wilkins et al, the synthesis of a new backing material that would be stiffer to more adequately support the ceramic and delay the onset of ceramic tensile failure is accomplished with the Kevlar laminates. At 19 million psi, it has the highest modulus of elasticity of any synthetic fiber, and is twice as stiff as E-Glass the most commonly used reinforcing fiber. Its high tensile strength and high modulus combined with its extremely low weight (1.45 g/cc - 40% less than the weight of glass), along with low elongation (2.8% at break vs. 4.0% at break for glass), high stress rupture, excellent impact strength and good vibration damping characteristics make it a natural for use as an armor backing.

SUMMARY

The development of the ceramic composite turbine disc protection panels for the A300B was a direct application of Norton's armor technology to a commercial application. In this case, the analytical predictions for modifying the ballistic projectile armor system were more than verified by the test program conducted to qualify the rotor containment system. In fact, with only a slight change in the areal density of the armor system a more than two-fold increase in kinetic energy protection level was achieved.

The assumption that guards used to protect against disc fragment damage to either the engine or aircraft components from failed turbine discs would impose intolerable weight and cost penalties upon the aircraft is disputed by this design. In fact, this concept is only slightly heavier than an integrally contained turbine engine but significantly less expensive on both a recurring and non-recurring cost basis.

Additional improvements in the state-of-the-art of armor technology also can now be incorporated into the rotor containment system to make this alternative even more attractive on a weight comparison basis to integral containment. The use of Kevlar-49 as a backing for the boron carbide ceramic has already been proven and qualified for use in the projectile armor systems, and its use for the rotor containment system could achieve a 12% weight savings over the current system.

Based on the successful application of Norton's Armor technology to this commercial application, and the significant increase in protection level that has been achieved, Norton has filed for patent rights in the U. S. and several foreign countries under Application Number 329,046. Patents rights are now pending in the U.S., U.K., France, Germany and Japan. This application is also covered in Italy under Patent Number 1004855.

REFERENCES

1. Wilkins, Mark L., Third Progress Report of Light Armor Program, UCRL-50460, Lawrence Radiation Laboratory, Univ. of California/Livermore, July 9, 1968.

2. Wilkins, M. L., Cline, C. F., and Honodel, C.A., Fourth Progress Report of Light Armor Program, UCRL 50694, Lawrence Radiation Laboratory, Univ. of California/Livermore, June 4, 1969.

3. Wilkins, M. L., Landingham, R.L., and Honodel, C.A., Fifth Progress Report of Light Armor Program, UCRL 50980, Lawrence Radiation Laboratory, Univ. of California/Livermore, January 1971.

4. Gardner, Paul B., Ceramic Armor - A Status Report, National Defense, September-October 1973.

5. Murphy, Jack, Making A Name For Itself, DuPont Magazine, July - August 1973.

6. Editor, Strongest Synthetic Fiber Yet Fills A Host Of Design Needs, Product Engineering, September 1974.

7. Gardner, Paul B., Advances in Ceramic Composite Armor Technology, Paper Presented at the American Defense Preparedness Association Symposium of Survivability and Vulnerability, October 1975.

8. Deutsche Airbus GmbH, Test Report VB No. 1856, 1973.

ABOUT THE AUTHOR

Paul B. Gardner is currently Business Manager for Armor and Spectramic Products in Norton Company's Industrial Ceramics Division. He joined the company in 1971 as a Project Engineer in Ceramic Components and in 1972 he was named Product Manager for the Armor Products Department. In his current position since late 1974, he has the responsibility for the business planning, marketing, sales and engineering of the Company's ARMOR, CRYSTAR and NORBIDE Product Lines. Prior to 1971 he held Experimental and Senior Experimental Engineering positions in Hamilton Standard Division of United Technologies' Aircraft Systems Department.

He received a BSME from the University of Rhode Island and an MSME from the Rensselaer Polytechnic Institute. He is currently a candidate for a Master of Science Degree in Management Science from the Worcester Polytechnic Institute. He holds a Registered Professional Engineers License in the Commonwealth of Massachusetts and is a member of the American Helicopter Society.

DISCUSSION

P. Gardner, Norton Co.

The compressor segment weight was 1.25 kilograms and the velocities varied from 175 to 260 meters per second.

G.J. Mangano, NAPTC

Paul, you made reference to high temperature. Could you tell me what the temperature was, how high?

P. Gardner, Norton Co.

We qualified the system at 300°F.

Question

How was the shield supported?

P. Gardner, Norton Co.

Only the four straps that I showed on the viewgraph supported the shield. These straps were attached to the aircraft structure at the Z-frame inside the firewall. The system weighed about 50 pounds, not including the weight of the straps. I do not recall the weight of the straps.

D. McCarthy, Rolls-Royce

Did you test a titanium shield mounted on the straps in exactly the same way?

P. Gardner, Norton Co.

No, we did not do any of the testing, it was done by Air Bus Industry, Hamburger, Flugzeugbau. Their test report indicates that they tested over 25 different materials, and had very little success, or had some very little success they could afford the weight for.

D. McCarthy, Rolls-Royce

I had the impression that the straps made quite a difference to the results.

P. Gardner, Norton Co.

The straps made some difference in the results. The initial test work was done with the armor panels mounted directly to the Z-frame of the simulated aircraft structure. The panels stopped the rotor segment, but the transmitted energy into the structure sheared the bolts off and the panel dropped away. So the straps were there to distribute that load more uniformly into the structure. That was not our design, that was designed by Hamburger Flugzeubau. If the actuators had not been in the wrong position relative to the APU, we probably wouldn't have had to contain anything.

CONCEPTS FOR THE DEVELOPMENT OF LIGHT-WEIGHT COMPOSITE STRUCTURES FOR ROTOR BURST CONTAINMENT*

by Arthur G. Holms

National Aeronautics and Space Administration
Lewis Research Center
Cleveland, Ohio 44135

ABSTRACT

Based on published results on rotor burst containment with single materials, and on body armor using composite materials, a set of hypotheses is established as to what variables might control the design of a weight - efficient protective device. Based on modern concepts for the design and analysis of small optimum seeking experiments, a particular experiment for evaluating the hypotheses and materials was designed. The design and methods for the analysis of results are described.

SUMMARY

The purpose of the research reported herein was to plan an experimental program, the results of which could provide a basis for the design of weight efficient full circumferential containment devices to protect passengers and critical aircraft systems from the devastating effects of turbine engine disk bursts. The conclusions about the needed experiment were synthesized from three areas of information, namely, (1) prior disk burst protection experiments, (2) personnel body armor research, and (3) modern concepts in the design and analysis of small optimum seeking experiments.

Based on both the prior disk burst experiments and the body armor research, a list of hypotheses was established as to what factors might be controlling in the design of a weight efficient protective device. The consequence of such hypotheses is that the device should consist of as many as four concentric rings, each to consist of a material uniquely chosen for its position in the penetration sequence. Four unique classes of materials are proposed for the four rings and

*Also published as NASA TM X-73633, 1977.

particularly attractive examples of each are identified. Experimenting is proposed to evaluate the hypotheses and material choices.

Because the materials are expensive, because their processing is difficult to control, and because the results of disk burst containment experiments are difficult to evaluate, some modern concepts for the design and analysis of small optimum seeking experiments were examined and are discussed. Based on such concepts, a particular experiment for evaluating the hypotheses and materials was designed, and the design and the method for the analysis of results is described.

INTRODUCTION

Recent statistics on turbine engine rotor failures in commercial aviation show that failures of several types occur (Mangano and De Lucia (1975)). The probability of successful containment of such failures depends on whether the failures to contain the fragments are due to: (1) full wheel bursts, (2) failed rim segments, or (3) failed blades. Engine containment of full wheel bursts (Table 1) has never occurred. Containment of rim fragments occurs in only a minority of failures. Containment of failed blades usually occurs, but this is not surprising because the FAA requires (Federal Regulations, Title 14) that failed blades be contained. Another FAA requirement is that failed disks be contained if the turbine is internal to the fuselage, as in the case of auxiliary power units.

The results of a long series of rotor burst protection experiments have been described by Mangano (1972). These results seem to imply that the weight penalties associated with full circumferential disk burst containment are prohibitive. The problem must be regarded as a research problem for which a major breakthrough is needed.

The possibility of using something less than full circumferential containment is currently being explored. Devices are under investigation to protect just a sector of a full circumference. The technique is called shadow shielding and the devices that have been proposed are called deflectors. Future research will undoubtedly separate those design situations (small angle of protection) where deflectors have the best weight efficiency from those situations (large angle of protection) where full circumferential containment has the best efficiency. Such a delineation cannot properly be made until optimization studies have been completed for both types.

The purpose of the present research was to plan some rotor burst containment experimenting that could result in procedures of general applicability for the design of weight efficient full circumferential rotor burst containment devices. To that end three areas of information were examined. The first was that provided by the bursting of turbine rotors into containment rings in a spin pit (Mangano (1972)). That investigation presented the results of a large amount of testing of mostly similar (steel) containment materials. The second area of information is that provided by the ballistic materials research of the Department of Defense to develop weight efficient personnel body armor. Although the response of targets to projectiles is basically different from the response of containment rings to disk bursts, the research does compare the ballistic properties of very dissimilar materials.

The joint examination of these two areas of research provides a list of physical hypotheses on how materials of widely different ballistic properties might be used in combination (composite rings) to product a more weight efficient containment than could be achieved with monolithic rings.

The main hypothesis from the rotor burst tests (Mangano (1972)) is that the containment device should absorb large amounts of energy in tensile straining. The main hypotheses from the body armor research (Rolston(1968)) is that the material properties should vary through the thickness of the device. In military armor, such variations are exemplified by dual hardness steel and by ceramics backed by fiber reinforced plastics.

The physical hypotheses should be subjected to critical experimentation so that they can be evaluated. Because the materials are expensive, because their processing is difficult to control, and because the results of disk burst containment experiments are difficult to evaluate, some modern concepts for the design and analysis of small optimum seeking experiments were reviewed. A specific design of an experiment is proposed. Because the materials and their processing are expensive, the experiment was designed so that preliminary conclusions can be drawn on completing just one half of the total design. On completion of the first half, the results can be examined to see whether the composite rings are superior to, or inferior to, the simpler monolithic rings (which have been extensively investigated). If the composite rings are not clearly superior to monolithic rings, the investigation can be terminated and further costs avoided. If the composite rings are superior, then the second half should be performed. Because the experiment is a telescoping design (Holms (1967)) or Addelman (1969) the data from both halves can be combined to produce valid estimates of the direct effects of the variables and their synergistic combinations.

In addition to providing containment design methods, a second purpose of the proposed experiment is to determine the weight penalty associated with a weight efficient containment system.

The results of the experiment might also identify concepts and materials applicable to the lesser problems of fan, compressor, and turbine blade containment.

IMPLICATIONS OF BODY ARMOR RESEARCH FOR ROTOR BURST CONTAINMENT

A basic concept that has proven widely useful in the design of weight efficient armor is the concept that the material properties should vary through the thickness of the armor. An elementary example is provided by the use of dual-hardness steel. The projectile first encounters a hard material that contributes to the deformation of the projectile, but because the hard material cannot be ideal in energy absorption, it is backed up by tougher material that sacrifices hardness in favor of better energy absorption. Such a concept was further investigated by Wong and Prifti (1972) at the Army Mechanics and Materials Research Center, Watertown, MA, who showed the existence of synergistic combinations of metals.

More complex systems were described by Rolston, Bodine, and Dunleavy (1968). They described some body armor in which a very hard material (a ceramic) is used in combination with a very strong material (a fiber reinforced plastic).

Materials that have proven weight efficient in protecting against slower moving projectiles have included nylon cloths (MIL-C-12369F(GL) (1974)) nylon felts (MIL-C-43635 (1969)) and aramid cloths (LP/P DES 32-75 (1975)). The use of aramid cloth for rotor burst protection was discussed by Gerstle (1975), in which he suggested that multi-material devices might be superior to monolithic devices.

PHYSICAL HYPOTHESES

The process by which a projectile is defeated by body armor is assumed to have some characteristics in common with, and some characteristics which

differ from, the process of a full circumferential disk burst containment. The common characteristics are assumed to occur in the initial stages where resistance to shear and resistance to spalling are important. The stage of disk burst containment that is assumed to be different from the operation of body armor is the final stage where the protective ring undergoes very large circumferential tensile and bending strains (Mangano (1972)).

The literature of body armor and the literature of rotor burst protection thus suggest a large number of physical hypotheses that might describe the rotor burst protection process. If all of these hypotheses were operative, the most efficient devices would be quite complex. The appropriate research would seem to consist of investigating the indicated complex device with a view to determining which features contribute to weight efficiency and which features do not.

Thus the long list of hypotheses to be considered should not be viewed as listing factors to be included in a design manual, but instead should be regarded as listing factors to be included in a research program. Many of the factors might prove to be insignificant and could be so identified in a design manual.

The hypotheses are as follows:

1. The protective device should consist of a nested set of four concentric cylinders, each having unique ballistic properties.

2. The innermost cylinder should be very strong in shear because:
   a. It should provide some blunting of the sharp edges of the projectile.
   b. It should dissipate some energy through projectile deformation.
   c. It should resist penetration by achieving a wider distribution of the load.

3. The first and second layers function in the immediate vicinity of the impact points as beams in bending. The first layer acts as the compressively stressed part of the beam and the second layer acts as that part of a beam that sustains high tensile stresses. The bond between them must sustain the "neutral axis shear stresses" and should also delay the spalling failure of the hard layer. The first layer should be very strong in compression and the second layer should be very strong in tension, and the combination should be of very low mass so as to minimize the distortions from circularity that result from inertia effects. The preservation of circularity would improve the uniformity of the load that is transferred to the outer layers. The particular desirability of low inertia for these layers suggests that hardness in the first layer is to be sought from a ceramic or a glass instead of a metal, and that strength in the second layer should be sought from a fiber reinforced plastic.

4. The third layer should be the result of a "hedge" strategy, that is, it should be a material proven weight efficient in tests of monolithic rings, namely, a high-toughness metal. As such, it would have some of the attributes of the other three layers.

5. The fourth layer should be chosen solely for its ability to absorb large amounts of energy in tensile straining. It should be a ballistic fabric or felt.

The experiment should serve two types of objectives.

1. It should test the truth or falsity of each of the preceding hypotheses.

2. It should show whether an optimum device (on a weight basis) would consist of more than one of the previously defined layers, and on a rough quantitative basis, it should give the optimum proportions of each.

So that the experiment will be representative of the weight efficiencies that are appropriate to aircraft usage, the four layers should each consist of materials that have maximum probability of performing the hypothesized-function on a weight efficient basis. Classes of materials that are though to be appropriate are as follows:

Layer	Class of material
First	Ceramic or glass
Second	Fiber reinforced plastic
Third	Metal
Fourth	Ballistic fabric or felt

Some materials that are regarded as being illustrative of the preceding four classes of materials are listed in Table 2. The listing does not differentiate between materials as to their practicality for the cold section or the hot section of a turbine engine. The assumption is that the experiment will evaluate basic interactions among the disk burst and containment material variables. When this has been done, the containment designer must then select materials that will retain the appropriate dynamic properties at the engine temperature conditions. For example, if an aramid fiber reinforced epoxy were found to be weight efficient in the second layer, then a containment device in the turbine hot section might use a tungsten fiber reinforced nickel in the second layer.

A high strength adhesive is proposed to be used between the first and the second layers. Detailed information on high strength adhesives was given by Shields (1970). High strength adhesives are specified by MMM-A-132. Some examples of high strength adhesives are provided by the cyanoacrylates (MIL-A-46050) and the epoxy-nylons.

DESIGN AND ANALYSIS OF SMALL OPTIMUM SEEKING EXPERIMENTS

Many strategies for the experimental attainment of optimum conditions have been investigated and described in the literature. Of them, the particular set of concepts known as "Box-Wilson methods" (Box and Wilson (1951)) or "Response Surface Methodology" (Box and Hunter (1957)) is now well established as the most rational and efficient approach. These methods have a flow sequence as depicted by Fig. 1 and as described as follows.

Step 1. - Using all prior knowledge, select a set of independent variables that are to be investigated for their effect on the dependent variable that is to be optimized. (In the present instance the dependent variable could be chosen as the ratio of rotor burst energy divided by the containment weight for just marginal containment, or it could be chosen as the ratio of rotor burst momentum divided by the containment weight for just marginal containment, or it could be chosen as some other function of the rotor variables and the containment weight).

The independent variables would be chosen to represent the environment of the impact process together with the design and material variables of the containment device. The test levels chosen for the independent variables would be based on prior knowledge of the physical process. A statistically optimal design of experiment is then selected to be maximally efficient for the model fitting. The data is to be fitted with a simple mathematical model (which is usually a polynlmial equation of first degree augmented by a few higher degree terms as may be permitted by the small experiment).

The experiment is performed and a statistically optimal procedure is used to select a mathematical model of maximum predictive accuracy in terms of the actual data. The next step depends upon the nature of the selected model, as displayed by the relative magnitudes of the first degree and higher order terms. If the first degree terms are clearly predominant the response function is essentially planar and the "method of steepest ascents" is appropriate. The next step is therefore Step 2. If the second degree terms cannot be ignored, the response surface is warped or curved and the "method of local exploration" is appropriate, and the next step is therefore Step 3.

Step 2. - The situation is that a planar surface represents the response as a first degree equation in the independent variables and the equation is used to determine the direction of steepest ascent in terms of the independent (coordinate) variables. The situation is analogous to a mountain climber at a river's edge who decides to walk in a straight line over the meadow in its direction of steepest ascent (for example, 30 degrees east of north, which is to say, some fixed ratio of the independent variables "miles east" and "miles north").

Having established such a direction, a sequence of experimental points is laid out in that direction. With the completion of the indicated experimenting, the location in the experiment space is identified for the maximum of the dependent variable. If the achieved maximum is adequate or if experimenting must be stopped for other reasons, the next step is Step 4. Otherwise the next step is to go back to Step 1 (but with newly acquired empirical and other information).

Step 3. - The experiment plan of "Step 1" was minimally adequate for a first degree equation. It must be augmented by sufficient "hypercube blocks" (Box and Hunter (1957)) or (Holms (1967)) to evaluate two-factor-interaction terms. It must also be augmented by a "star block" (Box and Wilson (1951)) or (Box and Hunter (1957)). Performance of the experiment allows the fitting and selection of a model that is a statistically optimal representation of the data. The practical interpretation of the equation can be performed as described by Box and Wilson (1951), by Davies (1960), or by Myers (1971).

The predictive model and its geometrical interpretation (often by the "method of canonical reduction") can be used to decide that a true maximum has been located, or that it has not. If a true maximum has been located, or if experimenting is to be discontinued for other reasons, the next step is Step 4. If not, then the canonical reduction would be used to identify a line of steepest ascents along a "rising ridge", and the procedure would otherwise be that of Step 2.

Step 4. - Stop the experimenting and write the report, or build the prototype, or both.

ILLUSTRATIVE EXAMPLE - A PARTICULAR EXPERIMENT FOR PRELIMINARY OPTIMIZATION OF A ROTOR BURST CONTAINMENT DEVICE USING COMPOSITE MATERIALS

To test the stated hypotheses, and to evaluate the listed materials, the experimenting would consist of spin-pit burst containment testing using a representative turbine wheel. The wheel to be burst is surrounded by the containment ring assembly to be tested. The number of equally sized wheel fragments and the burst speed are controlled by saw cuts radially oriented in the rim of the test wheel. The result of each burst test would be measured by the weight of the containment assembly, the wheel speed at burst, and whether the ring assembly contained or did not contain the wheel fragments.

In the design and analysis of a sequence of optimum seeking experiments, one object function, such as the protective efficiency, would be selected as the dependent variable. In any case, in the fitting of models to the data from a single experiment, more than one dependent variable can be tried. One dependent variable that might be tried is the ratio of kinetic energy stored in the rotor just prior to burst divided by that weight of containment that provides marginal or threshold containment. Another dependent variable that might be tried is the ratio of angular momentum stored in the rotor just prior to burst divided by that weight of containment that provides marginal or threshold containment. If two or more such dependent variables are compared for their correlation with a set of independent variables, the comparison might show that one of them is superior as a containment design variable.

Two classes of independent variables can be defined.

1. Variables that involve the attacking fragments such as (a) the number of them, (b) their mass, (c) their speed, and (d) the initial clearance between the rotor and the protective device.

2. Variables that involve the containment design such as the mechanical properties of the containment materials and the weight of each material used.

The experiment should provide some information on what might approximate an optimum condition among the second class of variables. It should also provide some information on how the conditions within the first class of variables might affect the optimum among the second class. The experiment

should be designed so that it can be fitted by a model equation containing first degree terms in all the variables and containing cross product terms involving independent variables both within and between these two classes of variables.

Fragment Variables

The fragment variables selected for the experiment are (a) the number of equally sized sectors and (b) the initial radial clearance between the rotor and the inside surface of the containment device. The test wheels will be modified so that on a controlled basis, the nature of the bursts will include two, three, and six piece bursts. Thus the sector sizes will be, respectively, 180^{o}, 120^{o}, and 60^{o}. These pieces will differ widely in their masses, so that their speeds for threshold containment will probably be different.

Differing speeds are likely to require differing relative weights of the different layers for maximum overall weight efficiency. Such a result is equivalent to saying that there are interactions between the sector size variable and the variables expressing the relative weights of the layers.

The radial clearance is defined as the radial distance between the outer surface of the disk and the inner surface of the container. This definition ignores the presence of the blades. Blades were concluded to be relatively unimportant by Mangano (1972) who wrote as follows:

"Therefore, the blades on a rotor fragment do not significantly influence the distribution of the impact loads that are induced in a ring (provided the ring thickness approaches that required to effect containment and the fragment hub to blades mass ratio is large), nor do the blades absorb significant amounts of energy through their deformation during the containment process. The blades serve only to influence the fragment trajectory during the initial stages of impact. This also means that in cases where the rotor tip-to-ring clearance is small (test or operational clearances) the blade radial length becomes in effect the radial clearance that influences the orientation of the hub or disk portion of the fragment."

As defined, the radial clearance would be relatively small for the last stage of a compressor and for the first stage of a turbine, and would be relatively large for the first stage of a compressor or for the last stage of a turbine.

The radial clearance determines the amount that a disk sector rotates before contacting the container. Thus making the radial clearance an independent variable will vary the orientation of the attacking fragment to the inner surface. This variation might affect the optimum fraction of total weight that is assigned to the inner layer. Thus there might be an interaction between clearance and first layer weight.

Container Variables

The container consists of four layers. The fractions of the total weight assigned to three of the layers are independent variables. The fraction of total weight assigned to the fourth layer is correlated with the other three and is therefore not an independent variable. Such a variable is sometimes called a slack variable.

Two variations of a basic experiment plan will be described. In one variation of the plan, the fraction of total weight assigned to the third (metallic) layer will be the balance of weight variable, while in the other variation, the fraction of total weight assigned to the fourth (cloth) layer will be the balance of weight variable. In any case, the materials for each layer would be selected from Table 2.

Plan of Experiment

The plan of the experiment is indicated in Table 3. The treatment symbols represent the combinations of independent variable conditions in Yates notation and they are listed in the first column. They are the same as those in Table 7 of Holms (1967) which also describes the notation and further characterizes the plan.

The independent variables x_A, x_B, x_C, x_D, and x_E are to be assigned relative levels that are consistent with the levels implied by the treatment symbols in the first column. In Table 3 the plan variables have the meanings listed in Appendix A.

As listed in Table 7 of Holms (1967) all the treatments are intended to be performed in a single time span, or stage, or block. As such, the experiment is highly efficient in producing orthogonal estimates of all direct effect coefficients and all two-factor interaction coefficients. As such the experiment would

not ordinarily be subdivided. For the purposes of multi-layer rotor burst containment experimenting, each specimen will be terribly expensive. Furthermore, as described in Appendix B, each treatment (each combination of independent variables) will require about four specimens to produce a single value of the associated dependent variable.

Because the evaluation of the treatments will be so terribly expensive, the experiment plan as listed in Table 3 has been divided into two blocks, so that depending on the results from the first block, a decision can be made to either continue or not continue with the second block. This division means that on completion of the experiment, one two-factor interaction effect will not be capable of being estimated. To improve the precision of each block and to improve the precision of the combined experiment, some center point treatments not in Table 7 of Holms (1967) have been added to each block of Table 3.

One basis for deciding whether or not to continue from the first to the second block of Table 3 could consist of a comparison of the performance of the multi-material containers with the performance of monolithic containers. The standard of comparison might be the performance of a metal container, or it might be the performance of a cloth container. In either case, the standard of comparison need not be established by data external to the experiment. It could be established from results obtained from the first block. If a metal were desired as the standard of comparison, then the variable x_C would be assigned to the weight fraction of ballistic cloth, and the variable z would be assigned to the weight fraction of metal, namely z would be the weight fraction of metal in the third layer which would be specified by the z-column of Table 3 (and the metal would be chosen from Table 2(c)).

If the standard of comparison were to be a ballistic cloth, then the weight fraction of metal in the third layer would be specified by x_C of Table 3 and the weight fraction of cloth would be as specified by the z column of Table 3. (The cloth would be chosen from Table 2(d).)

The criteria used in assigning the treatments of Table 3 to the two blocks are given in Appendix C. Also given in Appendix C is an illustration of how the results from the first block, and from the combined blocks, would be interpreted if the standard of comparison were a metal.

Model Selection and Interpretation

If the experiment were that given by both blocks of Table 3 then the model initially fitted to the data would be that given by equation (5) of Appendix C. Such an equation might contain a few coefficients consisting mostly of experimental error, and the equation could be improved by deleting such terms as described by Holms (1974). Terms could also be deleted using a more conventional deletion procedure such as that given by Sidik (1972).

Suppose equation (5) has been fitted to the data and the insignificant terms deleted. The coefficients of x_A, x_B, and x_C would be examined for negative signs. Any such term having a negative sign would thereby suggest that the associated material was less weight efficient than the "others". (The "others" would always include the "balance of weight" material that is not explicitly represented in the model.) The larger positive coefficients of x_A, x_B, and x_C (if any are found) identify associated materials as being particularly weight efficient.

Numerically large coefficients of the two factor interactions would show important interaction (synergistic) effects. Their interpretation would follow from the definitions given to the independent variables.

CONCLUDING REMARKS

Preliminary to some proposed empirical development of design methods for weight efficient full circumferential rotor burst containment devices, three areas of information were reviewed, namely: (1) rotor burst protection experiments, (2) personnel body armor materials, and (3) modern methods for the design and analysis of small optimum seeking experiments.

Review of the information on rotor burst protection and body armor suggested that the following hypotheses should be evaluated:

1. The device should consist of four concentric cylinders, each having unique ballistic properties.

2. The innermost cylinder should be strong in shear to: (a) provide blunting of the sharp edges of the rotor fragments (b) dissipate some energy through fragment deformation, and (c) resist penetration by achieving a wider distribution of the load.

3. In the vicinity of each impact point the first and second layers should act as a beam in bending with: (a) the first layer having high compressive strength, (b) the second layer having high tensile strength, (c) the bond between them (the neutral axis shear area) having high shear strength, and (d) the combination should be of low mass to minimize distortions from the original shape due to inertia effects. The bond and the second layer should also be strong to inhibit spalling in the first layer.

4. The third layer should be the result of a "hedge" strategy, that is, it should be a material proven weight efficient in tests of monolithic rings. Thus it would have some of the attributes of the other three layers.

5. The concentrated loads of the attacking fragments should be assumed to be well distributed by the first three layers, and the fourth layer should be chosen solely for its weight efficiency in absorbing large amounts of energy in tensile straining.

Based on the preceding hypotheses and based on the ballistic properties of different types of armor materials, the four concentric cylinders should consist of materials from inner to outer as follows:

1. A light hard layer, such as a ceramic or a glass.
2. A light high tensile strength layer, such as a fiber reinforced plastic.
3. A tough layer, such as a metal.
4. A stretchable layer, such as a ballistic nylon cloth.

To test the stated hypotheses, and to evaluate the listed materials, the experimenting would consist of spin-pit burst containment testing using a representative turbine wheel. The wheel to be burst is surrounded by the containment ring assembly to be tested. The number of equally sized wheel fragments and the burst speed are controlled by saw cuts radially oriented in the rim of the test wheel. The result of each burst test would be measured by the weight of containment assembly, the wheel speed at burst, and whether the ringassembly contained or did not contain the wheel fragments. In addition to the containment system variables, other variables (representing engine design) were included in the experiment. Thus interactions can be observed between engine variables and containment material variables. The engine variables consist of the radial distance between the disk and the inner containment ring, and the combined effects of the mass and speed of the attacking fragments.

The attributes of the proposed experiment plan are as follows:

1. The experiment can be performed in two stages. Completion of the first stage results in a direct comparison of the weight efficiency of the composite ring concept with that of a monolithic ring.

2. If the comparison is unfavorable to the composite ring, the investigation can be terminated.

3. If the investigation is continued to the completion of the second stage, then the major hypotheses will be quantitatively evaluated. That is, the fitted model equation will contain 14 empirical coefficients and their values will provide 14 conclusions about the direct influences of the variables together with the ways that they combine (interact) to produce synergistic effects.

4. The orthogonal design of the experiment results in the observed effects of the variables being free of error correlations with each other and free from variations entering the experiment between the performances of the two stages.

APPENDIX A

SYMBOLS

x_A	weight fraction of first (innermost) layer
x_B	weight fraction of second layer
x_C	weight fraction of third (or fourth) layer
x_D	number of equally sized sector fragments of test rotor
x_E	radial clearance (-1 means small clearance, +1 means large, and 0 means mean of other two)
z	balance of weight (weight fraction not included in x_A, x_B, and x_C)
Y	dependent variable. SFE_{50} is a possible dependent variable
SFE_{50}	ratio of kinetic energy stored in the rotor at burst divided by the weight of containment providing marginal, or threshold, or 50 percent probability of containment

APPENDIX B

TEST STRATEGY

Threshold containment is to be evaluated for each of the treatment conditions of Table 3. The dependent variable could be the stored kinetic energy prior to burst divided by the container weight, or it might be the angular momentum prior to burst divided by the container weight, or it might be otherwise defined. In any case, the threshold condition is defined here as that condition which results in a 50-percent probability of containment. The object of the testing is therefore to determine a rotor speed representing a 50-percent probability of containment. Each test usually has an identifiable result that can be called contained and labeled "C" or not contained labeled "NC". The NC results will usually occur at higher speeds than the C results (although material property variations can sometimes result in a C at a higher speed (RPM) than one or more speeds that resulted in NC). From the data, a quantity called rpm_{50} must be determined which will be an estimated speed for a 50-percent probability of containment. For the purposes of the experiment defined by Table 3, a good enough estimate of rpm_{50} is believed to be attainable if the experimenting includes four burst tests for every treatment. The test wheels would be modified with radial cuts to induce the 2, 3, and 6 sector bursts as listed in Table 3. The depths of the cuts would be such as to result in approximations to the desired burst speed. The first test at any given treatment condition should be at a speed which (based on all prior information) is equally likely to result in a C or an NC. Subsequent speeds are to be computed using a stepping factor, f_s. If the experimenter had good prior knowledge of the performance of the containment system, he might choose f_s such that $1 < f_s < 2$. With little prior information on the containment system, he might choose $f_s \geq 2$. If the first result is a C then each new speed rpm_{i+1} at point $i + 1$ in the sequence following a C at rpm_i should be

$$rpm_{i+1} = \sqrt{f_s} * rpm_i$$

If the first test in a sequence results in an NC, then each new test that follows an NC shall be at speed rpm_{i+1} determined from the previous speed rpm_i as follows:

$$rpm_{i+1} = rpm_i \Big/ \sqrt{f_s}$$

After a test result has been followed by a test result of opposite type (C followed by NC or NC followed by C) the next test shall be at rpm_{i+1} determined from the smallest speed for NC, $rpm_{min, NC}$ and from the largest speed for C, $rpm_{max, C}$ as follows:

$$rpm_{i+1} = \left[\left(rpm^2_{min, NC} + rpm^2_{max, C} \right) \Big/ 2 \right]^{1/2}$$

Illustrations of how such a test strategy might proceed are given by Fig. 2.

The final estimate of rpm_{50} would be obtained from the preceding equation with $i = 4$, except that if all four results were only C or only NC, then rpm_{50} would not be estimable.

APPENDIX C

DESIGN OF TWO-STAGE EXPERIMENT

This section presents some background information on the design of the experiment for multi-material containment rings. The terminology and use of symbols is that of Davies (1960) or of Holms (1967).

The first block (eight treatments) might be planned as a resolution 3 design to provide estimates of first-order coefficients for a model equation that would include the five variables. The defining contrasts must then include two three-letter words and one four-letter word. The four-letter word would be the defining contrast for the experiment with two blocks and 16 treatments. The experiment with two blocks would be a resolution 4 design, and therefore, it would be almost worthless with respect to the estimateion of the coefficients of the two-factor interactions. Such a design would be of little value because the physical basis for the research is the hypothesis that certain materials, when used in combination, might interact beneficially, and that furthermore, the beneficial effects of certain materials might be critically dependent on such ballistic variables as fragment orientation and speed. Correspondingly, the estimation of most of the two-factor interaction coefficients is essential to the answering of the main questions of the research.

In line with the preceding criteria, the objective of obtaining a resolution 3 design at the end of the first block will be sacrificed, and as a benefit of that sacrifice a nearly resolution 5 design can be achieved at the conclusion of the two blocks. For the two blocks, the defining contrast will be a five-letter word (which would ordinarily provide a resolution 5 design) but for the priviledge of having the option to stop or to continue the investigation beyond the first block we must pay the price of confounding one two-factor interaction with the block effect.

The defining contrasts for the first block can be

$$I = -ABD = CE = -ABCDE \qquad (1)$$

and the defining contrasts for the first two blocks can be

$$I = -ABCDE \qquad (2)$$

Let the variables be chosen and labeled as in Appendix A and in particular let x_C be the weight fraction of the fourth layer (cloth) and let z_M be the weight fraction of the third layer (metal). In such a labeling of variables, the variable z_M is obviously a first-degree function of x_A, x_B, and x_C and is therefore not an independent variable. It is called a slack variable or a "balance of weight" variable and would be omitted from any model fitting that included the variables x_A, x_B, and x_C. The association of particular plan variables (letters) with the physical variables might have been arbitrary, but it should not be, because the interaction $x_C x_E$ is confounded with the block effect. Because the coefficient of $x_C x_E$ is in error by the amount of the block effect, the letters C and E should be assigned to the variables thought least likely to interact.

The assignment of physical variables to the letters C and E is based on the following considerations. The impact process begins with the wheel fragments traveling through the clearance distance and the process ends with the transfer of some minor or major strain to the outer layer. This sequence suggests that the physical variables consisting of the initial clearance and the weight fraction of outer layer are the two physical variables least likely to interact. Correspondingly, these variables should be given the symbols C and E, and the order is arbitrary. (As suggested by the body armor data, the speed of impact is a variable that can change the mode of fracture. Thus the speed of impact has a high probability of interacting with the other variables. It was for this reason that the number of fragments is introduced as a controlled variable into the experiment, thus forcing the experiment into differing ranges of speed. Correspondingly, the variables x_C and x_E should not be used to represent the number of fragments.) Some additional concepts for the matching of physical variables to plan variables were given by Sidik (1971).

With the defining contrasts given by equation (1), the treatments and the aliased first- and second-degree model parameters are as shown in Table 4. Performance of the experiment with such treatments and acquisition of the associated observations would permit the numerical evaluation of eight model coefficients. Let these coefficients be labeled b_0, b_1, b_2, b_3, b_4, b_5, b_6, and b_7. Referring to the alias combinations of Table 4, the predictive equation could be written

$$Y = b_0 + b_1 x_A + b_2 x_B - b_3 x_D + b_4 x_C + b_5 x_A x_C + b_6 x_B x_C - b_7 x_C x_D \qquad (3)$$

Reference to the aliased pairs in Table 4 shows that any one or more of the terms in the preceding equation can be arbitrarily replaced by its alias as listed in Table 4. (The choices of algebraic signs are based on the assumption that the b's are computed by Yates' method.)

Note that the first degree terms in x_C and x_E are indistinguishable. Furthermore, a basic assumption of the multi-material concept is that the right combination of several materials will provide containment that is more weight efficient than the best material used singly. Consistent with this assumption is the assumption that the two-factor interactions will be large and that the ambiguities among the terms of Table 4 will not permit any conclusions to be drawn with respect to the effects of the variables. What will be achieved is the performance of eight or nine milti-material combinations to be compared with the performance of single material containment rings.

The performance of single material containment rings could be obtained from direct tests with single material rings, however, a crude indirect comparison of the performance of single material rings with multiple material rings is obtainable from just the first block data of Table 3. The crude comparison is obtained by fitting the model

$$Y = \alpha + \beta_M z_M \tag{4}$$

to the data, where α and β_M are the only constants fitted to the nine observations of Y. If the coefficient of correlation were low, or if the coefficient β_M were concluded to be insignificant, then no useful comparison could be drawn between the weight efficiency of metal rings and the weight efficiency of multi-material rings. The experimenter might proceed with block 2 or he might look to other sources of information. On the other hand, if the coefficient of correlation were high, of if the coefficient β_M were tested as significant, the immediate conclusions would be that the variation of the weight fraction of the metallic content was important and that the variations of the weight fractions of the nonmetallic materials were unimportant. (As listed in Table 3, the weight fraction of the metal would have been 0/12, 2/12, 3/12, 4/12, and 6/12.) If in the model fitting, β_M were concluded to be significant, then a negative value would show that the nonmetallic materials were weight efficient and that the investigation should be continued through the second block (at which point the effects of the nonmetallic materials would probably become clear - significant interactions would be displayed). A significant and positive value for β_M from the first block would show that the performance of the metal was

superior to that of the other materials. The implication of such a result would be that all the concepts leading to the design of the experiment should be re-examined, and that the next step should not include a performance of the second block.

If a second block is performed, the basic treatments and the first- and second-degree parameter estimates for the two blocks would be as shown in Table 5. Such an experiment would be described as a two-level, half-replicate, fractional-factorial experiment on five variables in two blocks.

Based on the structure exhibited by Table 5, a prediction equation obtained from the parameter estimates from the data observed from the two blocks would be written:

$$Y = b_0 + b_1x_A + b_2x_B + b_3x_Ax_B + b_4x_C + b_5x_Ax_C + b_6x_Bx_C - b_7x_Dx_E + b_8x_D$$

$$+ b_9x_Ax_D + b_{10}x_Bx_D - b^*_{11}x_Cx_E + b_{12}x_Cx_D - b_{13}x_Bx_E - b_{14}x_Ax_E - b_{15}x_E \qquad (5)$$

The estimate b^*_{11} is not necessarily the correct value for the coefficient of x_Cx_E. The estimate will be in error by the average performance shift in Y caused by any changes that may have occurred between the two blocks. The term in x_Cx_E would be deleted if equation (5) (or any simplification of it) were used as a containment design equation.

The experiment with the two blocks, as just described, can be doubled to a full factorial experiment with parameters estimated for all interactions up to the five variable interaction. If this were done, the coefficients of x_Cx_E, $x_Ax_Bx_D$, and $x_Ax_Bx_Cx_Dx_E$ would still contain any errors caused by block effects. *Confounded with block effect.

REFERENCES

Addelman, Sidney: Sequences of Two-Level Fractional Factorial Plans. Technometrics, vol. 11, 1969, pp. 477-509.

Box, G. E. P.; and Wilson, K. B.: On the Experimental Attainment of Optimum Conditions. R. Stat. Soc. J., Ser. B, vol. 13, 1951, pp. 1-45.

Box, G. E. P.; and Hunter, J. S.: Multi-Factor Experiment Designs for Exploring Response Surfaces. Ann. Math. Stat., vol. 28, 1957, pp. 195-241.

Davies, Owen L., ed.: The Design and Analysis of Industrial Experiments. 2nd ed., Hafner Publ. Co., 1956.

Airworthiness Standards; Aircraft Engines. Section 33.75 "Safety Analysis". Federal Regulations, Title 14, Pt. 33, 1976.

Gerstle, J. H.: Analysis of Rotor Fragment Impact on Ballistic Fabric Engine Burst Containment Shields. J. Aircraft, vol. 12, no. 4, Apr. 1975, pp. 388-393.

Holms, Arthur G.: Designs of Experiments as Telescoping Sequences of Blocks for Optimum Seeking (as intended for alloy development). NASA TN D-4100, 1967.

Holms, Arthur G.: Chain Pooling to Minimize Prediction Error in Subset Regression. NASA TM X-71645, 1974.

Mangano, G. J.: Rotor Burst Protection Program - Phases VI and VII: Exploratory Experimentation to Provide Data for the Design of Rotor Burst Fragment Containment Rings. NAPTC-AED-1968, Naval Air Propulsion Test Center, 1972.

Mangano, G. J.; and DeLucia, R. A.: Rotor Burst Protection Program: Statistics on Aircraft Gas Turbine Engine Rotor Failures that Occurred in U.S. Commercial Aviation During 1973. ASME Paper 75-GT-12, Mar. 1975.

Adhesives, Cyanoacrylate, Rapid Room Temperature Curing, Solventless. Spec. MIL-A-46050, Army Mater. Mech. Res. Center, Dec. 11, 1970.

Adhesives, Heat Resistant, Metal to Metal. Spec. MMM-A-132, Naval Air Systems Command, Apr. 30, 1965.

Myers, Raymond H.: Response Surface Methodology, Allyn and Bacon, Inc., 1971.

Rolston, Robert F.; Bodine, Edward; and Dunleavy, Joseph: Breakthrough in Armor. Space Aeron., July 1968, pp. 55-63.

Shields, J.: Adhesives Handbook. Chemical Rubber Co. Press, 1970.

Sidik, Steven M.; and Holms, Arthur G.: Optimal Design Procedures for Two-Level Fractional Factorial Experiments Given Prior Information about Parameters. NASA TN D-6527, 1971.

Sidik, Steven M.: An Improved Multiple Linear Regression and Data Analysis Computer Program Package. NASA TN D-6770, 1972.

TABLE 1. - DISK BURSTS

	1971	1972	1973	1974
Fan	1	1	0	0
Compressor	7	2	2	1
Turbine	5	2	1	4
Total	13	5	3	5

TABLE 2. - MATERIAL AND PROCESS OPTIONS

(a) Layer 1

Option	Requirements	Description
a	MIL-A-46103 (class 4)	Boron carbide ceramic, monolithic ring.
b	MIL-A-46103 (class 4)	Boron carbide ceramic, adhesively bonded tiles.
c	MIL-A-46103 (class 3)	Boron carbide/silicon carbide/silicon ceramic, monolithic ring.
d	MIL-A-46103 (class 3)	Boron carbide/silicon carbide/silicon ceramic, adhesively bonded tiles.
e	MIL-A-46103 (class 2)	Silicon carbide ceramic, monolithic ring.
f	MIL-A-46103 (class 2)	Silicon carbide ceramic, adhesively bonded tiles.
g	MIL-A-46103 (class 1) and/or MIL-T-46098	Aluminum oxide ceramic, monolithic ring.
h	MIL-A-46103 (class 1) and/or MIL-T-46098	Aluminum oxide ceramic adhesively bonded tiles.
i		Borosilicate glass (Pyrex 7740 or equal) monolithic ring
	MIL-A-46050	Adhesive, cyanoacrylate.
	MMM-A-132	Adhesive, epoxy-nylon.

TABLE 2. - Continued.

(b) Layer 2

Option	Requirements	Description
a	SAE-AMS 3832	Glass roving, filament wound, S-glass, epoxy resin.
b	MIL-A-46103B or MIL-I-17368*	Glass cloth reinforced, polyester resin.
c		Aramid fiber filament wound, phenolic-polyvinyl butyral resin.
d		Aramid cloth reinforced, phenolic-polyvinyl butyral resin.
e		Aramid fiber filament wound, epoxy resin.
f		Aramid cloth reinforced epoxy resin.

*Doron: Glass MIL-C-9084, resin MIL-R-7575.

TABLE 2. - Continued.

(c) Layer 3

Option	Requirements	Description
a	MII-S-17758	Hadfield steel rings. Billets pierced and roll formed. Fully austentized.
b	MIL-S-13259	Hadfield steel, rolled strip. Fully austentized. Spirally wrapped and tack welded.
c	MIL-S-17249 (ASTM 128, B-3)	Hadfield steel rings, centrifugally cast and finish machined.
d	SAE-AMS 5639 Fed QQ-S-763 (AISI 304)	Stainless steel rings, billets pierced and roll formed, solution treated.
e	SAE-AMS 5515 (AISI 301 or 302)	Stainless steel, rolled strip. Hot rolled and solution treated. Spirally wrapped and tack welded.
f	SAE-AMS 5370 (ACI-CF-8)	Stainless steel rings, centrifugally cast and finish machined.
g		TRIPP steel. Billets pierced and roll formed.
h		TRIPP steel, rolled strip. Spirally wrapped and tack welded.

TABLE 2. - Concluded.

(d) Layer 4

Option	Requirements	Description
a	MIL-C-43635	Felt, ballistic, nylon.
b		Felt, aramid (Kevlar 29).
c	MIL-C-12369	Fabric, ballistic, nylon.
d	LP/P DES 32-75*	Fabric, ballistic, aramid.
e		Polypropelene plastic film, Phillips XP or equal.

* Natick limited use specification.

TABLE 3. - PLAN OF EXPERIMENT AND LEVELS OF VARIABLES

Treatment symbol	Block	Fractions of total weight				Number of sectors, x_D	Disk to ring clearance, x_E
		x_A	x_B	x_C	z		
Center	1	1/4	1/4	1/4	1/4	3	0
(1)	1	1/6	1/6	1/6	3/6	2	-1
ae	2	2/6	1/6	1/6	2/6	2	1
be	2	1/6	2/6	1/6	2/6	2	1
ab	1	2/6	2/6	1/6	1/6	2	-1
ce	1	1/6	1/6	2/6	2/6	2	1
ac	2	2/6	1/6	2/6	1/6	2	-1
bc	2	1/6	2/6	2/6	1/6	2	-1
abce	1	2/6	2/6	2/6	0	2	1
de	2	1/6	1/6	1/6	3/6	6	1
ad	1	2/6	1/6	1/6	2/6	6	-1
bd	1	1/6	2/6	1/6	2/6	6	-1
abde	2	2/6	2/6	1/6	1/6	6	1
cd	2	1/6	1/6	2/6	2/6	6	-1
acde	1	2/6	1/6	2/6	1/6	6	1
bcde	1	1/6	2/6	2/6	1/6	6	1
abcd	2	2/6	2/6	2/6	0	6	-1
Center	2	1/4	1/4	1/4	1/4	3	0

TABLE 4. - FIRST BLOCK ALIASES

Treatments	Parameter aliases		Term aliases	
(1)	β_I	$+\beta_{CE}$	b_0	$b_0 x_C x_E$
ad	β_A	$-\beta_{BD}$	$b_1 x_A$	$-b_1 x_B x_D$
bd	β_B	$-\beta_{AD}$	$b_2 x_B$	$-b_2 x_A x_D$
ab	β_{AB}	$-\beta_D$	$-b_3 x_D$	$b_3 x_A x_B$
ce	β_C	$+\beta_E$	$b_4 x_C$	$b_4 x_E$
acde	β_{AC}	$+\beta_{AE}$	$b_5 x_A x_C$	$b_5 x_A x_E$
bcde	β_{BC}	$+\beta_{BE}$	$b_6 x_B x_C$	$b_6 x_B x_E$
abce	$-\beta_{CD}$	$-\beta_{DE}$	$-b_7 x_C x_D$	$-b_7 x_D x_E$

TABLE 5. - TREATMENTS AND ESTIMATES

FOR TWO BLOCKS

Block	Treatment	Parameter estimated
1	(1)	β_I
2	ae	β_A
2	be	β_B
1	ab	β_{AB}
1	ce	β_C
2	ac	β_{AC}
2	bc	β_{BC}
1	abce	$-\beta_{DE}$
2	de	β_D
1	ad	β_{AD}
1	bd	β_{BD}
2	abde	$-\beta^*_{CE}$
2	cd	β_{CD}
1	acde	$-\beta_{BE}$
1	bcde	$-\beta_{AE}$
2	abcd	$-\beta_E$

* Confounded with block effect.

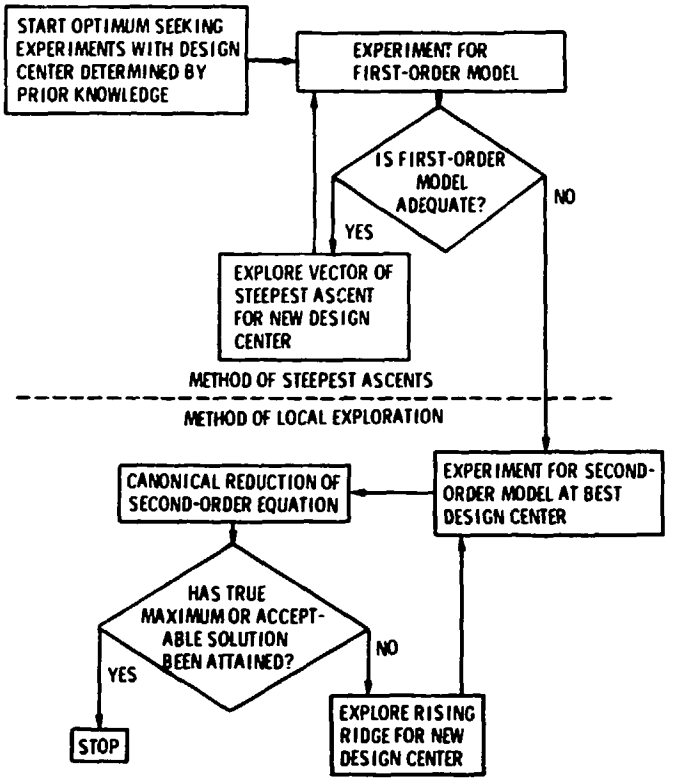

Figure 1. - Box-Wilson methods.

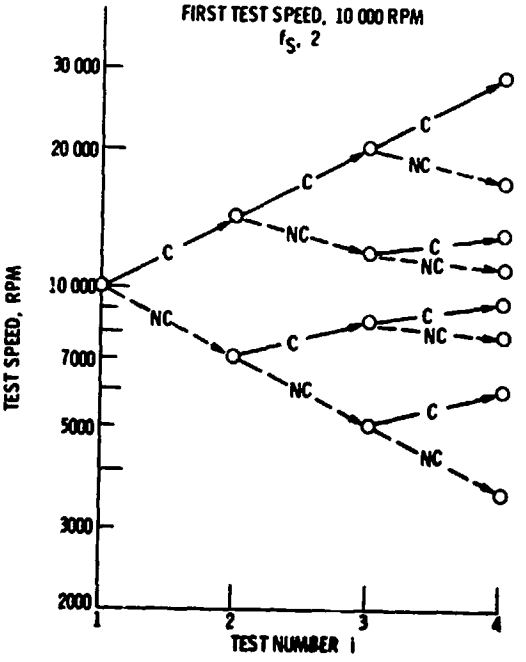

Figure 2. - Illustration of test strategy.

DISCUSSION

R. Bristow, Boeing

It looks like you had to have picked that equation, or the form of the equation, beforehand. Do you feel very comfortable there or could it be some other form in real life, perhaps a higher order, for example?

A.G. Holms, NASA-Lewis

I've shown what I call the lowest conceivable order equation that would utilize all of the data. It shows the unknown coefficients in a linear combination, and that is the type of thing that we can do a good job of fitting, particularly with the method of least squares, which is a time-honored technique and has never been questioned for 150 years.

The x's don't have to be in the first degree for this procedure to work well. The b's must be in the first degree, but the x's need not be. This means that if we had a physical reason for wanting to change the degrees of the x's we could; we could put in an x_a squared instead of an x_a: we have all of these options of varying the polynomial function of the x's. The plan has sixteen orthogonal experimental conditions. That means that we cannot evaluate more than sixteen b's. But we can always use any prior physical knowledge to make transfomrations on the x's.

G.L. Gunstone, CAA-UK

The factor that you call SFE, you said that you would calculate the fifty percent level. That is really not a very useful figure. It tells you that the fragment is just as likely to go through as not. To be useful to us, we need something giving a fairly high confidence level of containment. We would like perhaps 99 per cent.

A.G. Holms, NASA-Lewis

Yes, the containment should be designed for high reliability such as 99 per cent. But, our four test points for each condition only tell us "success" or "failure" for each trial energy. Thus, we cannot even estimate a standard deviation, let alone a probability distribution. Neither do we know what kind of a probability distribution would come out of the final manufacturing process. The evaluation of the probability distribution for the manufacturing process would really be up to the production engineers. But our fifty per cent point gives the containment designer a fix on his fifty per cent point. This would also be the mean value if he assumed normality. Then the desired level of reliability could be achieved by subtracting the appropriate number of standard deviations, where the standard deviation would be estimated for the final manufacturing process.

A. Weaver, P&W

The program you propose is a very complex one. It may not take into account all of the variables that are actually present. I don't think that we (collectively) really understand the simple mechanisms of containment with two materials, even similar materials, placed side by side, let alone putting four dissimilar ones there.

I'm very concerned that the proposed configuration and materials confirmation is so complex that it is far beyond the state of the art. I think you're talking about an answer that's many years away, and not really aimed at present-day problems. From a research standpoint, I think that there are other more reachable goals to attack first.

A.G. Holms, NASA-Lewis

I agree that a program like this would not develop understanding, if you use the word understanding to mean that you have a complete physical explanation of all the processes. I think what a program like this does when it incorporates a lot of variables is to give you this big equation and then you can look at those coefficients and say: "now here is a bunch of concepts that are interesting and surprising and here is another bunch of concepts that we can throw away; now that we have seen some of these concepts that are quite a surprise to us, let's design some smaller critical experiments that will give us a better physical understanding of what's going on". But if you go at it in the other order, of just investigating one variable at a time, then the existence of these interactions will forever remain unknown.

J.H. Gerstle, Boeing

Yes, first, I'd like to follow up on what Al said. I guess I don't understand why one would not pursue this on perhaps a two-material ring to start, to see if this kind of approach, in fact, will work, and how much value will come out of this. I guess I can't disassociate the physical understanding from the statistics of the experiment. To me they must go hand in hand.

A.G. Holms, NASA-Lewis

I had pointed out with my first slide that, if we are going to investigate a single test condition, we should ask ourselves how many specimens should we use to evaluate such a condition. Then I think the next thing to be thought of is that if you're going to do your experimentation on a small scale and only investigate a limited number of conditions, then I would want to increase the number of specimens that I tested for each condition. So what I have described here is an experiment where I have (depending on how you look at the center point) either sixteen conditions or eighteen conditions. I am saying let's use four specimens for each condition and that will give me a total experiment size of 72 specimens. Then, if you wanted to experiment with much smaller numbers of variables (and hence smaller numbers of conditions), I would want to increase the number of specimens for each condition so that we still might wind up with sixty to eighty specimens, with a lot less information acquired. Does that bear on the question or would you restate it?

J.H. Gerstle, Boeing

I guess I'm having difficulty understanding the answer. To pose the question another way, it seems to me a number of serious concerns have been voiced here about this method of testing and what will evolve from it in terms of useful information. This seems to me a tremendous investment in going down one road with four materials, only two of which acting together we don't yet understand very well, if at all. To summarize, it seems to me much too big a bite at one time. My intuition is that this is not the best way to go at this time. I think we ought to be thinking more about the test conditions, what would be more useful, and you might want to revise the test. I'd be concerned

about how the rings would be made, whether that's practical and meaningful. We have to think in terms of the engineering aspects of this, although I must say I share your concern for having a statistically meaningful experiment.

A.G. Holms, NASA-Lewis

Perhaps the question is not whether we are looking at this in an engineering manner or a statistical manner. Maybe the question is are we looking at it in an engineering manner or a physicists manner? It seems to me that if we're doing something like this, we could discover that certain concepts are good, that we can say lo and behold, this is good in an engineering sense. After that, you might be dissatisfied with the results in terms of physical understanding, and then having seen some ideas of what's good and what's not good on a quick basis, you can then go into more intelligently designed tests; that is to say, tests that are more intelligently designed to illuminate the physical processes. As far as doing a large massive experiment like this, I said that we were evaluating sixteen coefficients, when we evaluate each of those coefficients, we evaluate them in terms of the sixteen values of y. The consequence of that is that if for one of those conditions the y value is slightly in error, then only one-sixteenth of that error goes into our coefficients. So that's one reason for having a large orthogonal design of experiment like this, that even though you have only four specimens for each condition, every one of those informative coefficients that we're going after is averaged over the whole sixteen y values. And, therefore, it has a much lower error content. But the payoff is that we can get comparative information on many potentially beneficial materials interactions; namely, AB, AC, and BC instead of just AB, and they are compared precisely because they are all compared for the same experimental conditions.

D. McCarthy, Rolls-Royce

I was surprised that one of your parameters was the clearance between the disk and the containment ring. I would have thought the clearance between the blades and the containment ring was more significant because in the event of a piece of disk and a group of blades being released, the blades do the initial distortion of the containment ring; therefore, they do play a big part in the process.

A. Holms, NASA-Lewis

There is a report written by Mangano and his associates in 1972, which seemed to say that blades on the wheel that he was working with, were a very negligible factor in energy absorption. I think it's also true that the thermodynamicists try to keep that tip clearance just about as small as they can get it so that tip clearance is not really much of a variable. If we take the attitude that the blades are really negligible as far as absorbing energy is concerned, then the important clearance is the clearance between the disk outer diameter and the inner diameter of the turbine casing, and that clearance will determine how much the disk fragment rotates before it hits the container. It will determine whether a smooth curved surface of the fragment hits the container braodside or whether the fragment goes up against the container with a sharp penetrating edge.

DESIGN OF ROTORS FOR IMPROVED STRUCTURAL LIFE

J. T. Hill

Pratt & Whitney Aircraft Group
Commercial Products Division
United Technologies

ABSTRACT

Failure of any large portion of a jet engine rotor structure poses a threat of uncontained case penetration; therefore, considerable care and study is directed to the design, analysis, manufacture and inspection of these components to ensure that rotor failure is avoided over the full life of the engine. In this presentation, major rotor design criteria will be discussed with particular emphasis on those aspects of rotor design that ensure long life component integrity. Included will be a review of dynamic considerations, that necessitate tuning of bladed disk and seal assemblies to avoid excessive vibratory stress at both design and off-design conditions; and low cycle fatigue considerations, which have resulted in detailed analysis procedures to establish part temperature and stress variation throughout an operating cycle and extensive specimen and component fatigue testing to establish safe cyclic operating limits. Undetected, subsurface flaws can cyclically grow to failure if smooth section stresses are not restricted; therefore, investigations to characterize the frequency, size and behavior of intrinsic material defects have been implemented and results will be reviewed.

Manufacturing process improvements, including the application of increasingly sophisticated inspection techniques and quality control procedures will be reviewed in light of their impact on component durability.

UNCONTAINED DISK AND SEAL FAILURES

Major causes

- **High cycle fatigue**
- **Material or manufacturing defects**
- **Low cycle fatigue**

STAGE RESONANCE DIAGRAM

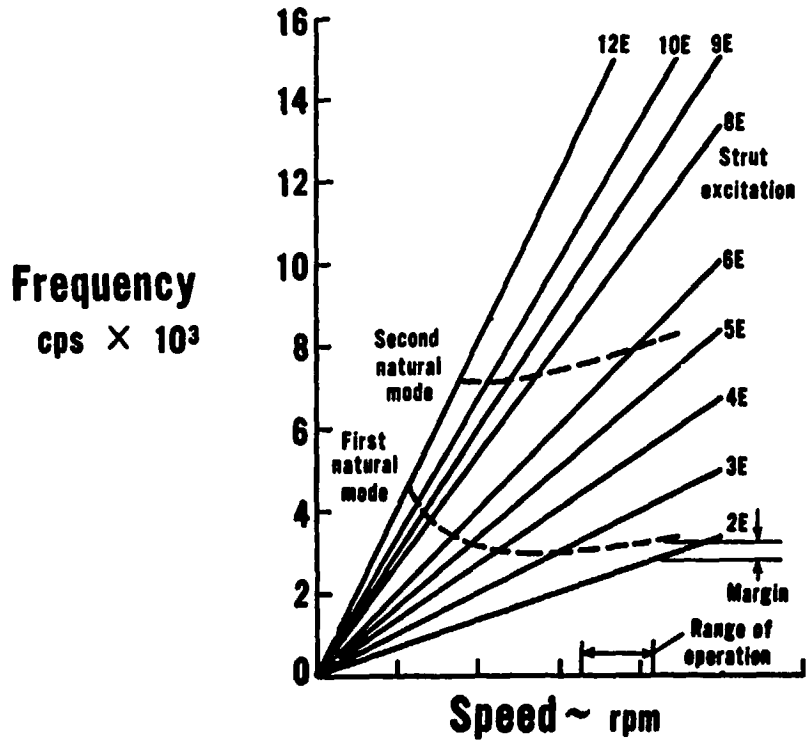

FLUTTER BOUNDARIES FOR FOUR FLUTTER TYPES

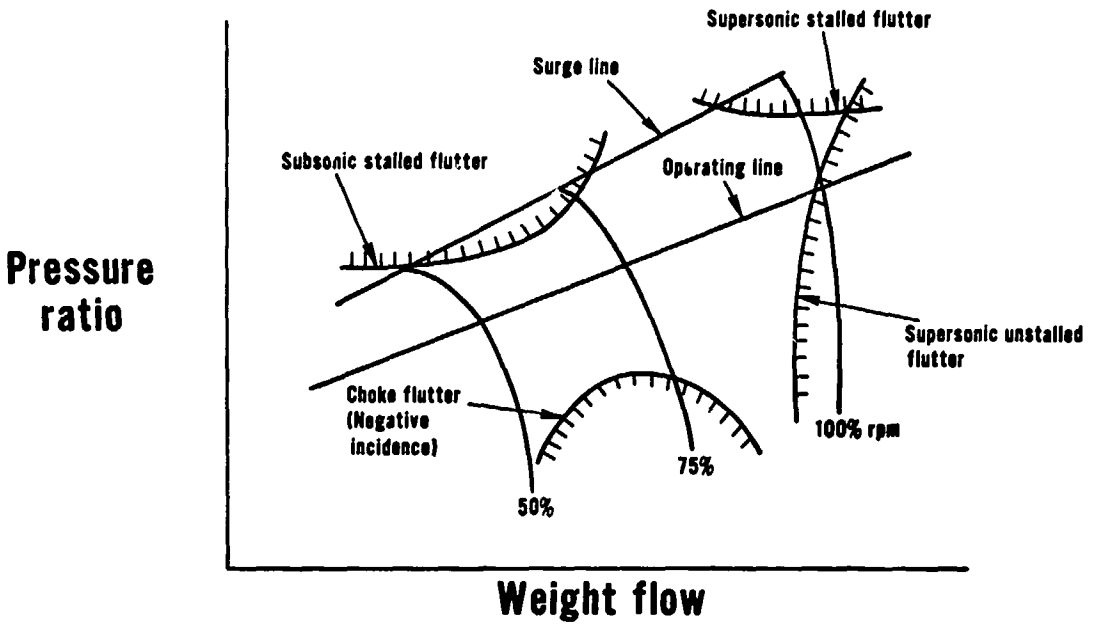

SUPERSONIC UNSTALLED FLUTTER ANALYSIS - CORRELATION

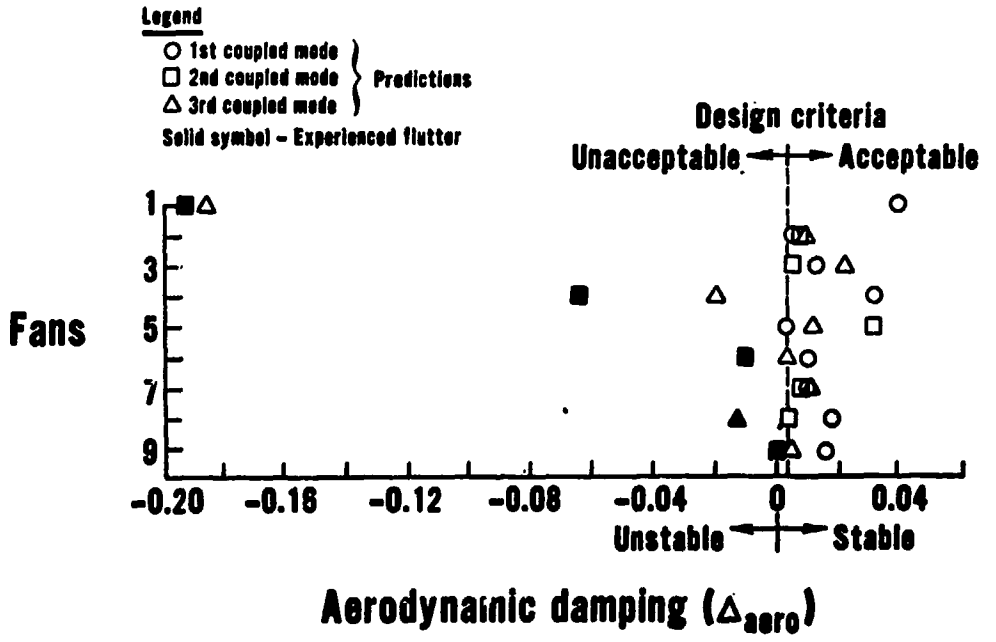

HIGH FREQUENCY FATIGUE

Summary

- Rotor resonance frequencies predictable
- Analytical systems exist to predict flutter in rotor components
- Engine development programs minimize vibratory problems
- Advanced analytical systems in development
  - Stalled and unstalled flutter predictions
  - Airfoil resonant stress predictions

FRACTURE ORIGINATING FROM MATERIAL DEFECT

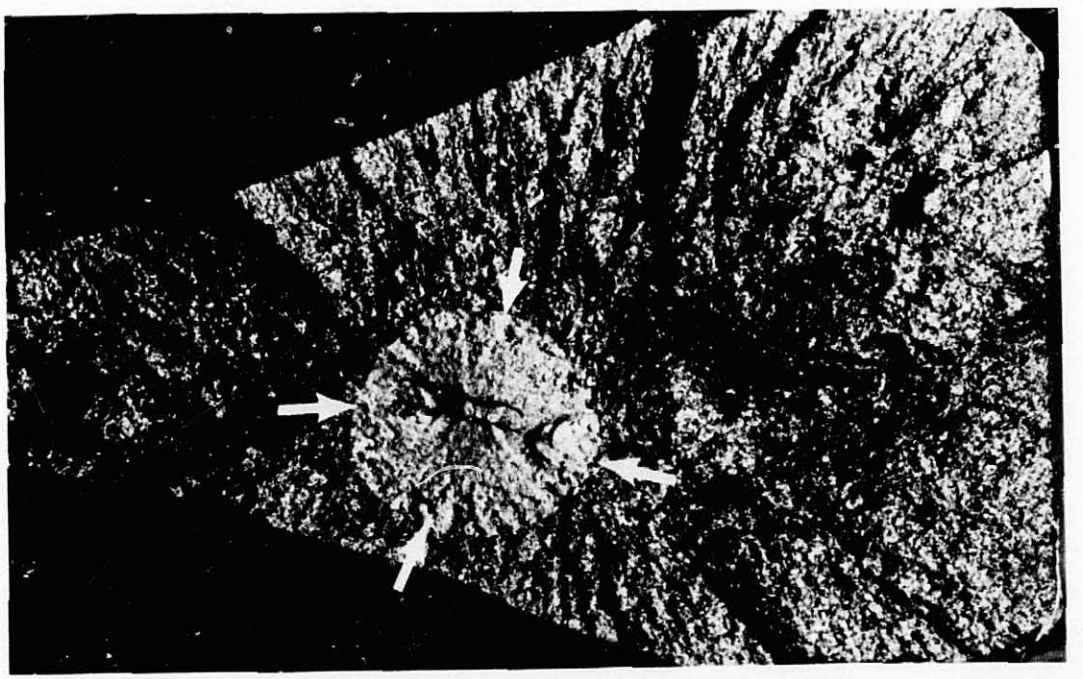

Mag: 11X

ANALYTICAL PROGRAM

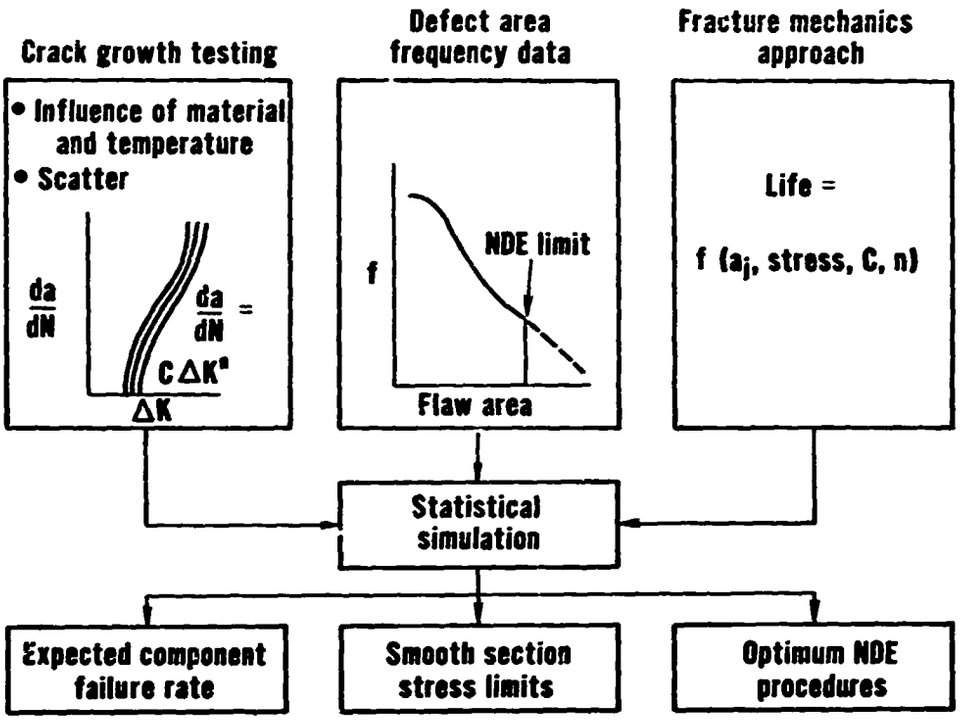

FRACTURE MECHANICS LIFE CURVES

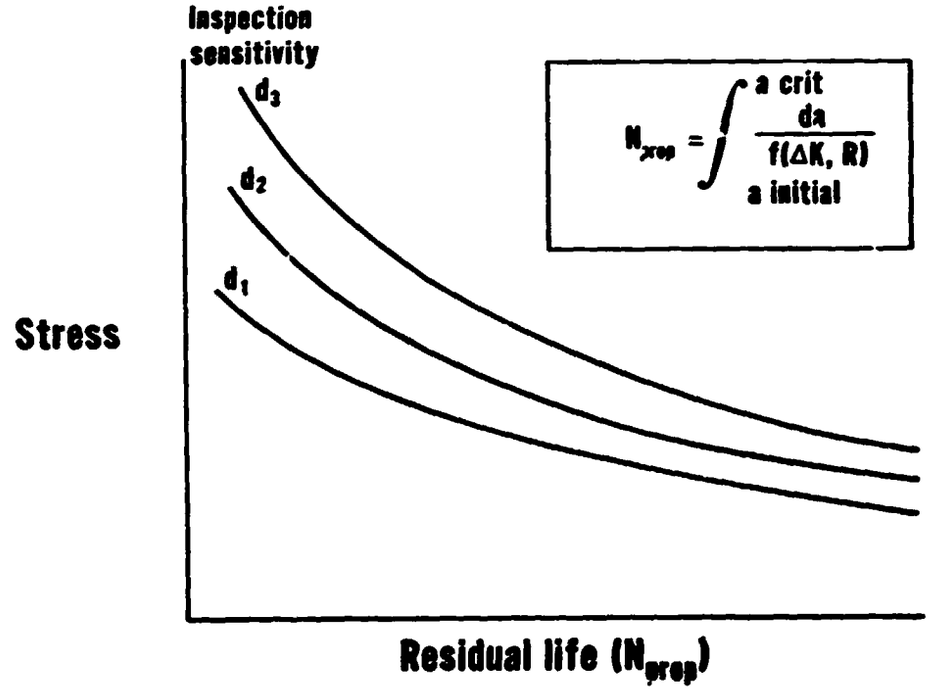

FRACTURE MECHANICS LIFE CURVES

Correlation with experience

JT4 steel disk failure predictions

	Disks supplied by suspect vendor		Disks supplied by other vendors	
P/N	Predicted to fail	Failures	Predicted to fail	Failures
360112	2 (1.89)	3	0	0
360113	0	0	0	0
360114	1 (0.284)	0	0	0
405715	0	0	0	0
242915	0	0	0	0

HOT ISOSTATICALLY PRESSED SUPERALLOYS

- Prealloyed powder eliminates segregation
- Powder screening controls defect size
- HIP produces homogeneous structures
- NDE sensitivity greatly enhanced

MATERIAL DEFECTS

Summary

- Smooth section stress limits for current alloys to prevent failures from subsurface defects
- Cleanliness improvements in current alloys through modified processing and controls
- Improved durability thru direct HIP of powder metal superalloys

LOW CYCLE FATIGUE

Definition of life

- Number of cycles to 1/32 inch long crack
- Statistical probability of 1 out of 1000

Details of concern

- Smooth disk bores and webs
- Disk bolt holes, flange holes, and rim slots

DISK LCF LIFE DETERMINATION

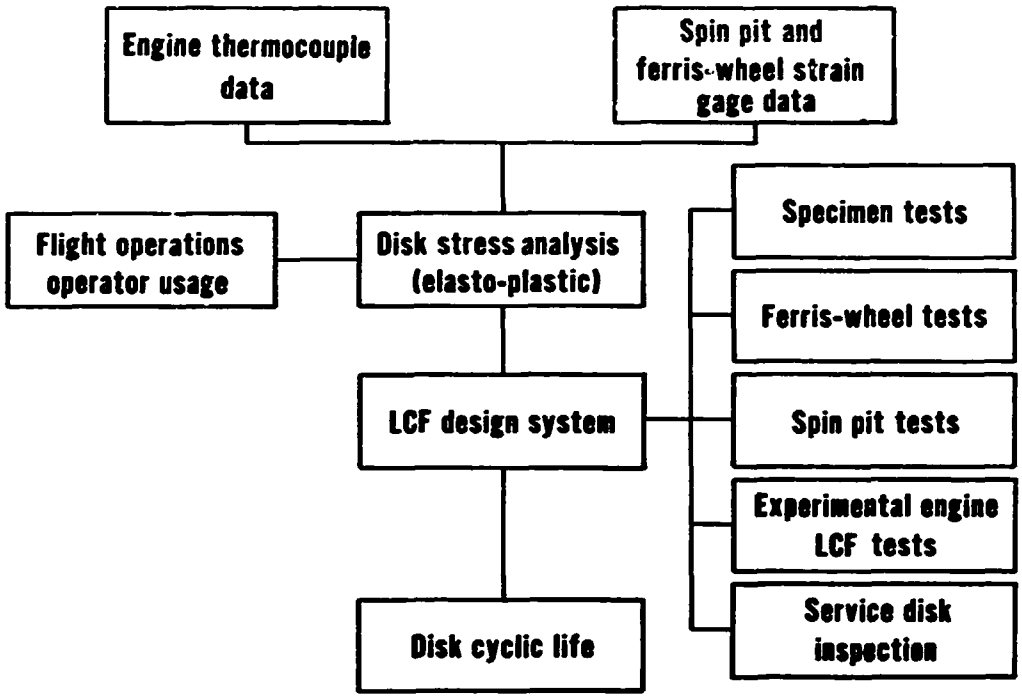

DISK COMPUTER PROGRAMS

- Plastic/elastic disk stress analysis
- Generalized shell analysis

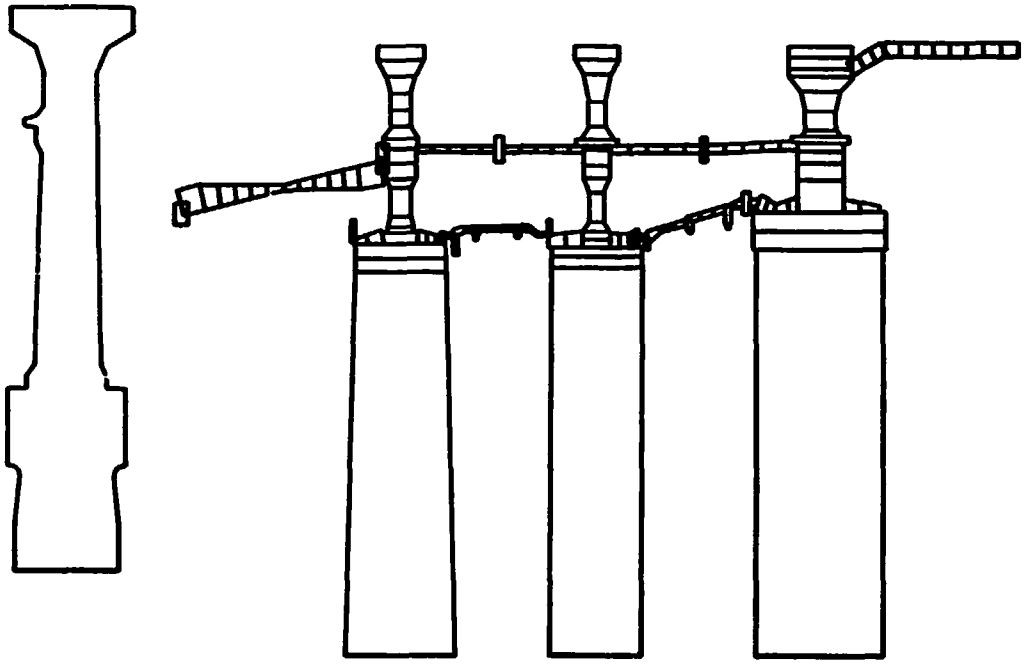

DISK COMPUTER PROGRAMS

Mixed element F/E code

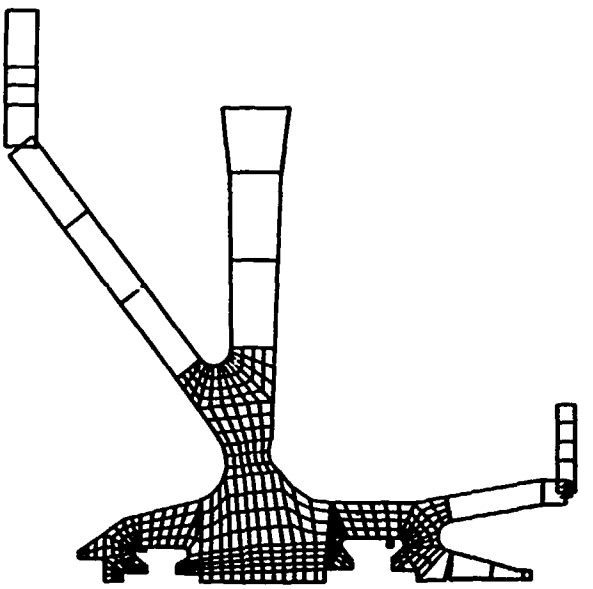

LOCAL STRESS DETERMINATION

- **Closed form solution for stress concentration**
- **2D and 3D finite element analysis**
- **2D and 3D boundary-integral equation techniques**

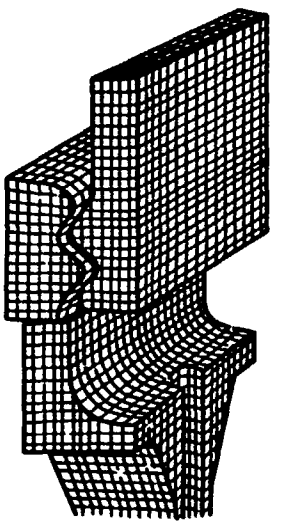

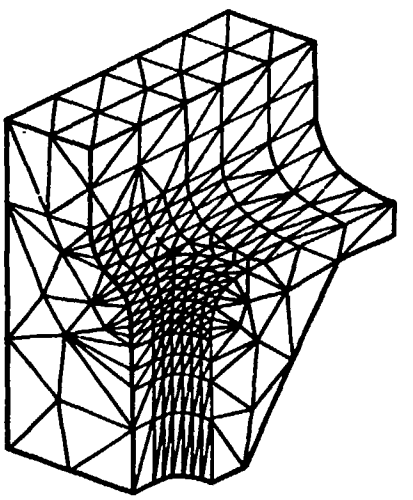

EFFECT OF RELAXATION

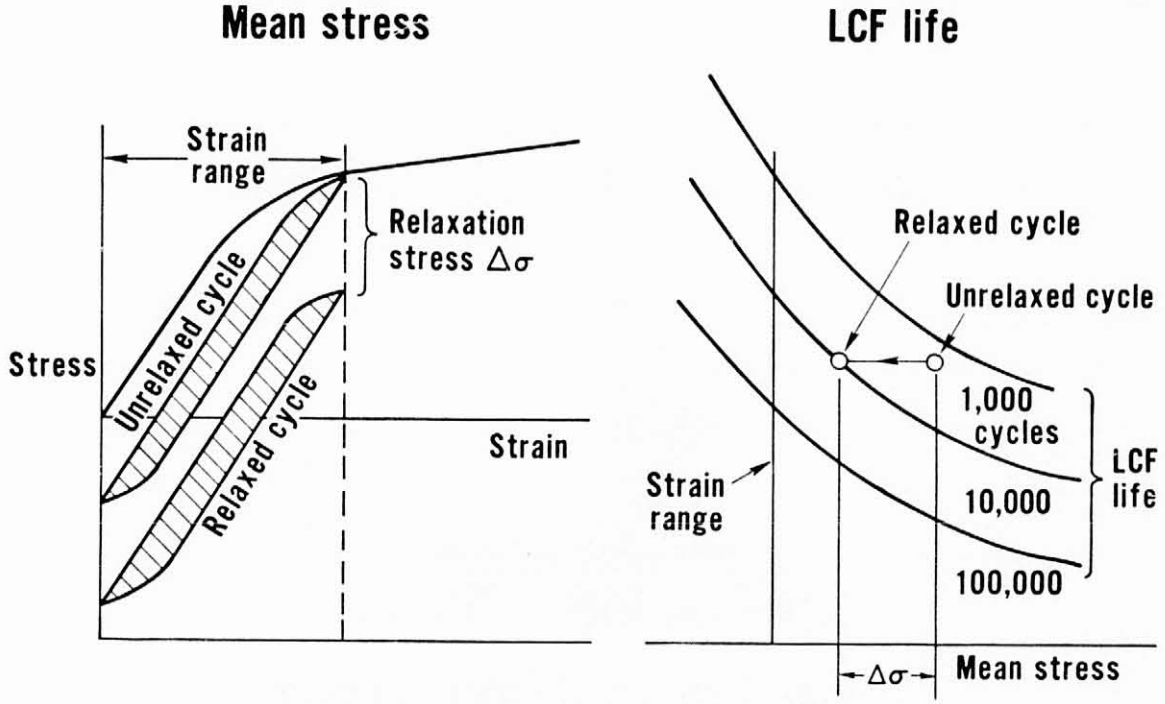

BASIC FORM OF SONNTAG TEST SPECIMENS USED IN LABORATORY EVALUATION OF MATERIAL PROPERTIES

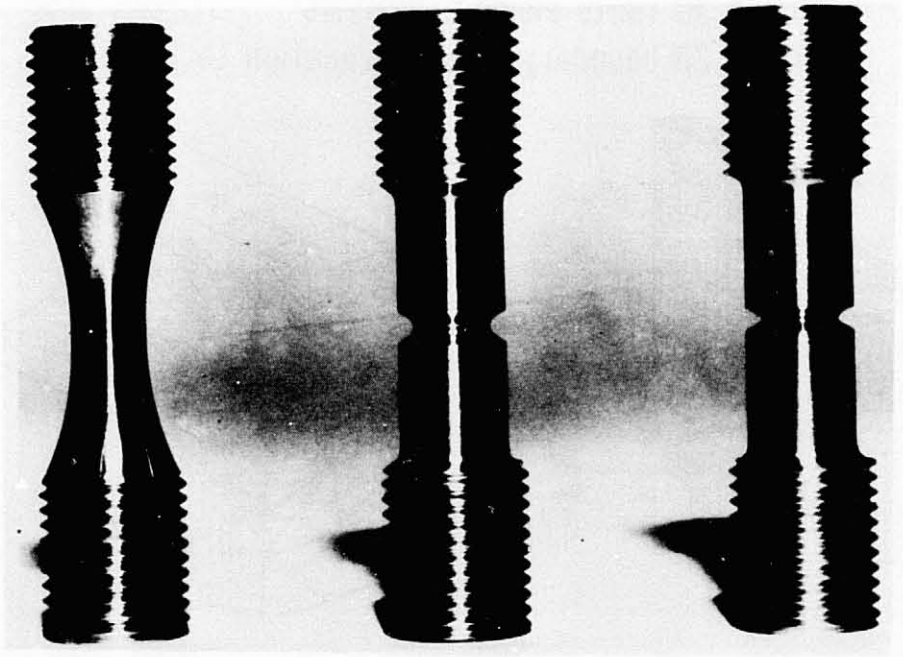

LCF DWELL TEST CYCLE

Equivalent to flight cycle

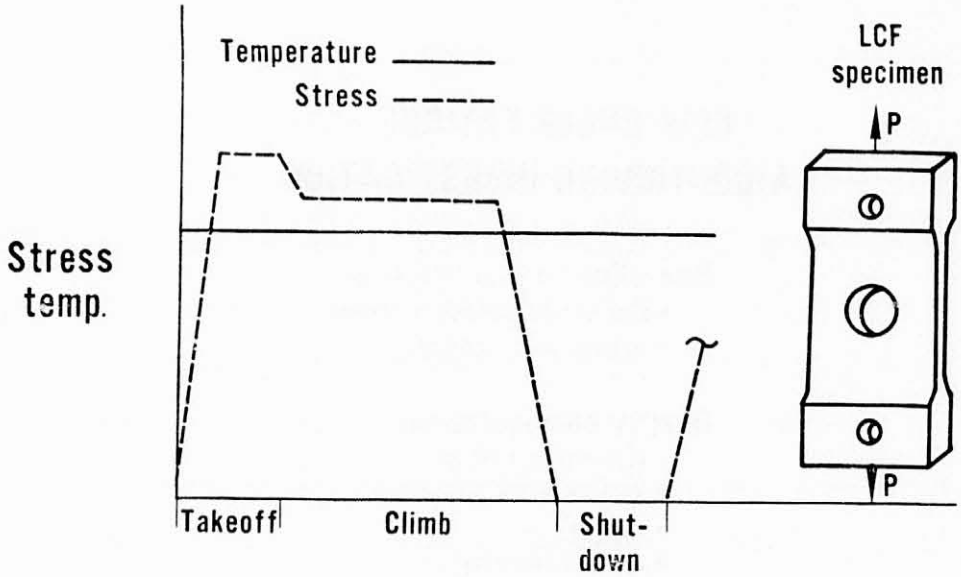

Equivalent testing time

1180 specimens tested

FERRIS-WHEEL TEST RIG FOR HYDRAULIC LOADING OF ROTOR DISKS

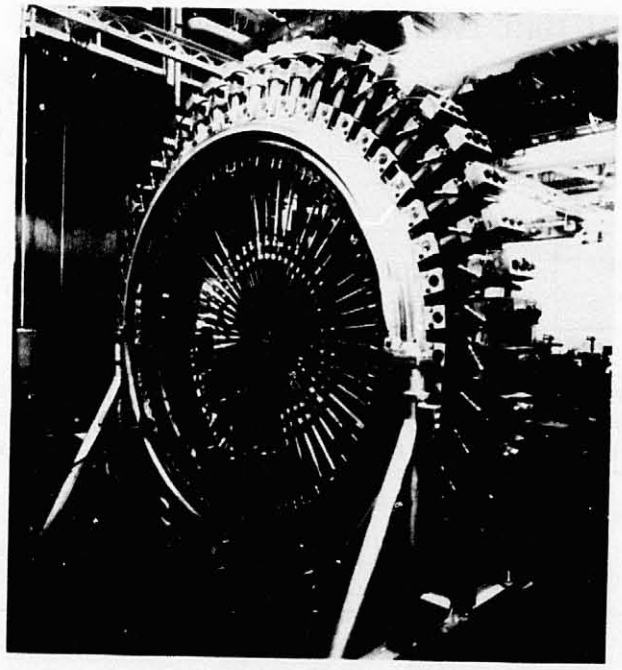

LOW CYCLE FATIGUE – A CONTINUING INVESTIGATION

New alloy characterization

- High creep strength titaniums
- Powder metal superalloys

Quality considerations

- Material variability
- Surface finish preparation
- Coatings
- Surface integrity

Basic fatigue studies

- Cumulative damage
- Multi-axial fatigue
- Creep -fatigue interaction
- Fatigue mechanisms

FRACTURE MECHANICS DESIGN SYSTEM

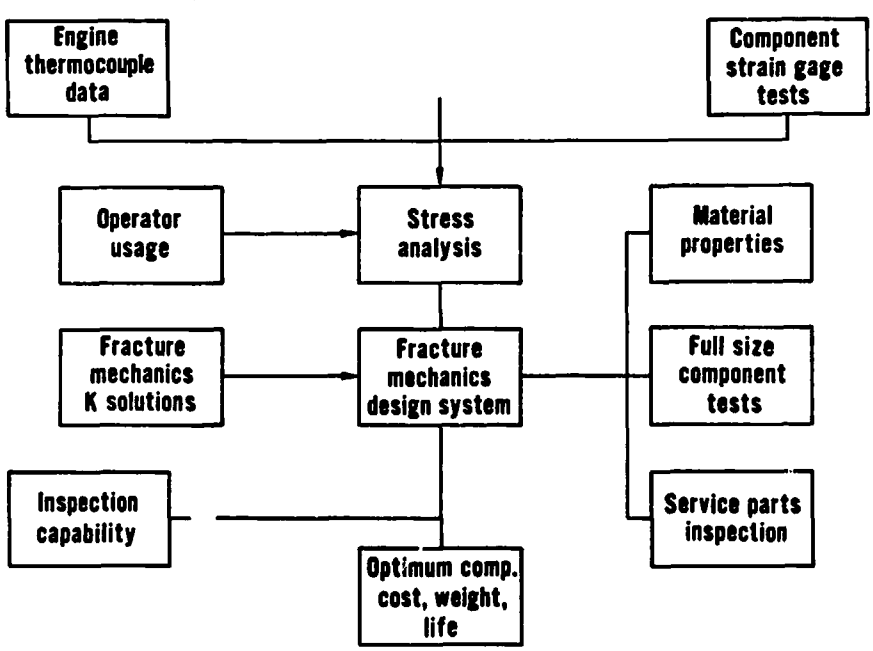

ΔK CALCULATION METHODS

- Numerical procedures

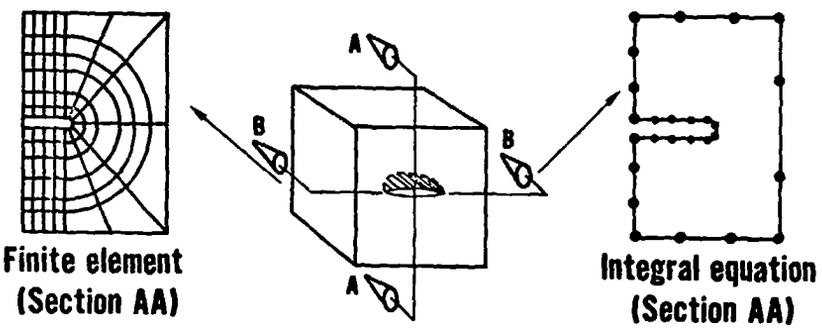

- Influence function method

$$K_j = \int_S h_j\,(X_i, \text{geometry})\;\sigma(X_i)\,dS$$

MATERIAL DATA BASE

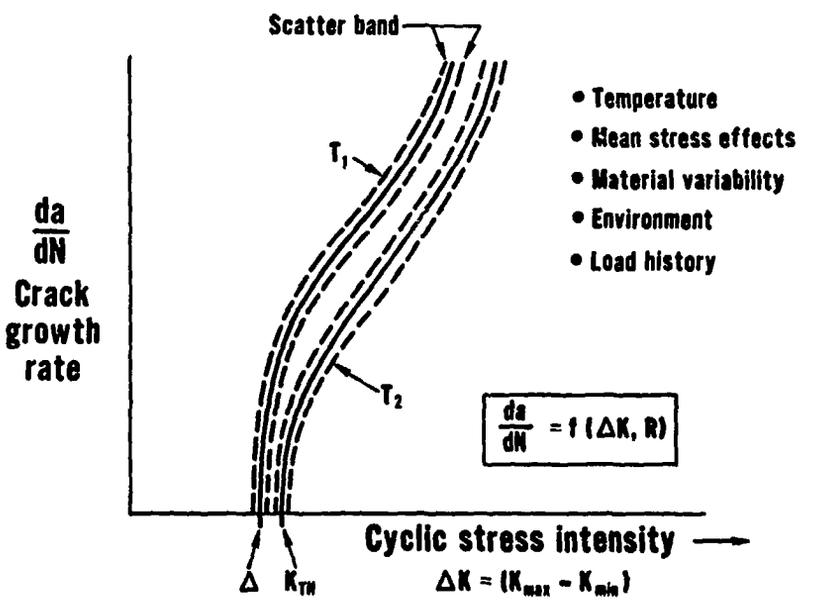

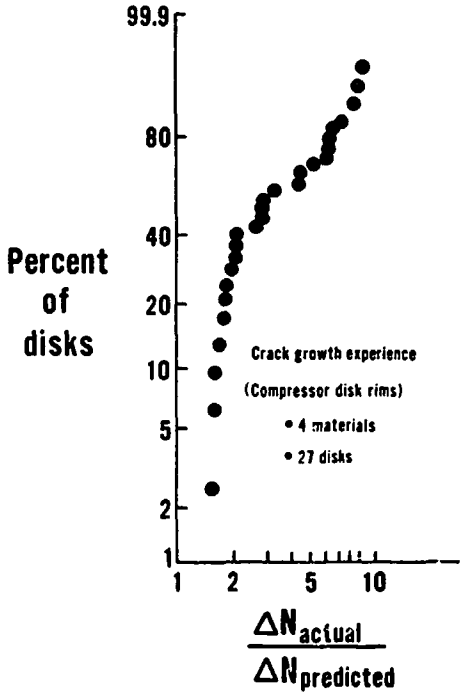

FRACTURE MECHANICS

Calibration

- Residual life predictions calibrated against crack behavior in specimens and components
  - Smooth sections
  - Bolt holes
  - Rim slots

LOW CYCLE FATIGUE/FRACTURE MECHANICS

Summary

- Well calibrated design procedures minimize low cycle fatigue cracking
- Fracture mechanics considerations assure crack tolerant designs and material selections
- No uncontained disk failures due to LCF in P&WA parts shipped since 1965

DISCUSSION

H. Rubel, Lockheed-Ga.

You have confirmed the SAE findings that progress has been made on low cycle fatigue, and I hope that this effort will be continued. I am concerned about HCF and flutter.

The airplane manufacturer, as we discussed earlier, must show that when certain things go wrong, the system still is operable. I am thinking along these same lines for engines. In a turbine, clogging of the nozzles may occur, which could excite a resonance in the running range, and could lead to failure. As another example, stator vanes in the rear end of the compressor could have its incidence angle changed due to attachment loosening and hence drive a particular disk to flutter. Would it be desirable to put some effort along those lines to ascertain margins for various deteriorated engine parts? In this way the airframe manufacturer and the user could know what degrees of safety exist in particular cases. A small incidence change may be more critical in some stages than in others. Should we not look at old cracked parts as well as virgin parts as is done for LCF? Could we advise the airlines which stages are most critical so that disk rim failures could be minimized?

J.T. Hill, PWA

In the course of an engine development program, extensive compressor and turbine rig testing is conducted at both design and off-design operating conditions. This testing establishes the success of the design effort by mapping the location of both positive and negative flutter boundaries and monitoring the level of resonance stage stress at all intermediate operating conditions. Modifications to the stator geometry, to improve component efficiency, are normally a part of the development effort. The sensitivity of dynamic stage response to such variations are routinely monitored.

As we are well aware, despite our best attempts to identify and solve vibration problems during the development program, HCF remains the major cause of uncontained disk failures. A review of PWA service experience, however, indicates that gas path blockages are not the major cause of such incidents. The presentation indicated that there is a resonant stress prediction system under development at PWA. When developed it will be possible to simulate blockages upstream or downstream of a particular stage, establish the resultant distortion pattern, and the effect on stage resonant stress. Such an analysis program, when developed, will permit the designer to assess the sensitivity of a particular design to the limits of gas path deterioration.

G.L. Gunstone, CAA-UK

I think we all started out worrying mostly about LCF and I think because we have done a very good job on that we nearly have it solved. High cycle fatigue is now the next major problem.

We are proposing to introduce a recommendation in our requirements which is being prepared right now, and it will read something like this. The blades should be designed in this order of strength from weakest to strongest: the airfoil, the blade root, the disk root, and the disk rim. Hence, any high cycle

effect is more likely to bring out a blade than break the disc. I'd be interested to know if anybody has any comments on that.

G.J. Mangano, NAPTC

That particular matter is scheduled to be discussed tomorrow. Thank you.

MATERIALS AND MANUFACTURING PROCESSES FOR INCREASED LIFE/RELIABILITY

R. E. Duttweiler

Aircraft Engine Group
General Electric Co.
Cincinnati, Ohio 45215

During the early 60's, improvements in both quality and durability of disk raw material were considered necessary for both military and commercial engines. Vacuum melting technology proved to be the breakthrough that spawned a new series of "superalloys", but it offered many process challenges. These new, tougher to forge alloys were developed to run at stress levels 50% above then existing commercial disk experience and simultaneously meet greatly increased low cycle fatigue life capabilities. After addressing to the low probability of being able to rely on Non-Destructive Testing (NDT) to sort for "good" parts - including the then emerging improved ultrasonic techniques - General Electric set an objective to provide material free of harmful indications for engine parts.

The challenge was met by introducing an entirely new concept in raw material process control which was defined as Premium Quality (PQ) material. It imposes careful selection, screening and sampling of the basic alloy ingredients, followed by careful monitoring of the melting parameters in all phases of the Vacuum Melting (VIM/VAR) sequence. Special care is taken to preclude solidification conditions that produce adverse levels of segregation. Melt furnaces are routinely cleaned and inspected for contamination. Ingots are also cleaned and inspected before entering the final melt step.

The ingot to billet conversion steps are closely controlled and monitored to maintain melt traceability and ingot position. Special Non-Destructive Evaluation (NDE) routines are applied to the final billet. Questionable indications are cut out for metallurgical evaluation. Disposition of such a billet depends on the nature, frequency and distribution of the indication. Occasionally an entire ingot, or even the entire heat, is rejected.

Billets that meet standards are then sent to the forging house where those to be used for rotating disks undergo further NDE. Those passing this stage are cut into forging multiples - each multiple producing one part - and the end faces of each multiple are etched as a final check for segregation before forging begins. When unacceptable indications are observed, correlation is made to the location of the affected billet in the ingot, and if not found to meet certain criteria, the entire ingot product is again subject to rejection.

Forging and heat treat operations are performed to very detailed practices with tight controls on forging pre-heat and reduction schedules, as well as the quench rates from solution heat-treatment. Metallurgical control is maintained over morphology, grain size and mechanical properties. Once accepted as Premium Quality material, the disks are shipped to the shop and skim-cut to a configuration suitable for immersion ultrasonic inspection. A three-mode scan is performed with Numerically Controlled (NC) equipment capable of finding randomly oriented indications in the part. Rejections are less than one part in one thousand for significant ultrasonic indications, and few of these have proven to be actual flaws.

These processing and inspection actions on the part of the supplier and manufacturer provide reasonable assurance that high quality parts are delivered. As a result, General Electric CF6 engines have not experienced a materials related failure of a fan, compressor or turbine disk where the prescribed controls have been followed.

PREVENTION OF ROTOR FAILURES IS A PRIMARY OBJECTIVE OF THE ENGINE MANUFACTURER.

MATERIAL PROCESS CONTROL IS THE MOST IMPORTANT KEY ELEMENT IN THE PREVENTION OF MATERIAL DEFECT RELATED FAILURES.

BACKGROUND

THE HIGH BYPASS TURBOFAN ENGINE PRESENTED MANY NEW CHALLENGES TO ROTOR MATERIALS INTEGRITY NEEDS:

- 50% INCREASE IN MECHANICAL PROPERTY LEVELS
- MORE MASSIVE COMPONENTS
- MAINTAIN DESIGN MARGINS (BURST/LCF)
- MAINTAIN VERY HIGH RELIABILITY
- EXTENDED LIFE REQUIREMENTS
- COMPLETE KNOWLEDGE OF OPERATING STRESS AND ENVIRONMENT

GE ROTOR MATERIAL INTEGRITY PERSPECTIVE

IN MORE DETAIL

MATERIAL DEFECT EXPERIENCE

I. LOW NUMBER OF "MATERIAL DEFECT" RELATED CRACKS IN COMMERCIAL ENGINE ROTOR EXPERIENCE

COMMERCIAL ENGINE ROTOR EXPERIENCE (1962-1975)

MATERIAL DEFECT RELATED FLAWS

GE - FLAWS FOUND IN FIELD ROTORS

	NUMBER	INITIAL FLAW SIZE
• ROTOR FLAWS	20	0.25 - 2.5 INCHES
• UNCONTAINED INCIDENTS	1	0.25 - 0.5 INCHES

TOTAL INDUSTRY - SAE AD HOC COMMITTEE (SATTAR)

- 137 UNCONTAINED DISK INCIDENTS
  - 19 (14%) MATERIAL DEFECT RELATED
- 38 OF THESE WERE SEVERITY CATEGORY III AND IV
  - 10 (26%) MATERIAL DEFECT RELATED

NDE EXPERIENCE

II. NDE IS A GOOD PROCESS CONTROL TOOL,
BUT IS NOT AN ADEQUATE FINAL SCREEN.

NDE DETECTION CAPABILITY
90% PROBABILITY

SYSTEM	SEMI-CIRCULAR CRACK LENGTH (MILS) 50% CONFIDENCE CRACK SIZE	95% CONFIDENCE CRACK SIZE
FPI	40	65
EDDY CURRENT	10	25
ULTRASONICS		
- NEAR SURFACE (1/4")	25	50
- BULK (2")	60	120

ULTRASONIC CAPABILITY

COMPARISON OF NEEDED VS REAL WORLD NDE CAPABILITY FOR ROTOR COMPONENTS

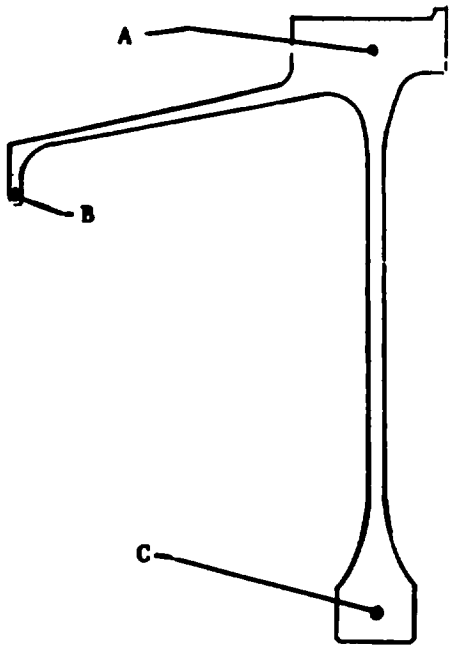

SEMI-CIRCULAR CRACK LENGTH (MILS)
90% PROBABILITY

AREA	NEED FOR DESIGN LIFE	PRODUCTION CAPABILITY(1) (95% CONF.)	LABORATORY CAPABILITY(1)	LABORATORY CAPABILITY(2)
A	25	135	90	60
B	60	70	25	15
C	15	100	25	15
		NORMAL SENSITIVITY SCAN	HIGH SENSITIVITY SCAN	

(1) RANDOM FLAW ORIENTATION

(2) PREFERRED FLAW ORIENTATION

NDE PROBLEMS

(ULTRASONIC INSPECTION)

EQUIPMENT - PRODUCTION EQUIPMENT PUSHED BEYOND LIMITS AT HIGH SENSITIVITY

DISKS - SURFACE FINISH/MICROSTRUCTURE PREVENTED HIGH SENSITIVITY INSPECTION

OPERATOR - MOST SYSTEMS MANUAL OPERATION, I.E. MANUAL SIGNAL RECOGNITION/EVALUATION

TIAL SYSTEM - (OPERATOR/EQUIPMENT/PART) REQUIRED TO OPERATE BEYOND LIMITS

TYPICAL NDE EXPERIENCE

ULTRASONIC INSPECTION

INSPECTION SOURCE	READINGS AS REPORTED BY OPERATOR LOW SENSITIVITY AMP. % *	 HIGH SENSITIVITY AMP. % *
INITIAL SCAN PRODUCTION	20	85
REPEAT SCAN PRODUCTION	10	80
NDT LAB PRODUCTION	8	35-55
NDT LAB ENGINEERING	10-12	55-60

80% AMPLITUDE = SIDE OF 20 MIL DIAMETER HOLE

* DEFECT IN PREFERRED ORIENTATION FOR DETECTION

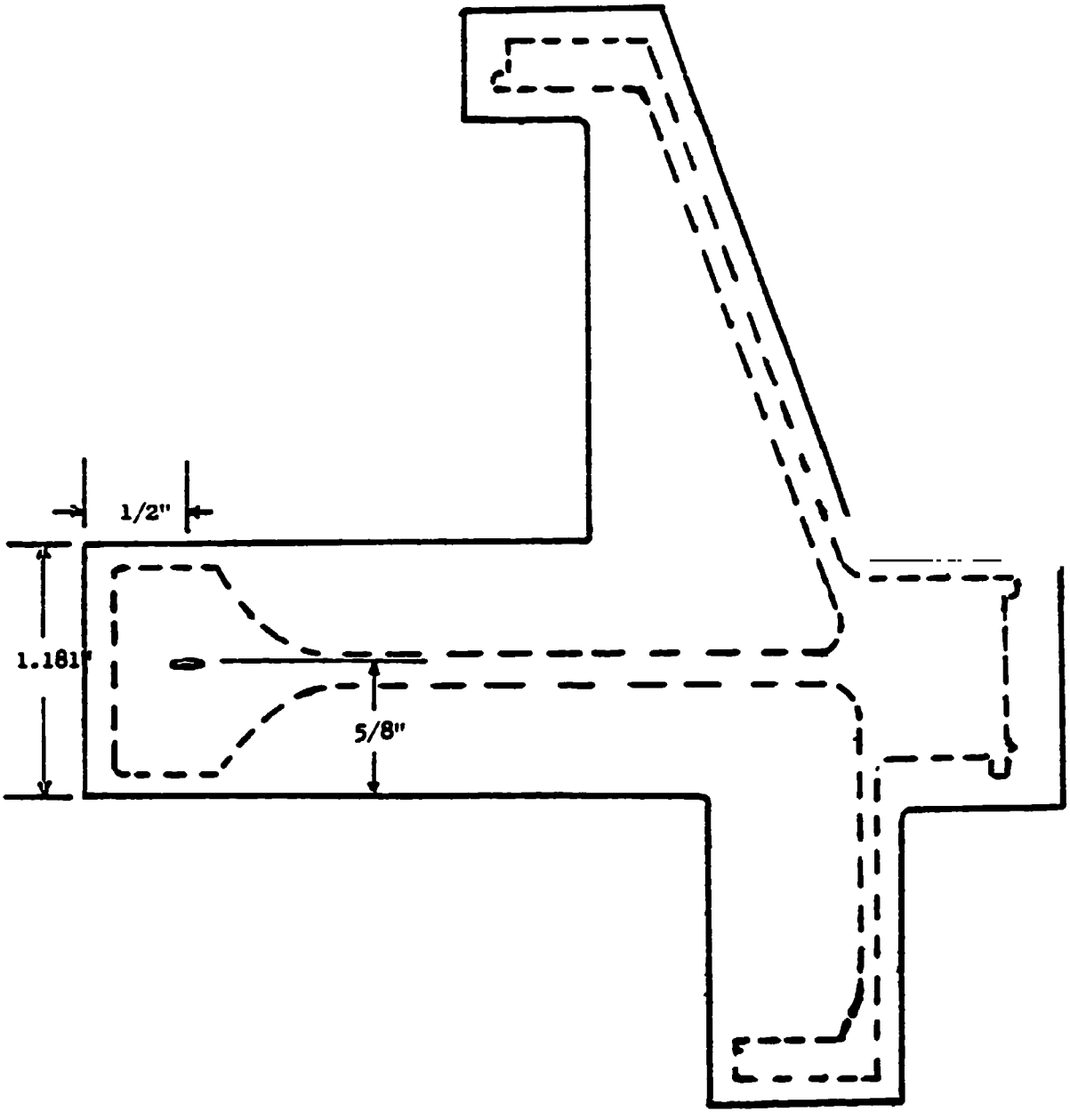

CROSS-SECTION OF DISK SHOWING
LOCATION OF FLAW

GOALS FOR NDE CAPABILITY
(90% PROBABILITY/95% CONFIDENCE)

PRODUCTION INSPECTION MODE	NEAR TERM GOAL FLAW SIZE, MILS	LONG TERM GOAL FLAW SIZE, MILS
FPI	40	25
EDDY CURRENT	10	5
ULTRASONICS	20	5

- MAJOR EFFORT AT GE TO IMPROVE ULTRASONICS
  - TRANSDUCER
  - PULSER/RECEIVER
  - SIGNAL ANALYSIS
  - COMPUTER AIDED CONTROL/EVALUATION

  GOAL: REMOVE OPERATOR JUDGEMENT FROM SYSTEM

GE ROTOR MATERIAL INTEGRITY PERSPECTIVE
RECAP

I. 50% INCREASE IN MATERIAL PROPERTIES PLUS INCREASE IN LIFE DEMANDS

II. VERY LOW INCIDENCE OF MATERIAL DEFECTS

III. MAINTAIN DESIGN MARGINS AND VERY HIGH RELIABILITY

CONCLUSION:

- WE HAVE EXPERIENCED VERY FEW MATERIALS RELATED DEFECT FAILURES.
- THE FACT IS WE ACHIEVE FAILURE PREVENTION BY MATERIALS AND MANUFACTURING CONTROL ---- JUST MAINTAIN IT.

"PREMIUM QUALITY" MATERIAL AND PROCESS SPECIFICATIONS

P.Q. SYSTEM GOAL

- MAINTAIN HIGH CONFIDENCE IN ESTABLISHED PROCESSES
- PREVENT MATERIAL DEFECTS

CONTROL PROCESS - PREVENT DEVIATION

AUDIT SYSTEM - ADEQUATE CONTROL/CORRECTIVE ACTION

AUDIT PROCESS - UNIFORM/CONSISTANT PRACTICE DRAWING

INSPECT PRODUCT - DRAWING CONFORMANCE
- NDE AS A PROCESS CONTROL TOOL

MAJOR EMPHASIS: EARLY PROBLEM RECOGNITION

P.Q. MATERIAL SYSTEM

IN-DEPTH CONTROL FOR CRITICAL ROTATING PARTS

- TRACEABILITY - ALL RAW MATERIAL
- DOUBLE OR TRIPLE VACUUM MELTING
- CONTROLLED MELTING AND CONVERSION
- BILLET AND FORGING MULTIPLE NDE
- FORGING AND HEAT TREATMENT
- FINISHED PART NDE

- APPROVED VENDOR LIST/REPORT CARD
- VENDOR AGREEMENT - PROCESS CHANGE APPROVAL
- DOWNGRADE VENDOR - POOR PERFORMANCE

TITANIUM BASE ALLOY

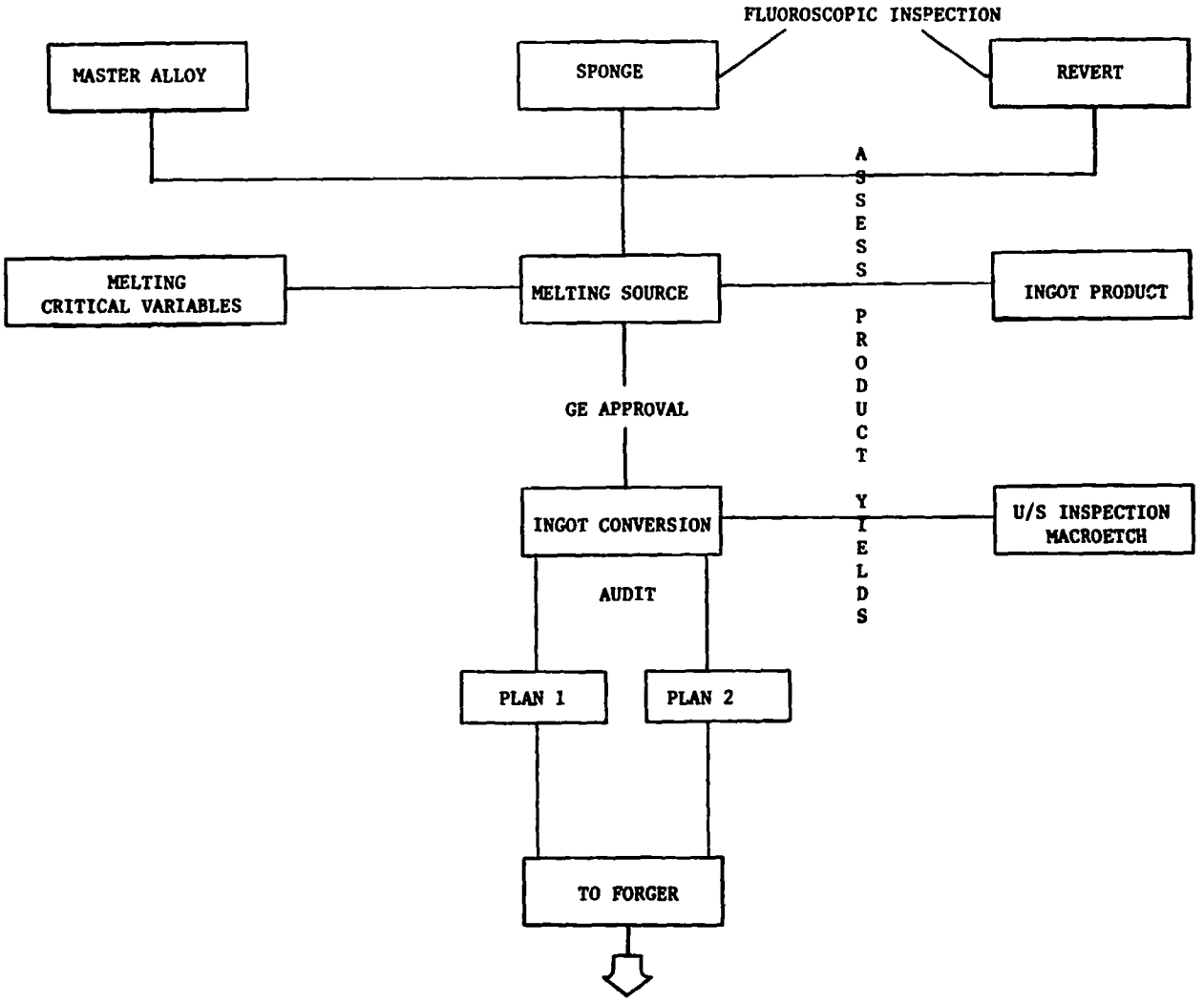

PREMIUM QUALITY TITANIUM ALLOY CONTROLS

M

I

L

L

- MELT RAW MATERIAL/SOURCES
  - TI SPONGE
  - MASTER ALLOY
  - REVERT ALLOY
  - TI DIOXIDE
  - COMPACT WELDING
- MELT FURNACE CLEANLINESS
- MELT INTERRUPTIONS/PRELIMINARY AND FINAL CYCLES
- VACUUM/WATER LEAKS
- REMELT ELECTRODE SURFACE CLEANLINESS
- INGOT CONVERSION PRACTICE
- BILLET ACCEPTANCE PLAN
  - ULTRASONIC INSPECTION PLAN
  - MACROETCH BAR ENDS
  - FORGE-DOWN PROPERTIES

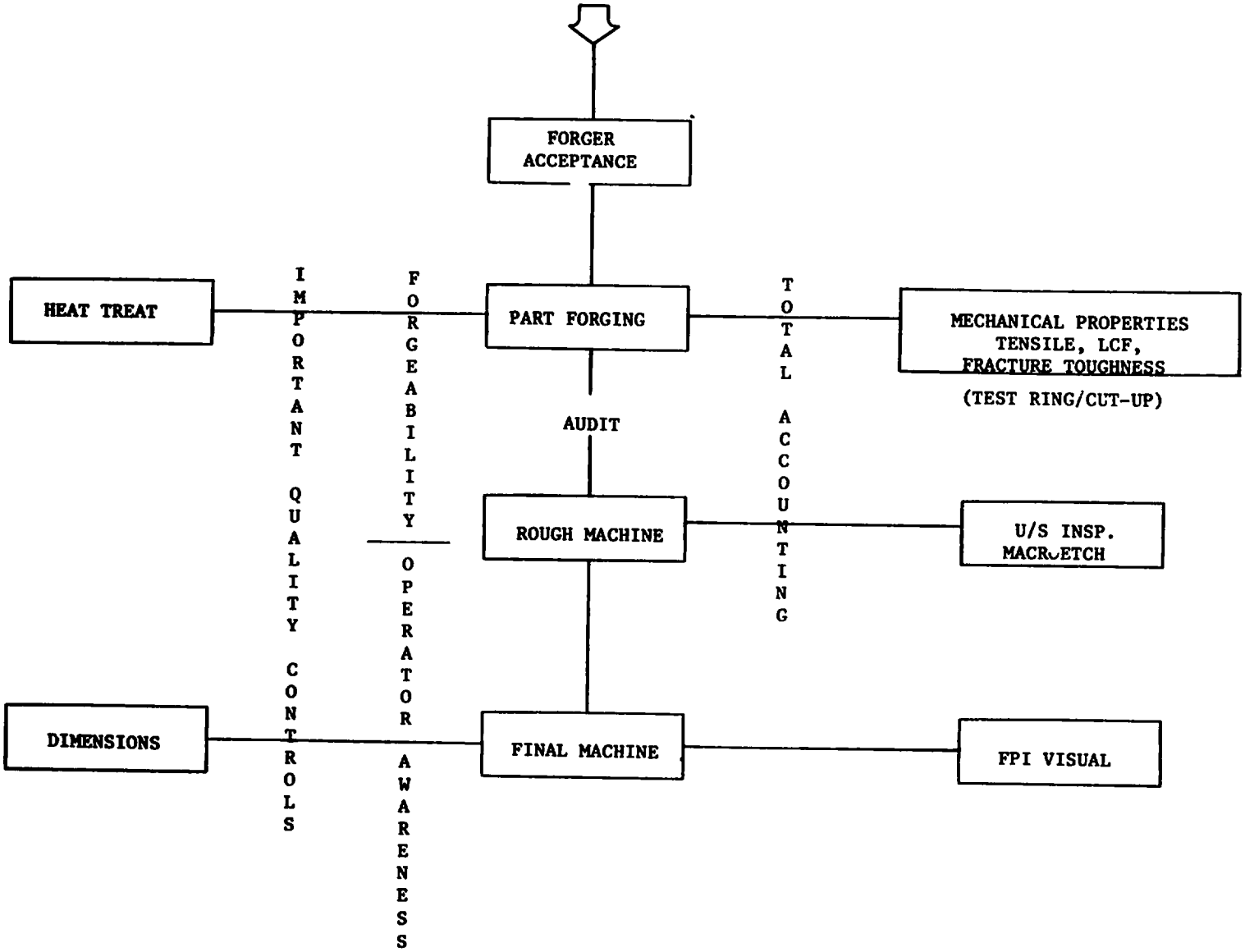
FORGER ACCEPTANCE
HEAT TREAT
IMPORTANT QUALITY CONTROLS
FORGEABILITY
OPERATOR AWARENESS
PART FORGING
TOTAL ACCOUNTING
MECHANICAL PROPERTIES TENSILE, LCF, FRACTURE TOUGHNESS
(TEST RING/CUT-UP)
AUDIT
ROUGH MACHINE
U/S INSP. MACRO ETCH
DIMENSIONS
FINAL MACHINE
FPI VISUAL

PREMIUM QUALITY TITANIUM ALLOY CONTROLS

FORGING QUALITY

- FORGING MULTIPLE MACROETCH
- FORGING PROCESS
  - PRE-HEAT
  - UPSET RATIO
  - HEAT TREATMENT
  - MICROSTRUCTURE
  - MACROETCH
- MECHANICAL PROPERTIES
  - TENSILE
  - FRACTURE TOUGHNESS
  - LOW CYCLE FATIGUE
- PROCESS DOCUMENTATION
- TOTAL MATERIAL/PROCESS CONTROL
  - TRACEABILITY
  - ACCOUNTABILITY

TYPICAL TITANIUM MELTING PRACTICE

(SIMILAR PRACTICE FOR IRON AND NICKEL BASE ALLOYS)

TRIPLE VACUUM MELTED

● WELDED COMPACTS	MELTED TO 24" DIAMETER ELECTRODE
● 24" DIAMETER ELECTRODE	MELTED TO 30" DIAMETER ELECTRODE
● 30" DIAMETER ELECTRODE	MELTED TO 36" INGOT

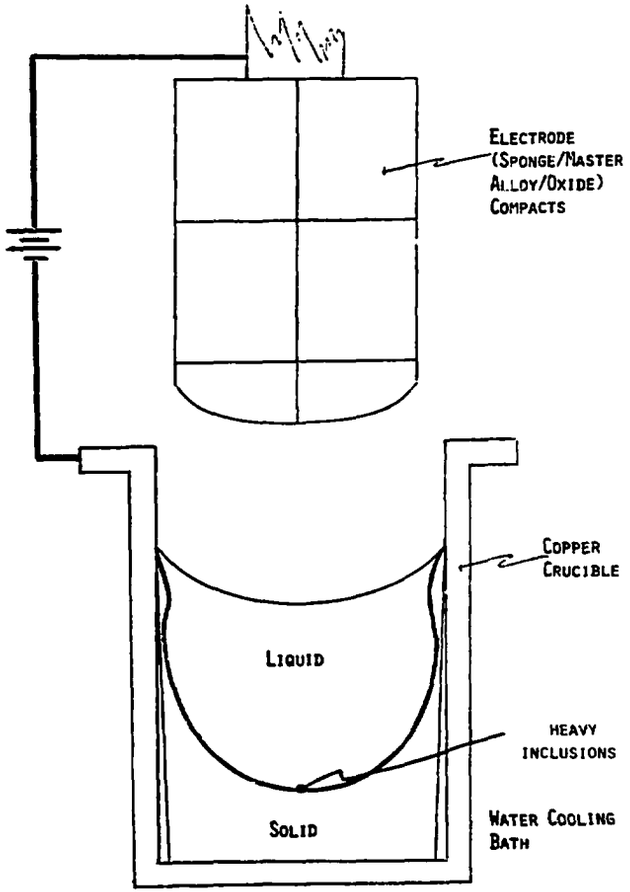
ELECTRODE
(SPONGE/MASTER
ALLOY/OXIDE)
COMPACTS
COPPER
CRUCIBLE
LIQUID
HEAVY
INCLUSIONS
SOLID
WATER COOLING
BATH

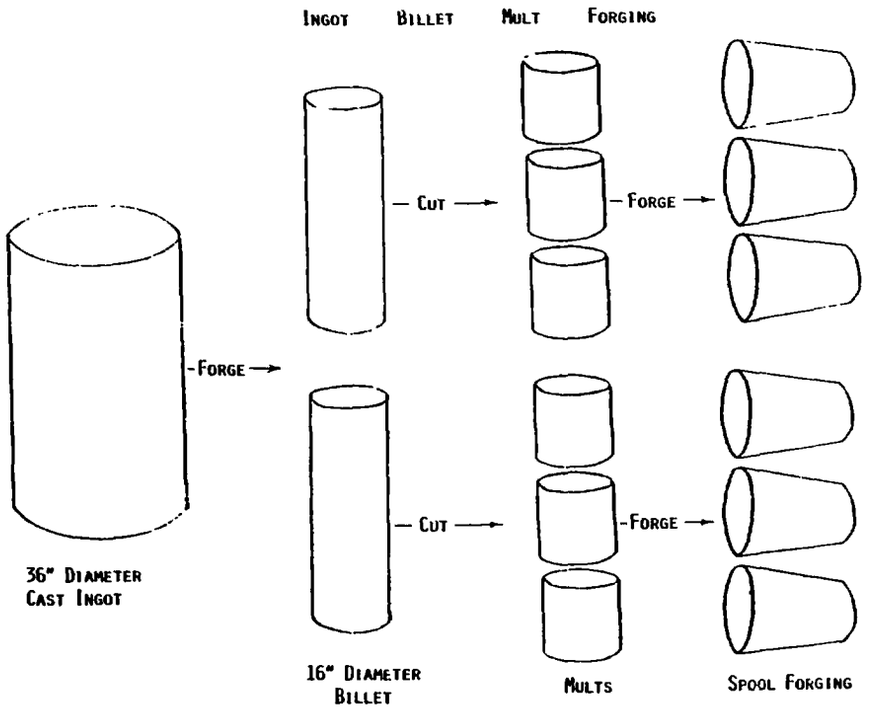
INGOT
BILLET
MULT
FORGING
FORGE
CUT
CUT
FORGE
FORGE
36" DIAMETER
CAST INGOT
16" DIAMETER
BILLET
MULTS
SPOOL FORGING

A HORROR STORY

INCIDENT:

- STAGE 3-9 Ti-6-2-4-2 SPOOL
  - HARD ALPHA ZONE PLUS OXIDE INCLUSIONS

RESULT: A LATENT MELT RELATED HIGH OXYGEN ZONE PASSED THROUGH THE SYSTEM UNDETECTED.

STAGE 3-9 SPOOL CONTOUR

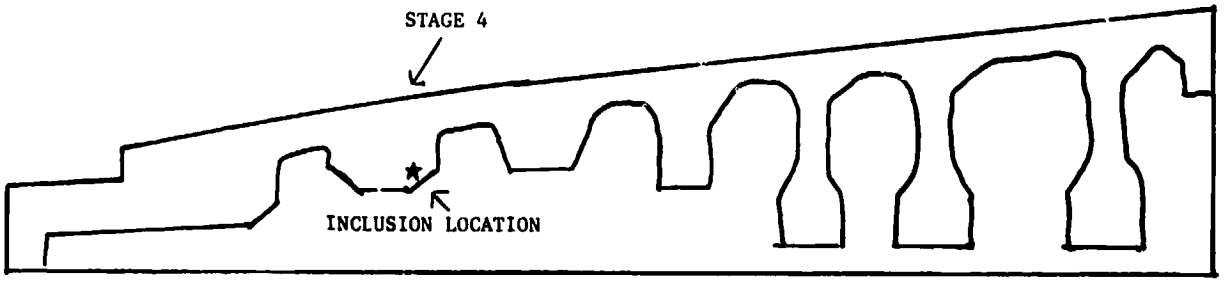

ENGINE INCIDENT INVESTIGATION

- PRIMARY CAUSE

  TYPE I OXYGEN STABILIZED HARD "ALPHA" INCLUSION WITH POROSITY

- FAILURE MECHANISM

  CYCLIC CRACK PROPAGATION FROM THE INCLUSION TO SPOOL SEPARATION

INVESTIGATION AT MILL

- MILL ON STRIKE
- POST STRIKE START-UP PROBLEMS IN INGOT CONVERSION
  - HARD ALPHA INCLUSIONS
  - CENTER BURST (POROSITY)
  - LOW BILLET YIELDS (ULTRASONIC REJECTS)
  - DELAYED SHIPMENTS
- FORGER REQUESTED TO CONVERT INGOTS - EXPEDITE DELIVERY
- AT MILL: OF TWELVE INGOTS CONVERTED AND INSPECTED,
  - 9 CONTAINED ULTRASONIC INDICATION
  - 3 WENT TO FORGER - NO INDICATIONS IDENTIFIED BY HIS ULTRASONIC INSPECTION
  - THE FAILED SPOOL CAME FROM ONE OF THESE THREE INGOTS

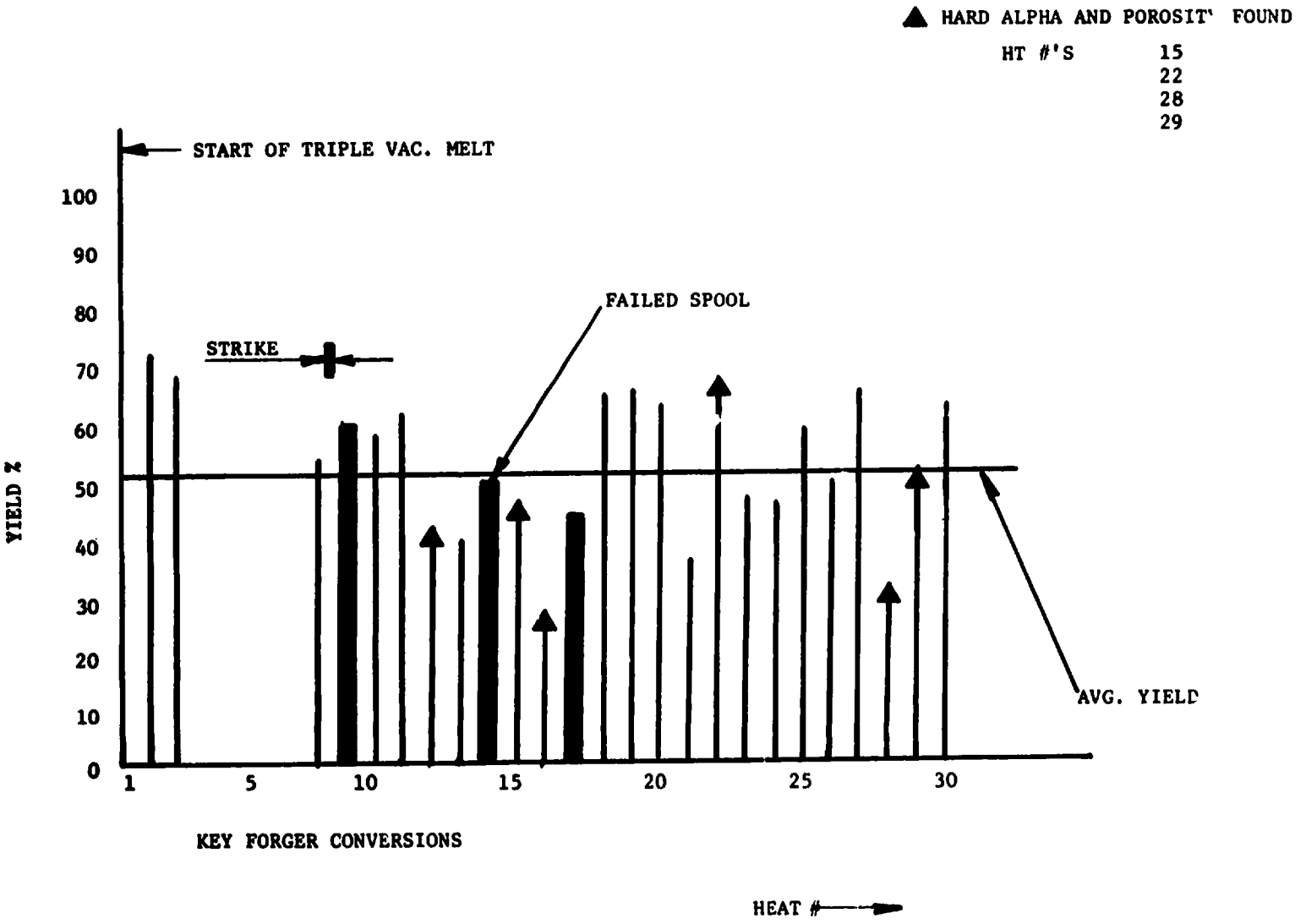
▲ HARD ALPHA AND POROSITY FOUND
HT #'S 15
22
28
29
START OF TRIPLE VAC. MELT
FAILED SPOOL
STRIKE
AVG. YIELD
YIELD %
100
90
80
70
60
50
40
30
20
10
0
1
5
10
15
20
25
30
KEY FORGER CONVERSIONS
HEAT #

% ULTRASONIC REJECTS

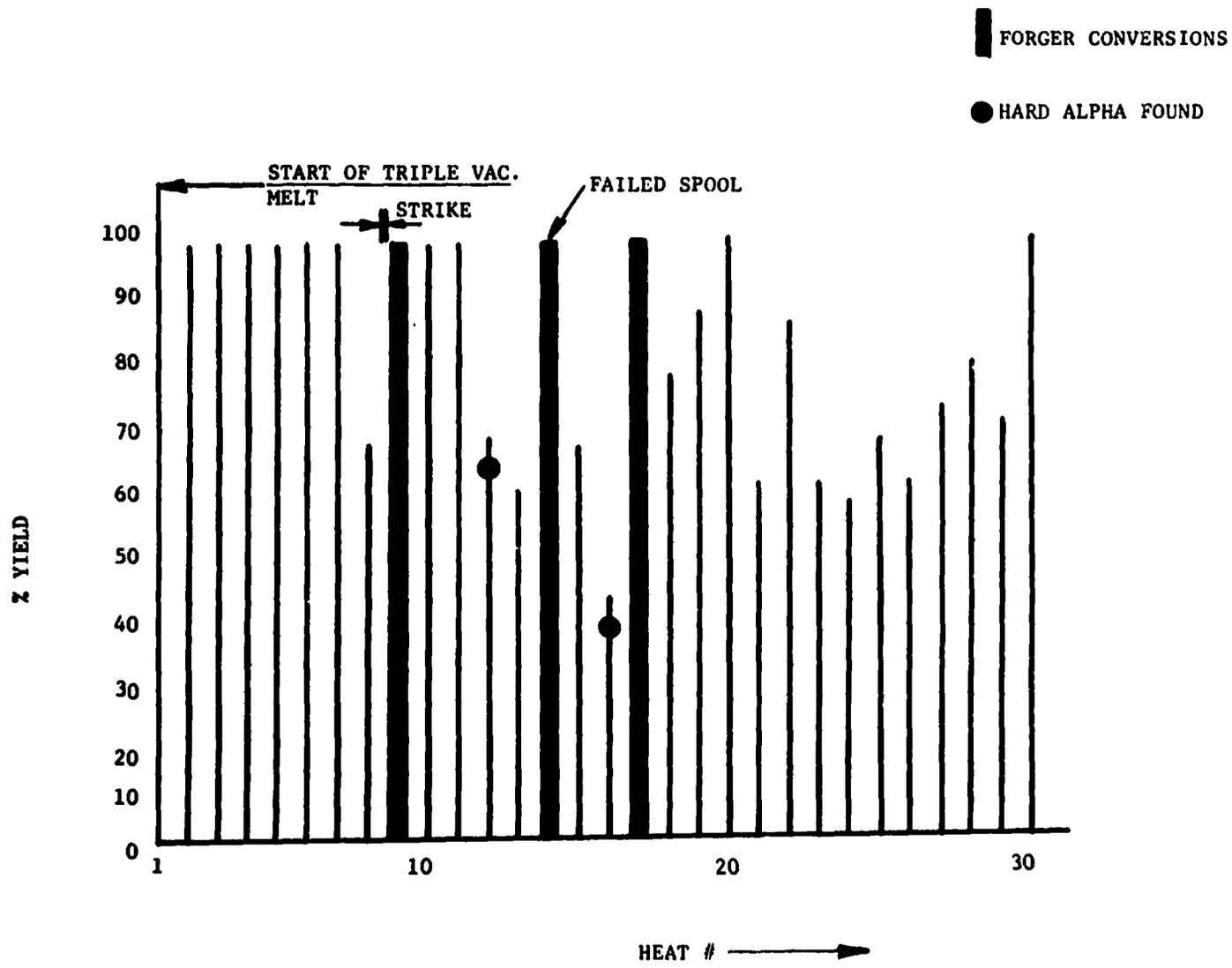

INVESTIGATION CONCLUSIONS:

- LOW PROCESS YIELDS NOT TRACKED BY MILL OR GE
- NO IMMEDIATE CORRECTIVE ACTION TAKEN
- PROCESS CHANGED AFTER STRIKE (?) START-UP PLAN (?)
- MATERIAL BYPASSED MILL ULTRASONIC INSPECTION - FORGER PERFORMED (AN UNAPPROVED SOURCE FOR THIS OPERATION)

LESSON LEARNED

VIOLATE A P.Q. CONTROLLED PROCESS, AND RISK AN INCIDENT OF SIGNIFICANT PROPORTIONS.

PREMIUM QUALITY MATERIAL TRACK RECORD
(1972 THROUGH 1976)

	POUNDS OF ALLOY	
	TITANIUM BASE	NICKEL BASE
TOTAL PQ BILLET PRODUCED	10,000,000	10,000,000
HEATS REJECTED AT MELTER	20,000	20,000
BILLET REJECTS AT MILL/FORGER	150,000	150,000
TOTAL PQ PARTS PRODUCED	7,000	16,000
FORGING/ROTOR REJECTS	5	75

GE EXPERIENCE: ONLY ONE SIGNIFICANT INCIDENT

- NONE WHEN PQ ROUTINE RIGOROUSLY FOLLOWED.

MATERIAL PROCESS CONTROL IS THE MOST IMPORTANT KEY ELEMENT FOR PREVENTION OF MATERIAL DEFECT RELATED ROTOR FAILURES.

DISCUSSION

G.J. Mangano, NAPTC

I have one question. Who enforces this procedure -- General Electric, or people that you have at the mill?

R. Duttweiler, GE-Cincinnati

It is all of them -- steel supplier people and our quality engineering as well as resident people who visit and audit the mills. Every six months we do an audit and every year we renew our agreement as to how things will be processed.

A lot of enforcement is done by the vendor himself; he writes down the rules that he will live by, and we simply audit against them. If he merely depends on us to catch him, he is not doing his job. He is failing to do what we both need to assure premium quality. We have simply set up a self-policing system.

One thing I'd like to add is that this system was forced by engineering on the manufacturer, with great reluctance because manufacturing told us that this would be an extremely expensive way to go. It really hasn't proved to be the case. It has developed into an accepted discipline. At first it was expected that these requirements would add an additional 8-10 per cent to raw materials cost, but it has not amounted to anything near that figure in recent years.

NDE - A KEY TO ENGINE ROTOR LIFE PREDICTION

by J. E. Doherty
Pratt & Whitney Aircraft Group
Commercial Products Div.
Middletown, Conn.

Abstract

A key ingredient in the establishment of safe life times for critical components is the means of reliably detecting flaws which may potentially exist. Although currently used NDE procedures are successful in detecting life limiting defects, the development of automated and computer aided NDE technology will permit even greater assurance of flight safety.

INTRODUCTION

The ability to predict and monitor the useful and safe lifetime of critical components in turbine engines is a current requirement. A key ingredient in the procedure for establishing the safe lifetimes for critical components is the means of reliably detecting potential flaws which may exist in these components. As evidenced by component performance, currently used flaw detection procedures are successfully screening out components with life limiting defects. New developments in nondestructive evaluation (NDE) technology now being made will permit the adoption of more strict flaw detection requirements thereby giving even greater assurance of flight safety. The primary key to this advance in NDE technology is the adoption of automation and/or computer aided techniques which will reduce or eliminate the dependence on human operators for the performance of NDE procedures. This paper will indicate how these gains are being made by showing how the sensitivity of inspection is operator dependent and by example show how the introduction of automation can permit significant improvements in inspection sensitivity.

A SIMPLE MODEL OF AN NDE SYSTEM

In the simplest case, an inspection system can be described by two distributions - a defect and a noise or false defect distribution, and by two quantities - the inspection threshold and the inspection uncertainty. The defect and noise distributions are simply the number of either present in a given population or the likelihood of occurrence for a given size defect (indication); both distributions are usually (but not always) monotonically decreasing functions with increasing defect size. The inspection threshold is the discrimination level or decision

point which is set to differentiate between defects (indications) of different sizes. A measure of how well a particular inspection system can make discriminations is the inspection uncertainty. For example, if a system were sorting a population of balls into boxes of white ones and boxes of black ones, there would be numerous black balls in the white box and white balls in the black box if the inspection uncertainty were large. If the inspection were perfect, with no uncertainty, there would be no alien balls in either box.

It is clear that for an inspection to perform satisfactorily, that is reliably, it must have a low inspection uncertainty at the inspection threshold of interest. Figure 1 shows schematically how the defect and noise distributions and the inspection threshold and uncertainty would appear in a typical case.

DETERMINATION OF INSPECTION UNCERTAINTY

It is a practical problem of much interest to determine the true proportion of defects of a given size that can be detected by an NDE system. In particular, one is usually most interested in the defect size where the probability of detection drops below some critical level. Current convention identifies reliable inspections as those where the probability of detection exceeds 90 percent at the inspection threshold of interest.

An exact determination of the probability of detection would require a full knowledge of the statistical description of the inspection system which only can be obtained by making an infinite number of measurements. The best one can do is to estimate the probability of detection and depending upon the procedure used, one can make this estimate with any degree of confidence. Current convention considers

estimates of the detection probability which have greater than 95 percent confidence level to be acceptable.

During the last five years, the measurement of inspection reliability has been one of the major interests of NDE practitioners. It has been found that proper measurements of inspection reliability are difficult, expensive and are, unfortunately, unique only to the specific application or case studied. To make proper measurement of inspection reliability, one must use: real flaws in real parts, representative inspectors, multiple sets of equipment, multiple reference standards and unbiased measurement techniques. The latter is most difficult of all. Despite the difficulties, measurements of minimum flaw sizes with 0.9 probability of detection at 95 percent confidence have been made for some specialized cases. Typical results are shown in Figure 2 which summarizes the evaluation of four different inspection procedures that were used to find cracks near a fillet in a round steel bar; as noted above these results apply only to this case. A detailed scrutiny of these results and others like them show that the chief contributor to the inspection uncertainty is the inspection operator. This is shown, for example, in Table I which compares the effectiveness of six different operators performing an eddy current inspection designed to detect small (0.015" long) cracks in a titanium component. Analysis of this and other similar experiments suggests that 75 percent or more of the source of inspection uncertainty is operator related. The message is clear - improved, more sensitive inspections may be had by reducing or eliminating the dependence on human inspection operators.

AUTOMATION - THE OPPORTUNITY FOR IMPROVED NDE

There is a concerted effort in the NDE field to develop automation and computer aided inspection techniques. The expressed purpose of these efforts is to increase

Table I

Summary Of Operator Performance In A
High Resolution Eddy Current Inspection

Operator	Misses/Trials
1	0/14
2	1/14
3	1/9
4	3/14
5	4/8
6	6/9

inspection sensitivity of the currently used effective inspection systems by increasing the probability of detection for small defects. This is illustrated in Fig. 3 which shows that a reduction in inspection uncertainty of an NDE system lowers the defect size where the probability of detection drops below 90 percent. This ability to detect smaller defects reliably is an improvement of inspection sensitivity.

There are many examples which could be used to demonstrate how the introduction of automation will permit improved NDE procedures but two which relate to turbine disks seem to be most appropriate.

COMPUTER AIDED INSPECTION OF NEAR NET SHAPE DISKS

Fabrication techniques are currently being developed to permit the manufacture of disks for gas turbine engines to shapes very close to their final shape. These near net shape techniques will permit considerable cost savings over the current techniques. To permit maximum cost savings, near net shape disk preforms must be only slightly larger than the final shape, thereby requiring improved resolution of defects near surfaces. In addition, increased sensitivity to smaller defects is required, since the new fabrication techniques will permit the use of advanced alloys. A primary cost saving in near net fabrication approaches is derived from the elimination of machining operations before ultrasonic inspection. Accordingly, the advanced inspection system must have the capability of contour following non-regular surfaces while still maintaining normalcy of the ultrasonic beam, since near net shapes will, as a rule, possess tapered and curved surfaces.

An ultrasonic inspection system for near net turbine disk shapes is currently under development at P&WA with the support of Air Force funding. This system is an

automated computer aided inspection system, Fig. 4. It has the ability to sense and contour follow disk shapes with as-processed surfaces, while requiring only a minimal pre-knowledge of the shape under inspection. It has high sensitivity ultrasonics that can resolve a 1/64 flat bottomed hole (FBH) 0.050 from the surface.

The inspection system has been configured about a small mini-computer and is designed to minimize the dependence on human operators. Unlike conventional disk inspection systems, this new system can detect and record the presence of indications with sizes much smaller than those at the inspection threshold. This information can be ordered into distributions such as number vs. size, as shown in Fig. 5, which can be used to monitor the fabrication process or possibly eventually could be used to estimate the statistical lifetime of the part. Being computer aided, this inspection system can recall at any future time the detailed inspection records for any part if required in the event of a disk service problem. The system has also been designed to permit the use of selective or variable rejection criteria that can be tailored to the anticipated local stress levels in the component.

The eventual introduction of computer aided and automated technology into production inspection will permit a more detailed and sensitive inspection of turbine disks because it has eliminated the major sources of operator generated inspection sensitivity. In addition, it offers significant advantages over conventional approaches, since it can collect order and store information beyond that just required to make go-no-go decisions.

AUTOMATED BOLT AND TIEROD HOLE INSPECTION OF DISKS

Occasionally during the static ferris wheel testing of disks, eddy current inspection of bolt holes and tierod holes is occasionally performed along with the regular wink fluorescent penetrant inspection. A potential advantage of eddy current testing is that it can be performed in situ and does not require any dismantling of the test apparatus. Unfortunately, most conventional eddy current inspection being manual inspections have larger inspection uncertainties than wink penetrant inspections at the small defect sizes which are of interest in static testing. For example, Fig. 6 shows the results of a conventional manual eddy current inspection for axial cracks in two disk bolt holes. The figure shows the eddy current scans of the circumference of the hole at nine equally spaced locations through the hole. The presence of a crack would be indicated by rightward-going peaks as seen in scan #5 of hole #5 and on this basis both holes would be judged to be cracked. In fact, wink penetrant inspection shows hole #5 to contain a very small crack and hole #9 to be uncracked.

Currently, P&WA is developing automated eddy current inspection techniques for the evaluation of holes. One approach being used, shown in Fig. 7, places the eddy current sensing device on the tip of a small rotating probe which is automatically indexed through the hole. Inspection information is recorded on a strip chart such that the results of each circumferential scan sequentially follows the previous one. The results of evaluations of holes 5 and 9 using this automatic system are compared with the manual scans and wink penetrant results in Fig. 8. In the automatic system, the circumferential scans are spaced 0.02" apart and the presence of a crack is indicated by an upward peak; the results of the hand scans shown in Fig. 6 have been linked sequentially in Fig. 8 for comparative purposes.

Figure 8 shows that unlike the manual inspection, the automatic inspection properly distinguishes the cracked hole from the uncracked one. In addition to identifying the crack, the automatic inspection indicates that the crack has some structure and that it has variable depth along its length. The use of other displays and analysis techniques with automatic eddy current inspection, Fig. 9, will eventually permit a quantitative determination of crack length and depth, something which is not possible using wink penetrant inspection. Again, this example demonstrates how the inspection sensitivity of a current inspection can be improved using automation techniques.

CONCLUSION

Improvement in flight safety is a continuing goal and a key to establishing flight safety is the reliable inspection of rotating components for potential defects. The development of new automated and computer aided NDE techniques will permit increased flight safety margins by improving the reliability of already reliable and effective NDE procedures.

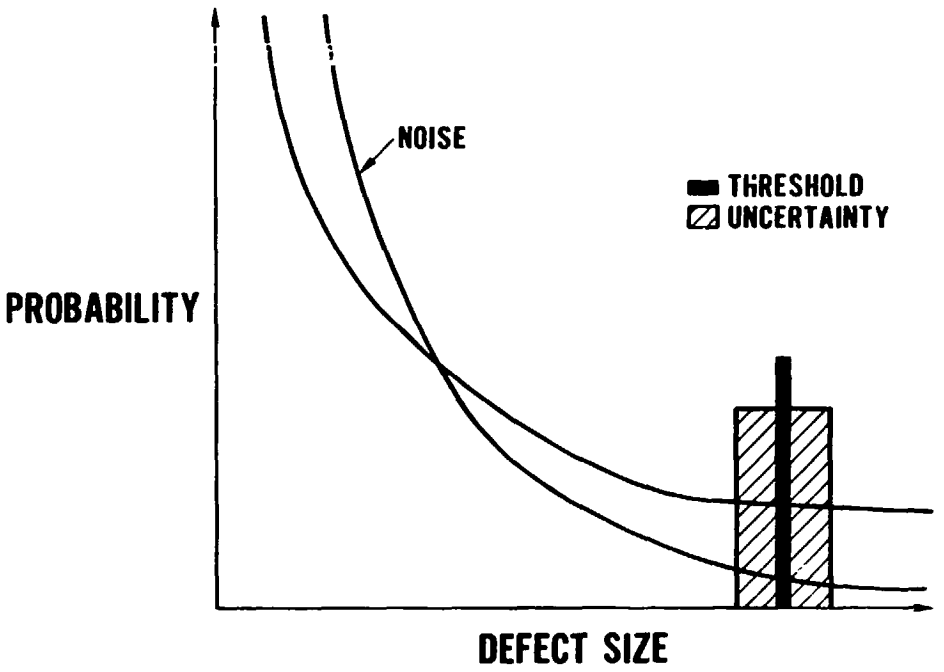

Figure 1. - The defect distribution for typical inspection. The noise distribution is low at the inspection threshold, signifying a practical signal to noise ratio. On the average the inspection threshold has the value indicated, however for a specific application of the inspection the actual inspection threshold lies somewhere in the band of inspection uncertainty.

MPI	0.06 to 0.08
Ultrasonic	0.06 to 0.07
Eddy current	0.10 to 0.12
FPI	0.14 to 0.16

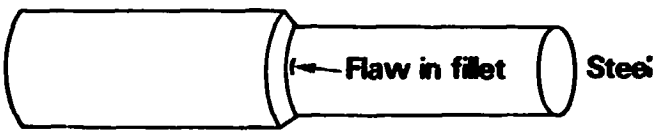

Boeing – AFML Contract F33615-72-C-2202

Figure 2. - The results of the measurement of minimum size crack near a fillet in a steel bar with 0.9 probability of detection at 95 percent confidence. The crack lengths are given in inches. It should be emphasized that these results apply only to this special case and that other inspection systems in other applications will have different minimum detectable flaws.

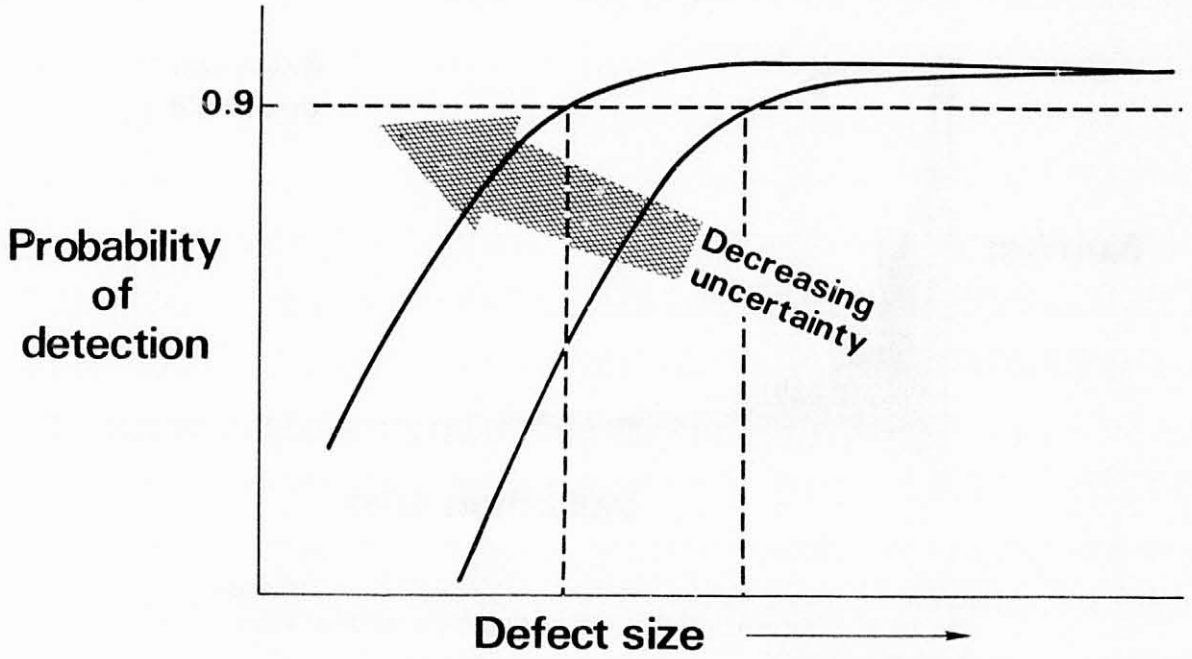

Figure 3. - The probability of detection at 95 percent confidence for different defect sizes for a typical NDE system. As the inspection uncertainty is reduced, the minimum reliably detectable defect decreases in size, and the reliability of detection at a given size increases.

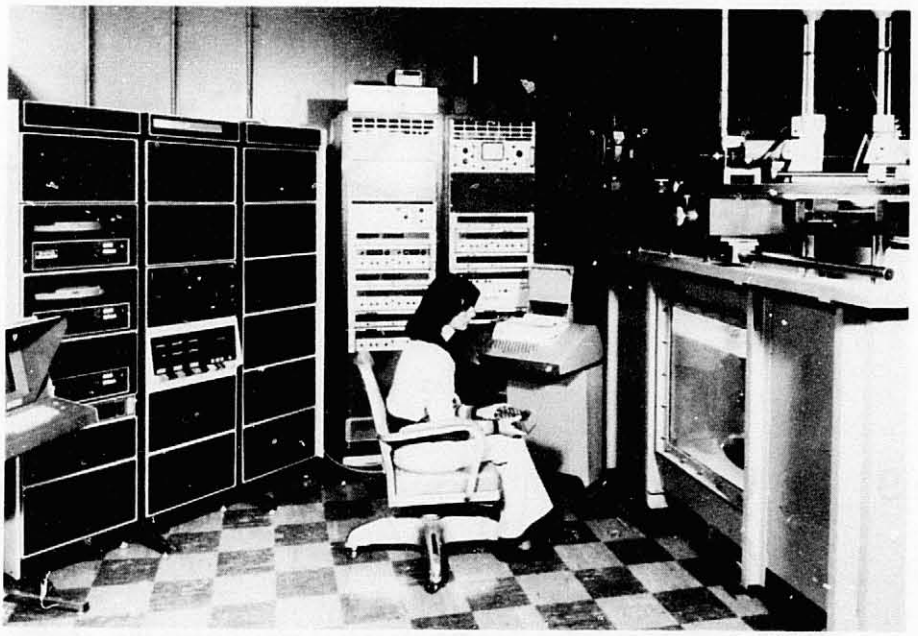

Figure 4. - The computer aided ultrasonic inspection system for near net shape disk. This system will permit more sensitive inspection of turbine disks during production.

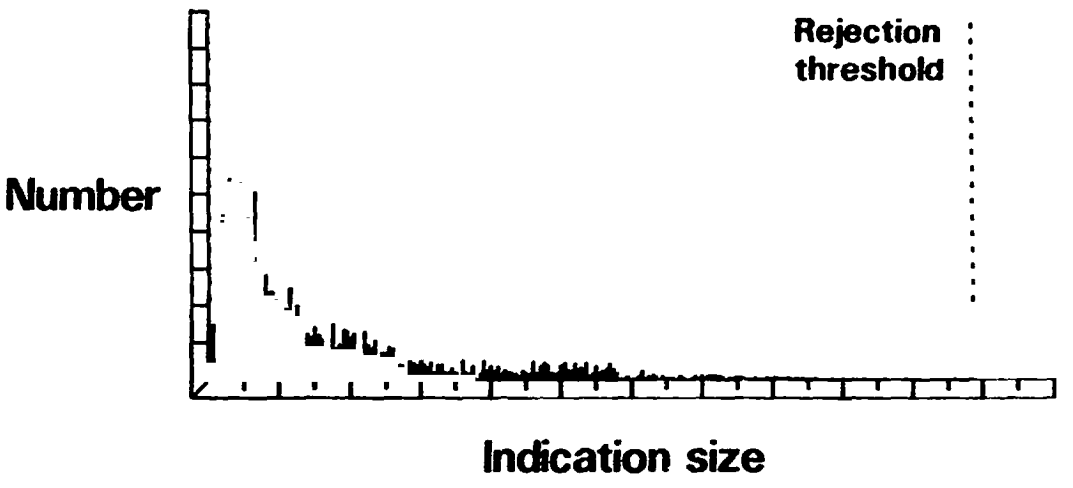

Figure 5. - A summary plot of the number of indications vs indication size for an ultrasonic inspection of a disk using a computer aided inspection system.

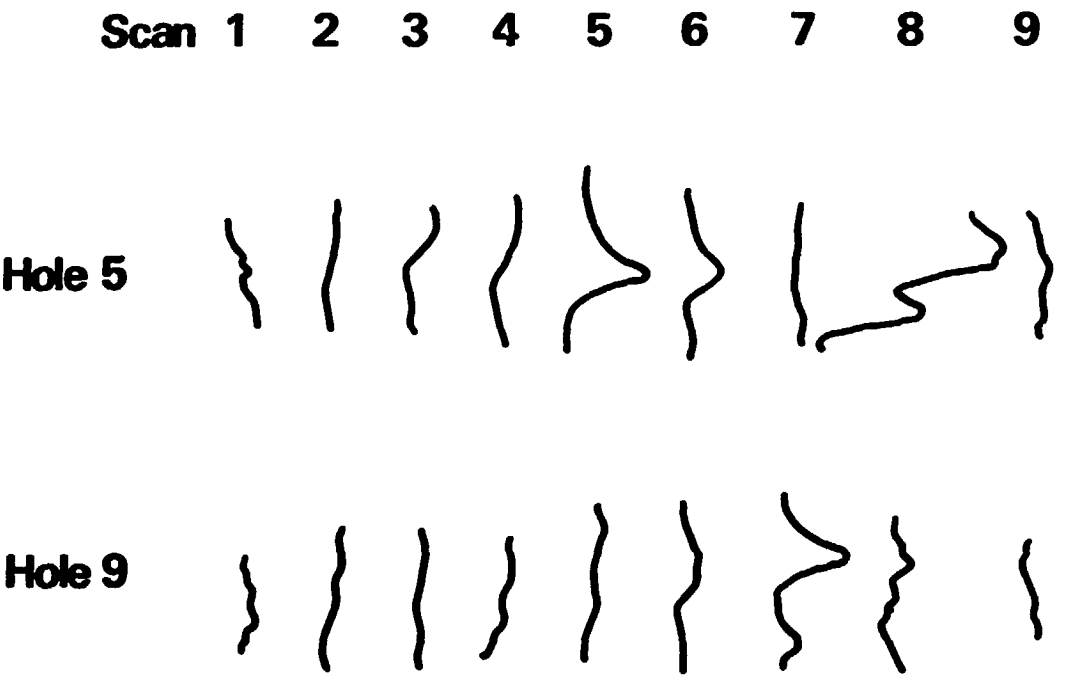

Figure 6. - The results of a conventional manual eddy current inspection of bolt holes. The eddy current scans the circumference of the hole at 9 equally spaced (0.1" apart) locations. A rightward peak as in scan no. 5 of hole 5 indicates a crack. Although the results show both holes to be cracked only hole 5 is cracked.

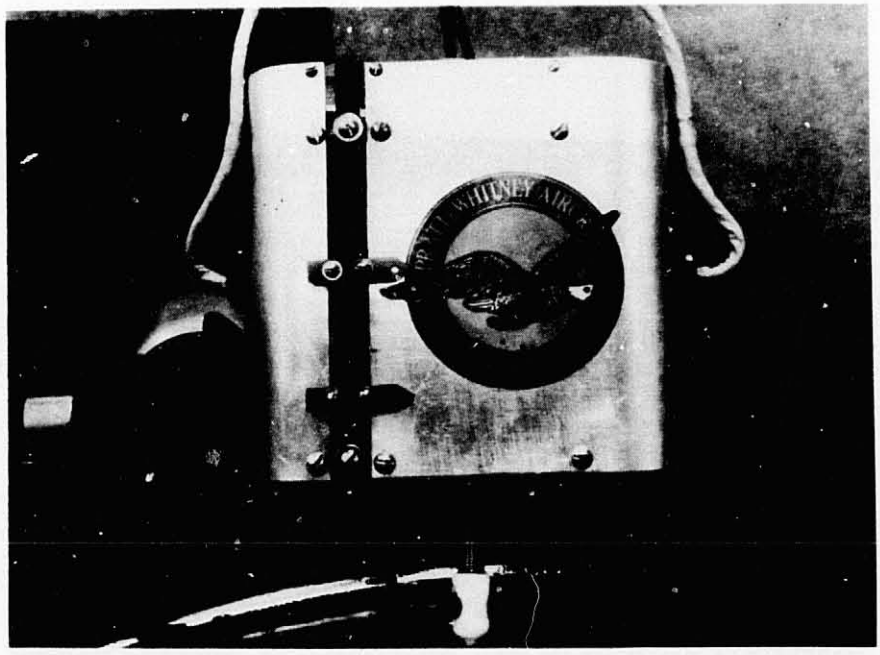

Figure 7. - An apparatus for automatically eddy current scanning a hole. The eddy current probe rotates while it continuously indexes into the hole.

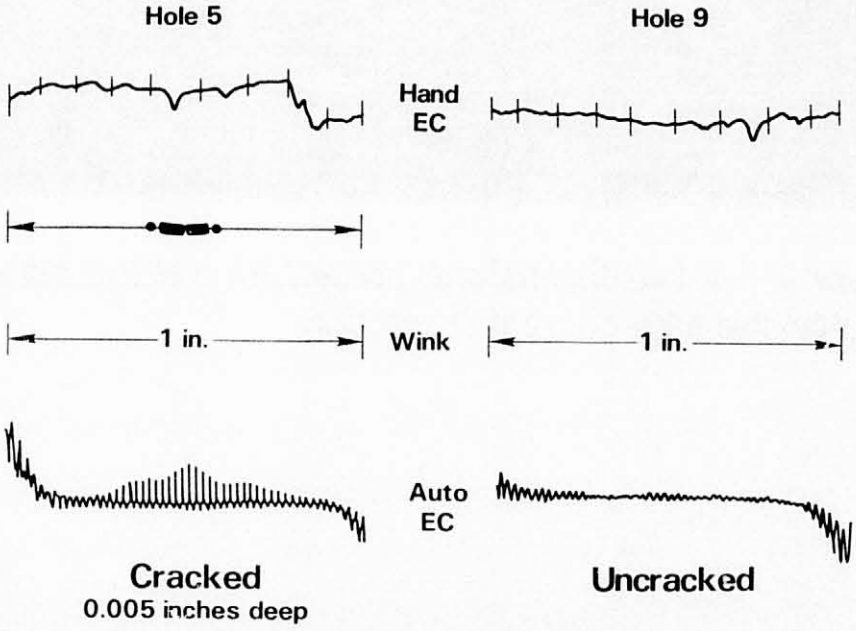

Figure 8. - The comparison of the inspection of two holes using manual eddy current wink penetrant and automatic eddy current techniques. The automatic correctly distinguishes between the cracked and uncracked hole. The scans of figure 6 have been linked for comparison.

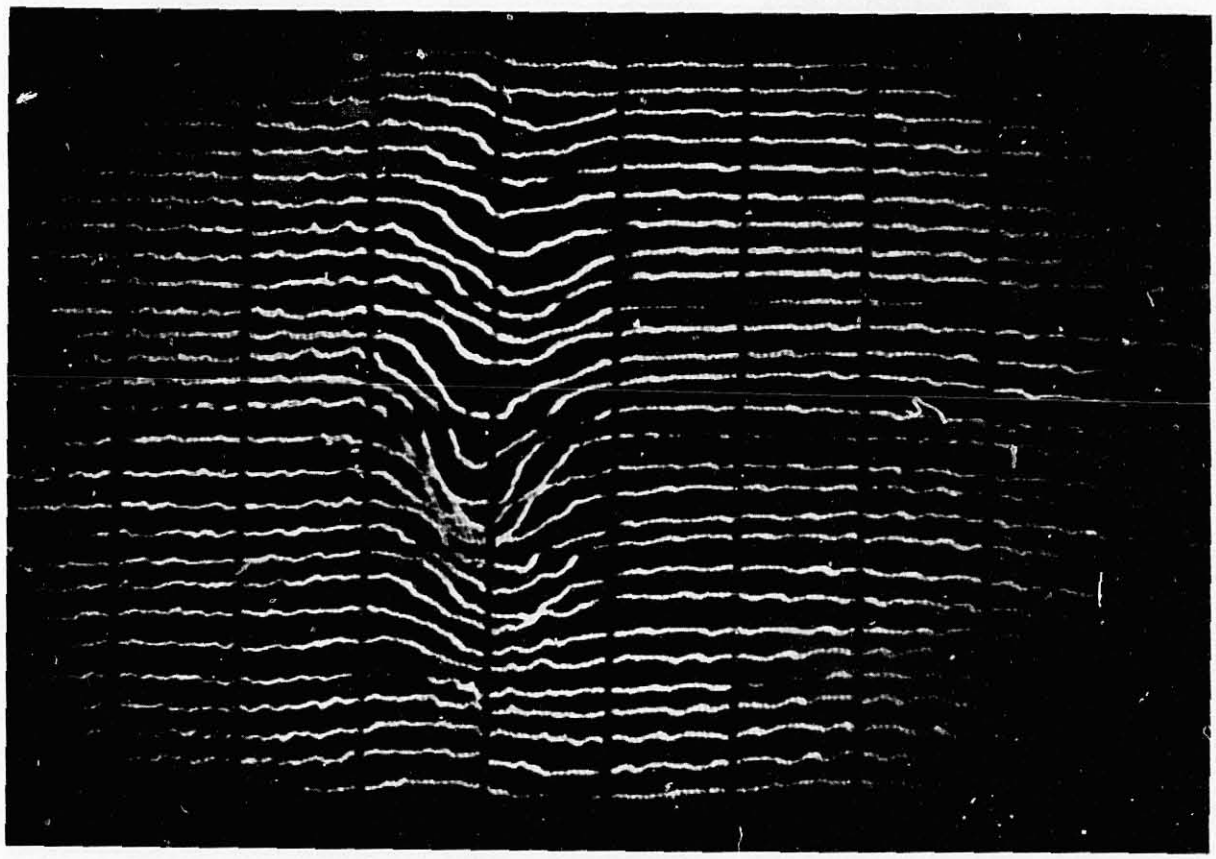

Figure 9. - A two dimensional presentation of the results of an automated eddy current inspection.

APPLICATION OF A FLIGHT-LINE DISK CRACK DETECTOR TO A SMALL ENGINE

John P. Barranger
NASA Lewis Research Center, Cleveland, Ohio

A disk crack detector has been developed which is intended to operate while in flight or at the flight line (ref.) The detector is being applied to a small military engine for use as a flight-line turbine crack monitor. The system consists of an eddy current type sensor and its cables within the engine, external connecting cables, and a remotely located electrical capacitance-conductance bridge and signal analyzer. As the turbine spins, the rotor is monitored by the sensor for radial surface cracks emanating from the interblade region of the rotor.

The sensor is a coil of insulated wire wound on a ceramic bobbin mounted in the nozzle. It is located approximately 2 1/2 millimeters (3/32 inch) away from the face of the downstream side of the first stage turbine wheel where experience has shown cracks are likely to occur. The coil has 100 turns of silver palladium ceramic coated wire with a coil inside diameter of 3.18 millimeters (0.125 inch), an outside diameter of 12.7 millimeters (0.50 inch), and a length of 1.59 millimeters (0.062 inch). The coil leads pass through cored nozzle vanes and are brazed to the sensor cables. The coil and coil leads are cooled by air through the core passage in the vanes.

A commercial bridge is used in the monitoring system and is designed to measure capacitance and conductance. By adding

designed to measure capacitance and conductance. By adding capacitance in series with the sensor coil, the combined reactance is made capacitive. The bridge cable length is limited to 3 3/4 meters (12 feet) because of the decreased bridge sensitivity resulting from the combination of high carrier frequency (1 MHz) and excessive cable capacitance. The capacitance-conductance bridge is self-balancing, automatically adjusting to changes in average coil inductance and resistance caused by temperature effects and variations in disk-to-sensor spacing.

A test cell at Lewis is being prepared to evaluate the monitor system under full scale engine conditions. Disks that have been removed from service because of time expiration will be installed in the test engine. Bench tests indicate that the system is able to detect a crack 3 millimeters (1/8 inch) long in these disks. This length is considerably shorter than the critical crack length.

Reference: Barranger, John P.: Flight Monitor for Jet Engine Disk Cracks and the Use of Critical Length Criterion of Fracture Mechanics, NASA TN D-7483, November 1973

DISCUSSION

H. Garten, GE-Lynn

How big a crack do you think you can detect? Also must it be on the surface?

J. Barranger, NASA-Lewis

The crack must be a minimum of 1/8-inch long for this system. The crack must be on the surface because this is a high frequency eddy current type detector.

I have a comment stemming from a number of inquiries. Everyone's trying to find that elusive crack that's always under the bolt head. This system cannot detect the disk crack until it propagates out beyond the boundaries of the bolt edge.

B.L. Koff, GE-Cincinnati

Is your plan to keep working until you can detect the crack that is under the bolt hole? What's your plan?

J. Barranger, NASA-Lewis

The present plan is to finish this program and turn the results over to the military. We do not plan to go any further beyond this program.

B.L. Koff, GE-Cincinnati

Do you plan to run this detector full time in the engine? Also, what kind of aerodynamics losses do you have with the step that you put in the flow path?

J. Barranger, NASA-Lewis

I'll answer the second question first. If we talk only about cross-sectional area, it's very small. For the total passage area, that step produced only a small change in the area. Concerning other aerodynamic situations, we really have not looked at it very hard. The detector may be monitored full time or may be monitored periodically. With regard to the testing program since we're putting a disk with a crack in it, which is verboten in most test programs, a high level of control will be exercised with continuous monitoring.

Unknown Questioner

Why was this engine used for this crack detector study?

J. Barranger, NASA-Lewis

We are looking at this particular engine because of the average disk life aspects of it. The disks have been taken out of service because someone says, after so many hours this disk comes out, regardless, cracked or uncracked -- this is the standard procedure. We looked at the disks that were taken out and found that there are cracks in some of the disks at the "end of life".

These are not critical cracks: that is, they are at least four times smaller than critical and, according to the manufacturer, are in a low stress region. What will be done with it in the future is again a matter of decision for the people who are the users, that is, the military. If they want to extend the program to its ultimate, one of these detectors would be installed on the engines that they have in existence. The electronics equipment would be ground based: it would be plugged in the side of the aircraft at the end of a flight or every month or whenever the testing interval might be. Then the decision would be made either to take a disk out earlier than its "end of life" because a crack shows up, or as an alternative, to continue to run the disk after the "end of life" (which is more risky) until a crack did show up. However, whether the average life would be less or greater than what it is now is hard to say. But that part of the program is uncertain at this particular time.

G.J. Mangano, NAPTC

Was that detector developed specifically for that application, or was it a general program, and you're using this particular engine as a test vehicle?

J. Barranger, NASA-Lewis

It was primarily a study program. The particular engine being used just happens to fit the test program needs.

S. Weiss, NASA-Lewis

This has been a concept study which is being further investigated by the Army.

W. Springer, Allison-GMC

The top of the disk is exposed to the gas flow pattern and a severe thermal stress concentration exists. After rapid crack propagation, that crack may become benign. Its growth rate drop off tremendously once the crack tip gets below the high stress field.

For the future do you think that you will ever get this device working for smaller cracks than an eighth of an inch and have it farther away from the disk than ninety mils?

J. Barranger, NASA-Lewis

The signal that I showed was a raw data signal, so without any further processing, it was pretty clear the crack was there. I've not tried to increase the sensitivity. I found that the blade root provides an undesirable signal, and a crack very often looks like an extension of one of the blade signals. To distinguish one from the other might be very difficult. In answer to the first part of your question, I do not think that we can get a substantial improvement in the small crack sensitivity unless the sensor is positioned very close to the disk. For the second part, the farther away you get, the less sensitive it is. More sensitivity with distance implies making the coil larger. However, as it becomes larger, a smaller fraction of the sensor area is exposed to the crack region so it becomes less sensitive to the crack. Thus,

it is a balance between those two situations. I do not think that we will do a whole lot better than this. But, I have not looked at the problem hard enough to determine what the answer to that question really is.

J. Doherty, P&W

Just a general comment. It would seem from an operational point of view, that you've chosen a very convenient problem: you know where the crack will be before you start looking. If you don't know where the crack is beforehand, you must have the engine full of sensors -- in every conceivable location. Many of us who have engines in the field know that when we have cracks in components, we must get those cracked parts out as fast as we can; we really don't have a lot of time to go around and find out where the next crack might be.

J. Barranger, NASA-Lewis

Yes, you're right. In this particular example, the cracks are chronic, which means that it is amenable to this sort of solution. If they're random, that's a much more difficult situation.

J. Morelli, TWA

I am going to summarize some comments tomorrow morning to put the meeting in perspective from an airline point of view. Quite honestly I would tend to agree with the gentleman who just spoke here this morning from Pratt & Whitney, that flying that kind of equipment is not the right way to go. But the thing that is important to us, I would like to point out tomorrow, is the ability of detecting cracks of any size installed in an engine. Because we quite honestly fall heir to problems that occur overnight and we're faced with a large fleet of engines and are faced with the problem of trying to segregate from those engines which are the ones we should worry about and which are all right. So I'm very happy to see that work is being done in this area, because I feel it's extremely important. But, perhaps, the flight application is not the one that we would choose as an airline, but instead something that could be done with the engine installed on the airplane (and again to help isolate, because we have had extremely good success in some applications), and I'd like to point that out as we talk tomorrow.

S. Weiss, NASA-Lewis

When we first got into the rotor burst protection problem, we set up a three-prong effort. The first thing that occurred to us was that you build a better wheel, but if you succeed, the designers concerned with increased performance will load it to its maximum and negate any safety benefits. Another concept was also pursued. That was to divert rotor fragments away from any vital parts of the airplane. Yet a third concept was to develop a system that would warn the operator that he has a wheel that is going to fail, before it actually does fail. This is the crack detector and it is not being developed as an NDE device for inspection. We had hoped to lay the groundwork for development of a sensor system that could be flight certified for installation on an engine.

Dr. Barringer suggested the idea of trying to modify eddy current devices for installation in flight engines which would detect a crack of some reasonable size. On the basis of fracture mechanics inspection, a critical crack length

criterion might be established. Continuous monitoring of the growth of a detected crack, with such a device, would permit removal of the wheel before the crack length grew to a danger threshold.

B.L. Koff, GE-Cinc.

In industry, we need to have fundamentally sound ideas in order to obtain funding and I doubt that such a program could gain support. We learn by doing but the scheme must be (a) practical in the end result and (b) one that will be accepted.

TURBINE DISKS FOR IMPROVED RELIABILITY

Albert Kaufman
NASA Lewis Research Center

SUMMARY

The trend toward higher turbine-blade tip speeds and inlet gas temperatures makes it increasingly difficult to design reliable turbine disks that can satisfy the life and performance requirements of advanced commercial aircraft engines. Containment devices to protect vital areas such as the passenger cabin, the fuel lines, and the fuel tanks against high-energy disk fragments would impose a severe performance penalty on the engine. The approach taken in this study was to use advanced disk structural concepts to improve the cyclic lives and reliability of turbine disks. Analytical studies were conducted under NASA contracts by the General Electric Company and Pratt & Whitney Aircraft to evaluate bore-entry disks as potential replacements for the existing first-stage turbine disks in the CF6-50 and JT8D-17 engines. Results of low-cycle fatigue, burst, fracture mechanics, and fragment energy analyses are summarized for the advanced disk designs and the existing disk designs with both conventional and advanced disk materials. Other disk concepts such as composite, laminated, link, multibore, multidisk, and spline disks were also evaluated for the CF6-50 engine.

INTRODUCTION

A disk burst is one of the most catastrophic failures possible in an aircraft engine. Flight failures of disks in commercial airliners have caused fires, rupture of fuel tanks, penetration of passenger cabins, wing damage, ingestion of disk fragments by other engines, and aircraft control problems (ref. 1).

Aircraft engine companies generally endeavor to use conservative design practices and modern quality control procedures in producing turbine disks. However, failures occur because of design errors, undetected manufacturing defects, uncontrollable operating factors, errors in engine maintenance and assembly, and failure of other engine components. To attempt to design turbine disks to preclude failure from any of these causes would result in prohibitively low allowable stresses. Containment devices to protect vital areas of the aircraft against high-energy disk fragments would impose severe performance penalties on the engine.

The approach taken in this program was directed toward improving turbine disk reliability by using more advanced structural concepts to increase low-cycle fatigue life, to impede crack propagation, and to reduce fragment energies that could be generated

event of a disk failure. This paper reports the results of NASA-sponsored analytical studies by the General Electric Company and Pratt & Whitney Aircraft (refs. 2 and 3) to evaluate bore-entry disks as potential replacements for the existing first-stage turbine disks in the CF6-50 and JT8D-17 engines, respectively; these engines were selected because of their extensive use in commercial passenger aircraft. Other concepts such as composite, laminated, and multidisk designs were also studied for the operating conditions of the CF6-50 engines.

The bore-entry disks were compared with the existing disks (henceforth called the "standard disks") on the basis of cycles to crack initiation and overspeed capability for initially unflawed disks and on the basis of cycles required to propagate initial flaws to failure. Comparisons were also made of the available kinetic energies of possible burst fragments. All of these comparisons were also made for the standard disk with the material of the bore-entry disk so that improvements resulting from changes in material properties could be distinguished from those resulting from structural design changes.

DISK CONCEPTS

CF6-50 Turbine Disk Designs

The standard disk and the disk concepts considered as potential replacements are illustrated in figure 1. The standard disk (fig. 1(a)) is machined from an Inconel 718 (Inc-718) forging. Local bosses on both sides of the disk provide reinforcement around the bolt holes to increase the low-cycle fatigue life at the hole rims. Cooling air from the compressor is channeled through the shaft, cools the disk bore, is pumped up radially between the stage 1 and 2 rotors, cools the aft side of the disk between the bolt holes and rim, and then enters the blades through openings in the dovetails.

The bore-entry disk (fig. 1(b)) is a two-part disk of integral construction. The two disk halves are connected by radial webs for channeling coolant up the center of the disk from the bore to the blades. Among the advantages of the bore-entry concept are improved cooling effectiveness, reduced axial thermal gradients, and increased resistance to crack propagation in the axial direction. One of the main attractions of the bore-entry concept for the CF6 program was that it lent itself to a redundant construction where the disk would be overdesigned so that if half was failing, the undamaged disk half would be able to assume a larger portion of the load and sustain the damaged part; however, this would require a substantial increase in total disk weight. The integral bore-entry disk would be fabricated from a single-piece forging of René 95 alloy with the material between disk halves removed by electrochemical machining.

The composite disk (fig. 1(c)) uses high-strength filament or wire hoops to provide most of the load-carrying ability of the disk except at the dovetail attachments. The

hoops would have to be pretensioned in order to assure an even load distribution among the filaments; this could be accomplished by filament winding, by interference fitting, or by the selection of filament and matrix materials so that the desired hoop pretension would be applied by differential thermal expansion under engine operating conditions.

In the laminated design (fig. 1(d)), a disk is constructed by bolting together a large number of sheet-metal laminates. A stepwise variation in thickness provides more laminates at the rim and bore but leaves gaps between laminates in the web region. In the link design (fig. 1(e)) a disk is constructed of pinned sheet-metal link segments. Both the laminate and link concepts are directed toward low-cost fabrication, isolation of propagating cracks, and generation of small burst fragments rather than toward improving disk life.

The multibore disk (fig. 1(f)) separates the highly stressed bore region into a number of circumferential ribs in order to prevent a crack or flaw at the bore from propagating axially. At the ends of the ribs, the tangential stresses due to centrifugal loading would be less and, therefore, the crack propagation rate should be slower than at the bore of the standard disk.

The purpose of the multidisk design (fig. 1(g)) is to obtain improved disk cooling and to provide for a redundant construction by transference of loads from a failed disk member to the undamaged ones through the bolts. The spline disk (fig. 1(h)) is essentially a two-piece design where the members are coupled through splines on their center faces. In order to counter the tendency of each disk-half to straighten out due to the lack of axial symmetry, the splines would have to be radially interlocked through pins. The mechanical coupling of the multidisk and spline designs prevents cracks in one disk member from propagating to another.

These concepts are described in more detail in reference 2.

JT8D-17 Turbine Disk Designs

The standard disk shown in figure 2(a) is machined from a Waspaloy forging. Cooling air is bled from the combustion chamber liner and discharged at high velocity through nozzles toward the front side of the disk near the rim. The cooling air is delivered to the blades through angled holes at the disk rim. These holes result in elliptical exit openings with high stress concentrations; these are the limiting low-cycle fatigue locations.

A split-bonded, bore-entry concept was selected as a possible replacement for the standard disk. As with the integral bore-entry disk (fig. 1(b)) for the CF6-50 turbine, cooling air would be introduced at the bore, would be pumped up radially through channels formed by radial webs, and would enter the blades through openings in the bases. The two halves of the bonded bore-entry disk would be fabricated from separate forgings

of Astroloy and diffusion brazed together at the center surfaces of the radial webs. Dovetail broaching and final machining operations would be performed on the bonded disk assembly. The emphasis in the design of the bonded bore-entry disk was on improving the cyclic life without providing redundancy or increasing the disk weight.

DESIGN CONDITIONS

Design properties of the materials for the standard and bore-entry disks are presented in table I. The simplified flight cycles used for the cyclic heat transfer and stress analyses are shown in figure 3 for the CF6-50 engine and in figure 4 for the JT8D-17 engine. The flight cycle shown in figure 4 was the cycle used in the original design of the first-stage turbine disk for the JT8D-17 engine. The analytical methods are discussed in references 2 to 4.

DISCUSSION OF RESULTS

Preliminary Analyses of CF6-50 Disk Concepts

The results of preliminary analyses of the seven candidate design disk concepts are summarized in table II. Two of the designs, the laminated and link disks, proved to have excessive mechanical stresses and to be unsuitable for the CF6 operating conditions. The multibore design exhibited high transient thermal stresses in the region above the bore rims; therefore, the desired benefit of this design in retarding the propagation of rib flaws was not fully realized. Analysis of the multidisk design under various failure conditions revealed that the bolts could not contain a failed outer disk and that a crack in a center disk would reach critical length before the load could be redistributed to the undamaged members.

Only the bore-entry, composite, and spline disks appeared suitable for the CF6-50 turbine disk applications. From the standpoint of strength-to-density ratio, the composite disk was the most promising concept. However, the composite design is furthest removed from the current state-of-the-art of fabrication and material processing technology of any of the concepts considered. Because of the considerable fabrication development that would be required, the composite disk was not further considered. The spline disk presented special problems in analysis because the load distribution among the splines is dependent on the fabrication tolerances and it is not readily apparent how the loading would be redistributed should one disk-half fail. The integral construction of the bore-entry disk gives more assurance that the loading due to a failed disk member would be more evenly redistributed on the undamaged member. The integral bore-

entry concept was, therefore, selected for more detailed study to replace the CF6-50 standard disk.

Analyses of CF6-50 Standard and Bore-Entry Disks

The rim and bore average temperature responses during the flight cycle of the standard and bore-entry disks are shown in figure 5. Average effective stresses are also indicated at the start and end of takeoff, climb, cruise, and thrust reversal on descent. In both disks the maximum rim and bore temperatures occurred at the end of takeoff and climb, respectively; the maximum stresses also occurred in the bore at the end of climb.

Bore temperatures in the bore-entry disk are only slightly lower than bore-temperatures in the standard disk since the bore is cooled in both cases. Rim temperatures were somewhat higher in the bore-entry disk because the coolant picks up some heat from the center faces of the disk, whereas the coolant only comes into contact with the sides of the standard disk near the rim.

Figure 6 shows the predicted cyclic lives to crack initiation in the initially unflawed standard and bore-entry disks. The limiting fatigue life of 30 000 cycles in the Inc-718 standard disk was at the aft dovetail post rabbet, where the side plate is fastened to the disk. This location was not further considered in the study because fragment generation due to failure would be limited to the dovetail post and adjacent blades. The next most critical location in the Inc-718 standard disk was at the bore with a predicted crack initiation time of 63 000 cycles. The initial FAA certified life of the first-stage turbine disk was 7800 cycles based on one-third of the minimum design life for the original design cycle, which was somewhat different from the simplified cycle used in this study; this FAA approved life is subject to increase as the result of ground tests of three fleet leader engines.

Calculated crack initiation lives for the René 95 standard and bore-entry disks were over 100 000 cycles. Since the crack initiation analyses were based on minimum guaranteed material properties, it is evident that even the standard disk is very conservatively designed provided the design conditions are not exceeded and the disks are initially unflawed.

The cyclic lives for cracks propagating from initial semielliptical surface flaws 0.635 centimeter (0.250 in.) by 0.211 centimeter (0.083 in.) to critical crack size are shown in figure 7 for the most critical locations in the three disks. Manufacturing flaws of this size should be readily detectable by modern nondestructive evaluation techniques. However, in the past, large defects in turbine disks have occasionally escaped detection through human error and have caused problems in some military engines in flight.

The most critical locations for flaws were at the dovetail slot bottom in the Inc-718

standard disk and at the bore in the René 95 standard and bore-entry disks. Although the bore-entry disk showed an improvement in the minimum crack propagation life of more than 300 percent as compared with the Inc-718 standard disk, part of this increase was due to the superior strength properties of the René 95 alloy. If the effect of different materials was eliminated by comparing the bore-flawed bore-entry and René 95 standard disks, the improvement in crack propagation life resulting solely from the structural change was 136 percent.

The crack propagation lives given in figure 7 for the Inc-718 standard disk with a dovetail slot bottom flaw and the bore-entry disk with a bore flaw are only 5 and 20 percent of the FAA certified life of the disk. However, the probability of such large flaws occurring at critical locations and passing modern inspection procedures is statistically remote. Of greater significance is that a substantial improvement in the crack propagation life is added insurance against sudden catastrophic failure due to unforeseen design, manufacturing, maintenance, or operating problems. The overspeed burst margins of the bore-entry disk were 18 and 11 percent greater than for the Inc-718 and René 95 standard disks, respectively.

The redundant construction of the bore-entry disk resulted in an increase in weight of 66 percent over the standard disk. This extra weight is equivalent to an increase of 0.29 percent in installed specific fuel consumption (SFC) for an average DC10-30 aircraft flight.

The extra disk weight could also be added to the standard disk design to reduce the centrifugal stresses due to the blade loads. However, this mechanical stress reduction would probably be offset by the increased transient thermal stresses resulting from the slower thermal response of the bulkier disk. Also, a heavier standard disk would lack the redundancy of the bore-entry disk and would generate even higher fragment energies from a burst disk.

Some possible fragment patterns resulting from manufacturing flaws are illustrated in table III. The available kinetic energies that would be generated from these failures are also indicated. The highest energy fragments are caused by failures initiating at and propagating radially from the bore, as shown by the 120° disk and blade fragment pattern for the standard disk in table III. However, the redundant construction of the integral bore-entry disk would enable the undamaged member to contain such a failed part. The only possibility of a segment separating in this way would be if the radial failure propagated through a web to the opposite disk face; however, this is highly unlikely because the total thickness for all the webs is only 20 percent of the bore circumference and, as one web started failing, its load would be transferred to adjacent webs. The most likely mode of fragment generation is a rim fragment resulting from defects or crack initiation sites at the dovetail slot bottom or bolt hole rim. Based on spin pit experience, the rim-initiated crack would result in the loss of three dovetail posts and

four blades, as shown in table III. The fragment energy of the bore-entry disk rim fragment was only about 10 percent of the 120° disk segment that was assumed to be generated from a bore defect in the standard disk.

Analyses of JT8D-17 Standard and Bore-Entry Disks

The average temperature responses for the JT8D-17 turbine disks in figure 8 show consistently lower bore and rim temperatures throughout the cycle in the bore-entry disk as compared with the standard disk. The lower temperatures in the bore-entry disk were the result of its superior cooling effectiveness and the use of cooling air bled from the compressor midstage. Maximum temperatures and stresses occurred at the end of takeoff and climb, respectively.

Predicted cyclic lives for the initially unflawed standard and bore-entry disks are presented in figure 9. The FAA-certified life of the Waspaloy standard disk is 16 000 cycles based on the limiting low-cycle fatigue life at the exit of the cooling air hole. These results indicate an improvement in the cyclic crack initiation life of the Astroloy bore-entry disk of 88 percent over the Waspaloy standard disk and 67 percent over the Astroloy standard disk. The most critical location in the bore-entry disk was in the bore region at the entrance to the cooling air channel.

Defects and manufacturing flaws in the JT8D-17 turbine disks were considered for the critical locations indicated in figure 10. Subsurface flaws of 0.119 centimeter (0.047 in.) in diameter were assumed in the bore and web regions for all three disks; this diameter was selected because it is at the threshold of detectability by ultrasonic inspection. The web flaws shown in figure 10 were at the radius of maximum radial stress in the standard disks and at the radius of maximum axial stress at the bond surface in the bore-entry disks. The surface flaws at the disk rim or bore were assumed to be 0.081 centimeter (0.032 in.) in length.

The most critical location in the Waspaloy standard disk for a flaw was at the exit of the cooling air hole with a predicted crack propagation life of 2900 cycles. Substituting Astroloy properties for the Waspaloy reduced the calculated crack propagation life to 1150 cycles because of the lower ductility. However, there are indications that if the crack propagation data had included hold-time effects, the crack propagation life of the Astroloy standard disk would have been superior to that of the Waspaloy standard disk. This would also mean that the values given in figure 10 for the bore-entry disk are too low.

The calculated improvement in the minimum crack propagation life of the bore-entry disk over the Waspaloy standard disk was 124 percent. This improvement is significant in increasing the capability of the disk to survive uncontrollable factors that might result in catastrophic failure of conventionally designed disks. There was a

slight reduction in the overspeed burst margin of the bore-entry disk as compared with the standard disk because the overall disk weight was kept constant and that portion of it due to the radial webs was of small structural importance.

A substantial reduction in fragment energy is shown in table III for the JT8D-17 bonded bore-entry disk even though it was not designed for redundancy. This improvement would result from the confinement of the fragmentation from a bore flaw to one disk half; the other half would probably experience failure at the rim from the increased blade loading.

CONCLUDING REMARKS

Some advanced turbine-disk structural concepts have been analytically studied as potential replacements for the existing first-stage turbine disks in the CF6-50 and JT8D-17 engines. An integral bore-entry design was selected for more detailed evaluation for the CF6-50 engine as a result of preliminary analyses of seven disk concepts including composite, laminated, and multidisk designs. The integral bore-entry turbine disk was designed to improve disk life and to prevent high-energy fragmentation by using redundant construction at the expense of an increase in disk weight.

A split-bonded, bore-entry design was selected for evaluation for the JT8D-17 engine. This bore-entry disk was designed to improve disk life without redundance or an increase in disk weight.

Cyclic thermal, stress, and fracture mechanics analyses of the bore-entry and standard disks demonstrated that substantial improvements in the cyclic lives of both initially unflawed and flawed disks could be achieved with the bore-entry disk designs. The benefits of the advanced disk designs are influenced by differences in design philosophy, disk cooling method, fabrication procedure, and engine operating characteristics.

REFERENCES

1. National Transportation Safety Board Special Study: Turbine-Engine Rotor Disc Failures, 1975.

2. Barack, W. N.; and Domas, P. A.: An Improved Turbine Disk Design to Increase Reliability of Aircraft Jet Engines. NASA CR-135033 (R75AEG, General Electric Co.), 1976.

3. Alver, A. S.; and Wong, J. K.: Improved Turbine Disk Design to Increase Reliability of Aircraft Jet Engines. NASA CR-134985 (PWA-5329), 1976.

4. Kaufman, Albert: Advanced Turbine Disk Designs to Increase Reliability of Aircraft Engines. NASA TM X-71804, 1976.

TABLE I. - DESIGN PROPERTIES OF TURBINE DISK MATERIALS

Property	CF6-50 engine		JT8D-17 engine	
	Inc-718	René 95	Waspaloy	Astroloy
Ultimate tensile strength, N/cm^2:				
At 294 K	126 000	150 000	124 000	134 000
At 811 K	110 000	145 000	110 000	117 000
Yield strength (0.2 percent offset), N/cm^2:				
At 294 K	101 000	116 000	86 000	97 000
At 811 K	92 000	110 000	76 000	87 000
Elongation at failure, percent:				
At 294 K	20	8.5	24	19
At 811 K	30	8.5	21	14.5
1000-Hour rupture strength at 867 K, N/cm^2	68 000	103 000	79 000	84 000
Stress range for crack initiation in 10 000 cycles at 811 K (minimum stress, zero), N/cm^2	81 000	93 000	85 000	[a]85 000
Critical stress intensity factor at 894 K, $N/cm^{3/2}$	93 000	88 000	>68 000	[a]>68 000

[a]Estimated.

TABLE II. - RESULTS OF PRELIMINARY ANALYSES OF CF6-50 DISK CONCEPTS

Disk concepts	Advantages	Disadvantages
Bore entry	Redundancy, improved thermal response, longer life	Increased weight to provide redundant design
Composite	Reduced stress levels, longer cyclic life	Limited material possibilities, fabrication development required
Laminated	Redundancy, low fragment energy, low cost	Excessive weight, high stresses at bolts and bolt holes, thermal mismatches between laminates
Link	Redundancy, low fragment energy, low cost	Excessive link stresses, difficult to seal disk to prevent coolant leakage
Multibore	Ribs prevent axial flow propagation at bore	High transient thermal stresses at rib outer diameter
Multidisk	Improved thermal response, some redundancy	Increased weight, bolts would fail if outer disk failed, no load shift if inner disk failed
Spline	Redundancy, longer life	Increased weight to provide redundant design, difficult to analyze load shift with one failed disk

TABLE III. - FRAGMENT ENERGIES OF TURBINE DISK DESIGNS

Disk design	Fragment pattern	Available kinetic energy, J
CF6-50 standard disk	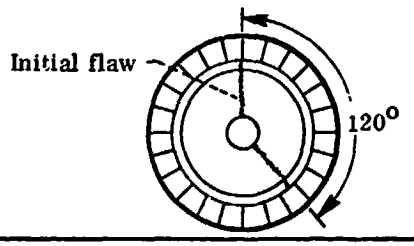	1 172 500
CF6-50 integral bore-entry disk	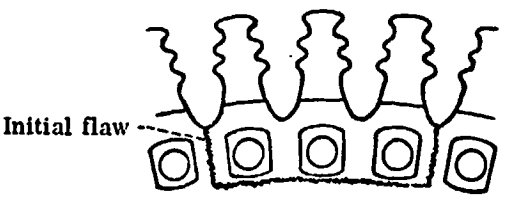	110 500
JT8D-17 standard disk	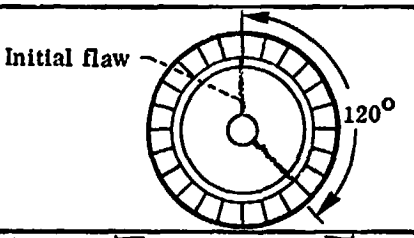	678 600
JT8D-17 bonded bore-entry disk	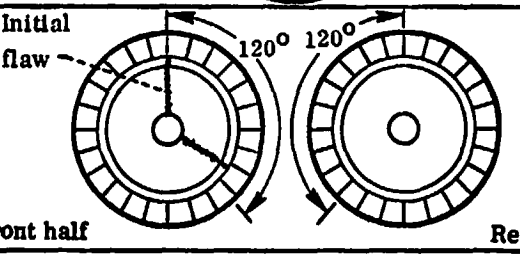	513 000

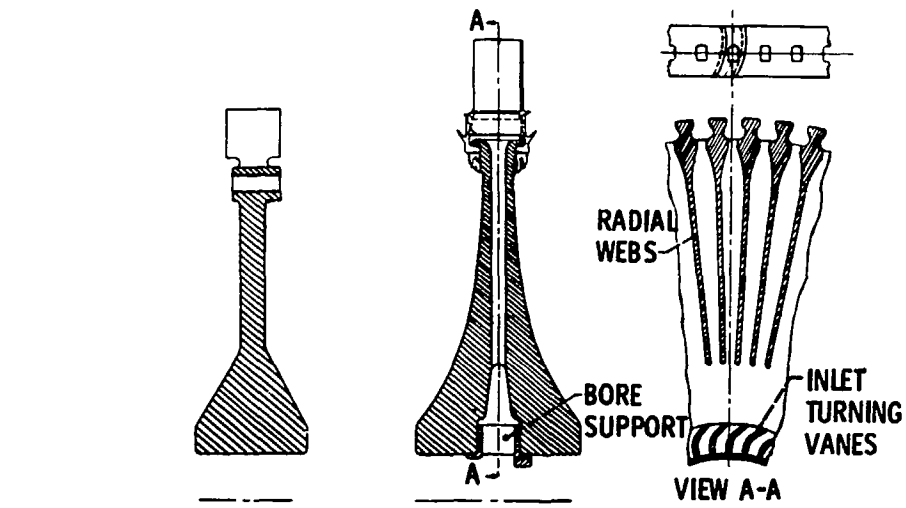

(a) Standard disk.

(b) Integral bore-entry disk.

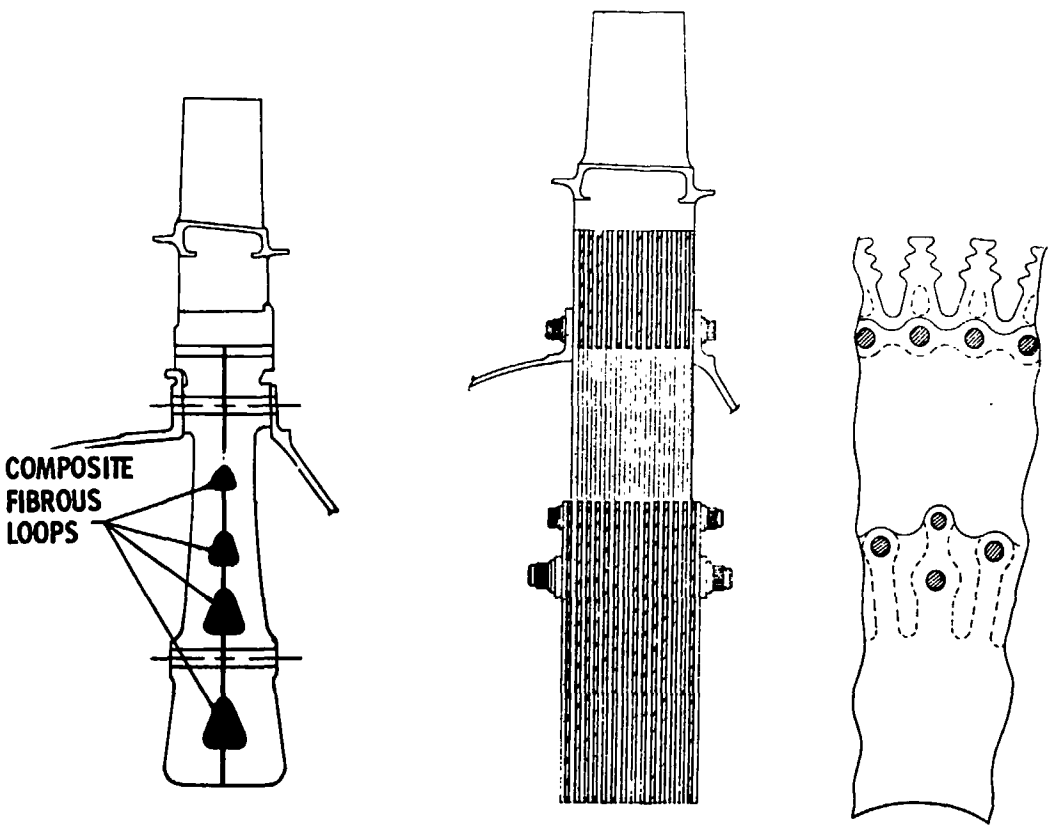

(c) Composite disk.

(d) Laminated disk.

Figure 1. - CF6-50 first-stage turbine disk designs.

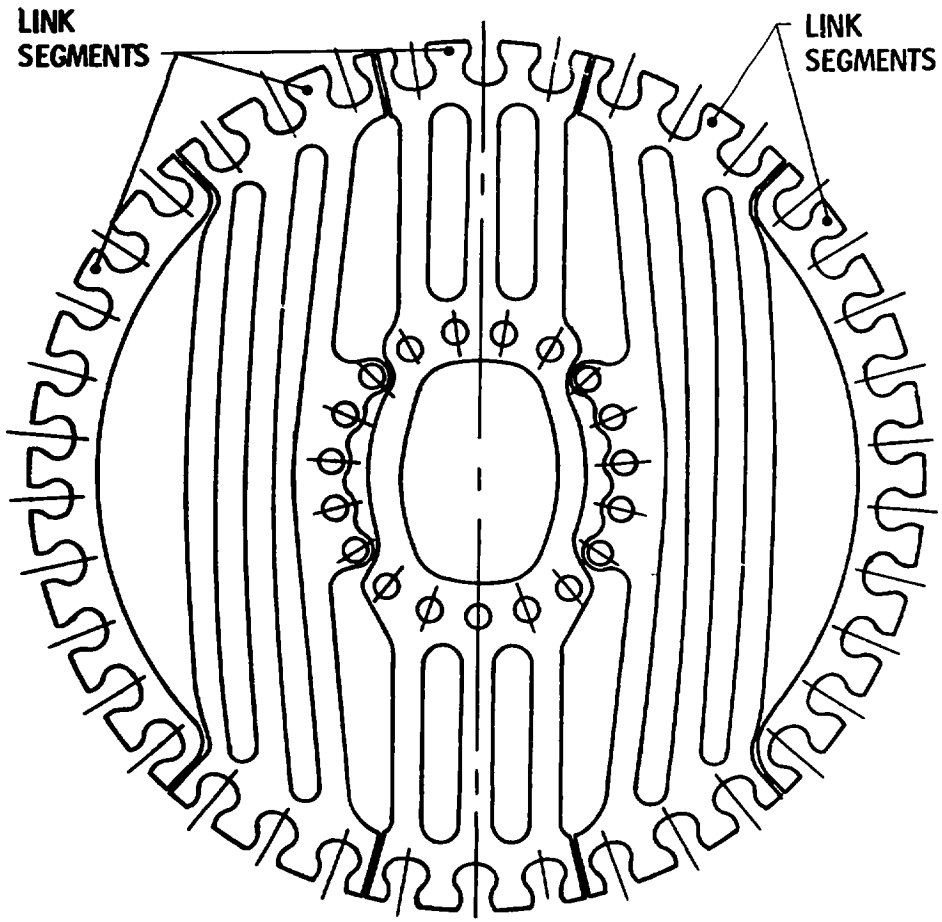

(e) Link disk (typically a disk would contain 20 to 40 layers each clocked axially relative to the next).

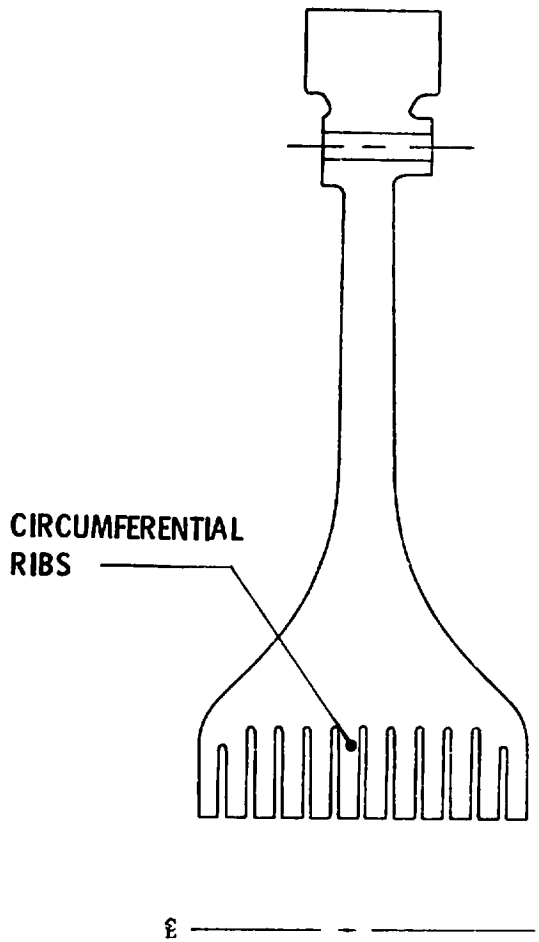

(f) Multibore disk.

Figure 1. - Continued.

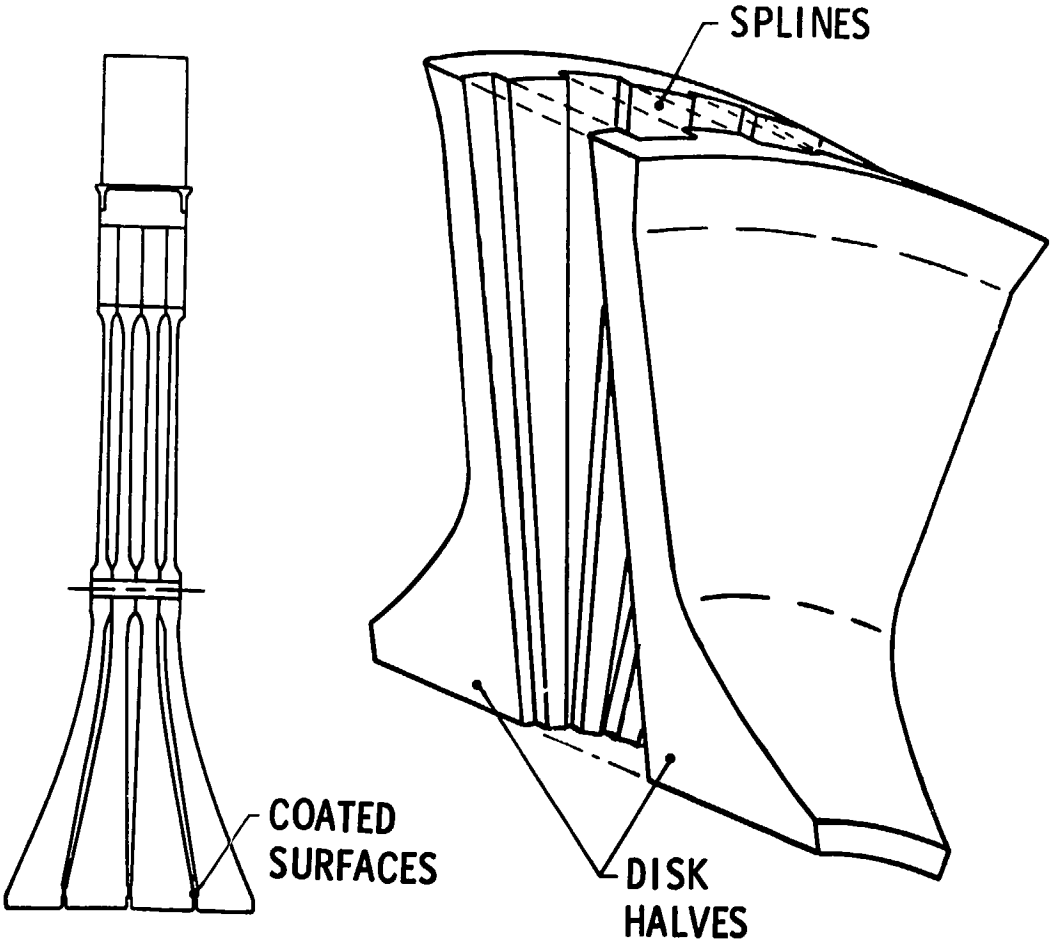

(g) Multidisk.

(h) Spline disk.

Figure 1. - Concluded.

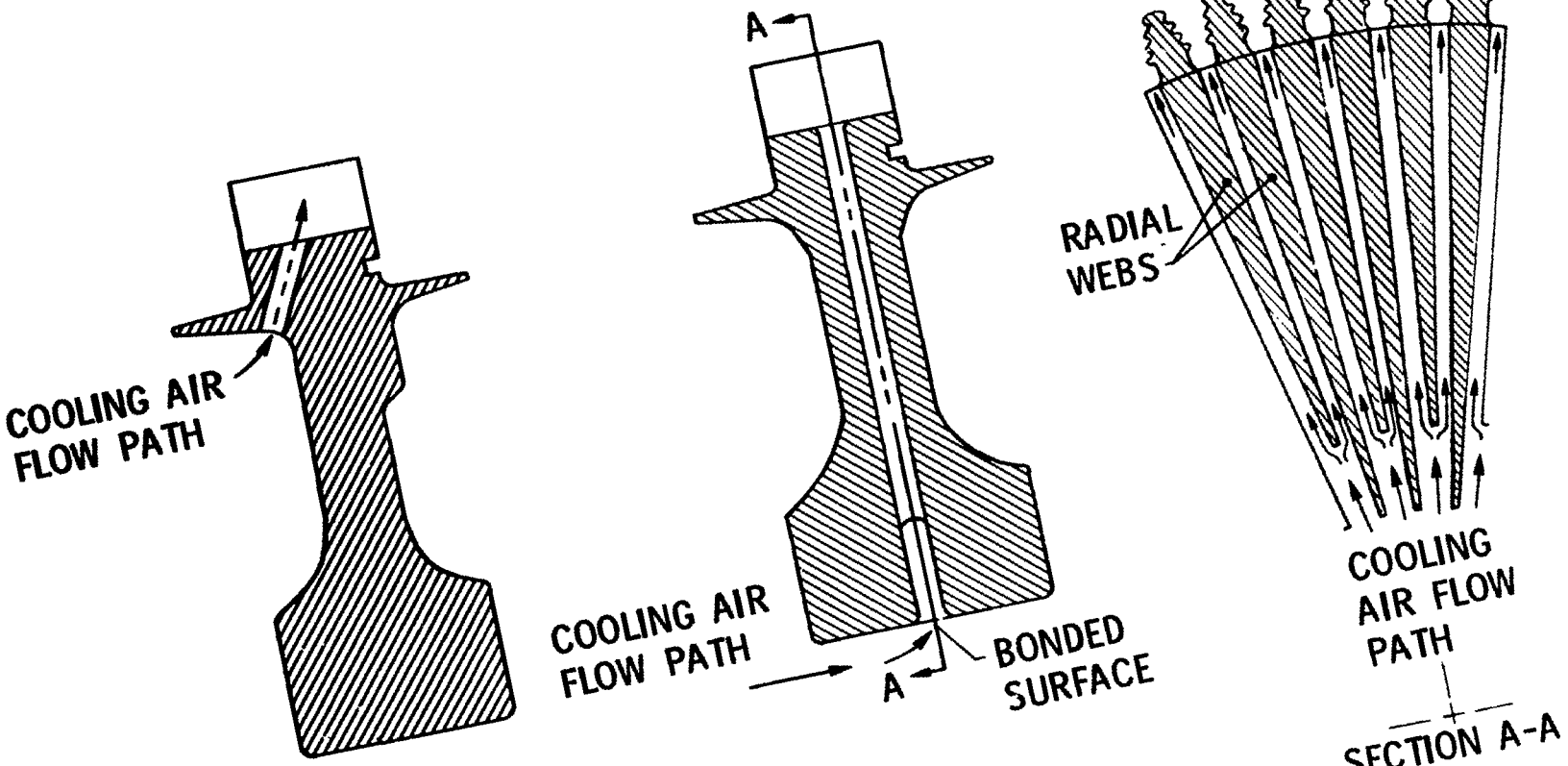

(a) Standard disk. (b) Bonded bore-entry disk.

Figure 2. - JT8D-17 first-stage turbine disk designs.

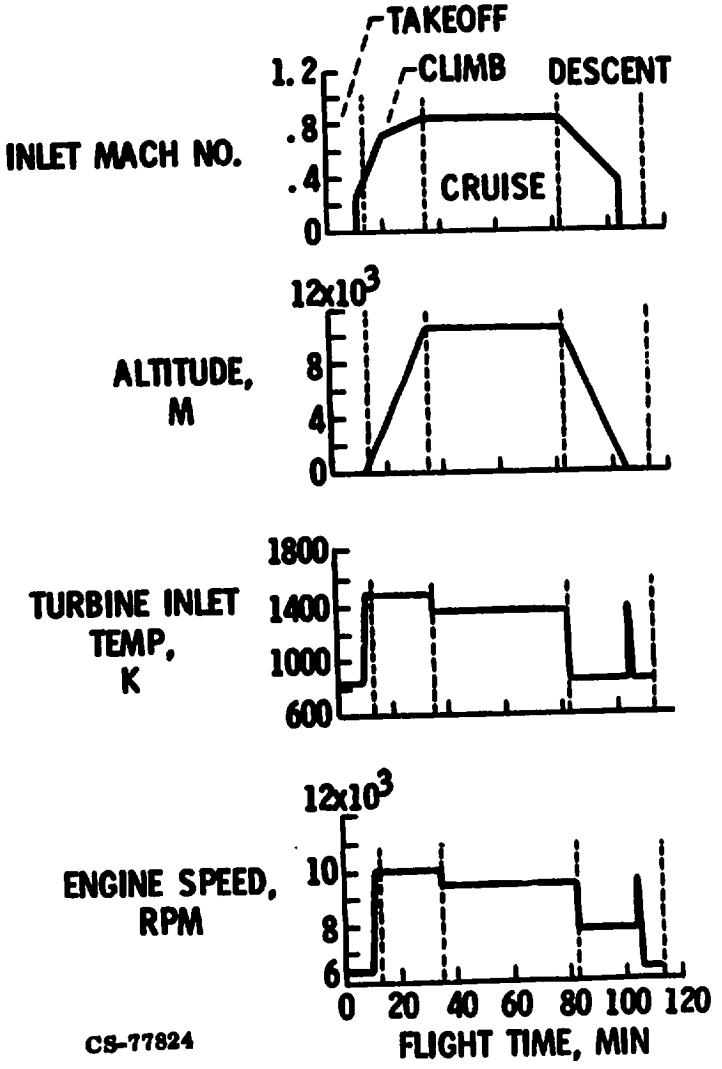

Figure 3. - CF6-50 simplified engine cycle.

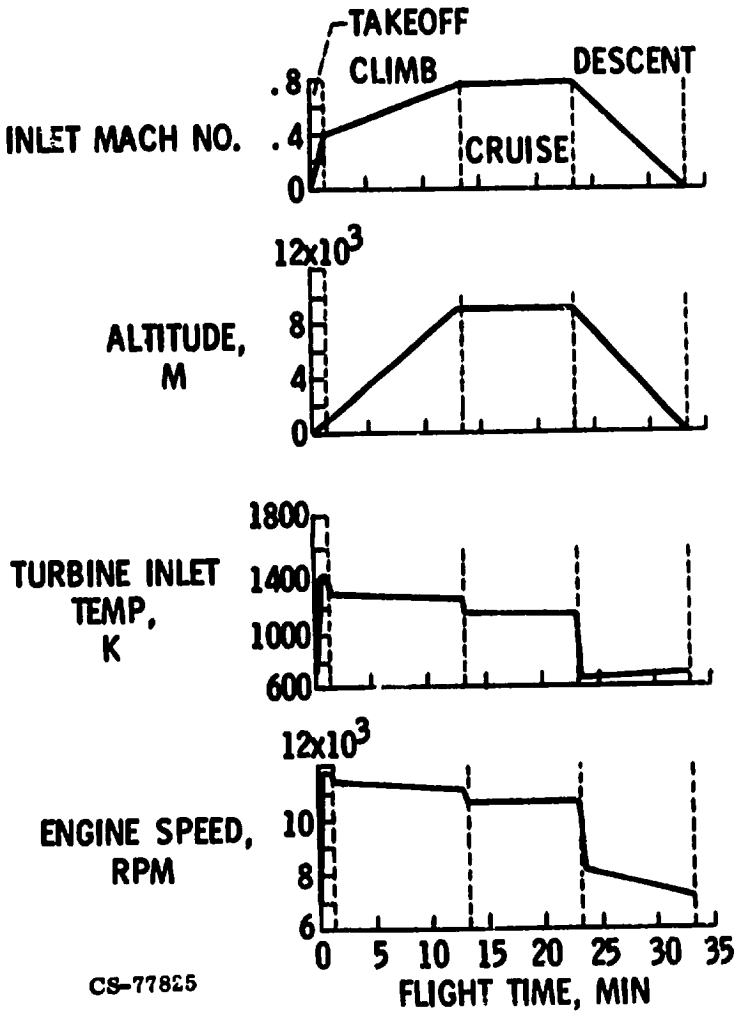

Figure 4. - JT8D-17 simplified engine cycle.

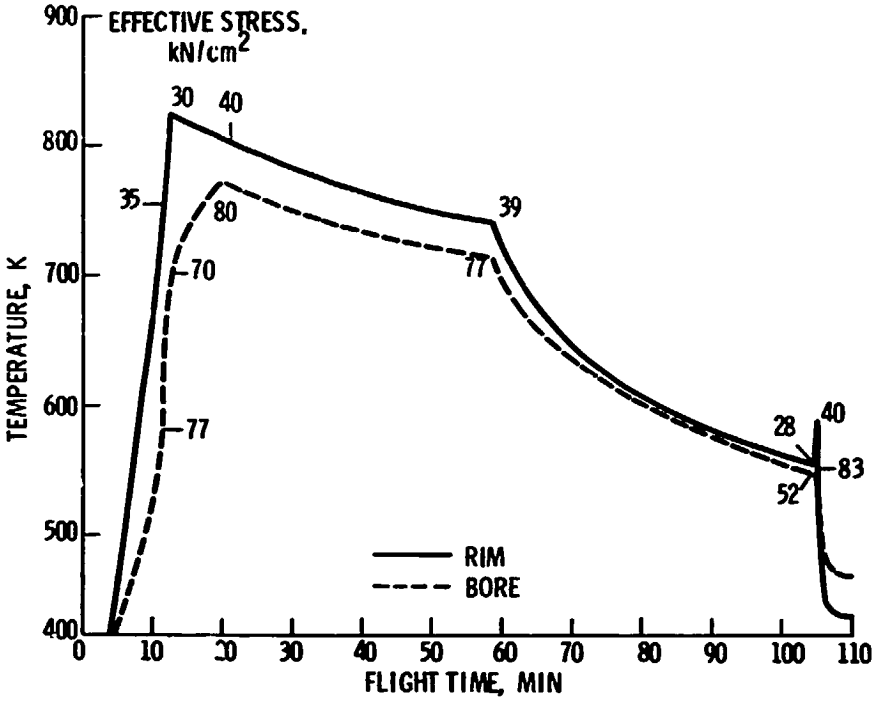

(a) INC-718 standard disk.

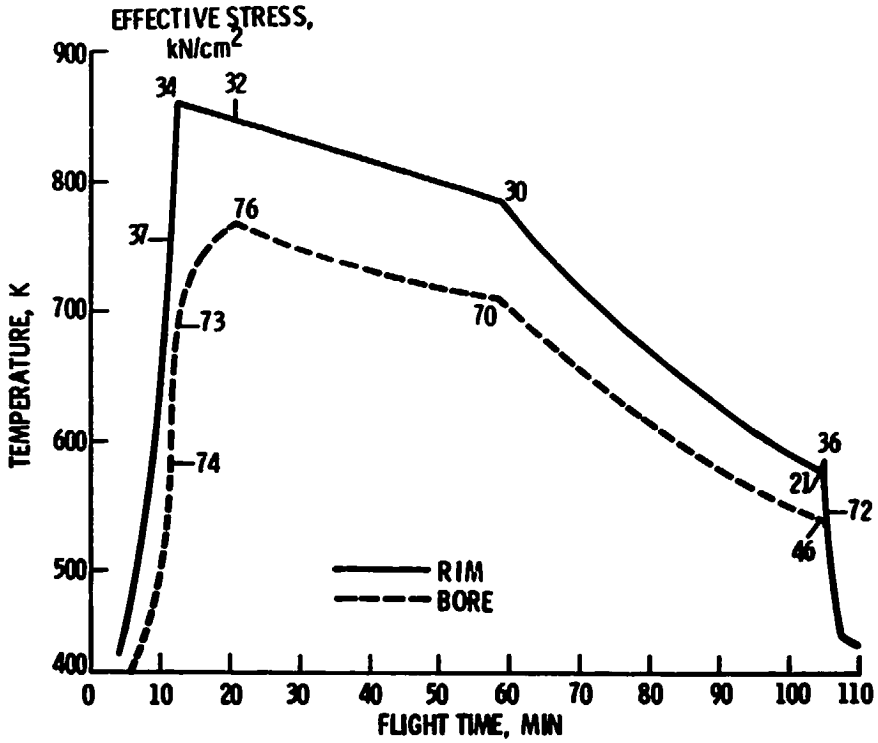

(b) Bore-entry disk.

Figure 5. - CF6-50 turbine disk temperature response.

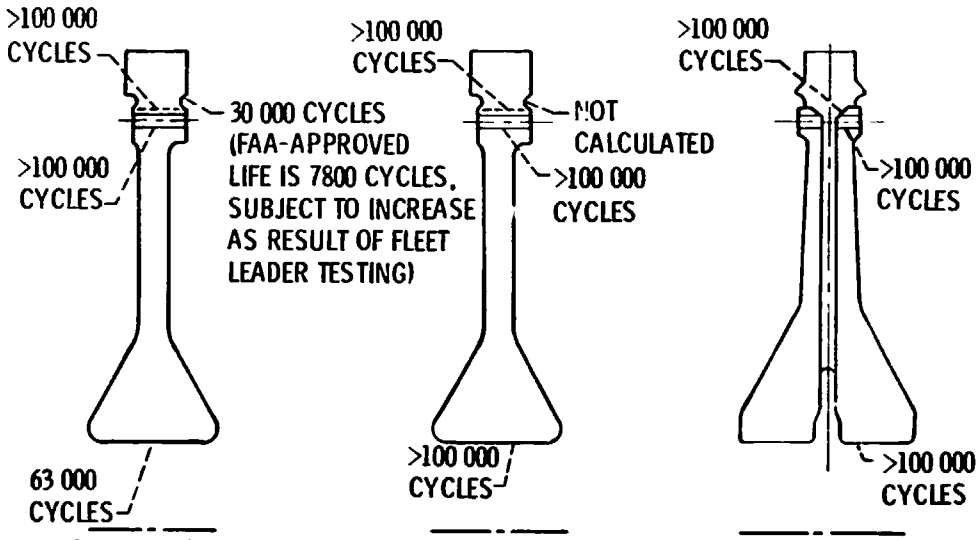

Figure 6. - Crack initiation lives of CF6-50 first-stage turbine disk designs.

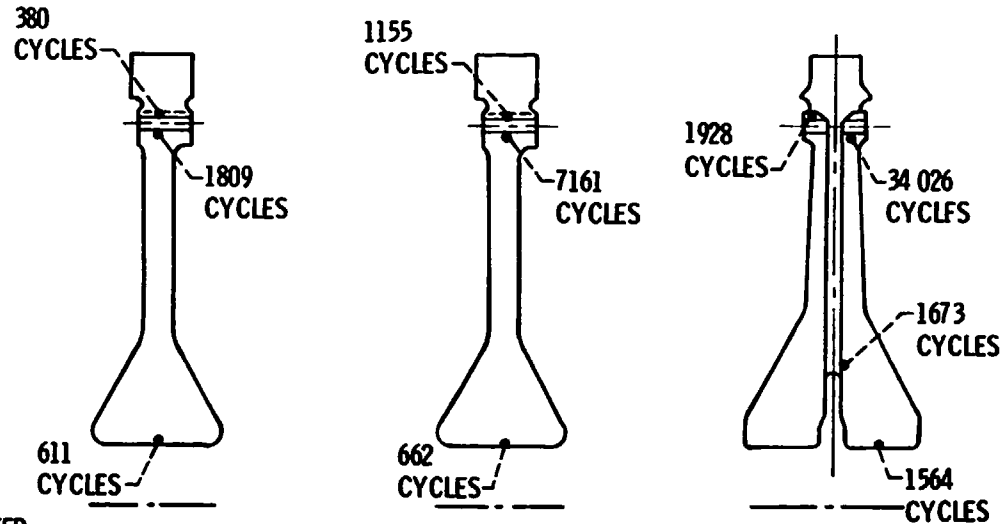

	(a) Standard disk (INC-718).	(b) Standard disk (Rene' 95).	(c) Integral bore-entry disk (Rene' 95).
BURST SPEED, PERCENT OF MAXIMUM TAKEOFF SPEED:	126	134	149
WEIGHT CHANGE, PERCENT OF STANDARD DISK WEIGHT:	---	0	+66

Figure 7. - Crack propagation lives of CF6-50 first-stage turbine disk designs.

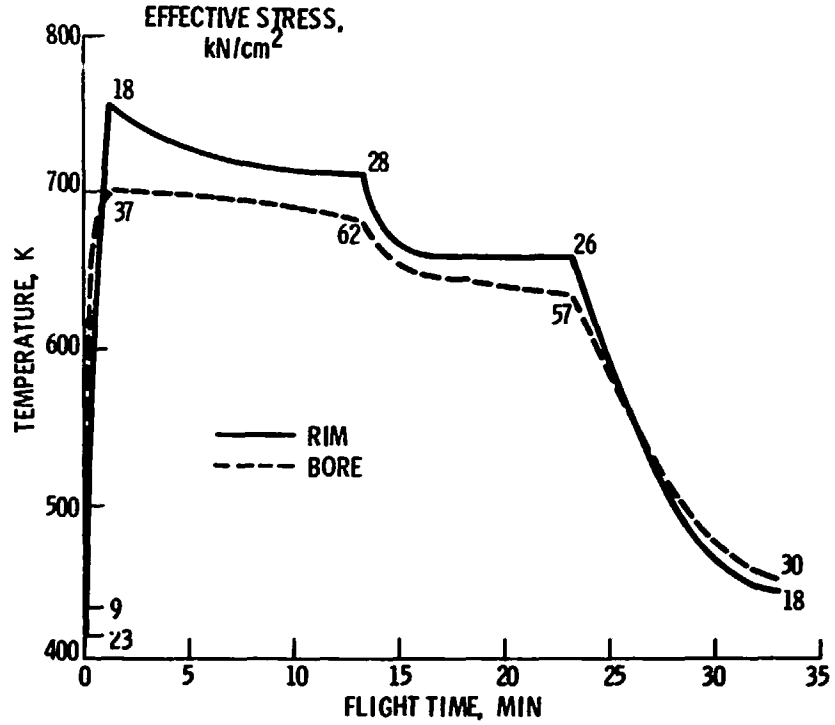

(a) Waspaloy standard disk.

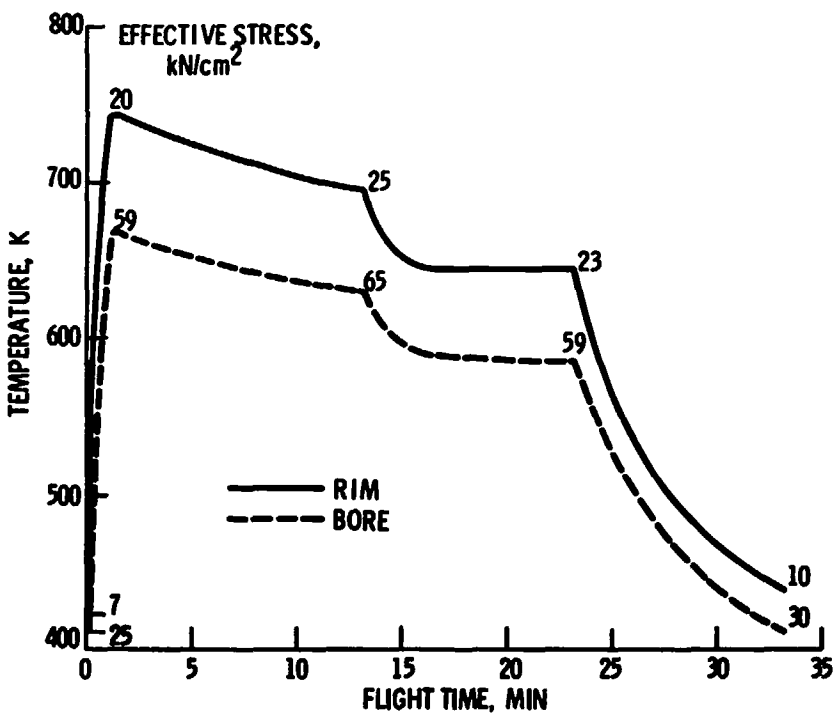

(b) Bore-entry disk.

Figure 8. - JT8D-17 turbine disk temperature response.

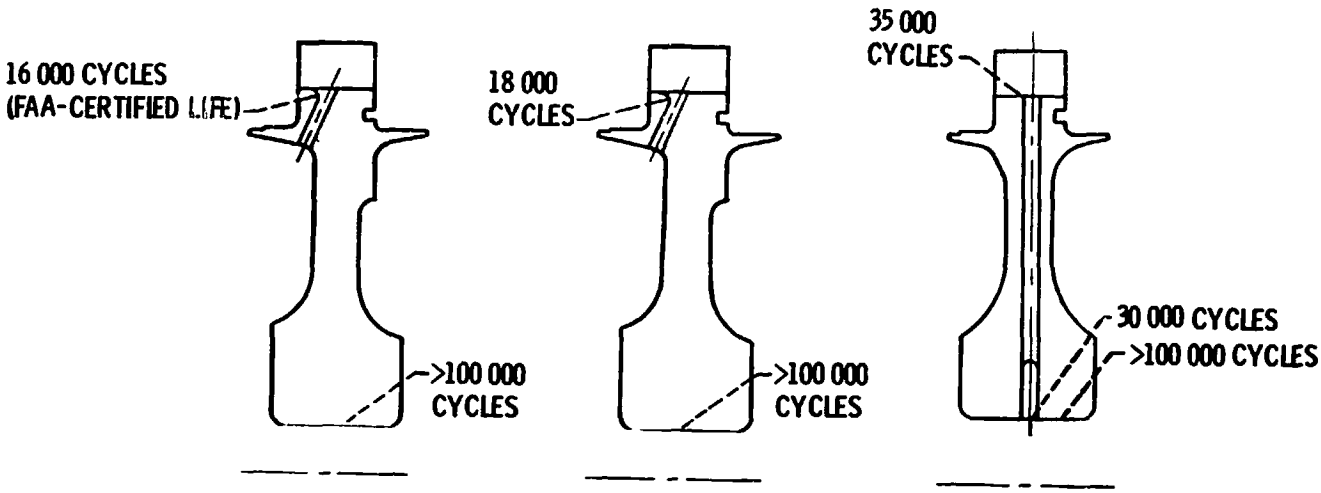

(a) Standard disk (Waspaloy).

(b) Standard disk (Astroloy).

(c) Bonded bore-entry disk (Astroloy).

Figure 9. - Crack initiation lives of JT8D-17 first-stage turbine disk designs.

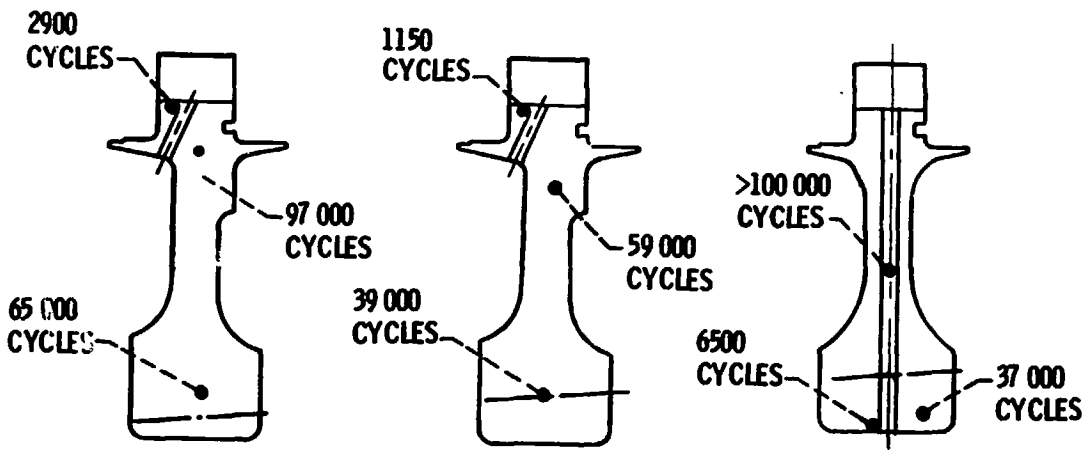

BURST SPEED, PERCENT OF MAXIMUM TAKEOFF SPEED:	136	136	133
WEIGHT CHANGE, PERCENT OF STANDARD DISK WEIGHT:	---	-4	0
	(a) Standard disk (Waspaloy).	(b) Standard disk (Astroloy).	(c) Bonded bore-entry disk (Astroloy).

Figure 10. - Crack propagation lives of JT8D-17 first-stage turbine disk designs.

DISCUSSION

J.H. Gerstle, Boeing

With respect to that bonded bore entry disk, it is a fortunate thing from an airframer's point of view that turbine disk failure fragments tend to always stay in the plane of rotation. If you remember Denis McCarthy's figure, he showed a dispersion of about ±3 degrees. We looked into it and saw something very similar: very narrow dispersion angles. I wonder if you would care to comment on if you had such a split disk design, whether the pieces would tend to fly out of the plane, which would gain us a little bit in reduced fragment energy, but from a configuration point of view the problem would be worse.

A. Kaufman, NASA-Lewis

Well, I really cannot comment much of that; that is kind of speculative. This isn't really answering your question but it's somewhat similar to it. One of the reasons that there is a disagreement between General Electric and PWA over whether you should bond disks or make them integrally is that GE is more worried about the bonded concept. I don't say this is right or wrong; but, they feel that a bonded disk is very likely to have an unbonded area which would propagate as you pile on cycles and create an unsymmetrical stress distribution. This would put some bending component on the disk, whereas an integral disk is more likely to be loaded uniformly and is more likely to do what your analysis predicts it will; it's more dependable. Pratt & Whitney seems to believe that this isn't a concern. I guess they have run some tests on this bonded design, but I don't think the tests are extensive enough to really set this concern to rest.

D.T. Poland, Lockheed-Calif.

One of the considerations in redundant structure is to have a safe-load life after you've experienced a failure so that safe operation will continue until we discover the failure. This means having a sufficient safe life to carry you between inspection periods so you can find cracks and failures on a scheduled inspection of the airframe and engines. I was wondering what considerations you had taken into account in this redundant design philosophy to allow for discovery of a failure in one of the redundant parts.

A. Kaufman, NASA-Lewis

This involved a little personal disagreement I have with the redundant design that GE did. I think it's a little over-redundant. The way they designed it was that in case of a failure, the undamaged disk could contain the failed part, and thus complete the operational life for which the disk was initially designed. I'm not sure that's not a dangerous concept because that could mean that the pilot would not be aware of the failure of part of the disk and could carry that failed part along. It seems to me that you want to have some redundancy but not too much. It would seem to me that the ideal redundant construction should be one in which you could contain the failed part long enough to get the airplane down to the ground, but by rubbing or some other means the pilot would have some warning that something is wrong. If you overdesign it so

it has a long life, the operator could be containing a failed part for thousands of cycles between overhauls, and then it could let go unexpectedly. I hope I've answered your question.

Unknown Speaker

I think it's worthwhile to point out that these pilots are very sensitive to any situation that happens. If you lose a piece of disk I do not think there is much doubt that he will not know it.

A. Kaufman, NASA-Lewis

In that redundant design if you initiate a crack in the bore, you're not going to lose a piece of disk. What you say is true if you lose a piece near the rim. But, I'm concerned that you may initiate a radial crack which may go up an inch or so and then be contained on the failed part. I don't think they have really wrung through that analysis. I'd be afraid that the pilot might not be aware of it, and the thing could come apart somewhere between overhauls. So, I think, a small amount of redundancy is what you want to aim for, and you don't want.that crack to ride along in the aircraft too long.

G.L. Gunstone, CAA-UK

It's quite a thought, Mr. Chairman, that in the whole airplane, the disks and the shafts in the engines are the only parts which are single-element items, failure of which is potentially catastrophic. On the engine side, we are 20 or 30 years behind the aircraft people in that particular respect. I think that getting redundancy or fail-safe systems is about the only solution I see as valid unless we adopt the other types of approaches we've talked about (that is, making the aircraft withstand the debris). If we're going actually to prevent the disks from failing in their own right, this is about the only way I see of it being possible.

J.C. Wallin, BAC

I just want to follow up briefly on the comments of the last two speakers. Following airframe practice, it is not going to be any good having redundancy in engines unless you have the inspection methods to go with it, so that you can detect the cracks before they become catastrophic. The way we use redundancy in the airframe structure is to have routine inspections which will pick up the flaws so you can do something about them before they get out of hand.

A. Kaufman, NASA-Lewis

I think we're talking of a redundant construction that when you get that plane down you're going to have a fairly good-size crack, maybe an inch long, maybe longer. There's always a possibility the failed part will be hidden but I would think (that aside) the inspector should be able to detect it readily.

J.T. Dixon, P&W-Florida

What the man from GE said, it's hard for me to believe, first off, that you can contain that portion with the estimated big eccentric load that you have there. But, if you do and if you can, I don't think you're going to worry about the pilot knowing. You're going to have such large deflection that those blades are going to contact the vanes, unless you're going to

increase engine length, and you add extra weight for extra engine length. So, I don't think you have to worry about excessive redundancy. A failure will be picked up pretty quick.

A. Kaufman, NASA-Lewis

It may not be detected readily but I can see what you're saying: if that flaw propagates really extensively, this will redistribute the stresses and throw an eccentric load on the disk. But suppose that the flaw grows to just an inch from the bore, I'm not sure you're going to get that much of an eccentric load that it is going to be felt.

SOME AIRLINE EXPERIENCE IN PREVENTING ENGINE ROTOR FAILURES

John J. Morelli

Director of Power Plant Maintenance*

Trans World Airlines, Inc.

Kansas City, Mo.

We have spent many hours discussing the disk and blade containment problems and have heard the viewpoints of the regulatory agencies, the engine manufacturers, and the airframe manufacturers.

The airlines' viewpoint has yet to be expressed, and I will take that on since through some misfortune of mine, I am the only airline representative here.

I have learned a great deal from the information presented here. The most important being, that no matter who accumulated and presented the data, there was virtual agreement with respect to the number of serious incidents of non-containment.

I would, however, hate to leave here having you think that it was a stroke of luck, or the will of God, that has kept the non-containment problem at such a low level that loss of life or aircraft has been remote or non-existant over the past 13 to 15 years.

The other side of the coin which must be talked to is that the airlines, with the assistance of the engine manufacturers, have achieved excellent control over the type of problems which lead to an uncontained failure--and have in fact, avoided many potential problems.

*Now retired.

I would not like to hazard a guess what the incident rate might look like if we had sat back and failed to respond or recognize incipient problems.

I can cite a few examples from memory--the JT4 engine developed a siege of third turbine blade failures which threw shrapnel out the tailpipe and into the wing flaps because most of the failures occurred on takeoff. I am sure that the statistics shown here included some JT4 damage incidents which occurred early in that period. I can tell you that this problem was effectively controlled with a very sophisticated tool, consisting of a broom stick with a rubber hose on the end of it. I don't know how many of you have heard of the "broom stick check", but it was a rather famous check across the industry. We did nothing more than put this broom stick up the tailpipe against the turbine blades while a mechanic turned the compressor. A clicking sound meant a loose turbine blade. Three clicks meant three loose blades, which was the limit we established for having the engine changed. We probably removed 100 wheels due to this problem, but I am certain you would not find an in-flight failure in the statistics since initiation of the "broom stick check". We even took a further step, we found that we could lower the back of the engine, take the exhaust case with the thrust reverser off, change the wheel while the engine was still on-the-wing, and get the job done in less time than it took us to change the engine.

Another problem that would have made headlines if left uncontrolled, was a deflection problem on the second stage nozzle guide vanes on the JT9D engine. In this case the inner platform would deflect into the second stage disk, scoring it, and causing a disk rupture. We attacked this problem with the help of Pratt and Whitney and some others in the industry, by taking X-rays of the affected area, using a radioactive isotope installed in the turbine shaft opposite the film which was wrapped around the outside of the engine. The photo permitted us to measure and monitor the gap between the two parts and to remove the engine when a given point was reached.

Again, we did not have a single failure that surely would have fallen into the "catastropic category". This type of control came about because of the initiative that we and others in the industry have taken and continue to take to avoid these kinds of problems.

The JT3D N1 Compressor rear hub failure is another excellent example. I bet there isn't anyone in the room who has heard of or has recognized that there has been a serious cracking problem with this hub over the past three to four years. This one wasn't easy to control, because it was so difficult to get to, being located between the N1 and N2 compressors with no exterior borescope holes readily available. We did, none-the-less, develop a good control system by inserting an eddy current probe on a long handle thru the N1 gearbox and compressor shaft. It took the finesse of a brain surgeon to detect a crack in such a difficult area, but once we mastered the technique we avoided having a single hub failure.

The last one that comes to mind is the RB211 problem which caused burn thru and release of the first stage nozzle guide vane. In addition to the safety aspects of this problem was the fact that the nozzle guide vane could cause downstream damage to the tune of about three to four hundred thousand dollars worth of turbine parts. In this case we simply used frequent borescope inspections through borescope holes that were strategically located to monitor and measure the rate of burning.

If my memory were better I could reach back for more examples, but gentlemen, if you multiply the TWA experience by the number of airlines, I believe you would have to acknowledge that we have pretty good control and have, in fact, minimized our exposure. You must understand, we do not wait for a spectacular failure to occur before reacting. We are constantly on the look out for incipient problems anytime an engine goes thru our engine shops. Additionally,

we trade experience with other airlines and with the engine manufacturers. Once a problem is identified, we establish a plan for the engines that are in service to avoid any inflight failures. It is our aim to develop the technology necessary to cull out the suspect engines while they are on the aircraft. To do so is vital, because there is no airline in the world that could put 400 engines on the ground and take them off to determine if they have a problem. So it is imperative that we categorically develop ways and means of finding problem engines quickly as a control and stop gap measure. It takes two to three years to cycle a given modification in a sizeable airline fleet--therefore these inspection measures are the only means of avoiding an economic catastrophy.

Quite honestly, I think we have pushed our diagnostic capability to a near limit. We need some new innovations. We need new holes in different places on the engines. We need some creative thinking that allows us to have greater visability within the engines and to test for problems that may be incipient.

We are somewhat more fortunate on the Jumbo Jets because at the insistence of the airlines, and by the good graces of the manufacturers, we do have a generous group of borescope holes, in addition to a modular concept of the major engine components, which allows for quick and more effective response in the field than we have with the older model jet engines. This is one of the reasons I get extremely nervous and extremely disturbed when I hear we are considering wrapping boiler plate around engines for better containment. It is my opinion that this is going the wrong way because, as I have stated, in order to control our problems, we must be able to see them--it is the problems we cannot see historically, that have hurt us.

I would like to continue my sales pitch for just a minute, since I am not certain that many in the industry recognize the job of the failure detection that the airlines have had in effect for a number of years. These procedures in fact allow us to anticipate and remove 85 percent of the engine failures long before they reach a critical stage. We can conveniently schedule the removal at our discretion, and in many cases maintenance and/or flight crews are not aware of the developing problems.

The first of these tools is an engine in-flight data analysis program developed twelve to thirteen years ago with the assistance of Pratt and Whitney. It involves a computer process which is nothing more than a gas path deterioration indicator. The data which is put into the computer daily is corrected to standard day conditions and is compared with a normal gas generator. The deviation for all engine parameters is then plotted. We simply look for the swing or trends in the data and it is possible to examine 1000 flying engines in 1½ hours, picking out those that appear to have a problem.

Spectographic analysis is another limited, but useful tool that can detect impending failures in some cases as far off as three to four months in advance.

We have for a number of years also been testing the AIDS system, which I'm sure some of you in the industry have heard about. We are the only domestic airline in the world who has decided to invest several million dollars in the installation of this equipment in our jumbo jet aircraft in order to capture dynamic information on not only the normal engine parameters which are observed by the flight engineers, but also into other areas of the engine to sample new parameters that we may someday find useful in furthering our engine failure detection capability. Unfortunately, we are not a research department, and we must limit the amount of Engineering we put into this kind of thing, since

we are basically in the business of carrying passengers.

We have made some great strides, but with the help of the type people available in this room, we could literally turn the world over in terms of advancing our diagnostic capability. This is one of the reasons I was pleased to hear John Barringer, yesterday, telling us about trying to install a crack detector in an operating engine. As I mentioned, the approach was wrong, but the ideas was beautiful! We don't necessarily need to build the diagnostics within the engine, since the environment is too hostile. What is needed is the ability to look inside the engine. I'm sure there are many innovative ways you gentlemen can think of to do this. I'm quite proud of an industry that can see 84 percent of its failures before they occur; so the 15 percent remaining can be a very fertile area for all of us to work in.

Aside from this, I certainly think we need to continue studying the trajectory of uncontained failures that do occur as it is obvious the risk of uncontained failures will be with us forever, irrespective of what containment approach we take. So therefore, we still need to learn as much as we can when a failure occurs so the airframe manufacturer, who apparently has done a fine job up to this point, can improve on locating vital systems.

APPENDIX A - AGENDA

Tuesday, March 29, 1977

INTRODUCTORY REMARKS AND MEETING OBJECTIVES: S. Weiss, NASA-Lewis

Session 1: PROBLEM DEFINITION; DESIGN CONSIDERATIONS, OBJECTIVES, AND APPROACHES

Chairman: J. H. Enders, FAA

1.1 A. K. Forney, FAA: Federal Aviation Association's Approach to Engine Rotor Integrity

1.2 G. L. Gunstone, CAA-UK: Engine Non-Containment -- the UK CAA View

1.3 S. A. Sattar, P&W-UTC: Aircraft Engine Containment -- SAE Committee Findings

1.4 R. B. McCormick, Boeing: Rotor Burst Protection Criteria and Implications

1.5 J. C. Wallin, BAC: Engine Non-Containment -- UK Risk Assessment Methods

Session 2: ROTOR BURST PROTECTION - STATE OF THE ART

Chairman: J. H. Gerstle, Boeing

2.1 D. McCarthy, Rolls-Royce Ltd.: Types of Rotor Failure and Characteristics of Fragments

2.2 M. A. O'Connor, Jr., McD-Douglas: Blade Fragment Energy Analysis

2.3 J. E. Wignot, Lockheed-Cal.: Designing the L-1011 to Minimize Rotor Failure Effects

2.4 M. A. O'Connor, Jr., McD-D: Approaches to Rotor Fragment Protection

2.5 D. F. Haskell, Army-BRL: Metallic Armor for Ballistic Protection from Steel Fragments

Wednesday, March 30, 1977

2.6 G. J. Mangano, NAPTC: Rotor Burst Protection Program -- Experimentation to Provide Guidelines for the Design of Turbine Rotor Burst Fragment Containment Rings

2.7 E. A. Witmer, MIT: Analysis of Simple 2-D and 3-D Metal Structures Subjected to Fragment Impact

2.8 R. J. Bristow, Boeing: Development of Fiber Shields for Engine Containment

2.9 A. T. Weaver, P&W-UTC: Kevlar for Blade Containment

2.10 D. Roylance, MIT: Numerical Analyses of Impact in Woven Textile Structures

2.11 J. H. Gerstle, Boeing: Analysis of Methods for Kevlar Shield Response to Rotor Fragments

2.12 P. B. Gardner, Norton Co.: Ceramic Composite Protection for Turbine Disc Bursts

2.13 A. G. Holms, NASA-Lewis: Concepts for the Development of Light-Weight Composite Structures for Rotor Burst Containment

Session 3: ROTOR BURST PREVENTION - STATE OF THE ART

Chairman: G. J. Mangano, NAPTC

3.1 J. T. Hill, P&W-UTC: Design of Rotors for Improved Structural Life

3.2 R. E. Duttweiler, GE: Materials and Manufacturing Process for Increased Life/Reliability

3.3 J. E. Doherty, P&W-UTC: NDE -- A Key to Engine Rotor Life Prediction

3.4 J. Barranger, NASA-Lewis: Application of a Flight-Line Disk Crack Detector to a Small Engine

Thursday, March 31, 1977

3.5 A. Kaufman, NASA-Lewis: Turbine Disks for Improved Reliability

3.6 J. J. Morelli, TWA, Inc.: Some Airline Experience in Preventing Engine Rotor Failures

Session 4: SUMMARY OF TOPICS 1, 2, AND 3

Chairman: S. Weiss, NASA-Lewis

4.1 A. K. Forney and J. J. Shea, FAA: Summary of Design Considerations, Objectives, and Approaches

4.2 S. A. Sattar, P&W-UTC: Rotor Burst Protection -- Status of Analysis and Experiments, Prospects, and Needed Research

4.3 B. L. Koff, GE: Rotor Burst Prevention -- Status, Prospects, and Needed Research

CLOSING REMARKS: S. Weiss, NASA-Lewis

APPENDIX B - ATTENDEES

Dr. John P. Barranger
Mail Stop 77-1
NASA Lewis Research Center
21000 Brookpark Road
Cleveland, OH 44135

Mr. Leonard Beitch
General Electric Co.
Interstate 75, Bldg. 500
M.D. K221
Cincinnati, OH 45215

Mr. Robert Berman
Federal Aviation Administration
Code ANE-214, Propulsion Section
12 New England Executive Park
Burlington, MA 01803

Dr. R.J. Bristow
Boeing Aerospace Co.
Impact Mechanics Lab.
P.O. Box 3999
Seattle, WA 98124

Mr. George E. Buron
Chief Project Engineer
Armor & Spectramic Products
Norton Company
Industrial Ceramics Div.
Worcester, MA 01606

Mr. E.G. Carrington
Canadair, Ltd.
P.O. Box 6087
Montreal, Canada H3C 3G9

Mr. Robert DeLucia
Naval Air Propulsion Test Center
Aeronautical Engine Dept.
Trenton, NJ 08628

Mr. J. Thomas Dixon
Government Products Division
Pratt & Whitney Aircraft, UTC
Box 2691
West Palm Beach, FL 33402

Dr. J.E. Doherty
Pratt & Whitney Aircraft Group
United Technology Corp.
400 Main Street
East Hartford, CT 06108

Professor John Dugundji
MIT, Room 33-313
Cambridge, MA 02139

Dr. R.E. Duttweiler
Aircraft Engine Group
General Electric Co.
Cincinnati, OH 45215

Mr. John H. Enders
Federal Aviation Administration, DOT
Office of Aviation Safety, FOB 10A
800 Independence Ave., S.W.
Washington, DC 20591

Mr. A.K. Forney
Federal Aviation Administration
AFS-140
Washington, DC 20591

Mr. Paul B. Gardner
Industrial Ceramics Div.
Norton Company
1 New Bond Street
Worcester, MA 01606

Mr. Herbert Garten
General Electric Company
Aircraft Engine Group
Lynn, MA 01902

Mr. Joseph Gausselin
D 422/402 AB71
Rockwell International Corp.
Los Angeles International Airport
Los Angeles, CA 90009

Dr. John H. Gerstle
Propulsion Technology Staff
Boeing Commercial Airplane Co.
P.O. Box 3707
Seattle, WA 98124

Mr. G.L. Gunstone
Civil Aviation Authority
Airworthiness Division
Brabazon House
Redhill Surrey RH 1 1 SQ
ENGLAND

Dr. Donald F. Haskell
U.S. Army Ballistics Research Lab.
Aberdeen Proving Ground, MD 21005

Attn: DRXBR-BM

Mr. Arthur G. Holms
Mail Stop 500-204, ASRDI
NASA Lewis Research Center
21000 Brookpark Road
Cleveland, OH 44135

Dr. Thomas G. Horeff
Chief, Propulsion Branch
FAA, AFS-140
800 Independence Ave., S.W.
Washington, DC 20591

Mr. Herbert Kaehler
AVCO, Lycoming Division
550 South Main Street
Stratford, CT 06497

Mr. Albert Kaufman
Mail Stop 77-2
NASA Lewis Research Center
21000 Brookpark Road
Cleveland, OH 44135

Dr. B.L. Koff
Chief Engineer
Aircraft Engine Group
General Electric Co.
Cincinnati, OH 45215

Dr. Kyohei Kondo
MIT, Room 41-211
Cambridge, MA 02139

Dr. John W. Leech
Solar Energy Division
Energy Research and Development Admin.
200 Mass. Ave., N.W.
Washington, DC 20545

Mr. Allen Lush
MIT, Room 41-219
Cambridge, MA 02139

Mr. G.J. Mangano
Naval Air Propulsion Test Center
Aeronautical Engine Department
Trenton, NJ 08628

Mr. Denis M. McCarthy
Chief Engineer, Staff Engineering
Rolls-Royce (1971) Limited
Moor Lane, P.O. Box 31
Derby DEZ 8 BJ
UNITED KINGDOM

Dr. Ralph B. McCormick
Propulsion Design
Boeing Commercial Airplane Co.
P.O. Box 3707
Seattle, WA 98124

Dr. Thomas McDonough
Aeronautical Research Associates of
Princeton, Inc.
P.O. Box 2229
Princeton, NJ 08540

Mr. John Meaney
Rohr Industries
Foot of H Street
Chula Vista, CA 92010

Mr. Fred Merlis
MIT, Room 33-122
Cambridge, MA 02139

Professor Rene H. Miller
MIT, Room 33-207
Cambridge, MA 02139

Mr. John J. Morelli
Director, Power Plant Maintenance
TWA, Inc.
Kansas City International Airport
P.O. Box 20126
Kansas City, MO 64195

Mr. M.A. O'Connor, Jr.
Douglas Aircraft Co.
3855 Lakewood Blvd.
Mail Code 36-41
Long Beach, CA 90846

Mr. M.K. O'Connor
Senior Design Engineer
Beech Aircraft Corp., Plant 1
Wichita, KA 67201

Dr. Donald W. Oplinger
Mechanics Research Lab.
Army Materials and Mechanics
Research Center
Watertown, MA 02172

Mr. D.T. Poland
Dept. 73-31, Bldg. 90, PL. A-1
Lockheed California Co.
P.O. Box 551
Burbank, CA 91520

Mr. David T. Powell
Chief, Propulsion Research Staff
Beoing Commercial Airplane Co.
P.O. Box 3707
M/S 73-01
Seattle, WA 98124

Mr. José J.A. Rodal
MIT, Room 41-219
Cambridge, MA 02139

Dr. David Roylance
MIT, Room 6-202
Cambridge, MA 02139

Mr. Herbert J. Rubel
1451 Holly Lane, N.E.
Atlanta, GA 30329

Dr. S.A. Sattar
Pratt & Whitney Aircraft Group
United Technology Corp.
400 Main Street
East Hartford, CT 06108

Mr. James Salvino
Naval Air Propulsion Test Center
Aeronautical Engine Department
Trenton, NJ 08628

Mr. John Schneider
General Electric Co. - I75
Gimson Road - K59
Cincinnati, OH 45215

Cdr. John J. Shea
FAA, ARD-520
2100 2nd Street, S.W.
Washington, DC 20591

Dr. Robert L. Spilker
University of Illinois at
Chicago Circle
Dept. of Materials Engineering
Box 4348
Chicago, IL 60680

Mr. Thomas R. Stagliano
MIT, Room 41-219
Cambridge, MA 02139

Mr. William Springer
Detroit Diesel Allison
General Motors Corp.
Speed Code T3, Box 894
Indianapolis, IN 46206

Dr. George P. Townsend
Hamilton Standard Division of
United Technologies Corp.
Mail Stop IA-3-3
Windsor Locks, CT 06096

Mr. John Veneri
AVCO, Lycoming Division
550 South Main Street
Stratford, CT 06497

Mr. Curtiss Walker
U.S. Army Air Mobility Research
and Development Lab.
NASA Lewis Research Center
Cleveland, OH 44134

Mr. J.C. Wallin
British Aircraft Corp., Ltd.
Chief Propulsion Engineer
Commercial Aircraft Division
Filton House, Bristol BS 99 7AR
ENGLAND

Dr. Alan T. Weaver
Pratt & Whitney Aircraft Group
United Technology Corp.
400 Main Street
East Hartford, CT 06108

Mr. Solomon Weiss
Mail Stop 500-204, ASRDI
NASA Lewis Research Center
21000 Brookpark Road
Cleveland, OH 44135

Mr. Jack E. Wignot
Dept. 75-71, Bldg. 63, PL. A-1
Lockheed California Co.
P.O. Box 551
Burbank, CA 91520

Professor Emmett A. Witmer
MIT, Room 41-219
Cambridge, MA 02139

Mr. Edward P. Wizniak, TE-20
National Transportation Safety Board
800 Independence Ave., S.W.
Washington, DC 20594

1 Report No	2 Government Accession No	3 Recipient's Catalog No
NASA CP-2017		

4 Title and Subtitle	5 Report Date
AN ASSESSMENT OF TECHNOLOGY FOR TURBOJET ENGINE ROTOR FAILURES	August 1977
	6 Performing Organization Code
7. Author(s)	8 Performing Organization Report No E-8305
9. Performing Organization Name and Address Aeroelastic and Structures Research Laboratory Department of Aeronautics and Astronautics Massachusetts Institute of Technology Cambridge, Massachusetts 02139	10. Work Unit No
	11 Contract or Grant No
12. Sponsoring Agency Name and Address National Aeronautics and Space Administration Washington, D.C. 20546	13. Type of Report and Period Covered Conference Publication
	14. Sponsoring Agency Code

15. Supplementary Notes Editor, Emmett A. Witmer, Massachusetts Institute of Technology, Cambridge, Massachusetts 02139; Coordinator, Arthur G. Holms, NASA Lewis Research Center, Cleveland, Ohio 44135.

16. Abstract

The nature and scope of the safety problems posed by turbojet engine rotor burst fragments are reviewed. The current state of the art of providing protection from engine rotor burst fragments is described. Included are structural and aircraft system redundancies, local shield protection, and engine mounted fragment control systems, together with methods for the design and development of these techniques. Descriptions are given of a variety of measures to reduce the frequency and severity of engine rotor bursts. They include nondestructive inspection by engine manufacturers and by airline operators including in-flight, at air terminals, and during overhaul. Also included are design concepts to reduce the energy of fragments when failures occur.

17. Key Words (Suggested by Author(s))	18. Distribution Statement
Air transportation and safety; Structural mechanics; Rotor burst protection; Quality assurance; Reliability; Fragment impact; Transient structural response	Unclassified - unlimited STAR Category 03

19. Security Classif. (of this report)	20. Security Classif. (of this page)	21. No. of Pages	22. Price*
Unclassified	Unclassified	434	A19

* For sale by the National Technical Information Service, Springfield, Virginia 22161

*U.S. GOVERNMENT PRINTING OFFICE 1977-757-070/6306